

DISSERTATION ZUR ERLANGUNG DES DOKTORGRADES
DER FAKULTÄT FÜR CHEMIE UND PHARMAZIE
DER LUDWIG-MAXIMILIANS-UNIVERSITÄT MÜNCHEN

**SYNTHESIS AND CHARACTERIZATION OF
NITROGEN-RICH ENERGETIC MATERIALS
BASED ON AZOLES**



PHILIPP CHRISTOPH SCHMID

aus

München

2016

Erklärung:

Diese Dissertation wurde im Sinne von § 7 der Promotionsordnung vom 28. November 2011 von Herrn Professor Dr. Thomas M. Klapötke betreut.

Eidesstattliche Versicherung:

Diese Dissertation wurde eigenständig und ohne unerlaubte Hilfe erarbeitet.

München,

.....
Philipp Schmid

Dissertation eingereicht am: 26.02.2016

1. Gutachter: Prof. Dr. Thomas M. Klapötke

2. Gutachter: Prof. Dr. Konstantin Karaghiosoff

Mündliche Prüfung am: 14.04.2016

Acknowledgement

First of all, I would like to thank Prof. Dr. Thomas M. Klapötke for offering me the opportunity to carry out my Ph.D. study in his laboratory and for giving me the freedom to pursue the topics of my interest. As a devoted mentor in many ways, Prof. Dr. Thomas M. Klapötke has been always supportive, understanding, and available for discussions and advice. In addition, I thank him for encouraging me to attend several conferences to present my research results and to work at Nalas Engineering in the United States, where I gained enormous working experience in industrial problems.

I also would like to thank Prof. Dr. Konstantin Karaghiosoff for helping me with numerous crystal structure measurements, even on the weekend and late at night. He has always contributed positively to our laboratory from not only his advice about NMR spectroscopy and X-ray structures, but also from his friendly and optimistic personality. He is also greatly acknowledged for his valuable suggestions on this thesis.

In addition, I would like to thank Prof. Dr. Manfred Heuschmann, Prof. Dr. Andreas Kornath, Prof. Dr. Wolfgang Beck, and Prof. Dr. Ingo-Peter Lorenz for being on the Ph.D. defense committee.

I would like to express my sincere appreciation to Dr. Jörg Stierstorfer for his help with solving X-ray crystal structures, calculating heats of formation, proofreading many manuscripts and this thesis, as well as providing much guidance and advice during the past three years.

Many thanks to Jerry Salan for the fruitful collaboration between Nalas Engineering and our laboratory, and for giving me the opportunity to work with him on large scale preparation of energetic materials during the summer 2015. Furthermore, I also would like to thank Dr. Pascal Dubé for mentoring and guiding me during my time at Nalas Engineering.

Chemistry can be dangerous, especially when dealing with energetic materials. I would like to thank Dr. Burkhard Krumm for answering all questions related to lab safety and for maintaining the highest possible safety standards within our laboratory.

Irene Scheckenbach is thanked for her helpfulness, for taking care of all bureaucratic problems, and for providing helpful information about alternative funding possibilities.

I would like to thank all my labmates in D3.110, including Marc Bölter, Dr. Dennis Fischer, Maurus Völkl, and Tomasz Witkowski, who have created a pleasant and productive working atmosphere. Our discussions about chemistry, soccer, and everything else have always been wonderful facets during my Ph.D. study.

I would like to thank several people for their scientific input and for introducing me to the field of energetic materials. I am deeply indebted to my colleague Dr. Dennis Fischer, who guided me not only in the beginning of my thesis, but always answered questions regarding the synthesis of energetic materials. I also want to thank him for the fun moments, when he talked himself into a frenzy. Moreover, I would like to thank Dr. Davin Piercey for sharing his views on energetic materials, the economy, and other things, as well as for taking me to work during my time in New Haven. Many more thanks go to Dr. Andreas Preimesser for answering any questions related to nitration reactions and Carolin Pflüger for introducing me to the pycnometer and helping me with X-ray crystallographic questions. Dr. Fang Wang is also greatly acknowledged for mentorship and guidance, answering any questions related to chemistry or China, and for many inspiring lively discussions about chemistry and life.

I also want to thank my bachelor and research students Matthias Kurz, Simon Kießling, Simon Schnell, Katherina Hafner, Marcel Leroux for their contributions and the good teamwork in our laboratory.

Stefan Huber is thanked for introducing me to the BAM fallhammer and friction tester, and for measuring the sensitivities of numerous materials. The X-ray and the analytical teams are thanked for measuring countless single crystals, NMR, MS, and elemental analysis samples.

Certainly the life during Ph.D. study is more than just chemistry. I feel fortunate to have shared a lot of time with present and past members of the weekly "Kochrunde" for various delicious meals and enjoyable talks during lunch time. Among them are Dr. Camilla Evangelisti, Johann Glück, Ivan Gospodinov, Martin Härtl, Dr. Marcos Kettner, Carolin Pflüger, Regina Scharf, Dr. Jörg Stierstorfer, Norbert Szimhardt, and Maurus Völkl. It was also my great pleasure to spend some entertaining Friday afternoons and evenings in the "Kaffeeküche" with Josh Bauer, Johann Glück, Ivan Gospodinov, Tobias Hermann, Dr. Dániel Izsák, Dr. Andreas Preimesser, Dr. Jörg Stierstorfer, Norbert Szimhardt, and Maurus Völkl. Dominykas Juknelevicius is thanked for interesting discussions about fireworks and the memorable skiing trips to Austria. Moreover, I thank Josh Bauer for proofreading this thesis.

I also want to thank all other members of the Klapötke and Karaghiosoff laboratories for their good collaboration and amusing free time activities over the past three years.

I would like to thank Pamela "Pam" Hathway, Simon Peschke, Thomas Riffelmacher, Frank Tambornino, and Daniel Terwilliger, for the amusing learning sessions during my undergraduate studies. Special thanks goes to Simon Peschke, Frank Tambornino, and Daniel Terwilliger for holding on to the tradition of our weekly lunch meetings discussing not only chemistry but also many other important aspects in life.

I would like to thank the people that I am proud to have as my friends (I hope that it is also true the other way around). Some of them have been there for me for two decades. This long list includes Daniela Beer, Katrin Dylla, Thomas Flügel, Johanna Groß, Katrin Groß, Bernhard Grzonka, Mirco Haupt, Gesine Hübner, Malte Niklaß, Benjamin Pointner, Oliver Reith, Daniel Rossmann, Patrick Ströthoff, Johannes Vitzagia, and Marcel Wiemann. I would like to thank you all for the fun time we spent together during school or later, for discussions, help, entertaining evenings and fun-filled holidays.

I would like to deeply thank my girlfriend Katrin Gaigl for her love and support during my study.

I am deeply indebted to my mother Jutta Schmid, my sister Sarah Schmid and my grandmother Helga Mund for their endless support during my entire life.

Contents

1.	Introduction.....	1
2.	Summary and Conclusion.....	15
3.	Synthesis of 5-(1 <i>H</i> -Tetrazolyl)-1-hydroxy-tetrazole and Energetically Relevant Nitrogen-Rich Ionic Derivatives.....	24
4.	5-(1 <i>H</i> -Tetrazolyl)-2-Hydroxy-Tetrazole: A Selective 2 <i>N</i> -Monoxidation of Bis(1 <i>H</i> -Tetrazole)	52
5.	Synthesis and Characterization of the Asymmetric 1,2-Dihydroxy-5,5'-bitetrazole and Selected Nitrogen-Rich Derivatives	77
6.	Energetic Improvements by <i>N</i> -Oxidation: Insensitive Amino-Hydroximoyl-Tetrazole-2 <i>N</i> -Oxides	103
7.	Energetic Complexes of 5-(4-Amino-1,2,4-triazol-3-on-5-yl)tetrazole and Ionic Derivatives of its 2 <i>N</i> -Oxide	122
8.	Thermal Stabilization of Energetic Materials by the Aromatic Nitrogen-Rich 4,4',5,5'-Tetraamino-3,3'-Bi-1,2,4-Triazolium Cation	142
9.	3,6,7-Triamino-[1,2,4]triazolo[4,3- <i>b</i>][1,2,4]triazolium - a non-toxic, high performance energetic building block with excellent stabilities.....	189
10.	Energetic Materials Based on 5,5'-Diamino-4,4'-nitramino-3,3'-bi-1,2,4-triazole.....	235
11.	Crystal Structures of Furazanes	258
12.	Appendix: General Information.....	279
13.	List of publications	284

1. Introduction

1.1. Milestones in the Development of Energetic Materials

The development of energetic materials began with the serendipitous discovery of *black powder* in ancient China. One of the first documents explicitly describing the ingredients of black powder dates back to 808 AD (Figure 1).^[1] Instead of exploiting the explosive nature of black powder, Taoist monks used such mixtures to "tame" the violent nature of the key components in medicines for immortality.^[2]



Figure 1. A procedure for making gun powder described in an ancient Chinese book 太上圣祖金丹秘诀, Taishang (Top high) Shengzu (Holy ancestor) Jindan (Gold ball, Chinese monks used to make medicine into small balls) Mijue (Secret recipes) by the Taoist monk Qing Xu Zi (Clear Unreal/Empty Gentleman).

Even though modern black powder still contains the same ingredients (sulfur, salpeter (KNO_3), and a carbon source), the ratio significantly differs from the original Chinese recipe with the optimal ratio found to be 75% salpeter, 10% sulfur and 15% charcol. It took 400 – 500 years before European monks, such as the English Roger Bacon, the German Berthold Schwarz, and the fictive author Marcus Graecus, described black powder in the 12th and 13th centuries.

In the following centuries, *black powder* remained the only explosive for military and civil applications. In 1847, the Italian chemist Ascanio Sobrero synthesized *nitroglycerin* (NG), which was not applicable due to its high sensitivity. Alfred Nobel, on the other hand, developed the nitroglycerin-based *dynamite* (75% nitroglycerin, 25% kieselgur). This explosive was patented in 1867^[3] and commercialized afterwards.

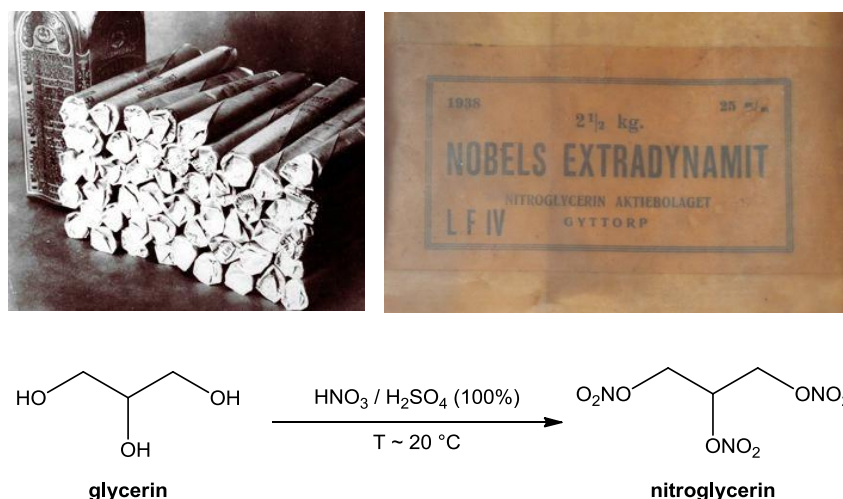


Figure 2. Alfred Nobel's Extradynamit^[4,5] (top) and the synthetic route toward nitroglycerin (bottom).

Picric acid (PA) was first reported by the alchemist Johann Glauber in 1742, who treated wool or horn with nitric acid and obtained potassium picrate. It took more than 100 years until its application as an explosive was found by Sprengel, who detonated PA in 1871 and filed the related patents.^[6] Thereafter, PA replaced black powder in nearly all military applications. However, the high acidity of PA causes the corrosion of metal shell walls, resulting in the formation of highly sensitive metal salts that can explode unpredictably, which made alternative explosives desirable.

Trinitrotoluene (TNT), first synthesized by Julius Wilbrand in 1863,^[7] replaced more sensitive PA in the early 20th century. TNT is melt-castable, allowing it to be melted without decomposition and casted into any form required by military or civil applications. Today, TNT is still used by construction and mining companies, as well as the US Military. Due to its melt-castability, TNT is a key component in many explosive mixtures, such as *composition B* (60% *hexogen* (RDX), 39% TNT, and 1% wax as binder) or *pentolite* (50% TNT and 50% *nitropenta* (PETN)).

Besides TNT, several robust nitroaromatic-based explosives have also been synthesized:

Nitropenta (PETN) was synthesized by Bernhard Tollens in 1891^[8] and widely exploited after the 1920s. PETN has a moderate thermal stability ($T_m = 143\text{ }^{\circ}\text{C}$, $T_{dec.} = 208\text{ }^{\circ}\text{C}$) and can accidentally be initiated by mechanical stimuli. PETN is used today in blasting caps and wires as a booster explosive to detonate a secondary explosive. Furthermore, PETN is utilized in explosive mixtures, such as *Semtex*, which contains RDX and PETN.

Hexogen (RDX) was discovered by Georg Henning in 1898.^[9] After the synthesis was improved by Bachmann,^[10] it was widely used during World War II. RDX remains one of the most commonly used secondary explosive in the military, due to its high detonation velocity and thermal stability up to $210\text{ }^{\circ}\text{C}$. It has also been applied in many polymer bonded explosives, such as *Composition A*, *Composition C4*, and *Torpex*.

Octogen (HMX) was also obtained in Bachmann's synthesis of RDX as a side product (8–12%).^[10,11] HMX has a slightly higher density than RDX and is somewhat more powerful. HMX is used in military applications, such as shaped charges and in detonators for nuclear weapons.

Triaminotrinitrobenzene (TATB) was first synthesized by C. L. Jackson and J. F. Wing in 1888.^[12] This compound started to draw more attention in the 1950s as an explosive from the Naval Ordnance Laboratories and its large-scale synthesis was later improved and reported in 1976.^[13] TATB has a high stability against thermal and physical stimuli, due to inter- and intramolecular hydrogen-bonding, making it useful in nuclear warheads.

Hexanitrostilbene (HNS), first prepared by Shipp in 1964,^[14] is another highly stable nitroaromatic-compound. Due to its high melting point around $315\text{ }^{\circ}\text{C}$, HNS is used as a heat resistant high explosive for oil exploration and in the Apollo Lunar Active Seismic Experiments.^[15]

The next milestone in energetic materials was the preparation of *hexanitroisowurtzitan* (CL-20) by Nilsen *et al.* at the Naval Air Warfare Center Weapons Division in China Lake, CA in 1987.^[16] The caged nitramine CL-20 exists as five polymorphs but only the ϵ -polymorph has potential applications because it has the highest density.

Similar caged energetic materials include *octanitrocubane* (ONC), which was synthesized by Eaton *et al.* in 1999.^[17] ONC has not found any applications yet because of its challenging and expensive multiple-step synthesis.

The Swedish FOI made progress in the area of highly stable energetic materials by preparing the insensitive and thermally stable *diaminodinitroethene* (FOX-7) in 1998.^[18]

In 2012 Klapötke and coworkers prepared *dihydroxylammonium 5,5'-bistetrazole-1,1'-dioxide* (TKX-50),^[19] a nitrogen-rich energetic salt with a detonation velocity higher than RDX.

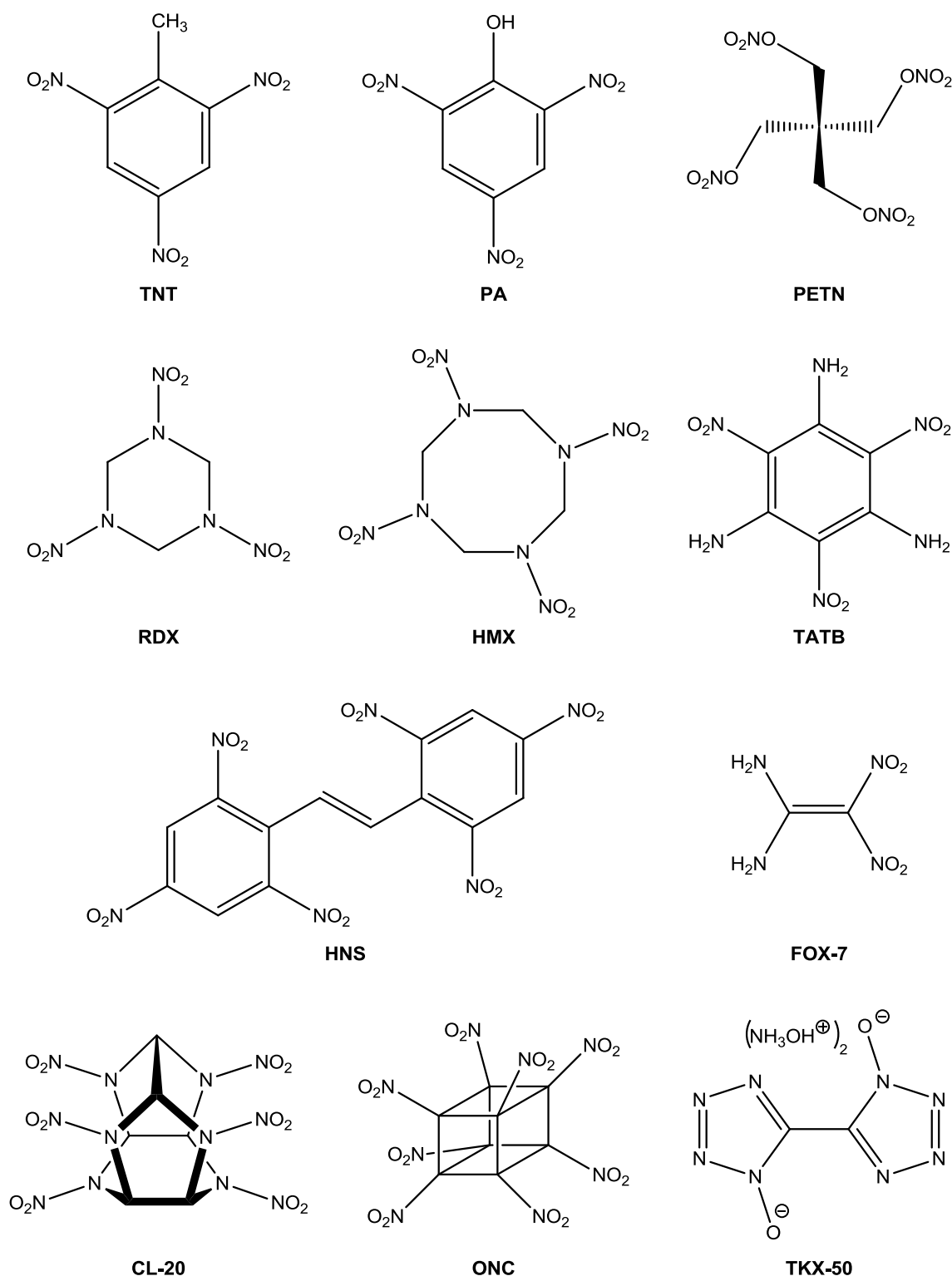


Figure 3. Selected explosives from the 19th century until today: 2,4,6-trinitrotoluene (**TNT**); 2,4,6-trinitrophenol, picric acid (**PA**); pentaerythritol tetranitrate, nitropenta (**PETN**); 1,3,5-trinitro-1,3,5-triazinane, hexogen, research department explosive (**RDX**), 1,3,5,7-tetranitro-1,3,5,7-tetrazocane, octogen, high-melting explosive (**HMX**); 2,4,6-triamino-1,3,5-trinitrobenzene (**TATB**); hexanitrostilbene (**HNS**); 1,1-diamino-2,2-dinitroethene, (**FOX-7**), 2,4,6,8,10,12-hexanitro-2,4,6,8,10,12-hexaazaisowurtzitane (**CL-20**), octanitrocubane (**ONC**), dihydroxylammonium 5,5'-bistetrazole-1,1'-dioxide (**TKX-50**).

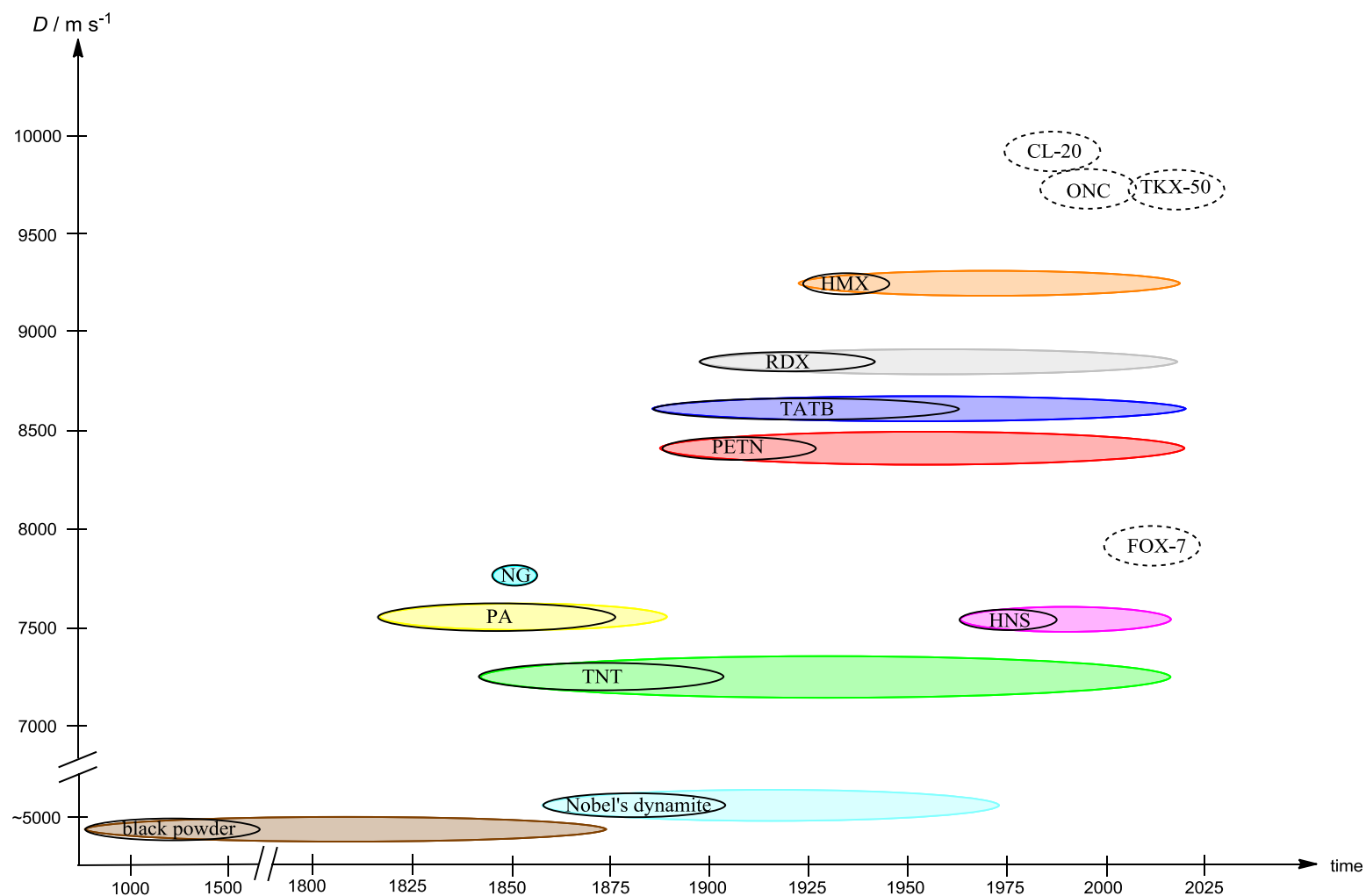


Figure 4. Illustration of the performance development of selected explosives or mixtures (as detonation velocity D) over the last centuries. Continuous circles: time span from the first preparation of the material to its application. Colored fields: time span of the explosive used in military or civil application. Dashed circles: compounds not practically exploited yet.

1.2 Definition and Classification

The first attempt to systematically study the functional groups in molecules with explosive properties was made by Van't Hoff.^[20] Numerous functional groups were classified, including a) the O–O bonds in peroxides, ozone, and ozonides; b) the O–Cl bonds in chlorates and perchlorates; c) the N–Cl bonds in nitrogen chlorides; d) the N=O bonds in nitro compounds, nitric acid esters and its salts; e) the N=N bonds in diazo compounds, hydrazoic acid, its salts and esters; f) the N=C bonds in fulminates and cyanogen; and g) the C≡C bonds in acetylenes and acetylides.

Later, Plets^[21] neologized the term *explosophores*, where *explos* derives from the Latin term *explodere* (to drive off or cast out) and *phores* from the Greek term *pherein* (to carry or bring). Plets defined groupings of atoms that can confer explosive properties on a substance,^[20] including a) the –NO₂ and –ONO₂ groups in both inorganic and organic substances; b) the –N=N– and –N=N=N groups in inorganic and organic azides; c) the –NX₂ group, where X is a halogen, for example in NCl₃; d) the –N=C group in fulminates; e) the –OClO₂ and –OClO₃ groups in inorganic and organic chlorates and perchlorates, respectively; f) the –O–O– and –O–O–O– groups in inorganic and organic peroxides and ozonides, respectively; g) the –C≡C– groups in acetylenes and metal acetylides; and h) the metal-carbon bonds in some organometallic compounds. Many of these moieties are indeed present in the aforementioned energetic materials.

Substances that Plets described as *explosophores* are nowadays referred to as energetic materials, which include explosives, propellants, and pyrotechnics (Figure 5). Defined by the American Society for Testing and Materials, energetic materials are “substance or composition that contain both fuel and oxidizer and rapidly react to release energy and gas”.^[22] In my opinion, a more accurate definition of energetic materials is, however, suggested by my colleague Dr. Davin Piercey, who describes energetic materials as “a metastable compound or mixture capable of the rapid release of stored potential energy.”^[23] On this basis, we now classify and subdivide different kinds of energetic materials (Figure 5).

- A. Explosives** (high explosives) are energetic materials that detonate, which means upon combustion, they propagate a detonation front that is faster than the speed of sound in the corresponding material (e.g. air 340 m s⁻¹).
- a. Primary explosives** (PEs) are (extremely) sensitive explosives that can be easily initiated by external stimuli, such as friction, impact, spark or heat. PEs are used to initiate a main charge in a energetic device. They need to undergo a fast deflagration

to detonation transition (DDT), so that a stable shock front caused by the PE can initiate the main charge. As a general rule, explosives more sensitive than PETN are considered as PEs.

- b. Secondary explosives** are used as the main ingredient in an explosive charge and ignited by a (usually small amount of) PE. In general, SEs are less sensitive toward impact, heat and friction and contain a higher energy density than PEs. SEs can be subdivided in three categories:
 - i. High performance explosives**, used in many military applications, should have a certain stability against mechanical and thermal stimuli. One of the most prominent and widely used high performance explosives is RDX, which sets the current benchmark for these types of materials. Other examples include HMX or CL-20, ONC, and TKX-50, while the latter three have not been broadly employed yet.
 - ii. Insensitive high explosives** are extremely insensitive against external stimuli and difficult to initiate. Such properties make them applicable in devices that must not be set off by accident. For example, the highly insensitive TATB is used in nuclear warheads, where an accidental detonation would present extreme danger. Another insensitive high explosive is FOX-7, which has very high resistance against mechanical stimuli and heat.
 - iii. Heat resistant high explosives** are, as described, resistant to heat and are mostly used for civilian applications, where high thermal stabilities are required. HNS ($T_{\text{dec.}} \geq 315\text{ }^{\circ}\text{C}$) has applications as explosive, such as deep oil drilling or in space missions. Another high temperature stable explosive is 2,6-bis(picrylamino)-3,5-dinitropyridine (PYX, $T_{\text{dec.}} \geq 370\text{ }^{\circ}\text{C}$), which is also used in deep oil drilling.
- B. Propellants** (low explosives) are materials that burn or deflagrate, i.e. they propagate a shock wave slower than the speed of sound. Propellants can be subdivided into gun propellants and rocket propellants. The former is used to accelerate munitions in pistols, artillery or mortars, and the latter is used to create a thrust to provide spacecraft propulsion.
- C. Pyrotechnics** can be divided into three categories: decoy flares, signal flares, and fireworks. Decoy flares contain pyrotechnic compositions. They can imitate the infrared signal of a plane and guide the enemy infrared-guided missile away from its original target. Signal flares emit light for signaling or illumination in civilian and military applications. Another type of pyrotechnics are fireworks, mostly used for their aesthetic in cultural events.

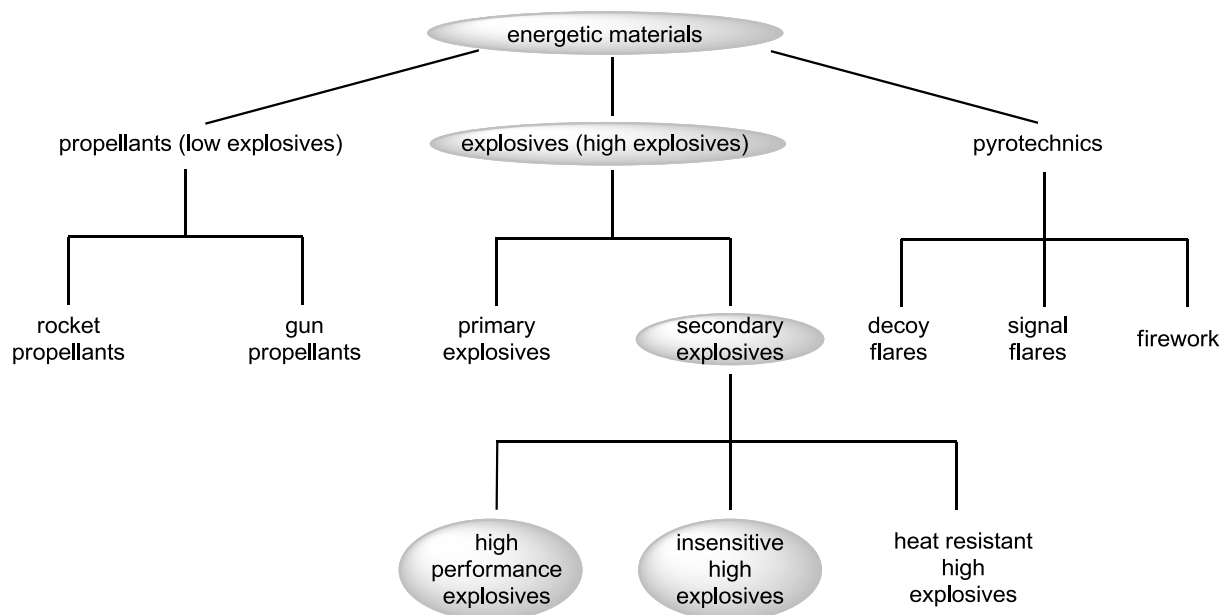


Figure 5. Classification of energetic materials. The areas investigated in this thesis are highlighted in grey.

1.3 Strategies for the design of new explosives

For secondary explosives, the power of an explosive is often described by the detonation velocity (D) and the detonation pressure (p_{CJ} , named after Chapman and Jouguet). D is a experimentally measurable value reflecting the velocity of the shockwave propagated by the explosive during detonation. The detonation pressure p_{CJ} can only be calculated and is the peak dynamic pressure in the shock front. The calculation of D and p_{CJ} is described by Eq. 1 and 2.^[24]

$$p_{CJ} = K \delta_0^2 \Phi / \text{kbar} \quad (\text{Eq. 1})$$

$$D = A \Phi^{0.5} (1 + B \delta_0) / \text{m s}^{-1} \quad (\text{Eq. 2})$$

with $K = 15.88$, $A = 1.01$, $B = 1.30$, δ_0 = loading density and $\Phi = N (M)^{0.5} (Q)^{0.5}$ with N = number of moles of gas released per gram of explosive [mol/g], M = mass of gas in gram per mole of gas [g/mol], Q = heat of explosion [cal/g]

As shown in Eq. 1 and Eq. 2, both detonation velocity and pressure are dependent on the loading density and its square, respectively. On this basis, one can consider that the density is the most important parameter for designing new explosives. Moreover the parameter Φ is dependent on the molecular formula of the substance and its heat of explosion Q . Therefore, other than a high density, a powerful secondary explosive should possess a high heat of explosion, which is dependent on the heat of formation $\Delta_f H^\circ$ and the oxygen balance of the

material. Lately, concerns have been raised about the environmental impact of explosives. Thus, explosive materials should ideally only release environmentally benign decomposition products upon detonation.^[25] Apart from a high density, high heat of formation, and low toxicity, there are many other requirements for new explosives, as depicted in Figure 6.

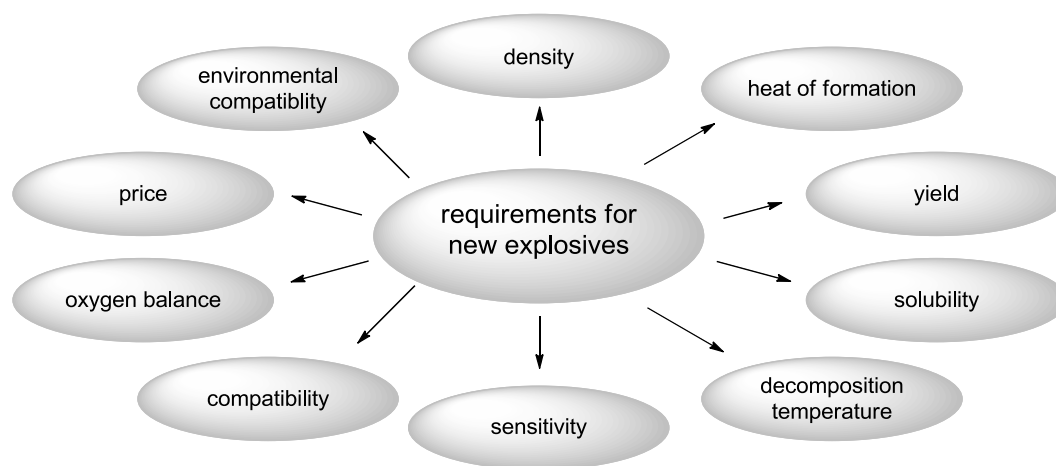


Figure 6. Requirements for new secondary explosives.

When designing new secondary explosives, several strategies^[26] are adopted to obtain target molecules with a high densities and high heat of formations (Figure 7). The material should possess enough oxygen to fully oxidize the carbon backbone (desirably to carbon monoxide) as in NG or PETN. Moreover, it is preferred to construct strained cages or rings that release energy upon decomposition, such as in CL-20 or ONC. Another widely used concept is the introduction of nitrogen-rich compounds as in ABTe and BT1O (Figure 7). These substances expel mainly non-toxic N_2 upon decomposition and the explosion is facilitated by the energy released from the formation of the $N\equiv N$ triple bond. Within the nitrogen-rich compounds, there is the possibility to improve the performance by introduction of *N*-oxides as in BT1O, of which the details were studied in this thesis.

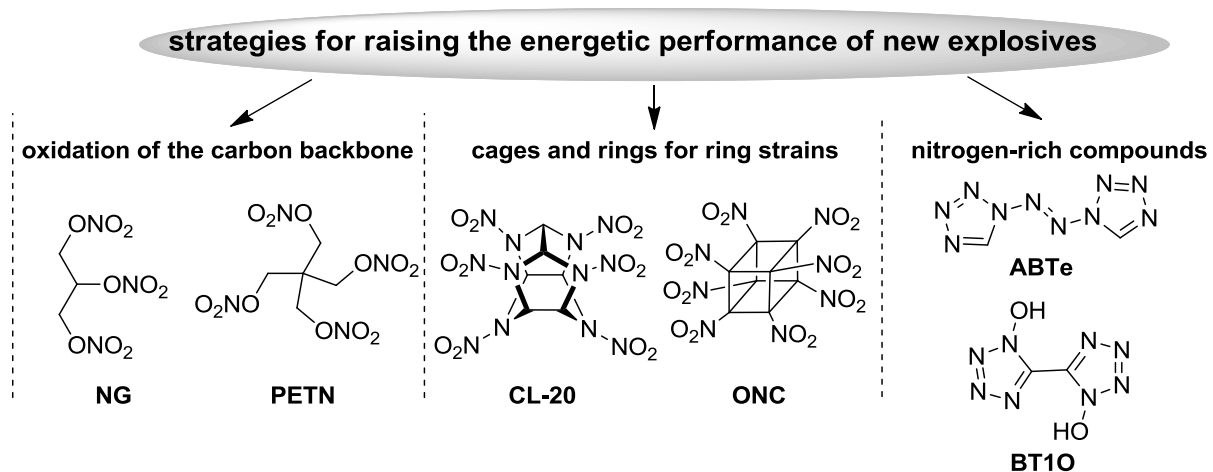


Figure 7. Different strategies for raising the energetic performance when designing new explosives with selected examples.

Since new secondary explosives need to have not only high explosive power but also a certain stability, several strategies^[27] can be used to raise the stability against thermal and mechanical stimuli (Figure 8). The formation of salts generally improves the thermal stability and in some cases even the stability toward shock and friction. One has to differentiate metal salts, such as K_2DNABT (Figure 8), of which the cation usually is an alkaline or earth alkaline metal, from nitrogen-rich salts, such as TKX-50. The latter ones comprise nitrogen-rich cations and anions. These salts have drawn increasing attention because their stability can be improved without attenuating their energetic performance. Incorporation of alternating amino and nitro groups can stabilize the system by forming inter- and/or intramolecular hydrogen bonds. Very stable compounds can be obtained with such a strategy, such as FOX-7 and TATB. Another stabilizing tactic is to introduce extended conjugation throughout the whole molecule structure as in the thermally stable HNS.

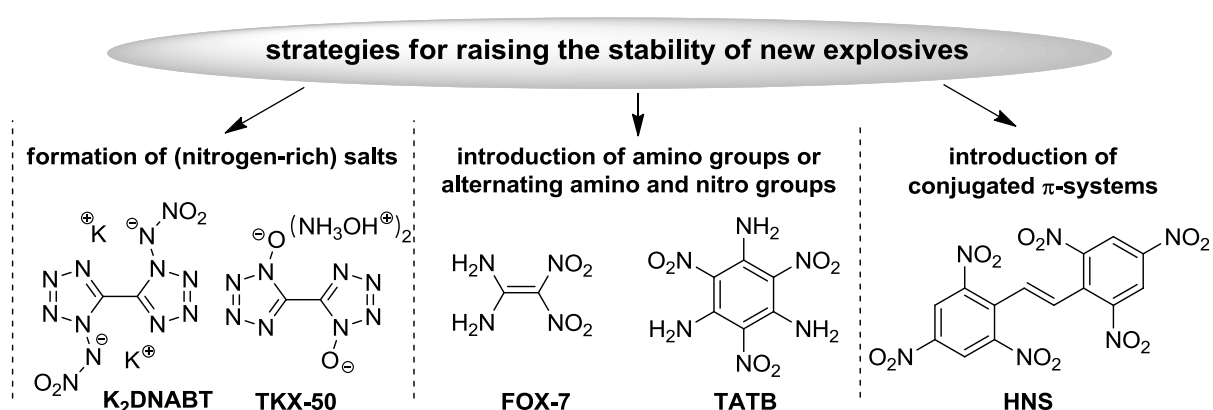


Figure 8. Different strategies for raising the stability when designing new explosives with selected examples.

1.4 Motivation and Objectives

RDX is widely used because of its feasible preparation, low cost, and extraordinary power as a secondary explosive. Due to its toxicity and carcinogenicity,^[28] the need for alternatives has been raised in recent years. Potential RDX replacements are expected to have several key features, including a thermal stability over 200 °C, a comparable or higher performance with $D \geq 8800 \text{ m s}^{-1}$ and $p_{\text{CJ}} \geq 340 \text{ kbar}$, comparable or lower sensitivities, such as impact sensitivity $\geq 7.5 \text{ J}$ and friction sensitivity $\geq 120 \text{ N}$, and a lower toxicity.

The objectives of this thesis are to synthesize, characterize, and investigate new secondary explosives that could replace RDX. Moreover, much effort is made on exploring ways to improve the performance of a molecule while retaining or improving its stability.

In order to achieve these goals, azole-based heterocycles, including tetrazoles, triazoles, and furazanes (Figure 9) are investigated in this thesis. The skeleton of these azoles is suitable to achieve new high energetic density materials comprising a high nitrogen content. To these three types of azoles, the foregoing strategies are applied.

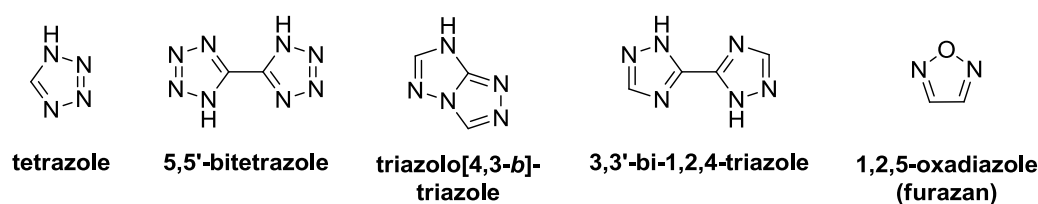


Figure 9. Chemical structures of selected nitrogen-rich heterocycles.

Through selective tailoring, new materials with enhanced energetic properties can be synthesized. The strategies for improving explosive performance can be combined with retaining or raising the stability (Figure 10).

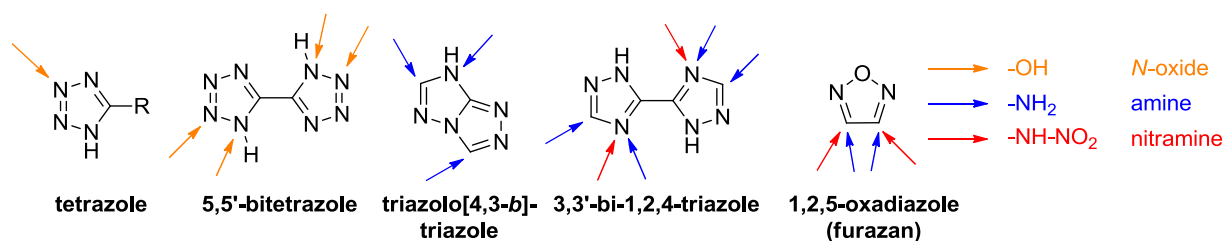


Figure 10. Chemical structures of selected nitrogen-rich heterocycles. The positions that are altered in this thesis are marked with the corresponding colored arrows. By introducing different functional groups, such as *N*-oxides, amines and nitramines, the properties of the molecules can be altered in a desired way.

The target molecules include conjugated π -systems, several nitrogen-rich ionic compounds, and some molecules possessing *N*-oxides, amino- and/or alternating amino- and nitro(amino)-motifs.

Additional efforts are made to synthesize novel bitetrazoles featuring *N*-oxide groups (Figure 11). By comparing their properties with those of their parent compounds, we will gain a deeper insight into the impact of the *N*-oxide motif on the crucial properties of tetrazoles, such as (thermal) stability, density and energetic performance. This systematic study can pave the way to further improve nitrogen-rich energetic materials.

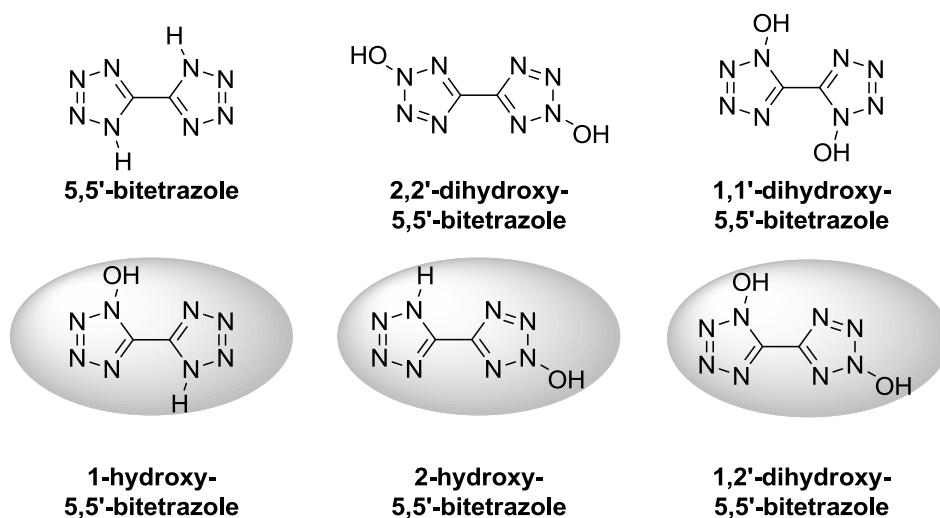


Figure 11. 5,5'-Bitetrazole and hydroxy derivatives: highlighted compounds are newly synthesized in this thesis and compared with other 5,5'-bitetrazole derivatives.

1.5 References

- [1] 太上圣祖金丹秘诀, Taishang (Top high) Shengzu (Holy ancestor) Jindan (Gold ball,) Mijue (Secret recipes) by Qing Xu Zi, available online at http://www.chinabaike.com/article/sort0525/sort0540/2007/20070729156297_12.html (accessed 26.01.2016)
- [2] Fang Wang, private communication.
- [3] http://www.nobelprize.org/alfred_nobel/biographical/patents.html (accessed 26.01.2016)
- [4] http://www.nobelprize.org/alfred_nobel/biographical/articles/vinterviken/images/vv-6.jpg (accessed 26.01.2016)
- [5] https://upload.wikimedia.org/wikipedia/commons/4/47/Nobels_Extradynamit_label.jpg (accessed 26.01.2016)
- [6] H. Sprengel, British Patent #901, **1871**.
- [7] J. Wilbrand, *Annalen der Chemie und Pharmacie* **1863**, 128, 178–179.
- [8] B. Tollens, P. Wigand, *Justus Liebigs Annalen der Chemie* **1891**, 265, 316–340.
- [9] G. F. Henning, *Vol. Patent DE 104280*, **1898**.
- [10] W. E. Bachmann, J. C. Sheehan, *J. Am. Chem. Soc.* **1949**, 71, 1842–1845.
- [11] H. Fischer, *Chem. Ber.* **1949**, 82, 192–193.
- [12] C. L. Jackson, J. F. Wing, *Amer. Chem. J.* **1888**, 10, 283.
- [13] T. M. Benzinger, *US Pat.* 4032377, **1976**.
- [14] K. G. Shipp, *J. Org. Chem.* **1964**, 29, 2620–2623.
- [15] J. R. Bates, W. W. Lauderdale, H. Kernaghan, ALSEP Termination Report, NASA Reference Publication 1036, available online at <http://www.lpi.usra.edu/lunar/documents/NASA%20RP-1036.pdf> (accessed 26.01.2016)
- [16] A. T. Nielsen, A. P. Chafin, S. L. Christian, D. W. Moore, M. P. Nadler, R. A. Nissan, D. J. Vanderah, R. D. Gilardi, C. F. George, J. L. Flippen-Anderson, *Tetrahedron* **1998**, 54, 11793–11812.

- [17] M.-X. Zhang, P. E. Eaton, R. Gilardi, *Angew. Chem.* **2000**, *112*, 422–426; *Angew. Chem. Int. Ed.* **2000**, *39*, 401–404.
- [18] N.V. Latypov, J. Bergman, A. Langlet, U. Wellmar, U. Bemm, *Tetrahedron* **1998**, *54*, 11525–11536.
- [19] N. Fischer, D. Fischer, T. M. Klapötke, D. G. Piercey, J. Stierstorfer, *J. Mater. Chem.* **2012**, *22*, 20418–20422.
- [20] T. Urbanski, *Chemistry and Technology of Explosives*, Vol. I, Pergamon Press, Oxford, London, New York, Paris, **1964**.
- [21] V. Plets, *Zh. Obshch. Khim.* **1953**, *5*, 173–178.
- [22] www.astm.org (accessed 26.01.2016)
- [23] D. Piercey, *Dissertation*, Ludwig-Maximilians Universität München, **2013**, p. 4.
- [24] M. J. Kamlet, S. J. Jacobs, *J. Chem. Phys.* **1968**, *48*, 23–35.
- [25] a) J. Giles, *Nature* **2004**, *427*, 580–581; b) M. B. Talawar, R. Sivabalan, T. Mukundan, H. Muthurajan, A. K. Sikder, B. R. Gandhe, A. Subhananda Rao, *J. Hazard. Mat.* **2008**, *161*, 589–607.
- [26] T. M. Klapötke, *Chemistry of High-Energy Materials*, 3rd ed., De Gruyter, Berlin, **2015**.
- [27] A. K. Sikder, N. Sikder, *J. Hazard. Mat.* **2004**, *112*, 1–15.
- [28] R. L. Muhly, Update on the Reevaluation of the Carcinogenic Potential of RDX, U.S: Army Center for Health Promotion and Preventive Medicine, **2001**, available online at <http://web.archive.org/web/20091112035039/http://www.mass.gov/dep/cleanup/compliance/rdxwhite.pdf> (accessed 26.01.2016)

2. Summary and Conclusion

Chapters 3–11 have been published in a peer-reviewed scientific journals. The layout of the articles was slightly modified to properly fit in this thesis. An overview of the results is presented here, followed by a brief summary of each chapter, presenting the best compound(s) of each publication.

Chapters 3–7 investigate the performance increment of the *N*-oxide group in tetrazoles and demonstrate the effect of introducing the *N*-oxide group into different types of tetrazoles. In general the introduction of *N*-oxides in tetrazoles:

- improves the sensitivities toward mechanical stimuli,
- slightly decreases the decomposition temperature and calculated heat of formation,
- results in a significant increase in densities, and
- improves the detonation velocity and detonation pressure

Chapters 8 and 9 describe two different types of cationic triazoles. The introduction of the amino-substituted moieties allows for the formation of energetic cations and hydrogen-bonding networks that can increase the thermal stability of energetic materials.

Chapter 10 discusses the novel 5,5'-diamino-4,4'-nitramino-3,3'-bi-1,2,4-triazole that comprises of amino groups adjacent to nitro groups. This compound shows an improved performance while retaining the thermal stability through a strong hydrogen-bonding network.

Chapter 11 studies energetic furazanes and improves their thermal and mechanical stability by introducing various nitrogen-rich cations.

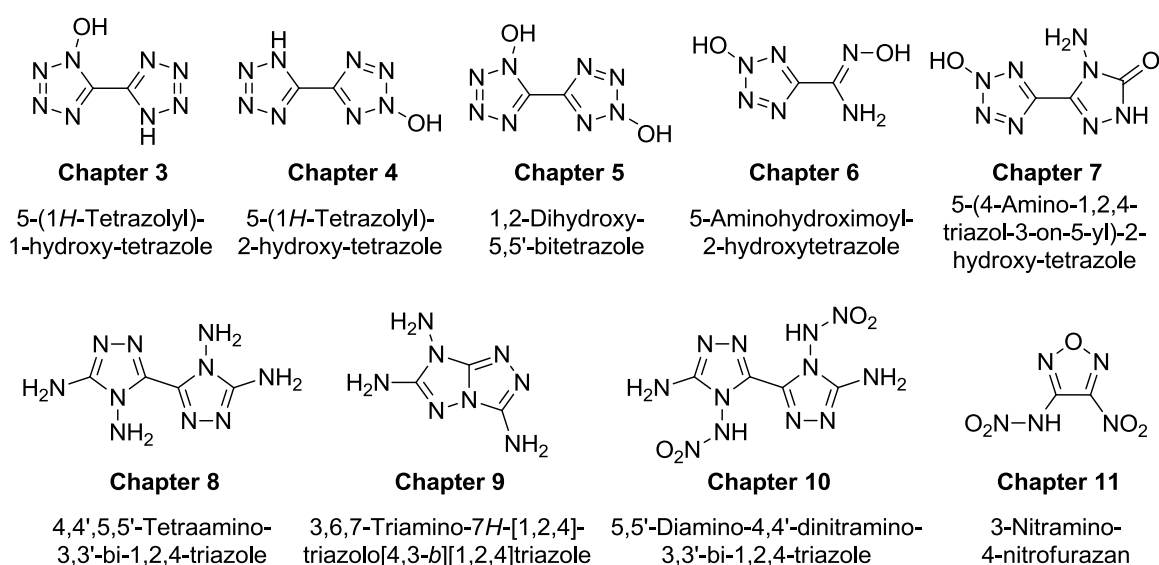


Figure 1. Overview of the energetic compounds presented in this thesis in their neutral form.

Table 1. Comparison of the properties of selected bitetrazole-*N*-oxides investigated in Chapters 3–7 and synthetic route toward compounds **1**–**5**.

	1	2	3	4	5	RDX
Formula	C ₂ H ₈ N ₁₀ O ₃	C ₂ H ₈ N ₁₀ O ₃	C ₂ H ₈ N ₁₀ O ₄	C ₂ H ₇ N ₇ O ₃	C ₃ H ₇ N ₉ O ₃	C ₃ H ₆ N ₆ O ₆
FW [g mol ⁻¹]	220.15	220.15	236.15	177.12	217.15	222.12
<i>IS</i> [J] ^a	12	20	10	>40	15	7.5
<i>FS</i> [N] ^b	216	160	240	360	360	120
<i>ESD</i> [J] ^c	0.75	0.7	1.0	0.7	0.25	0.20
<i>N</i> [%] ^d	63.62	63.62	59.31	55.36	58.87	37.84
<i>Q</i> [%] ^e	-36.33	-36.33	-27.10	-40.36	-37.36	-21.61
<i>T</i> _{dec.} [°C] ^f	200	183	192	164	178	210
<i>ρ</i> [g cm ⁻³] (298 K) ^g	1.731	1.696	1.75	1.704	1.73 (pyc.)	1.806
<i>Δ_fH</i> ^o [kJ mol ⁻¹] ^h	469.0	443.6	451.8	281.9	355.9	70.3
<i>Δ_fU</i> ^o [kJ kg ⁻¹] ⁱ	2248.5	2092.2	2028.6	1710.4	1747.5	417.0
EXPLO V6.01 values:						
- <i>Δ_EU</i> ^o [kJ kg ⁻¹] ^j	5546	5426	5869	5707	5020	5734
<i>T_E</i> [K] ^k	3490	3459	3727	3522	3304	3800
<i>p_{CJ}</i> [kbar] ^l	323	303	341	309	288	352
<i>D</i> [m s ⁻¹] ^m	9117	8916	9187	8934	8656	8815
<i>V₀</i> [L kg ⁻¹] ⁿ	924	926	920	917	862	792
SSRT:						
weight [mg]	474	-	-	474	-	504
dent [mg SiO ₂]	723	-	-	587	-	858
Toxicity assessment:						
EC ₅₀ (15 min) [g L ⁻¹]	1.634	0.386	0.320	-	-	0.327
EC ₅₀ (30 min) [g L ⁻¹]	0.330	0.180	0.240	-	-	0.239

^a impact sensitivity (BAM drophammer, 1 of 6); ^b friction sensitivity (BAM friction tester, 1 of 6); ^c electrostatic discharge device (OZM); ^d nitrogen content; ^e oxygen balance; ^f decomposition temperature from DSC ($\beta = 5^\circ\text{C}$); ^g recalculated from low temperature X-ray densities ($\rho_{298\text{K}} = \rho_{\text{T}} / (1 + \alpha_{\text{V}}(298 - T_0))$; $\alpha_{\text{V}} = 1.5 \cdot 10^{-4} \text{ K}^{-1}$); ^h calculated (CBS-4M) heat of formation; ⁱ calculated energy of formation; ^j energy of explosion; ^k explosion temperature; ^l detonation pressure; ^m detonation velocity; ⁿ assuming only gaseous products.

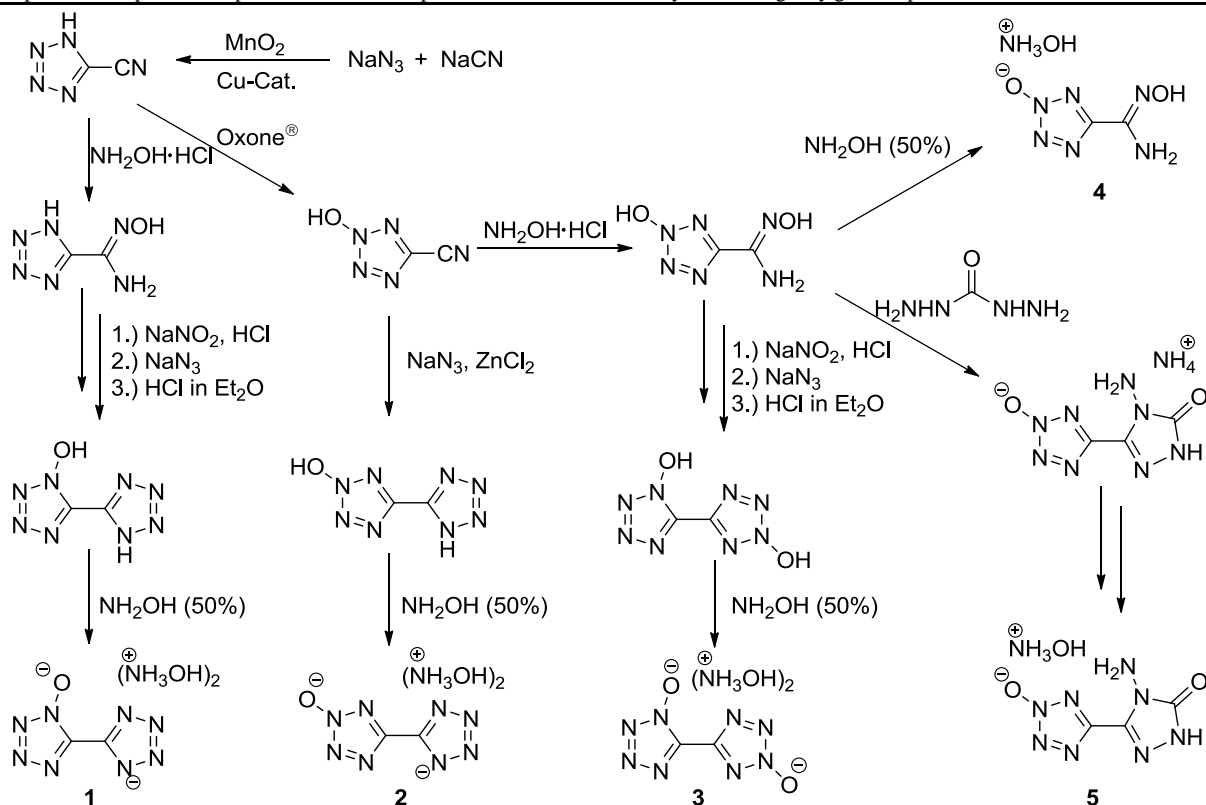
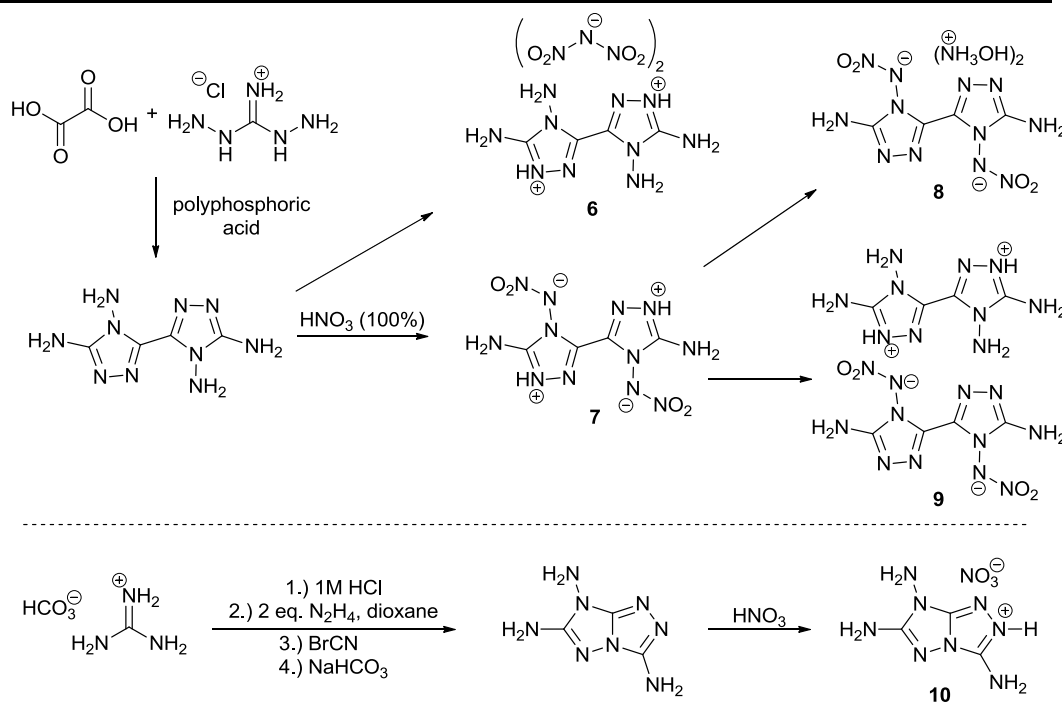


Table 2. Comparison of the properties of different triazoles investigated in Chapters 8–11 and synthetic route toward compounds **6–10**.

	6	7	8	9	10
Formula	C ₄ H ₁₀ N ₁₆ O ₈	C ₄ H ₆ N ₁₂ O ₄	C ₄ H ₁₂ N ₁₄ O ₆	C ₈ H ₁₄ N ₂₂ O ₄	C ₃ H ₇ N ₉ O ₃
FW [g mol ⁻¹]	410.22	286.17	352.23	482.34	217.15
<i>IS</i> [J] ^a	5	9	8	35	40
<i>FS</i> [N] ^b	360	120	288	360	360
<i>ESD</i> [J] ^c	0.8	0.15	1.5	0.75	0.75
<i>N</i> [%] ^d	54.63	58.73	55.67	63.89	58.05
<i>Ω</i> [%] ^e	-19.50	-39.14	-36.34	-63.03	-47.89
<i>T</i> _{dec.} [°C] ^f	200	259	210	296	280
<i>ρ</i> [g cm ⁻³] (298 K) ^g	1.826	1.756	1.763	1.816	1.779
<i>Δ_fH</i> ^o [kJ mol ⁻¹] ^h	301.5	691.9	654.5	922.9	261.5
<i>Δ_fU</i> ^o [kJ kg ⁻¹] ⁱ	837.7	2513.1	1970.7	2016.1	1312.7
EXPLO V6.02 values:					
- <i>Δ_EU</i> ^o [kJ kg ⁻¹] ^j	4955	5520	5936.2	4169	4663
<i>T_E</i> [K] ^k	3407	3771	3679	2774	3062
<i>p_{Cl}</i> [kbar] ^l	338	312	340	310	302
<i>D</i> [m s ⁻¹] ^m	9053	8846	9313	9191	9005
<i>V</i> ₀ [L kg ⁻¹] ⁿ	843	808	897	822	870
SSRT:					
weight [mg]	524	504	506	512	-
dent [mg SiO ₂]	772	633	664	475	-
Toxicity assessment:					
EC ₅₀ (15 min) [g L ⁻¹]	-	0.129	0.751	-	3.564
EC ₅₀ (30 min) [g L ⁻¹]	3.780	0.065	0.346	-	3.363

^a impact sensitivity (BAM drophammer, 1 of 6); ^b friction sensitivity (BAM friction tester, 1 of 6); ^c electrostatic discharge device (OZM); ^d nitrogen content; ^e oxygen balance; ^f decomposition temperature from DSC ($\beta = 5^\circ\text{C}$); ^g recalculated from low temperature X-ray densities ($\rho_{298\text{K}} = \rho_T / (1 + \alpha_V(298 - T_0))$; $\alpha_V = 1.5 \cdot 10^{-4} \text{ K}^{-1}$); ^h calculated (CBS-4M) heat of formation; ⁱ calculated energy of formation; ^j energy of explosion; ^k explosion temperature; ^l detonation pressure; ^m detonation velocity; ⁿ assuming only gaseous products.



2.1 Chapter 3: 5-(1*H*-Tetrazolyl)-1-hydroxy-tetrazole

5-(1*H*-Tetrazolyl)-1-hydroxytetrazole and various nitrogen-rich ionic derivatives, such as the bis(hydroxylammonium) salt were synthesized in five steps using sodium azide, sodium cyanide, and MnO₂ as starting materials. The most energetic compound of this study is the hydroxylammonium salt (Figure 2) that possesses energetic properties similar to RDX.

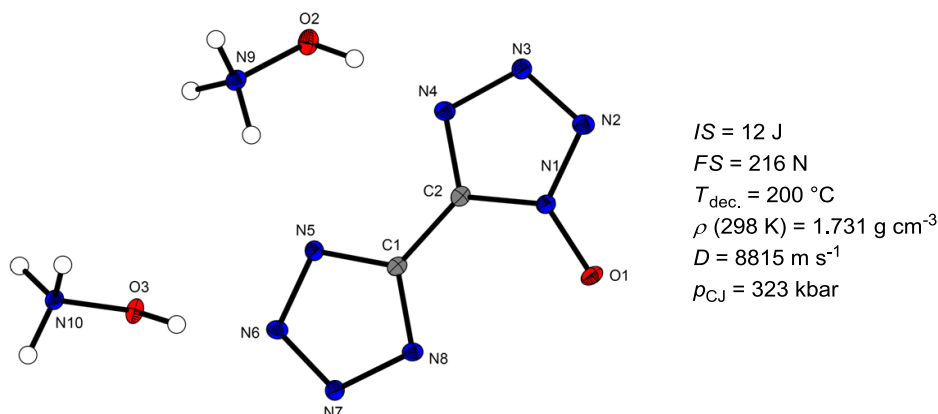


Figure 2. Molecular unit of bis(hydroxylammonium) 5-(1-oxidotetrazolyl)-tetrazolate and its energetic properties.

2.2 Chapter 4: 5-(1*H*-Tetrazolyl)-2-hydroxy-tetrazole

In order to gain insight into the performance increment of tetrazole *N*-oxides, 5-(1*H*-tetrazolyl)-2-hydroxytetrazole and its ionic derivatives were synthesized and characterized for the first time. The hydroxylammonium salt (Figure 3) shows a somewhat inferior thermal stability and slightly lower density than the corresponding 1-*N*-oxide from the previous study.

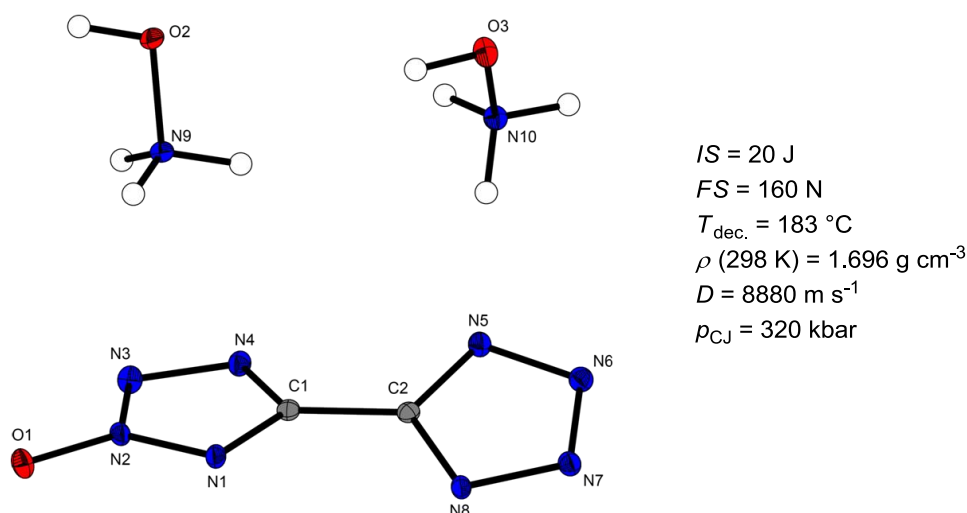


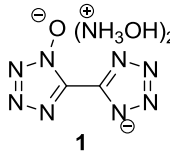
Figure 3. Molecular unit of bis(hydroxylammonium) 5-(2-oxidotetrazolyl)-tetrazolate and its energetic properties.

2.3 Chapter 5: 1,2'-Dihydroxy-5,5'-bitetrazole

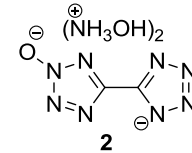
The synthesis of the asymmetric 1,2'-dihydroxy-5,5'-bitetrazole tetrazole and its energetic derivatives completes the study on 5,5'-bitetrazole-*N*-oxides. The energetic properties of hydroxylammonium salt **1** are listed in Table 3 and compared to other tetrazole-*N*-oxides from the previous studies.

Table 3. Comparison of the properties of different bitetrazole-*N*-oxides

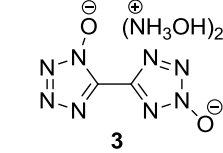
	1	2	3	11 ^[1]	TKX-50 ^[2]	RDX
Formula	C ₂ H ₈ N ₁₀ O ₃	C ₂ H ₈ N ₁₀ O ₃	C ₂ H ₈ N ₁₀ O ₄	C ₂ H ₈ N ₁₀ O ₄	C ₂ H ₈ N ₁₀ O ₄	C ₃ H ₆ N ₆ O ₆
<i>IS</i> [J]	12	20	10	3	20	7.5
<i>FS</i> [N]	216	160	240	60	120	120
<i>ESD</i> [J]	0.75	0.70	1.0	0.25	0.10	0.20
<i>N</i> [%]	63.62	63.62	59.30	59.30	59.30	37.84
<i>T</i> _{dec.} [°C]	200	183	192	172	221	210
ρ [g cm ⁻³] (298 K)	1.731	1.696	1.75 (pyc.)	1.822	1.877	1.806
$\Delta_f H^\circ$ [kJ mol ⁻¹]	469.0	443.6	451.8	390.7	458.7	70.3
$\Delta_f U^\circ$ [kJ kg ⁻¹]	2248.5	2092.2	2028.6	1769.7	2057.8	417.0
EXPLO V6.01 values:						
$-\Delta_E U^\circ$ [kJ kg ⁻¹]	5546	5426	5869	5652	5939	5734
<i>p</i> _{CJ} [kbar]	323	303	341	366	401	352
<i>D</i> [m s ⁻¹]	9117	8916	9187	9439	9781	8815
<i>V</i> ₀ [L kg ⁻¹]	924	926	920	917	913	792



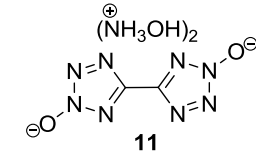
1



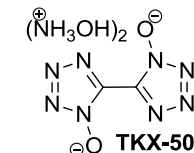
2



3



11



TKX-50

The densities, physiochemical properties, and sensitivities show a general trend regarding the introduction of *N*-oxides in bitetrazoles (Figure 4). The energetic performance of the bitetrazoles increases with the number of *N*-oxide substituents and symmetry of the structure. In addition, bitetrazole 1-*N*-oxides show higher performances than the corresponding 2-*N*-oxide derivatives. 5,5'-Bitetrazole exhibits lower energetic properties than 1-hydroxy- and 2-hydroxy-5,5'-bitetrazole, whereas the energetic performance of dihydroxy-5,5'-bitetrazoles exceeds that of the mono-substituted derivatives.

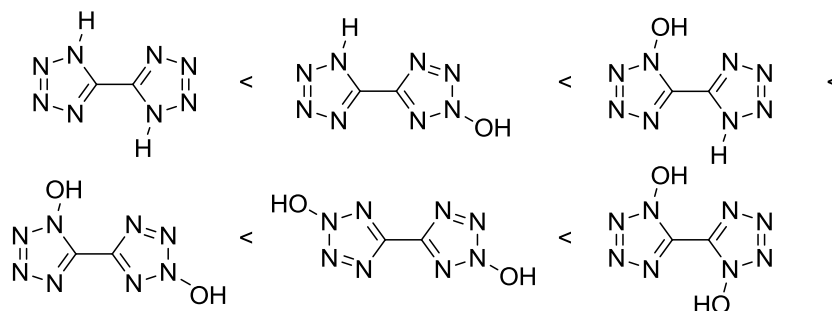


Figure 4. Illustration of the performance increment caused by the introduction of *N*-oxides to 5,5'-bitetrazole.

2.4 Chapter 6: Amino-Hydroximoyl-2-Hydroxy-Tetrazole

5-Aminohydroximoyl-2-hydroxytetrazole and its energetic derivatives were obtained from inexpensive starting materials following a facile three-step route. For example, the hydroxylammonium salt displayed in Figure 5 contains the *N*-oxide group in the tetrazole skeleton. Such a structural modification leads to improved sensitivities to mechanical stimuli, a slight decrease in the decomposition temperature, an increase in density, and an improvement in detonation velocity and detonation pressure.

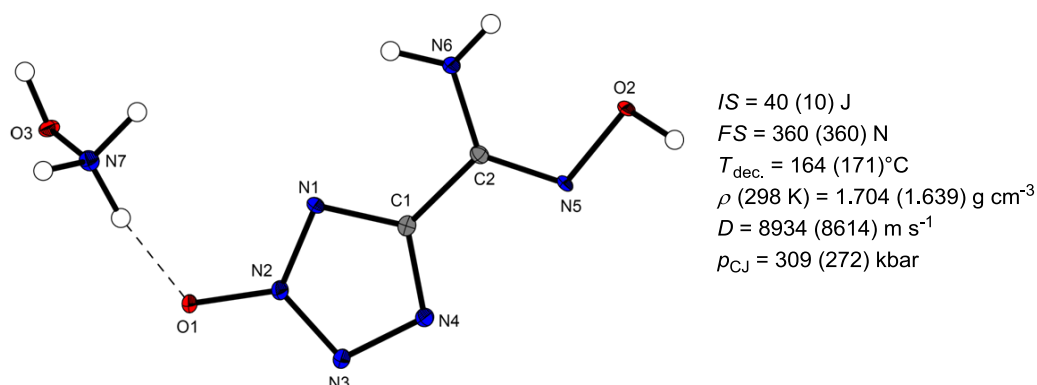


Figure 5. Molecular unit of hydroxylammonium amino-hydroximoyl-tetrazole-2-oxide and its energetic properties. The values of the corresponding tetrazole lacking the *N*-oxide moiety are given in parantheses.

2.5 Chapter 7: 5-(4-Amino-1,2,4-triazol-3-on-5-yl)-2-hydroxy-tetrazole

Selected ionic derivatives of the 5-(4-amino-1,2,4-triazol-3-on-5-yl)-2-hydroxy-tetrazole were prepared and their properties were compared with the corresponding compounds without the *N*-oxide group. The detonation parameters of the ammonium and hydroxylammonium salt (Figure 6) confirm that tetrazole-*N*-oxides are superior over the parent tetrazoles.

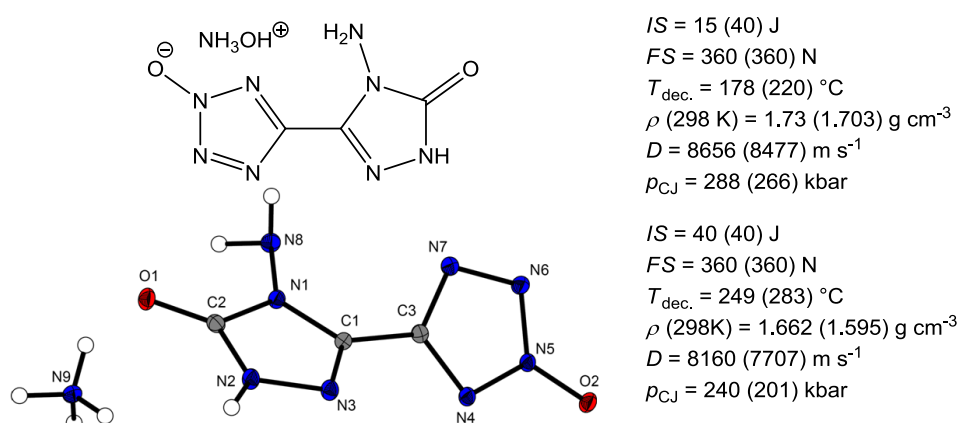


Figure 6. Chemical structure and molecular unit of hydroxylammonium and ammonium 5-(4-amino-1,2,4-triazol-3-on-5-yl)-tetrazole-2-oxide with their energetic properties. The values of the corresponding tetrazoles without the *N*-oxide group are given in parantheses.

2.6 Chapter 8: 4,4',5,5'-Tetraamino-3,3'-bi-1,2,4-triazole

4,4',5,5'-Tetraamino-3,3'-bi-1,2,4-triazole was prepared and used as a new nitrogen-rich cation. Numerous energetic salts were prepared and stabilized by the four amino groups of the 4,4',5,5'-tetraamino-3,3'-bi-1,2,4-triazolium cation. The dinitramide salt (Figure 7) has a decomposition temperature of 200 °C. This result is notable because dinitramides usually show lower decomposition temperatures despite their good energetic performances.

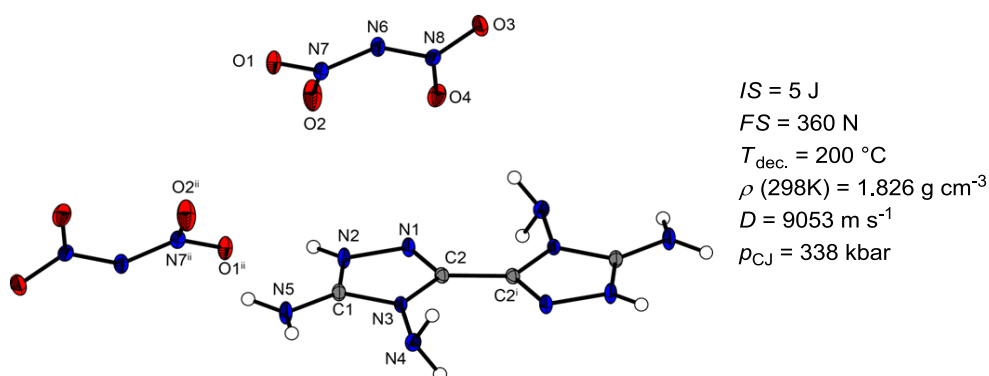


Figure 7. Molecular unit of 4,4',5,5'-tetraamino-3,3'-bi-1,2,4-triazolium dinitramide with its energetic properties.

2.7 Chapter 9: 3,6,7-Triamino-[1,2,4]triazolo[4,3-b][1,2,4]triazole

It has been demonstrated that the 3,6,7-triamino-[1,2,4]triazolo[4,3-b][1,2,4]triazolium (TATOT) cation (Figure 8) can be used as an inexpensive alternative to commonly employed nitrogen-rich cations. The TATOT cation is distinguished by its stability toward high temperatures and mechanical stimuli, very low toxicity, and high energetic performance. The synthesized compounds in this study show the advantage of energetic ionic systems that are able to form multiple hydrogen bonds.

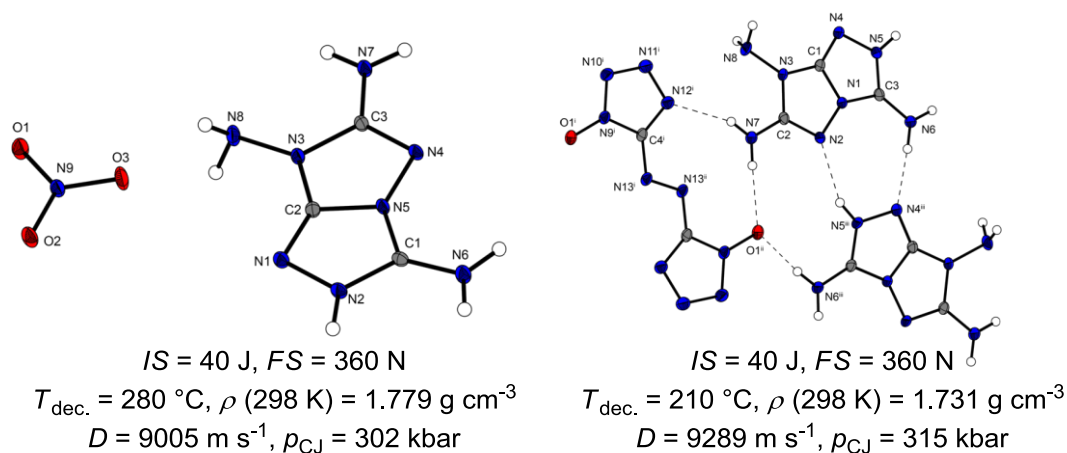


Figure 8. Molecular units of TATOT nitrate and di-TATOT 5,5'-azotetrazolate-1,1'-dioxide with its energetic properties.

2.8 Chapter 10: 5,5'-Diamino-4,4'-dinitramino-3,3'-bi-1,2,4-triazole

4,4',5,5'-Tetraamino-3,3'-bi-1,2,4-triazole was selectively nitrated at the *N*-amino groups to furnish 5,5'-diamino-4,4'-dinitramino-3,3'-bi-(1,2,4-triazole) in high purity and good yields. The introduction of the N-NO₂ group adjacent to the C-NH₂ group was found to effectively improve the density while retaining the thermal stability through a hydrogen-bonding network. The most energetic derivative in this study was the hydroxylammonium salt (Figure 9). Also notable is the high thermal stability of the 4,4',5,5'-tetraamino-3,3'-bi-1,2,4-triazolium salt (Figure 9), which is not expected for a triazole with an N-NO₂ motif.

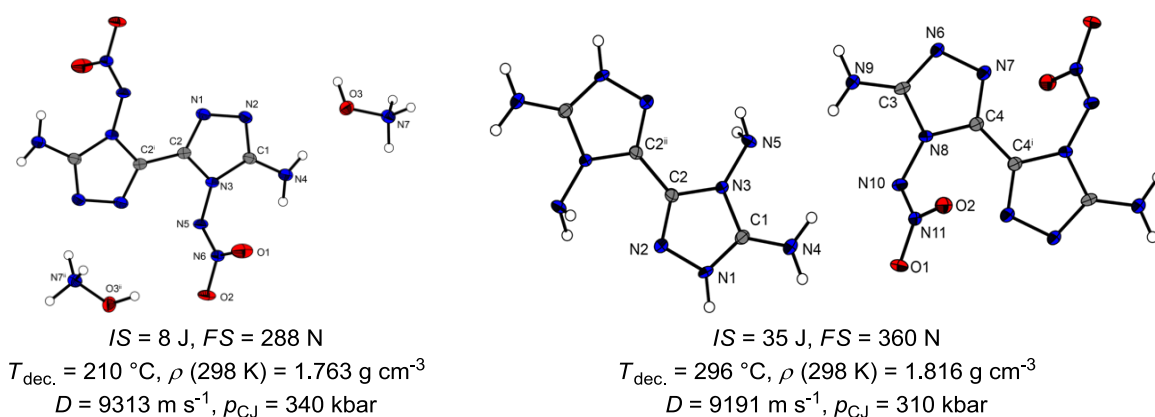


Figure 9. Molecular unit of di(hydroxylammonium) 5,5'-diamino-4,4'-dinitramino-3,3'-bi-(1,2,4-triazolate) and tetraamino-3,3'-bi-1,2,4-triazolium 5,5'-diamino-4,4'-dinitramino-3,3'-bi-(1,2,4-triazolate) with their energetic properties.

2.9 Chapter 11: 3-Nitramino-4-nitrofurazan

Energetic derivatives of 3-nitramino-4-nitrofurazan and dinitraminoazoxyfurazan were investigated in the search for more thermally stable materials in these families of energetic anions. Even though the hydroxylammonium salt (Figure 10) has excellent detonation parameters, its practical application may be limited because of its low thermal stability. However, the TATOT salt of dinitraminoazoxyfurazan (Figure 10) showed high thermal and mechanical stabilities due to an extensive hydrogen bonding network.

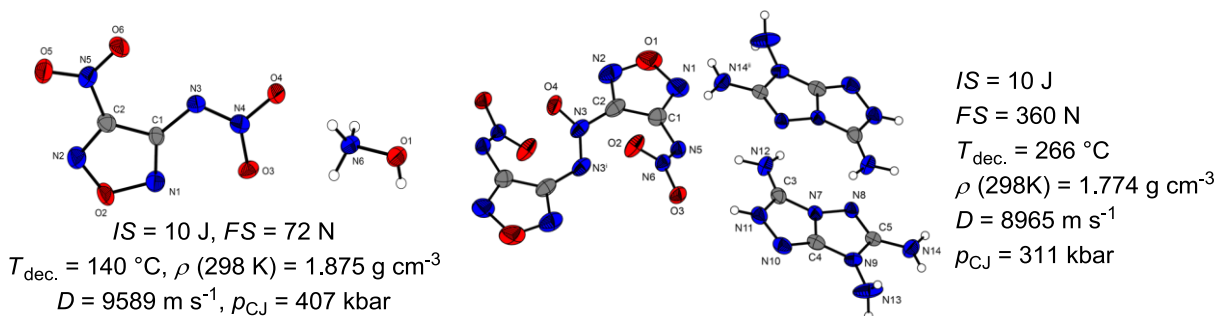


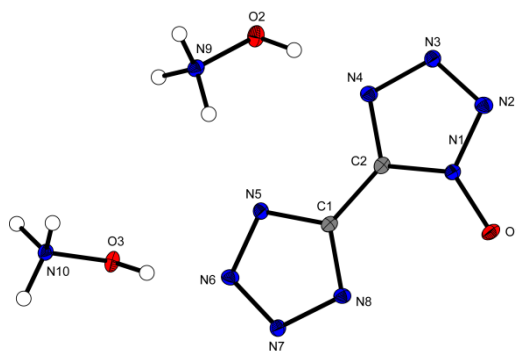
Figure 10. Molecular unit of hydroxylammonium 3-nitramino-4-nitrofurazan and di-TATOT dinitraminoazoxyfurazan with their energetic properties.

2.10 References

- [1] N. Fischer, L. Gao, T. M. Klapötke, J. Stierstorfer, *Polyhedron* **2013**, *51*, 201–210.
- [2] N. Fischer, D. Fischer, T. M. Klapötke, D. G. Piercey, J. Stierstorfer, *J. Mater. Chem.* **2012**, *22*, 20418–20422.

Synthesis of 5-(1*H*-Tetrazolyl)-1-hydroxy-tetrazole and Energetically Relevant Nitrogen-Rich Ionic Derivatives

published in *Propellants Explos. Pyrotech.* **2014**, 39, 550–557. (DOI: 10.1002/prop.201300152)



Abstract: Sodium 5-cyanotetrazolate sesquihydrate (**1**) was prepared from sodium azide and two equivalents of sodium cyanide under acidic conditions. Sodium 5-cyanotetrazolate sesquihydrate (**1**) reacts with hydroxylammonium chloride to form 5-aminohydroximoyl tetrazole (**2**). 5-Aminohydroximoyl tetrazole (**2**) is treated with sodium nitrite and hydrochloric acid to form 5-chlorohydroximoyltetrazole (**3**). The chloride azide exchange yields 5-azidohydroximoyltetrazole monohydrate (**4**). When compound **4** is treated with hydrochloric acid, 5-(1*H*-tetrazolyl)-1-hydroxytetrazole (**5**) is obtained in good yield. Compound **5** can be deprotonated twice by various bases. Different ionic derivatives such as bis(hydroxylammonium) (**6**), bis(hydrazinium) (**7**), bis(guanidinium) (**8**), bis(aminoguanidinium) (**9**), bis(ammonium) (**10**), and diaminouronium (**11**) 5-(1-oxidotetrazolyl)-tetrazolate were synthesized and characterized. With respect to energetic use salts **6** and **7** are most relevant. Compounds **3–9** and **11** were characterized using low temperature single-crystal X-ray diffraction. All compounds were investigated by NMR and vibrational (IR, Raman) spectroscopy, mass spectrometry and elemental analysis. The thermal properties were determined by differential scanning calorimetry (DSC). The sensitivities towards impact (4: 4 J, 5: 40 J, 6: 12 J, 7: 40 J), friction: (4: 60N, 5: 240 N, 6: 216 N, 7: 240 N), and electrical discharge (5: 0.40 J, 6: 0.75 J, 7: 0.75 J), were investigated using BAM standards and a small scale electrostatic discharge tester. The detonation parameters of **5–7** were calculated using the EXPLO5.06 code and calculated (CBS-4 M) enthalpy of formation values.

Keywords: Energetic materials · Tetrazoles · *N*-Oxides · Crystal structures · Nitrogen-rich

3.1 Introduction

The research of new secondary explosives in the 20th century was focused on cyclic and caged nitramines such as RDX^[1], HMX^[2], bicyclo-HMX^[3], and CL-20^[4]. In our days, these compounds are the most prevalent in civil and military applications^[5] (Figure 1). In recent years concerns about the environmental impact of energetic materials have grown, demanding new green energetic materials, which are based on a high nitrogen content that releases mainly environmentally friendly N₂ after decomposition^[6].

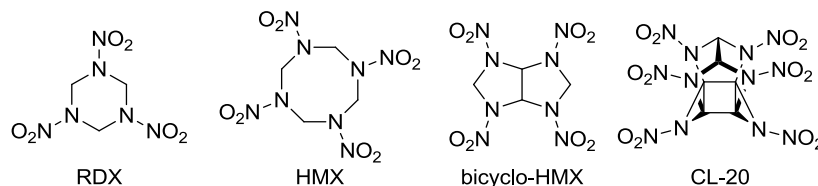


Figure 1. The cyclic or caged high explosives 1,3,5-trinitro-1,3,5-triazinane (RDX), 1,3,5,7-tetranitro-1,3,5,7-tetrazocane (HMX), cis-1,3,4,6-tetranitrooctahydroimidazo-[4,5-d]imidazole (bicycle-HMX), and 2,4,6,8,10,12-hexanitro-2,4,6,8,10,12-hexaazaisowurtzitane (CL-20).

Generally compounds based on azoles^[6a] can be considered as basic structures for new environmentally friendly, nitrogen-rich, strained compounds. Unfortunately, tetrazoles without oxygen-rich groups such as nitro mostly lack in high densities. Although being interesting energetic materials with respect to propellant applications their use as explosives is very limited. Recently it has been observed that the introduction of *N*-oxides in tetrazoles results in superior energetic performance.^[7] This strategy can even be increased by using bistetrazoles, which show high densities and moderate sensitivities.^[8] With this knowledge in hand, the highly energetic bis(hydroxylammonium) bistetrazole-1,1'-di-*N*-oxide^[9] and other nitrogen-rich bistetrazole-1,1'-di-*N*-oxide salts^[10], as well as bistetrazole-2,2'-di-*N*-oxide salts^[11] have been synthesized by our group. They show much better energetic properties than the corresponding oxygen-free bistetrazoles, latter one also being described as a useful ligand in metal complexes^[12]. The bis(hydroxylammonium) salt of 5,5'-bistetrazole has a low temperature (173 K) density of only 1.742 g cm⁻³^[8a]. Bis(hydroxylammonium) bistetrazole-1,1'-*N*-oxide has a density of 1.915 g cm⁻³ at this temperature, which results in much higher calculated detonation parameters (e.g. $V_{\text{det}} = 8854 \text{ m s}^{-1}$ vs. 9698 m s^{-1}). So far, bistetrazole-*N*1-monoxide, which will be referred to as 5-(1*H*-tetrazolyl)-1-hydroxytetrazole is missing in the literature. We would like to investigate whether there is a density or performance increment in the introduction of *N*-oxide to the bis(tetrazole) system (Figure 2).

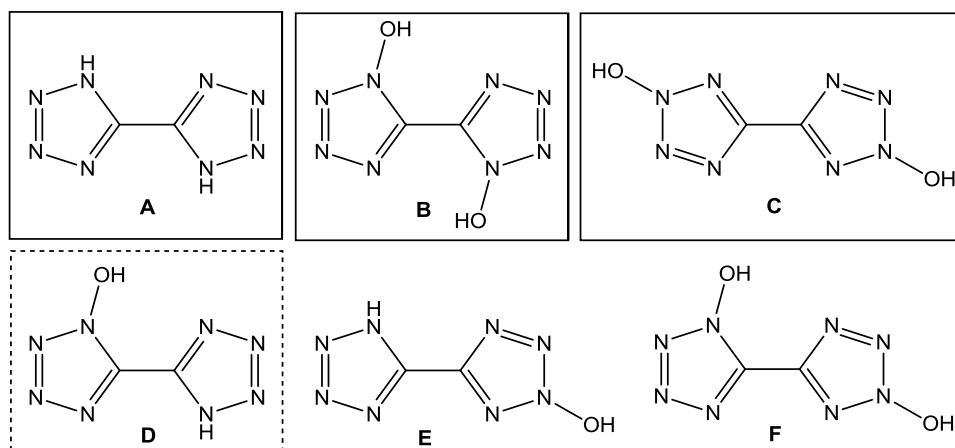


Figure 2. 5,5'-Bistetrazole and potential hydroxy-derivatives. A) 5,5'-Bistetrazole, B) Bis(1-hydroxytetrazole), C) Bis(2-hydroxytetrazole), D) 5-(1H-Tetrazolyl)-1-hydroxytetrazole, E) 5-(1H-Tetrazolyl)-2-hydroxytetrazole, F) 5-(2-Hydroxytetrazolyl)-1-hydroxytetrazole. Continuous box: known compounds. Dashed box: investigated in this work. No box: unknown yet.

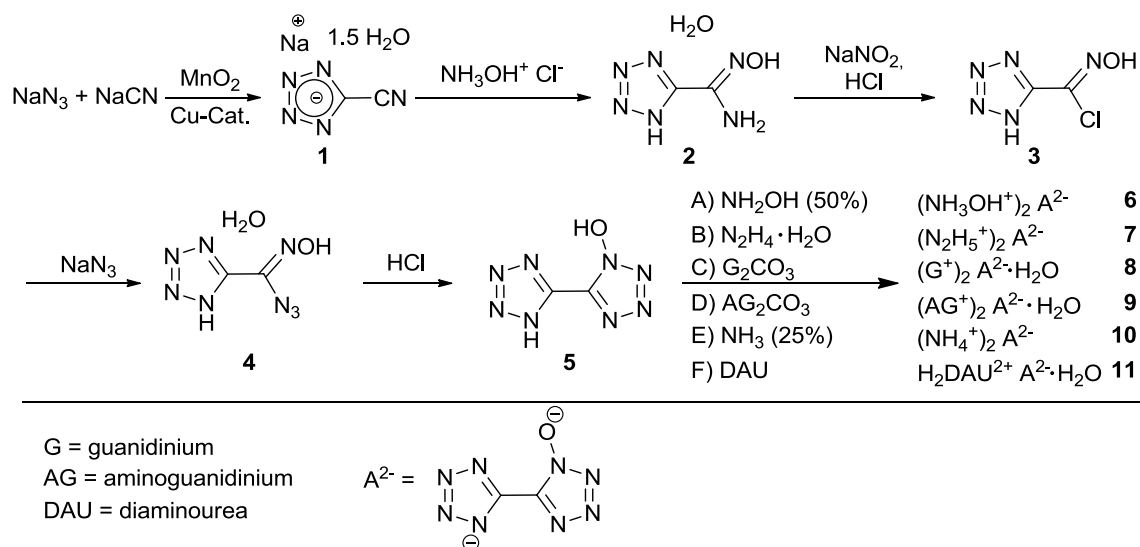
Herein we report the synthesis and characterization of the first anionic bistetrazole 1*N*-monoxide 5-(1*H*-tetrazolyl)-1-hydroxytetrazole, as well as its bis(hydroxylammonium) and bis(hydrazinium) salts. We further characterized two new intermediates, 5-chlorohydroximoyl-tetrazole and 5-azidohydroximoyl-tetrazole monohydrate, that were precursors of the target molecule.

3.2 Results and Discussion

3.2.1 Synthesis

Sodium 5-cyanotetrazolate sesquihydrate (**1**) and 5-aminohydroximoyl tetrazole (**2**) were synthesized as described in the literature^[14] in a two step synthetic protocol according to Scheme 1. In the first step NaN_3 , NaCN , and MnO_2 are reacted to give sodium 5-cyanotetrazolate sesquihydrate, which is then converted to compound **2** by reaction with aqueous hydroxylamine solution. The 5-chlorohydroximoyl-tetrazole **3** is obtained by diazotization of compound **2**, using sodium nitrite and concentrated hydrochloric acid. The mixture has been cooled to 0 °C and the addition of the sodium nitrite should be carried out slowly to ensure a clean reaction and complete conversion. 5-Azidohydroximoyl-tetrazole monohydrate **4** is prepared via a chlorine-azide exchange by dissolving **3** in ice-cooled ethanol and adding an aqueous solution of sodium azide. Azide **4** is the most sensitive compound and should be handled with care (impact sensitivity: 4 J, friction sensitivity: 60 N). This can be attributed to the highly energetic covalent azide group. In the last step an acid-catalyzed (HCl) cyclization of **4** could be accomplished in good yields. The product was

extracted and recrystallized with ethyl acetate to yield colorless crystals of 5-(1*H*-tetrazolyl)-1-hydroxytetrazole **5**. Mono-*N*-oxidation of 5,5'-bistetrazole by Oxone as an alternative reaction to this selective process yielded a mixture of different products. Addition of aqueous hydroxylamine or hydrazine solution to the acid **5** yielded bis(hydroxylammonium) 5-(1-oxidotetrazolyl)-tetrazolate (**6**) and bis(hydrazinium) 5-(1-oxidotetrazolyl)-tetrazolate (**7**), respectively. All compounds can easily be identified by NMR and vibrational spectroscopy, which is shown in the Supporting Information.



Scheme 1. Synthetic route towards compounds **4–11**.

3.2.2 Crystal Structures

During this work the crystal structures of compounds **3–9** and **11** were determined. Selected data and parameter of the X-ray determinations for compounds **3–9** and **11** are given in Table S1 (Supporting Information). The X-ray structures of **3**, **8**, **9**, and **11** are described in the Supporting Information as well.

5-Azidohydroximoyl-tetrazole monohydrate (**4**) crystallizes from water in the orthorhombic space group $P2_12_12_1$ with a density of 1.745 g cm^{-3} and with four molecules per unit cell. The molecular unit of **4** is illustrated in Figure 3.

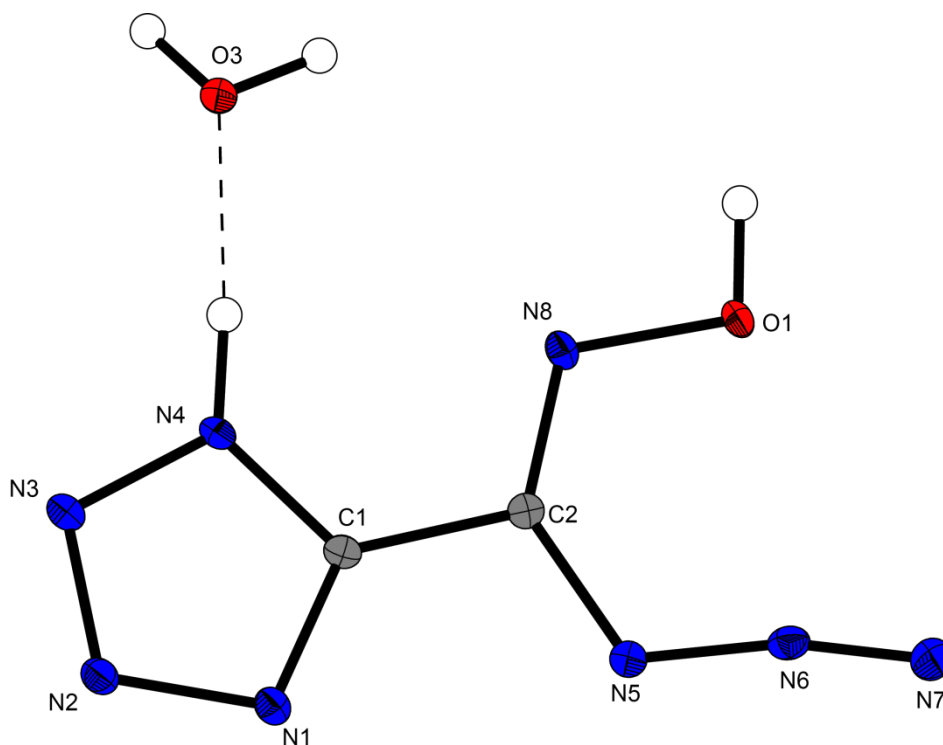


Figure 3. Molecular unit of **4**, showing the atom-labeling scheme. Thermal ellipsoids represent the 50% probability level and hydrogen atoms are shown as small spheres of arbitrary radius.

5-(1*H*-Tetrazolyl)-1-hydroxytetrazole (**5**) crystallizes with and without inclusion of crystal water. The water free structure was solved in the orthorhombic space group *Pbca* with eight molecular moieties in the unit cell. Its density of 1.814 g cm⁻³ is lower to that of 5,5'-bis(1-hydroxy)tetrazole dihydrate (1.881 g cm⁻³)^[9] and higher than that of salts **6** and **7**. However, in comparison to 5,5-bistetrazole (1.738 g cm⁻³)^[13] the density is significantly higher. These values insistently demonstrate the influence of introducing *N*-oxides towards tetrazoles. The tetrazole and tetrazole-1-oxide ring planes are tilted against each other by a torsion angle N4–C1–C2–N5 of 14.3(2)8°. The molecular unit is shown in Figure 4.

Interestingly, the two hydrogen atoms are located at the nitrogen atoms N4 and N6. The oxidized ring should be described as a zwitterionic system. This is in contrast to the structure of the corresponding monohydrate (Figure 5). There the protons are located at oxygen atom O1 as well as at nitrogen atom N5.

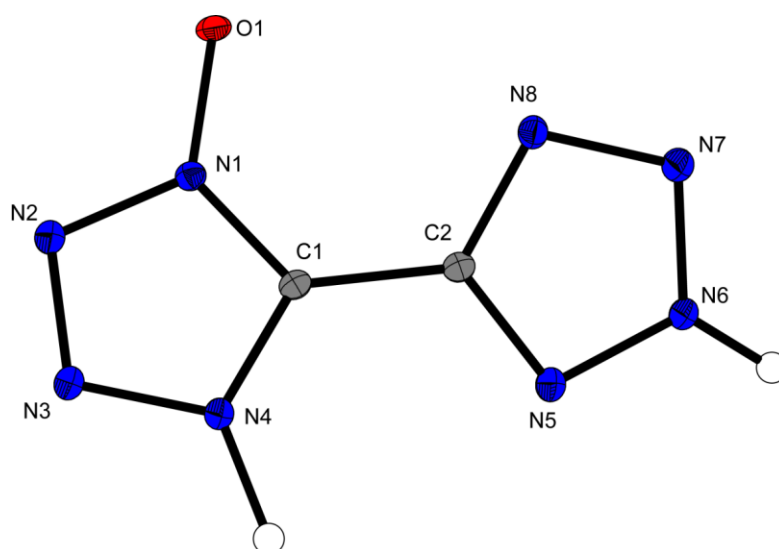


Figure 4. Molecular moiety of 5-(2*H*-tetrazolyl)-4*H*-tetrazole-1-oxide (**5**). Thermal ellipsoids are drawn at the 50% probability level and hydrogen atoms are shown as small spheres of arbitrary radius.

5-(1*H*-Tetrazolyl)-1-hydroxytetrazole monohydrate (**5**·H₂O) crystallizes in the monoclinic space group $P2_1/n$ with a lower density of 1.756 g cm⁻³. Eight molecules are found per unit cell. With a torsion angle N1–C1–C2–N5 of 15.5(2)°, the two heterocyclic ring systems are only slightly stronger tilted against each other in comparison to those of the anhydrous structure. The molecular unit of **5**·H₂O is shown in Figure 5.

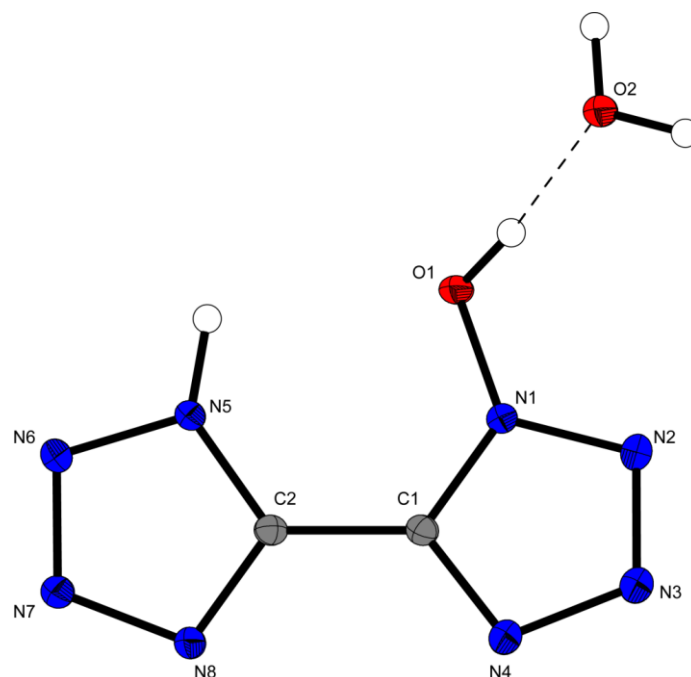


Figure 5. Molecular unit of 5-(1*H*-tetrazolyl)-1-hydroxytetrazole monohydrate (**5**·H₂O), showing the atom-labeling scheme. Thermal ellipsoids represent the 50% probability level and hydrogen atoms are shown as small spheres of arbitrary radius.

The bis(hydroxylammonium) salt **6** crystallizes anhydrously from water in the triclinic space group $P\bar{1}$ with two molecular moieties in the unit cell. Its density of 1.782 g cm^{-3} is lower than that of **5** and also of bis(hydroxylammonium) bis(tetrazolyl-1-oxide) (1.918 g cm^{-3})^[9] but higher than that of bis(hydroxylammonium) 5,5'-bistetrazolate (1.742 g cm^{-3})^[8a]. This is a lower value than the expected average value of 1.85 g cm^{-3} . The two aromatic ring systems are perfectly planar (torsion angle $\text{N8-C1-C2-N1}=0.12(27)^\circ$). The molecular unit of **6** is shown in Figure 6.

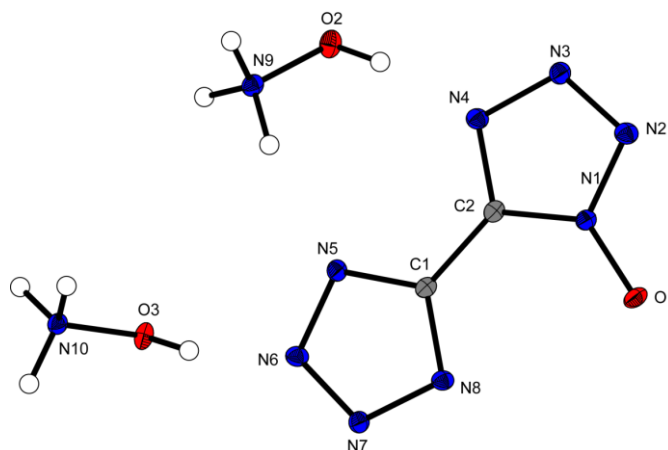


Figure 6. Molecular moiety of **6**. Ellipsoids of non-hydrogen atoms are drawn at the 50% probability level. Selected bond lengths /pm: O1–N1 132.84(18), N1–C2 134.4(2), N1–N2 134.6(2), N2–N3 130.5(2), N3–N4 134.9(2), N4–C2 134.0(2).

The bis(hydrazinium) salt **7** crystallizes anhydrously from water in the triclinic space group $P\bar{1}$ with two molecular moieties in the unit cell and a density of 1.704 g cm^{-3} . With a torsion angle N1-C1-C2-N8 of $7.7(2)^\circ$, the two aromatic ring systems are tilted against each other. The molecular unit of **7** is shown in Figure 7.

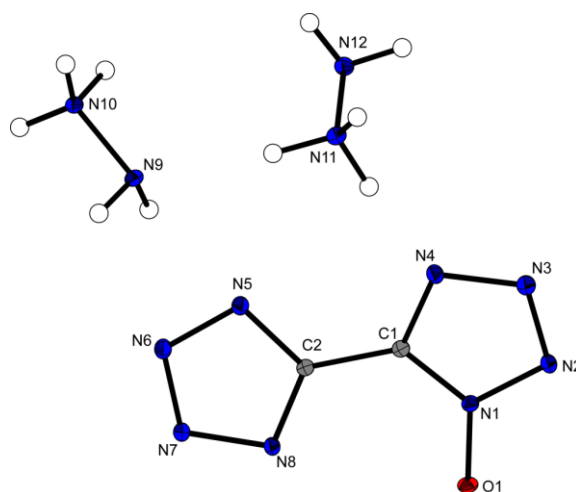


Figure 7. Molecular moiety of **7**. Ellipsoids of non-hydrogen atoms are drawn at the 50% probability level. Selected bond lengths /pm: O1–N1 132.56(16), N1–C1 134.24(19), N1–N2 134.46(18), N2–N3 131.92(18), N3–N4 134.89(18), N4–C1 133.78(19).

3.2.3 Physiochemical and Energetic Properties

The heats and energies of formation are given in Table 1. The values were calculated by the atomization method using electronic energies (CBS-4M method). Details are given in the Supporting Information. Compounds **5–7** have a large positive heat of formation. The highest value of 663 kJ mol^{-1} was calculated for the hydrazinium salt **7**. The calculation of the detonation parameters was performed with the program package EXPLO5 (version 6.01)^[19]. The program is based on the chemical equilibrium, steady-state model of detonation. It uses the Becker-Kistiakowsky-Wilson's equation of state (BKW EOS) for gaseous detonation products and Cowan-Fickett's equation of state for solid carbon.

The EXPLO5 detonation parameters calculated of compounds **5–7** using the room temperature recalculated X-ray densities^[20] are summarized in Table 1 and compared to the values calculated for TKX-50 and RDX.

The detonation velocities ($D = 8843$ (**5**), 9117 (**6**), 8979 (**7**) m s^{-1}) of the two salts are slightly higher than that of the acid **5**. All of them are higher than the detonation velocity of RDX, ($D = 8815 \text{ m s}^{-1}$). However, the detonation pressure of compounds **5–7** ($p_{\text{CJ}} = 31.4$ (**5**), 32.3 (**6**), 29.0 (**7**) GPa) is lower than that of RDX ($p_{\text{CJ}} = 35.2$ GPa). Both trends fit to the equations of Kamlet and Jacob^[21].

A small-scale reactivity test (SSRT) was carried out to assess the explosive performance of **6** in comparison to the previous measured TKX-50, CL-20 and RDX (for a detailed set up description, see reference [9]). From measuring the volumes of the dents (Table 1), it can be concluded that the small scale explosive performance of **6** is slightly lower than the performance of commonly used RDX.

3.2.4 Sensitivities

The impact and friction sensitivities were explored by BAM methods (method 1 of 6). The CHNO-based energetic compounds **4–7** reveal strong differences regarding their impact and friction sensitivity. The azido-based compound **4** has to be classified as very sensitive towards impact (4 J) and sensitive towards friction (60 N). The free acid **5** and its hydrazinium salt **7** can both be considered as insensitive as each reveals a value of 240 N for the friction test and 40 J for the impact test. The hydroxylammonium salt **6** exhibits a friction sensitivity of 216 N and an impact sensitivity of 12 J. Therefore it has to be classified as sensitive, however compound **5–7** are still less sensitive than commonly used RDX ($IS = 7.5 \text{ J}$, $FS = 120 \text{ N}$).

Table 1. Energetic properties, detonation parameters and toxicity.

	5	6	7	TKX-50^[9]	RDX
Formula	C ₂ H ₂ N ₈ O	C ₂ H ₈ N ₁₀ O ₃	C ₂ H ₁₀ N ₁₂ O	C ₂ H ₈ N ₁₀ O ₄	C ₃ H ₆ N ₆ O ₆
FW [g mol ⁻¹]	154.09	220.15	218.18	236.15	222.12
IS [J] ^a	40	12	40	20	7.5 ^[16]
FS [N] ^b	240	216	240	120	120 ^[16]
ESD [J] ^c	0.40	0.75	0.75	0.10	0.20
N [%] ^d	72.27	63.62	77.04	59.30	37.84
Ω [%] ^e	-41.53	-36.33	-58.67	-27.10	-21.61
T _{dec.} [°C] ^f	192	200	208	221	210 ^[17]
ρ [g cm ⁻³] (298K) ^g	1.762	1.731	1.655	1.877	1.806 ^[18]
Δ _f H° [kJ mol ⁻¹] ^h	636.6	469.0	662.6	458.7	70.3
Δ _f U° [kJ kg ⁻¹] ⁱ	4219.6	2248.5	3167.4	2057.8	417.0
EXPLO V6.01 values:					
-Δ _E U° [kJ kg ⁻¹] ^j	5611	5546	4755	5939	5734
T _E [K] ^k	4043	3490	2903	3642	3800
p _{CJ} [kbar] ^l	314	323	290	401	352
D [m s ⁻¹] ^m	8843	9117	8979	9781	8815
V ₀ [L kg ⁻¹] ⁿ	797	924	939	913	792
SSRT:					
weight [mg]	-	474	-	509	504
dent [mg SiO ₂]	-	723	-	857	858
Toxicity assessment:					
EC ₅₀ (15 min) [g L ⁻¹]	-	1.634	-	1.172	0.327
EC ₅₀ (30 min) [g L ⁻¹]	-	0.330	-	0.580	0.239

^a impact sensitivity (BAM drophammer, 1 of 6); ^b friction sensitivity (BAM friction tester, 1 of 6); ^c electrostatic discharge device (OZM); ^d nitrogen content; ^e oxygen balance; ^f decomposition temperature from DSC (β = 5°C); ^g recalculated from low temperature X-ray densities (ρ_{298K} = ρ_T / (1+α_V(298-T₀); α_V = 1.5 · 10⁻⁴ K⁻¹); ^h calculated (CBS-4M) heat of formation; ⁱ calculated energy of formation; ^j energy of explosion; ^k explosion temperature; ^l detonation pressure; ^m detonation velocity; ⁿ assuming only gaseous products.

3.2.5 Toxicity Assessment

The toxicity to aquatic life was investigated using the luminescent marine bacterium *Vibrio fischeri* using the commercially available bioassay system *LUMISTox*[®]. *Vibrio fischeri* is a representative species for other aquatic life and therefore a useful indicator when it comes to groundwater pollution. Being the most important toxicological parameter, the EC₅₀ value of the sample was determined. EC₅₀ is the effective concentration of the examined compound, at which the bioluminescence of the strain *Vibrio fischeri* is decreased by 50% after a defined period of exposure as compared to the original bioluminescence of the sample before being treated with the differently diluted solutions of the test compound. For the bis(hydroxylammonium) salt **6** we observed an EC₅₀ value of 1.634 g L⁻¹ after an incubation time of 15 min as well as an EC₅₀ value of 0.330 g L⁻¹ after an incubation time of 30 min. The toxicity test demonstrates the low toxicity of compound **6** compared to RDX (Table 1).

3.3 Experimental Section

The analytical methods and general procedures are described in the appendix of this thesis. Sodium cyanotetrazole sesquihydrate **1** and 5-aminohydroximoyl tetrazole **2** were synthesized according to the literature.^[14]

Synthesis of 5-Chlorohydroximoyl-tetrazole (3)

5-Aminohydroximoyl-tetrazole (1.80 g, 12.3 mmol) was dissolved in fuming hydrochloric acid (33.4 mL, 404 mmol). The solution was cooled with an ice bath and additionally 50 g of ice were added. An aqueous solution of sodium nitrite (2.42 g, 35.1 mmol) was added dropwise over 1 h while the temperature was kept below 0 °C. Afterwards the solution was allowed to warm to ambient temperature and diluted by addition of 100 mL of ice water. The product was extracted three-times with diethyl ether (50mL) and after removal of the solvent 5-chlorohydroximoyl-tetrazole precipitated to give 1.65 g (11.2 mmol, 91%) of a white powder.

¹H NMR ([D₆]DMSO): δ = 13.39 (s, 1H, –NOH), 7.78 ppm (br. s, 1H, NH); **¹³C NMR** ([D₆]DMSO): δ = 152.4 (CN₄), 124.9 ppm (CClNOH); **MS** m/z (DEI⁺): 147.0 [M⁺]; **EA** (C₂H₂ClN₅O·H₂O, 172.11) calcd.: C 14.51, H 2.44, N 42.31%; found: C 14.59, H 2.41, N 41.88%.

Synthesis of 5-Azidohydroximoyl-tetrazole monohydrate (4)

5-Chlorohydroximoyl-tetrazole (1.48 g, 10 mmol) was dissolved in ethanol (50mL) and cooled with an ice bath. An aqueous solution of sodium azide (1.30 g, 20 mmol) was added dropwise over 1 h while the temperature was kept below 5 °C. Afterwards, an aqueous solution of sodium hydrogencarbonate (840 mg, 10 mmol) was added slowly, the reaction mixture was stirred for 1 h and diluted with water (175 mL). The solution was adjusted to pH 1 by addition of conc. hydrochloric acid and the product was extracted three-times with diethyl ether (50 mL). During removal of the solvent, 5-azidohydroximoyl-tetrazole monohydrate crystallized to give colorless rods. Yield: 1.27 g, 7.4 mmol, 74%.

DSC (5 °C min⁻¹, °C): 126 °C (dec.); **IR** (ATR, cm⁻¹): $\tilde{\nu}$ = 3546(w), 3223(w), 3173(m), 3020(w), 2876(w), 2470(w), 2175(m), 2116(m), 1890(w), 1614(m), 1581(m), 1421(m), 1293(s), 1256(m), 1152(w), 1129(w), 1086(w), 1060(w), 1021(vs), 948(s), 863(s), 760(m), 696(s), 609(m); **Raman** (1064 nm, 300 mW, 25 °C, cm⁻¹): $\tilde{\nu}$ = 2180(8), 2120(7), 1617(100), 1583(76), 1473(25), 1437(17), 1294(13), 1259(23), 1132(8), 1088(9), 1062(5), 1024(19), 960(9), 866(13), 750(6), 603(4), 575(3), 465(7), 404(9), 631(10), 315(15), 230(23), 194(9),

146(84), 125(45), 110(38), 69(45); **¹H NMR** ([D₆]DMSO): δ = 12.54 (s, 1H, –NOH), 6.39 ppm (br. s, 1H, NH); **¹³C NMR** ([D₆]DMSO): δ = 150.0 (CN₄), 133.3 ppm (C(N₃)NOH); **MS** m/z (DEI⁺): 154.0 [M⁺]; **EA** (C₂H₄N₈O₂, 172.11) calcd.: C 13.96, H 2.34, N 65.11%; found: C 14.61, H 2.33, N 64.29%; **Sensitivities**: IS: 4 J, FS: 60 N (at grain size <100 μ m).

Synthesis of 5-(1*H*-Tetrazolyl)-1-hydroxytetrazole (5)

5-Azidohydroximoyl-tetrazole monohydrate (5.15 g, 29.9 mmol) was dissolved in hydrochloric acid (100 mL, 37%) and stirred at ambient temperature for 24 h. The mixture is diluted with water and the product was extracted with ethyl acetate. The solution was left for crystallization to yield colorless crystals. Yield: 4.19 g, 27.2 mmol, 91%.

DSC (5 °C min⁻¹): 192 °C (dec.); **IR** (ATR, cm⁻¹): $\tilde{\nu}$ = 3046(s), 2775(s), 2122(w), 1993(w), 1731(m), 1637(m), 1535(m), 1527(m), 1470(m), 1453(m), 1424(m), 1398(m), 1389(m), 1316(s), 1243(s), 1208(s), 1184(s), 1174(vs), 1137(vs), 1120(vs), 1080(s), 1048(vs), 1033(s), 1033(s), 1008(m), 882(s), 757(m), 717(m), 708(m), 700(m), 693(m), 672 (w); **Raman** (1064 nm, 300 mW, 25 °C, cm⁻¹): $\tilde{\nu}$ = 1638(63), 1413(5), 1275(19), 1253(9), 1197(14), 1185(16), 1178(13), 1137(41), 1123(13), 1085(13), 1047(6), 1036(5), 1023(5), 1009(8), 882(3), 760(11), 682(4), 584(3), 407(22), 325(17), 220(10), 174(31), 149(30), 149(30), 133(80), 103(61), 89(44), 71(100); **¹H NMR** ([D₆]DMSO): δ = 7.87 ppm (s, 1H, OH); **¹³C NMR** ([D₆]DMSO): δ = 146.2 (s, CN₄), 138.1 ppm (s, CN₄O); **MS** m/z (DEI⁺): 155.1 (M⁺); **EA** (C₂H₂N₈O, 154.09) calcd.: C 15.59, H 1.31, N 72.72%; found: C 16.29, H 1.37, N 71.99%; **Sensitivities**: IS: 40 J, FS: 240 N, ESD: 750 mJ (at grain size 100–500 μ m).

Synthesis of Bis(hydroxylammonium) 5-(1-oxidotetrazolyl)-tetrazolate (6)

5-(1*H*-Tetrazolyl)-1-hydroxytetrazole (500 mg, 3.24 mmol) was dissolved in 20 mL of water. Hydroxylamine (428 mg of a 50% w/v solution in H₂O, 6.48 mmol) was added. The solution was left for crystallization and bis(hydroxylammonium) 5-(1-oxidotetrazolyl)-tetrazolate precipitated as colorless needles. Yield: 614 mg, 2.79 mmol, 86%.

DSC (5 °C min⁻¹): 200 °C (dec.); **IR** (ATR, cm⁻¹): $\tilde{\nu}$ = 3090(m), 2922(m), 2860(m), 2660(s), 2186(m), 2112(m), 2062(m), 2050(m), 1648(m), 1622(m), 1600(m), 1562(m), 1532(s), 1510(s), 1458(s), 1386(m), 1334(s), 1248(s), 1228(vs), 1190(s), 1156(s), 1114(m), 1082(m), 1082(m), 1050(m), 1038(m), 1014(m), 1000(s), 760(m), 726(s), 712(s), 682 (vs); **Raman** (1064 nm, 300 mW, 25 °C, cm⁻¹): $\tilde{\nu}$ = 3085(4), 2923(5), 2727(5), 1617(9), 1602(100), 1586(9), 1574(5), 1526(6), 1461(5), 1389(4), 1336(4), 1242(17), 1225(5), 1192(9), 1158(7), 1140(11), 1115(14), 1082(5), 1053(8), 1039(10), 1003(18), 761(7), 587(4), 587(4), 422(10),

368(6), 325(6), 284(5), 253(6), 171(8), 154(9), 139(9), 123(35), 102(38), 79(27), 66(13); **¹H NMR** ([D₆]DMSO): δ = 9.38 ppm (s, br, NH₃OH⁺); **¹³C NMR** ([D₆]DMSO): δ = 149.3 (s, CN₄); 138.2 ppm (s, CN₄O); **MS** m/z (FAB⁻): 153.1 (C₂HN₈O⁻), m/z (FAB⁺): 33.1 (NH₃O⁺); **EA** (C₂H₈N₁₀O₃, 220.15) calcd.: C 10.91, H 3.66, N 63.62%; found: C 11.37, H 3.59, N 63.42%; **Sensitivities**: IS: 12 J, IS: 216 N, ESD: 750 mJ (at grain sizes 100–500 μ m).

Synthesis of Bis(hydrazinium) 5-(1-oxidotetrazolyl)-tetrazolate (7)

5-(1*H*-Tetrazolyl)-1-hydroxytetrazole (770 mg, 5.0 mmol) was dissolved in ethanol (10mL). A solution of hydrazine (10.0 mmol, 501 mg) in water was added and a white solid precipitated instantaneously. The solution was stirred for 5 min at ambient temperature, the white precipitate was filtered off and the filtrate was rinsed with ethanol and ether. The crude product was recrystallized from about 5 mL of water to give bis(hydrazinium) 5-(1-oxidotetrazolyl)-tetrazolate as colorless needles. Yield: 1.01 mg, 4.6 mmol, 93%.

DSC (5 °Cmin⁻¹): 208 °C (dec.); **IR** (ATR, cm⁻¹): $\tilde{\nu}$ = 3310(s), 3263(s), 3185(m), 2961(s), 2944(s), 2920(s), 2769(s), 2615(s), 2505(s), 2168(m), 2164(m), 2131(m), 1948(w), 1800(w), 1668(w), 1630(s), 1624(s), 1597(s), 1585(s), 1564(s), 1528(s), 1497(m), 1455(vs), 1455(vs), 1439(s), 1415(m), 1374(s), 1332(s), 1234(vs), 1216(s), 1176(s), 1134(m), 1093(vs), 1033(s), 999(s), 975(vs), 957(vs), 754(s), 720 (m); **Raman** (1064 nm, 300 mW, 25 °C, cm⁻¹): $\tilde{\nu}$ = 3310(2), 3268(3), 1599(100), 1527(4), 1456(3), 1333(4), 1235(15), 1217(13), 1175(5), 1130(12), 1112(12), 1099(9), 1071(3), 1035(11), 977(7), 959(5), 764(7), 758(4), 579(2), 421(9), 361(5), 332(4), 243(3), 243(3), 159(7), 135(9), 118(9), 98(60), 79(20), 65(11); **¹H NMR** ([D₆]DMSO): δ = 6.66 ppm (s, br, N₂H₅⁺); **¹³C NMR** ([D₆]DMSO): δ = 150.5 (s, CN₄); 138.2 ppm (s, CN₄O); **MS** m/z (FAB⁻): 153.1 (C₂HN₈O⁻); m/z (FAB⁺) 33.1 (N₂H₅⁺); **EA** (C₂H₁₀N₁₂O, 218.18) calcd.: C 11.01, H 4.62, N 77.04%; found: C 11.57, H 4.55, N 75.71%; **Sensitivities**: IS: 40 J; FS: 240 N; ESD: 750 mJ (at grain sizes 100-500 μ m).

3.4 Conclusions

5-(1*H*-Tetrazolyl)-1-hydroxytetrazole (**5**) and various nitrogen-rich ionic derivatives (e.g. bis(hydroxylammonium) salt **6**, bis(hydrazinium) salt **7**) were synthesized in five steps, starting from commercially available starting materials sodium azide, sodium cyanide and MnO₂.

The crystal structures of **3–7** were determined by low temperature single-crystal X-ray diffraction. The compounds crystallize in the space groups *P*2₁/*n* (**3**), *P*2₁2₁2₁ (**4**), *Pbca* (**5**), *P*-1 (**6**, **7**) with densities of 1.449 (**3**), 1.745 (**4**), 1.814 (**5**), and 1.782 (**6**), 1.704 g cm⁻³ (**7**),

respectively. Additionally all compounds were fully characterized by vibrational spectroscopy (IR and Raman), ^1H and ^{13}C NMR, mass spectroscopy, and elemental analysis. Furthermore, a ^{15}N NMR was obtained of compound **5** and **6** and all resonances were assigned.

Thermal stabilities of compounds **4–7** were investigated by DSC. They decompose at 126 °C (**4**), 192 °C (**5**), 200 °C (**6**), and 208 °C (**7**), respectively.

The sensitivities towards friction impact and electrostatic discharge were investigated by BAM methods. Compounds **4–7** were found to have impact sensitivities of 4 J (very sensitive) (**4**), 40 J (insensitive) (**5**, **7**), and 12 J (sensitive) (**6**), friction sensitivities of 60 N (sensitive) (**4**), 240 N (insensitive) (**5**, **7**), and 216 N (sensitive) (**6**), and ESD sensitivities of 0.40 J (**5**), 0.75 J (**6**), and 0.75 J (**7**).

Using calculated heats of formation and experimentally obtained crystal densities, the detonation parameters (heat of explosion, explosion temperature, detonation pressure, and velocity) were calculated for compounds **5–7** [$D = 8843 \text{ m s}^{-1}$ (**5**), 9117 m s^{-1} (**6**), 8979 m s^{-1} (**7**)]. The sensitivities and detonation velocity of the newly synthesized 5-(1*H*-tetrazolyl)-1-hydroxytetrazole (**5**) and its salts outperform commonly used RDX ($IS = 7.5 \text{ J}$, $FS = 120 \text{ N}$, $ESD = 0.2 \text{ J}$, $D = 8815 \text{ m s}^{-1}$). The low toxicity of compound **6** was determined, which makes compound **6** a potential “green” RDX replacement.

3.5 References

- [1] a) W. E. Bachmann, J. C. Sheehan, A New Method of Preparing the High Explosive RDX, *J. Am. Chem. Soc.* **1949**, *71*, 1842–1845. b) E. P. Burrows, E. E. Brueggemann, Reversed-phase gradient high-performance liquid chromatography of nitramine munitions and characterization of munitions process samples by gas chromatography-mass spectrometry, *J. of Chromatogr.* **1985**, *329*, 285–289.
- [2] a) H. Fischer, Notiz über die Darstellung von Oktogen (Cyclo-tetramethylentetranitramin), *Chem. Ber.* **1949**, *82*, 192–193; b) Y. Wang, W. Jiang, X. Song, G. Deng, F. Li, Insensitive HMX (Octahydro-1,3,5,7-tetranitro-1,3,5,7-tetrazocine) Nanocrystals Fabricated by High-Yield, Low-Cost Mechanical Milling, *Cent. Eur. J. Energ. Mater.* **2013**, *10*, 277–287.
- [3] (a) P. F. Pagoria, A. R. Mitchell, R. D. Schmidt, C. L. Coon, E. S. Jessop, Nitration, *Am. Chem. Soc. Symp. Ser.* **1996**, *623*, 151–164. (b) R. Gilardi, J. L. Flippen-Anderson, R. Evans, cis-2,4,6,8-Tetranitro-1*H*,5*H*-2,4,6,8-tetraazabicyclo[3.3.0] octane, the Energetic Compound 'bicyclo-HMX', *Acta Crystallogr.* **2002**, *E58*, o972–o974.

- [4] A. T. Nielsen, A. P. Chafin, S. L. Christian, D. W. Moore, M. P. Nadler, R. A. Nissan, D. J. Vanderah, R. D. Gilardi, C. F. George, J. L. Flippen-Anderson, Synthesis of Polyazapolycyclic caged polynitramines, *Tetrahedron* **1998**, *54*, 11793–11812.
- [5] T. M. Klapötke, *Chemie Der Hochenergetischen Materialien*, Walter De Gruyter GmbH & Co. KG, Berlin, **2009**.
- [6] a) H. Gao, J. M. Shreeve, Azole-Based Energetic Salts, *Chem. Rev.* **2011**, *111*, 7377–7436; b) R. Haiges, S. Schneider, T. Schroer, K. O. Christe, New High Energy Density Materials. Synthesis and Characterization of $\text{N}_5^+\text{P}(\text{N}_3)_6^-$, $\text{N}_5^+\text{B}(\text{N}_3)_4^-$, $\text{N}_5^+\text{HF}_2^- \cdot n \text{HF}$, $\text{N}_5^+\text{BF}_4^-$, $\text{N}_5^+\text{PF}_6^-$, and $\text{N}_5^+\text{SO}_3\text{F}^-$, *Angew. Chem.* **2004**, *116*, 5027–5032; *Angew. Chem. Int. Ed.* **2004**, *43*, 4919–4924; c) D. E. Chavez, M. A. Hiskey, D. L. Naud, D. Parrish, Synthesis of an Energetic Nitrate Ester, *Angew. Chem.* **2008**, *120*, 8431–8433; *Angew. Chem. Int. Ed.* **2008**, *47*, 8307–8309; d) M. B. Talawar, R. Sivabalan, T. Mukundan, H. Muthurajan, A. K. Sikder, B. R. Gandhe, A. Subhananda Rao, Environmentally compatible next generation green energetic materials (GEMs), *J. Hazard. Mater.* **2009**, *161*, 589–607; e) O. S. Bushuyev, P. Brown, A. Maiti, R. H. Gee, G. R. Peterson, B. L. Weeks, L. J. Hope-Weeks, Ionic Polymers as a New Structural Motif for High Energy-Density Materials, *J. Am. Chem. Soc.* **2012**, *134*, 1422–1425.
- [7] a) M. Göbel, K. Karaghiosoff, T. M. Klapötke, D. G. Piercey, J. Stierstorfer, Nitrotetrazolate-2*N*-oxides and the Strategy of *N*-Oxide Introduction, *J. Am. Chem. Soc.* **2010**, *132*, 17216–17226. b) J. C. Bottaro, M. Petrie, P. E. Penwell, A. L. Dodge, R. Malhotra, NANA/HEDM Technology: Late Stage Exploratory Effort, Report No. A466714; SRI International: Menlo Park, CA, **2003**; DARPA/AFOSR funded, contact no. F49629-02-C-0030.
- [8] a) N. Fischer, D. Izsák, T. M. Klapötke, S. Rappenglück, J. Stierstorfer, Nitrogen-Rich 5,5'-Bistetrazolates and their Potential Use in Propellant Systems: A Comprehensive Study, *Chem. Eur. J.* **2012**, *18*, 4051–4062; b) N. Fischer, T. M. Klapötke, K. Peters, M. Rusan, J. Stierstorfer, Alkaline Earth Metal Salts of 5,5'-Bistetrazole – from Academical Interest to Practical Application, *Z. Anorg. Allg. Chem.* **2011**, *637*, 1693–1701.
- [9] N. Fischer, D. Fischer, T. M. Klapötke, D. G. Piercey, J. Stierstorfer, Pushing the limits of energetic materials – the synthesis and characterization of dihydroxylammonium 5,5'-bistetrazole-1,1'-diolate *J. Mater. Chem.* **2012**, *22*, 20418–20422.

- [10] N. Fischer, T. M. Klapötke, M. Reymann, J. Stierstorfer, Nitrogen-Rich Salts of 1*H*,1'*H*-5,5'-Bitetrazole-1,1'-diol: Energetic Materials with High Thermal Stability, *Eur. J. Inorg. Chem.* **2013**, 2167–2180.
- [11] N. Fischer, L. Gao, T. M. Klapötke, J. Stierstorfer, Energetic salts of 5,5'-bis(tetrazole-2-oxide) in a comparison to 5,5'-bis(tetrazole-1-oxide) derivatives, *Polyhedron* **2013**, *51*, 201–210.
- [12] P. J. Eulgem, A. Klein, N. Maggiorosa, D. Naumann, R. W. H. Pohl, New Rare Earth Metal Complexes with Nitrogen-Rich Ligands: 5,5'-Bitetrazolate and 1,3-Bis(tetrazol-5-yl)triazene - On the Borderline between Coordination and the Formation of Salt-Like Compounds, *Chem. Eur. J.* **2008**, *14*, 3727–3736.
- [13] P. J. Steel, Heterocyclic tauomerism. XI. Structures of 5,5'-bitetrazole and 1-methyl-5-(2'-pyridyl)tetrazole at 130 K, *J. Chem. Crystallogr.* **1996**, *26*, 399–402.
- [14] N. Fischer, T. M. Klapötke, S. Rappenglück, J. Stierstorfer, The Reactivity of 5-Cyanotetrazole towards Water and Hydroxylamine, *ChemPlusChem* **2012**, *77*, 877–888.
- [15] <http://www.linseis.com>
- [16] R. M. Vrcelj, J. N. Sherwood, A. R. Kennedy, H. G. Gallagher and T. Gelbrich, Polymorphism in 2-4-6 Trinitrotoluene, *Cryst. Growth Des.* **2003**, *3*, 1027–1032.
- [17] R. Mayer, J. Köhler and A. Homburg, Explosives, Wiley-VCH, Weinheim, 5th edn, **2002**.
- [18] C. S. Choi and E. Prince, The Crystal Structure of Cyclotrimethylene-trinitramine, *Acta Crystallogr., Sect. B* **1972**, *28*, 2857–2862.
- [19] M. Sućeska, *EXPLO5.06 program*, Zagreb, Croatia, **2012**.
- [20] C. Xue, J. Sun, B. Kang, Y. Liu, X. Liu, The β - δ -Phase Transition and Thermal Expansion of Octahydro-1,3,5,7-Tetranitro-1,3,5,7-Tetrazocine, *Propellants, Explos., Pyrotech.* **2010**, *35*, 333–338.
- [21] M. J. Kamlet, S. J. Jacobs, Chemistry of Detonations I. A simple Method for Calculating Detonation Properties of C-H-N-O Explosives, *J. Chem. Phys.* **1968**, *48*, 23–35.

3.6 Supplementary Information

The analytical methods and general procedures are described in the appendix of this thesis.

3.6.1 Experimental work

Sodium cyanotetrazolate sesquihydrate (1)

To an aqueous solution (400 mL) of sodium cyanide (50.0 g, 1.02 mol) and sodium azide (32.5 g, 500 mmol) was added MnO_2 (50.0 g, 575 mmol). A mixture of sulfuric acid (100 mL of a 50% solution in H_2O , 936 mmol), formic acid (60.0 g, 1.11 mol) and $\text{CuSO}_4 \times 5 \text{H}_2\text{O}$ (1.00 g, 4.01 mmol) was added dropwise to the brown suspension within 30 min. The temperature was kept between 38 and 43 °C by cooling the reaction mixture with an ice bath. Afterwards the mixture was heated to 60 °C for 2 h before it was allowed to cool to ambient temperature. The resulting brownish slurry was filtered off and the filtrate was adjusted to pH 10 by addition of sodium carbonate (106 g, 1.00 mol). The solution was diluted with water (300 mL), the thus formed manganese formate was filtered off and the filtrate was neutralized with formic acid (7.00 mL). The solvent was removed under reduced pressure and the residue was extracted with boiling acetone. Removal of the solvent under reduced pressure and recrystallization from an ethanol ethyl acetate mixture to give slightly green crystals. Yield: 25.3 g (175.6 mmol, 35%).

Carboxymidoximoyl-tetrazole monohydrate (2)

Sodium cyanotetrazolate sesquihydrate (2.00 g, 14.0 mmol) was dissolved in 5 mL of water and treated with an aqueous solution of hydroxylammonium chloride (4 mL water, 1.04 g, 15.0 mmol). The solution was heated to reflux for 10 min, until precipitation of the product. The crude product was filtered off and recrystallized from hot water. The filtrate was left to stand for a few more days to give colorless crystals. Yield: 0.84 g (5.75 mmol, 41%).

Bis(guanidinium) 5-(1-oxidotetrazolyl)-tetrazolate monohydrate (8)

5-(1*H*-Tetrazolyl)-1-hydroxytetrazole (770.2 mg, 5.0 mmol) was dissolved in 10 mL of ethanol. A solution of guanidinium carbonate (900.9 mg, 5.0 mmol) in water was added and the solution was refluxed for 1 h. Then solution was left for crystallization to give bis(guanidinium) 5-(1-oxidotetrazolyl)-tetrazolate monohydrate. Yield: 1.18 g (4.07 mmol, 81%).

DSC (5 °C min⁻¹): 285°C (dec.); **IR** (ATR, cm⁻¹): $\tilde{\nu}$ = 3496(w), 3328(s), 3114(s), 2194(w), 2170(w), 2130(w), 2048(vw), 1652(vs), 1600(s), 1450(s), 1376(m), 1332(m), 1238(s),

1222(m), 1184(m), 1150(m), 1136(m), 1118(m), 1084(m), 1048(m), 1030(m), 1002(m), 880(m), 880(m), 814(m), 752(m), 718(m), 688 (s); **Raman** (1064 nm, 300 mW, 25 °C, cm⁻¹): $\tilde{\nu}$ = 3217(2), 1647(4), 1602(100), 1452(4), 1379(4), 1334(5), 1239(11), 1224(15), 1185(5), 1148(14), 1120(12), 1084(5), 1049(10), 1033(15), 1011(31), 757(6), 549(9), 537(5), 516(4), 424(8), 412(5), 357(6), 318(4), 318(4), 197(6), 152(24), 128(20), 89(25), 71(5); **¹H NMR** ([D₆]DMSO): δ = 6.56 ppm (br s, 6H, C-NH₂); **¹³C NMR** ([D₆]DMSO): δ = 158.4 (s, G⁺), 150.4 (s, CN₄), 137.9 ppm (s, CN₄O); **MS** m/z (FAB⁻): 153.1 (C₂N₈HO⁻), m/z (FAB⁺): 60.1 (G⁺); **EA** (C₄H₁₄N₁₄O₂, 290.25) calcd.: C 16.55, H 4.86, N 67.56%; found: C 16.97, H 4.88, N 67.02%; **Sensitivities**: IS: > 40 J, FS: >360 N.

Bis(aminoguanidinium) 5-(1-oxidotetrazolyl)-tetrazolate monohydrate (9)

5-(1*H*-Tetrazolyl)-1-hydroxytetrazole (428 mg, 2.78 mmol) was dissolved in 10 mL of water. Aminoguanidinium bicarbonate (756 mg, 5.66 mmol) was added and the mixture was heated to 90 °C for 1 h. The solution was left for crystallization to yield bis(aminoguanidinium) 5-(1-oxidotetrazolyl)-tetrazolate monohydrate as colorless, slightly brownish crystals. Yield: 690 mg (2.15 mmol, 76%).

DSC (5 °C min⁻¹): 201 °C (mp.), 230 °C (dec.); **IR** (ATR, cm⁻¹): $\tilde{\nu}$ = 3414(m), 3338(m), 3310(m), 3266(m), 3120(s), 3000(m), 2766(w), 2194(w), 1690(s), 1662(vs), 1600(m), 1568(m), 1526(w), 1450(s), 1376(m), 1338(m), 1238(s), 1224(s), 1182(s), 1148(m), 1116(m), 1072(m), 1048(m), 1048(m), 1032(m), 986(s), 962(s), 762(vs), 752(s), 718(s), 686(s), 658 (s); **Raman** (1064 nm, 300 mW, 25 °C, cm⁻¹): $\tilde{\nu}$ = 3249(3), 1666(3), 1602(100), 1455(3), 1379(4), 1340(4), 1244(11), 1227(10), 1183(6), 1142(13), 1113(9), 1076(7), 1048(17), 1036(6), 994(5), 972(14), 765(7), 755(4), 632(4), 579(3), 513(7), 427(6), 405(7), 405(7), 341(7), 308(4), 130(45), 116(47), 107(46); **¹H NMR** ([D₆]DMSO): δ = 9.36 (s, 1H, C-NH-N), 7.53 (br, 4H, C-NH₂), 4.71 ppm (s, 2H, N-NH₂); **¹³C NMR** ([D₆]DMSO): δ = 159.2 (s, AG⁺), 150.4 (s, CN₄), 138.0 ppm (s, CN₄O); **MS** m/z (FAB⁻): 153.1 (C₂N₈HO⁻); m/z (FAB⁺): 75.1 (AG⁺); **EA** (C₄H₁₆N₁₆O₂, 320.28) calcd.: C 15.00, H 5.04, N 69.97%; found: C 15.53, H 4.86, N 69.77%; **Sensitivities**: IS: 40 J, FS: 360 N.

Bis(ammonium) 5-(1-oxidotetrazolyl)-tetrazolate (10)

5-(1*H*-Tetrazolyl)-1-hydroxytetrazole (770.2 mg, 5.0 mmol) was dissolved in water (10 mL) and 25% NH₃ (0.8 mL) was added. 30 mL of ethanol were added and the white precipitate was filtered off to give a colorless powder of bis(ammonium) 5-(1-oxidotetrazolyl)-tetrazolate. Single crystals could not be obtained, using solvents as water, ethanol, DMF, THF, ACN, ethyl acetate and diethyl ether. Yield: 0.81 g (4.31 mmol, 86%).

DSC (5 °C min⁻¹): 250 °C (dec.); **IR** (ATR, cm⁻¹): $\tilde{\nu}$ = 3179(m), 3041(s), 3027(s), 2876(s), 2132(w), 1870(w), 1735(w), 1689(m), 1595(w), 1444(vs), 1422(vs), 1374(s), 1329(m), 1240(vs), 1222(s), 1180(s), 1147(m), 1139(m), 1111(w), 1043(w), 1034(m), 1002(s), 761(m), 761(m), 732(w), 719 (m); **Raman** (1064 nm, 300 mW, 25 °C, cm⁻¹): $\tilde{\nu}$ = 3039(4), 2820(2), 2702(2), 1596(100), 1525(2), 1330(3), 1241(10), 1223(8), 1142(10), 1113(9), 1073(7), 1045(7), 1035(10), 763(8), 588(2), 418(6), 356(5), 191(8), 84(46); **¹H NMR** ([D₆]DMSO): δ = 7.47 ppm (s, br, NH₄⁺); **¹³C NMR** ([D₆]DMSO): δ = 150.4 (s, CN₄), 138.4 ppm (s, CN₄O); **MS** m/z (FAB⁻): 153.1 (C₂HN₈O⁻); m/z : (FAB⁺) 18.0 (NH₄⁺); **EA** (C₂H₈N₁₀O, 188.15) calcd.: C 12.77, H 4.29, N 74.44%; found: C 13.40, H 4.30, N 73.92%; **Sensitivities**: IS: 40 J, FS: 360 N.

Diaminouronium 5-(1-oxidotetrazolyl)-tetrazolate monohydrate (11)

5-(1*H*-Tetrazolyl)-1-hydroxytetrazole (462.0 mg, 3.0 mmol) was dissolved in 10 mL of water and added to a solution of diaminourea (540 mg, 6.0 mmol). The solvent was left for crystallization and the product was recrystallized in water to give colorless crystals. Yield: 0.72 g (2.75 mmol, 92%).

DSC (5 °C min⁻¹): 210 °C (dec.); **IR** (ATR, cm⁻¹): $\tilde{\nu}$ = 3348(m), 3088(s), 2995(s), 2877(s), 2662(s), 2493(s), 2241(m), 2181(m), 2041(m), 1725(s), 1628(s), 1607(s), 1590(s), 1570(vs), 1520(vs), 1450(vs), 1439(vs), 1377(m), 1335(m), 1305(s), 1239(vs), 1222(vs), 1214(vs), 1214(vs), 1180(vs), 1129(s), 1044(m), 1032(s), 1002(s), 799(m), 749(s), 720(s); **Raman** (1064 nm, 300 mW, 25 °C, cm⁻¹): $\tilde{\nu}$ = 1727(5), 1598(100), 1526(5), 1338(4), 1240(13), 1224(10), 1183(9), 1130(15), 1116(15), 1076(7), 1046(10), 1034(4), 982(7), 764(5), 752(4), 594(3), 512(4), 425(8), 336(5), 256(3), 208(6); **¹H NMR** ([D₆]DMSO): δ = 7.12 ppm (s, br, 7H, H₃N⁺-NH-CO-NH-NH₃⁺); **¹³C NMR** ([D₆]DMSO): δ = 159.9 (C=O), 147.0 (s, CN₄), 137.1 ppm (s, CN₄O); **MS** m/z (FAB⁻): 153.1 (C₂HN₈O⁻); **EA** (C₂H₈N₁₀O, 262.19) calcd.: C 13.74, H 3.84, N 64.11%; found: C 14.25, H 3.85, N 63.76%; **Sensitivities**: IS: 15 J, FS: 360 N.

3.6.2 X-ray diffraction

5-Chlorohydroximoyl-tetrazole (**3**), depicted in Figure S1, crystallizes from isopropanol with inclusion of one solvent molecule isopropanol in the monoclinic space group *P*2₁/*n* with a density of 1.449 g cm⁻³. The molecular unit of **3** (Figure S1) reveals a high level of planarity of the tetrazole ring, indicated by a torsion angle N1-N2-N3-N4 of 0.2(2)°, whereas the almost planar chloroxime group with an angle of 0.35(22)° (Cl-C2-N5-O1) is tilted against

the tetrazole ring plane by $4.0(3)^\circ$ (N1–C1–C2–N5). With a bond length of 172.7(8) pm the chlorine carbon distance is only slightly shorter than the expected Cl–C bond length of 177 pm.

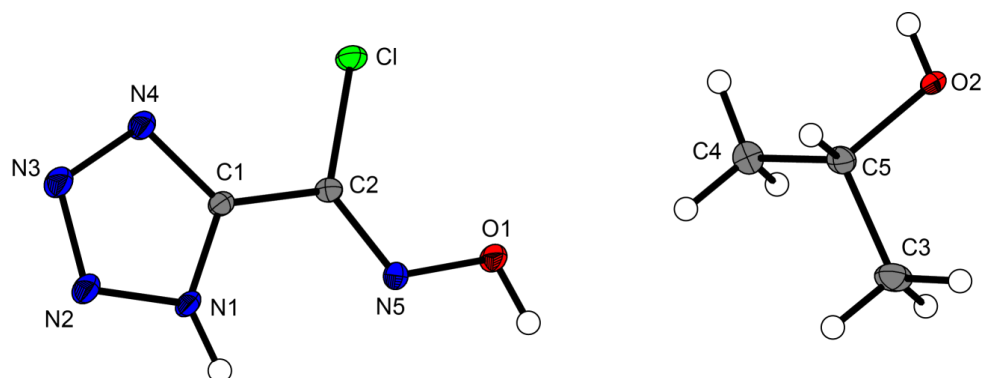


Figure S1. Representation of the molecular unit of **3**, showing the atom-labeling scheme. Thermal ellipsoids represent the 50% probability level and hydrogen atoms are shown as small spheres of arbitrary radius.

As mentioned in the main part, **5** forms a zwitterionic arrangement of the oxidized tetrazole ring. This could be also a solid state effect due to the hydrogen bond network. Figure S2 illustrates the coordination geometry of compound **5**.

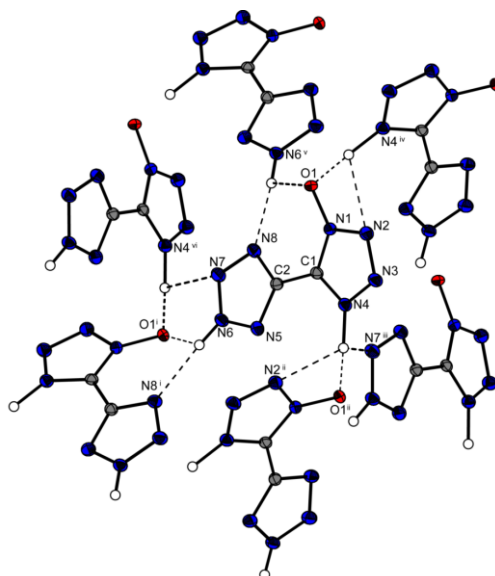


Figure S2. Selected view on the hydrogen bond network of **5**. Thermal ellipsoids represent the 50% probability level and hydrogen atoms are shown as small spheres of arbitrary radius. Symmetry codes: (i) $-x, 0.5+y, 0.5-z$; (ii) $0.5-x, 0.5+y, z$; (iii) $-0.5+x, y, 0.5-z$; (iv) $-0.5+x, -0.5+y, z$; (v) $1-x, -0.5+y, 0.5+z$; (vi) $0.5+x, y, 0.5-z$.

Bis(guanidinium) 5-(1-oxidotetrazolyl)-tetrazolate monohydrate (**8**) crystallizes from water with one solvent moiety in the monoclinic space group $P2_1/n$ with a density of 1.592 g cm^{-3} . Four molecules are found per unit cell. The two aromatic ring systems are slightly tilted

against each other with a torsion angle N1–C1–C2–N8 = 6.8(2)°. The molecular unit of **8** is shown in Figure S3.

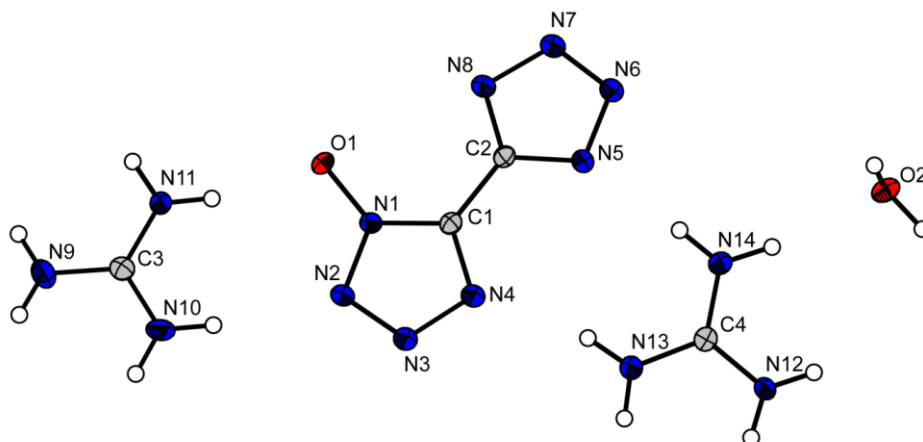


Figure S3. Molecular unit of bis(guanidinium) 5-(1-oxidotetrazolyl)-tetrazolate monohydrate (**8**), showing the atom-labeling scheme. Thermal ellipsoids represent the 50% probability level and hydrogen atoms are shown as small spheres of arbitrary radius.

Bis(aminoguanidinium) 5-(1-oxidotetrazolyl)-tetrazolate monohydrate (**9**) crystallizes from water with one solvent moiety in the triclinic space group $P\bar{1}$ with a density of 1.553 g cm⁻³. Four molecules are found per unit cell. The two aromatic ring systems are slightly tilted against each other with a torsion angle N1–C1–C2–N8 = 5.0(2)°. The molecular unit of **9** is shown in Figure S4.

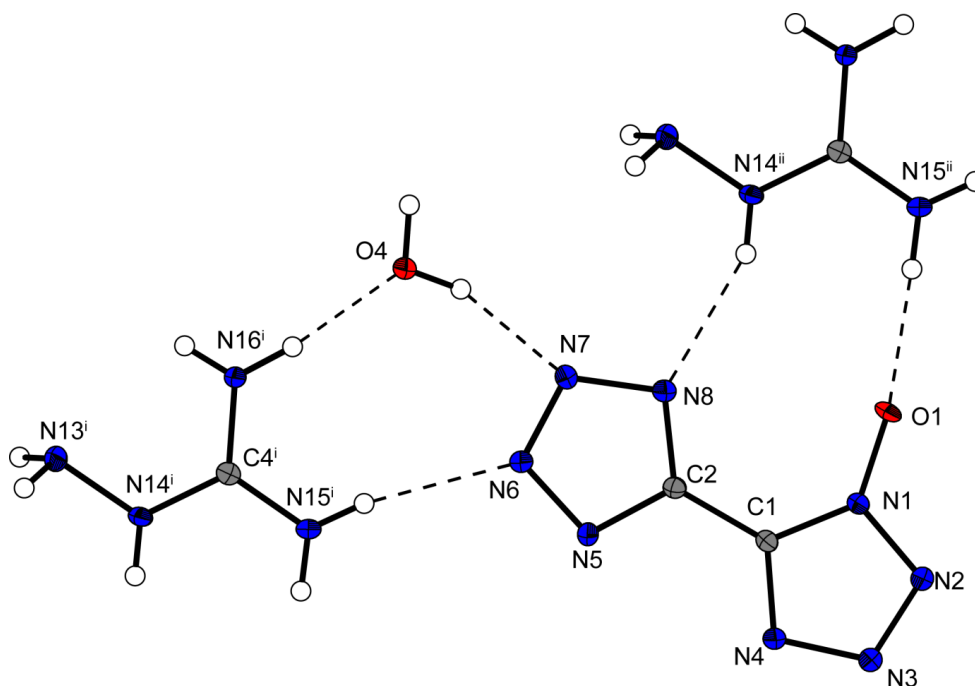


Figure S4. Molecular unit of bis(aminoguanidinium) 5-(1-oxidotetrazolyl)-tetrazolate monohydrate (**9**), showing the atom-labeling scheme. Thermal ellipsoids represent the 50% probability level and hydrogen atoms are shown as small spheres of arbitrary radius.

Diaminouronium 5-(1-oxidotetrazolyl)-tetrazolate monohydrate (**11**) crystallizes from water with one solvent moiety in the monoclinic space group *Cc* with a density of 1.802 g cm⁻³. Four molecules are found per unit cell. The two aromatic ring systems are tilted against each other with a torsion angle N1–C1–C2–N8 = 11.0(4)°. The molecular unit of **11** is shown in Figure S5.

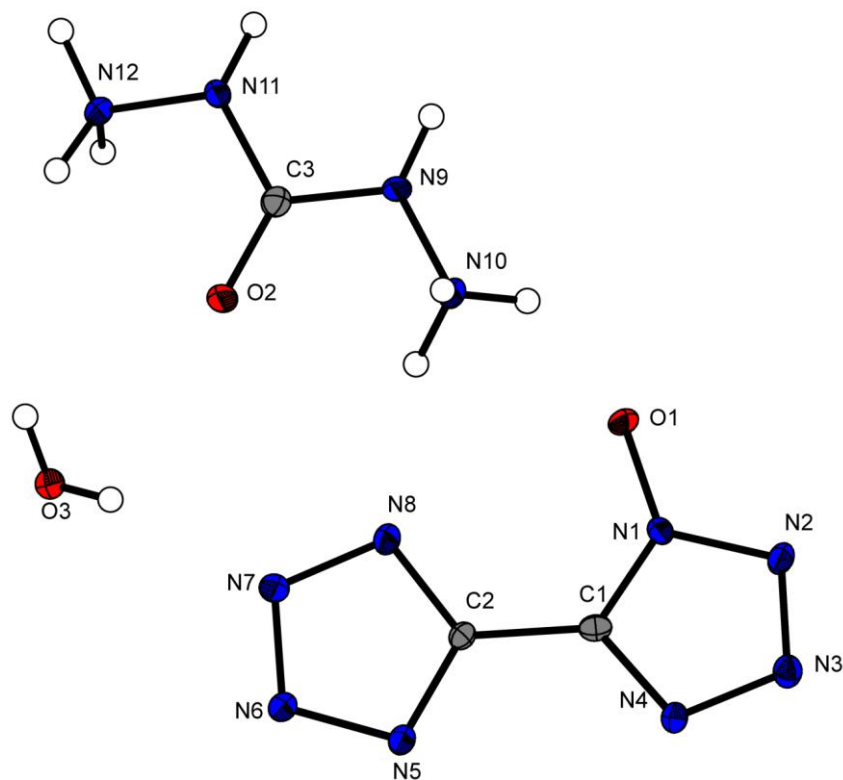


Figure S5. Molecular unit of diaminouronium 5-(1-oxidotetrazolyl)-tetrazolate monohydrate (**11**), showing the atom-labeling scheme. Thermal ellipsoids represent the 50% probability level and hydrogen atoms are shown as small spheres of arbitrary radius.

Table S1. X-ray data and parameters of **3–6**.

	3 · iPrOH	4	5	5 · H₂O	6
Formula	C ₅ H ₁₀ Cl N ₅ O ₂	C ₂ H ₄ N ₈ O ₂	C ₂ H ₂ N ₈ O	C ₂ H ₄ N ₈ O ₂	C ₂ H ₈ N ₁₀ O ₃
FW [g/mol]	207.63	172.13	376.30	172.13	220.18
Crystal system	monoclinic	orthorhombic	orthorhombic	monoclinic	triclinic
Space Group	<i>P</i> 2 ₁ / <i>n</i> (No. 14)	<i>P</i> 2 ₁ 2 ₁ 2 ₁ (No. 19)	<i>Pbca</i> (No. 19)	<i>P</i> 2 ₁ / <i>n</i> (No. 14)	<i>P</i> −1 (No. 2)
Color / Habit	colorless block	colorless block	colorless block	colorless plate	colorless needle
Size [mm]	0.05 × 0.30 × 0.40	0.10 × 0.20 × 0.30	0.19 × 0.23 × 0.48	0.09 × 0.31 × 0.32	0.05 × 0.05 × 0.40
<i>a</i> [pm]	770.18(7)	466.09(3)	934.33(5)	1438.51(8)	360.63(3)
<i>b</i> [pm]	680.12(5)	482.97(3)	960.67(5)	648.42(4)	801.89(7)
<i>c</i> [pm]	1821.32(19)	2909.70(18)	1257.32(6)	1448.69(7)	1479.80(13)
α [°]	90	90	90	90	105.053(8)
β [°]	93.910(9)	90	90	105.557(5)	91.716(7)
γ [°]	90	90	90	90	96.035(7)
<i>V</i> [nm ³]	0.95181(15)	0.65500 (7)	1.12855(10)	1.30177(13)	0.41023(6)
<i>Z</i>	4	4	8	8	2
$\rho_{\text{calc.}}$ [g cm ^{−3}]	1.449	1.746	1.814	1.757	1.783
μ [mm ^{−1}]	0.380	0.151	0.151	0.152	0.157
<i>F</i> (000)	432	352	624	704	228
$\lambda_{\text{MoK}\alpha}$ [pm]	71.073	71.073	71.073	71.073	71.073
<i>T</i> [K]	100	100	100	123	100
ϑ min-max [°]	4.1, 26.0	4.2, 27.0	4.2, 26.5	4.2, 26.0	4.3, 26.5
Dataset <i>h</i> ; <i>k</i> ; <i>l</i>	−9:9; −8:7; −20:22	−4:5; −6:6; −37:37	−11:11; −12:11; −15:15	−17:17; −7:7; −17:16	−4:4; −10:10; −18:18
Reflect. coll.	4682	5437	8311	9543	4211
Independ. refl.	1867	889	1161	2537	1697
<i>R</i> _{int}	0.036	0.027	0.034	0.028	0.043
Reflection obs.	1867	889	1161	2537	1697
No. parameters	158	125	108	249	168
<i>R</i> ₁ (obs)	0.0339	0.0265	0.0296	0.0306	0.0406
<i>wR</i> ₂ (all data)	0.0833	0.0617	0.0739	0.0807	0.1091
<i>S</i>	1.02	1.13	1.09	1.03	1.06
Resd.	−0.025, 0.027	−0.017, 0.023	−0.026, 0.025	−0.021, 0.028	−0.030, 0.026
Dens.[e nm ^{−3}]					
Device type	Oxford Xcalibur3 CCD	Oxford Xcalibur3 CCD	Oxford Xcalibur3 CCD	Oxford Xcalibur3 CCD	Oxford Xcalibur3 CCD
Solution	SIR-92	SIR-92	SIR-92	SIR-92	SIR-92
Refinement	SHELXL-97	SHELXL-97	SHELXL-97	SHELXL-97	SHELXL-97
Absorpt. corr.	multi-scan	multi-scan	multi-scan	multi-scan	multi-scan
CCDC	966800	966799	966802	966801	966804

Table S2. X-ray data and parameters of **7–9** and **11**.

	7	8	9	11
Formula	C ₂ H ₁₀ N ₁₂ O ₁	C ₄ H ₁₄ N ₁₄ O ₂	C ₄ H ₁₄ N ₁₆ O	C ₃ H ₁₀ N ₁₂ O ₃
FW [g/mol]	218.22	290.25	302.33	262.19
Crystal system	triclinic	monoclinic	triclinic	monoclinic
Space Group	<i>P</i> –1 (No. 2)	<i>P</i> 2 ₁ / <i>n</i> (No. 14)	<i>P</i> –1 (No. 2)	<i>Cc</i> (No. 9)
Color / Habit	colorless block	colorless block	yellow plate	colorless plate
Size [mm]	0.40 × 0.20 × 0.20	0.20 × 0.25 × 0.45	0.40 × 0.40 × 0.12	0.17 × 0.16 × 0.02
<i>a</i> [pm]	365.49(4)	682.07(3)	941.60(4)	761.64(4)
<i>b</i> [pm]	843.61(7)	1792.40(6)	1185.42(5)	1977.84(9)
<i>c</i> [pm]	1433.78(13)	1010.16(4)	1332.38(6)	645.70(3)
α [°]	103.552(7)	90	104.622(4)	90
β [°]	96.583(8)	101.198(4)	90.626(4)	96.531(5)
γ [°]	93.298(7)	90	107.029(4)	90
<i>V</i> [nm ³]	0.42530(7)	1.21145(8)	1.37013(10)	0.96637(8)
<i>Z</i>	2	4	4	4
$\rho_{\text{calc.}}$ [g cm ^{–3}]	1.704	1.592	1.553	1.802
μ [mm ^{–1}]	0.140	0.130	0.127	0.155
<i>F</i> (000)	228	608	672	544
$\lambda_{\text{MoK}\alpha}$ [pm]	71.073	71.073	71.073	71.073
<i>T</i> [K]	100	100	100	100
ϑ min-max [°]	4.3, 26.5	4.3, 26.0	4.2, 26.0	4.1, 28.0
Dataset <i>h</i> ; <i>k</i> ; <i>l</i>	–4:4; –10:10; –17:17	–8:8; –22:21; –12:11	–11:11; –14:14; –16:16	–10:8; –26:25; –8:8
Reflect. coll.	4504	9416	13756	2909
Independ. refl.	1764	2372	5362	1164
<i>R</i> _{int}	0.029	0.036	0.045	0.038
Reflection obs.	1764	2372	5362	1164
No. parameters	176	237	525	203
<i>R</i> ₁ (obs)	0.0358	0.0297	0.0341	0.031
<i>wR</i> ₂ (all data)	0.0889	0.0783	0.0959	0.0655
<i>S</i>	1.04	1.05	1.04	1.04
Resd. Dens. [e nm ^{–3}]	–0.023, 0.027	–0.020, 0.021	–0.026, 0.023	–0.020, 0.019
Device type	Oxford Xcalibur3 CCD	Oxford Xcalibur3 CCD	Oxford Xcalibur3 CCD	Oxford Xcalibur3 CCD
Solution	SIR-92	SIR-92	SIR-92	SIR-92
Refinement	SHELXL-97	SHELXL-97	SHELXL-97	SHELXL-97
Absorpt. corr.	multi-scan	multi-scan	multi-scan	multi-scan
CCDC	966971	966803	966805	966806

3.6.3 Spectroscopy

NMR Spectroscopy

All compounds **1–7** were investigated using proton and carbon NMR spectroscopy. For **5** and its hydroxylammonium salt **6**, also a ¹⁵N NMR spectrum was recorded. Chemical shifts are given with respect to TMS (¹H, ¹³C) and MeNO₂ (¹⁵N) in *d*6-DMSO as the solvent.

The analysis of compound **1** and **2** was identical to that previously reported in the literature.^[1] 5-Chlorohydroximoyl-tetrazole **3** reveals a sharp signal at 13.39 ppm and a broad signal at 7.78 ppm, contributing to the acidic oximic proton and the proton of the tetrazole ring. In the ¹³C NMR spectrum two signals are found and can be assigned to the carbon atom of the tetrazole ring (152.4 ppm) and to the chloroxime group (124.9 ppm).

In the ^1H NMR spectrum of compound **4**, a sharp signal at 12.54 ppm and a broader signal at 6.39 ppm are observed, contributing to the acidic oximic proton and to the proton of the tetrazole ring. Regarding the ^{13}C NMR spectrum, two chemical shifts are found, whereby the one at 150.0 ppm can be assigned to the carbon atom of the tetrazole ring and the other signal at a higher field of 133.3 ppm refers to the azidoxime group.

In the proton NMR spectra of compound **5** only a broad signal at 7.87 ppm can be observed due to fast proton exchanges, whereas compound **6** and **7** show a broad signal at 9.38 ppm and 6.66 ppm, respectively, which can be assigned to the hydroxylammonium group and the hydrazinium group. The ^{13}C NMR spectra reveals two singlets at 146.2 ppm (CN_4H) and 138.1 ppm (CN_4OH) for compound **5**, two singlets which are slightly shifted to 149.3 ppm (CN_4^-) and 138.2 ppm (CN_4O^-) for compound **6** and two singlets at 150.5 ppm (CN_4^-) and 138.2 ppm (CN_4O^-) for compound **7**. The assignment is reconfirmed by comparison to similar literature known structures as bistetrazole salts^[2] and TKX-50^[3].

Only for the free acid **5** and the hydroxylammonium salt **6** it was worthwhile running a ^{15}N NMR spectrum (Figure S6). Compound **5** reveals six signals, from which the two signals at -53.7 (N5/8) and at -2.7 ppm (N6/7) are slightly shifted compared to shifts of bistetrazole salts (-66 ppm) (3 ppm).^[4] The peaks at from the tetrazole-*N*-oxide at -115.8 (N1), -86.4 ppm (N4), -19.8 (N2) and -17.6 (N3) match the pattern from the signals of cyanotetrazolate-1-oxide, which we published earlier.^[5] The bis(hydroxylammonium) 5-(1-oxidotetrazolyl)-tetrazolate **6** reveals a set of seven chemical shifts. The resonance at -297.3 (N9) refers to the hydroxylammonium cation. The three signals at 5.2 ppm (N6/7), -13.5 (N3) and -17.7 ppm (N2) are shifted only slightly compared to the free acid **5**. In contrast to that, the resonances at -90.1 (N1), -72.5 ppm (N4) and -64.3 ppm (N5/8) are shifted more than 10 ppm compared to the free acid. Nevertheless all signals can be assigned by comparing to the chemical shifts of cyanotetrazolate-1-oxide^[5] and bistetrazole salts.^[2]

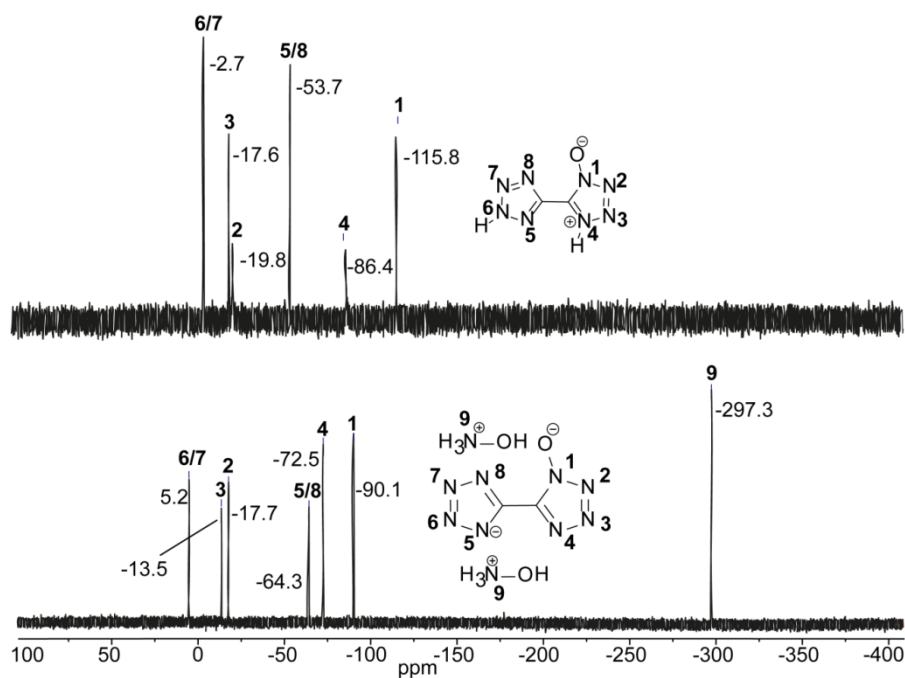


Figure S6. ^{15}N NMR spectrum of 5-(1*H*-tetrazolyl)-1-hydroxytetrazole **5** and bis(hydroxyl-ammonium) 5-(1-oxidotetrazolyl)-tetrazolate (**6**).

Vibrational Spectroscopy

IR and Raman spectra of compounds **4–7** were measured and the absorptions were assigned according to commonly observed values found in literature.^[6]

Regarding the IR and Raman spectra of compounds **4–7**, all of them reveal tetrazole framework vibrations at $1293\text{--}964\text{ cm}^{-1}$ and asymmetric as well as symmetric stretching vibrations of the N1--C1--N4 fragment,^[7] being observed in the range from $1385\text{--}1316\text{ cm}^{-1}$. The stretching vibration of the cyclic C=N bond collide with the C=N stretching vibration of the oxime subunit, in case of compound **4**, which occurs in a range from $1688\text{--}1521\text{ cm}^{-1}$. Moreover, these vibrations are dominant in the Raman spectrum and only weakly represented in the IR spectrum.

In the IR spectrum of compound **4**, additional absorption bands are observed in a range from $2178\text{--}2116\text{ cm}^{-1}$, which contribute to vibrations of the azide subunit. Apart from that, the IR and Raman spectrum of the free acid **4** shows no significant differences. Only the absorption bands for the tetrazole frame work change, due to the changed electronic structure in the tetrazolate unit. Furthermore, valence vibrations of the O--H bond, and also N--H valence vibrations in case of **4**, occur in a range from $3546\text{--}2852\text{ cm}^{-1}$.

Regarding the IR and Raman spectra of the acid **5**, as well as those of its nitrogen-rich salts **6**–**7**, besides the tetrazole framework vibrations also the tetrazole-1-oxide groups show vibrations of the aromatic ring system at $1550\text{--}1350\text{ cm}^{-1}$ and $1350\text{--}700\text{ cm}^{-1}$ [$\nu(\text{NN})$, $\nu(\text{NCN})$, $\gamma(\text{CN})$, δ aromatic tetrazole-oxide ring], which complicates a clear assignment without any quantum chemical calculations. For the two nitrogen-rich salts, asymmetric and symmetric valence vibrations are observed, being specific for the respective cation. Valence vibrations of the ammonium group of the hydroxylammonium cation in compound **6** and of the hydrazinium cation in compound **7** can be observed in a range of $3496\text{--}2660\text{ cm}^{-1}$ [$\nu_{\text{asym}}(\text{NH}_2/\text{NH}_3^+)$] and also deformational vibrations in a range of $1617\text{--}1524\text{ cm}^{-1}$ [$\delta_{\text{sym}}(\text{NH}_2/\text{NH}_3^+)$, $\delta_{\text{asym}}(\text{NH}_2/\text{NH}_3^+)$]. O–H deformation vibrations can be observed in the IR spectrum of compound **6** in form of two additional sharp vibration bands at 1510 cm^{-1} and 1458 cm^{-1} .

Mass Spectrometry

For detection of the different ions via mass spectrometry, either the DEI or the FAB technique was used. The spectra were recorded using 3-nitrobenzyl alcohol as liquid matrix. In the DEI⁺ mode the molecule peak of compound **4** (m/z 154.0) is observed. In the DEI⁺ spectra the protonated molecule [$\text{M}+\text{H}^+$] of compound **5** (m/z 155.1) could be detected. In the FAB[−] spectra of compound **6** and **7** the bistetrazole-1-olate anion (m/z 153.1) could be detected. In the FAB⁺ spectra of compound **6** and **7** the corresponding cation NH_3O^+ (m/z 33.1) and N_2H_5^+ (m/z 33.1) appears.

3.6.4 Explosive performance: Heat of formation calculations

General information about the heat of formation calculations can be found in the appendix of this thesis. The calculation results are summarized in Table S3.

Table S3. Calculation results.

M	$-H^{298}$ [a] / a.u.	$\Delta_f H^\circ(\text{g}, \text{M})$ / kJ mol^{-1} [b]	V_M / nm^3 [c]	$\Delta U_L, \Delta H_L$ (6,7); ΔH_{sub} [e] (5) / kJ mol^{-1} [d]	$\Delta_f H^\circ(\text{s})$ [f] / kJ mol^{-1}	Δn [g]	$\Delta_f U(\text{s})$ [f] / kJ kg^{-1}
5	589.716739	723.7		87.1	636.6	5.5	4219.9
5 dianion	588.599429	592.1					
NH_4O^+	131.863249	687.2					
N_2H_5^+	112.030523	774.1					
6		1966.6	0.211	1497.5	469.0	10.5	2248.2
7		2140.3	0.219	1477.8	662.6	11.5	3167.4

[a] CBS-4M electronic enthalpy; [b] gas phase enthalpy of formation; [c] molecular volumes taken from X-ray structures and corrected to room temperature; [d] lattice energy and enthalpy (calculated using Jenkins and Glasser equations); [e] enthalpy of sublimation (calculated by Trouton rule); [f] standard solid state enthalpy of formation; [g] solid state energy of formation.

3.6.5 Toxicity assessment

Liquid-dried luminescent bacteria of the strain *Vibrio fischeri* NRRL-B-11177 obtained from HACH LANGE GmbH (Düsseldorf, Germany) were used for the luminescent bacteria inhibition test. The measurements were performed on a *LUMIStox 300* obtained by HACH LANGE GmbH (Düsseldorf, Germany) and were carried out as described by the provider at 15 °C. Each sample was tested after 15 min and 30 min.

The sample dilution sequence corresponds to DIN 38412 L34, which ranges from 1:2 to 1:32 dilution of the compound in the test system. For better reproducibility, all dilution steps were made in duplicate. The change of intensity of bacterial luminescence in the absence (controls) and in the presence (samples) of the tested substances after different incubation times (15 min, 30 min) were recorded. The controls (2% NaCl only) were measured for calculating the correction factor, which is necessary to consider the normal decrease of luminescence without any toxic effect per time.

The EC₅₀ value can be determined by plotting log Γ against log c , where Γ = inhibition (in %) / 100 – inhibition (in %) and c = concentration of the test sample. The EC₅₀ value is identical with the intersection of the resulting graph with the X-axis ($\Gamma = 0$). For better comparison of the resulting toxicities we also determined the toxic effect of RDX and TKX-50 to the bacterial strain under the same conditions applied for the toxicity assessment of the dihydroxylammonium salt **6**.

To imitate the natural environment of the employed marine bacterium as good as possible, the samples need to be diluted with a 2% (w/v) sodium chloride solution. Since RDX is barely soluble in water, a stock solution in acetone was prepared, which was further diluted with the sodium chloride solution to a mixture containing 200 ppm RDX in water/acetone 99/1 (v/v).

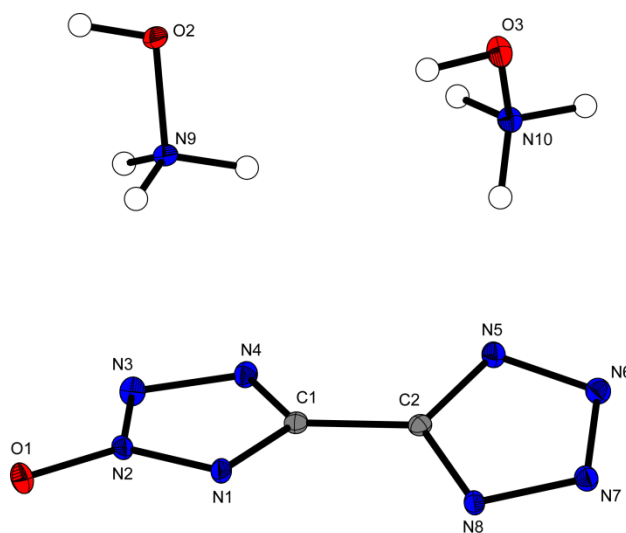
The poor water solubility of 5,5'-bistetrazole-1,1'-diolates also sets problems during the toxicity tests of TKX-50. Here, an aqueous solution containing 1467 ppm TKX-50 was prepared and sodium chloride was added to adjust the final sodium chloride concentration of the stock solution to 2 % (w/v). Since disodium 5,5'-bistetrazole-1,1'-diolate shows nearly as poor water solubility as TKX-50, no higher concentration of the investigated compound could be used without precipitating disodium 5,5'-bistetrazole-1,1'-diolate tetrahydrate from the stock solution.

3.6.6 References

- [1] N. Fischer, T. M. Klapötke, S. Rappenglück, J. Stierstorfer, The Reactivity of 5-Cyanotetrazole towards Water and Hydroxylamine, *ChemPlusChem* **2012**, 77, 877–888.
- [2] N. Fischer, T. M. Klapötke, K. Peters, M. Rusan, J. Stierstorfer, Alkaline Earth Metal Salts of 5,5'-Bistetrazole – from Academical Interest to Practical Application, *Z. Anorg. Allg. Chem.* **2011**, 637, 1693–1701.
- [3] N. Fischer, D. Fischer, T. M. Klapötke, D. G. Piercey, J. Stierstorfer, Pushing the limits of energetic materials – the synthesis and characterization of dihydroxylammonium 5,5'-bistetrazole-1,1'-diolate *J. Mater. Chem.* **2012**, 22, 20418–20422.
- [4] N. Fischer, D. Izsák, T. M. Klapötke, S. Rappenglück, J. Stierstorfer, Nitrogen-Rich 5,5'-Bistetrazolates and their Potential Use in Propellant Systems: A Comprehensive Study, *Chem. Eur. J.* **2012**, 18, 4051–4062.
- [5] F. Boneberg, A. Kirchner, T. M. Klapötke, D. G. Piercey, M. J. Poller, J. Stierstorfer, A Study of Cyanotetrazole Oxides and Derivatives thereof, *Chem. Asian J.* **2013**, 8, 148–159.
- [6] M. Hesse, H. Meier, B Zeeh, *Spektroskopische Methoden in der Organischen Chemie*, 7th ed., Thieme, Stuttgart, New York **2005**.
- [7] T. M. Klapötke, P. Mayer, C. Miro Sabate, J. M. Welch, N. Wiegand, Simple, Nitrogen-Rich, Energetic Salts of 5-Nitrotetrazole, *Inorg. Chem.* **2008**, 47, 6014–6027.

5-(1*H*-Tetrazolyl)-2-Hydroxy-Tetrazole: A Selective 2*N*-Monoxiditation of Bis(1*H*-Tetrazole)

published in *ChemPlusChem* **2015**, 80, 97–106. (DOI: 10.1002/cplu.201402124)

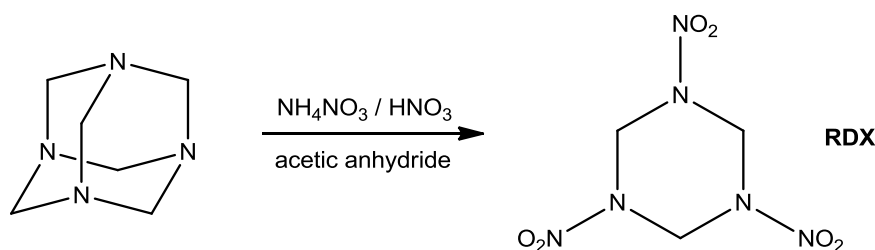


Abstract: Sodium 5-cyanotetrazolate sesquihydrate (**1**) is prepared from sodium azide and two equivalents of sodium cyanide under acidic conditions. Sodium 5-cyanotetrazolate sesquihydrate (**1**) is *N*-oxidized with Oxone to sodium 5-cyanotetrazolate monohydrate (**2**). Compound **2** is treated with sodium azide and a Lewis acid to form 5-(1*H*-tetrazolyl)-2-hydroxytetrazole monohydrate (**3**). Compound **3** can be deprotonated twice by various bases to give ionic derivatives such as bis(hydroxylammonium) (**4**), bis(hydrazinium) (**6**), bis(guanidinium) (**7**), bis(aminoguanidinium) (**8**), bis(ammonium) (**9**) and diaminouronium (**11**). In addition, compound **3** can only be deprotonated once as demonstrated by hydroxylammonium (**4**) and triaminoguanidinium (**10**) salts. Compounds **2–5** and **10–11** are structurally characterized by single-crystal X-ray diffraction. Additionally, compounds **2–11** were characterized by using NMR and vibrational (IR, Raman) spectroscopy as well as mass spectrometry and elemental analysis. Their thermal behavior was studied from differential thermal analysis measurements, and the sensitivities of the compounds towards shock, friction and electrostatic discharge were determined. In addition, the heats of formation are calculated (atomization method, CBS-4M enthalpies), and several detonation/propulsion parameters are computed with the EXPLO5 code.

Keywords: Energetic materials · Tetrazoles · *N*-Oxides · Heterocycles · X-ray diffraction

4.1 Introduction

Hexogen (RDX) was first synthesized by Georg F. Henning in 1898.^[1] Through the improved synthesis by Bachmann (Scheme 1),^[2] it found broad application in World War Two. Owing to the high detonation velocity of about 8750 m s^{-1} and its thermal stability of 210°C , RDX still is the most common secondary explosive today. It is used in many explosive applications such as Composition A, Composition C4 or Torpex.^[3]



Scheme 1. Synthesis of RDX after the Bachmann process^[2]

Since the discovery of RDX, the requirements for new energetic materials have altered. In addition to performance and stability, the environmental impact must now also be taken into account in the synthesis of novel secondary explosives. As a result, nitrogen-rich compounds have moved into the focus of research, as during decomposition, they mainly release non-toxic dinitrogen.^[4] Nitrogen-rich energetic materials possess highly positive heats of formation, which can be attributed to the large number of N–N bonds.^[5] In addition, a nitrogen-rich compound containing a strained ring system releases even more energy during decomposition. Tetrazoles with high heats of formation (e.g. *5H*-tetrazole: $\Delta_f H^\circ = 237.2 \text{ kJ mol}^{-1}$) seem superior to other heterocyclic aromatic ring systems such as 1,2,4-triazole ($109.0 \text{ kJ mol}^{-1}$) and imidazole (58.5 kJ mol^{-1}).^[6] Additionally, the high thermal stability of tetrazoles compared to other nitrogen-rich heterocycles makes them very promising energetic precursors. However, tetrazoles without proper substitution will hardly find application owing to their low density. Introduction of *N*-oxides improves the density and thus, the performance of tetrazoles.^[7]

Recently, the introduction of an *N*-oxide led to a very potent explosive: the bistetrazole-1,1'-di-*N*-oxide and its hydroxylammonium salt (TKX-50). TKX-50 ($V_{\text{Det}} = 9781 \text{ m s}^{-1}$) exceeds the energetic properties of RDX. The toxicity values of the decomposition products of TKX-50 are acceptable, and even its stability towards temperature and mechanical stimuli are slightly better than that of RDX.^[8] In addition to TKX-50, bistetrazole-2,2'-di-*N*-oxides and 5-(1*H*-tetrazolyl)-1-hydroxytetrazole have been synthesized in our group, as illustrated in Figure 1.^[9] Bistetrazole-*N*-oxides show good energetic properties, so it is worth taking a

closer look at the system. Interestingly, bistetrazole-2,2'-di-*N*-oxides (**C**) show slightly worse detonation parameters and sensitivities, than in their corresponding bistetrazole-1,1'-di-*N*-oxides (**B**). With the synthesis of 5-(1*H*-tetrazolyl)-2-hydroxytetrazole (**E**), which is missing in the literature, we will be able to investigate further the influence of the oxygen position in the bistetrazole-*N*-oxide system.

Herein, we report the synthesis and characterization of the first anionic bistetrazole 2*N*-monoxide 5-(1*H*-tetrazolyl)-2-hydroxytetrazole. Various energetic salts (e.g., hydroxylammonium, triaminoguanidinium, diaminouronium) of this compound, as well as sodium 5-cyanotetrazolate-2-oxide monohydrate, a precursor towards the target molecule, are synthesized and fully characterized.

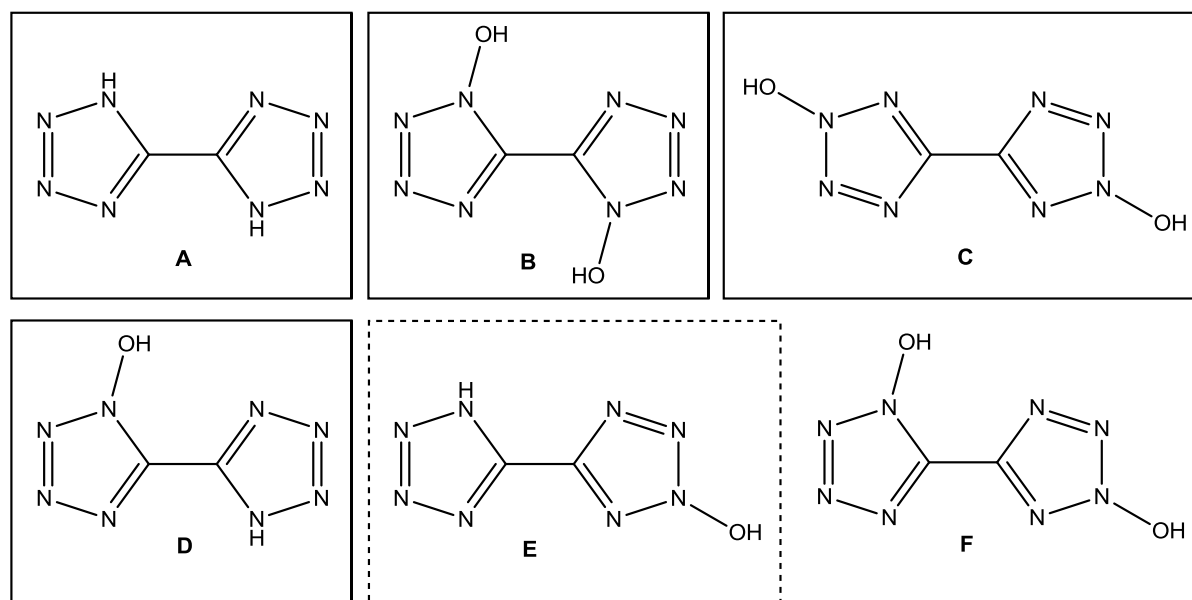


Figure 1. 5,5'-Bistetrazole and potential hydroxy-derivatives. A) 5,5'-Bistetrazole, B) Bis(1-hydroxytetrazole), C) Bis(2-hydroxytetrazole), D) 5-(1*H*-Tetrazolyl)-1-hydroxytetrazole, E) 5-(1*H*-Tetrazolyl)-2-hydroxytetrazole, F) 5-(2-Hydroxytetrazolyl)-1-hydroxytetrazole. Continuous box: known compounds. Dashed box: investigated in this work. No box: unknown yet.

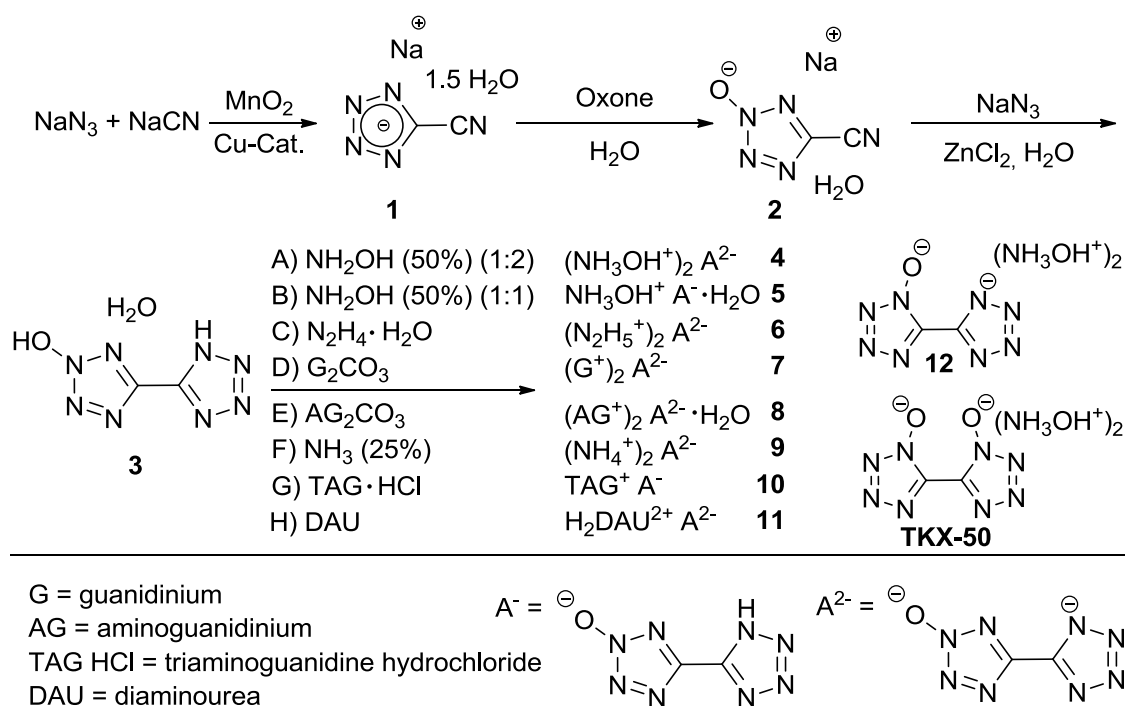
4.2 Results and Discussion

4.2.1 Synthesis

Scheme 2 illustrates the preparation of 5-(1*H*-tetrazolyl)-2-hydroxytetrazole monohydrate (**3**). In the first step, sodium 5-cyanotetrazolate sesquihydrate (**1**) is synthesized by the reaction of sodium azide with sodium cyanide in the presence of manganese dioxide and catalytic amounts of copper, as described in literature.^[10]

The *N*-oxidation of sodium 5-cyanotetrazolate sesquihydrate (**1**) was accomplished with saturated aqueous solution of Oxone. The oxidation proceeded at 40 °C in an aqueous potassium acetate buffer, and resulted in sodium 5-cyanotetrazolate-2-oxide monohydrate (**2**). The reaction was highly selective toward position 2 of the tetrazole-ring.^[7b] Compound **2** was treated with sodium azide and zinc chloride to form the second tetrazole ring through a “click-reaction”.^[11] Compound **3** is sensitive towards friction and impact, and thus, it should be handled with care (impact sensitivity: 4 J; friction sensitivity: 30 N; ESD: 50 mJ).

From **3**, salts were obtained as illustrated in Scheme 2, namely bis(hydroxylammonium) 5-(2-oxidotetrazolyl)-tetrazolate (**4**), bis(hydrazinium) 5-(2-oxidotetrazolyl)-tetrazolate monohydrate (**6**), bis(ammonium) 5-(2-oxidotetrazolyl)-tetrazolate (**9**), triaminoguanidinium 5-(2-oxidotetrazolyl)-tetrazolate (**10**) and diaminouronium 5-(2-oxidotetrazolyl)-tetrazolate (**11**). The diaminouronium salt **11** and the triaminoguanidinium salt **10** crystallize in a 1:1 stoichiometry despite a reactant stoichiometric ratio of 2:1. Hydroxylammonium 5-(2-oxidotetrazolyl)-tetrazolate monohydrate (**5**) was synthesized using a 1:1 stoichiometric ratio.



Scheme 2. Synthetic route towards compounds **1–11** as well as chemical structures of bis(hydroxylammonium)5-(1-oxidotetrazolyl)-tetrazolate (**12**) and TKX-50.

4.2.2 Crystal Structures

The crystal structures of compounds **2–5**, **10** and **11** were determined single crystal X-ray diffraction. Selected data and parameters of the X-ray measurements for these compounds are

given in Table S1 in the Supporting Information. The cif files were deposited with CCDC 999287(**2**), 999288 (**3**), 999291 (**4**), 999289 (**5**), 999292 (**10**), and 999290 (**11**).

Compound **2** crystallizes from ethanol in the monoclinic space group $P2_1/c$ with a density of 1.758 g cm^{-3} and four molecules per unit cell. The molecular moiety of compound **2** is shown in Figure 2.

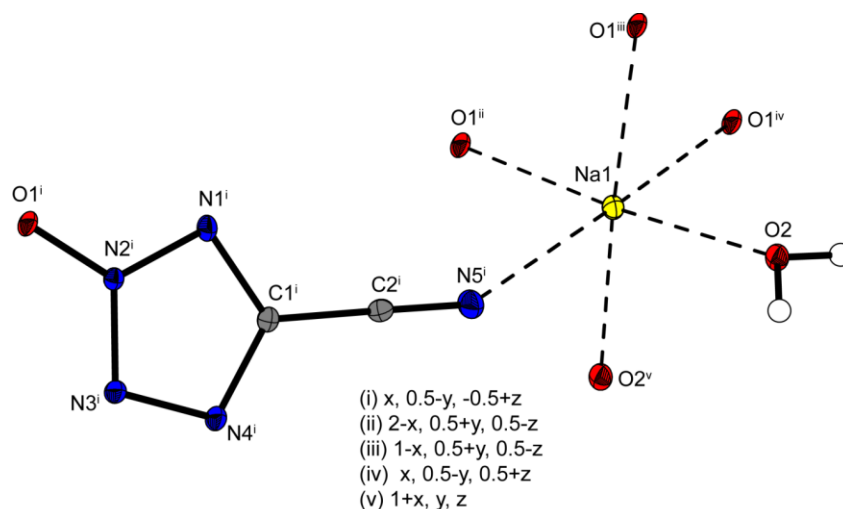


Figure 2. Molecular unit of **2**. Thermal ellipsoids of nonhydrogen atoms represent the 50% probability level. Hydrogen atoms are drawn as small spheres of arbitrary radius.

Compound **3** crystallizes from 2 M hydrochloric acid in the monoclinic space group $P2_1/c$ with a density of 1.844 g cm^{-3} and with four molecules per unit cell. With a torsion angle N1-C1-C2-N8 of $-0.7(3)^\circ$, the two tetrazole rings form an almost planar system. The molecular unit of **3** is illustrated in Figure 3.

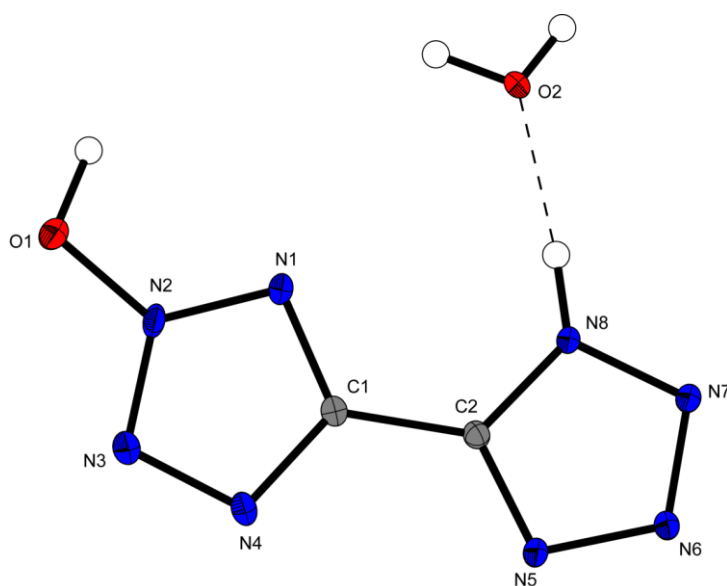


Figure 3. Molecular moiety of **3**. Thermal ellipsoids show the 50% probability level and hydrogen atoms are drawn as small spheres of arbitrary radius.

The salt **4** crystallizes anhydrously from methanol in the monoclinic space group $P2_1/n$ with four molecules per unit cell and a density of 1.746 g cm^{-3} . The two tetrazole rings are strongly tilted against each other and show a torsions angle N1-C1-C2-N8 of -21.6° which is in strong contrast to the corresponding 1*N*-monoxide where both tetrazole rings are perfectly planar.^[9b] The molecular unit of **4** is shown in Figure 4. For better comparison, the density of **4** and other bistetrazoles were recalculated to room temperature densities in this paragraph ($\rho_{298\text{K}} = \rho_{\text{T}} / (1 + \alpha_{\text{V}}(298 - T_0))$; $\alpha_{\text{V}} = 1.5 \cdot 10^{-4} \text{ K}^{-1}$). The room temperature density of compound **4** (1.696 g cm^{-3}) is lower compared to TKX-50 (1.877 g cm^{-3})^[8] and slightly lower compared to compound **12** (1.731 g cm^{-3}).^[9b] Unexpectedly, the density of bis(hydroxylammonium) 5,5'-bistetrazolate (1.742 g cm^{-3}) is slightly higher than compound **4**.^[12] This shows that the introduction of 2*N*-oxides does not necessarily lead to an improvement in density. Anyhow, as anticipated, the density of bis(hydroxylammonium) 5,5'-bis(tetrazole-2-oxide) (1.822 g cm^{-3}) is higher than the density of compound **4**.^[9a]

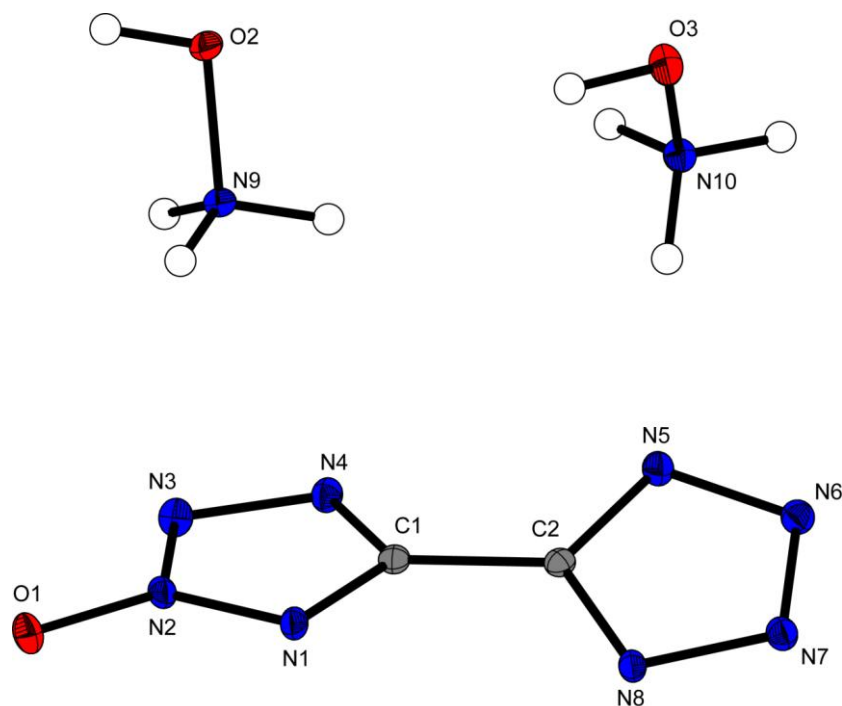


Figure 4. Molecular unit of **4** represents the atom-labeling scheme. Thermal ellipsoids illustrate the 50% probability level and hydrogen atoms are shown as small spheres of arbitrary radius.

Compound **5** crystallizes from water in the triclinic space group $P\bar{1}$ with the inclusion of one water moiety. The density of 1.764 g cm^{-3} is slightly higher than the density of **4**. The two tetrazole rings are tilted against each other with a torsion angle N4-C1-C2-N8 of $-7.1(6)^\circ$. The crystal structure (Figure 5) reveals that the proton of O1 is probably more acidic than the

N5 proton. The hydroxylammonium cation forms hydrogen bridges to the N8 and N4 nitrogen atoms.

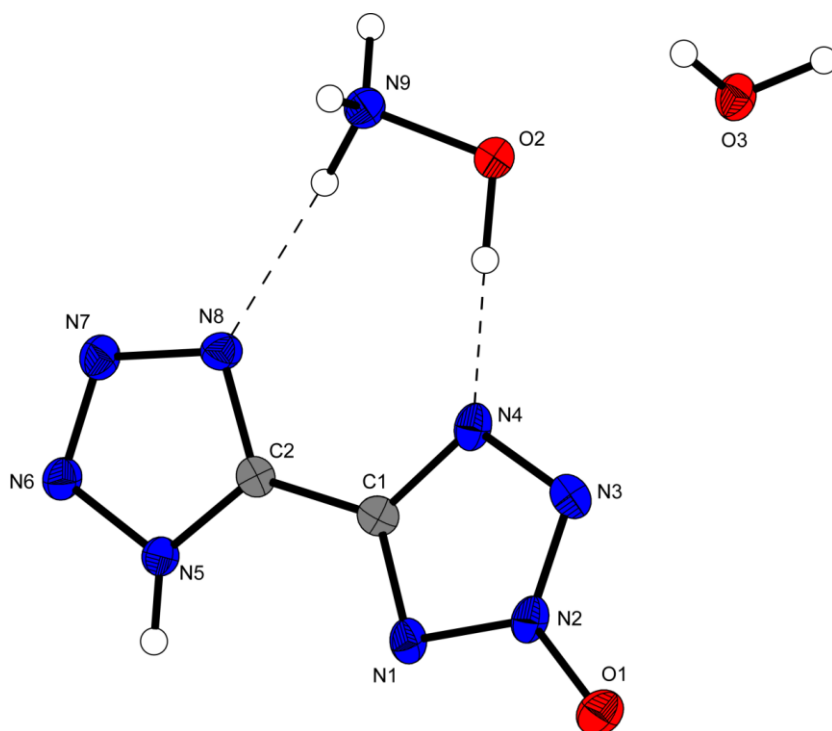


Figure 5. Representation of the molecular moiety of **5**, showing the atom-labeling scheme. Thermal ellipsoids represent the 50% probability level and hydrogen atoms are shown as small spheres of arbitrary radius.

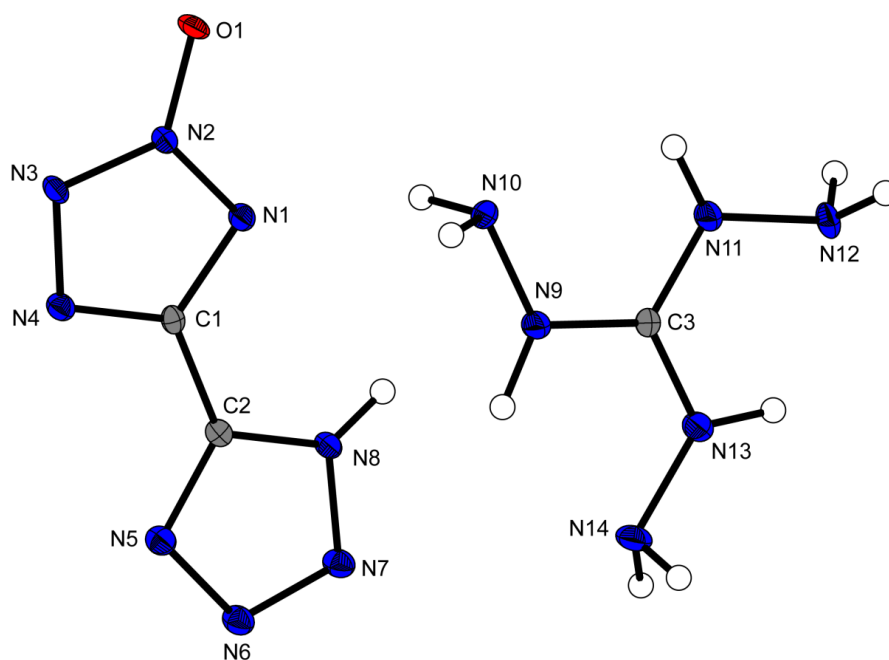


Figure 6. Molecular unit of **10**, showing the atom labeling scheme. Ellipsoids of non-hydrogen atoms are drawn at the 50% probability level and hydrogen atoms are shown as small spheres of arbitrary radius.

Despite a reactant stoichiometric ratio of 2:1 it was not possible to obtain a bis(triaminoguanidinium) salt of **3**. Compound **10** crystallizes anhydrously from water in the triclinic space group $P\bar{1}$. It has the lowest density (1.695 g cm^{-3}) of the present compounds investigated by XRD. The crystal structure confirms the O1 proton is more acidic than the proton at the tetrazole ring. The molecular unit of **10** is illustrated in Figure 6. Compound **11** crystallizes anhydrously from water in the monoclinic space group $P2_1/n$ with a density of 1.789 g cm^{-3} , which is the highest density in this article. Similar to compound **10**, we were not able to obtain a salt in a 2:1 ratio. Although diaminourea is able to deprotonate the bistetrazole system twice, salt **11** was received in a 1:1 ratio, as shown in Figure 7.

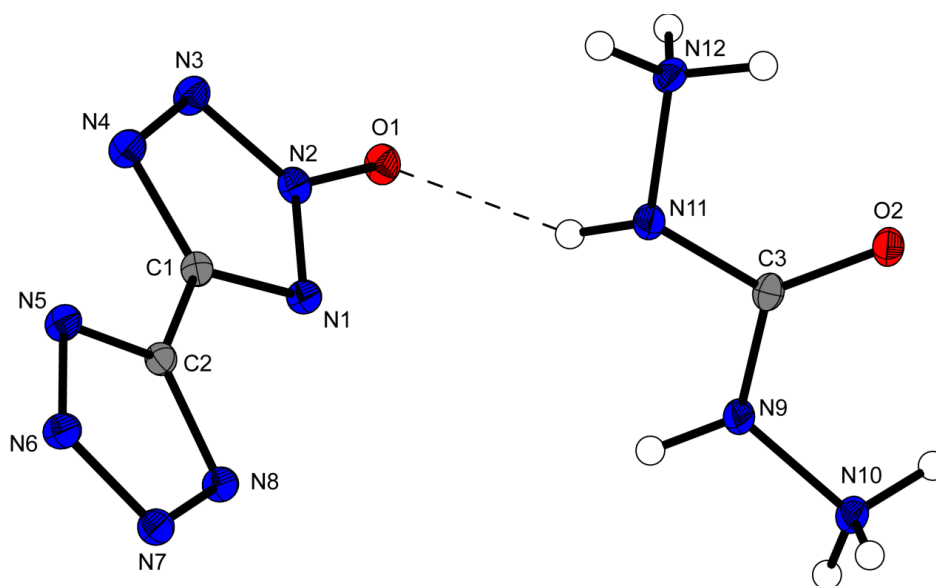


Figure 7. View on one molecular unit of **11** and its atom-labeling scheme. Ellipsoids are drawn at the 50% probability level and hydrogen atoms are shown as small spheres of arbitrary radius.

4.2.3 Thermal Analysis and Sensitivities

Compounds **2**, **3**, **5** and **8** dehydrate between 98°C (**2**) and 107°C (**5**). Compound **2** decomposes at 276°C . The acid **3** decomposes at 175°C . Virtually the same decomposition temperature could be measured for **5** (176°C). With a decomposition onset at 183°C , compound **4** has a higher decomposition temperature than bis(hydroxylammonium) 5,5'-bis(tetrazole-2-oxide) (172°C).^[9a] Nevertheless, RDX (210°C)^[13] and **12** (200°C)^[9b] possess slightly higher decomposition temperatures. The highest decomposition point was observed for the guanidinium salt **7** at 324°C , which exceeds the decomposition temperature of RDX and even is in the range of the high-temperature-stable hexanitrostilbene ($T_{\text{dec.}} = 316^\circ\text{C}$).^[14] Besides compound **7**, the ammonium salt **9** (onset: 255°C) and the hydrazinium salt **6** (onset:

249 °C) show remarkably high thermal stability. The decomposition onset temperatures of 201 °C (**10**), 214 °C (**11**) and 221 °C (**8**) are in the range of RDX.

The impact and friction sensitivities were explored by BAM methods. The CHNO-based energetic compounds **2–11** reveal strong differences in their impact and friction sensitivities.

The salts of **3** show a wide variation of sensitivities towards friction and impact. Surprisingly, the acid **3** is very sensitive to impact (4 J; anhydrous: 1 J) and friction (30 N; anhydrous: <5 N) and highly sensitive towards electrostatic discharge (50 mJ; anhydrous: 10 mJ), and is the most sensitive compound investigated in this work. The hydroxylammonium salt **4** shows low friction sensitivity (160 N), and can be considered as less sensitive towards impact (20 J). RDX shows lower sensitivities to impact (7.5 J) and friction (120 N).^[13] With regard to impact sensitivity, compound **4** (20 J, 160 N) is superior to **12** (12 J, 216 N), but is inferior in terms of the friction sensitivity.^[9b] Even though the hydroxylammonium 5-(2-oxidotetrazolyl)-tetrazolate monohydrate contains one crystal water, it shows the lowest friction sensitivity among the salts, with a value of 120 N. The triaminoguanidinium salt **10** and the diaminourea salt **11** are very sensitive to impact (3 J) and sensitive to friction (240 N). Compounds **6–9** are insensitive to impact (>40 J) and less sensitive to friction (360 N). The ESD test shows that all salts **4–11** are less sensitive toward electrostatic discharge (**4–6**, **10**: 700 mJ; **9**, **11**: 1000 mJ; **7**, **8** : 1500 mJ) than the free acid **3** (50 mJ).

4.2.4 Heat of formation

Older energetic materials such as TNT suffer their energy content by oxidation of their carbon backbone, and mostly have negative heats of formation. Our new materials, which are based on tetrazoles, show very large positive heats and energies of formation. This energy is released during detonation forming molecular dinitrogen. Often, nitrogen-rich materials tend to detonate (instead of ideal burning) in bomb calorimeter measurements. Therefore, heats of formation are usually computed theoretically. In this study, we used the atomization method [Eq. (1)] to calculate the room-temperature gas phase heat of formation ($\Delta_f H^\circ_{(g, M, 298)}$) in combination with CBS-4M calculated electronic enthalpies. Details of these calculations are given in the Supporting Information.^[15] All quantum chemical calculations are performed using the Gaussian G09 program package.^[16]

$$\Delta_f H^\circ_{(g, M, 298)} = H_{(Molecule, 298)} - \sum H^\circ_{(Atoms, 298)} + \sum \Delta_f H^\circ_{(Atoms, 298)} \quad (1)$$

For neutral **3**, the sublimation enthalpy (ΔH_{sub}), which is needed to convert the gas-phase enthalpy of formation [Eq. (2)] to the solid-state one, was calculated from Equation (3).^[17]

$$\Delta_f H^\circ_{(s)} = \Delta_f H^\circ_{(g)} - \Delta H_{sub} \quad (2)$$

$$\Delta H_{sub} (\text{kJ mol}^{-1}) = 188 \cdot T_m (\text{K}) \quad (3)$$

In the case of the ionic compounds, the lattice energy (U_L) and lattice enthalpy (ΔH_L) were calculated from the corresponding room temperature X-ray molecular volumes according to the equations provided by Jenkins and Glasser.^[18] The lattice enthalpy was used in order to convert the gas-phase enthalpy of formation into the molar solid state enthalpy of formation $\Delta_f H^\circ(s)$ as shown in Equation (4), in which Δn is the change of moles of gaseous components. With respect to the significance in energetic materials chemistry, the enthalpies were converted to mass related energies of formation.

$$\Delta_f U(s) = \Delta H_m - \Delta n RT \cdot 1000 \text{ kg} / M \quad (4)$$

The anhydrous acid **3** possesses a heat of formation of 575.4 kJ mol⁻¹. The corresponding 1*N*-oxide 5-(1*H*-tetrazolyl)-1-hydroxytetrazole shows a higher value for the heat of formation (636.6 kJ mol⁻¹).^[9b] 5,5'-Bis-(1-hydroxytetrazole) (689.1 kJ mol⁻¹)^[19] also reaches a higher value for the heat of formation. Thus, the *N*1-position for the *N*-oxide seems to increase the heat of formation. In contrast, the 5,5'-bis-(2-hydroxytetrazole) (559.7 kJ mol⁻¹) has a lower heat of formation than compound **3**,^[9a] which means that the 2*N*-monoxide has a higher heat of formation than the 2*N*-dioxide.

The heat of formation of the 1*N*-oxides **12** (469.0 kJ mol⁻¹)^[9b] and TKX-50 (458.7 kJ mol⁻¹)^[8] differ in about 10 kJ mol⁻¹. Comparison with the heat of formation of the 2*N*-oxides the bis(hydroxylammonium) salt **4** (443.6 kJ mol⁻¹) shows that **4** has a heat of formation almost 50 kJ mol⁻¹ higher than that of bis(hydroxylammonium) 5,5'-bis(tetrazole-2-oxide) (390.7 kJ mol⁻¹).^[9a]

The highest value for the heat of formation (809.1 kJ mol⁻¹) was obtained for the triaminoguanidinium salt **10**. The diaminourea salt **11** reveals the lowest heat of formation (240.7 kJ mol⁻¹).

4.2.5 Physiochemical and energetic properties

Table 1 details the theoretically calculated heats of formation of the compounds **3**, **4**, **10** and **11**.

The calculation of the detonation parameters was performed with the program package EXPLO5 (version 6.01).^[20] The program is based on the chemical equilibrium, steady-state

model of detonation. It uses the Becker–Kistiakowsky–Wilson's equation of state (BKW EOS) for gaseous detonation products and Cowan–Fickett's equation of state for solid carbon.

The EXPLO5 detonation parameters of compounds **3**, **4**, **10**, and **11** were calculated using the room-temperature recalculated X-ray densities^[21] (summarized in Table 1) and compared to the values calculated for **12**, TKX-50 and RDX.

Table 1. Energetic properties and detonation parameters of **3–4** and **10–11** compared to **12**, TKX-50, and RDX.

	3 (3·H₂O)	4	10	11	12^[9b]	TKX-50^[8]	RDX^[13]
Formula	C ₂ H ₂ N ₈ O ₁	C ₂ H ₈ N ₁₀ O ₃	C ₃ H ₁₀ N ₁₄ O ₁	C ₃ H ₈ N ₁₂ O ₂	C ₂ H ₈ N ₁₀ O ₃	C ₂ H ₈ N ₁₀ O ₄	C ₃ H ₆ N ₆ O ₆
FW [g mol ⁻¹]	154.09	220.15	258.20	244.17	220.15	236.15	222.12
IS [J] ^a	1 (4)	20	3	3	12	20	7.5
FS [N] ^b	<5 (30)	160	240	240	216	120	120
ESD [J] ^c	0.01 (0.05)	0.7	0.7	1.0	0.75	0.10	0.20
N [%] ^d	73.73 (65.11)	63.62	75.95	68.84	63.62	59.30	37.84
Ω [%] ^e	−37.19 (−41.53)	−36.33	−61.97	−52.42	−36.33	−27.10	−21.61
T _{dec.} [°C] ^f	172	183	201	214	200	221	210
ρ [g cm ⁻³] (298K) ^g	1.77 (pyc.) (1.791)	1.696	1.646	1.756	1.731	1.877	1.806
Δ _r H° [kJ mol ⁻¹] ^h	575.4	443.6	809.1	240.7	469.0	458.7	70.3
Δ _r U° [kJ kg ⁻¹] ⁱ	3822.2	2092.2	3253.5	1097.4	2248.5	2057.8	417.0
EXPLO V6.01 values:							
−Δ _E U° [kJ kg ⁻¹] ^j	5237	5426	4589	3281	5546	5939	5734
T _E [K] ^k	3826	3459	2940	2426	3490	3642	3800
p _{C-J} [kbar] ^l	304	303	267	244	323	401	352
D [m s ⁻¹] ^m	8749	8916	8635	8239	9117	9781	8815
V ₀ [L kg ⁻¹] ⁿ	796	926	890	870	924	913	792

^a impact sensitivity (BAM drophammer, 1 of 6); ^b friction sensitivity (BAM friction tester, 1 of 6); ^c electrostatic discharge device (OZM); ^d nitrogen content; ^e oxygen balance; ^f decomposition temperature from DSC (β = 5°C); ^g recalculated from low temperature X-ray densities (ρ_{298K} = ρ_T / (1 + α_V(298-T₀)); α_V = 1.5 · 10⁻⁴ K⁻¹); ^h calculated (CBS-4M) heat of formation; ⁱ calculated energy of formation; ^j energy of explosion; ^k explosion temperature; ^l detonation pressure; ^m detonation velocity; ⁿ assuming only gaseous products.

The detonation velocity of compound **4** (8916 m s⁻¹) is the highest detonation velocity of all investigated compounds, as well as RDX (8815 m s⁻¹).^[13] However, **4** has a lower detonation velocity than **12** (9117 m s⁻¹)^[9b] and TKX-50 (9781 m s⁻¹)^[8] because of its lower density in the solid state. The replacement of RDX with TKX-50 is still an ongoing research topic, and various compatibility and performance tests must be performed. Although compound **4** is a further outstanding secondary explosive based on tetrazole-*N*-oxides, we expect no advantages over TKX-50 with respect to performance and thermal stability. The detonation velocity of the acid **3** (8749 m s⁻¹) is higher than those of the salts **10** (8635 m s⁻¹) and **11** (8239 m s⁻¹). A similar trend is also observed for the calculated detonation pressure (**3**: 304 kbar, **10**: 267 kbar, **11**: 244 kbar). The detonation pressure of compound **4** (303 kbar) is

lower than those of RDX (352 kbar)^[13] and **12** (323 kbar).^[9b] It seems that the bistetrazole 1*N*-oxides have higher densities and better energetic properties than the 2*N*-oxides.

4.2.6 NMR spectroscopy

The ¹³C NMR resonances of **2** (131.3 (CN₄O), 112.2 (CN) ppm) are comparable to values found for other salts of cyanotetrazolate-2-oxides.^[22] For **3**, the ¹³C resonances are found at 148.4 ppm for the carbon in the tetrazole ring with the 2*N*-oxide and 152.4 ppm for the carbon in the tetrazole ring without oxide. We observed that the peaks of compound **3** are slightly downshifted compared to 5-(1*H*-tetrazolyl)-1-hydroxytetrazole.^[9b] In the ¹H NMR spectrum, one signal is observed and assigned to the hydroxyl group at 10.24 ppm. The hydroxylammonium salt **4** exhibits ¹³C resonances at 149.8 (CN₄O) and 152.1 (CN₄) ppm, which are also slightly downshifted compared with the corresponding 1*N*-oxide.^[9b] The anions of compounds **5–11** each show two shifts in the ¹³C NMR spectra similar to those observed for **4**, and can easily be assigned accordingly.

4.2.7 Vibrational Spectroscopy

IR- and Raman spectra for compounds **3–11** were measured, and the frequencies were assigned according to commonly observed values in the literature.^[23]

For compound **2**, we observed the characteristic pattern of vibrations in the Raman spectra as described in literature for other salts of cyanotetrazole-2-oxide.^[22] The C=N stretch occurs at 2275 cm⁻¹ as the strongest band observed. As other characteristic bands, the N3–N4 tetrazole stretch is observed at 1014 cm⁻¹, and the C1–N4 stretch arises at 1454 cm⁻¹.^[22] The Raman spectra of compounds **4–11** show absorptions in the range 1540–700 cm⁻¹, which can be assigned to the vibrations of the tetrazole and the tetrazole-2-oxid rings [ν (NN), ν (NCN), γ (CN), δ aromatic ring].^[24] The acid **3** shows the most intense absorption at 1636 cm⁻¹, which indicates the symmetrical stretching mode between the C–C linked tetrazole rings. This stretching mode can be observed at 1599 cm⁻¹ for the anion of the hydroxylammonium salt **4** and in similar regions for the other salts **5–11** (1624 cm⁻¹ to 1593 cm⁻¹). Valence vibrations of the ammonium group of the hydroxylammonium cation in compound **4** can be observed as two broad bands at 2948 cm⁻¹ and 2736 cm⁻¹ [$\nu_{\text{asym}}(\text{NH}_2/\text{NH}_3^+)$]^[9b] and in similar regions for the other salts (3291 (**10**), 3254 (**8**), 3249 (**7**), 3170 and 3025 (**9**), 3139 (**6**), 2685 (**11**) cm⁻¹).

The IR spectra of compound **2** contains broad and strong bands between 3493 cm⁻¹ and 2877 cm⁻¹, which indicates the O–H vibration of the compound and the crystal water. The N–O (1661 cm⁻¹), the C=N (2272–2263 cm⁻¹), the N2–N3 (1014 cm⁻¹) and the N3–N4 (1412–

1368 cm⁻¹) stretches match to the values found in literature.^[22] The typical tetrazole vibrations for the compounds **3–11** are found in the range 1528–700 cm⁻¹,^[24] which complicates a detailed assignment without any quantum chemical calculations. The IR spectra of compound **3** shows two strong absorptions at 3522 cm⁻¹ and 3373 cm⁻¹, which indicates the OH and NH valence vibrations and the O–H stretching vibrations of the crystal water. In the range 1541–1696 cm⁻¹, we observed the asymmetrical C=N stretching modes of the tetrazole ring system for the acid **3** and the salts **4–11** [e.g. 1529 cm⁻¹ (**6**)].

4.2.8 Toxicity

Besides the high energetic properties required for the replacements of RDX, research must also focus on environmental friendliness. The *Luminescent Bacteria Inhibition Test* offers the possibility to determine the environmental acceptability of new energetic materials to aquatic organisms, with marine bacteria used as a representative marine organisms.

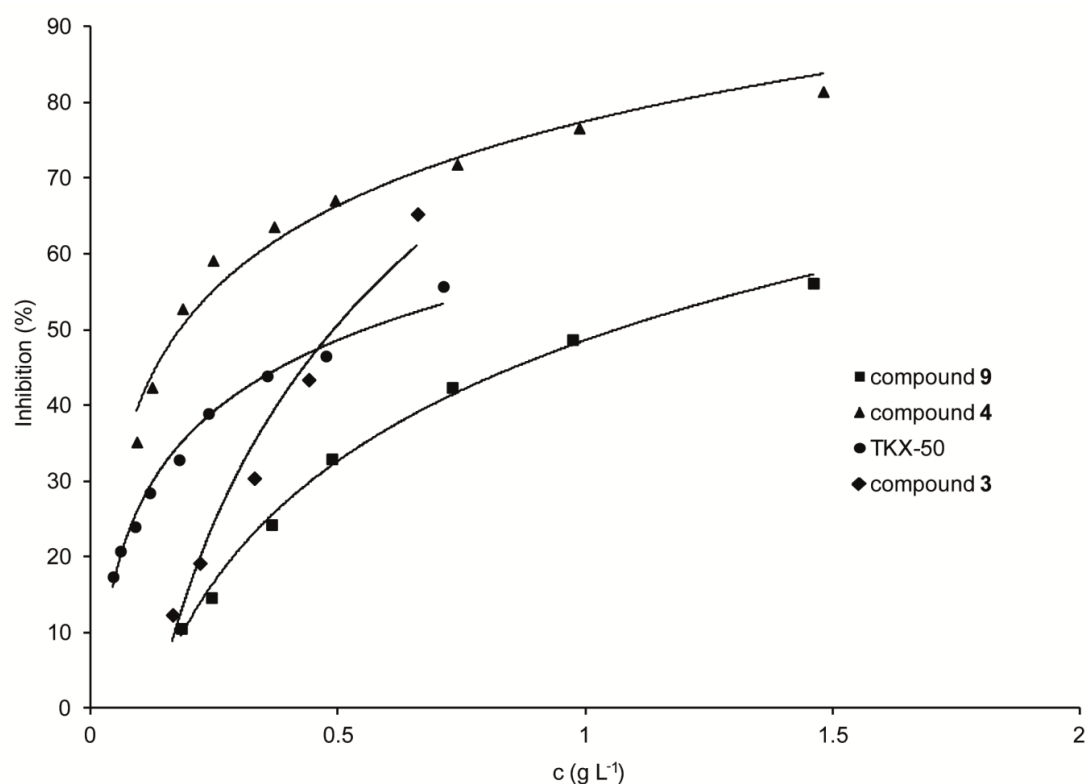
In this test, the decrease of the luminescence of the liquid-dried bacteria is determined after 15 and 30 min at different concentrations of the test compounds, and is compared to a control measurement of a 1% NaCl stock solution. The EC₅₀ value gives the concentration of each compound at which the bacterial luminescence is inhibited by 50%, and is calculated by plotting *I* against the concentration of the test substance in a diagram with a logarithmic scale [Eq. (5)].

$$I = \text{inhibition (\%)} / (100 - \text{inhibition (\%)}) \quad (5)$$

The toxicity of acid **3** to aquatic life is lower than that of RDX, and lies in the range of that of TKX-50. For better comparability of the toxicities of the anions 5-(2-oxidotetrazolyl)-tetrazolate and 5-(1-oxidotetrazolyl)-tetrazolate, the EC₅₀ values of the corresponding ammonium salts as well as hydroxylammonium salts were determined. The EC₅₀ values listed in Table 2 indicate that the 2*N*-oxide anions exhibits a higher toxicity than the corresponding 1*N*-oxide anions. However, both ammonium salts show a low toxicological potential towards marine organism, whereas the toxicity of the hydroxylammonium salts are in the range of the RDX toxicity. The higher toxicity of hydroxylammonium salts compared to the corresponding ammonium salts indicates that hydroxylammonium cations generally exhibit a higher toxicity toward marine organism, as illustrated in Figure 8.

Table 2. Toxicity data of compounds **3**, **4**, **9**, in comparison to **12**, bis(ammonium) 5-(1-oxidotetrazolyl)-tetrazolate (**13**), TKX-50, and RDX.

compound	EC50 (15 min.) [g/L]	EC50 (30 min.) [g/L]
3	0.601	0.491
4	0.386	0.180
9	1.727	1.027
12 ^[9b]	1.634	0.330
13	4.210	3.678
TKX-50 ^[8]	1.172	0.580
RDX ^[8]	0.327	0.239

**Figure 8.** Inhibition of compounds **3**, **4**, **9**, and TKX-50 at different concentrations of the substances after 30 min.

4.3 Conclusions

5-(1*H*-Tetrazolyl)-2-hydroxytetrazole monohydrate (**3**) and the precursor sodium 5-cyanotetrazolate-2-oxide hydrate (**2**) were synthesized and characterized for the first time. Different nitrogen-rich bases were used for deprotonation of compound **3** in aqueous media. The compounds crystallize in the space groups $P2_1/c$ (**2**, **3**), $P2_1/n$ (**4**, **11**) and $P-1$ (**5**, **10**) with densities of 1.707 (**2**), 1.791 (**3**), 1.696 (**4**), 1.713 (**5**), 1.646 (**10**), 1.756 g cm⁻³ (**11**). Surprisingly, the density of bis(hydroxylammonium) 5,5'-bistetrazolate (1.742 g cm⁻³) is

slightly higher than that of **4**.^[25] This shows that the introduction of 2*N*-oxides does not necessarily lead to an improve in densities.

The detonation velocities were calculated for compounds **3**, **4**, **10** and **11** [$D = 8749$ (**3**), 8916 (**4**), 8635 (**10**), 8239 m s⁻¹ (**11**)], by using the calculated heats of formation and recalculated crystal densities from the X-ray experiments. The most promising compound in terms of explosive performance is compound **4**, which is in the range of RDX ($IS = 7.5$ J, $FS = 120$ N, $ESD = 0.2$ J, $D = 8815$ m s⁻¹).^[13]

This study confirms the assumption that tetrazole 1*N*-oxides are superior to tetrazole 2*N*-oxides in terms of temperature stability, density, and performance. This applies for bistetrazole dioxides as well as bistetrazole monoxides.

The toxicity test indicates anions of bistetrazole-1*N*-monoxides have lower toxicity to aquatic than anions of bistetrazole-2*N*-monoxides. Furthermore, the ammonium cation seems to be less toxic than the hydroxylammonium cation.

4.4 Experimental Section

The analytical methods and general procedures are described in the appendix of this thesis. Sodium 5-cyanotetrazolate sesquihydrate (**1**) was synthesized according to the literature.^[10]

Sodium 5-cyanotetrazole-2-oxide monohydrate (**2**)^[7b]

Sodium cyanotetrazolate sesquihydrate (2.50 g, 17.35 mmol) was dissolved in 35 mL of distilled water, and potassium acetate (1.49 g, 151.81 mmol) was added. The solution was stirred at room temperature, and Oxone (3.34 g, 108.66 mmol) added slowly. After stirring of the suspension for 20 h at 40 °C, the solution was poured into 800 mL of acetone and the precipitated salts were filtered off. After evaporation of the solvent under reduced pressure, the remaining solid was dissolved in ethanol. The insoluble residues were filtered off, and the filtrate was left for crystallization to give colorless crystals of sodium cyanotetrazolate-2-oxide monohydrate (2.23 g, 14.76 mmol, 85%).

DTA (5 °C min⁻¹) onset: 98 °C (–H₂O), 276 °C (dec.); **IR** (ATR, cm⁻¹): $\tilde{\nu} = 3496(\text{m})$, 3392(m), 3272(w), 2273(m), 1662(m), 1612(w), 1569(w), 1445(vs), 1431(m), 1414(s), 1399(vs), 1385(m), 1370(vs), 1238(s), 1077(m), 1014(m), 805(s), 722(s); **Raman** (1064 nm, 300 mW, 25 °C, cm⁻¹): $\tilde{\nu} = 2275(100)$, 1454(42), 1416(4), 1386(5), 1381(4), 1241(4), 1109(18), 1078(2), 1014(53), 810(11), 723(3), 581(5), 501(7), 475(5), 352(2), 191(11), 180(9), 144(10), 118(24), 105(37), 94(56), 79(7), 67(10); **¹³C NMR** ([D₆]DMSO): $\delta = 131.3$ (s, CN₄O), 112.2 ppm (s, CN); **MS** m/z (FAB⁻): 110.1 (C₂N₅O⁻), m/z (FAB⁺): 23.1 (Na⁺); **EA**

(C₂H₂NaN₅O₂, 151.06) calcd.: C 15.90, H 1.33, N 46.36%; found: C 15.93, H 1.42, N 45.61%; **Sensitivities**: IS: >40 J; FS: 360 N; ESD: 1500 mJ (at grain sizes <100 μm).

5-(1*H*-Tetrazolyl)-2-hydroxytetrazole monohydrate (3)^[11]

Sodium cyanotetrazolate-2-oxide monohydrate (2.80 g, 18.53 mmol) was dissolved in 150 mL of distilled water. To the solution sodium azide (1.45 g, 22.25 mmol) and zinc chloride (3.03 g, 22.25 mmol) were added. The solution was heated at reflux for 3 h, then the precipitating white solid was filtered off, solved in conc. hydrochloric acid, and extracted with diethyl ether to give 5-(1*H*-tetrazolyl)-2-hydroxytetrazole monohydrate (1.85 g, 10.75 mmol, 58%). Recrystallization in 2 M hydrochloric acid yielded colorless needles (1.35 g, 7.84 mmol, 42%).

DTA (5 °C min⁻¹) onset: 104 °C (–H₂O), 175 °C (dec.); **IR** (ATR, cm⁻¹): $\tilde{\nu}$ = 3522(m), 3373(m), 2342(m), 1916(m), 1632(m), 1560(m), 1490(m), 1450(m), 1380(s), 1349(s), 1333(s), 1285(m), 1260(s), 1247(m), 1223(m), 1172(w), 1158(m), 1121(s), 1069(s), 1039(m), 1003(m), 980(vs), 835(m), 835(m), 829(m), 754(m), 716(s), 703(m), 667(m); **Raman** (1064 nm, 300 mW, 25 °C, cm⁻¹): $\tilde{\nu}$ = 1636(100), 1495(11), 1383(4), 1354(2), 1336(2), 1263(15), 1251(4), 1228(4), 1160(12), 1126(5), 1068(7), 1042(43), 1029(6), 766(4), 755(10), 562(4), 422(3), 408(5), 388(4), 298(2); **¹H NMR** ([D₆]DMSO): δ = 10.24 ppm (s, 1H, CN₄OH); **¹³C NMR** ([D₆]DMSO): δ = 152.4 (s, CN₄), 148.4 ppm (s, CN₄O); **MS** *m/z* (FAB⁻): 153.1 (C₂HN₈O⁻); **EA** (C₂H₄N₈O₂, 172.11) calcd.: C 13.96, H 2.34, N 65.11 %; found: C 14.54, H 2.44, N 64.64%; **Sensitivities**: IS: 4 J, FS: 30 N, ESD: 50 mJ (at grain sizes <100 μm for C₂H₂N₈O·H₂O); IS: 1 J; FS: <5 N; ESD: 10 mJ (at grain sizes <100 μm for C₂H₂N₈O).

Bis(hydroxylammonium) 5-(2-oxidotetrazolyl)-tetrazolate (4)

5-(1*H*-Tetrazolyl)-2-hydroxytetrazole monohydrate (0.67 g, 3.89 mmol) was dissolved in 10 mL of water. Hydroxylamine (0.51 g 50% w/v in water, 7.78 mmol) was added. Bis(hydroxylammonium) 5-(2-oxidotetrazolyl)-tetrazolate precipitated as white powder. Recrystallization in methanol yielded colorless crystals (0.80 g, 3.62 mmol, 93%).

DTA (5 °C min⁻¹) onset: 88 °C (–NH₃OH⁺), 183 °C (dec.); **IR** (ATR, cm⁻¹): $\tilde{\nu}$ = 3206(w), 3082(w), 2928(m), 2831(m), 2666(s), 2518(m), 2349(w), 2246(w), 2130(w), 2059(w), 1640(w), 1613(w), 1598(w), 1528(m), 1441(w), 1386(m), 1367(s), 1349(s), 1306(vs), 1257(m), 1225(m), 1200(s), 1166(m), 1166(m), 1139(w), 1120(w), 1089(w), 1055(w), 1030(w), 1011(s), 996(m), 777(vs), 721(s), 691(w); **Raman** (1064 nm, 300 mW, 25 °C, cm⁻¹): $\tilde{\nu}$ = 2948(3), 2736(3), 1624(5), 1613(10), 1599(100), 1585(9), 1574(5), 1545(4),

1370(5), 1228(5), 1169(4), 1156(3), 1142(18), 1090(13), 1033(18), 1012(19), 998(6), 773(4), 600(2), 429(3), 395(3), 318(3), 229(5), 229(5), 194(6), 170(8), 144(14), 128(30), 88(29), 73(11); **¹H NMR** ([D₆]DMSO): δ = 8.78 ppm (br s, NH₃OH⁺); **¹³C NMR** ([D₆]DMSO): δ = 152.1 (s, CN₄), 149.8 ppm (s, CN₄O); **MS** m/z (FAB⁻): 153.1 (C₂HN₈O⁻), m/z (FAB⁺): 34.0 (NH₃OH⁺); **EA** (C₂H₈N₁₀O₃, 220.15) calcd.: C 10.91, H 3.66, N 63.62%; found: C 11.47, H 3.64, N 63.35%; **Sensitivities**: IS: 20 J; FS: 160 N; ESD: 700 mJ (at grain sizes <100 μ m).

Hydroxylammonium 5-(2-oxidotetrazolyl)-tetrazolate monohydrate (5)

5-(1*H*-Tetrazolyl)-2-hydroxytetrazole monohydrate (0.86 g, 5.00 mmol) was dissolved in 10 mL of water. Hydroxylamine (0.33 g, 50% w/v in water, 5.00 mmol) was added. The solution was left for crystallization and hydroxylammonium 5-(2-oxidotetrazolyl)-tetrazolate monohydrate precipitated as colorless crystals (1.00 g, 4.87 mmol, 97%).

DTA (5 °C min⁻¹) onset: 107 °C (-H₂O), 176 °C (dec.); **IR** (ATR, cm⁻¹): $\tilde{\nu}$ = 2713(m), 1622(m), 1517(m), 1461(m), 1377(s), 1361(s), 1291(m), 1245(m), 1212(m), 1186(s), 1131(w), 1086(s), 1053(m), 1002(s), 990(vs), 789(vs), 765(s), 755(vs), 701(vs), 689(s); **Raman** (1064 nm, 300 mW, 25 °C, cm⁻¹): $\tilde{\nu}$ = 1624(100), 1562(3), 1476(10), 1470(10), 1366(6), 1293(2), 1247(12), 1225(2), 1133(17), 1099(21), 1059(6), 1024(31), 1006(9), 789(3), 763(3), 592(2), 421(3), 388(6), 329(5), 213(5), 173(8), 150(24), 134(11), 134(11), 118(18), 102(19), 83(35); **¹H NMR** ([D₆]DMSO): δ = 9.58 ppm (br s, NH₃OH⁺); **¹³C NMR** ([D₆]DMSO): δ = 148.0 (s, CN₄), 145.5 ppm (s, CN₄O); **MS** m/z (FAB⁻): 153.1 (C₂N₈HO⁻); m/z (FAB⁺): 34.0 (NH₃OH⁺); **EA** (C₂H₇N₉O₃, 205.14) calcd.: C 11.71, H 3.44, N 61.45%; found: C 12.27, H 3.34, N 61.62%; **Sensitivities**: IS: 10 J, FS: 120 N; ESD: 500 mJ (at grain sizes <100 μ m).

Bis(hydrazinium) 5-(2-oxidotetrazolyl)-tetrazolate monohydrate (6)

5-(1*H*-Tetrazolyl)-2-hydroxytetrazole monohydrate (0.67 g, 3.89 mmol) was dissolved in 10 mL of water. A solution of hydrazinium hydroxide (0.39 g, 7.78 mmol) was added. The solution was stirred for 5 min at ambient temperature and left stand to yield bis(hydrazinium) 5-(2-oxidotetrazolyl)-tetrazolate monohydrate as a colorless solid (0.77 g, 3.53 mmol, 91%).

DTA (5 °C min⁻¹) onset: 249 °C (dec.); **IR** (ATR, cm⁻¹): $\tilde{\nu}$ = 3503(w), 3323(m), 3227(m), 3057(m), 2957(m), 2863(m), 2793(m), 2735(s), 2656(s), 2254(w), 2115(w), 1926(vw), 1635(m), 1620(m), 1591(m), 1529(m), 1445(w), 1393(s), 1375(vs), 1350(s), 1308(vs), 1223(m), 1182(m), 1182(m), 1155(m), 1130(vs), 1092(vs), 1073(m), 1046(m), 1031(w), 1012(m), 973(vs), 788(s), 722(m); **Raman** (1064 nm, 300 mW, 25 °C, cm⁻¹): $\tilde{\nu}$ = 3139(3),

1594(100), 1548(4), 1446(2), 1409(2), 1377(3), 1226(5), 1184(5), 1136(11), 1093(15), 1048(15), 1034(13), 1014(5), 975(8), 789(2), 774(5), 598(2), 446(3), 433(3), 387(5), 320(4), 227(5), 192(4), 192(4), 176(8), 166(6), 149(5), 107(22), 92(26), 78(24), 61(4); **¹H NMR** ([D₆]DMSO): δ = 6.91 ppm (br s, N₂H₅⁺); **¹³C NMR** ([D₆]DMSO): δ = 153.3 (s, CN₄), 150.9 ppm (s, CN₄O); **MS** m/z (FAB⁻): 153.1 (C₂HN₈O⁻), m/z (FAB⁺): 33.1 (N₂H₅⁺); **EA** (C₂H₁₀N₁₂O, 218.18) calcd.: C 11.01, H 4.62, N 77.04%; found: C 11.48, H 5.03, N 76.08%; **Sensitivities**: IS: >40 J; FS: 360 N; ESD: 700 mJ (at grain sizes <100 μ m).

Bis(guanidinium) 5-(2-oxidotetrazolyl)-tetrazolate (7)

5-(1*H*-Tetrazolyl)-2-hydroxytetrazole monohydrate (0.86 g, 5.00 mmol) was dissolved in 10 mL of water. A solution of guanidinium carbonate (0.90 g, 5.00 mmol) in water was added and the solution refluxed for 1 h. The solution was cooled to ambient temperature and bis(guanidinium) 5-(2-oxidotetrazolyl)-tetrazolate precipitated as colorless powder (1.20 g, 4.41 mmol, 88%).

DTA (5 °C min⁻¹) onset: 324 °C (dec.); **IR** (ATR, cm⁻¹): $\tilde{\nu}$ = 3392(m), 3302(m), 3233(m), 3081(s), 2825(m), 2759(w), 1677(s), 1637(vs), 1590(s), 1445(w), 1397(s), 1382(s), 1344(s), 1312(vs), 1225(m), 1185(m), 1160(m), 1133(m), 1095(m), 1071(w), 1045(w), 1032(w), 1010(s), 1010(s), 788(vs), 719(s), 696(w); **Raman** (1064 nm, 300 mW, 25 °C, cm⁻¹): $\tilde{\nu}$ = 3249(3), 1595(100), 1569(5), 1546(3), 1446(2), 1386(2), 1228(4), 1187(4), 1136(16), 1096(11), 1073(10), 1046(27), 1034(11), 1011(33), 790(6), 773(6), 548(9), 435(3), 384(6), 318(5), 132(42), 93(23), 62(6); **¹H NMR** ([D₆]DMSO): δ = 7.39 ppm (s, 6H, CH₆N₃⁺); **¹³C NMR** ([D₆]DMSO): δ = 158.2 (s, CH₆N₃⁺), 153.4 (s, CN₄), 150.9 ppm (s, CN₄O); **MS** m/z (FAB⁻): 153.1 (C₂HN₈O⁻), m/z (FAB⁺): 60.1 (CH₆N₃⁺); **EA** (C₄H₁₂N₁₄O, 272.23) calcd.: C 17.65, H 4.44, N 72.03%; found: C 18.06, H 4.41, N 71.46%; **Sensitivities**: IS: >40 J; FS: 360 N; ESD: 1500 mJ (at grain sizes <100 μ m).

Bis(aminoguanidinium) 5-(2-oxidotetrazolyl)-tetrazolate monohydrate (7)

5-(1*H*-Tetrazolyl)-2-hydroxytetrazole monohydrate (0.86 g, 5.00 mmol) was dissolved in 10 mL of water. A solution of aminoguanidine bicarbonate (1.36 g, 10.00 mmol) in water was added and the solution was heated to 90 °C for 1 h. Then the solution was cooled to ambient temperature and bis(aminoguanidinium) 5-(2-oxidotetrazolyl)-tetrazolate monohydrate precipitated as a white powder (1.29 g, 4.03 mmol, 81%).

DTA (5 °C min⁻¹) onset: 99 °C (-H₂O), 210 °C (m.p.), 228 °C (dec.); **IR** (ATR, cm⁻¹): $\tilde{\nu}$ = 3388(m), 3310(m), 3148(m), 3065(s), 1688(vs), 1669(vs), 1656(vs), 1592(w), 1444(w),

1394(s), 1378(s), 1347(vs), 1310(s), 1220(m), 1194(m), 1177(w), 1146(m), 1100(w), 1075(w), 1038(m), 1028(m), 1010(s), 957(vw), 957(vw), 784(s), 740(w), 719(m), 694(w); **Raman** (1064 nm, 300 mW, 25 °C, cm^{-1}): $\tilde{\nu}$ = 3254(7), 1671(3), 1632(16), 1596(100), 1579(9), 1543(4), 1453(3), 1387(2), 1349(2), 1234(5), 1222(5), 1179(5), 1133(16), 1095(17), 1076(10), 1040(24), 1013(7), 964(20), 789(7), 772(5), 625(4), 594(3), 519(8), 431(7), 431(7), 384(9), 311(8), 129(60), 117(56), 88(30); **^1H NMR** ($[\text{D}_6]$ DMSO): δ = 9.14 (s, 1H, CNHNH₂), 7.34 (br s, 4H, CNH₂), 4.74 ppm (br s, 2H, CNHNH₂); **^{13}C NMR** ($[\text{D}_6]$ DMSO): δ = 159.0 (s, CH₇N₄⁺), 153.4 (s, CN₄), 150.9 ppm (s, CN₄O); **MS** m/z (FAB⁻): 153.1 (C₂HN₈O⁻), m/z (FAB⁺): 75.1 (CH₇N₄⁺); **EA** (C₄H₁₆N₁₆O₂, 320.28) calcd.: C 15.00, H 5.04, N 69.97%; found: C 15.54, H 4.86, N 69.92%; **Sensitivities**: IS: >40 J; FS: 360 N; ESD: 1500 mJ (at grain sizes <100 μm).

Bis(ammonium) 5-(2-oxidotetrazolyl)-tetrazolate (9)

5-(1*H*-Tetrazolyl)-2-hydroxytetrazole monohydrate (0.86 g, 5.00 mmol) was dissolved in 10 mL of water and 0.8 mL of 25% NH₃ was added. The solution was left for crystallization, yielding a white powder of bis(ammonium) 5-(2-oxidotetrazolyl)-tetrazolate (0.76 g, 4.04 mmol, 81%).

DTA (5 °C min⁻¹) onset: 255 °C (dec.); **IR** (ATR, cm^{-1}): $\tilde{\nu}$ = 3173(m), 3006(s), 2849(s), 2133(w), 1879(w), 1697(w), 1425(vs), 1383(s), 1341(s), 1306(vs), 1221(m), 1185(m), 1140(m), 1095(w), 1050(w), 1017(m), 1006(s), 793(m), 732(m), 723(s), 700(w); **Raman** (1064 nm, 300 mW, 25 °C, cm^{-1}): $\tilde{\nu}$ = 3170(4), 3025(11), 2865(8), 1593(89), 1566(13), 1548(4), 1466(3), 1413(5), 1225(5), 1203(14), 1187(6), 1140(16), 1103(18), 1072(25), 1029(20), 1008(8), 808(5), 775(5), 595(3), 419(9), 392(11), 311(5), 199(15), 199(15), 117(53), 92(100), 74(68); **^1H NMR** ($[\text{D}_6]$ DMSO): δ = 7.56 ppm (s, 4H, NH₄⁺); **^{13}C NMR** ($[\text{D}_6]$ DMSO): δ = 153.7 (s, CN₄), 151.5 ppm (s, CN₄O); **MS** m/z (FAB⁻): 153.1 (C₂HN₈O⁻), m/z (FAB⁺): 18.1 (NH₄⁺); **EA** (C₂H₈N₁₀O, 188.16) calcd.: C 12.77, H 4.29, N 74.44%; found: C 12.25, H 4.12, N 73.76%; **Sensitivities**: IS: >40 J; FS: 360 N; ESD: 1000 mJ (at grain sizes <100 μm).

Triaminoguanidinium 5-(2-oxidotetrazolyl)-tetrazolate (10)

5-(1*H*-Tetrazolyl)-2-hydroxytetrazole monohydrate (0.86 g, 5.00 mmol) was dissolved in water (10 mL) and triaminoguanidinium chloride (1.41 g, 10.00 mmol) was added. The solution was left for crystallization to give triaminoguanidinium 5-(2-oxidotetrazolyl)-tetrazolate as colorless blocks (1.19 g, 4.61 mmol, 92%).

DTA (5 °C min⁻¹) onset: 192 °C (m.p.), 201 °C (dec.); **IR** (ATR, cm⁻¹): $\tilde{\nu}$ = 3360(w), 3344(w), 3289(m), 3255(m), 2955(w), 2767(w), 2636(w), 2525(w), 2483(w), 2136(w), 1683(vs), 1616(m), 1594(m), 1558(w), 1449(w), 1399(m), 1393(m), 1378(s), 1361(s), 1273(m), 1214(m), 1146(s), 1130(s), 1130(s), 1083(m), 1054(m), 1028(m), 991(s), 897(s), 781(s), 721(m), 703(w); **Raman** (1064 nm, 300 mW, 25 °C, cm⁻¹): $\tilde{\nu}$ = 3291(6), 1691(3), 1676(3), 1629(9), 1614(100), 1599(10), 1477(8), 1462(6), 1450(6), 1363(7), 1332(3), 1236(12), 1218(3), 1204(2), 1147(4), 1108(22), 1089(14), 1059(5), 1032(35), 986(5), 888(8), 779(5), 760(4), 760(4), 638(2), 580(3), 442(4), 416(7), 379(14), 314(3), 253(4), 201(3), 153(14), 119(28), 96(50); **¹H NMR** ([D₆]DMSO): δ = 8.63 (s, 3H, CNH₂NH₂), 5.28 ppm (br s, 6H, CNH₂NH₂); **¹³C NMR** ([D₆]DMSO): δ = 159.2 (s, CH₉N₆⁺), 147.8 (s, CN₄), 144.5 ppm (s, CN₄O); **MS** m/z : (FAB⁻): 153.1 (C₂HN₈O⁻), m/z (FAB⁺): 105.1 (CH₉N₆⁺); **EA** (C₃H₁₀N₁₄O, 258.21) calcd.: C 13.95, H 3.90, N 75.95%; found: C 14.55, H 3.81, N 76.31%; **Sensitivities**: FS: 3 J, IS: 240 N, ESD: 700 mJ (at grain sizes 100-500 μ m).

Diaminouronium 5-(2-oxidotetrazolyl)-tetrazolate (11)

5-(1*H*-Tetrazolyl)-2-hydroxytetrazole monohydrate (0.86 g, 5.00 mmol) was dissolved in 100 mL water and diaminourea (0.90 g, 10.00 mmol) was added. The solution was left for crystallization to give diaminouronium 5-(2-oxidotetrazolyl)-tetrazolate as colorless blocks (1.09 g, 4.46 mmol, 89%).

DTA (5 °C min⁻¹) onset: 214 °C (dec.); **IR** (ATR, cm⁻¹): $\tilde{\nu}$ = 3137(m), 2974(m), 2811(m), 2613(m), 2488(m), 2124(w), 2072(w), 1904(w), 1731(m), 1693(vw), 1639(m), 1616(m), 1593(m), 1546(vs), 1542(vs), 1374(s), 1359(s), 1349(vs), 1304(vs), 1292(s), 1218(s), 1190(vs), 1139(s), 1139(s), 1086(m), 1063(w), 1049(w), 1033(w), 1005(s), 978(w), 813(w), 768(m), 752(m), 719(m), 685(w), 664(w); **Raman** (1064 nm, 300 mW, 25 °C, cm⁻¹): $\tilde{\nu}$ = 2685(1), 1732(3), 1597(100), 1546(5), 1444(2), 1361(3), 1226(5), 1196(6), 1142(15), 1090(8), 1052(5), 1035(14), 1022(1), 1008(14), 980(3), 774(4), 583(2), 505(3), 425(2), 402(3), 327(3), 291(2), 248(2), 248(2), 183(9), 131(17), 112(39), 99(27), 67(5); **¹H NMR** ([D₆]DMSO): δ = 7.33 ppm (br s, CH₈N₄O²⁺); **¹³C NMR** ([D₆]DMSO): δ = 160.4 (s, CH₈N₄O²⁺), 149.4 (s, CN₄), 146.4 ppm (s, CN₄O); **MS** m/z (FAB⁻): 153.1 (C₂HN₈O⁻), m/z (FAB⁺): 91.1 (CH₇N₄O⁺); **EA** (C₃H₈N₁₂O₂, 244.17) calcd.: C 14.76, H 3.30, N 68.84%; found: C 15.13, H 3.38, N 68.15%; **Sensitivities**: FS: 3 J, IS: 240 N, ESD: 1000 mJ (at grain sizes <100 μ m).

4.5 References

- [1] G. F. Henning, *Vol. Patent DE 104280*, **1898**.
- [2] W. E. Bachmann, J. C. Sheehan, *J. Am. Chem. Soc.* **1949**, *71*, 1842–1845.
- [3] T. M. Klapötke, *Chemie der hochenergetischen Materialien*, Walter de Gruyter GmbH & Co. KG, Berlin, **2009**.
- [4] M. B. Talawar, R. Sivabalan, T. Mukundan, H. Muthurajan, A. K. Sikder, B. R. Gandhe, A. S. Rao, *J. Hazard. Mater.* **2009**, *161*, 589–607.
- [5] R. P. Singh, R. D. Verma, D. T. Meshri, J. M. Shreeve, *Angew. Chem.* **2006**, *118*, 3664–3682.
- [6] A. M. Churakov, V. A. Tartakovsky, *Chem. Rev.* **2004**, *104*, 2601–2616.
- [7] a) J. C. Bottaro, M. Petrie, P. E. Penwell, A. L. Dodge, R. Malhotra, NANA/HEDM Technology: Late Stage Exploratory Effort, Report No. A466714; SRI International: Menlo Park, CA, 2003; DARPA/AFOSR funded, contact no. F49629-02-C-0030; b) M. Göbel, K. Karaghiosoff, T. M. Klapötke, D. G. Piercey, J. Stierstorfer, *J. Am. Chem. Soc.* **2010**, *132*, 17216–17226; c) D. Fischer, T. M. Klapötke, D. G. Piercey, J. Stierstorfer, *Chem. Eur. J.* **2013**, *19*, 4602–4613.
- [8] N. Fischer, D. Fischer, T. M. Klapötke, D. G. Piercey, J. Stierstorfer, *J. Mater. Chem.* **2012**, *22*, 20418–20422.
- [9] a) N. Fischer, L. Gao, T. M. Klapötke, J. Stierstorfer, *Polyhedron* **2013**, *51*, 201–210; b) D. Fischer, T. M. Klapötke, M. Reymann, P. C. Schmid, J. Stierstorfer, M. Sućeska, *Propellants Explos. Pyrotech.* **2014**, *in press*, doi: 10.1002/prop.201300152.
- [10] N. Fischer, T. M. Klapötke, S. Rappenglück, J. Stierstorfer, *ChemPlusChem* **2012**, *77*, 877–888.
- [11] A. Chafin, D. J. Irvin, M. H. Mason, S. L. Mason, *TetrahedronLett.* **2008**, *49*, 3823–3826.
- [12] N. Fischer, D. Izsák, T. M. Klapötke, S. Rappenglück, J. Stierstorfer, *Chem. Europ. J.* **2012**, *18*, 4051–4062.
- [13] E. P. Burrows, E. E. Brueggemann, *J. Chromatogr. A* **1985**, *329*, 285–289.
- [14] K. G. Shipp, *J. of Org. Chem.* **1964**, *29*, 2620–2623.

- [15] (a) J. W. Ochterski, G. A. Petersson, J. A. Montgomery Jr., *J. Chem. Phys.* **1996**, *104*, 2598; (b) J. A. Montgomery Jr., M. J. Frisch, J. W. Ochterski G. A. Petersson, *J. Chem. Phys.* **2000**, *112*, 6532; (c) L. A. Curtiss, K. Raghavachari, P. C. Redfern, J. A. Pople, *J. Chem. Phys.* **1997**, *106*, 1063; (d) E. F. C. Byrd, B. M. Rice, *J. Phys. Chem. A* **2006**, *110*, 1005–1013; (e) B. M. Rice, S. V. Pai, J. Hare, *Comb. Flame* **1999**, *118*, 445–458.
- [16] M. J. Frisch, G. W. Trucks, H. B. Schlegel, G. E. Scuseria, M. A. Robb, J. R. Cheeseman, G. Scalmani, V. Barone, B. Mennucci, G. A. Petersson, H. Nakatsuji, M. Caricato, X. Li, H.P. Hratchian, A. F. Izmaylov, J. Bloino, G. Zheng, J. L. Sonnenberg, M. Hada, M. Ehara, K. Toyota, R. Fukuda, J. Hasegawa, M. Ishida, T. Nakajima, Y. Honda, O. Kitao, H. Nakai, T. Vreven, J. A. Montgomery, Jr., J. E. Peralta, F. Ogliaro, M. Bearpark, J. J. Heyd, E. Brothers, K. N. Kudin, V. N. Staroverov, R. Kobayashi, J. Normand, K. Raghavachari, A. Rendell, J. C. Burant, S. S. Iyengar, J. Tomasi, M. Cossi, N. Rega, J. M. Millam, M. Klene, J. E. Knox, J. B. Cross, V. Bakken, C. Adamo, J. Jaramillo, R. Gomperts, R. E. Stratmann, O. Yazyev, A. J. Austin, R. Cammi, C. Pomelli, J. W. Ochterski, R. L. Martin, K. Morokuma, V. G. Zakrzewski, G. A. Voth, P. Salvador, J. J. Dannenberg, S. Dapprich, A. D. Daniels, O. Farkas, J.B. Foresman, J. V. Ortiz, J. Cioslowski, D. J. Fox, Gaussian 09 A.02, Gaussian, Inc., Wallingford, CT, USA, **2009**.
- [17] M. S. Westwell, M. S. Searle, D. J. Wales, D. H. Williams, *J. Am. Chem. Soc.* **1995**, *117*, 5013–5015; (b) F. Trouton, *Philos. Mag.* **1884**, *18*, 54–57.
- [18] (a) H. D. B. Jenkins, H. K. Roobottom, J. Passmore, L. Glasser, *Inorg. Chem.* **1999**, *38*, 3609–3620; (b) H. D. B. Jenkins, D. Tudela, L. Glasser, *Inorg. Chem.* **2002**, *41*, 2364–2367.
- [19] N. Fischer, T. M. Klapötke, M. Reyman, J. Stierstorfer, *Europ. J. of Inorg. Chem.* **2013**, 2167–2180.
- [20] M. Sućeska, EXPLO5.06 program, Zagreb, Croatia, **2012**.
- [21] C. Xue, J. Sun, B. Kang, Y. Liu, X. Liu, G. Song, Q. Xue, *Propellants Explos. Pyrotech.* **2010**, *35*, 333–338.
- [22] F. Boneberg, A. Kirchner, T. M. Klapötke, D. G. Piercey, M. J. Poller, J. Stierstorfer; *Chem Asian J.* **2013**, *8*, 148–159.
- [23] a) M. Hesse, H. Meier, B. Zeeh, *Spektroskopische Methoden in der Organischen Chemie*, 7th edn., Thieme, Stuttgart, New York, **2005**; b) G. Socrates, *Infrared and*

Raman Characteristic Group Frequencies: Tables and Charts, 3rd edn., John Wiley & Sons, Chichester, **2004**.

- [24] T. M. Klapötke, P. Mayer, C. Miró Sabaté, J. M. Welch, N. Wiegand, *Inorg. Chem.* **2008**, 47, 6014–6027.

4.6 Supplementary information

4.6.1 XRD data and parameters

Table S1. XRD data and parameters.

	2	3	4	5	10	11
Formula	C ₂ H ₂ N ₅ NaO ₂	C ₂ H ₄ N ₈ O ₂	C ₂ H ₈ N ₁₀ O ₃	C ₂ H ₇ N ₉ O ₃	C ₃ H ₁₀ N ₁₄ O	C ₃ H ₈ N ₁₂ O ₂
FW [g mol ⁻¹]	151.08	172.13	220.18	205.17	258.25	244.21
Crystal system	monoclinic	monoclinic	monoclinic	triclinic	triclinic	monoclinic
Space Group	<i>P</i> 2 ₁ / <i>c</i>	<i>P</i> 2 ₁ / <i>c</i>	<i>P</i> 2 ₁ / <i>n</i>	<i>P</i> −1	<i>P</i> −1	<i>P</i> 2 ₁ / <i>n</i>
Color / Habit	colorless, needle	colorless, plate	colorless, rhomb	colorless, plate	colorless, plate	colorless, block
Size [mm]	0.03 x 0.08 x 0.40	0.44 x 0.12 x 0.07	0.22 x 0.19 x 0.02	0.24 x 0.16 x 0.09	0.40 x 0.25 x 0.06	0.44 x 0.25 x 0.18
<i>a</i> [Å]	3.5759(3)	4.8998(4)	9.0461(5)	6.7588(9)	7.3223(9)	8.4384(5)
<i>b</i> [Å]	16.1740(13)	13.0808(10)	8.4585(4)	7.9235(13)	7.3625(8)	5.4398(3)
<i>c</i> [Å]	9.9739(7)	9.8927(9)	11.0958(5)	8.2845(12)	9.8189(12)	19.7862(10)
α [°]	90	90.00	90.00	105.745(14)	85.379(9)	90.00
β [°]	98.207(8)	102.070(9)	99.371(5)	98.464(12)	74.156(10)	93.384(5)
γ [°]	90	90.00	90.00	110.187(14)	84.561(9)	90.00
<i>V</i> [Å ³]	570.95(8)	620.04(9)	837.68(7)	386.28(12)	506.11(10)	906.67(9)
<i>Z</i>	4	4	4	2	2	4
ρ_{calc} [g cm ⁻³]	1.758	1.844	1.746	1.764	1.695	1.789
μ [mm ⁻¹]	0.212	0.160	0.154	0.156	0.137	0.150
<i>F</i> (000)	304	352	456	212	268	504
$\lambda_{\text{MoK}\alpha}$ [Å]	0.71073	0.71073	0.71073	0.71073	0.71073	0.71073
<i>T</i> [K]	100	100	100	298	100	173
θ min-max [°]	4.3, 26.0	4.21, 26.50	4.44, 26.24	4.26, 26.49	4.17, 26.25	4.28, 26.50
Dataset <i>h</i> ; <i>k</i> ; <i>l</i>	−4:4 ; −19:13; −12:12	−5:6; −16:15; −7:12	−11:10; −6:10; −7:13	−8:3; −9:9; −10:10	−9:9; −9:9; −12:12	−10:10; −6:6; −24:24
Reflect. coll.	2902	3292	3079	2126	3715	6759
Independ. refl.	1128	1284	1687	1573	2032	1878
<i>R</i> _{int}	0.0264	0.0253	0.0257	0.0371	0.0303	0.0289
Reflection obs.	934	1090	1388	938	1573	1607
No. parameters	99	125	168	155	203	186
<i>R</i> ₁ (obs)	0.0334	0.0362	0.0394	0.0708	0.0455	0.0397
<i>wR</i> ₂ (all data)	0.0917	0.0923	0.0930	0.1806	0.1153	0.0984
<i>S</i>	1.05	1.100	1.048	1.039	1.058	1.093
Resd.	−0.21, 0.26	−0.305, 0.240	−0.295, 0.288	−0.344, 0.495	−0.313, 0.367	−0.209, 0.357
Dens.[e Å ⁻³]						
Device type	Oxford XCalibur3 CCD	Oxford XCalibur3 CCD	Oxford XCalibur3 CCD	Oxford XCalibur3 CCD	Oxford XCalibur3 CCD	Oxford XCalibur3 CCD
Solution	SIR-92	SIR-92	SIR-92	SIR-92	SIR-92	SIR-92
Refinement	SHELXL-97	SHELXL-97	SHELXL-97	SHELXL-97	SHELXL-97	SHELXL-97
Absorpt. corr.	multi-scan	multi-scan	multi-scan	multi-scan	multi-scan	multi-scan
CCDC	999287	999288	999291	999289	999292	999290

4.6.2 Calculation of heats of formation

General information about the heat of formation calculations can be found in the appendix of this thesis. The calculation results are summarized in Table S2.

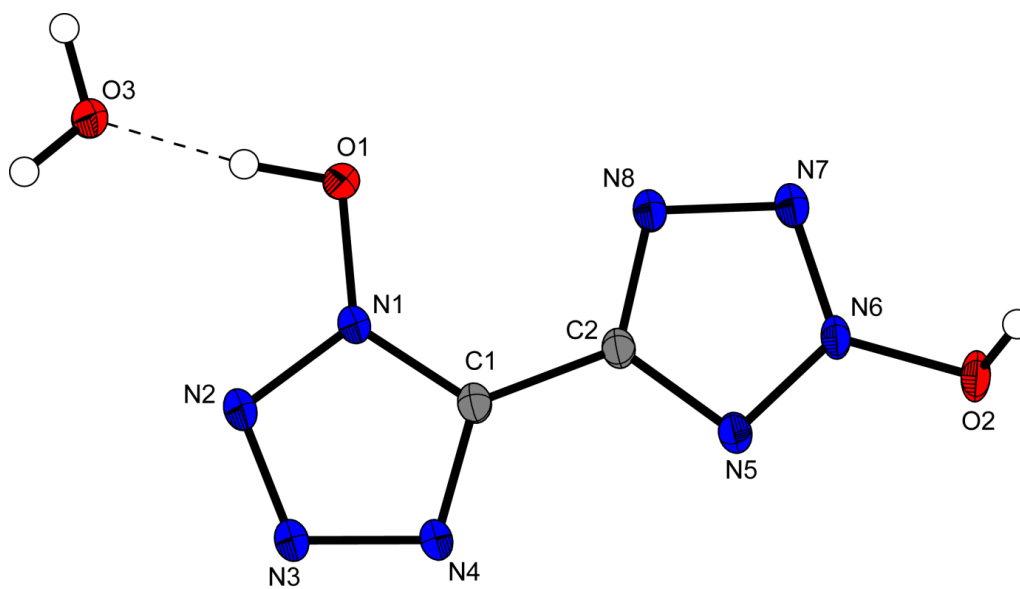
Table S2. Heat of formation calculation results.

M	$-H^{298}$ ^[a] / a.u.	$\Delta_f H^\circ(\text{g}, \text{M})$ / kJ mol ⁻¹ ^[b]	V_M / Å ³ ^[c]	$\Delta U_L, \Delta H_L$; ^[d] ΔH_{sub} ^[e] (3) / kJ mol ⁻¹	$\Delta_f H^\circ(\text{s})$ ^[f] / kJ mol ⁻¹	Δn ^[g]	$\Delta_f U(\text{s})$ ^[f] / kJ kg ⁻¹
3	589.741361	659.0		83.7	575.4	5.5	589.0
3 anion	589.251393	412.1					
3 dianion	588.617028	544.3					
NH₄O⁺	131.863249	687.2					
4		1917.1	215.6	1475.1, 1482.6	434.6	10.5	2092.2
TAG⁺	371.197775	874.3					
10		1285.2	260.6	471.1, 476.1	809.1	12.5	3253.5
H₂DAU²⁺	335.970626	1726.2					
11		2268.7	233.4	2023.0, 2027.9	240.7	11.0	1097.4

^[a] CBS-4M electronic enthalpy; ^[b] gas phase enthalpy of formation; ^[c] molecular volumes taken from X-ray structures and corrected to room temperature; ^[d] lattice energy and enthalpy (calculated using Jenkins and Glasser equations); ^[e] enthalpy of sublimation (calculated by Trouton rule); ^[f] standard solid state enthalpy of formation; ^[g] solid state energy of formation.

Synthesis and Characterization of the Asymmetric 1,2-Dihydroxy-5,5'-bitetrazole and Selected Nitrogen-Rich Derivatives

published in *Eur. J. Inorg. Chem.* **2015**, 17, 2794–2803. (DOI: 10.1002/ejic.201500338)



Abstract: A selective synthesis of asymmetric 1,2'-dihydroxy-5,5'-bitetrazole monohydrate (**4**·H₂O) from inexpensive starting materials is presented. This bitetrazole derivative contains two *N*-oxides at the N1 and at the N2' position, which both increase the energetic performance. Various energetic salts, such as hydroxylammonium (**5**), tetraaminobitriazolium (**10**), and triaminotriazolotriazolium (**11**) were synthesized. Neutral **4** and hydroxylammonium salt **5** were compared in detail with other tetrazole mono- and di-*N*-oxides to gain a deeper insight into the performance increment of *N*-oxides in tetrazoles. Compounds **3–5**, **9**, and **11** were structurally characterized by using single-crystal X-ray diffraction. Additionally, all new compounds were characterized by using NMR, IR and Raman spectroscopy, mass spectrometry, elemental analysis as well as differential thermal analysis (DTA) measurements. The sensitivities of the compounds toward shock, friction, and electrostatic discharge were determined. Finally, the heats of formation were calculated and several detonation parameters were computed with the EXPLO5 v. 6.01 code.

Keywords: *N*-oxides · tetrazoles · structure elucidation · energetic materials · nitrogen heterocycles

5.1 Introduction

In the 20th century the main research focus in the fields of energetic materials was on cyclic and caged nitramines with high energetic performance. Such materials derive most of their energy from the oxidation of a carbon backbone by incorporating the oxidizer in the same molecule. Traditional substances, such as RDX (Hexogen) and HMX (Octogen) (Figure 1) are commonly used, although a replacement is strongly desired because of their toxicity. Modern alternatives could include CL-20 and TKX-50^[1] (Figure 1), which are still under investigation.

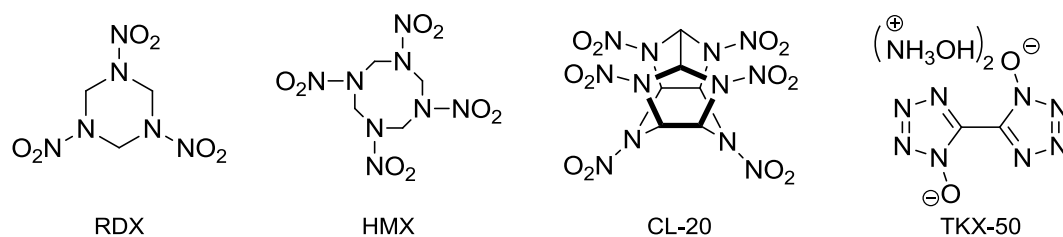


Figure 1. Cyclic and caged nitramines 1,3,5-trinitro-1,3,5-triazinane (RDX), 1,3,5,7-tetranitro-1,3,5,7-tetrazocane (HMX), and 2,4,6,8,10,12-hexanitro-2,4,6,8,10,12-hexaazaisowurtzitane (CL-20) as well as nitrogen-rich, ionic dihydroxylammonium bitetrazole 1-oxide (TKX-50).

A good compromise between high energetic properties and low environmental pollution was achieved through the synthesis of nitrogen-rich compounds that provide high ring- or cage-strain as well as high heats of formation and release nontoxic dinitrogen upon decomposition.^[2,3] One of the most promising energetic building blocks are tetrazoles, which can be combined with oxygen-rich nitro and nitramine groups to compensate for the low oxygen balance of the ring.^[4] Furthermore, bitetrazoles show very high potential due to the high nitrogen content and consequently large number of N–N bonds, leading to high positive heats of formation.^[5,6] The introduction of *N*-oxides in tetrazoles^[7–9] and bitetrazoles resulted in superior energetic performance compared with tetrazoles lacking the *N*-oxide, in particular higher densities and lower sensitivities.^[1] The energetic properties of these compounds partially exceed those of the commonly used RDX and could potentially be used as an environmentally friendly replacement for RDX.

Several bitetrazole *N*-oxides shown in Figure 2 have been synthesized, namely 5,5'-bitetrazole (A),^[5] 1,1'-dihydroxy-5,5'-bitetrazole (B),^[1] 2,2'-dihydroxy-5,5'-bitetrazole (C),^[6] 1-hydroxy-5,5'-bitetrazole (D),^[10] and 2-hydroxy-5,5'-bitetrazole (E).^[11] Bitetrazole B, which crystallizes as a dihydrate, and, particularly, its dihydroxylammonium salt TKX-50, presented an exceptionally high energetic performance compared with RDX and HMX.^[1] The high density of TKX-50 (1.915 g cm⁻³ at 173 K), heat of formation ($\Delta_f H^\circ = 446.6$ kJ mol⁻¹) and high

calculated detonation velocity and pressure ($D = 9698 \text{ m s}^{-1}$, $p_{C-J} = 424 \text{ kbar}$) as well as low sensitivities provide an impetus to study further tetrazole *N*-oxides. These studies on the influence of the position of the *N*-oxide in bitetrazoles resulted in the development of compounds **C**, **D**, and **E**, which all exhibit good energetic performance.^[6,10,11]

In order to complete the study on the performance increment of the *N*-oxide group in bitetrazole ring systems, the synthesis route toward asymmetric 1,2'-dihydroxy-5,5'-bitetrazole **F**, which is still missing in the literature, is reported in this work. Along with the neutral compound, selected energetic nitrogen-rich salts were synthesized and fully characterized. Furthermore, 1,2'-dihydroxy-5,5'-bitetrazole as well as its energetic salts were compared with various hydroxy- and dihydroxy-5,5'-bitetrazoles in order to determine its potential as a secondary explosive.

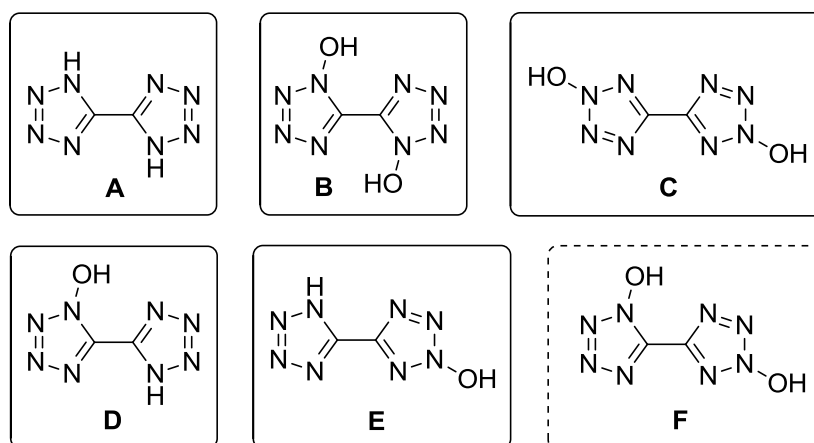


Figure 2. 5,5'-Bitetrazole and hydroxy derivatives: 5,5'-bitetrazole (**A**), 1,1'-dihydroxy-5,5'-bitetrazole (**B**), 2,2'-dihydroxy-5,5'-bitetrazole (**C**), 1-hydroxy-5,5'-bitetrazole (**D**), 2-hydroxy-5,5'-bitetrazole (**E**), and 1,2'-dihydroxy-5,5'-bitetrazole (**F**). Continuous box: reported compounds. Dashed box: investigated in this work.

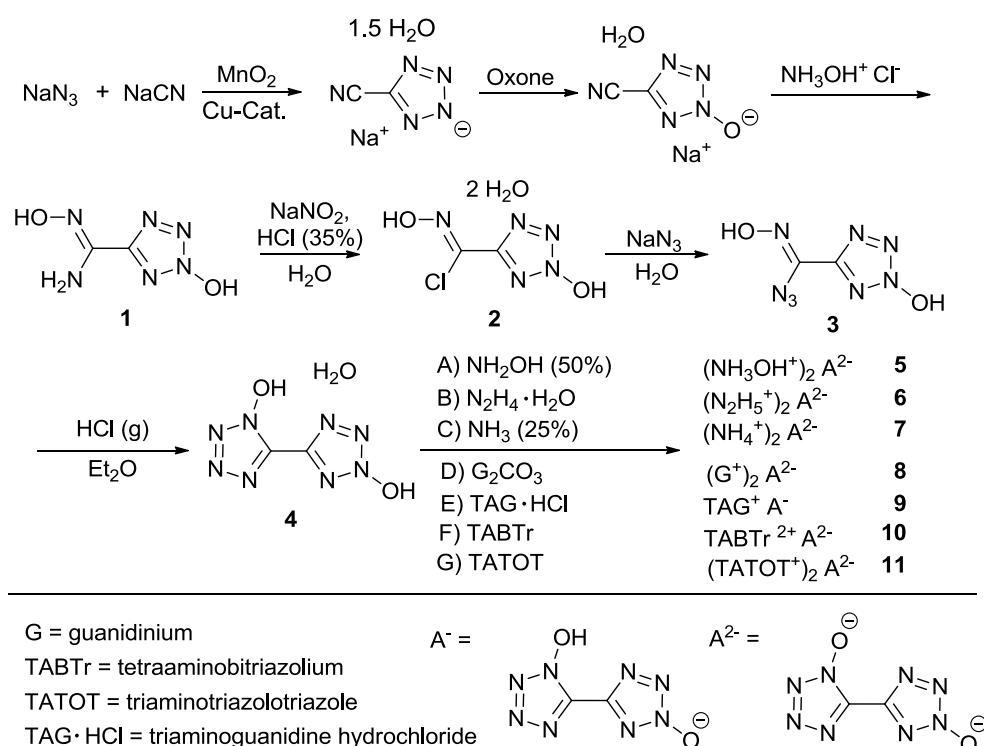
5.2 Results and Discussion

5.2.1 Synthesis

The preparation of 1,2'-dihydroxy-5,5'-bitetrazole monohydrate (**4**·H₂O) and its energetic salts is illustrated in Scheme 1. 5-Aminohydroximoyl-2-hydroxytetrazole (**1**)^[11,12,36] was dissolved in fuming hydrochloric acid and treated with sodium nitrite under cooling to obtain 5-chlorohydroximoyl-2-hydroxytetrazole dihydrate (**2**·2H₂O). In the next step, 5-azidohydroximoyl-2-hydroxytetrazole (**3**) was synthesized by reacting **2**·2H₂O with sodium azide in aqueous solution under constant cooling below 5 °C. Compound **3** is highly sensitive toward friction and impact and should be handled very carefully (impact sensitivity: 1 J,

friction sensitivity: < 5 N, ESD: 10 mJ). Azide **3** was dissolved in diethyl ether and gaseous HCl was bubbled through the solution to close the second tetrazole ring. In this way it was possible to selectively obtain the 1,2'-dihydroxy-5,5'-bitetrazole as the monohydrate **4**·H₂O. Oxidation of 5,5'-bitetrazole with Oxone gave a mixture of 1,1'-, 2,2'-, and 1,2'-dihydroxy-5,5'-bitetrazole.^[6]

The energetic salts were formed by reactions of **4** and selected bases, as illustrated in Scheme 1, which yielded dihydroxylammonium 5,5'-bitetrazole 1,2'-dioxide monohydrate (**5**·H₂O), dihydrazinium 5,5'-bitetrazole 1,2'-dioxide (**6**), diammonium 5,5'-bitetrazole 1,2'-dioxide (**7**), diguanidinium 5,5'-bitetrazole 1,2'-dioxide (**8**), triaminoguanidinium 1-hydroxy-5,5'-bitetrazole 2'-oxide (**9**), 4,4',5,5'-tetraamino-3,3'-bi-1,2,4-triazolium 5,5'-bitetrazole 1,2'-dioxide (**10**), and di-3,6,7-triamino-7*H*-[1,2,4]triazolo[4,3-*b*][1,2,4]triazolium 5,5'-bitetrazole 1,2'-dioxide dihydrate (**11**·2H₂O). Compounds **5**–**8** and **11** were synthesized by adding two equivalents of the corresponding base to one equivalent of 1,2'-dihydroxy-5,5'-bitetrazole monohydrate (**4**·H₂O) under aqueous conditions. In case of **10**, a 1:1 stoichiometric ratio was applied. Compound **9** crystallized in a 1:1 stoichiometry as a monohydrate (**9**·H₂O). Anhydrous **9** was obtained by drying at 80 °C for 2 h.



Scheme 1. Synthetic route toward compounds **1**–**11**.

5.2.2 Crystal Structures

The crystal structures of compounds **2**·2H₂O, **4**·H₂O, **5**·H₂O, **9**·H₂O, and **11**·2H₂O were determined. Table S1 in the Supporting Information illustrates selected data and parameters of the X-ray measurements. To determine the molecular structures of these five compounds in the crystalline state, an Oxford Xcalibur3 diffractometer with a Spellman generator (voltage 50 kV, current 40 mA) and a KappaCCD detector was used. The data collection and reduction was performed with CrysAlisPro software.^[13] The solution and refinement of all structures were performed with the programs SIR-92,^[14] SHELXS-97,^[15] and SHELXL-97^[16] implemented in the WinGX software package^[17] and finally checked with the Platon software.^[18] In all crystal structures, the hydrogen atoms were located and refined. The absorptions were corrected with the SCALE3 ABSPACK multiscan method.^[19] Further crystallographic data for the structures have been deposited with the Cambridge Crystallographic Data Centre (see Table S1).^[20]

5-Chlorohydroximoyl-2-hydroxytetrazole dihydrate (**2**·2H₂O) crystallizes from water in the orthorhombic space group *Pca*2₁ with a density of 1.769 g cm⁻³ at 173 K and four molecules per unit cell. The molecular unit of **2**·2H₂O is illustrated in Figure 3. The length of the C1–C2 bond is 1.465(3) Å and is shorter in comparison to a C–C single bond (1.54 Å), but is in the same range as the previously reported sodium 5-cyanotetrazolate 2-oxide monohydrate, the precursor of **1**.^[9] The O2–N5 bond, with a length of 1.374(2) Å, is only slightly longer than the O1–N2 bond [1.309(2) Å]. The proton between O4 and O1 is located closer to O4 [O4–H4B 0.91(4) Å] than to O1 [O1–H4B 1.67(4) Å], resulting in the protonation of one water molecule and formation of an oxonium ion. The oxygen atom O1 is deprotonated and forms a hydrogen bond, as indicated in Figure 3. The torsion angles N1–C1–C2–N5 [0.0(3)°] and N4–C1–C2–C11 [–0.9(2)°] reveal the planarity of compound **2**·2H₂O.

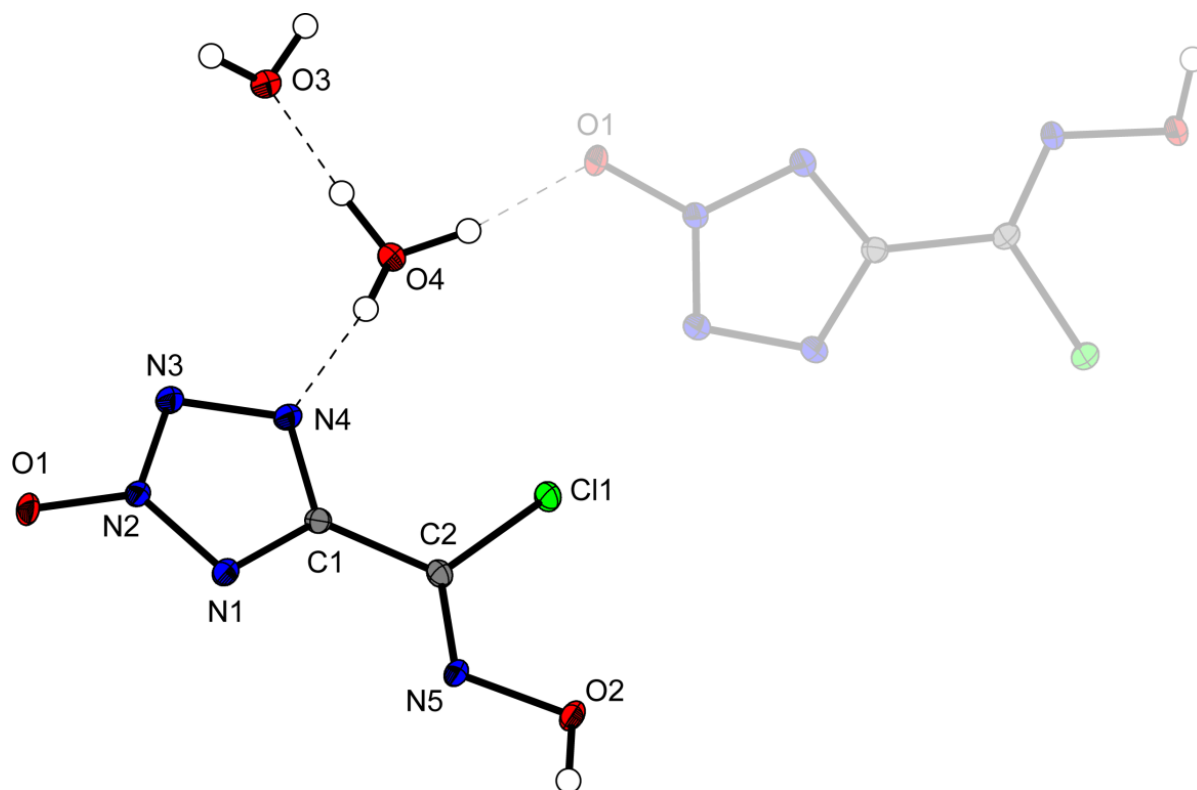


Figure 3. Molecular unit of $2 \cdot 2\text{H}_2\text{O}$. Ellipsoids are drawn at the 50 % probability level. Selected bond lengths (Å): N1–N2 1.328(2), N2–N3 1.318(2), N3–N4 1.342(2), N1–C1 1.332(2), N4–C1 1.338(2), C1–C2 1.465(3), O1–N2 1.309(2), O2–N5 1.374(2); selected bond angles (°): N1–N2–N3 115.17(14), N2–N3–N4 104.63(14), N3–N4–C1 106.42(15), N1–C1–N4 112.74(16), N2–N1–C1 101.03(14); selected hydrogen bond lengths (Å): O4...H4B...O1 0.91(4), 1.67(4), 2.564(2), 169(3); selected torsion angles (°): C1–N1–N2–N3 0.00(19), N1–C1–C2–N5 0.0(3), N4–C1–C2–Cl1 –0.9(2), O2–N5–C2–Cl1 0.6(2).

1,2'-Dihydroxy-5,5'-bitetrazole monohydrate ($4 \cdot \text{H}_2\text{O}$) crystallizes from water in the monoclinic space group $P2_1/n$ with a density of 1.783 g cm^{-3} at 173 K and four molecules per unit cell. The molecular unit of $4 \cdot \text{H}_2\text{O}$ is illustrated in Figure 4. In $4 \cdot \text{H}_2\text{O}$, both tetrazole rings have similar bond lengths and angles of approximately 1.3 Å and 108° , respectively. The torsion angle of N1–C1–C2–N8 is $-4.9(3)^\circ$, showing that the two tetrazole rings are tilted against each other. The length of the connecting C–C bond is 1.449(2) Å and is shorter in comparison to a C–C single bond (1.54 Å). Similar C–C bond lengths can be observed in $5 \cdot \text{H}_2\text{O}$, $9 \cdot \text{H}_2\text{O}$, and $11 \cdot 2\text{H}_2\text{O}$, as well as in the previously reported 5,5'-bitetrazole,^[21] 1,1'-dihydroxy-5,5'-bitetrazole dihydrate^[1] (1.434 Å), and 2,2'-dihydroxy-5,5'-bitetrazole (1.45 Å).^[6] Both N–O bonds are almost equally long [O1–N1 1.3398(17) Å, O2–N6 1.3474(18) Å], as also observed in the case of 1,1'-dihydroxy-5,5'-bitetrazole dihydrate^[1] and 2,2'-dihydroxy-5,5'-bitetrazole.^[6] When comparing the density of $4 \cdot \text{H}_2\text{O}$ at 173 K with other 5,5'-bitetrazoles, $4 \cdot \text{H}_2\text{O}$ shows higher density than 5,5'-bitetrazole but lower density than the more symmetrical 1,1'- and 2,2'-dihydroxy-5,5'-bitetrazole: 5,5'-bitetrazole $1.738^{[21]} < 4 \cdot \text{H}_2\text{O} \ 1.783 < 1,1'$ -dihydroxy-5,5'-bitetrazole dihydrate $1.811^{[1]} < 2,2'$ -dihydroxy-5,5'-bitetrazole 1.953 g cm^{-3} .^[6]

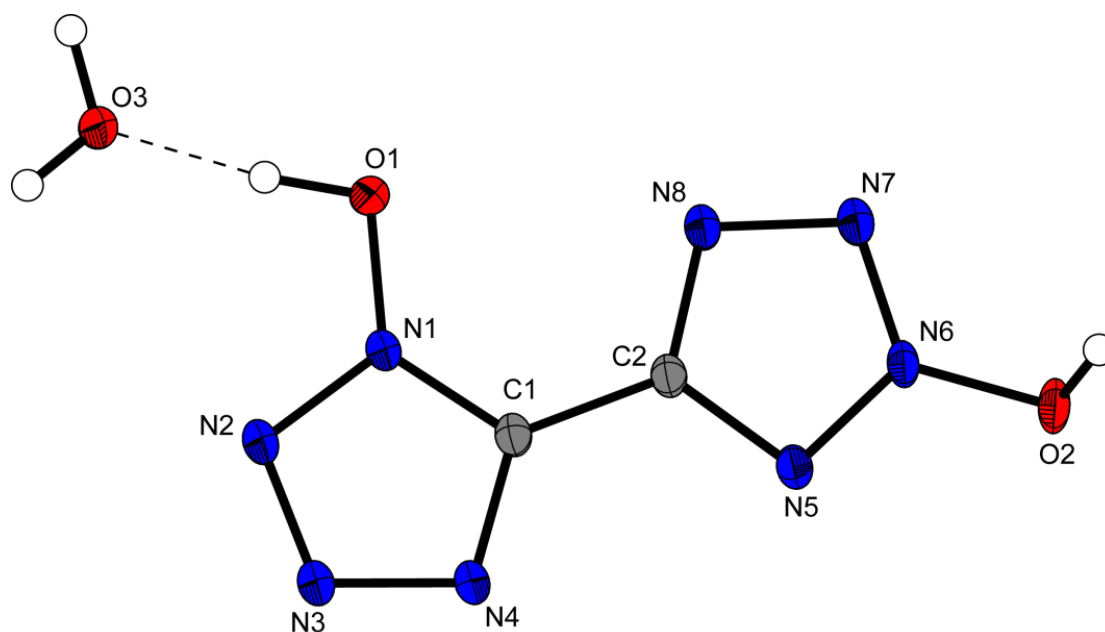


Figure 4. Molecular unit of **4**·H₂O. Ellipsoids are drawn at the 50 % probability level. Selected bond lengths (Å): N2–N3 1.302(2), N4–C1 1.326(2), N5–C2 1.332(2), N6–N7 1.307(2), C1–C2 1.449(2), O1–N1 1.3398(17), O2–N6 1.3474(18); selected bond angles (°): N1–N2–N3 105.55(13), N2–N3–N4 110.69(13), N3–N4–C1 106.52(13), N6–N7–N8 104.61(13), N7–N8–C2 106.08(13), N5–C2–N8 112.96(13); selected torsion angles (°): N1–C1–C2–N8 –4.9(3).

Dihydroxylammonium 5,5'-bitetrazole 1,2'-dioxide monohydrate (**5**·H₂O) crystallizes from water in the monoclinic space group $P2_1/n$ with a density of 1.736 g cm^{–3} at 173 K and four molecules per unit cell. The molecular unit of **5**·H₂O is illustrated in Figure 5. The bond lengths and the angles in both tetrazole rings match the values of compound **4**. The tetrazole rings are tilted against each other by a torsion angle N1–C1–C2–N8 of 7.6(3)°. The N–O bonds in **5**·H₂O have similar lengths; namely O1–N1 1.319(2) Å and O2–N6 1.305(2) Å. In comparison to the densities at 173 K of other dihydroxylammonium salts, the following can be observed: **5**·H₂O 1.736 < dihydroxylammonium 2,2'-dihydroxy-5,5'-bitetrazole 1.832^[6] < TKX-50 1.915 g cm^{–3}.^[1]

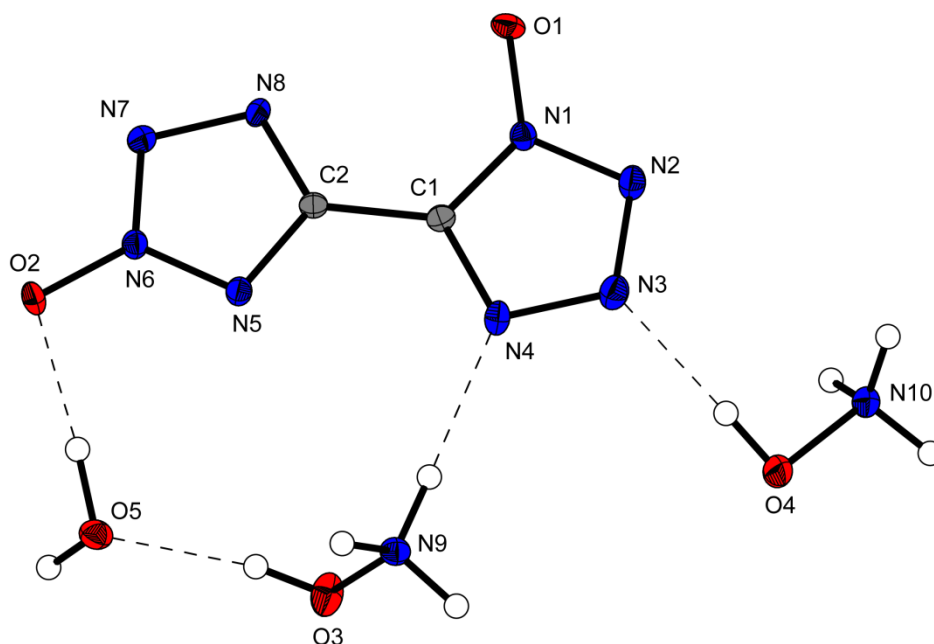


Figure 5. Molecular unit of **5**·H₂O. Ellipsoids are drawn at the 50 % probability level. Selected bond lengths (Å): N1–N2 1.340(2), N4–C1 1.334(3), N7–N8 1.337(2), N5–C2 1.341(3), O1–N1 1.319(2), O2–N6 1.305(2), C1–C2 1.441(3); selected bond angles (°): N1–N2–N3 105.39(16), N3–N4–C1 105.34(17), N6–N7–N8 105.94(16), N7–N8–C2 105.29(18); selected torsion angles (°): N1–C1–C2–N8 7.6(3).

Triaminoguanidinium 1-hydroxy-5,5'-bitetrazole 2'-oxide monohydrate (**9**·H₂O) crystallizes from water in the triclinic space group *P*–1 with two molecules per unit cell. It has a density of 1.704 g cm^{–3} at 173 K, which is higher than the density of the reported bi(triaminoguanidinium) 2,2'-dihydroxy-5,5'-bitetrazole dihydrate (1.600 g cm^{–3}).^[6]

Di-3,6,7-triamino-7*H*-[1,2,4]triazolo[4,3-*b*][1,2,4]triazolium 5,5'-bitetrazole 1,2'-dioxide dihydrate (**11**·2H₂O) crystallizes from water in the monoclinic space group *P*2₁/*c* with a density of 1.729 g cm^{–3} at 173 K and four molecules per unit cell. The bond lengths and angles of the anion and the cation are consistent with the previous structures of **5**·H₂O and **9**·H₂O, and the literature.^[22] The many hydrogen bonds that build up between the amino groups and *N*-oxides could explain the high thermal stability of compound **11**.

The molecular units of **9**·H₂O and **11**·2H₂O are illustrated in Figures 6 and 7, respectively.

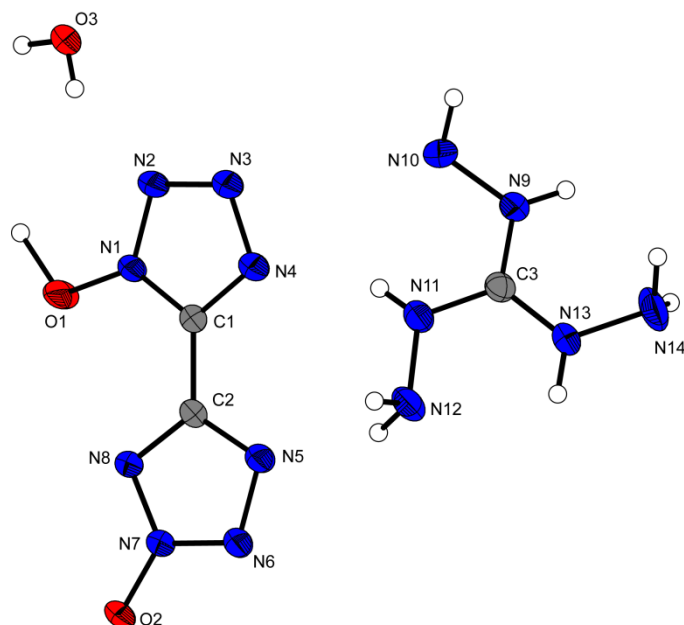


Figure 6. Molecular unit of **9**·H₂O. Ellipsoids are drawn at the 50 % probability level. Selected bond lengths (Å): N1–C1 1.336(2), N2–N3 1.306(2), N5–N6 1.340(2), N8–C2 1.340(2), O1–N1 1.328(2), O2–N7 1.287(2), C1–C2 1.448(2); selected bond angles (°): N1–N2–N3 105.77(13), N3–N4–C1 106.10(14), N6–N5–C2 105.42(14), N5–N6–N7 105.89(14); selected torsion angles (°): N1–C1–C2–N8 –4.0(3).

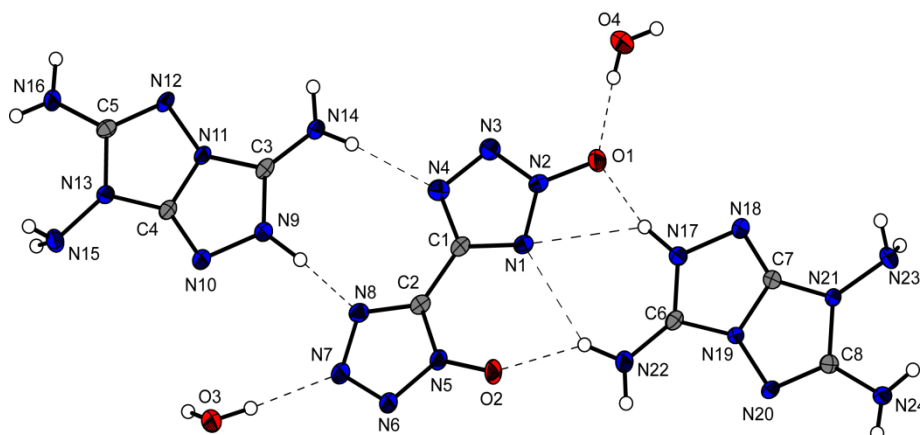


Figure 7. Molecular unit of **11**·2H₂O. Ellipsoids are drawn at the 50 % probability level. Selected bond lengths (Å): N1–N2 1.328(3), N4–C1 1.343(4), N7–N8 1.343(4), N8–C2 1.329(4), O1–N2 1.304(3), O2–N5 1.305(3), C1–C2 1.446(4); selected bond angles (°): N2–N3–N4 105.6(2), N3–N4–C1 105.4(2), N5–N6–N7 106.1(2), N5–C2–N8 107.7(2); selected torsion angles (°): N4–C1–C2–N8 4.0(5).

5.2.3 Thermal Analysis and Sensitivities

The impact and friction sensitivities were explored by BAM methods. The energetic compounds **1–11** reveal strong differences regarding their sensitivities. The impact sensitivity tests were carried out according to STANAG 4489^[23] modified instruction,^[24] using a BAM (Bundesanstalt für Materialforschung) drop hammer.^[25] The friction sensitivity tests were carried out according to STANAG 4487^[26] modified instruction,^[27] using the BAM friction tester. The classification of the tested compounds is based on the “UN Recommendations on

the Transport of Dangerous Goods”.[28] All compounds were tested for their sensitivity toward electrical discharge, using the Electric Spark Tester ESD 2010 EN.[29]

The starting material **1** showed no friction sensitivity (>360 N), but was sensitive toward impact (20 J) and electrostatic discharge (1.0 J). Compound **2**·2H₂O was less sensitive than **1** (IS: 40 J, FS: 360 N). Compounds **3** and **4** showed the highest sensitivities of all measured compounds, and the former was highly sensitive toward impact (1 J), friction (<5 N), and electrostatic discharge (10 mJ) and should be handled very carefully. Compound **3** is more sensitive than 5-azidohydroximoyl-tetrazole monohydrate (IS: 4 J, FS: 60 N).[10] Compound **4** (IS: 3 J, FS: 60 N) shows higher sensitivities than 1,1'-dihydroxy-5,5'-bitetrazole dihydrate (IS: > 40 J, FS: 216 N),[1] but lower sensitivities than 2,2'-dihydroxy-5,5'-bitetrazole (IS: 3 J, FS: < 5 N).[6] When comparing the sensitivities of dihydroxylammonium salts of 5,5'-bitetrazoles, dihydroxylammonium 5,5'-bitetrazole 2,2'-dioxide showed the most sensitive values (IS: 3 J, FS: 60 N).[6] Compound **5** shows higher sensitivity toward impact (10 J) than dihydroxylammonium 5,5'-bitetrazole 1,1'-dioxide (20 J);[1] on the other hand, TKX-50[1] was more sensitive toward friction (120 N).

Differential thermal analysis (DTA) measurements to determine the melting- and decomposition temperatures of compounds **3–11** were performed at a heating rate of 5 °C min⁻¹; the results are illustrated in Figure 8. The decomposition temperatures are given as absolute onset temperatures. Compounds **4** and **5** dehydrate at 86 and 88 °C, respectively. The decomposition temperature of **3** was 127 °C, which is comparable to the decomposition value of 5-azidohydroximoyl-tetrazole monohydrate ($T_{\text{dec}} = 126$ °C).[10] Compound **4**·H₂O ($T_{\text{dec}} = 136$ °C) shows a lower decomposition temperature than 2,2'-dihydroxy-5,5'-bitetrazole ($T_{\text{dec}} = 165$ °C)[6] and 1,1'-dihydroxy-5,5'-bitetrazole dihydrate ($T_{\text{dec}} = 214$ °C).[1] Compound **5**·H₂O decomposed at 192 °C, which is lower than the value of TKX-50 ($T_{\text{dec}} = 221$ °C),[1] but higher than dihydroxylammonium 5,5'-bitetrazole 2,2'-dioxide ($T_{\text{dec}} = 172$ °C).[6] Compounds **6**, **7**, **8**, **10**, and **11** have higher decomposition temperatures than RDX ($T_{\text{dec}} = 210$ °C) and TKX-50 ($T_{\text{dec}} = 221$ °C). Diguanidinium salt **8** had the highest decomposition temperature (300 °C) of the present set of compounds, which is comparable to diguanidinium 5,5'-bitetrazole 2,2'-dioxide with an even higher value (331 °C).[6] For triaminoguanidinium 1-hydroxy-5,5'-bitetrazole 2'-oxide (**9**) the melting point was measured at 162 °C and the decomposition temperature was 180 °C. Ammonium salt **7** showed higher thermal stability ($T_{\text{dec}} = 280$ °C) than diammonium 5,5'-bitetrazole 2,2'-dioxide ($T_{\text{dec}} = 265$ °C).[6]

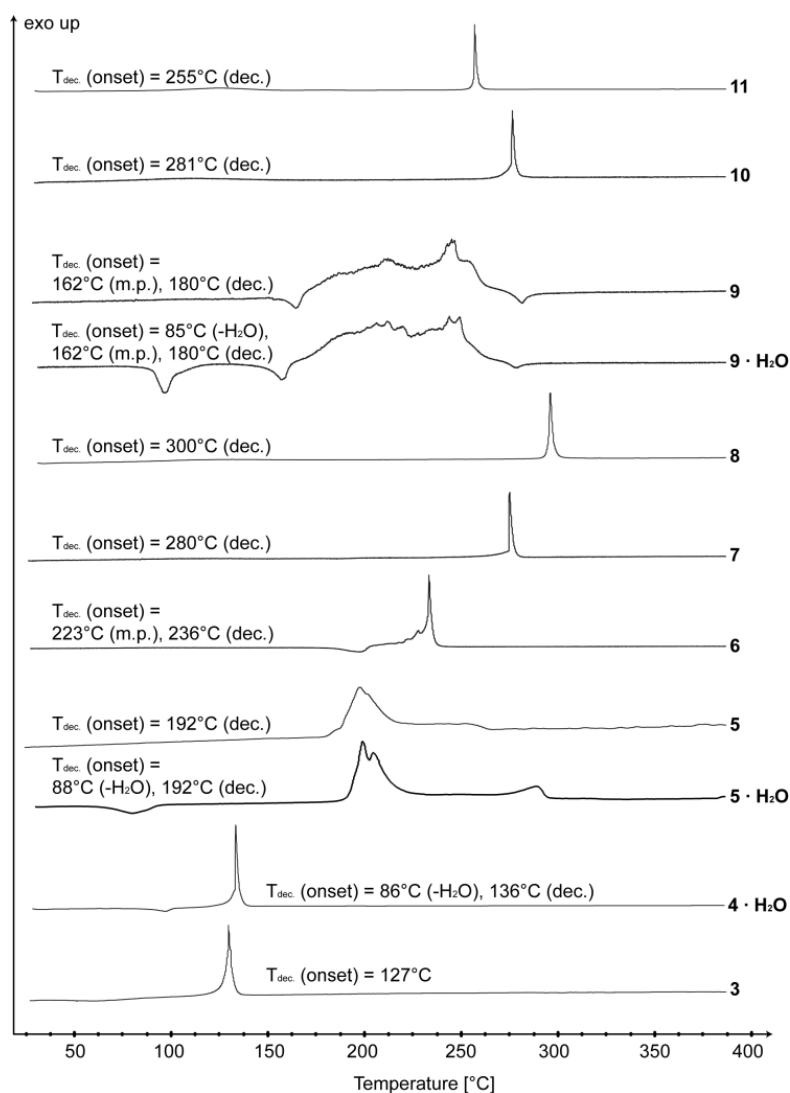


Figure 8. DTA plots of compounds **3–11** measured with a heating rate of $5^{\circ}\text{C min}^{-1}$.

5.2.5 Physiochemical and energetic properties

The calculation of the detonation parameters was performed with the program package EXPLO5 v. 6.01.^[30] The detonation parameters of **4–11**, calculated by using the pycnometrical measured densities of the water-free compounds at room temperature,^[31] are summarized in Table 1 and compared with the values calculated for RDX.

Compounds **4–11** reveal highly diverse results regarding the heats of formation. Compounds **5**, **7**, and **8** have lower heats of formation than the neutral compound **4** ($\Delta_f H^{\circ} = 566.5 \text{ kJ mol}^{-1}$), which is comparable to that of 2,2'-dihydroxy-5,5'-bitetrazole ($559.7 \text{ kJ mol}^{-1}$).^[6] On the other hand, compounds **9**, **10**, and **11** have remarkably high heats of formation of 833.6, 810.9, and $1574.9 \text{ kJ mol}^{-1}$, respectively, with **11** being by far the highest. When comparing other dihydroxylammonium salts of 5,5'-bitetrazoles,

Table 1. Energetic Properties and detonation parameters of anhydrous compounds **4–11** in comparison to RDX.

	4	5	6	7	8	9	10	11	RDX
Formula	C ₂ H ₂ N ₈ O ₂	C ₂ H ₈ N ₁₀ O ₄	C ₂ H ₁₀ N ₁₂ O ₂	C ₂ H ₈ N ₁₀ O ₂	C ₄ H ₁₂ N ₁₄ O ₂	C ₃ H ₁₀ N ₁₄ O ₂	C ₆ H ₁₀ N ₁₈ O ₂	C ₈ H ₁₄ N ₂₄ O ₂	C ₃ H ₆ N ₆ O ₆
FW [g mol ⁻¹]	170.09	236.15	234.18	204.15	288.24	274.21	366.27	478.37	222.12
<i>IS</i> [J] ^a	3	10	10	40	40	3	40	40	7.5
<i>FS</i> [N] ^b	60	240	324	360	360	288	360	360	120
<i>ESD</i> [J] ^c	0.50	1.0	0.5	1.5	1.5	0.7	0.3	1.5	0.20
<i>N</i> [%] ^d	65.88	59.31	71.77	68.61	68.03	71.51	68.84	70.27	37.84
<i>Ω</i> [%] ^e	-28.22	-27.10	-47.83	-47.02	-66.61	-52.52	-65.53	-70.24	-21.61
<i>T</i> _{dec.} [°C] ^f	136	192	236	280	300	180	281	255	210
<i>ρ</i> [g cm ⁻³] (298K) ^g	1.78	1.75	1.70	1.72	1.59	1.59	1.79	1.66	1.806
<i>Δ_fH</i> ^o [kJ mol ⁻¹] ^h	566.5	451.8	591.1	275.9	346.7	833.6	810.9	1574.9	70.3
<i>Δ_fU</i> ^o [kJ kg ⁻¹] ⁱ	3418.1	2028.6	2651.0	1473.0	1323.4	3157.5	2315.6	3396.0	417.0
EXPLO5 V6.01 values:									
- <i>Δ_EU</i> ^o [kJ kg ⁻¹] ^j	5638	5869	5027	4078	3358	5154	3841	4658	5845
<i>T_E</i> [K] ^k	4153	3727	3088	2736	2382	3326	2696	3107	3810
<i>p_{C-J}</i> [kbar] ^l	331	341	308	278	203	258	270	249	345
<i>D</i> [m s ⁻¹] ^m	8932	9187	9123	8696	7759	8440	8545	8297	8861
<i>V₀</i> [L kg ⁻¹] ⁿ	808	920	943	921	882	901	803	808	785
a impact sensitivity (BAM drophammer, 1 of 6); b friction sensitivity (BAM friction tester, 1 of 6); c electrostatic discharge device (OZM); d nitrogen content; e oxygen balance; f decomposition temperature from DTA (<i>β</i> = 5°C); g measured pycnometrically at room temperature; h in parenthesis values for the density obtained from the X-ray measurement at 298K; i calculated (CBS-4M) heat of formation; j calculated energy of formation; k energy of explosion; l explosion temperature; m detonation pressure; n detonation velocity; o assuming only gaseous products.									

as TKX-50 ($\Delta_f H^\circ = 446.6 \text{ kJ mol}^{-1}$)^[11] and dihydroxylammonium 5,5'-bitetrazole 2,2'-dioxide ($\Delta_f H^\circ = 390.7 \text{ kJ mol}^{-1}$),^[6] compound **5** presents the highest heat of formation ($451.8 \text{ kJ mol}^{-1}$). In comparison to the values reported for diammonium 5,5'-bitetrazole 2,2'-dioxide ($\Delta_f H^\circ = 257.3 \text{ kJ mol}^{-1}$)^[6] and diguanidinium 5,5'-bitetrazole 2,2'-dioxide ($\Delta_f H^\circ = 322.0 \text{ kJ mol}^{-1}$),^[6] compounds **7** ($\Delta_f H^\circ = 275.9 \text{ kJ mol}^{-1}$) and **8** ($\Delta_f H^\circ = 346.7 \text{ kJ mol}^{-1}$) have similar heats of formation. The synthesized compounds **4–11** all have much higher heats of formation than RDX (70.3 kJ mol^{-1}). The neutral compound **4** has a relatively high detonation velocity of 8932 m s^{-1} and detonation pressure of 331 kbar. Both values are lower than those of the more symmetric 2,2'-dihydroxy-5,5'-bitetrazole ($D = 9364 \text{ m s}^{-1}$, $p_{C-J} = 409 \text{ kbar}$)^[6] but are in the same range as those of RDX ($D = 8861 \text{ m s}^{-1}$, $p_{C-J} = 345 \text{ kbar}$). The diguanidinium salt **8** has the lowest detonation velocity of 7759 m s^{-1} and detonation pressure of 203 kbar of all measured energetic salts, which is consistent with the reported diguanidinium 5,5'-bitetrazole 2,2'-dioxide ($D = 7752 \text{ m s}^{-1}$, $p_{C-J} = 221 \text{ kbar}$).^[6] Compound **5** has a lower detonation velocity ($D = 9187 \text{ m s}^{-1}$) and detonation pressure ($p_{C-J} = 341 \text{ kbar}$) than dihydroxylammonium 5,5'-bitetrazole 2,2'-dioxide ($D = 9264 \text{ m s}^{-1}$, $p_{C-J} = 372 \text{ kbar}$)^[6] and TKX-50 ($D = 9698 \text{ m s}^{-1}$, $p_{C-J} = 424 \text{ kbar}$).^[11] However, **5** exceeds the energetic properties of dihydroxylammonium 5,5'-bitetrazole 1-oxide^[10] and dihydroxylammonium 5,5'-bitetrazole 2-oxide^[11] and has a similar detonation pressure, but higher detonation velocity than RDX.

5.2.6 NMR spectroscopy

All compounds described were characterized by using multinuclear NMR spectroscopy. Chemical shifts are given with respect to TMS (^1H , ^{13}C) in $[\text{D}_6]\text{DMSO}$ as the solvent.

The ^1H NMR spectrum of **4**· H_2O shows one broad peak at $\delta = 9.93 \text{ ppm}$, which indicates the hydroxy groups. The two sharp carbon signals at 146.0 (CN₄O with the 2-*N*-oxide) and 137.9 ppm (CN₄O with the 1-*N*-oxide) were assigned by comparison to other hydroxy-5,5'-bitetrazoles: chemical shifts of the carbon in the tetrazole ring with the 1-*N*-oxide are reported at $\delta = 135.8 \text{ ppm}$ for 1,1'-dihydroxy-5,5'-bitetrazole dihydrate^[1] and at $\delta = 138.1 \text{ ppm}$ for 1-hydroxy-5,5'-bitetrazole,^[10] whereas the 2-*N*-oxide carbon signals are shifted downfield to 151.6 ppm for 2,2'-dihydroxy-5,5'-bitetrazole^[6] and to $\delta = 148.4 \text{ ppm}$ for 2-hydroxy-5,5'-bitetrazole.^[11] The carbon signals of salts **5–11** were observed between 142.2 and 146.1 ppm for the tetrazole ring comprising the 2-*N*-oxide group and between 136.0 and 140.4 ppm for the tetrazole ring comprising the 1-*N*-oxide. Proton signals of **6**, **7**, and **8** between 7.18 and

7.42 ppm are comparable to other reported salts of 2,2'-dihydroxy-5,5'-bitetrazole^[6] and 1-hydroxy- or 2-hydroxy-5,5'-bitetrazoles.^[10,11]

5.2.7 Vibrational Spectroscopy

IR and Raman spectra were measured and used for identification of structural elements and functional groups of compounds **1–11**. The frequencies were assigned according to commonly observed values in the literature.^[32,33]

The characteristic IR vibrations of bitetrazoles in the neutral compound **4** along with its energetic salts **5–11** are observed in the range of 1600–700 cm⁻¹, including the N1–C1–N4 symmetric and asymmetric deformation vibrations, the N2–N3 and N3–N4 stretches as well as the stretching vibration of the cyclic C=N bond reported in the literature.^[9,12] Strong bands in the range of 1500–1400 cm⁻¹ of all investigated compounds represent the N–O stretching vibrations. Additionally, the spectrum of **4**·H₂O shows a strong band at 3196 cm⁻¹, indicating the O–H vibration of the compound and the crystal water. The asymmetric stretching vibrations of the ammonium cation in **7** can be found at 3011 cm⁻¹, with deformation vibrations around 1400 cm⁻¹. The C=N stretching vibrations of the guanidinium salt **8** as well as the triaminoguanidinium salt **9** can be assigned to very strong absorption bands at 1645 (**8**) and 1679 (**9**) cm⁻¹. Furthermore, compounds **8–10** exhibit N–H stretching vibrations of the amino groups in the range of 3500–3300 cm⁻¹ and N–H deformation vibrations, ranging from 1645 to 1689 cm⁻¹.

The Raman spectra of **4–11** show distinctive absorptions for bitetrazole *N*-oxides. The valence vibrations of the C–C bonds of compounds **4–11** are visible in the strongest bands at 1614 (**4**), 1603 (**5**), 1604 (**6**), 1605 (**7**), 1601 (**8**), 1611 (**9**), 1602 (**10**), and 1615 (**11**) cm⁻¹. The absorptions from 1048 to 1002 cm⁻¹ additionally indicate the N–O valence vibrations of all measured compounds.

5.3 Conclusions

Compound **4**·H₂O was synthesized and characterized with various methods: differential thermal analysis, NMR, IR, and Raman spectroscopy, mass spectrometry, elemental analysis and sensitivity tests. Furthermore single-crystal structures of compounds **2**, **4**, **5**, **9**, and **11** were measured and the results reveal that these compounds crystallize in the monoclinic space groups *P*2₁/*n* (**4**·H₂O, **5**·H₂O), *P*2₁/*c* (**11**·2H₂O), orthorhombic space group *Pca*2₁ (**2**·H₂O), and triclinic space group *P*–1 (**9**·H₂O) with densities between 1.704 g cm⁻³ (**9**·H₂O) and 1.783 g cm⁻³ (**4**·H₂O) at 173 K. The diammonium salt **7** and the diguanidinium salt **8** exhibit

remarkably high decomposition temperatures of 280 °C (**7**) and 300 °C (**8**), which is common for ammonium and guanidinium salts of bitetrazoles. The dihydroxylammonium salt **5** seems to be less sensitive toward physical impact than dihydroxylammonium 5,5'-bitetrazole 2,2'-dioxide and TKX-50,^[1] which makes it safer to handle. The detonation parameters of the dihydroxylammonium salt **5** are the highest among all the synthesized compounds, the detonation pressure of **5** ($p_{C-J} = 341$ kbar) is in the same range and the detonation velocity ($D = 9187$ m s⁻¹) is even higher than that of RDX.

The discussed densities, physiochemical properties and sensitivities show a general trend regarding the introduction of *N*-oxides in bitetrazoles (Figure 9): the energetic performance of the bitetrazoles increases with the number of *N*-oxide substituents and the symmetry of the structure. In addition, bitetrazole 1-*N*-oxides show higher performance than the corresponding 2-*N*-oxide derivatives. 5,5'-Bitetrazole exhibits lower energetic properties than 1-hydroxy- and 2-hydroxy-5,5'-bitetrazole, whereas the energetic performance of dihydroxy-5,5'-bitetrazoles exceeds that of the mono-substituted derivatives.

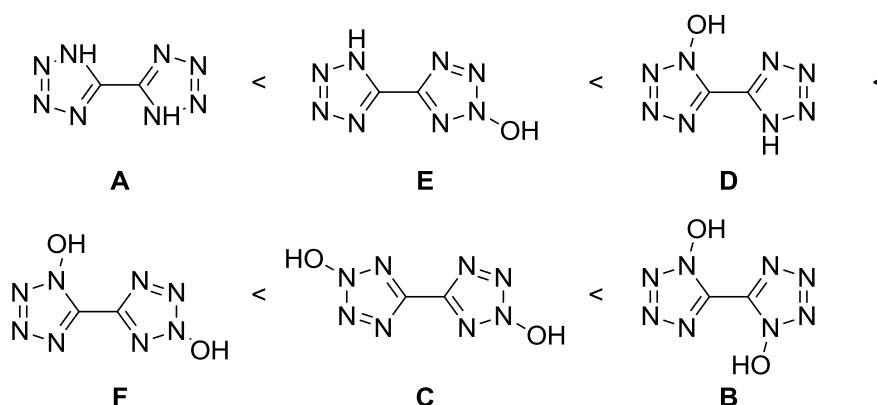


Figure 9. Illustration of the performance increment caused by the introduction of *N*-oxides to 5,5'-bitetrazole.

5.4 Experimental Section

General Information

Caution! 5-Azidohydroximoyl-2-hydroxytetrazole (**3**), 1,2'-dihydroxy-5,5'-bitetrazole monohydrate (**4**·H₂O), and the salts thereof are energetic materials with increased sensitivities toward shock and friction. **Special caution is recommended for working with azide 3 (IS = 1 J, FS < 5 N).** Therefore, suitable safety precautions (safety glass, face shield, ear protection, Kevlar[®] gloves, and earthed equipment) must be applied while synthesizing and handling the described compounds.

General Information: All chemicals and solvents were employed as received (Sigma–Aldrich, Fluka, Acros). ^1H and ^{13}C NMR spectra were recorded with a JEOL Eclipse 270, JEOL EX 400, or a JEOL Eclipse 400 instrument. The chemical shifts quoted in ppm in the text refer to typical standards such as tetramethylsilane (^1H , ^{13}C). To determine the melting and decomposition temperatures of the described compounds a Linseis PT 10 DSC (heating rate $5\text{ }^\circ\text{C min}^{-1}$) was used. Infrared spectra were measured with a Perkin–Elmer Spectrum One FTIR spectrometer as KBr pellets. Transmittance values are described as strong (s), medium (m), and weak (w). Raman spectra were recorded with a Bruker MultiRAM Raman Sample Compartment D418 equipped with a Nd-YAG-Laser (1064 nm) and a LN-Ge diode as detector. The intensities are reported as percentages of the most intense peak and are given in parentheses. Mass spectra of the described compounds were measured with a JEOL MStation JMS 700 using either FAB or DEI technique. To measure elemental analyses a Netsch STA 429 simultaneous thermal analyzer was employed. Sensitivity data were determined with a BAM drop hammer and a BAM friction tester. The electrostatic sensitivity tests were carried out with an electric spark tester ESD 2010 EN (OZM Research).

All quantum chemical calculations were carried out with the Gaussian G09 program package.^[34] The detonation parameters were calculated with the program EXPLO5 v. 6.01. The program is based on the steady-state model of equilibrium detonation and uses Becker–Kistiakowsky–Wilson's equation of state (BKW EOS) for gaseous detonation products and Cowan–Fickett EOS for solid carbon. The calculation of the equilibrium composition of the detonation products is done by applying modified White, Johnson and Dantzig's free energy minimization technique. The program is designed to enable the calculation of detonation parameters at the CJ point.

Precursors sodium 5-cyanotetrazolate sesquihydrate, sodium cyanotetrazole 2-oxide monohydrate, and 2-hydroxy-5-aminohydroximoyl-tetrazole were synthesized according to reported procedures.^[11,12,36]

5-Chlorohydroximoyl-2-hydroxytetrazole dihydrate ($2\cdot 2\text{H}_2\text{O}$)

5-Aminohydroximoyl-2-hydroxytetrazole (**1**; 5.85 g, 40.60 mmol, 1.0 equiv.) was dissolved in hydrochloric acid (150 mL). The solution was cooled with an ice bath and additionally 30 g of ice were added. An aqueous solution of sodium nitrite (8.40 g, 121.80 mmol, 3.0 equiv.) in H_2O (20 mL) was added dropwise over 1 h. The solution was then warmed to ambient temperature and stirred for 30 min under a constant N_2 flow to expel nitrous gasses. The solution was diluted with water (150 mL) and extracted with diethyl ether ($3 \times 100\text{ mL}$) to

give **2** (4.94 g, 24.76 mmol, 61%) as colorless needles. Recrystallization from acetone gave colorless needles of **2**·2H₂O that were suitable for X-ray analysis.

IR (ATR, cm⁻¹): $\tilde{\nu}$ = 3518 (w), 2822 (w), 1632 (w), 1523 (w), 1465 (m), 1428 (w), 1402 (m), 1357 (s), 1232 (m), 1153 (w), 1127 (w), 1042 (vs), 961 (s), 855 (w), 776 (s), 751 (s), 735 (s), 687 (m); **Raman** (1064 nm, 300 mW, 25 °C, cm⁻¹): $\tilde{\nu}$ = 1627 (65), 1515 (89), 1476 (13), 1430 (5), 1405 (9), 1387 (6), 1235 (23), 1156 (21), 1124 (12), 1036 (86), 964 (17), 738 (10), 692 (21), 597 (12), 558 (12), 446 (12), 405 (4), 365 (4), 292 (10), 281 (13), 212 (10), 186 (18), 156 (20), 156 (20), 133 (45), 117 (100), 90 (67), 69 (22); **¹H NMR** (270 MHz, [D₆]DMSO, 25 °C, TMS): δ = 13.01 (s, 1 H, CN₄OH), 5.66 (s, 1 H, C(NO₂)Cl) ppm; **¹³C NMR** (68 MHz, [D₆]DMSO, 25 °C, TMS): δ = 154.7 (s, CN₄OH), 125.5 (s, C(NO₂)Cl) ppm; **EA** (C₂H₆ClN₅O₄, 199.55) calcd.: C 12.04, H 3.03, N 35.10%; found C 12.26, H 3.04, N 35.05%; **Sensitivities**: IS: 40 J; FS: 360 N (at grain size 100–500 μm).

5-Azidohydroximoyl-2-hydroxytetrazole (**3**)

Compound **2**·2H₂O (1.84 g, 9.22 mmol, 1.0 equiv.) was dissolved in water and cooled with an ice bath. An aqueous solution of sodium azide (1.32 g, 20.28 mmol, 2.2 equiv.) was added dropwise over 1 h while the temperature was kept below 5 °C. An aqueous solution of sodium bicarbonate (0.93 g, 11.06 mmol, 1.2 equiv.) was then added slowly and the reaction mixture was stirred for 1 h. The solution was adjusted to pH 1 by addition of conc. hydrochloric acid (solution colour turned from orange to yellow). The product was extracted with diethyl ether (3 × 50 mL) to give **3** (0.71 g, 4.17 mmol, 45 %) as slightly yellow crystals.

DTA (5 °C min⁻¹) onset: 127 °C (dec.); **IR** (ATR, cm⁻¹): $\tilde{\nu}$ = 3136 (w), 3015 (m), 2821 (m), 2557 (m), 2362 (w), 2184 (m), 2134 (m), 1693 (w), 1632 (m), 1590 (w), 1468 (m), 1405 (vs), 1280 (vs), 1176 (s), 1132 (m), 1039 (m), 991 (m), 958 (s), 879 (m), 789 (vs), 730 (m), 694 (m); **Raman** (1064 nm, 300 mW, 25 °C, cm⁻¹): $\tilde{\nu}$ = 2841 (5), 2192 (11), 2137 (12), 1632 (75), 1594 (90), 1536 (95), 1490 (17), 1470 (25), 1412 (18), 1304 (9), 1283 (12), 1251 (10), 1187 (25), 1129 (12), 1055 (24), 1030 (20), 994 (39), 984 (22), 959 (12), 876 (18), 788 (11), 734 (8), 595 (9), 595 (9), 442 (16), 370 (15), 305 (23), 239 (39), 120 (98), 106 (100); **¹H NMR** (270 MHz, [D₆]DMSO, 25 °C, TMS): δ = 12.22 (s, 1 H, CN₄OH), 6.95 (s, 1 H, C(NO₂)N₃) ppm; **¹³C NMR** (68 MHz, [D₆]DMSO, 25 °C, TMS): δ = 153.4 (s, CN₄OH), 133.7 (s, C(NO₂)N₃) ppm; **MS** *m/z* (FAB⁻): 169.1 (C₂HN₈O₂⁻); **EA** (C₂H₄N₈O₂, 170.09) calcd.: C 13.96, H 2.34, N 65.11%; found: C 14.54, H 2.44, N 64.64%. **Sensitivities**: IS: 1 J; FS: < 5 N; ESD: 10 mJ (at grain sizes < 100 μm).

1,2'-Dihydroxy-5,5'-bitetrazole monohydrate ($4 \cdot \text{H}_2\text{O}$)

Compound **3** (1.68 g, 9.88 mmol) was suspended in diethyl ether (100 mL). Gaseous hydrochloric acid was bubbled through the reaction mixture at 0 to 5 °C while stirring for 1 h. The reaction was observed carefully and HCl addition was paused when the temperature rose above 10 °C. The round-bottomed flask was sealed and stirred at room temperature overnight. The solvent was then evaporated to give $4 \cdot \text{H}_2\text{O}$ (1.50 g, 7.97 mmol, 81%) as a pale-yellowish solid. Recrystallization from diethyl ether gave yellowish crystals (1.10 g, 5.85 mmol, 59%) that were suitable for X-ray diffraction. Compound $4 \cdot \text{H}_2\text{O}$ can be dried at 90 °C for 1 h to give anhydrous 1,2'-dihydroxy-5,5'-bitetrazole (**4**).

DTA (5 °C min⁻¹) onset: 86 °C ($-\text{H}_2\text{O}$), 136 °C (dec.); **IR** (ATR, cm⁻¹): $\tilde{\nu}$ = 3196 (s), 1681 (s), 1601 (w), 1503 (m), 1405 (m), 1357 (s), 1333 (s), 1321 (vs), 1253 (s), 1220 (s), 1116 (m), 1047 (m), 1010 (s), 997 (s), 790 (m), 733 (m) cm⁻¹; **Raman** (1064 nm, 300 mW, 25 °C, cm⁻¹): $\tilde{\nu}$ = 1614 (75), 1371 (12), 1324 (6), 1251 (42), 1177 (23), 1145 (24), 1040 (38), 1018 (21), 755 (20), 502 (5), 422 (10), 388 (12), 274 (14), 253 (9), 226 (9), 177 (16), 128 (27), 105 (100), 84 (65) cm⁻¹; **¹H NMR** (270 MHz, [D₆]DMSO, 25 °C, TMS): δ = 9.93 (br. s, 2 H, OH) ppm; **¹³C NMR** (68 MHz, [D₆]DMSO, 25 °C, TMS): δ = 146.0 (s, CN₄OH (2*N*-oxide)), 137.9 (s, CN₄OH (1*N*-oxide)) ppm; **MS** *m/z* (FAB⁻): 169.1 (C₂HN₈O₂⁻). **EA** (C₂H₂N₈O₂·H₂O, 188.11) calcd.: C 12.77, H 2.14, N 59.57%; found C 13.44, H 2.38, N 60.50%; **Sensitivities**: IS: 3 J; FS: 60 N; ESD: 500 mJ (at grain sizes 100–500 μm).

Dihydroxylammonium 5,5'-bitetrazole-1,2'-dioxide monohydrate ($5 \cdot \text{H}_2\text{O}$)

To a solution of $4 \cdot \text{H}_2\text{O}$ (700 mg, 3.72 mmol, 1 equiv.) in ethanol (30 mL), a solution of hydroxylamine (50 % w/v, 0.49 g, 7.44 mmol, 2 equiv.) was added. A colorless precipitate started to form immediately. After stirring for 20 min, the solution was filtered to give **5** (770 mg, 3.03 mmol, 81%). Recrystallization from water gave colorless crystals of $5 \cdot \text{H}_2\text{O}$.

DTA (5 °C min⁻¹) onset: 88 °C ($-\text{H}_2\text{O}$), 192 °C (dec.); **IR** (ATR, cm⁻¹): $\tilde{\nu}$ = 3159 (m), 2917 (m), 2711 (m), 2360 (w), 1628 (w), 1601 (w), 1539 (w), 1495 (w), 1458 (m), 1393 (m), 1370 (s), 1330 (m), 1243 (s), 1237 (vs), 1194 (s), 1042 (w), 1016 (w), 999 (s), 828 (vw), 782 (m), 752 (m), 708 (m); **Raman** (1064 nm, 300 mW, 25 °C, cm⁻¹): $\tilde{\nu}$ = 3114 (5), 2985 (5), 2700 (5), 1603 (100), 1328 (5), 1236 (16), 1141 (10), 1124 (15), 1026 (36), 1004 (20), 785 (4), 756 (9), 749 (9), 439 (7), 414 (8), 284 (7), 99 (56); **¹H NMR** (270 MHz, [D₆]DMSO, 25 °C, TMS): δ = 8.54 (br. s, NH₃OH⁺) ppm; **¹³C NMR** (68 MHz, [D₆]DMSO, 25 °C, TMS): δ = 146.1 (s, CN₄O (2*N*-oxide)), 136.5 (s, CN₄O (1*N*-oxide)) ppm; **MS** *m/z* (FAB⁻): 169.1 (C₂HN₈O₂⁻); *m/z* (FAB⁺): 34.0 (NH₃OH⁺); **EA** (C₂H₁₀N₁₀O₅, 254.16) calcd.: C 9.45, H 3.97,

N 55.11%; found: C 9.31, H 4.09, N 56.97%; **Sensitivities**: IS: 10 J, FS: 240 N, ESD: 1000 mJ (at grain sizes < 100 μm).

Dihydrazinium 5,5'-bitetrazole-1,2'-dioxide (6)

Compound **4**·H₂O (0.94 g, 5 mmol, 1 equiv.) was dissolved in H₂O (20 mL). Hydrazinium hydroxide (0.50 g, 10 mmol, 2 equiv.) was added and the mixture was heated to 80 °C for 20 min. The solution was filtered and the solution left open to the air to slowly evaporate the solvent to give **6** (0.92 g, 3.93 mmol, 79%) as a white powder.

DTA (5 °C min⁻¹) onset: 223 °C (m.p.), 236 °C (dec.); **IR** (ATR, cm⁻¹): $\tilde{\nu}$ = 3283 (m), 3094 (m), 2929 (m), 2656 (m), 1652 (w), 1611 (m), 1557 (m), 1461 (s), 1350 (s), 1232 (s), 1193 (m), 1131 (vs), 1119 (s), 968 (vs), 778 (m), 753 (m); **Raman** (1064 nm, 300 mW, 25 °C, cm⁻¹): $\tilde{\nu}$ = 3193 (4), 1604 (100), 1462 (5), 1393 (4), 1383 (6), 1364 (5), 1233 (24), 1123 (12), 1041 (9), 1016 (56), 969 (11), 753 (15), 546 (3), 446 (5), 380 (8), 349 (6), 186 (8), 96 (82); **¹H NMR** (270 MHz, [D₆]DMSO, 25 °C, TMS): δ = 7.31 ppm (br s, 5H; N₂H₅⁺); **¹³C NMR** (68 MHz, [D₆]DMSO, 25 °C, TMS): δ = 145.9 (s, CN₄O (2*N*-oxide)), 136.3 ppm (s, CN₄O (1*N*-oxide)); **MS** *m/z* (FAB⁻): 169.2 (C₂HN₈O₂⁻); *m/z* (FAB⁺): 33.1 (N₂H₅⁺); **EA** (C₂H₁₀N₁₂O₂, 234.18) calcd.: C 10.26, H 4.30, N 71.77%; found: C 10.27, H 4.16, N 71.56%; **Sensitivities**: IS: 10 J; FS: 324 N; ESD: 500 mJ (at grain sizes <100 μm).

Diammonium 5,5'-bitetrazol-1,2'-dioxide (7)

Compound **4**·H₂O (0.94 g, 5 mmol, 1 equiv.) was dissolved in H₂O (20 mL). A 2 M NH₃ solution (5 mL, 10 mmol, 2 equiv.) was added and the mixture was stirred for 10 min. The solution was filtered and the solution left open to the air to slowly evaporate the solvent to give **7** (0.91 g, 4.46 mmol, 89 %) as a white powder.

DTA (5 °C min⁻¹) onset: 280 °C (dec.); **IR** (ATR, cm⁻¹): $\tilde{\nu}$ = 3156 (w), 3011 (m), 2814 (m), 1730 (w), 1673 (w), 1433 (vs), 1404 (s), 1376 (vs), 1330 (s), 1232 (s), 1197 (m), 1101 (m), 1038 (m), 998 (s), 780 (s), 751 (m), 716 (m), 614 (m); **Raman** (1064 nm, 300 mW, 25 °C, cm⁻¹): $\tilde{\nu}$ = 3028 (3), 1605 (100), 1381 (3), 1234 (12), 1141 (8), 1128 (8), 1040 (4), 1025 (22), 1001 (5), 782 (3), 756 (4), 616 (1), 535 (1), 413 (2), 310 (4), 176 (5), 105 (30); **¹H NMR** (270 MHz, [D₆]DMSO, 25 °C, TMS): δ = 7.42 ppm (br s, NH₄⁺); **¹³C NMR** (68 MHz, [D₆]DMSO, 25 °C, TMS): δ = 146.0 (s, CN₄O (2*N*-oxide)), 136.6 ppm (s, CN₄O (1*N*-oxide)); **MS** (FAB⁻) *m/z*: 169.1 (C₂HN₈O₂⁻); **MS** *m/z* (FAB⁺): 18.1 (NH₄⁺); **EA** (C₂H₈N₁₀O₂, 204.15): C 11.77, H 3.95, N 68.61%; found: C 12.06, H 3.89, N 68.48%; **Sensitivities**: IS: 40 J, FS: 360 N, ESD: 1.5 J (at grain sizes <100 μm).

Diguanidinium 5,5'-bitetrazol-1,2'-dioxide (8)

Compound **4**·H₂O (0.94 g, 5 mmol, 1 equiv.) was dissolved in H₂O (20 mL). Guanidinium carbonate (0.90 g, 5 mmol, 1 equiv.) was added and the mixture was heated to reflux for 1 h. The solution was filtered and the solution left open to the air to slowly evaporate the solvent to give **8** (1.16 g, 4.02 mmol, 80%) as a white powder.

DTA (5 °C min⁻¹) onset: 300 °C (dec.); **IR** (ATR, cm⁻¹): $\tilde{\nu}$ = 3445 (m), 3345 (m), 3140 (m), 2804 (w), 1645 (vs), 1594 (m), 1459 (m), 1402 (m), 1386 (s), 1335 (m), 1251 (s), 1194 (w), 1156 (m), 995 (m), 783 (m), 766 (w), 748 (w), 714 (w), 698 (vw); **Raman** (1064 nm, 300 mW, 25 °C, cm⁻¹): $\tilde{\nu}$ = 3248 (3), 1601 (100), 1389 (4), 1336 (3), 1230 (10), 1156 (8), 1119 (10), 1029 (50), 1010 (21), 785 (4), 768 (7), 748 (6), 540 (8), 445 (4), 414 (5), 281 (8), 122 (30), 100 (30); **¹H NMR** (270 MHz, [D₆]DMSO, 25 °C, TMS): δ = 7.18 ppm (br s, 12 H; NH₂); **¹³C NMR** (68 MHz, [D₆]DMSO, 25 °C, TMS): δ = 158.1 (s, CN₃H₆), 146.0 (s, CN₄O (2N-oxide)), 136.0 ppm (s, CN₄O (1N-oxide)); **MS** m/z (FAB⁻): 169.2 (C₂HN₈O₂⁻); m/z (FAB⁺): 60.1 (CH₆N₃⁺); **EA** (C₄H₁₂N₁₄O₂, 288.24): C 16.67, H 4.20, N 68.03%; found: C 17.31, H 4.10, N 67.53%; **Sensitivities**: IS: 40 J; FS: 360 N; ESD: 1.5 J (at grain sizes <100 μm).

Triaminoguanidinium 1-hydroxy-5,5'-bitetrazole-2'-oxide (9)

Compound **4**·H₂O (0.75 g, 4 mmol, 1 equiv.) was dissolved in H₂O (20 mL). Triaminoguanidinium chloride (1.12 g, 8 mmol, 2 equiv.) was added and the mixture was heated for 30 min. The solution was filtered and left for crystallization to give **9**·H₂O (0.99 g, 3.39 mmol, 85%) as colorless crystals. The product was dried at 80 °C for 2 h to yield white powder of anhydrous **9**.

DTA (5 °C min⁻¹) onset: 162 °C (m.p.), 180 °C (dec.); **IR** (**9**·H₂O, ATR, cm⁻¹): $\tilde{\nu}$ = 3514 (m), 3333 (m), 3194 (s), 2832 (m), 1688 (s), 1679 (vs), 1581 (m), 1414 (m), 1381 (s), 1347 (s), 1130 (s), 1057 (m), 873 (s), 791 (s); **Raman** (**9**·H₂O, 1064 nm, 300 mW, 25 °C, cm⁻¹): $\tilde{\nu}$ = 3240 (4), 1611 (100), 1421 (3), 1389 (5), 1255 (20), 1207 (4), 1135 (19), 1117 (14), 1048 (4), 1020 (41), 1002 (7), 882 (6), 801 (3), 767 (6), 749 (7), 641 (4), 587 (3), 424 (5), 378 (6), 281 (11), 226 (5), 132 (19), 113 (30), 91 (34); **¹H NMR** (270 MHz, [D₆]DMSO, 25 °C, TMS): δ = 8.59 (br s, 4H; NH, OH), 5.27 ppm (br s, 6H; NH₂); **¹³C NMR** (68 MHz, [D₆]DMSO, 25 °C, TMS): δ = 159.1 (s, CN₆H₉⁺), 143.1 (s, CN₄O (2N-oxide)), 140.2 ppm (s, CN₄OH (1N-oxide)); **MS** m/z (FAB⁻): 169.2 (C₂HN₈O₂⁻); m/z (FAB⁺): 105.0 (CH₉N₆⁺); **EA** (C₃H₁₀N₁₄O₂, 274.21): C 13.14, H 3.68, N 71.51%; found: C 13.38, H 4.16, N 70.23%; **Sensitivities**: IS: 3 J; FS: 288 N; ESD: 700 mJ (at grain sizes <100 μm).

4,4',5,5'-Tetraamino-3,3'-bi-1,2,4-triazolium 5,5'-bitetrazole-1,2'-dioxide (10)

Compound **4**·H₂O (0.56 g, 3 mmol, 1 equiv.) was dissolved in H₂O (400 mL). 4,4',5,5'-Tetraamino-3,3'-bi-1,2,4-triazole^[36] (0.59 g, 3 mmol, 1 equiv.) was added and the mixture was heated to reflux until a clear solution formed. The solution was cooled to ambient temperature and the precipitate was filtered to give **10** (0.72 g, 1.97 mmol, 66%) as a white powder.

DTA (5 °C min⁻¹): onset: 281 °C (dec.); **IR** (ATR, cm⁻¹): $\tilde{\nu}$ = 3306 (w), 3201 (w), 2967 (m), 2680 (w), 2290 (w), 1711 (s), 1689 (s), 1600 (w), 1455 (m), 1392 (m), 1344 (s), 1300 (m), 1237 (s), 1198 (m), 1103 (w), 1000 (m), 976 (s), 909 (m), 851 (m), 779 (s), 744 (s), 666 (vs); **Raman** (1064 nm, 300 mW, 25 °C, cm⁻¹): $\tilde{\nu}$ = 3154 (3), 1628 (100), 1602 (71), 1457 (10), 1375 (5), 1287 (18), 1237 (14), 1142 (11), 1078 (6), 1045 (5), 1020 (39), 801 (25), 750 (7), 708 (12), 618 (7), 388 (7), 365 (8), 301 (7), 277 (7), 183 (11), 98 (21); **¹H NMR** (270 MHz, [D₆]DMSO, 25 °C, TMS): δ = 7.37 (br s, 5H; C₄H₁₀N₁₀²⁺), 5.99 ppm (br s, 5H; C₄H₁₀N₁₀²⁺); **¹³C NMR** (68 MHz, [D₆]DMSO, 25 °C, TMS): δ = 153.9 (s, CNH₂), 142.2 (s, CN₄O (2N-oxide)), 140.4 (s, CN₄O (1N-oxide)), 138.5 (s, C-C); **MS** *m/z* (FAB⁻): 169.1 (C₂HN₈O₂⁻); *m/z* (DEI): 196.2 (C₄H₈N₁₀); **EA** (C₆H₁₀N₁₈O₂, 366.27): C 19.68, H 2.75, N 68.84%; found: C 20.21, H 2.90, N 68.41%; **Sensitivities**: IS: 40 J; FS: 360 N; ESD: 300 mJ (at grain sizes <100 μm).

Di-3,6,7-triamino-7H-[1,2,4]triazolo[4,3-*b*][1,2,4]triazolium 5,5'-bitetrazole-1,2'-dioxide dihydrate (11·2H₂O)

Compound **4**·H₂O (0.56 g, 3 mmol, 1 equiv.) was dissolved in H₂O (30 mL). 3,6,7-Triamino-7H-[1,2,4]triazolo[4,3-*b*][1,2,4]triazole^[22] (0.92 g, 6 mmol, 2 equiv.) was added and the mixture was heated until the compounds dissolved. The solution was filtered and left for crystallization to give **11**·2H₂O (1.12 g, 2.34 mmol, 78 %) as a gray powder. Recrystallization of **11**·2H₂O in water yielded crystals that were suitable for X-ray measurements. **11**·2H₂O was dried at 90 °C for 2 h to obtain water-free **11**.

DTA (5 °C min⁻¹): 255 °C (dec.); **IR** (ATR, cm⁻¹): $\tilde{\nu}$ = 3556 (w), 3437 (w), 3335 (m), 3155 (m), 2990 (m), 2684 (m), 1698 (s), 1646 (vs), 1582 (m), 1516 (m), 1470 (m), 1416 (m), 1355 (s), 1245 (s), 1202 (m), 1111 (w), 996 (w), 974 (w), 838 (w), 703 (m); **Raman** (1064 nm, 300 mW, 25 °C, cm⁻¹): $\tilde{\nu}$ = 3167 (3), 1709 (8), 1673 (9), 1615 (45), 1472 (8), 1397 (11), 1386 (9), 1296 (10), 1251 (22), 1149 (9), 1112 (18), 1018 (42), 849 (23), 766 (14), 684 (10), 629 (22), 601 (28), 422 (12), 406 (11), 354 (11), 317 (12), 174 (14), 92 (100), 92 (100); **¹H NMR** (270 MHz, [D₆]DMSO, 25 °C, TMS): δ = 7.89 (br s, 4H; C₃H₇N₈⁺), 7.15 (br s, 4H; C₃H₇N₈⁺), 5.77 ppm (br s, 4H; C₃H₇N₈⁺); **¹³C NMR** (68 MHz, [D₆]DMSO, 25 °C, TMS): δ = 160.0 (s,

$\text{C}_3\text{H}_7\text{N}_8^+$), 147.6 (s, $\text{C}_3\text{H}_7\text{N}_8^+$), 145.3 (s, CN_4O (2*N*-oxide)), 141.6 (s, $\text{C}_3\text{H}_7\text{N}_8^+$), 137.5 ppm (s, CN_4O (1*N*-oxide)); **MS** m/z (FAB⁻): 169.2 ($\text{C}_2\text{HN}_8\text{O}_2^-$); m/z (FAB⁺): 155.0 ($\text{C}_3\text{H}_7\text{N}_8^+$); **EA** ($\text{C}_8\text{H}_{18}\text{N}_{24}\text{O}_4$, 514.40): C 18.68, H 3.53, N 65.35%; found: C 19.28, H 3.53, N 65.54%; **Sensitivities**: IS: 40 J; FS: 360 N; ESD: 1.5 J (at grain sizes <100 μm).

5.5 References

- [1] N. Fischer, D. Fischer, T. M. Klapötke, D. G. Piercey, J. Stierstorfer, *J. Mater. Chem.* **2012**, 22, 20418–20422.
- [2] R. A. Carboni, J. C. Kauer, J. E. Castle, H. E. Simmons, *J. Am. Chem. Soc.* **1967**, 89, 2618–2625.
- [3] M. B. Talawar, R. Sivabalan, T. Mukundan, H. Muthurajan, A. K. Sikder, B. R. Gandhe, A. S. Rao, *J. Hazard. Mater.* **2009**, 161, 589–607.
- [4] a) R. P. Singh, R. D. Verma, D. T. Meshri, J. M. Shreeve, *Angew. Chem. Int. Ed.* **2006**, 45, 3584–3601; *Angew. Chem.* **2006**, 118, 3664–3682; b) H. Gao, J. M. Shreeve, *Chem. Rev.* **2011**, 111, 7377–7436.
- [5] N. Fischer, D. Izsák, T. M. Klapötke, S. Rappenglück, J. Stierstorfer, *Chem. Eur. J.* **2012**, 18, 4051–4062.
- [6] N. Fischer, L. Gao, T. M. Klapötke, J. Stierstorfer, *Polyhedron* **2013**, 51, 201–210.
- [7] M. Göbel, K. Karaghiosoff, T. M. Klapötke, D. G. Piercey, J. Stierstorfer, *J. Am. Chem. Soc.* **2010**, 132, 17216–17226.
- [8] J. C. Bottaro, M. Petrie, P. E. Penwell, A. L. Dodge, R. Malhotra, NANA/HEDM Technology: Late Stage Exploratory Effort, Report No. A466714; SRI International: Menlo Park, CA, **2003**; DARPA/AFOSR funded, Contact No. F49629-02-C-0030.
- [9] F. Boneberg, A. Kirchner, T. M. Klapötke, D. G. Piercey, M. J. Poller, J. Stierstorfer, *Chem. Asian J.* **2013**, 8, 148–159.
- [10] D. Fischer, T. M. Klapötke, M. Reymann, P. C. Schmid, J. Stierstorfer, M. Sućeska, *Propellants Explos. Pyrotech.* **2014**, 39, 550–557.
- [11] T. M. Klapötke, M. Q. Kurz, R. Scharf, P. C. Schmid, J. Stierstorfer, M. Sućeska, *ChemPlusChem* **2015**, 80, 97–106.

- [12] N. Fischer, T. M. Klapötke, S. Rappenglück, J. Stierstorfer, *ChemPlusChem* **2012**, 77, 877–888.
- [13] *CrysAlisPro*, Agilent Technologies, version 1.171.35.11, **2011**.
- [14] A. Altomare, G. Cascarano, C. Giacovazzo, A. Guagliardi, *Appl. Cryst.* **1993**, 26, 343.
- [15] G. M. Sheldrick, *SHELXS-97, Program for Crystal Structure Solution*, Universität Göttingen, **1997**.
- [16] G. M. Sheldrick, *SHELXL-97, Program for the Refinement of Crystal Structures*, University of Göttingen, Germany, **1994**.
- [17] L. Farrugia, *J. Appl. Cryst.* **1999**, 32, 837–838.
- [18] Spek, A. L. Platon, Utrecht University, Utrecht, The Netherlands, **1999**.
- [19] Empirical absorption correction using spherical harmonics, implemented in SCALE3 ABSPACK scaling algorithm (CrysAlisPro Oxford Diffraction Ltd., Version 171.33.41, **2009**).
- [20] CCDC-1056567 (for **2**•2H₂O), -CCDC-1056566 (for **4**•H₂O), -CCDC-1056565 (for **5**•H₂O), -CCDC-1056568 (for **9**•H₂O), and -CCDC-1056569 (for **11**•2H₂O) contain the supplementary crystallographic data for this paper. These data can be obtained free of charge from The Cambridge Crystallographic Data Centre via www.ccdc.cam.ac.uk/data_request/cif.
- [21] P. J. Steel, *J. Chem. Crystallogr.* **1996**, 26, 399–402.
- [22] T. M. Klapötke, P. C. Schmid, S. Schnell, J. Stierstorfer, *Chem. Eur. J*, *submitted*.
- [23] NATO standardization agreement (STANAG) on explosives, *impact sensitivity tests*, no. 4489, 1st ed., Sept. 17, **1999**.
- [24] WIWEB-Standardarbeitsanweisung 4-5.1.02, *Ermittlung der Explosionsgefährlichkeit, hier der Schlagempfindlichkeit mit dem Fallhammer*, Nov. 8, **2002**.
- [25] <http://www.bam.de>.
- [26] NATO standardization agreement (STANAG) on explosive, *friction sensitivity tests*, no. 4487, 1st ed., Aug. 22, **2002**.
- [27] WIWEB-Standardarbeitsanweisung 4-5.1.03, *Ermittlung der Explosionsgefährlichkeit oder der Reibeempfindlichkeit mit dem Reibeapparat*, Nov. 8, **2002**.

- [28] Impact: Insensitive > 40 J, less sensitive ≥ 35 J, sensitive ≥ 4 J, very sensitive ≤ 3 J; friction: Insensitive > 360 N, less sensitive = 360 N, sensitive < 360 N a. > 80 N, very sensitive ≤ 80 N, extreme sensitive ≤ 10 N; According to the UN Recommendations on the Transport of Dangerous Goods (+) indicates: not safe for transport.
- [29] <http://www.ozm.cz>.
- [30] M. Sućeska, EXPLO5, v. 6.01, Zagreb, Croatia, **2012**.
- [31] Before measuring the densities with a pycnometer, all compounds containing crystal water were dried in an oven until no more water was detected with a DTA control experiment.
- [32] M. Hesse, H. Meier, B. Zeeh, in *Spektroskopische Methoden in der Organischen Chemie*, 7th ed., Thieme, Stuttgart, Germany, **2005**.
- [33] G. Socrates, in *Infrared and Raman Characteristics Group Frequencies*, 3rd ed., John Wiley & Sons, The Atrium, Southern Gate, Chichester, West Sussex, UK, **2004**.
- [34] M. J. Frisch, G. W. Trucks, H. B. Schlegel, G. E. Scuseria, M. A. Robb, J. R. Cheeseman, G. Scalmani, V. Barone, B. Mennucci, G. A. Petersson, H. Nakatsuji, M. Caricato, X. Li, H. P. Hratchian, A. F. Izmaylov, J. Bloino, G. Zheng, J. L. Sonnenberg, M. Hada, M. Ehara, K. Toyota, R. Fukuda, J. Hasegawa, M. Ishida, T. Nakajima, Y. Honda, O. Kitao, H. Nakai, T. Vreven, J. A. Montgomery, Jr., J. E. Peralta, F. Ogliaro, M. Bearpark, J. J. Heyd, E. Brothers, K. N. Kudin, V. N. Staroverov, R. Kobayashi, J. Normand, K. Raghavachari, A. Rendell, J. C. Burant, S. S. Iyengar, J. Tomasi, M. Cossi, N. Rega, J. M. Millam, M. Klene, J. E. Knox, J. B. Cross, V. Bakken, C. Adamo, J. Jaramillo, R. Gomperts, R. E. Stratmann, O. Yazyev, A. J. Austin, R. Cammi, C. Pomelli, J. W. Ochterski, R. L. Martin, K. Morokuma, V. G. Zakrzewski, G. A. Voth, P. Salvador, J. J. Dannenberg, S. Dapprich, A. D. Daniels, Ö. Farkas, J. B. Foresman, J. V. Ortiz, J. Cioslowski, D. J. Fox, *Gaussian 09*, revision A.1, Gaussian, Inc., Wallingford CT, **2009**.
- [35] T. M. Klapötke, M. Q. Kurz, P. C. Schmid, J. Stierstorfer, *J. Energ. Mater.* **2015**, *33*, 191–201.
- [36] T. M. Klapötke, P. C. Schmid, S. Schnell, J. Stierstorfer, *J. Mater. Chem. A* **2015**, *3*, 2658–2668.

5.6 Supplementary information

5.6.1 Crystallographic data and refinement parameters

Table S1. Crystallographic data and refinement parameters of compounds **2·H₂O**, **4·H₂O**, **5·H₂O**, **9·H₂O** and **11·H₂O**.

	2·H₂O	4·H₂O	5·H₂O	9·H₂O	11·H₂O
Formula	C ₂ H ₆ ClN ₅ O ₄	C ₂ H ₄ N ₈ O ₃	C ₂ H ₁₀ N ₁₀ O ₅	C ₃ H ₁₂ N ₁₄ O ₃	C ₈ H ₁₈ N ₂₄ O ₄
FW [g mol ⁻¹]	199.57	188.13	254.20	292.27	514.46
Crystal system	orthorhombic	monoclinic	monoclinic	triclinic	monoclinic
Space Group	<i>Pca</i> 2 ₁	<i>P</i> 2 ₁ / <i>n</i>	<i>P</i> 2 ₁ / <i>n</i>	<i>P</i> -1	<i>P</i> 2 ₁ / <i>c</i>
Color / Habit	colorless, stab	colorless, block	colorless, rod	colorless, block	colorless, rod
Size [mm]	0.10 × 0.10 × 0.40	0.15 × 0.21 × 0.45	0.03 × 0.10 × 0.40	0.17 × 0.29 × 0.32	0.02 × 0.02 × 0.10
<i>a</i> [Å]	17.4411(8)	6.5433(3)	11.3310(6)	3.6668(2)	6.3289(3)
<i>b</i> [Å]	3.5939(2)	5.7268(3)	6.4307(4)	12.1708(8)	13.2203(6)
<i>c</i> [Å]	11.9564(5)	18.7867(10)	13.6404(10)	13.5574(11)	24.0351(12)
<i>α</i> [°]	90	90	90	71.577(6)	90
<i>β</i> [°]	90	95.267(5)	101.929(7)	84.056(6)	100.611(1)
<i>γ</i> [°]	90	90	90	84.295(5)	90
<i>V</i> [Å ³]	749.45(6)	701.01(6)	972.46(11)	569.52(7)	1976.63(16)
<i>Z</i>	4	4	4	2	4
<i>ρ</i> _{calc.} [g cm ⁻³]	1.769	1.783	1.736	1.704	1.729
<i>μ</i> [mm ⁻¹]	0.498	0.160	0.159	0.145	0.142
<i>F</i> (000)	408	384	528	304	1064
<i>λ</i> _{MoKα} [Å]	0.71073	0.71073	0.71073	0.71073	0.71073
<i>T</i> [K]	173	173	173	173	173
<i>θ</i> min-max [°]	4.7, 26.5	4.2, 26.5	4.4, 26.5	4.3, 26.5	3.0, 26.4
Dataset <i>h</i> ; <i>k</i> ; <i>l</i>	−19:21; −4:4; −15:15	−7:8; −6:7; −23:23	−13:14; −8:8 ; −17:17	−4:4; −15:14; −16:11	−7:7; −16:0; −30:6
Reflect. coll.	5071	5122	7137	4308	4163
Independ. refl.	818	1447	2001	2354	4173
<i>R</i> _{int}	0.024	0.027	0.057	0.017	0.000
Reflection obs.	801	1166	1419	2041	3613
No. parameters	133	134	194	219	398
<i>R</i> ₁ (obs)	0.0167	0.0389	0.0427	0.0417	0.0576
<i>wR</i> ₂ (all data)	0.0445	0.0996	0.0905	0.1146	0.1562
<i>S</i>	1.10	1.03	1.03	1.06	1.18
Resd. Dens.[e Å ⁻³]	−0.16, 0.19	−0.51, 0.38	−0.25, 0.25	−0.48, 0.39	−0.29, 0.33
Device type	Oxford	Oxford	Oxford	Oxford	Oxford
	XCalibur3 CCD	XCalibur3 CCD	XCalibur3 CCD	XCalibur3 CCD	XCalibur3 CCD
Solution	SIR-2004	SIR-2004	SIR-2004	SIR-2004	SIR-2004
Refinement	SHELXL-97	SHELXL-97	SHELXL-97	SHELXL-97	SHELXL-97
Absorpt. corr.	multi-scan	multi-scan	multi-scan	multi-scan	multi-scan
CCDC	1056567	1056566	1056565	1056568	1056569

5.6.2 Heat of formation calculations

General information about the heat of formation calculations can be found in the appendix of this thesis. The calculation results are summarized in Table S2.

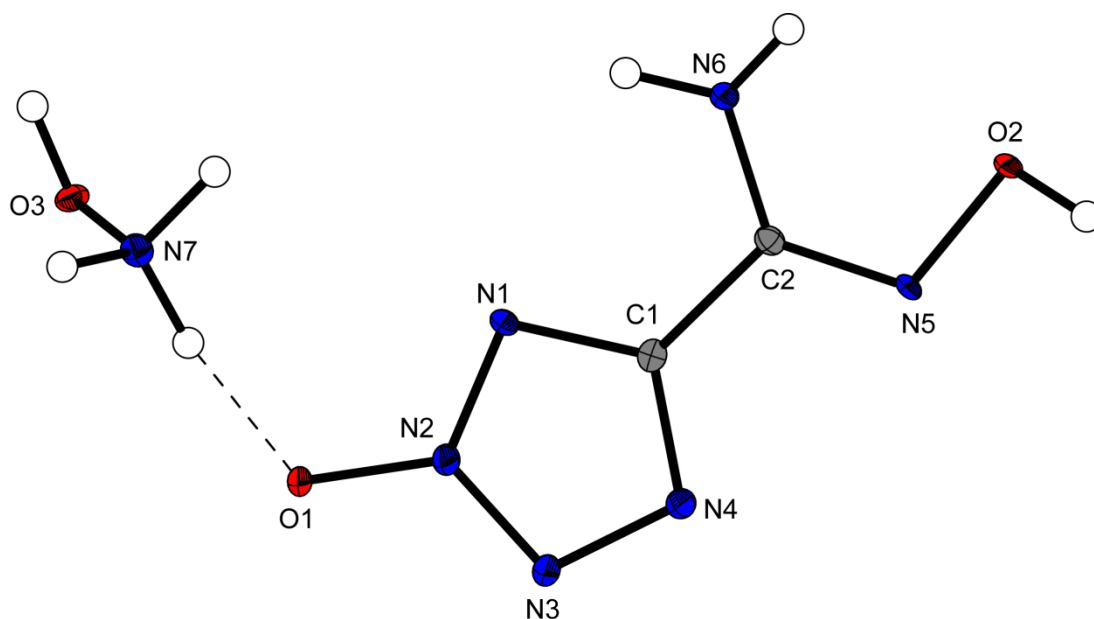
Table S2. Calculation results

M	$-H^{298}$ ^[a] / a.u.	$\Delta_f H^\circ(\text{g}, \text{M})$ / kJ mol ⁻¹ ^[b]	V_M nm ³ ^[c]	$\Delta U_L, \Delta H_L$ (4); ^[d] ΔH_{sub} ^[e] (3) / kJ mol ⁻¹	$\Delta_f H^\circ(\text{s})$ ^[f] / kJ mol ⁻¹	Δn ^[g]	$\Delta_f U(\text{s})$ ^[f] / kJ kg ⁻¹
4	664.829406	654.0		87.4	566.5	6.0	3418.1
NH₄O⁺	131.863249	687.2					
BT1O2O²⁻	663.703743	542.7					
5		1915.5	0.224	1455.1, 1462.5	451.8	11.0	2028.6
N₂H₅⁺	112.030523	774.1					
6		2089.5	0.210	1491.0, 1498.5	591.1	12.0	2651.0
NH₄⁺	56.796608	635.3					
7		1813.3	0.196	1530.0, 1537.4	275.9	10.0	1473.0
G⁺	205.453192	571.2					
8		1685.1	0.284	1330.9, 1338.3	346.7	14.0	1323.4
TAG⁺	371.197775	874.3					
BT1OH2O⁻	664.328169	436.6					
9		1309.7	0.261	471.1, 476.1	833.6	13.0	3157.5
TADTr²⁺	704.327388	2032.9					
10		2575.6	0.340	1759.7, 1764.7	810.9	15.0	2315.6
TATOT⁺	555.474133	1080.0					
11		2702.8	0.445	1120.4, 1127.9	1574.9	20.0	3396.0

^[a] CBS-4M electronic enthalpy; ^[b] gas phase enthalpy of formation; ^[c] molecular volumes taken from X-ray structures and corrected to room temperature; ^[d] lattice energy and enthalpy (calculated using Jenkins and Glasser equations); ^[e] enthalpy of sublimation (calculated by Trouton's rule); ^[f] standard solid state enthalpy of formation; ^[g] solid state energy of formation.

Energetic Improvements by *N*-Oxidation: Insensitive Amino-Hydroximoyl-Tetrazole-2*N*-Oxides

published in *J. Energ. Mat.* **2015**, *33*, 191–201. (DOI: 10.1080/07370652.2014.963743)

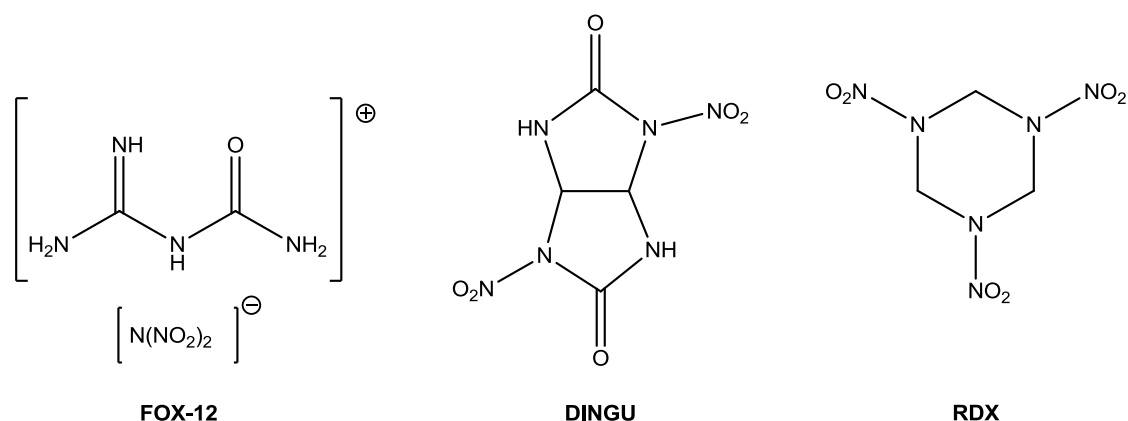


Abstract: 5-Aminohydroximoyl-2-hydroxytetrazole (**3**) was synthesized in a three-step synthesis from cheap starting materials. This novel tetrazole derivative contains two energetic moieties: an *N*-oxide as well as an aminohydroximoyl group. Various energetic nitrogen-rich salts as the hydroxylammonium (**4**), guanidinium (**5**), aminoguanidinium (**6**), ammonium (**7**), and triaminoguanidinium (**8**) were synthesized. Moreover, zwitterionic 5-amidrazonyl-tetrazole-2-oxide monohydrate (**9**) was synthesized. Compounds **4**, **5**, **8**, **9**, and **10** were structurally characterized using single-crystal X-ray diffraction. Additionally, all new compounds were characterized using nuclear magnetic resonance (NMR) and vibrational (infrared [IR], Raman) spectroscopy as well as mass spectrometry and elemental analysis. The thermal behavior was studied using differential thermal analysis (DTA) measurements and the sensitivities of the compounds towards shock, friction and electrostatic discharge were determined. Finally, the enthalpies of formation were calculated (atomization method, CBS-4M enthalpies) and several detonation/propulsion parameters computed with the EXPLO5 code.

Keywords: Insensitive Munitions · Explosives · Tetrazole · *N*-Oxide · Crystal Structure

6.1 Introduction

Research concerned with the improvement of secondary explosives has been mainly focused on reducing their environmental impact (green explosives) and improving their performance. Yet there is another important aspect that has been addressed: insensitive munitions^[1]. Insensitive munitions are devices comprising explosives that possess very low sensitivities toward outer stimuli. Therefore, the current aim is to create munitions that survive accidents and enemy attack. FOX-12^[2] and the 1988 developed DINGU^[3] are examples of explosives that can be used for insensitive munitions (Scheme 1). The sensitivity data of these compounds are significantly lower than those of hexogen (RDX), the most commonly used military explosive. However, new insensitive energetic materials, which are accessible through facile synthetic routes using only inexpensive and commercially available starting materials, are always desirable.



Scheme 2. Chemical structures of guanylurea dinitramide (FOX-12) and dinitroglucyl (DINGU) which are examples of insensitive munitions as well as the commonly used hexogen (RDX).

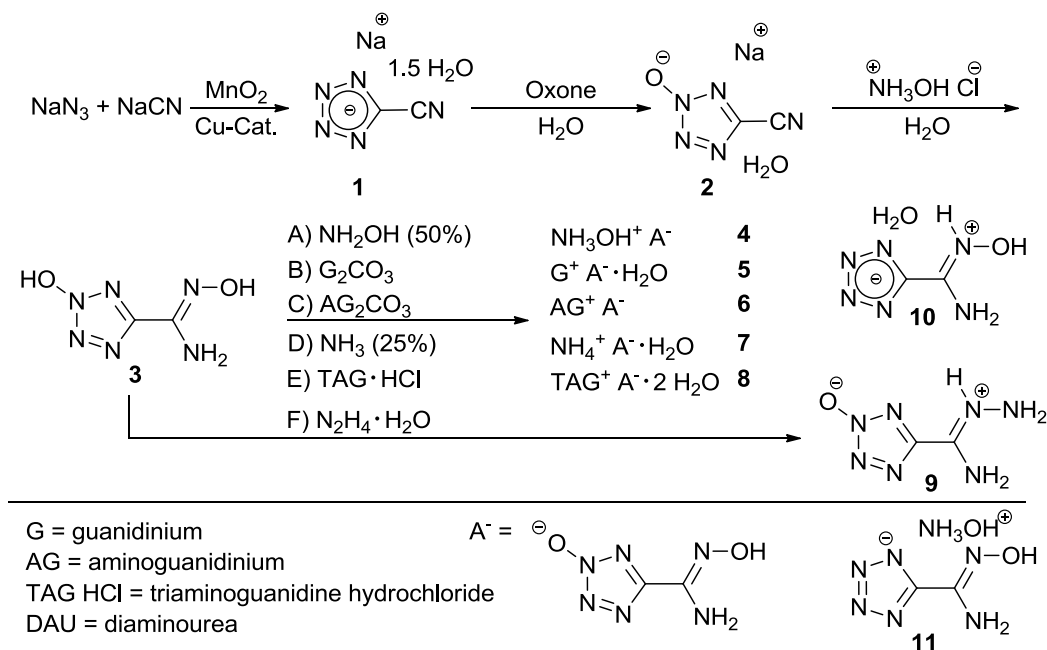
Our focus has recently been drawn to energetic materials that are based on tetrazoles because they mainly release nontoxic N_2 -gas on decomposition^[4], as well as to tetrazole *N*-oxides, because the inclusion of the *N*-oxide group is known to improve the performance of tetrazole derivatives^[5]. Aminohydroxyimoyl-1*H*-tetrazole monohydrate and its derivatives show potential for use as possible new energetic materials^[6]; however, there is still the possibility to improve the performance of 5-aminohydroxyimoyl-1*H*-tetrazole monohydrate and its energetic salts, by introducing the *N*-oxide group to this system. Therefore we developed a facile, three-step synthesis that allowed us to obtain 5-aminohydroxyimoyl-2-hydroxytetrazole as well as several energetic salts (e.g. hydroxylammonium, triaminoguanidinium, ammonium) containing the corresponding deprotonated anion, which enabled us to lower the sensitivity of

compounds **4–8** while at the same time boosting the energetic performance of the tetrazole system compared to the *N*-oxide free compounds.

6.2 Results and Discussion

6.2.1 Synthesis

The precursor sodium 5-cyanotetrazolate sesquihydrate (**1**) was synthesized from sodium azide and sodium cyanide in the presence of manganese dioxide and catalytic amounts of copper as described in the literature (Scheme 2).^[6] A saturated aqueous solution of Oxone, buffered with potassium acetate, selectively oxidized compound **1** to form sodium 5-cyanotetrazolate-2-oxide monohydrate (**2**).^[7] In the third step, compound **2** was treated with hydroxylammonium chloride, which reacted with the electrophilic nitrile group to form 5-aminohydroximoyl-2-hydroxytetrazole (**3**) after 15 min reflux.^[6,7] As is illustrated in Scheme 2, energetic salts of the acid **3** such as hydroxylammonium 5-aminohydroxyimoyl-tetrazole-2-oxide (**4**), guanidinium 5-aminohydroxyimoyl-tetrazole-2-oxide monohydrate (**5**), aminoguanidinium 5-aminohydroxyimoyl-tetrazole-2-oxide (**6**), ammonium 5-aminohydroxyimoyl-tetrazole-2-oxide monohydrate (**7**) and triaminoguanidinium 5-aminohydroxyimoyl-tetrazole-2-oxide dihydrate (**8**) were also prepared.



Scheme 3. Synthetic routes for the formation of compounds **1–9**, as well as the chemical structure of 5-aminohydroxyimoyltetrazole monohydrate (**10**) and hydroxylammonium 5-aminohydroxyimoyl-tetrazolate (**11**).

Attempts were made to synthesize the hydrazinium salt of **3**. However, when the neutral compound **3** was treated with aqueous hydrazine, crystals of 5-amidrazonyl-tetrazole-2-oxide

monohydrate (**9**) were obtained. In this reaction hydroxylamine was cleaved by the nucleophilic attack of hydrazine at the hydroximoyl-carbon atom. Finally, single crystals of precursor **10**, which is a zwitterion, were obtained in the literature synthesis of Fischer et al.^[6].

6.2.2 X-ray Analysis

The crystal structures of compounds **4**, **5** and **8–10** were determined. Selected data and parameters of the X-ray determinations for these compounds are illustrated in Table S1 (see online Supplementary Information).

Hydroxylammonium 5-aminohydroximoyl-tetrazole-2-oxide (**4**) crystallizes anhydrously from water in the monoclinic space group $P2_1/c$ with eight molecular moieties per unit cell. The density of compound **4** is 1.755 g cm^{-3} , which is higher than that of compound **11** (1.670 g cm^{-3})^[6]. This is consistent with the expected increase in the density on formation of the corresponding *N*-oxide. The N4–C1–C2–N5 torsion angle of $1.2(4)^\circ$, is consistent with the tetrazole ring and the 5-aminohydroximoyl forming an almost planar structure. This is in contrast to the strongly nonplanarity of compound **11** (N1–C1–C2–N5: 21.3°)^[6]. The molecular unit of **4** is shown in Figure 1.

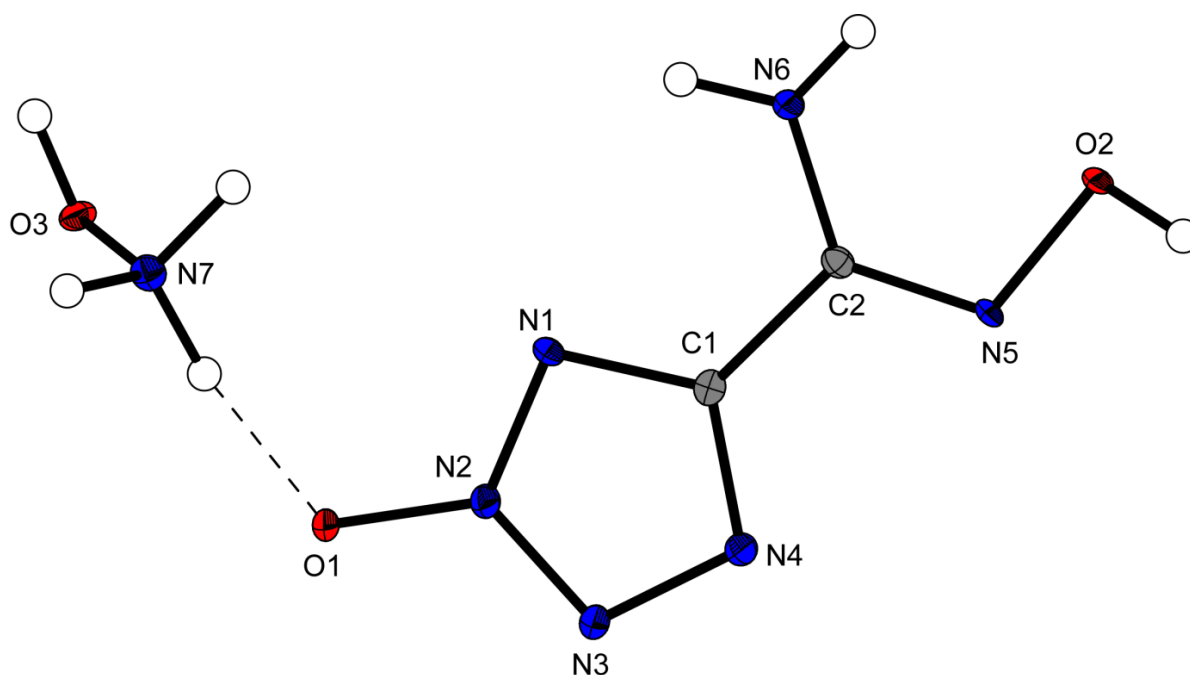


Figure 2. Molecular unit of **4** showing the atom-labeling scheme. Thermal ellipsoids show the 50% probability level and hydrogen atoms are shown as small spheres of arbitrary radius.

Guanidinium 5-aminohydroximoyl-tetrazol-2-oxide monohydrate (**5**) and triaminoguanidinium 5-aminohydroximoyl-tetrazole-2-oxide dihydrate (**8**) both crystallize from water as hydrates. The molecular units are illustrated in Figures 2 and 3. They crystallize

in the space groups $Pna2_1$ (**5**) and $C2/c$ (**8**). The density of the monohydrate **5** (1.594 g cm^{-3}) was observed to be higher than that of the dihydrate **8** (1.524 g cm^{-3}).

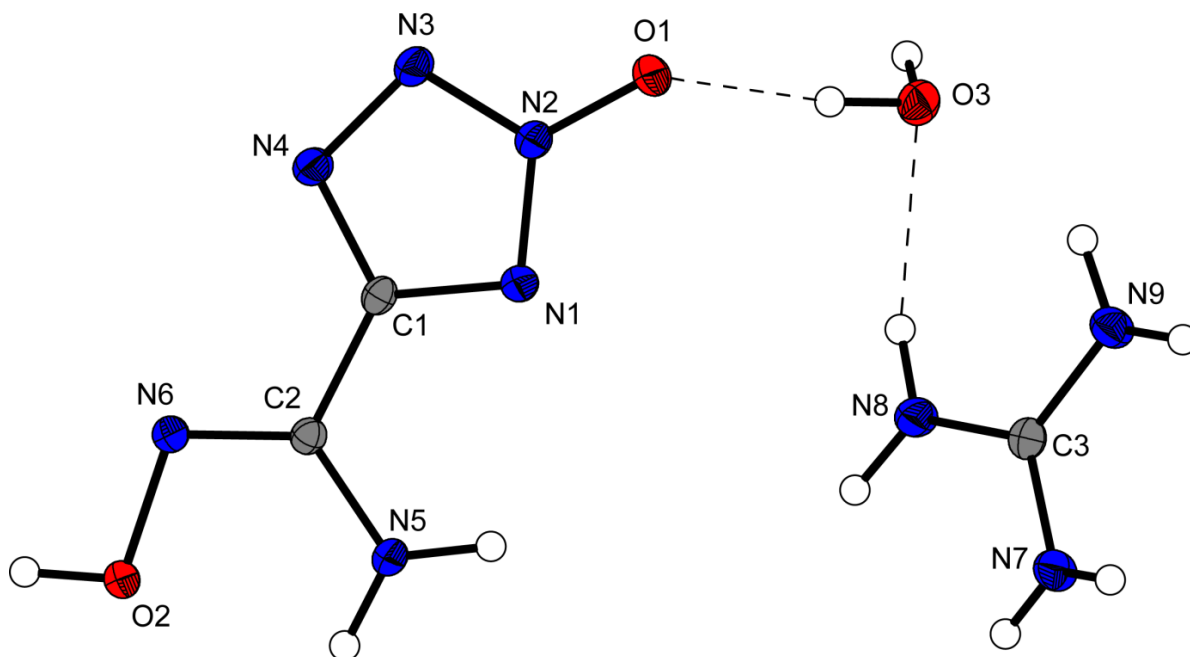


Figure 3. Molecular unit of **5** showing the atom-labeling scheme, hydrogen bridges between the water moiety and the anion as well as the guanidinium cation. Thermal ellipsoids illustrate the 50% probability level and hydrogen atoms are shown as small spheres of arbitrary radius

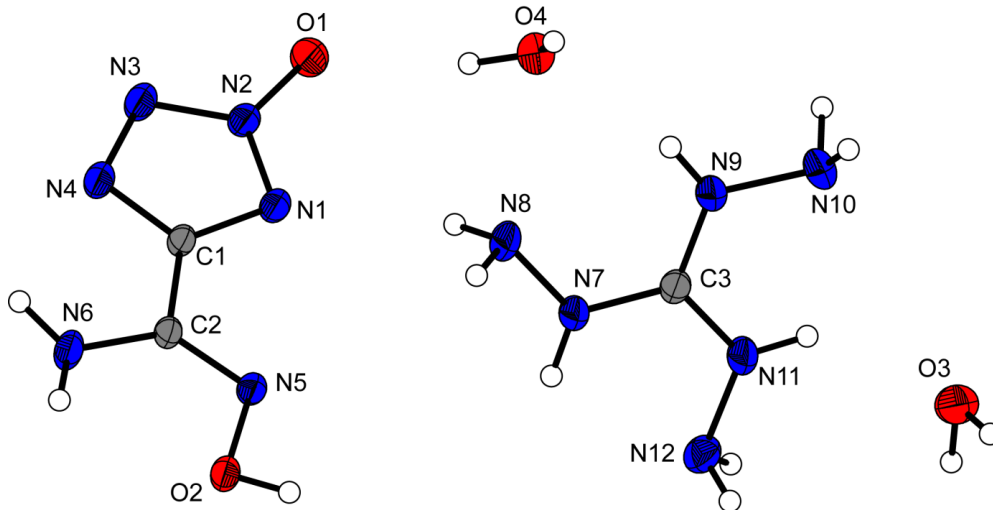


Figure 4. Molecular unit of **8** showing the atom-labeling scheme. Thermal ellipsoids illustrate the 50% probability level and hydrogen atoms are shown as small spheres of arbitrary radius.

Zwitterionic 5-amidrazonyl-tetrazole-2-oxide monohydrate (**9**) crystallizes from water as colorless plates. The molecular unit is illustrated in Figure 4. Compound **9** crystallizes in the orthorhombic space group $Pca2_1$ with four molecules per unit cell with a density of 1.665 g cm^{-3} . Though in most *N*-hydroxytetrazoles the acidic proton is bound to the O-atom of the *N*-oxide group, the basic amidrazonyl-moiety results in a zwitterionic structure where protonation takes place at the nitrogen atom N6. Because the bond lengths of N5–C2

(1.314(2) Å) and N6–C2 (1.310(2) Å) are similar, the positive charge is delocalized over atoms N6, C2 and N5.

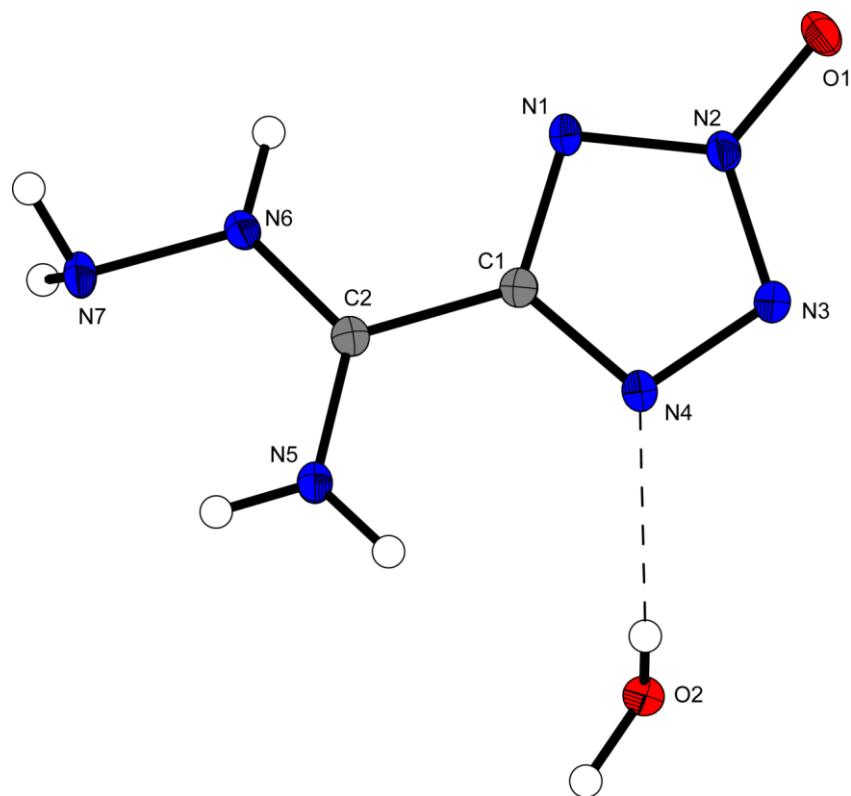


Figure 5. Chemical structure and molecular unit of **9** showing the atom-labeling scheme. Thermal ellipsoids illustrate the 50% probability level and hydrogen atoms are shown as small spheres of arbitrary radius.

A similar structure was obtained for 5-aminohydroximoyl-tetrazole monohydrate (**10**), which was recrystallized from 2 M hydrochloric acid and is illustrated in Figure 5. Compound **10** crystallizes in the monoclinic space group $P2_1/c$ with eight molecules per unit cell with a density of 1.689 g cm^{-3} . Interestingly, no proton is bound to one of the tetrazole ring atoms but is bound instead to the N6 atom, which results in a zwitterionic structure.

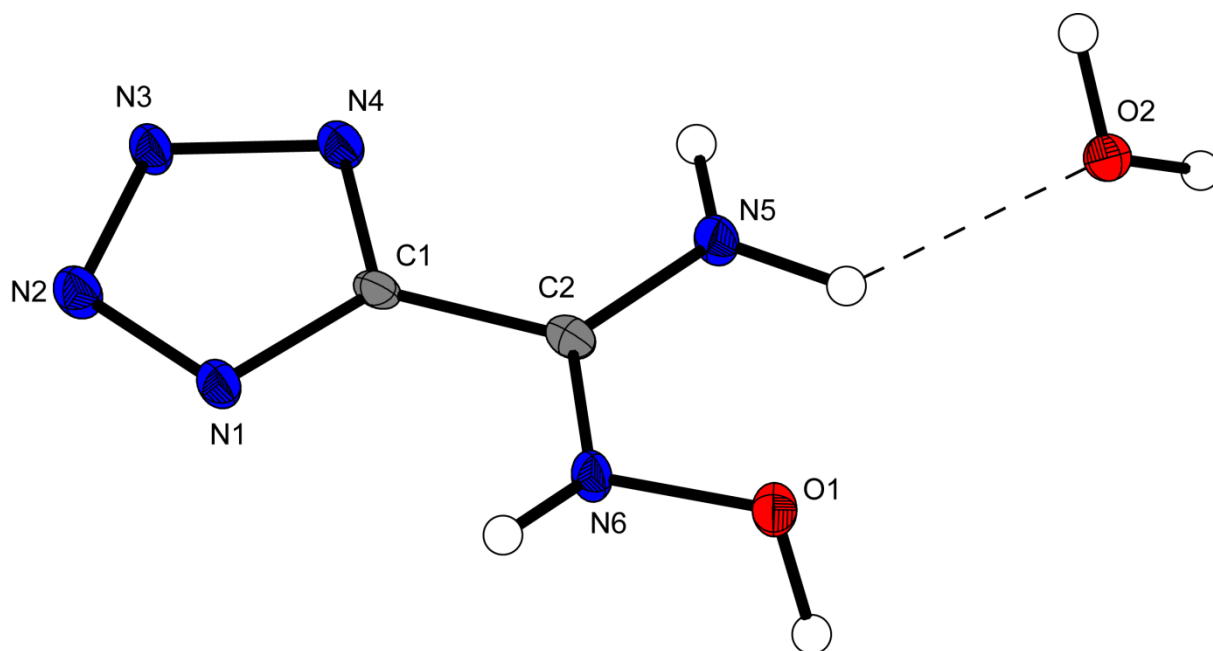


Figure 5. Chemical structure and molecular unit of **10** showing the atom-labeling scheme. Thermal ellipsoids illustrate the 50% probability level and hydrogen atoms are shown as small spheres of arbitrary radius.

6.2.3 Thermal Analysis and Sensitivities

Dehydration of compounds **5**, **7** and **9** was observed in the range of 69 °C (**7**, **9**) to 111 °C (**5**). The acid **3** decomposes at 192 °C, which means it has a lower decomposition temperature than 5-aminohydroxyimoyl-1*H*-tetrazole monohydrate (244 °C)^[6]. Compound **4** decomposes at 164 °C, which is similar to the decomposition temperature of compound **11** (171 °C)^[6]. Compounds **6–8** decompose at 181, 186, and 180 °C, respectively. Despite their relatively high decomposition temperature, RDX (210 °C)^[8] still shows a slightly higher decomposition temperature. The decomposition point for the guanidinium salt **5** at 179 °C is surprisingly low.

For the 5-amidrazonyl-tetrazole-2-oxide monohydrate **9**, the onset of decomposition was observed at 122 °C. 5-Aminohydroximoyl-2-hydroxytetrazole **3** and its energetic salts (**4–8**) as well as compound **9** show no sensitivity towards friction (**4–9**: 360 N) or sensitivity towards impact (**4–9**: >40 J, **3**: 20 J), and compounds **4–9** exceed the properties of RDX (impact: 7.5 J, friction: 120 N) by far, which is important for use as insensitive munitions^[8].

6.2.4 Physiochemical and energetic properties

The values for the heats of formation are calculated with the atomization method, using electronic energies (CBS-4M method) at room temperature. Details are given in the

Supplementary Information. The heats and energies of formation for compounds **3** and **4** are given in Table 1.

Table 1. Energetic properties and detonation parameters

	3	4	11 ^[6]	RDX ^[8]
Formula	C ₂ H ₄ N ₆ O ₂	C ₂ H ₇ N ₇ O ₃	C ₂ H ₇ N ₇ O ₂	C ₃ H ₆ N ₆ O ₆
FW [g mol ⁻¹]	144.09	177.12	161.12	222.12
IS [J] ^a	20	>40	10	7.5
FS [N] ^b	360	360	>360	120
ESD [J] ^c	1.0	0.7	0.30	0.20
N [%] ^d	58.32	55.36	60.85	37.84
Ω [%] ^e	-44.42	-40.36	-54.62	-21.61
T _{dec.} [°C] ^f	192	164	171	210
ρ [g cm ⁻³] (298K) ^g	1.65 (pyc.)	1.704	1.639	1.806
Δ _f H° [kJ mol ⁻¹] ^h	238.3	281.9	294.4	70.3
Δ _f U° [kJ kg ⁻¹] ⁱ	1757.2	1710.4	1950.1	417.0
EXPLO V6.01 values:				
-Δ _E U° [kJ kg ⁻¹] ^j	4894	5707	5132	5734
T _E [K] ^k	3395	3522	3173	3800
p _{CJ} [kbar] ^l	250	309	272	352
D [m s ⁻¹] ^m	8179	8934	8614	8815
V ₀ [L kg ⁻¹] ⁿ	849	917	916	792
SSRT:				
weight [mg]	-	474	-	504
dent [mg SiO ₂]	-	587	-	858

^a impact sensitivity (BAM drophammer, 1 of 6); ^b friction sensitivity (BAM friction tester, 1 of 6); ^c electrostatic discharge device (OZM); ^d nitrogen content; ^e oxygen balance; ^f decomposition temperature from DTA (β = 5°C); ^g recalculated from low temperature X-ray densities (ρ_{298K} = ρ_T / (1+α_V(298-T₀)); α_V = 1.5 · 10⁻⁴ K⁻¹); ^h calculated (CBS-4M) heat of formation; ⁱ calculated energy of formation; ^j energy of explosion; ^k explosion temperature; ^l detonation pressure; ^m detonation velocity; ⁿ assuming only gaseous products.

Calculation of the detonation parameters was performed with the program package EXPLO5 (version 6.01).^[9] The program is based on the chemical equilibrium, steady-state model of detonation. It uses the Becker–Kistiakowsky–Wilson equation of state (BKW EOS) for gaseous detonation products and Cowan–Fickett's equation of state for solid carbon.

The calculated EXPLO5 detonation parameters of compounds **3** and **4** using values for the room temperature X-ray densities obtained as described in Table 1^[10] are summarized in Table 1 and compared to the values calculated for compound **11** and RDX.

The detonation velocity of the acid **3** is 8179 m s⁻¹, whereas compound **4** has a detonation velocity of 8934 m s⁻¹ which is slightly higher than that of RDX (8815 m s⁻¹)^[8]. A small-scale reactivity test (SSRT) was carried out to assess the explosive performance of **4** in comparison with RDX (for a detailed set up description, see supplementary information in Fischer et al. [11]). From measuring the volumes of the dents (Table 1), it can be concluded that the small scale explosive performance of **4** is lower than the performance of commonly used RDX. This

might be due to the lower calculated detonation pressure (p_{CJ} (**4**) = 309 kbar vs. p_{CJ} (RDX) = 352 kbar).

The study exemplifies the effect of introducing the *N*-oxide group to tetrazoles. A comparison of **4** and **11** confirms the observations that were previously reported for related compounds^[5,11,12]. In terms of stability, the *N*-oxide raises the sensitivity (IS (**4**) > 40J, IS (**11**) = 10 J) while slightly lowering the decomposition temperature ($T_{dec.}$ (**4**) = 164 °C, $T_{dec.}$ (**11**) = 171 °C). In terms of energetic parameters, the *N*-oxide insignificantly decreases the calculated heat of formation ($\Delta_f H^\circ$ (**4**) = 281.9 kJ mol⁻¹, $\Delta_f H^\circ$ (**11**) = 294.4 kJ mol⁻¹) in comparison with the related *N*-oxide free compound. On the other hand, a significant increase in the density can be observed (ρ (**4**) = 1.704 g cm⁻³ (298K), ρ (**11**) = 1.639 g cm⁻³ (298K)). This results in an improvement in the detonation velocity by 3.6% (D (**4**) = 8934 m s⁻¹, D (**11**) = 8643 m s⁻¹) and more remarkably in an increase in the detonation pressure by 12% (p_{CJ} (**4**) = 309 kbar, p_{CJ} (**11**) = 272 kbar). These trends fit the equation of Kamlet and Jacobs^[13] and clearly illustrate the improvement in performance through the addition of an *N*-oxide groups to the corresponding tetrazoles.

5.2.5 NMR spectroscopy

Nuclear magnetic resonance (NMR) is a suitable method to identify compounds **3–9**. Compound **3** shows two resonances in the ¹H NMR spectrum. The broad signal at 11.04 ppm corresponds to the *N*-oxide proton of the tetrazole ring and at 9.04 ppm to the OH moiety of the 5-aminohydroximoyl group. The signal for the hydroxy group of the 5-aminohydroximoyl moiety can be observed for all of the energetic salts **4–8** with a slight downshift in the range of 10.15–9.47 ppm (**4**: 10.15; **5**: 9.68; **6**: 9.66; **7**: 9.61; **8**: 9.47 ppm). Compound **9** shows two signals at 7.36 (–NHNH₂) and 5.57 ppm (–C(NH₂)).

The ¹³C NMR spectrum of **3** possesses two sharp signals at 149.4 ppm (–CN₄O) and at 143.8 ppm (–C(NH₂)NOH). Compared to 5-aminohydroxyimoyl tetrazolate monohydrate (150.7 and 144.9 ppm), the signals are slightly upshifted^[6]. For the salts **4–8** the signal for the tetrazole carbon (151.2–150.4 ppm), as well as the signal for the 5-aminohydroximoyl carbon (144.3–144.1 ppm) are in the same range. For the acid **3**, a slight downshift of both carbon signals is observed. The carbon atoms of the guanidinium, aminoguanidinium and triaminoguanidinium cations show signals with the typical chemical shifts at 158.2, 158.9, and 159.1 ppm, respectively. Compound **9** shows two carbon signals at 151.0 (–CN₄O) and at 144.2 ppm (–C(NH₂)NHNH₂).

6.2.6 Vibrational Spectroscopy

In addition to NMR spectroscopy, infrared (IR) and Raman spectroscopy are reliable methods to characterize all of the compounds described in this work. The measurements and absorptions were assigned according to literature values^[14].

The IR spectra of compounds **3–9** reveal characteristic tetrazole ring vibrations in the range 1238 (**3**) to 937 (**8**) cm^{-1} . Compounds **3–9** show symmetric stretching vibrations (N1–C1–N4) in the range from 1408–1367 cm^{-1} , which is comparable to those observed for 5-aminohydroximoyl tetrazolate monohydrate and its salts. The stretching vibration of the tetrazole C=N bond as well as the C=N stretching vibration of the 5-aminohydroximoyl moiety is observed in the 1663–1595 cm^{-1} range. Furthermore, the *N*-oxide of the aromatic tetrazole ring system shows vibrations at 1499–700 cm^{-1} [$\nu(\text{NN})$, $\nu(\text{NCN})$, $\gamma(\text{CN})$, δ aromatic ring]^[15].

The Raman spectra of salts **4–8** all show a characteristic pattern of three bands of high intensity at 1595–1542 cm^{-1} (C=N stretching), 1022–1041 cm^{-1} (N2–N3 stretch), and 132–82 cm^{-1} .^[16] The absorptions in the range of 3257–2900 cm^{-1} corresponds to the valence vibration of the nitrogen rich cations ($\nu_{\text{asym}}(\text{NH}_2/\text{NH}_3^+)$)^[12]. However, the spectrum of compound **3** also reveals an absorption at 3173 cm^{-1} , which can be attributed to the NH_2 group of 5-aminohydroximoyl. Compound **9** also possesses three diagnostic bands at 1542 cm^{-1} , 1025 cm^{-1} , and 92 cm^{-1} . Valence vibration of the amidrazonyl group can be observed at 3236 ($-\text{CNH}_2$) and at 2820 cm^{-1} ($-\text{CN}(\text{NH}_2)$).

6.3 Experimental Part

The analytical methods and general procedures are described in the appendix of this thesis. Sodium 5-cyanotetrazolate sesquihydrate (**1**), 5-aminohydroximoyltetrazole monohydrate (**10**)^[6], and sodium 5-cyanotetrazolate-2-oxide monohydrate (**2**)^[7] were synthesized according to the literature. Compound **10** was recrystallized from 2 M hydrochloric acid and left standing for several days to yield little colorless plates.

5-Aminohydroximoyl-2-hydroxytetrazole (**3**)

Hydroxylammonium chloride (0.48 g; 6.9 mmol, 1.04 eq.) was added to a solution of sodium cyanotetrazolate-2-oxide monohydrate (1.00g, 6.6 mmol) in water (10 mL). The solution was heated to reflux for 15 mins and was left to crystallize. The white solid was filtered off to give 0.61 g (4.26 mmol, 65%) of 5-aminohydroximoyl-2-hydroxytetrazole as a white powder.

DTA (5 °C min⁻¹): 192 °C (dec.); **IR** (atr, cm⁻¹): $\tilde{\nu}$ = 3496(m), 3392(m), 3272(w), 2273(m), 1662(m), 1612(w), 1569(w), 1445(vs), 1431(m), 1414(s), 1399(vs), 1385(m), 1370(vs), 1238(s), 1077(m), 1014(m), 805(s), 722(s); **Raman** (1064 nm, 300 mW, 25 °C, cm⁻¹): $\tilde{\nu}$ = 3173(4), 1682(9), 1641(33), 1569(44), 1467(12), 1415(8), 1365(10), 1309(5), 1224(6), 1135(30), 1122(36), 1070(9), 1039(9), 1022(100), 819(6), 754(14), 738(14), 632(4), 589(9), 440(19), 409(10), 345(17), 307(8), 307(8), 210(26), 186(23), 162(46), 129(63), 114(59), 90(31); **¹H NMR** ([D₆]-DMSO, 25 °C, ppm) δ = 11.04 (br s, 1H, CN₄OH), 9.04 (s, 1H, C(NH₂)NOH); **¹³C NMR** ([D₆]-DMSO 25 °C, ppm) δ = 149.4 (s, CN₄O), 143.8 (s, C(NH₂)NOH); **EA** (C₂H₄N₆O₂, 144.09) calcd.: C 16.67, H 2.80, N 58.32%; found: C 17.02, H 2.73, N 57.83 %; **Sensitivities**: IS: 20 J, FS: 360 N, ESD: 1.0 J (at grain sizes <100 μm).

Hydroxylammonium 5-aminohydroxyimoyl-tetrazole-2-oxide (4)

5-Aminohydroximoyl-2-hydroxytetrazole (1.44 g, 10 mmol) was dissolved in 30 mL of water and hydroxylamine (0.66 g of a 50% w/v solution in H₂O, 10 mmol) was added. The solution was left standing and hydroxylammonium 5-aminohydroxyimoyl-tetrazole-2-oxide precipitated as colorless crystals. Yield: 1.63 g, 9.20 mmol, 92%.

DTA (5 °C min⁻¹): 164 °C (dec.); **IR** (atr, cm⁻¹): $\tilde{\nu}$ = 3452(w), 3359(m), 3187(m), 3067(w), 3009(w), 2906(m), 2671(w), 1686(s), 1629(w), 1599(m), 1544(w), 1472(m), 1449(w), 1406(vs), 1381(s), 1369(vs), 1306(m), 1239(s), 1224(vs), 1144(w), 1118(w), 1071(w), 1011(s), 1011(s), 1001(s), 939(m), 831(w), 759(vs), 687(m), 668(m); **Raman** (1064 nm, 300 mW, 25 °C, cm⁻¹): $\tilde{\nu}$ = 2900(4), 1669(18), 1605(8), 1548(100), 1405(7), 1372(5), 1227(10), 1141(8), 1109(12), 1070(7), 1046(4), 1030(57), 1009(16), 833(6), 759(10), 597(5), 460(8), 428(10), 396(6), 355(10), 290(5), 251(5), 187(8), 187(8), 143(14), 103(54), 82(68); **¹H NMR** ([D₆]-DMSO, 25 °C, ppm) δ = 10.15 (br s, 1H, NH₃OH⁺), 5.72 (s, 2H C(NH₂)NOH); **¹³C NMR** ([D₆]-DMSO, 25 °C, ppm) δ = 151.2 (s, CN₄O), 144.2 (s, C(NH₂)NOH); **EA** (C₂H₇N₇O₃, 177.12) calcd.: C 13.56, H 3.98, N 55.36%; found: C 13.95, H 3.99, N 54.91%; **Sensitivities**. FS: >40 J; IS: 360 N; ESD: 0.7 J (at grain sizes <100 μm).

Compounds **5–9** were synthesized according to the procedures given in the Supplementary Information

6.4 Conclusions

5-Aminohydroximoyl-2-hydroxytetrazole (**3**) was obtained from inexpensive starting materials following a facile three-step route. Various nitrogen-rich salts (**4–8**) and the novel

zwitterionic 5-amidrazonyl-tetrazole-2-oxide monohydrate (**9**) were synthesized. Furthermore, the crystal structures of compounds **4**, **5**, **8**, **9**, and **10** were determined using single crystal X-ray diffraction. The densities are found in the range between 1.524 g cm⁻³ (**8**) and 1.755 g cm⁻³ (**4**). Surprisingly, compounds **3–9** showed no sensitivity towards friction (**4–9**: 360 N,) or impact (**4–9**: >40 J, **3**: 20 J). DTA measurements revealed that acid **3** has the highest thermal stability (192 °C), while its salts decompose below 190° C (**4**: 164 °C, **5**: 179 °C, **6**: 181 °C, **7**: 186 °C, **8**: 180 °C). The detonation parameters were calculated for compounds **3** and **4** by using the calculated heats of formation and experimentally obtained crystal densities, as well as CBS-4M and EXPLO5 (version 6.01; $D = \mathbf{3}$: 8179 m s⁻¹, **4**: 8934 m s⁻¹, RDX: 8815 m s⁻¹). The calculated detonation parameters show that compound **4** is in the range of RDX, while at the same time (**4**) shows improved sensitivity values toward friction and impact in comparison with RDX (IS = **4**: >40 J, RDX: 7.5 J; FS = **4**: 360 N, RDX: 120 N).

The study clearly demonstrates the effect of introducing the *N*-oxide group in tetrazoles. In general the introduction of *N*-oxides in tetrazoles:

- improves the sensitivities towards mechanical stimuli,
- slightly decreases the decomposition temperature and calculated heat of formation,
- results in a significant increase in densities, and
- improves the detonation velocity and detonation pressure

6.5 References

- [1] (a) Agrawal, J.P. 2010. Status of explosives. In *High Energy Materials*, 1st ed. Weinheim, Germany: Wiley-VCH; (b) Klapötke, T.M. 2011. *Chemistry of High-Energy Materials*, 1st ed. Berlin: de Gruyter.
- [2] Ostmark, H., U. Bemm, H. Bergman, and A. Langlet. 2002. N-guanylurea-dinitramide: A new energetic material with low sensitivity for propellants and explosives applications. *Thermochimica Acta*, 384: 253–259.
- [3] (a) Boileau, J., M. Carail, E. Wimmer, R. Gallo, and M. Pierrot. 1985. Dérivés nitrés acétylés du glycoluril. *Propellants, Explos. Pyrotech.*, 10: 118–120; (b) Boileau, J., E. Wimmer, R. Gilardi, M. M. Stineciphier, R. Gallo, and M. Pierrot. 1988. Structure of 1,4-dinitroglycoluril. *Acta Cryst. C*, 44: 696–699.

- [4] Talawar, M. B., R. Sivabalan, R., T. Mukundan, H. Muthurajan, A. K. Sikder, B. R. Gandhe, and A. S. Rao. 2009. Environmentally compatible next generation green energetic materials (GEMs). *J. Hazard. Mater.*, 161: 589–607.
- [5] Göbel, M., K. Karaghiosoff, T. M. Klapötke, D. G. Piercey, and J. Stierstorfer. 2010. Nitrotetrazolate-2*N*-Oxides and the Strategy of *N*-Oxide Introduction. *J. Am. Chem. Soc.*, 132: 17216–17226.
- [6] Fischer, N., T. M. Klapötke, S. Rappenglück, and J. Stierstorfer. 2012. The Reactivity of 5-Cyanotetrazole towards Water and Hydroxylamine. *ChemPlusChem*, 77: 877–888.
- [7] Klapötke, T. M., M. Q. Kurz, P. C. Schmid, and J. Stierstorfer. 2014. 5-(1*H*-Tetrazolyl)-2-Hydroxy-Tetrazole: A Selective 2*N*-Monooxidation of Bis(1*H*-Tetrazole). *ChemPlusChem*, *accepted*, doi: 10.1002/cplu.201402124R1
- [8] Burrows, E. P., and E. E. Brueggemann. 1985. Reversed-phase gradient high-performance liquid chromatography of nitramine munitions and characterization of munitions process samples by gas chromatography-mass spectrometry. *J. Chromatogr. A*, 329: 285–289.
- [9] Sućeska, M. 2012. EXPLO5.06 program. Zagreb, Croatia.
- [10] Xue, C., J. Sun, B. Kang, Y. Liu, X. Liu, G. Song, and Q. Xue. 2010. The β - δ -Phase Transition and Thermal Expansion of Octahydro-1,3,5,7-Tetranitro-1,3,5,7-Tetrazocine. *Propellants Explos. Pyrotech.*, 35: 333–338.
- [11] Fischer, N., D. Fischer, T. M. Klapötke, D. G. Piercey, and J. Stierstorfer. 2012. Pushing the limits of energetic materials - the synthesis and characterization of dihydroxylammonium 5,5'-bistetrazole-1,1'-diolate. *J. Mater. Chem.*, 22: 20418–20422.
- [12] Fischer, D., T. M. Klapötke, M. Reymann, P. C. Schmid, J. Stierstorfer, and M. Sućeska. 2014. Synthesis of 5-(1*H*-Tetrazolyl)-1-hydroxy-tetrazole and Energetically Relevant Nitrogen-Rich Ionic Derivatives. *Propellants Explos. Pyrotech.*, *in press*, doi: 10.1002/prop.201300152.
- [13] Kamlet, M. J., and S. J. Jacobs. 1968. Chemistry of Detonations I. A Simple Method for Calculating Detonation Properties of C–H–N–O Explosives. *J. Chem. Phys.*, 48: 23–35.
- [14] a) Hesse, M., H. Meier, and B. Zeeh. 2005. Spektroskopische Methoden in der Organischen Chemie, 5th ed. Stuttgart, New York: Thieme; b) Socrates, G. 2004.

Infrared and Raman Characteristic Group Frequencies: Tables and Charts, 3rd ed.
Chichester: John Wiley & Sons.

- [15] Klapötke, T. M., P. Mayer, C. Miró Sabaté, J. M. Welch, and N. Wiegand. 2008. Simple, Nitrogen-Rich, Energetic Salts of 5-Nitrotetrazole. *Inorg. Chem.*, 47: 6014–6027.
- [16] Boneberg, F., A. Kirchner, T. M. Klapötke, D. G. Piercey, M. J. Poller, and J. Stierstorfer. 2013. A Study of Cyanotetrazole Oxides and Derivatives thereof. *Chem. Asian J.*, 8: 148–159.

6.6 Supplementary information

6.6.1 Experimental

Guanidinium 5-aminohydroximoyl-tetrazole-2-oxide monohydrate (5)

5-Aminohydroximoyl-2-hydroxytetrazole (0.72 g, 5.0 mmol) was dissolved in 10 mL of water. A solution of guanidinium carbonate (0.45 g, 5.0 mmol) in water was added and the solution was refluxed for 1 h. The solution was left for crystallization to give guanidinium 5-aminohydroximoyl-tetrazole-2-oxide monohydrate as colorless crystals. Yield: 0.96 g, 4.35 mmol, 87%.

DTA (5 °C min⁻¹) onset: 111 °C (-H₂O), 166 °C(m.p.), 179 °C (dec.); **IR** (ATR, cm⁻¹): $\tilde{\nu}$ = 3449(m), 3342(s), 3146(s), 2814(w), 1663(s), 1637(vs), 1597(s), 1540(w), 1444(w), 1426(w), 1403(m), 1382(m), 1367(s), 1297(s), 1227(m), 1141(w), 1083(w), 1060(w), 1040(w), 1010(vw), 965(w), 948(m), 827(w), 827(w), 758(m), 736(w), 690(w), 658(vw); **Raman** (1064 nm, 300 mW, 25 °C, cm⁻¹): $\tilde{\nu}$ = 3228(3), 1667(9), 1640(13), 1600(13), 1539(100), 1512(11), 1405(5), 1373(4), 1231(6), 1142(10), 1087(6), 1058(7), 1041(49), 1026(6), 1010(28), 996(4), 967(6), 953(5), 828(5), 758(6), 588(3), 542(7), 447(4), 447(4), 405(8), 341(7), 316(4), 184(9), 146(29), 112(36), 90(58), 68(18); **¹H NMR** ([D₆]DMSO): δ = 9.68 (br s, 1H, C(NH₂)NOH), 7.17 (s, 4H, C(NH₂)₃⁺), 5.59 ppm (s, 2H, C(NH₂)₃⁺); **¹³C NMR** ([D₆]DMSO): δ = 158.2 (s, C(NH₂)₃⁺), 151.0 (s, CN₄O), 144.1 ppm (s, C(NH₂)NOH); **MS** *m/z* (FAB⁻): 143.1 (C₂H₃N₆O₂⁻), *m/z* (FAB⁺): 60.1 (CH₆N₃⁺); **EA** (C₃H₁₁N₉O₃, 221.18) calcd.: C 16.29, H 5.01, N 56.99%; found: C 16.63, H 4.92, N 56.52%; **Sensitivities**: IS: >40 J, FS: 360 N, ESD: 1.5 J (at grain sizes <100 μm).

Aminoguanidinium 5-aminohydroximoyl-tetrazole-2-oxide (6)

5-Aminohydroximoyl-2-hydroxytetrazole (0.72 g, 5.0 mmol) was dissolved in 10 mL of water. A solution of aminoguanidine bicarbonate (0.68 g, 5.0 mmol) in water was added and the solution was heated to 90 °C for 1 h. Aminoguanidinium 5-aminohydroximoyl-tetrazole-2-oxide crystallized as colorless needles. Yield: 0.89 mg, 4.08 mmol, 82%.

DTA (5 °C min⁻¹) onset: 181 °C (dec.); **IR** (ATR, cm⁻¹): $\tilde{\nu}$ = 3459(w), 3339(s), 3170(s), 2826(m), 1692(vs), 1667(vs), 1642(s), 1595(s), 1547(w), 1446(w), 1408(vs), 1390(s), 1377(s), 1312(s), 1216(m), 1137(w), 1090(w), 1069(m), 1053(m), 977(w), 938(vs), 762(s), 757(s), 757(s), 693(w), 662(m); **Raman** (1064 nm, 300 mW, 25 °C, cm⁻¹): $\tilde{\nu}$ = 3255(5), 1699(8), 1663(22), 1589(21), 1549(100), 1412(9), 1381(5), 1315(4), 1220(13), 1120(11), 1084(13), 1058(17), 1038(87), 954(32), 825(5), 758(14), 513(13), 440(13), 399(11), 353(11),

302(8), 214(18), 154(54), 154(54), 132(81), 97(61); **¹H NMR** ([D₆]DMSO): δ = 9.66 (s, 1H, C(NH₂)NOH), 8.92 (s, 1H, CNHN), 7.10 (s, br, 4H, CNH₂), 5.52 (s, 2H, C(NH₂)NOH), 4.72 ppm (s, 2H, NNH₂); **¹³C NMR** ([D₆]DMSO): δ = 158.9 (s, CH₇N₄⁺), 150.8 (s, CN₄O), 144.1 ppm (s, C(NH₂)NOH); **MS** m/z (FAB⁻): 143.1 (C₂H₃N₆O₂⁻), m/z (FAB⁺): 75.1 (CH₇N₄⁺); **EA** (C₃H₁₀N₁₀O₂, 218.18) calcd.: C 16.52, H 4.62, N 64.20%; found: C 16.92, H 4.47, N 63.21%; **Sensitivities**: IS: >40 J, FS: 360 N, ESD: 1.5 J (at grain sizes <100 μ m).

Ammonium 5-aminohydroximoyl-tetrazole-2-oxide monohydrate (7)

5-Aminohydroximoyl-2-hydroxytetrazole (0.72 g, 5.0 mmol) was dissolved in water (30 mL) and 25% NH₃ (0.4 mL) was added. The solution was stirred for 10 min and left standing. Ammonium 5-aminohydroximoyl-tetrazole-2-oxide monohydrate precipitated as a white powder. Yield: 0.68 g, 3.82 mmol, 76%.

DTA (5 °C min⁻¹) onset: 63 °C (-H₂O), 186 °C (dec.); **IR** (ATR, cm⁻¹): $\tilde{\nu}$ = 3435(m), 3296(m), 3172(m), 3058(m), 2896(m), 2751(m), 1863(w), 1679(s), 1648(m), 1609(m), 1499(w), 1451(s), 1421(m), 1406(vs), 1376(vs), 1303(m), 1213(s), 1132(vw), 1105(w), 1064(w), 1022(w), 951(s), 861(w), 861(w), 831(w), 808(w), 759(s), 718(m), 675(m); **Raman** (1064 nm, 300 mW, 25 °C, cm⁻¹): $\tilde{\nu}$ = 3066(3), 1670(24), 1602(13), 1576(5), 1563(11), 1548(100), 1535(14), 1519(9), 1410(11), 1309(2), 1217(9), 1127(14), 1067(5), 1038(5), 1024(60), 1009(6), 969(10), 829(6), 760(8), 698(2), 590(3), 449(4), 392(7), 392(7), 353(8), 323(6), 288(3), 186(9), 164(16), 144(15), 114(42), 105(47), 91(62), 81(49); **¹H NMR** ([D₆]DMSO): δ = 9.61 (br s, 1H, C(NH₂)NOH), 7.39 (br s, 4H, NH₄⁺), 5.56 ppm (s, 2H, C(NH₂)NOH); **¹³C NMR** ([D₆]DMSO): δ = 151.2 (s, CN₄O), 144.1 ppm (s, C(NH₂)NOH); **MS** m/z (FAB⁻): 143.1 (C₂H₃N₆O₂⁻), m/z (FAB⁺): 18.1 (NH₄⁺); **EA** (C₂H₉N₇O₃, 179.14) calcd.: C 13.41, H 5.06, N 54.73%; found: C 13.89, H 4.93, N 54.01%; **Sensitivities**: IS: >40 J, IS: 360 N, ESD: 1.0 J (at grain sizes <100 μ m).

Triaminoguanidinium 5-aminohydroximoyl-tetrazole-2-oxide dihydrate (8)

5-Aminohydroximoyl-2-hydroxytetrazole (0.72 g, 5.0 mmol) was dissolved in water (30 mL) and triaminoguanidine hydrochloride (0.70 g, 5.0 mmol) was added. The solution was left for crystallization. Triaminoguanidinium 5-aminohydroximoyl-tetrazole-2-oxide dihydrate crystallized as colorless needles. Yield: 1.05 g, 3.94 mmol, 79%.

DTA (5 °C min⁻¹) onset: 180 °C (dec.); **IR** (ATR, cm⁻¹): $\tilde{\nu}$ = 3426(w), 3327(m), 3185(m), 3042(m), 2792(m), 1681(vs), 1607(s), 1454(w), 1407(m), 1376(s), 1301(m), 1219(w), 1198(w), 1141(m), 1102(w), 1030(m), 937(s), 827(vw), 767(m), 695(vw), 662(vw); **Raman**

(1064 nm, 300 mW, 25 °C, cm^{-1}): $\tilde{\nu} = 3257(7)$, 1667(28), 1606(22), 1542(100), 1516(10), 1411(5), 1394(5), 1331(4), 1222(13), 1147(9), 1130(13), 1101(13), 1055(9), 1031(50), 950(14), 888(12), 758(10), 643(7), 480(6), 442(11), 418(12), 400(12), 356(12), 356(12), 307(9), 261(12), 234(15), 160(21), 139(37), 119(41), 92(98), 67(21); **^1H NMR** ($[\text{D}_6]$ DMSO): $\delta = 9.47$ (s, 1H, $\text{C}(\text{NH}_2)\text{NOH}$), 8.60 (s, 3H, CNHN), 5.41 (s, 2H, $\text{C}(\text{NH}_2)\text{NOH}$), 4.50 ppm (br s, 6H, NNH_2); **^{13}C NMR** ($[\text{D}_6]$ DMSO): $\delta = 159.1$ (s, CH_9N_6^+), 150.4 (s, CN_4O), 144.3 ppm (s, $\text{C}(\text{NH}_2)\text{NOH}$); **MS** m/z (FAB^-): 143.1 ($\text{C}_2\text{H}_3\text{N}_6\text{O}_2^-$), m/z (FAB^+): 105.1 (CH_9N_6^+); **EA** ($\text{C}_3\text{H}_{16}\text{N}_{12}\text{O}_4$, 284.24) calcd.: C 12.68, H 5.67, N 59.13%; found: C 12.98, H 5.61, N 58.83%; **Sensitivities**: IS: >40 J, FS: 360 N, ESD: 0.5 J (at grain sizes <100 μm).

5-Amidrazonyl-tetrazole-2-oxide monohydrate (9)

5-Aminohydroximoyl-2-hydroxytetrazole (0.72 g, 5.0 mmol) was dissolved in 30 mL of water. A solution of hydrazine (0.25 g, 5.0 mmol) in water was added. The solution was stirred for 5 min at ambient temperature and was left stand to yield 5-amidrazonyl-tetrazole-2-oxide monohydrate as colorless crystals. Yield: 0.16 g, 1.01 mmol, 20%.

DTA (5 °C min^{-1}) onset: 63 °C ($-\text{H}_2\text{O}$), 122 °C (dec.); **IR** (ATR, cm^{-1}): $\tilde{\nu} = 3454(\text{w})$, 3398(w), 3320(m), 3067(w), 2978(w), 2816(m), 2744(m), 2651(m), 2121(vw), 1669(m), 1636(w), 1607(m), 1564(w), 1452(w), 1409(s), 1393(m), 1372(vs), 1304(m), 1218(s), 1141(m), 1127(w), 1089(s), 1024(w), 1024(w), 964(vs), 832(m), 765(m), 756(m), 719(w), 695(m), 660(w); **Raman** (1064 nm, 300 mW, 25 °C, cm^{-1}): $\tilde{\nu} = 3236(4)$, 2820(3), 1660(27), 1588(18), 1542(88), 1474(5), 1411(10), 1376(6), 1303(2), 1218(9), 1118(19), 1065(7), 1042(6), 1025(87), 1008(12), 964(18), 826(8), 759(14), 698(3), 660(3), 596(7), 451(9), 400(18), 400(18), 343(11), 318(7), 263(4), 220(13), 164(34), 116(58), 92(100), 76(56); **^1H NMR** ($[\text{D}_6]$ DMSO): $\delta = 7.36$ (s, 2H, CNHNH_2), 5.57 ppm (s, 2H, $\text{C}(\text{NH}_2)$); **^{13}C NMR** ($[\text{D}_6]$ DMSO): $\delta = 151.0$ (s, CN_4O), 144.2 ppm (s, $\text{C}(\text{NH}_2)\text{NHNH}_2$); **MS** m/z (FAB^-): 142.1 ($\text{C}_2\text{H}_4\text{N}_7\text{O}^-$); **EA** ($\text{C}_2\text{H}_7\text{N}_7\text{O}_2$, 161.12) calcd.: C 14.91, H 4.38, N 60.85%; found: C 15.32, H 4.29, N 60.51%; **Sensitivities**: IS: >40 J, friction sensitivity: 360 N, ESD: 1.0 J (at grain sizes <100 μm).

6.6.2 XRD data and parameters

Table S1. XRD data and parameters

	4	5	8	9	10
Formula	C ₂ H ₇ N ₇ O ₃	C ₃ H ₁₁ N ₉ O ₃	C ₃ H ₁₆ N ₁₂ O ₄	C ₂ H ₇ N ₇ O ₂	C ₂ H ₆ N ₆ O ₂
FW [g mol ⁻¹]	177.15	221.21	284.28	161.15	146.13
Crystal system	monoclinic	orthorhombic	monoclinic	orthorhombic	monoclinic
Space Group	<i>P2₁/c</i>	<i>Pna2₁</i>	<i>C2/c</i>	<i>Pca2₁</i>	<i>C2/c</i>
Color / Habit	colorless, plate	colorless, block	colorless, plate	colorless, plate	colorless, plate
Size [mm]	0.02 x 0.05 x 0.13	0.06 x 0.24 x 0.31	0.04 x 0.15 x 0.20	0.04 x 0.15 x 0.25	0.02 x 0.10 x 0.40
<i>a</i> [Å]	16.8022(12)	20.6155(11)	30.3686(15)	21.2128(12)	19.286(4)
<i>b</i> [Å]	3.5611(3)	9.1001(7)	3.9469(2)	3.5347(2)	3.5699(3)
<i>c</i> [Å]	22.4560(17)	4.9135(5)	21.0147(11)	8.5711(4)	19.042(3)
α [°]	90	90.00	90	90.00	90
β [°]	93.401(2)	90.00	100.247(1)	90.00	118.720(19)
γ [°]	90	90.00	90	90.00	90
<i>V</i> [Å ³]	1341.27(18)	921.79(13)	2478.7(2)	642.67(6)	1149.7(4)
<i>Z</i>	8	4	8	4	8
$\rho_{\text{calc.}}$ [g cm ⁻³]	1.755	1.594	1.524	1.665	1.689
μ [mm ⁻¹]	0.156	0.137	0.132	0.143	0.146
<i>F</i> (000)	736	464	1200	336	608
$\lambda_{\text{MoK}\alpha}$ [Å]	0.71073	0.71073	0.71073	0.71073	0.71073
<i>T</i> [K]	100	173	293	173	173
θ min-max [°]	2.12, 26.40	4.48, 27.49	2.6, 26.1	4.52, 26.42	4.2, 26.5
Dataset <i>h</i> ; <i>k</i> ; <i>l</i>	−21:20; 0:4; 0:28	−25:26; −7:11; −6:5	−36:36; −4:4; −25:25	−26:22; −3:4; −10: 10	−23:24; −4:4; −23:17
Reflect. coll.	2759	5175	30319	3770	3420
Independ. refl.	2761	1180	2437	1329	1185
<i>R</i> _{int}	0.000	0.0355	0.0392	0.0265	0.051
Reflection obs.	2292	1049	1974	1267	1185
No. parameters	274	180	245	128	115
<i>R</i> ₁ (obs)	0.0477	0.0289	0.0354	0.0259	0.0539
<i>wR</i> ₂ (all data)	0.1009	0.0662	0.0926	0.0632	0.1333
<i>S</i>	1.086	1.049	1.072	1.047	1.052
Resd.	−0.291, 0.366	−0.148, 0.139	−0.259, 0.168	−0.121, 0.116	−0.286, 0.301
Dens.[e Å ⁻³]					
Device type	Oxford XCalibur3 CCD	Oxford XCalibur3 CCD	Oxford XCalibur3 CCD	Oxford XCalibur3 CCD	Oxford XCalibur3 CCD
Solution	SIR-92	SIR-92	SIR-92	SIR-92	SIR-92
Refinement	SHELXL-97	SHELXL-97	SHELXL-97	SHELXL-97	SHELXL-97
Absorpt. corr.	multi-scan	multi-scan	multi-scan	multi-scan	multi-scan
CCDC	1000369	1000365	1000368	1000366	1000367

6.6.3 Explosive performance: Heat of formation calculations

General information about the heat of formation calculations can be found in the appendix of this thesis. The calculation results are summarized in Table S2.

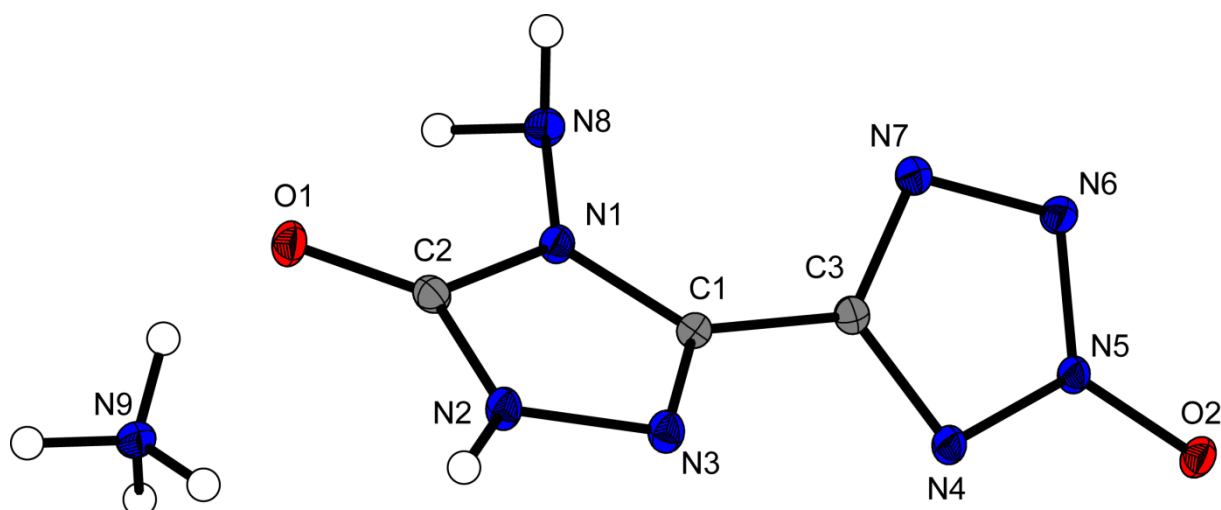
Table S2. Calculation results

M	$-H^{298}$ [a] / a.u.	$\Delta_f H^\circ(\text{g}, \text{M})$ / kJ mol^{-1} [b]	V_M / nm^3 [c]	ΔU_L , ΔH_L (4); [d] ΔH_{sub} [e] (3) / kJ mol^{-1}	$\Delta_f H^\circ(\text{s})$ [f] / kJ mol^{-1}	Δn [g]	$\Delta_f U(\text{s})$ [f] / kJ kg^{-1}
3	556.717459	325.8		87.4	238.3	6.0	1757.2
NH₄O⁺	131.863249	687.2					
AHT2O⁻	556.209692	125.6					
4		812.0	0.173	525.1, 530.1	281.9	8.5	1710.5

[a] CBS-4M electronic enthalpy; [b] gas phase enthalpy of formation; [c] molecular volumes taken from X-ray structures and corrected to room temperature; [d] lattice energy and enthalpy (calculated using Jenkins and Glasser equations); [e] enthalpy of sublimation (calculated by Trouton rule); [f] standard solid state enthalpy of formation; [g] solid state energy of formation.

Energetic Complexes of 5-(4-Amino-1,2,4-triazol-3-on-5-yl)tetrazole and Ionic Derivatives of its 2*N*-Oxide

published in *Z. Anorg. Allg. Chem.* **2014**, 640, 2759–2765. (DOI: 10.1002/zaac.201400417)



Abstract: 5-(4-Amino-1,2,4-triazol-3-on-5-yl)tetrazole (**HATT**) was used as a ligand for the two complexes $[\text{Cu}(\text{ATT})_2(\text{H}_2\text{O})_2] \cdot 2\text{H}_2\text{O}$ (**5**) and $\text{Co}(\text{HATT})_2(\text{H}_2\text{O})_2](\text{ClO}_4)_3 \cdot 4\text{H}_2\text{O}$ (**6**). Both were characterized by X-ray diffraction, elemental analysis and IR spectroscopy. Following the recent trend in energetic materials research of synthesis of heterocyclic 2*N*-oxides the corresponding 5-(4-amino-1,2,4-triazol-3-on-5-yl)tetrazole-2-oxide (**HATT2O**) was synthesized for the first time. Two ionic energetic derivatives (ammonium, hydroxylammonium) were prepared and an intensive characterization of their energetic properties and sensitivities is given. In addition heats of formation were computed and several detonation parameters calculated using the EXPLO5 6.01 computer code.

Keywords: Tetrazole · Triazolone · *N*-Oxides · X-ray · Coordination chemistry

7.1 Introduction

Unfortunately RDX (royal demolition explosive, hexahydro-1,3,5-trinitro-1,3,5-triazine),^[1] although demonstrated to be highly noxious,^[2] is still used as secondary explosive because of its performance and easy availability. Basically energetic materials can be classified by the origin of their release of energy: i) the oxidation of the carbon backbone like in TNT (trinitrotoluol) or PETN (pentaerythritol tetranitrate), ii) cages and strained ring systems e.g. in CL-20^[3] (2,4,6,8,10,12-hexanitro-2,4,6,8,10,12-hexaazaisowurtzitane) or ONC^[4] (octanitrocubane) (Figure 1), iii) nitrogen-rich materials such as triazoles, tetrazoles or tetrazines. The combination of all of these strategies would lead to nitrogen-rich, strained heterocycles containing C–NO₂ groups.

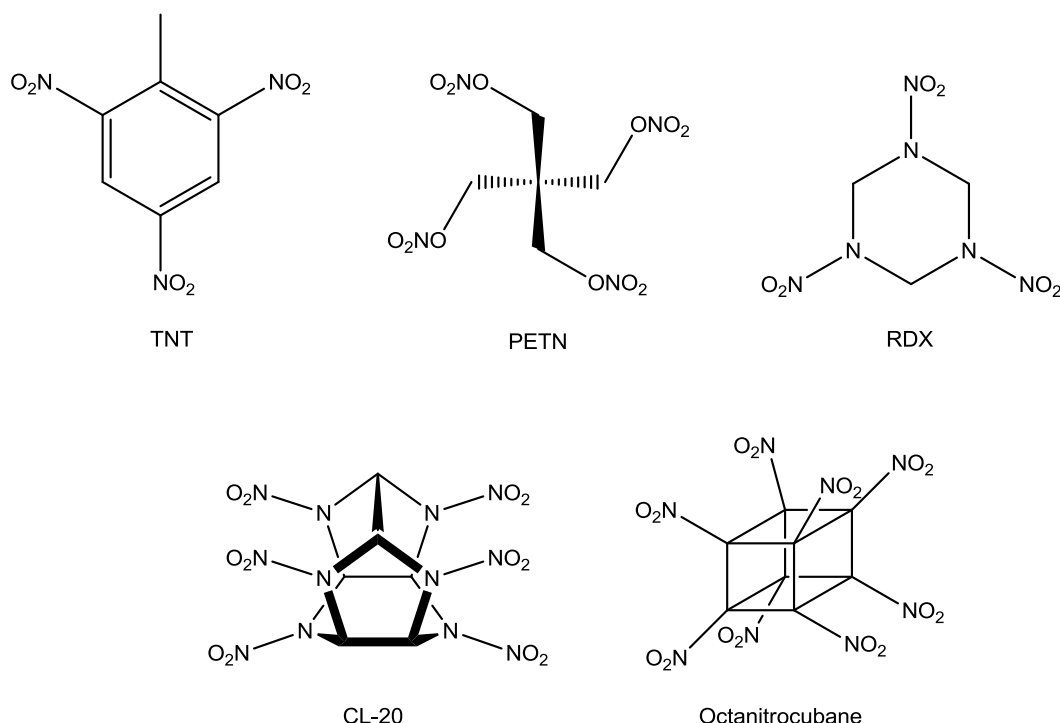


Figure 1. Chemical Structures of common energetic materials: TNT, PETN, RDX, CL-20 and ONC.

Tetrazoles possess a wide range of application in the fields of primary^[5] and secondary explosives^[6] as well as pyrotechnic fuels^[7]. Cyclic systems with aromatic characteristics and high-nitrogen content possess several advantages over conventional energetic materials as the enhancement of density, the decrease of sensitivity and high heats of formation.^[6] Nitrogen-rich heterocycles decompose mainly environmentally benign N₂-gas.^[6,8] Following this concept, we recently synthesized K₂DNABT, a suitable replacement for toxic lead azide, which is based on 1,1'-dinitramino-5,5'-bistetrazole.^[9] It has been shown many times that performance of energetic nitrogen-rich heterocycles can be improved by introduction of *N*-

oxides.^[10] Examples of energetic materials following this concept are TKX-50 (dihydroxylammonium 5,5'-bistetrazole-1,1'-diolate),^[11] MAD-X1 (dihydroxylammonium 3,3'-dinitro-5,5'-bis-1,2,4-triazole-1,1'-diolate),^[12] and DNBTDO (5,7-dinitrobenzo-1,2,3,4-tetrazine-1,3-dioxide)^[13] (Figure 2).

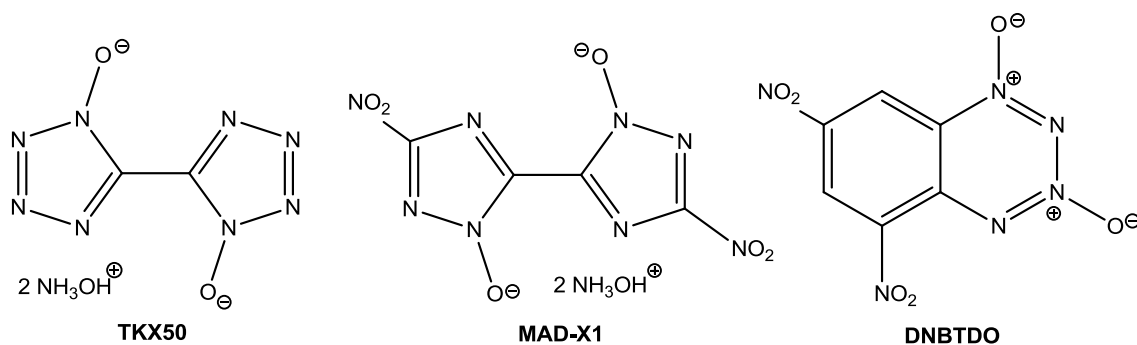


Figure 2. Chemical structures of the energetic *N*-oxides: **TKX-50** (dihydroxylammonium 5,5'-bistetrazole-1,1'-diolate), **MAD-X1** (dihydroxylammonium 3,3'-dinitro-5,5'-bis-1,2,4-triazole-1,1'-diolate) and **DNBTDO** (tetrazine-1,3-dioxide, 5,7-dinitrobenzo-1,2,3,4-tetrazine-1,3-dioxide).

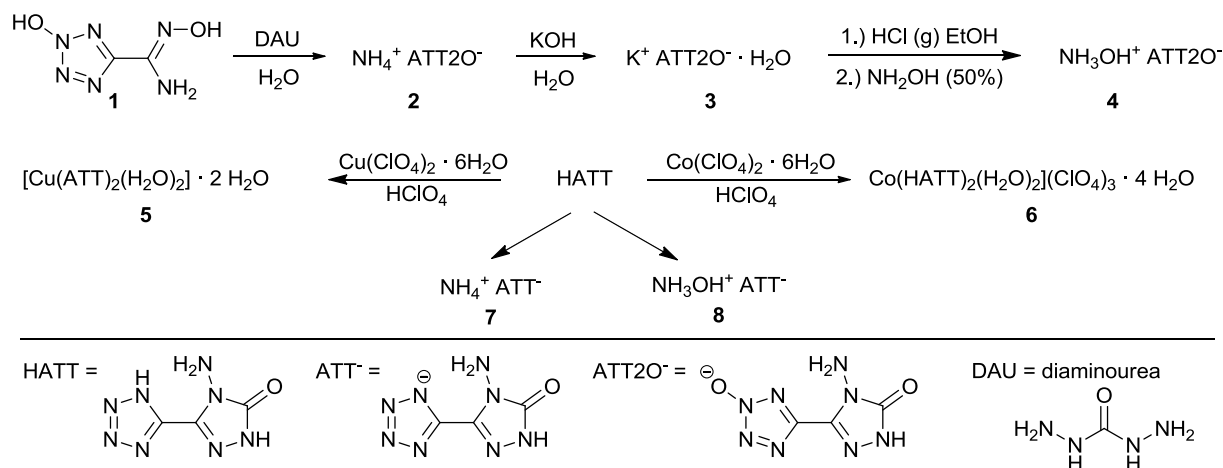
Recently, 5-(4-amino-1,2,4-triazol-3-on-5-yl)tetrazole (**HATT**) and its energetic salts **7** and **8** (see Scheme 1) were investigated.^[14] In this report we continue the investigation of *N*-oxide introduction. Therefore ammonium 5-(4-amino-1,2,4-triazol-3-on-5-yl)tetrazole-2-oxide (**2**) and hydroxylammonium 5-(4-amino-1,2,4-triazol-3-on-5-yl)tetrazole-2-oxide (**4**) have been prepared and compared to the corresponding compounds **7** and **8** without the *N*-oxide functionality. Further, the ability of **HATT** to act as a bidentate ligand was demonstrated with a copper(II) (**5**) and cobalt(III) perchlorate (**6**) complex. The complexes were tested on their potential as primary explosives.

7.2 Results and Discussion

7.2.1 Synthesis

A synthetic overview is depicted in Scheme 1. 5-Aminohydroxymoyltetrazole (**1**) and 5-(4-amino-1,2,4-triazol-3-on-5-yl)tetrazole(**HATT**) were synthesized according to Refs. [14,15]. Compound **1** was refluxed with diaminourea in water to give ammonium 5-(4-amino-1,2,4-triazol-3-on-5-yl)tetrazole-2-oxide (**2**). Potassium 5-(4-amino-1,2,4-triazol-3-on-5-yl)tetrazole-2-oxide dihydrate (**3**) was obtained by the reaction of **2** with potassium hydroxide. The reaction of **3** with HCl(g) in ethanol followed by a work-up with hydroxylamine (50%) solution yielded hydroxylammonium 5-(4-amino-1,2,4-triazol-3-on-5-yl)tetrazole-2-oxide (**4**).

Further, **HATT** was solved in 12 % perchloric acid and reacted with copper(II) perchlorate to obtain complex **5**. Due to the high acidity of the ligand, a copper(II) complex with anionic **ATT⁻** instead of the expected neutral **HATT** as ligand was obtained. In contrast, the reaction of **HATT** with cobalt(II) perchlorate in 15 % perchloric acid yielded a complex with neutral **HATT** as ligand and perchlorate as counterions. During the reaction the cobalt(II) was oxidized to cobalt(III) probably by air oxygen.



Scheme 1. Synthetic route towards compounds **2–6** as well as chemical structures of compounds **7** and **8**.

7.2.2 Crystal Structures

The crystal structures of compounds **2–6** were determined by low temperature X-ray diffraction. Selected parameters of the X-ray determinations are given in Table S1 in the Supporting Information. The cif files were deposited^[16] with the CCDC Nos. CCDC-1020001 (**2**), -1020002 (**3**), -1020003 (**4·H₂O**), -1000194 (**5**), -1000195 (**6**), and -1020004 (**9**).

The ammonium salt **2** crystallizes water-free in the triclinic space group *P*-1 with two molecular moieties in the unit cell. The calculated density of salt **2** is 1.711 g cm⁻³, which is higher than the density of compound **7** (1.625 g cm⁻³), the analogous compound without the *N*-oxide group.^[14] The two rings are strongly tilted against each other, the N3–C1–C3–N4 torsion angle is 35.6(18)°, which is in contrast to the almost planar system of compound **7**.^[14] The molecular unit of **2** is shown in Figure 3.

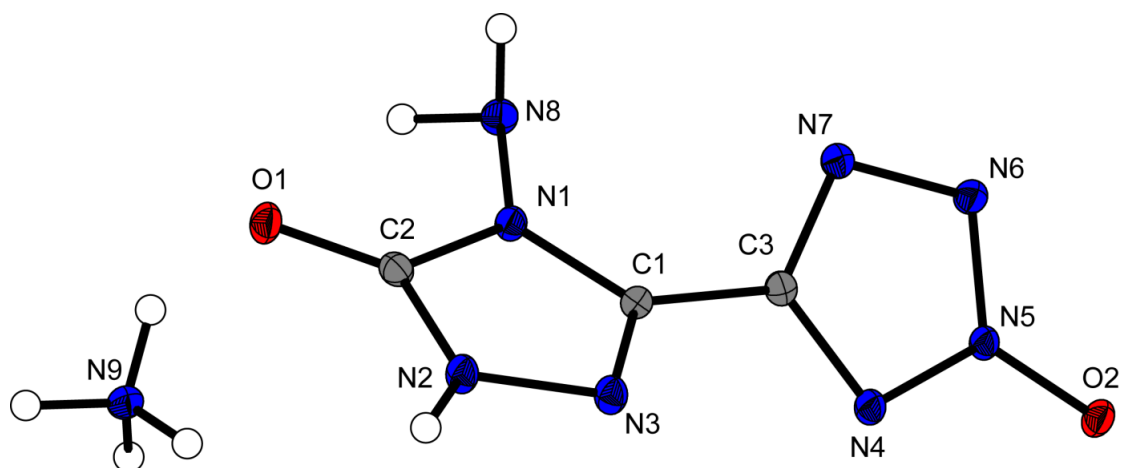


Figure 3. Molecular unit of ammonium 5-(4-amino-1,2,4-triazol-3-on-5-yl)tetrazole-2-oxide (**2**). Thermal ellipsoids show the 50% probability level and hydrogen atoms are shown as small spheres of arbitrary radius. Selected bond lengths: [Å]: O1–C2 1.239(3), N6–N7 1.344(2), O2–N5 1.310(2), N7–C3 1.331(3), N1–N8 1.415(2), N1–C1 1.369(3), N1–C2 1.384(3), N4–C3 1.343(3), C1–C3 1.459(3); selected bond angles [°]: N8–N1–C1 125.67(16), N8–N1–C2 125.84(16), C1–N1–C2 108.45(18), N3–N2–C2 112.69(16), N2–N3–C1 104.56(16).

Potassium 5-(4-amino-1,2,4-triazol-3-on-5-yl)tetrazole-2-oxide dihydrate (**3**) is illustrated in Figure 4. It crystallizes in the triclinic space group $P\bar{1}$ with two molecular moieties per unit cell. The calculated density of **3** is 1.775 g cm^{-3} . In contrast to the structure of **2** the torsion angle N5–C2–C5–N1 is $175.98 (17)^\circ$, which indicates an almost planar structure.

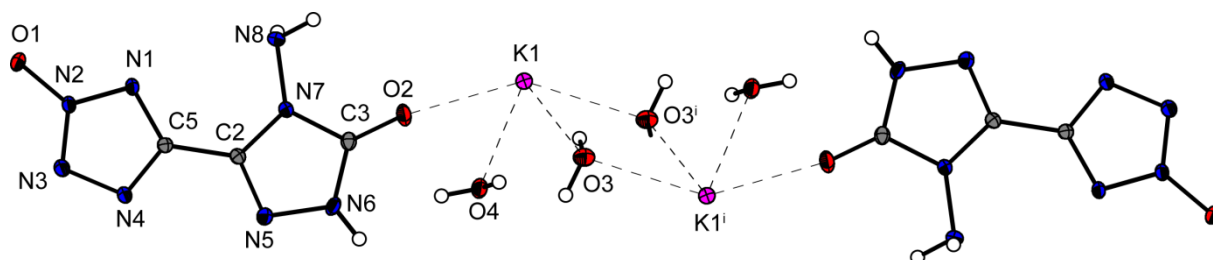


Figure 4. View on a selected section of the packing of potassium 5-(4-amino-1,2,4-triazol-3-on-5-yl)tetrazole-2-oxide dihydrate (**3**). Thermal ellipsoids show the 50% probability level and hydrogen atoms are shown as small spheres of arbitrary radius.

The hydroxylammonium salt **4** crystallizes from water as monohydrate ($\mathbf{4} \cdot \text{H}_2\text{O}$) in the triclinic space group $P\bar{1}$ with four molecular moieties per unit cell. The calculated density of $\mathbf{4} \cdot \text{H}_2\text{O}$ is 1.704 g cm^{-3} at 173K, which is only slightly lower than the pycnometrically measured density of the water free structure **4** (1.73 g cm^{-3} at 298 K). However, the density of the water-free hydroxylammonium salt **4** is higher than the density of compound **8** (1.703 g cm^{-3}), which does not exhibit an *N*-oxide group.^[14] Compound **2** and **4** are consistent examples demonstrating the effect of increasing densities by *N*-oxidation.^[10-13] The torsion angle N4–C1–C2–N5 in **4** is $175.2 (2)^\circ$, the two connected rings form an almost planar structure similar to compound **3**. The molecular unit of **4** is shown in Figure 5.

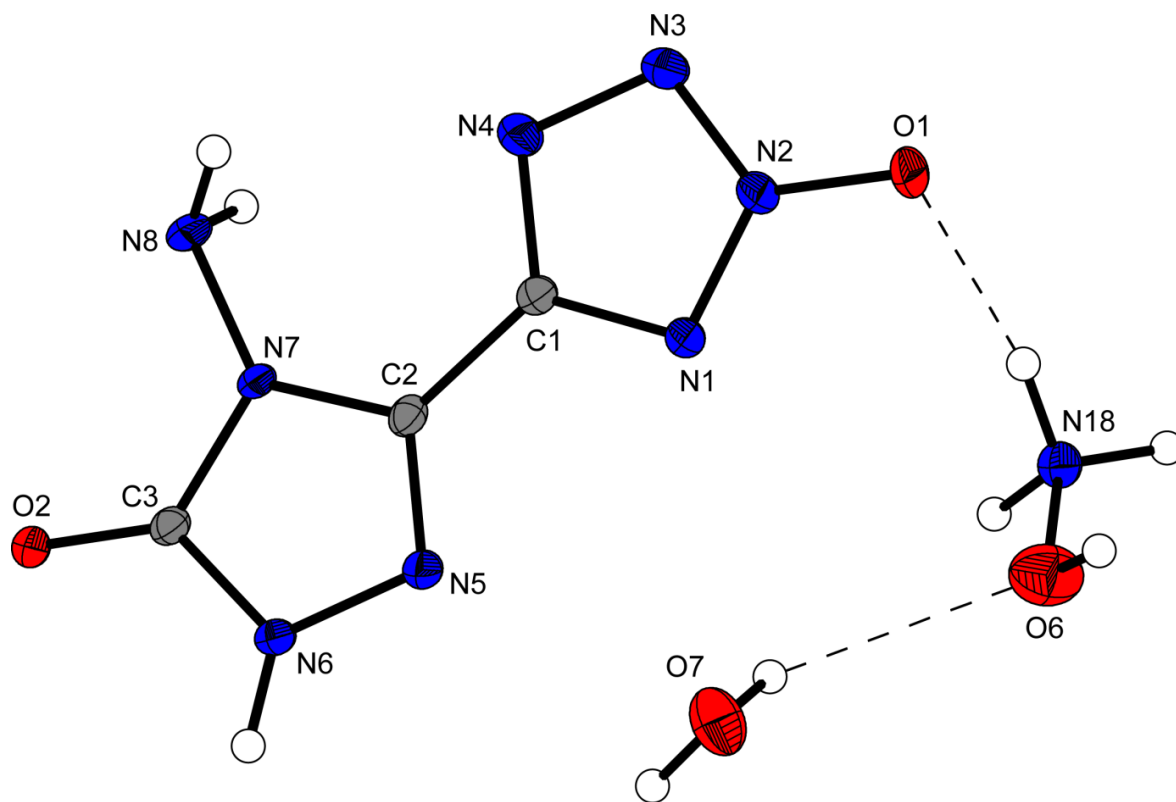


Figure 5. Molecular unit of hydroxylammonium 5-(4-amino-1,2,4-triazol-3-on-5-yl)tetrazole-2-oxide monohydrate (**4** · **H₂O**). Thermal ellipsoids show the 50% probability level and hydrogen atoms are shown as small spheres of arbitrary radius. Selected bond lengths: [Å]: O2–C3 1.239(3), N3–N4 1.344(3), O1–N2 1.302(3), N4–C1 1.333(3), N7–N8 1.407(3), N7–C2 1.378(3), selected bond angles [°]: N8–N7–C2 130.8(2), N8–N7–C3 121.55(19), C2–N7–C3 107.70(19).

The copper(II) complex **5** crystallizes in the monoclinic space group $P2_1/n$ with two formula units per unit cell and a calculated density of 2.009 g cm^{-3} at 100 K. The copper(II) atom exhibits an octahedral coordination sphere [$\angle(\text{N1–Cu1–N8}) = 92.31(7)^\circ$ and $\angle(\text{O2–Cu1–N1}) = 88.86(6)^\circ$] with Jahn-Teller distortion along the O2–Cu1–O2^i axis [$d(\text{Cu1–O2}) = 2.4911(15) \text{ \AA}$]. The Cu–N bonds in the equatorial position exhibit standard values of copper(II) complexes with about 2 \AA .^[17] The bond lengths and angles of the deprotonated tetrazole ring and the 4-amino-1,2,4-triazol-3-one are also in the range of literature known compounds.^[17a,18] The molecular unit of complex **5** is illustrated in Figure 6.

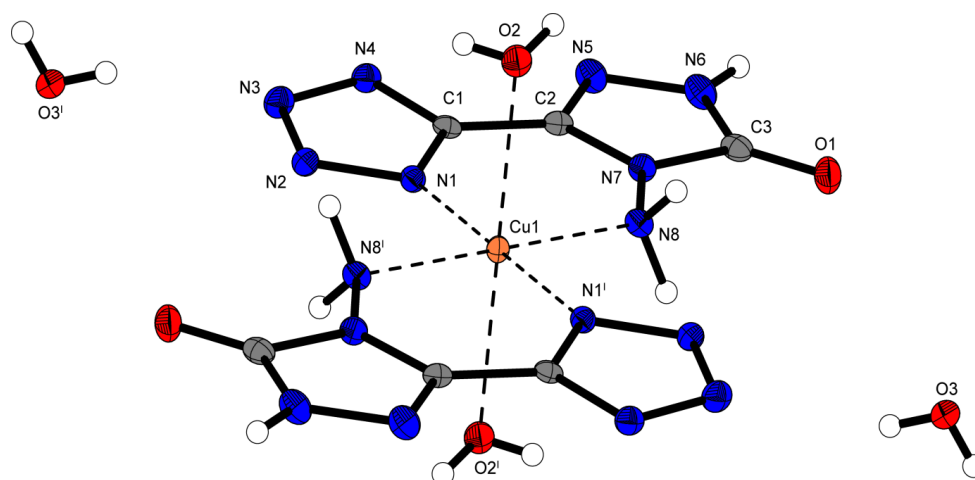


Figure 6. Formula unit of $[\text{Cu}(\text{ATT})_2(\text{H}_2\text{O})_2] \cdot 2 \text{H}_2\text{O}$ (**5**). Thermal ellipsoids of non-hydrogen atoms are drawn at the 50 % probability level. Selected bond lengths [\AA]: Cu1–N1 1.9729(17), Cu1–N8 2.0504(19), Cu1–O2 2.4911(15), C1–N1 1.338(3), N1–N2 1.353(3), N2–N3 1.312(3), C1–C2 1.447(3), C2–N7 1.372(3), C2–N5 1.301(3), N5–N6 1.371(3), C3–N7 1.392(3), C3–O1 1.224(3), N7–N8 1.408(2); selected bond angles [$^\circ$]: N1–Cu1–N8 92.31(7), O2–Cu1–N1 88.86(6), O2–Cu1–N8 89.49(7), C1–N1–Cu1 128.79(15), N2–N1–Cu1 125.27(14), N7–N8–Cu1 121.86(14), N3–N2–N1 107.93(18), N2–N3–N4 110.88(18), N1–C1–C2 123.93(19), C2–N5–N6 104.16(18), C2–N7–N8 128.12(18), O1–C3–N7 126.7(2); selected torsion angles [$^\circ$]: Cu1–N1–N2–N3 172.97(14), N8–Cu1–N1–C1 $-5.36(19)$, C1–N1–N2–N3 0.0(2), N1–C1–C2–N7 $-3.0(3)$, N6–N5–C2–N7 0.1(2), N8–N7–C2–C1 $-1.2(3)$, C2–N7–C3–O1 179.6(2). Symmetry code: i: $1-x, 1-y, -z$.

The two crystal water molecules are stabilized by strong hydrogen bonds (Table 1) between O3–H3A \cdots N3ⁱ, O3–H3B \cdots O2ⁱⁱ and N8–H8A \cdots O3ⁱⁱ (symmetry codes: i: $1-x, 1-y, -z$; ii: $0.5-x, -0.5+y, 0.5-z$). This explains why the dehydration process firstly occurs at 145 $^\circ\text{C}$ (onset).

Table 1. Distances and angles of selected hydrogen bonds in complex **5**.

D–H \cdots A	D–H / \AA	H \cdots A / \AA	D \cdots A / \AA	D–H \cdots A / $^\circ$
O3–H3A \cdots N3i	0.70(4)	2.20(4)	2.867(3)	160(3)
O3–H3B \cdots O2ii	0.71(4)	2.14(4)	2.833(3)	166(3)
N8–H8A \cdots O3ii	0.91(3)	1.97(3)	2.852(3)	163(3)
N8–H8B \cdots O1iii	0.76(3)	2.10(3)	2.841(3)	165(3)

Symmetry codes: i: $1-x, 1-y, -z$; ii: $0.5-x, -0.5+y, 0.5-z$; iii: $1.5-x, 0.5+y, 0.5-z$.

The cobalt(III) complex **6** crystallizes in the monoclinic space group $C2/c$ with four formula units per unit cell and a calculated density of 2.022 g cm^{-3} at 173 K. The coordination sphere is octahedral and the cobalt center is surrounded by two **HATT** and two aqua ligands. The Co–N bonds [$d(\text{Co1–N4}) = 2.08 \text{ \AA}$ and $d(\text{Co1–N8}) = 2.22 \text{ \AA}$] are longer than in comparable literature known cobalt(III) complexes (Co–N about $1.90\text{--}2.0 \text{ \AA}$).^[19] The bond lengths are more in the range of octahedral cobalt(II) complexes (Co–N about $2.1\text{--}2.2 \text{ \AA}$).^[17b, 20] The lengths and angles of the **HATT** ligand are similar to that of the anionic **ATT** in complex **5**. The triazolone units are nearly identical and for the tetrazole units, only small differences can be observed between the neutral [$d(\text{N2–N3}) = 1.312(3) \text{ \AA}$] and anionic [$d(\text{N2–$

N3) = 1.292(3) Å] form. The non-coordinating perchlorates exhibit normal values for the bond lengths and angles.^[21] The molecular unit of complex **6** is illustrated in Figure 7.

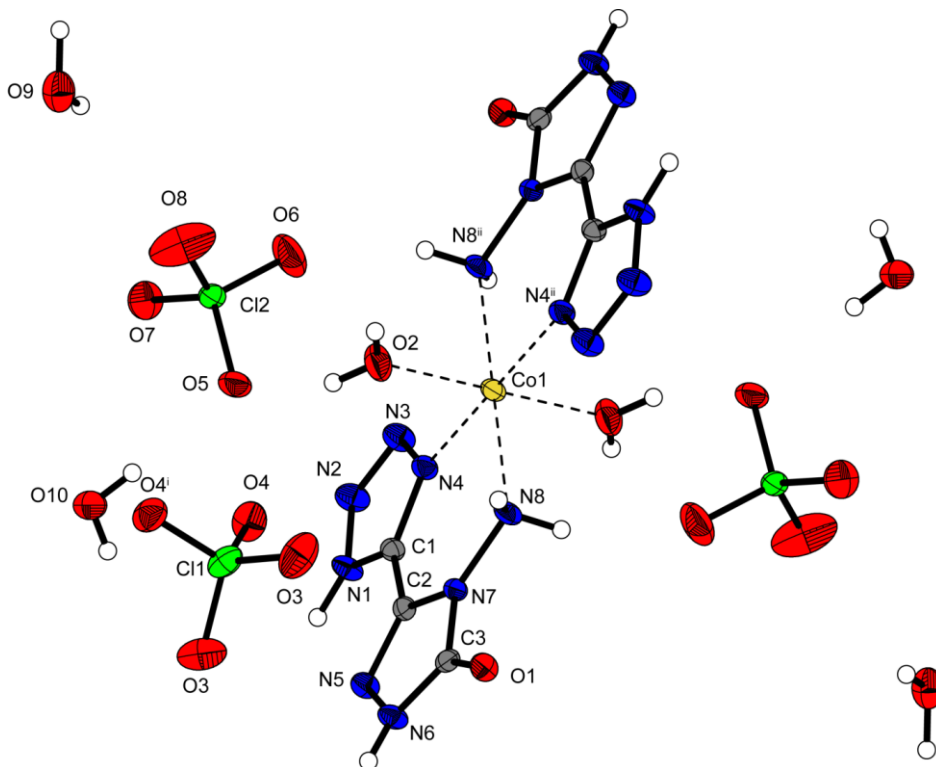


Figure 7. Formula unit of $[\text{Co}(\text{HATT})_2(\text{H}_2\text{O})_2](\text{ClO}_4)_3 \cdot 4 \text{H}_2\text{O}$ (**6**). Thermal ellipsoids of non-hydrogen atoms are drawn at the 50 % probability level. Selected bond lengths [Å]: Co1–O2 2.066(2), Co1–N4 2.080(2), Co1–N8 2.222(2), C1–N1 1.327(3), N1–N2 1.345(3), N2–N3 1.292(3), C1–C2 1.446(3), C2–N7 1.372(3), C2–N5 1.304(3), N5–N6 1.372(3), C3–N7 1.384(3), C3–O1 1.236(3), N7–N8 1.419(3), C11–O3 1.440(2), C11–O4 1.443(2); selected bond angles [°]: N4–Co1–N8 87.07(8), O2–Co1–N4 90.85(8), O2–Co1–N8 88.76(9), C1–N4–Co1 130.21(17), N3–N4–Co1 123.56(16), N7–N8–Co1 121.21(15), N3–N2–N1 106.8(2), N2–N3–N4 110.1(2), N4–C1–C2 125.7(2), C2–N5–N6 104.5(2), C2–N7–N8 128.4(2), O1–C3–N7 126.0(2), O3–C11–O4 108.99(12); selected torsion angles [°]: N2–N3–N4–Co1 –175.56(16), N8–Co1–N4–N3 –172.4(2), C1–N1–N2–N3 –0.9(3), N4–C1–C2–N7 –4.4(4), N6–N5–C2–N7 –0.4(3), N8–N7–C2–C1 –1.9(4), C2–N7–C3–O1 –179.8(2). Symmetry codes: i: 0.5–x, 0.5–y, 1–z; ii: –x, y, 0.5–z.

The perchlorate anions and crystal water molecules are stabilized by various hydrogen bonds which are formed between them and the ligands of the complex unit (Table 2).

Table 2. Distances and angles of selected hydrogen bonds in complex **6**.

D–H...A	D–H / Å	H...A / Å	D...A / Å	D–H...A / °
N1–H1...O1 ⁱⁱⁱ	0.89(3)	1.82(3)	2.697(3)	169(3)
O2–H2A...O7 ^{iv}	0.72(4)	2.15(4)	2.873(4)	176(5)
N6–H6...O9 ^v	0.83(3)	2.04(4)	2.857(3)	171(4)
N8–H8A...N5 ^{vi}	0.89(4)	2.47(4)	3.343(3)	168(3)
O9–H9B...O1 ^{vii}	0.92(4)	1.95(4)	2.805(3)	155(3)
O10–H10A...O9 ^{viii}	0.75(4)	1.96(5)	2.692(3)	166(5)
O10–H10B...O5	0.81(4)	2.07(4)	2.855(5)	161(4)

Symmetry codes: i: 0.5–x, 0.5–y, 1–z; ii: –x, y, 0.5–z; iii: x, –y, –0.5+z; iv: x, 1–y, 0.5+z; v: –x, –1+y, 0.5–z; vi: x, –y, 0.5+z; vii: x, 1+y, z; viii: x, 1–y, –0.5+z.

7.2.3 NMR, IR and Raman spectroscopy

Compounds **2–4** were investigated by ^1H and ^{13}C spectroscopy. The proton spectra of the ionic compounds **2–4** show peaks with similar chemical shifts for the single proton at the triazole moiety (11.92–11.79 ppm) and the two protons at the amino moiety (5.35–5.31 ppm). The ^{13}C spectra of compounds **2–4** each reveal three signals which do not differ significantly for each salt. The signals in the range from 154.1 to 154.0 ppm can be assigned to the carbonyl C-atom of the triazole ring. Compounds **7** and **8**, which lack the *N*-oxide reveal signals with similar chemical shifts at 154.1 and 154.2 ppm.^[14] The two other signals can be assigned to the C-atom of the tetrazole ring (146.3–145.8 ppm) and to the remaining C-atom of the triazole (139.3–139.1 ppm). Since these two carbons are located closer to the *N*-oxide, an influence can be observed when comparing the chemical shifts of compound **2–4** to those of compound **7** and **8**. The latter reveal the tetrazole carbon at 151.7–151.6 ppm and the remaining triazole carbon at 141.5–141.3 ppm.^[14]

Compounds **2–6** were investigated by using infrared and/or Raman spectroscopy. The measurements and absorptions were assigned according to literature values.^[22] In the IR spectra, the characteristic vibrations of the tetrazole framework of compounds **2–4** can be observed in the range from 1693–963 cm^{-1} , the fragment N1–C1–N4 possess asymmetric and symmetric stretching vibrations at 1416–1352 cm^{-1} , the N2–N3 match occurs at 963–965 cm^{-1} and finally the N3–N4 match is seen between 1401–1187 cm^{-1} . The cyclic C=N stretching vibrations show medium absorption in the range from 1693–1591 cm^{-1} . Furthermore, the typical observed band of the *N*-oxide of the synthesized salts **2–4** arises at 1533–1530 cm^{-1} .^[23] The carbonyl moiety of the connected triazole ring shows a strong absorption band at 1718–1693 cm^{-1} and the amino moiety is observed at 3348–3022 cm^{-1} .^[24]

The coordination compound **5** shows a sharp band at 3410 cm^{-1} and a broad one at 3364 cm^{-1} in the infrared spectrum for the O–H valence vibrations. Further, N–H valence vibrations can be observed at 3099 and 2971 cm^{-1} . The very strong C=O stretching vibration is shifted to higher wavenumbers compared to the free acid and can be observed at 1712 cm^{-1} . The N–H deformation vibrations and typical tetrazole and triazolone vibrations between 1640 and 712 cm^{-1} are shifted due to coordination. Considerable more O–H and N–H vibrations can be observed for complex **6**. Various signals are shown in the range between 3422 and 2450 cm^{-1} . Further, a very strong absorption band is observed at 1059 cm^{-1} which can be assigned to the perchlorate vibration.

In the Raman spectra of salts **2–4** appear two characteristic bands with high intensity, which match the corresponding literature known compounds that lack the *N*-oxide group.^[14] The band in the range from 1613–1602 cm⁻¹ can be assigned to the C=N stretching and the band in the range from 1034 to 1022 cm⁻¹ can be assigned a tetrazole N2–N3 stretch.^[23] The N–O valence vibration of the *N*-oxide moiety shows a band at 1034–1022 cm⁻¹.^[25] The band of the carbonyl moiety of the triazolone can be observed in the range from 1656 to 1642 cm⁻¹.^[26]

7.2.4 Physiochemical and energetic properties

Compounds **2** and complex **5** are classified as insensitive towards impact (40 J) and friction (360 N), whereas compound **4** is sensitive towards impact (15 J) and less sensitive towards friction (360 N). By introducing the *N*-oxide, the sensitivity towards impact was raised as demonstrated when comparing compounds **4** and **8**. However, the *N*-oxides **2** and **4** are less sensitive towards impact and friction compared to commonly used RDX (IS: 7.5 J; FS: 120 N). Compound **6** is classified as sensitive towards impact (4 J) and very sensitive towards friction (60 N).

Differential thermal analysis (DTA) was carried out to determine the decomposition temperatures of **2–6**. The decomposition temperatures are given as absolute onset temperatures. The thermal stability of the anhydrous ammonium salt (**2**) (249 °C) is significantly higher than that of the hydroxylammonium salt (**4**) (178 °C), however the potassium salt **3** (301 °C) possess the highest decomposition temperature. Following the trend that the presence of *N*-oxide decreases the thermal stability, **2** and **4** exhibit lower decomposition temperatures than their analogous salts **7** (283 °C) and **8** (220 °C), however ammonium salt **2** is still more temperature stable than commonly used RDX (210 °C). Compound **5** is dehydrated between 140 and 200 °C. The exothermal decomposition process starts at 264 °C (onset). The crystal water of compound **6** is removed between 90 and 130 °C. The coordinated aqua ligand is removed between 145 and 170 °C. The dehydration process is directly followed by exothermal decomposition ($T_{\text{dec. (onset)}} = 176$ °C). The cobalt(III) perchlorate complex is expected to exhibit an increased performance and sensitivity if water-free.

The values for the heats of formation are calculated with the atomization method, using electronic energies (CBS-4M method) at room temperature. Details are given in the SI. The heats and energies of formation for compounds **2** and **4** are compared to those of compounds **7**, **8** and RDX and given in Table 3. Calculation of the detonation parameters was performed with the program package EXPLO5 (version 6.01).^[27] The program is based on the chemical

equilibrium, steady-state model of detonation. It uses the Becker–Kistiakowsky–Wilson equation of state (BKW EOS) for gaseous detonation products and Cowan–Fickett's equation of state for solid carbon. The calculated EXPLO5 detonation parameters of compounds **2** and **4** using values for the room temperature X-ray densities are obtained as described in Table 3.^[28] The calculated detonation parameters are summarized in Table 3 and compared to the values calculated for compounds **7**, **8** and RDX.

Table 3. Energetic properties and detonation parameters

	2	4	7 ^[14]	8 ^[14]	RDX ^[1]
Formula	C ₃ H ₇ N ₉ O ₂	C ₃ H ₇ N ₉ O ₃	C ₃ H ₇ N ₉ O	C ₃ H ₇ N ₉ O ₂	C ₃ H ₆ N ₆ O ₆
FW [g mol ⁻¹]	201.15	217.15	185.15	201.15	222.12
IS [J] ^a	40	15	40	40	7.5
FS [N] ^b	360	360	360	360	120
ESD [J] ^c	1.2	0.25	1.50	0.50	0.20
N [%] ^d	62.67	58.87	68.09	52.67	37.84
Q [%] ^e	-59.66	-37.36	-73.45	-59.65	-21.61
T _{dec.} [°C] ^f	249	178	283	220	210
ρ [g cm ⁻³] (298K) ^g	1.662	1.73 (pyc.)	1.595	1.703	1.806
Δ _r H° [kJ mol ⁻¹] ^h	304.2	355.9	315.6	369.4	70.3
Δ _r U° [kJ kg ⁻¹] ⁱ	1623.1	1747.5	1818.1	1947.0	417.0
EXPLO V6.01 values:					
-Δ _E U° [kJ kg ⁻¹] ^j	4183	5020	3472	4505	5734
T _E [K] ^k	2856	3304	2456	2980	3800
p _{CJ} [kbar] ^l	240	288	201	266	352
D [m s ⁻¹] ^m	8160	8656	7707	8477	8815
V ₀ [L kg ⁻¹] ⁿ	855	862	842	854	792

^a impact sensitivity (BAM drophammer, 1 of 6); ^b friction sensitivity (BAM friction tester, 1 of 6); ^c electrostatic discharge device (OZM); ^d nitrogen content; ^e oxygen balance; ^f decomposition temperature from DTA (β = 5°C); ^g recalculated from low temperature X-ray densities (ρ_{298K} = ρ_T / (1+α_V(298-T₀)); α_V = 1.5 · 10⁻⁴ K⁻¹); ^h calculated (CBS-4M) heat of formation; ⁱ calculated energy of formation; ^j energy of explosion; ^k explosion temperature; ^l detonation pressure; ^m detonation velocity; ⁿ assuming only gaseous products.

Hydroxylammonium salt **4** reveals the highest detonation velocity (8656 m s⁻¹) and detonation pressure (288 kbar) of all investigated compounds in this report, the thermally more stable ammonium salt **2** reaches a detonation velocity of 8160 m s⁻¹ and a detonation pressure of 240 kbar. Even though compounds **2** and **4** have slightly worse energetic properties compared to RDX (*D* = 8815, *p*_{CJ} = 352 kbar), **2** and **4** exemplify the effect of the *N*-oxides in tetrazoles. Compared to their analogues **7** and **8**, which lack the oxide group, a raise of the detonation velocity by 2.1% (**4**) and 5.9% (**2**) as well as a raise of the detonation pressure by 8.3% (**4**) and 19.4% (**2**) can be observed. These trends fit the equation of *Kamlet and Jacobs*^[29] and are in the range of numbers that we reported previously for other tetrazole-*N*-oxides (*D* raised by 3.6% and *p*_{CJ} raised by 12%).^[15]

7.3 Conclusions

5-(4-Amino-1,2,4-triazol-3-on-5-yl)tetrazole was prepared and its ability as a bidentate nitrogen-rich ligand (neutral and anionic) was demonstrated. As expected, it coordinates involving N1 of the tetrazole as well as the N–NH₂ group of the triazolone ring. Moreover the *N*-oxide homologue 5-(4-amino-1,2,4-triazol-3-on-5-yl)tetrazole-2-oxide was synthesized and two new ionic energetic derivatives (ammonium and hydroxylammonium salts) were isolated, characterized, and compared to the corresponding compounds lacking the *N*-oxide group. The detonation parameters of compounds **2** ($D = 8160 \text{ m s}^{-1}$, $p_{\text{CJ}} = 240 \text{ kbar}$) and **4** ($D = 8656 \text{ m s}^{-1}$, $p_{\text{CJ}} = 288 \text{ kbar}$) confirm that tetrazole-*N*-oxides are superior over tetrazoles without the *N*-oxide group. The decomposition temperatures of the ammonium salt **2** (249 °C) exceeds the decomposition temperature of RDX (210 °C) by far, whereas the hydroxylammonium salt **4** decomposes already at 178 °C.

By a detailed comparison of the ammonium salts **2** and **7** as well as the hydroxylammonium salts **4** and **8**, it can be concluded that introducing the *N*-oxide group in tetrazoles decreases the decomposition temperature while at the same time increases the density. Moreover, we demonstrated that *N*-oxides introduction improves not only the calculated detonation velocity but also the detonation pressure. In the case of ammonium salt **2**, the detonation pressure can be raised by a remarkable 19% if the tetrazole is modified by *N*-oxide introduction. When designing novel nitrogen-rich energetic materials, the incorporation of *N*-oxides in a new system should always be considered.

7.4 Experimental Section

The analytical methods and general procedures are described in the appendix of this thesis. 5-Aminohydroximoyl-2-hydroxytetrazole (**1**) and the ligand **HATT** were prepared according to literature procedure.^[14, 15]

NH₄ ATT2O (**2**)

5-Aminohydroximoyl-2-hydroxytetrazole (**1**) (4.9 g; 34.2 mmol) was suspended in hot water, and DAU (3.1 g; 34.2 mmol) was added. Hydrochloric acid (37%; 0.51 mL; 17.1 mmol) was added and the suspension was refluxed for 2 h during which the reaction mixture turned from a colorless suspension to a clear and red solution. The solution was filtered, left for crystallization, and ammonium 5-(4-amino-1,2,4-triazol-3-on-5-yl)tetrazole-2-oxide (**2**) was isolated as light yellow crystals. Yield: 3.2 g (15.9 mmol, 47 %).

DTA (5 °C min⁻¹) onset: 249 °C (dec.); **IR** (ATR, cm⁻¹): $\tilde{\nu}$ = 3042(s), 2111(w), 1693(s), 1532(m), 1401(vs), 1352(vs), 1230(s), 1209(m), 1100(w), 1035(w), 1017(s), 965(s), 814(m), 772(s), 723(s), 707(vs); **Raman** (1064 nm, 300 mW, 25 °C, cm⁻¹): $\tilde{\nu}$ = 3185(2), 1642(10), 1613(100), 1535(4), 1390(4), 1359(3), 1268(2), 1210(9), 1126(10), 1026(29), 966(3), 818(14), 752(3), 709(6), 617(3), 564(2), 433(2), 359(4), 341(4), 263(5), 220(4), 157(13), 128(17), 128(17), 98(34), 75(14); **¹H NMR** ([D₆]DMSO): δ = 11.92 (s, 1H, NH), 7.35 (br s, 4H, NH₄⁺), 5.34 ppm (br s, 2H, NH₂); **¹³C NMR** ([D₆]DMSO): δ = 154.0 (C=O), 146.2 (ON₄C-CN₃HNH₂O), 139.2 ppm (ON₄C-CN₃HNH₂O); **MS** m/z (FAB⁻): 183.0 (C₃N₈H₃O₂⁻); m/z (FAB⁺): 18.1 (NH₄⁺); **EA** (C₃H₇N₉O₂, 217.15 g mol⁻¹) calcd.: C 17.91, H 3.51, N 62.67%; found: C 18.09, H 3.53, N 61.64%; **Sensitivities**: IS: 40 J, FS: 40 N, ESD: 1.2 J (at grain size 500–1000 μ m).

K ATT2O · H₂O (3)

To a solution of **2** (0.56 g, 2.78 mmol) in water (20 mL) potassium hydroxide (31 mL, 0.1 mol/L) was added. The solution was heated to reflux for 15 min and was left for crystallization to yield potassium 5-(4-amino-1,2,4-triazol-3-on-5-yl)tetrazole-2-oxide dihydrate (**3**) as colorless crystals. Yield: 0.54 g (2.43 mmol, 87%)

DTA (5 °C min⁻¹) onset: 301 °C (dec.); **IR** (ATR, cm⁻¹): $\tilde{\nu}$ = 3537(m), 3348(m), 3287(m), 3203(m), 2360(m), 2336(w), 2129(w), 1718(vs), 1644(m), 1530(m), 1391(m), 1354(s), 1230(m), 1211(s), 1041(m), 1019(m), 963(m), 859(w), 787(m), 734(s), 704(vs), 692(s), 692(s); **Raman** (1064 nm, 300 mW, 25 °C, cm⁻¹): $\tilde{\nu}$ = 3290(2), 3203(3), 1651(5), 1602(100), 1535(4), 1400(6), 1233(8), 1215(14), 1126(11), 1022(33), 962(4), 814(16), 750(6), 708(5), 631(3), 365(6), 311(5), 279(4), 112(20), 92(29), 68(18); **¹H NMR** ([D₆]DMSO): δ = 11.79 (s, 1H, NH), 5.35 ppm (br s, 2H, NH₂); **¹³C NMR** ([D₆]DMSO): δ = 153.98 (C=O), 145.83 (ON₄C-CN₃HNH₂O), 139.3 ppm (ON₄C-CN₃HNH₂O); **MS** m/z (FAB⁻): 183.0 (C₃N₈H₃O₂⁻); m/z (FAB⁺): 39.0 (K⁺); **EA** (C₃H₇KN₈O₄, 258.24 g mol⁻¹) calcd.: C 13.95, H 2.73, N 43.39%; found C 14.23, H 2.81, N 43.09%.

NH₃OH ATT2O (4)

Compound **3** (1.23 g, 5.54 mmol) was dissolved in ethanol and the solution was cooled with an ice bath. Gaseous hydrochloric acid was bubbled through the solution, the remaining precipitate was filtered off and the clear solution was reacted with a solution of hydroxylamine (0.34 mL of a 50% w/v solution in H₂O, 0.37 g, 11.2 mmol). The thus formed hydroxylammonium 5-(4-amino-1,2,4-triazol-3-on-5-yl)tetrazole-2-oxide (**4**) precipitated

from ethanol as a colorless powder. Yield: 0.56 g (2.9 mmol, 47%). Recrystallization from water yielded colorless crystals of **4** · H₂O, suitable for X-Ray diffraction.

DTA (5 °C min⁻¹) onset: 178 °C (dec.); **IR** (ATR, cm⁻¹): $\tilde{\nu}$ = 3196(w), 3102(m), 3022(m), 2738(m), 1698(s), 1662(s), 1591(m), 1533(m), 1416(m), 1381(m), 1357(s), 1240(m), 1212(m), 1187(m), 1026(m), 1002(m), 965(m), 820(m), 784(m), 726(s), 706(vs); **Raman** (1064 nm, 300 mW, 25 °C, cm⁻¹): $\tilde{\nu}$ = 3106(2), 1656(11), 1608(100), 1245(3), 1217(16), 1134(13), 1034(23), 1004(8), 965(4), 822(13), 708(6), 351(4), 241(4), 172(11), 141(18), 92(13), 69(9); **¹H NMR** ([D₆]DMSO): δ = 11.88 (s, 1H, NH), 10.25 (s, br, 4H, NOH₄), 5.31 ppm (br s, 2H, NH₂); **¹³C NMR** ([D₆]DMSO): δ = 153.96 (C=O), 146.28 (ON₄C-CN₃HNH₂O), 139.12 ppm (ON₄C-CN₃HNH₂O); **MS** *m/z* (FAB⁻): 183.0 (C₃N₈H₃O₂⁻); *m/z* (FAB⁺): 34.0 (NH₃OH⁺); **EA** (C₃H₇N₉O₃, 217.15 g mol⁻¹) calcd.: C 16.59, H 3.25, N 58.08%; found C 16.28, H 3.25, N 55.79%; **Sensitivities**: IS: 15 J, FS: 360 N, ESD: 0.25 J (at grain size 100–500 μm).

[Cu(ATT)₂(H₂O)₂] · 2 H₂O (**5**)

To a warm solution (70 °C) of HATT (168 mg, 1.0 mmol) in perchloric acid (12 %, 25 mL) was added an aqueous solution of copper(II) perchlorate hexahydrate (186 mg, 0.5 mmol). The solution was left for crystallization at ambient conditions. After two days, blue single crystals suitable for X-ray diffraction were obtained. Yield: 152 mg (0.32 mmol, 65%).

DTA (5 °C min⁻¹) onset: 145 °C (–H₂O), 264 °C (dec.); **IR** (ATR, cm⁻¹): $\tilde{\nu}$ = 3410 (s), 3364 (m), 3099 (w), 2971 (m), 2776 (w), 2608 (w), 1724 (vs), 1712 (vs), 1640 (s), 1528 (m), 1477 (m), 1425 (w), 1404 (s), 1346 (w), 1307 (m), 1252 (m), 1212 (s), 1140 (m), 1118 (m), 1097 (m), 1080 (s), 1035 (m), 985 (s), 815 (w), 756 (m), 737 (m), 712 (m), 669 (m); **EA** (C₆H₁₄CuN₁₆O₆, 469.79 g mol⁻¹) calcd.: C 15.34, H 3.00, N 47.70%; found: C 15.46, H 2.94, N 47.00%; **Sensitivities**: IS: 40 J, FS: 360 N, ESD: 1.5 J (at grain size 100–500 μm).

[Co(HATT)₂(H₂O)₂](ClO₄)₃ · 4 H₂O (**6**)

To a 70 °C warm solution of HATT (168 mg, 1.0 mmol) in perchloric acid (15%, 10 mL) was added an aqueous solution of cobalt(II) perchlorate hexahydrate (183 mg, 0.5 mmol). The solution was left for crystallization at ambient conditions. After one month, orange single crystals suitable for X-ray diffraction were obtained. Yield: 248 mg (0.31 mmol, 62%).

DTA (5 °C min⁻¹) onset: 109 °C (–H₂O), 176 °C (dec.); **IR** (ATR): $\tilde{\nu}$ = 3422 (m), 3238 (m), 3226 (m), 3147 (m), 3109 (m), 3014 (w), 2979 (w), 2948 (w), 2842 (w), 2801 (w), 2714 (w), 2687 (w), 2623 (w), 2540 (w), 2512 (w), 2450 (vw), 1703 (s), 1698 (s), 1682 (m), 1642 (m),

1633 (m), 1611 (s), 1543 (m), 1494 (vw), 1468 (vw), 1455 (vw), 1426 (w), 1362 (vw), 1267 (w), 1230 (w), 1169 (w), 1059 (vs), 972 (s), 934 (m), 903 (m), 817 (m), 780 (w), 732 (w), 710 (w), 704 (w), 661 cm^{-1} (vw); **EA** ($\text{C}_6\text{H}_{20}\text{Cl}_3\text{CoN}_{16}\text{O}_{20}$, 801.61 g mol^{-1}) calcd.: C 8.99, H 2.51, N 27.96%; found C 9.00, H 2.73, N 26.75%; **Sensitivities**: IS: 4 J, FS 60 N, ESD: 0.5 J (at grain size 500–1000 μm).

7.5 References

- [1] a) W. E. Bachmann, J. C. Sheehan, *J. Am. Chem. Soc.* **1949**, *71*, 1842–1845; b) E. P. Burrows, E. E. Brueggemann, *J. Chromatogr.* **1985**, *329*, 285–289.
- [2] RDX CAS # 121-82-4 - ToxFAQs™, <http://www.atsdr.cdc.gov/toxfaqs/index.asp>.
- [3] A. T. Nielsen, A. P. Chafin, S. L. Christian, D. W. Moore, M. P. Nadler, R. A. Nissan, D. J. Vanderah, R. D. Gilardi, C. F. George, J. L. Flippen-Anderson, *Tetrahedron* **1998**, *54*, 11793–11812.
- [4] M.-X. Zhang, P. E. Eaton, R. Gilardi, *Angew. Chem.* **2000**, *112*, 422–426; *Angew. Chem. Int. Ed.* **2000**, *39*, 401–404.
- [5] M. H. V. Huynh, M. A. Hiskey, T. J. Meyer, M. Wetzler, *Proc. Natl. Acad. Sci. USA* **2006**, *103*, 5409–5412.
- [6] H. Gao, J. M. Shreeve, *Chem. Rev.* **2011**, *111*, 7377–7436.
- [7] D. E. Chavez, M. A. Hiskey, D. L. Naud, *J. Pyrotech.* **1999**, *10*, 17–37.
- [8] a) R. Haiges, S. Schneider, T. Schroer, K. O. Christe, *Angew. Chem.* **2004**, *116*, 5027–5032; *Angew. Chem. Int. Ed.* **2004**, *43*, 4919–4924; b) D. E. Chavez, M. A. Hiskey, D. L. Naud, D. Parrish, *Angew. Chem.* **2008**, *120*, 8431–8433; *Angew. Chem. Int. Ed.* **2008**, *47*, 8307–8309; c) M. B. Talawar, R. Sivabalan, T. Mukundan, H. Muthurajan, A. K. Sikder, B. R. Gandhe, A. Subhananda Rao, *J. Hazard. Mater.* **2009**, *161*, 589–607; d) O. S. Bushuyev, P. Brown, A. Maiti, R. H. Gee, G. R. Peterson, B. L. Weeks, L. J. Hope-Weeks, *J. Am. Chem. Soc.* **2012**, *134*, 1422–1425.
- [9] D. Fischer, T. M. Klapötke, J. Stierstorfer, *Angew. Chem.* **2014**, *126*, 8311–8314; *Angew. Chem. Int. Ed.* **2014**, *53*, 8172–8175.
- [10] a) M. Göbel, K. Karaghiosoff, T. M. Klapötke, D. G. Piercey, J. Stierstorfer, *J. Am. Chem. Soc.* **2010**, *132*, 17216–17226. b) J. C. Bottaro, M. Petrie, P. E. Penwell, A. L. Dodge, R. Malhotra, NANA/HEDM Technology: Late Stage Exploratory Effort, Report

- No. A466714; SRI International: Menlo Park, CA, **2003**; DARPA/AFOSR funded, Contact No. F49629-02-C-0030.
- [11] D. Fischer, N. Fischer, T. M. Klapötke, D. G. Piercey, J. Stierstorfer, *J. Mater. Chem.* **2012**, 22, 20418–20422.
- [12] A. A. Dippold, T. M. Klapötke, *J. Am. Chem. Soc.* **2013**, 135, 9931–9938.
- [13] T. M. Klapötke, D. G. Piercey, J. Stierstorfer, M. Weyrauther, *Propellants Explos. Pyrotech.* **2012**, 37, 527–535.
- [14] N. Fischer, K. Hüll, T. M. Klapötke, J. Stierstorfer, *J. Heterocycl. Chem.* **2014**, 51, 85–95.
- [15] T. M. Klapötke, M. Q. Kurz, P. C. Schmid, J. Stierstorfer, *J. Energ. Mat.* accepted, ID UEGM-**2014**-1265
- [16] The cif files can be obtained free of charge from the Cambridge Crystallographic Data Centre via www.ccdc.cam.ac.uk/data_request/cif.
- [17] a) M. Joas, T. M. Klapötke, J. Stierstorfer, N. Szimhardt, *Chem. Eur. J.* **2013**, 19, 9995–10003; b) N. Fischer, M. Joas, T. M. Klapötke, J. Stierstorfer, *Inorg. Chem.* **2013**, 52, 13791–13802; c) T. M. Klapötke, P. Mayer, K. Polborn, J. Stierstorfer, J. J. Weigand, *9th New Trends in Research of Energetic Materials Seminar*, Pardubice, Czech, April 19–21, **2006**, 641–651.
- [18] a) M. Joas, T. M. Klapötke, J. Stierstorfer, *Crystals* **2012**, 2, 958–966; b) J. Zhang, T. Zhang, K. Yu, *Chem. Heterocycl. Compd. (N. Y., NY, U. S.)* **2003**, 39, 461–466.
- [19] a) N. V. Podberezskaya, N. V. Pervukhina, V. P. Doronina, *Zh. Strukt. Khim.* **1991**, 32, 34–39; b) B. Morosin, R. G. Dunn, R. Assink, T. M. Massis, J. Fronabarger, E. N. Duesler, *Acta Crystallogr., Sect. C: Cryst. Struct. Commun.* **1997**, C53, 1609–1611; c) A. Y. Zhilin, M. A. Ilyushin, I. V. Tselinskii, A. S. Kozlov, N. E. Kuz'mina, *Russ. J. Appl. Chem.* **2002**, 75, 1849–1851.
- [20] L. Tian, L. Yan, *J. Coord. Chem.* **2012**, 65, 1600–1609.
- [21] A. F. Holleman, N. Wiberg, *Lehrbuch der Anorganischen Chemie*, 102. ed., Walter de Gruyter, Berlin, New York, **2007**.
- [22] a) M. Hesse, H. Meier, B. Zeeh, *Spektroskopische Methoden in der Organischen Chemie*, 7th ed., Thieme, Stuttgart, New York, **2005**; b) G. Socrates, *Infrared and Raman Characteristic Group Frequencies: Tables and Charts*, 3rd ed., John Wiley &

- Sons, Chichester, **2004**; c) R. I. Hiyoshi, Y. Kohno, J. Nakamura, *J. Phys. Chem. A* **2004**, *108*, 5915–5920.
- [23] F. Boneberg, A. Kirchner, T. M. Klapötke, D. G. Piercey, M. J. Poller, J. Stierstorfer, *Chem. Asian J.* **2013**, *8*, 148–159.
- [24] S. Gunasekaran, E. Sailatha, S. Seshadri, S. Kumaresan, *Indian J. Pure Ap. Phy.* **2009**, *47*, 12–18.
- [25] N. Fischer, L. Gao, T. M. Klapötke, J. Stierstorfer, *Polyhedron* **2013**, *51*, 201–210.
- [26] R. I. Hiyoshi, Y. Kohno, J. Nakamura, *J. Phys. Chem. A* **2004**, *108*, 5915–5920.
- [27] M. Sućeska, EXPLO5.06 program, Zagreb, Croatia, **2012**.
- [28] C. Xue, J. Sun, B. Kang, Y. Liu, X. Liu, G. Song, Q. Xue, *Propellants Explos. Pyrotech.* **2010**, *35*, 333–338.
- [29] M. J. Kamlet, S. J. Jacobs, *J. Chem. Phys.* **1968**, *48*, 23–35.

7.6 Supplementary information

The analytical methods and general procedures are described in the appendix of this thesis.

7.6.1 XRD data, parameters and X-ray discussion of compound 9

Table S1. XRD data and parameters

	2	3	4 · H₂O
Formula	C ₃ H ₇ N ₉ O ₂	C ₃ H ₇ KN ₈ O ₄	C ₃ H ₉ N ₉ O ₄
FW [g mol ⁻¹]	201.18	258.27	235.19
Crystal system	triclinic	triclinic	triclinic
Space Group	<i>P</i> -1	<i>P</i> -1	<i>P</i> -1
Color / Habit	colorless, plate	colorless, block	colorless, block
Size [mm]	0.40 × 0.16 × 0.06	0.16 × 0.15 × 0.10	0.06 × 0.11 × 0.29
<i>a</i> [Å]	7.5149(8)	6.5838(5)	6.8500(7)
<i>b</i> [Å]	8.0822(9)	8.2722(6)	11.7730(11)
<i>c</i> [Å]	8.2340(10)	9.6273(7)	12.4647(10)
α [°]	117.256(12)	101.472(7)	104.376(8)
β [°]	92.367(9)	108.582(7)	105.624(9)
γ [°]	113.842(10)	92.956(6)	97.452(8)
<i>V</i> [Å ³]	390.56(11)	483.32(6)	916.71(16)
<i>Z</i>	2	2	4
$\rho_{\text{calc.}}$ [g cm ⁻³]	1.711	1.775	1.704
μ [mm ⁻¹]	0.144	0.569	0.151
<i>F</i> (000)	208	264	488
$\lambda_{\text{MoK}\alpha}$ [Å]	0.71073	0.71073	0.71073
<i>T</i> [K]	100	173	173
θ min-max [°]	4.79, 26.49	4.11, 26.49	4.28, 26.50
Dataset <i>h</i> ; <i>k</i> ; <i>l</i>	−9:9, −10:10, −10:10	−8:8, −10:10, −12:12	−8:8, −14:11, −13:15
Reflect. coll.	5743	3679	7163
Independ. refl.	1618	1997	3773
<i>R</i> _{int}	0.038	0.025	0.037
Reflection obs.	1302	1683	2799
No. parameters	155	173	361
<i>R</i> ₁ (obs)	0.0368	0.0337	0.0529
<i>wR</i> ₂ (all data)	0.0895	0.0801	0.1517
<i>S</i>	1.09	1.03	1.02
Resd. Dens.[e Å ⁻³]	−0.25, 0.20	−0.25, 0.35	−0.45, 1.10
Device type	Oxford XCalibur3 CCD	Oxford XCalibur3 CCD	Oxford XCalibur3 CCD
Solution	SIR-2004	SIR-2004	SIR-2004
Refinement	SHELXL-97	SHELXL-97	SHELXL-97
Absorpt. corr.	multi-scan	multi-scan	multi-scan
CCDC	1020001	1020002	1020003

Table S1. (continued) XRD data and parameters

	5	6	9
Formula	C ₆ H ₁₄ CuN ₁₆ O ₆	C ₆ H ₂₀ Cl ₃ CoN ₁₆ O ₂₀	C ₆ H ₁₈ KN ₁₆ O ₁₀
FW [g mol ⁻¹]	469.87	801.66	983.85
Crystal system	monoclinic	monoclinic	monoclinic
Space Group	<i>P</i> 2 ₁ / <i>n</i>	<i>C</i> 2/ <i>c</i>	<i>C</i> 2/ <i>c</i>
Color / Habit	blue, plate	yellow, block	colorless, plate
Size [mm]	0.37 × 0.18 × 0.03	0.34 × 0.33 × 0.21	0.38 × 0.14 × 0.06
<i>a</i> [Å]	7.4762(3)	21.4290(11)	28.9960(13)
<i>b</i> [Å]	6.9546(3)	11.2605(5)	6.4151(2)
<i>c</i> [Å]	15.008(6)	11.5542(6)	20.6002(11)
α [°]	90	90	90
β [°]	95.045(4)	109.154(5)	108.482(5)
γ [°]	90	90	90
<i>V</i> [Å ³]	776.93(6)	2633.7(2)	3634.3(3)
<i>Z</i>	2	4	4
$\rho_{\text{calc.}}$ [g cm ⁻³]	2.009	2.022	1.798
μ [mm ⁻¹]	1.48	1.08	0.271
<i>F</i> (000)	478	1624	2036
$\lambda_{\text{MoK}\alpha}$ [Å]	0.71073	0.71073	0.71073
<i>T</i> [K]	100	173	173
ϑ min-max [°]	4.2, 26.7	4.1, 26.4	4.1, 26.5
Dataset <i>h</i> ; <i>k</i> ; <i>l</i>	−9:9; −7:8; −14:18	−26:26; −10:14; −14:13	−36:36; −7:8; −20:25
Reflect. coll.	3223	6834	14822
Independ. refl.	1636	2685	3740
<i>R</i> _{int}	0.021	0.029	0.030
Reflection obs.	1442	2209	3244
No. parameters	161	266	366
<i>R</i> ₁ (obs)	0.031	0.035	0.0291
<i>wR</i> ₂ (all data)	0.084	0.090	0.0754
<i>S</i>	1.06	1.06	1.04
Resd. Dens.[e Å ⁻³]	−0.65; 0.39	−0.46; 0.77	−0.24; 0.30
Device type	Oxford XCalibur3 CCD	Oxford XCalibur3 CCD	Oxford XCalibur3 CCD
Solution	SIR-2004	SIR-2004	SIR-2004
Refinement	SHELXL-97	SHELXL-97	SHELXL-97
Absorpt. corr.	multi-scan	multi-scan	multi-scan
CCDC	1000194	1000195	1020004

Hydroxylammonium potassium 5-(4-amino-1,2,4-triazol-3-on-5-yl)tetrazole-2-oxide dihydrate (9)

During the attempts to obtain salt **4**, a small amount of crystals consisting of hydroxylammonium potassium 5-(4-amino-1,2,4-triazol-3-on-5-yl)tetrazole-2-oxide dihydrate (**9**) were obtained (Figure S1). The double salt crystallizes in the monoclinic space group $C2/c$ with four molecular moieties per unit cell. The calculated density is 1.798 g cm^{-3} at 173 K.

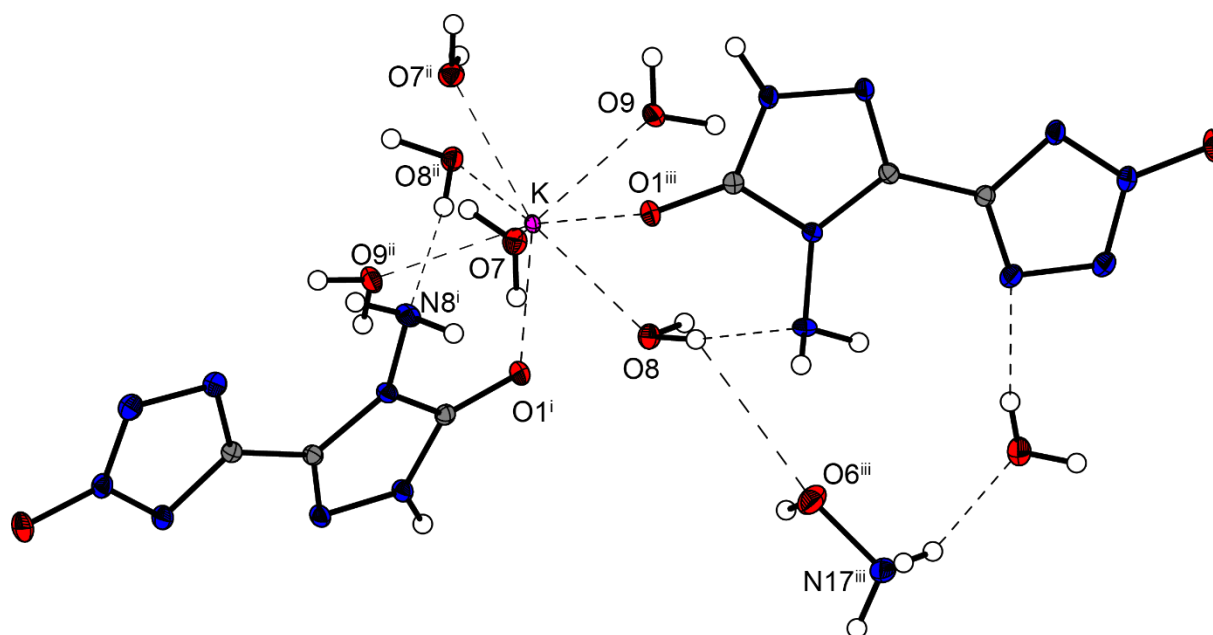


Figure S1. Molecular unit of hydroxylammonium potassium 5-(4-amino-1,2,4-triazol-3-on-5-yl)tetrazole-2-oxide dihydrate (**9**). Thermal ellipsoids show the 50% probability level and hydrogen atoms are shown as small spheres of arbitrary radius.

6.6.2 Heat of formation calculations

General information about the heat of formation calculations can be found in the appendix of this thesis. The calculation results are summarized in Table S2.

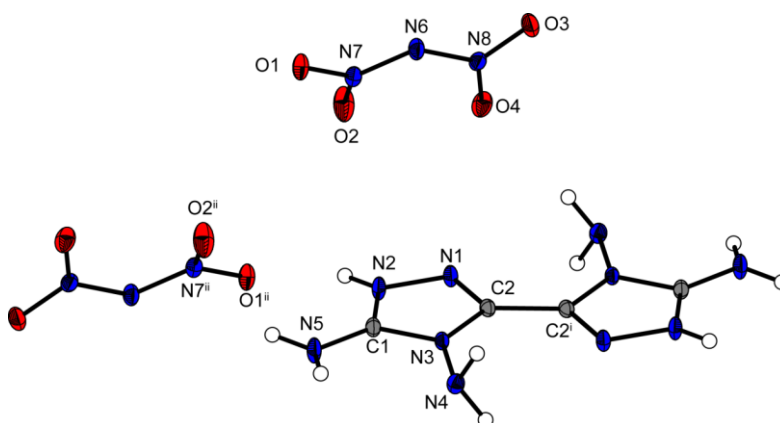
Table S2. Calculation results

M	$-H^{298}$ [a] / a.u.	$\Delta_f H^\circ(\text{g}, \text{M})$ / kJ mol^{-1} [b]	V_M / nm^3 [c]	$\Delta U_L, \Delta H_L$ (4); ΔH_{sub} [e] (3) / kJ mol^{-1}	$\Delta_f H^\circ(\text{s})$ [f] / kJ mol^{-1}	Δn [g]	$\Delta_f U(\text{s})$ [f] / kJ kg^{-1}
NH_4^+	56.796608	635.3					
ATT2O^-	703.65381	178.1					
2		813.4	0.201	504.2, 509.2	304.2	9.0	1623.1
NH_4O^+	131.863249	687.2					
4		864.5	0.202	503.6, 508.6	355.9	9.5	1747.5

[a] CBS-4M electronic enthalpy; [b] gas phase enthalpy of formation; [c] molecular volumes taken from X-ray structures and corrected to room temperature; [d] lattice energy and enthalpy (calculated using Jenkins and Glasser equations); [e] enthalpy of sublimation (calculated by Trouton rule); [f] standard solid state enthalpy of formation; [g] solid state energy of formation.

Thermal Stabilization of Energetic Materials by the Aromatic Nitrogen-Rich 4,4',5,5'-Tetraamino-3,3'-Bi-1,2,4-Triazolium Cation

published in *J. Mater. Chem. A* **2015**, 3, 2658–2668. (DOI: 10.1039/C4TA05964F)



Abstract: 4,4',5,5'-Tetraamino-3,3'-bi-1,2,4-triazole (**1**) was prepared from readily available starting materials by a one-step procedure. Compound **1** consists of two combined aromatic triazoles with four amino moieties, resulting in a compound which has (i) high temperature stability, (ii) a high heat of formation, (iii) a high density and iv) no sensitivity towards physical stimuli (friction, impact and electrostatic discharge). This compound has never previously been considered as building block in the development of new energetic materials. We investigated **1** in detail as a potential nitrogen-rich, temperature-stable cation for synthesis of energetic ionic derivatives (**2–13**) for the use as environmentally benign explosives. The cation was combined with oxygen-rich counter-anions such as dinitramide (**2**), 5-nitrotetrazole-2-oxide (**3**), 5-nitrotetrazolate (**4**), nitrate (**5**), tetranitrobisimidazole (**6**), 5,5'-bitetrazole-1,1'-dioxide (**7**), 1,1'-dinitramino-5,5'-bitetrazolate (**8**), 5-nitriminotetrazolate (**9**), 1-methyl-5-nitriminotetrazolate (**10**), perchlorate (**11**), picrate (**12**) and nitroformate (**13**). Compounds **2–10** and **13** were characterized by low-temperature single-crystal X-ray diffraction. All compounds were investigated by NMR and vibrational (IR, Raman) spectroscopy, mass spectrometry and elemental analysis. The excellent thermal properties were determined by differential thermal analysis. The sensitivities towards impact, friction, and electrical discharge were investigated using BAM standards and a small-scale electrostatic discharge tester. The detonation parameters of the compounds without inclusion of crystal water (**1–3**, **5–8**, **11** and **13**) were calculated using the EXPLO5 (V6.02) code and calculated (CBS-4M) values for the enthalpy of formation.

8.1 Introduction

Research on energetic materials has mainly considered cyclic or caged nitramines – for example 1,3,5-trinitro-1,3,5-triazinane (**RDX**) and 2,4,6,8,10,12-hexanitro-2,4,6,8,10,12-hexaazaisowurtzitane (CL-20) (Fig. 1.)^[1] Since the development of **RDX**, any newly synthesized energetic compounds have had to compete with **RDX**, particularly in terms of detonation pressure and detonation velocity, which are very important parameters in secondary explosives.^[2] Secondary explosives should also be stable with respect to temperature and have a high density, be safe to handle and cheap to synthesize. A high density is vital to the performance of an energetic material because the detonation pressure is proportional to the square of its density.^[2] In addition to enhanced physical properties, the demand for environmentally friendly nitrogen-rich energetic materials is steadily increasing. To reduce pollution of the environment through commonly used toxic and carcinogenic explosives such as **RDX** or lead azide, explosives that release mostly dinitrogen after decomposition are becoming increasingly important.^[3]

One approach for synthesizing new energetic compounds is the preparation of energetic salts, which mostly have a high density and high stability as a result of their high lattice energy.^[2] As an alternative to using alkali metals (Na^+ , K^+)^[4] as cations, nitrogen-rich cations have become more popular as a result of a potential hydrogen bond network, resulting in less sensitive materials,^[5] and a high positive heat of formation. This high positive heat of formation usually results in high energetic performance as well as a good oxygen balance.^[6]

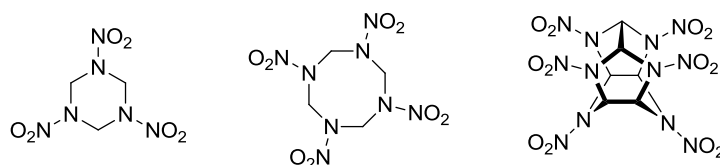


Figure 1. Chemical structure of the commonly used secondary explosive hexogen (**RDX**, left) and octogen (**HMX**, middle) as well as CL-20 (right), a potential high-performing alternative.

One approach for synthesizing new energetic compounds is the preparation of energetic salts, which mostly exhibit high densities and high stabilities, due to their high lattice energy.^[2] Other than employing alkali metals (Na^+ , K^+)^[4] as cations, the use of nitrogen-rich cations became more popular, due to (i) the potential hydrogen bond network resulting in less sensitive materials^[5] and (ii) a high positive heat of formation. Latter one mostly results in a high energetic performance as well as a decent oxygen balance.^[6]

Examples for commonly used nitrogen-rich cations are guanidinium (G^+), aminoguanidinium (AG^+), diaminoguanidinium (DAG^+), triaminoguanidinium (TAG^+), ammonium (NH_4^+),

hydroxylammonium (NH_3OH^+) and hydrazinium (N_2H_5^+) ions. They vary considerably in their temperature stability and in their energetic performance. A common observed trend in simple nitrogen-rich cations is the decrease in temperature stability in the order G^+ , AG^+ , DAG^+ and TAG^+ whereas the performance increases with increasing number of energetic N–N bonds.^[7] The use of NH_4^+ , NH_3OH^+ and N_2H_5^+ cations is a valuable strategy to improve the energetic performance of explosives. Unfortunately, this usually leads to an increase in the mechanical sensitivity and a decrease in temperature stability from NH_4^+ over N_2H_5^+ to NH_3OH^+ .^[5,8] As a high thermal stability seems to be accompanied by a decrease in the energetic performance of energetic salts, the currently used nitrogen-rich salts are limited by either their thermal stability or by their energetic performance compared with **RDX**.

It therefore seems that, in many energetic materials, a good energetic performance and low sensitivity are mutually exclude.^[8] This can be observed in the series of five-membered azoles from pyrazole to pentazole. Whereas pyrazole, containing only two nitrogen atoms, has a low performance but high stability, a pentazole heterocyclic compound with five nitrogen-atoms in the ring is too sensitive to be considered in any applications, but has a high performance.^[3a,3f]

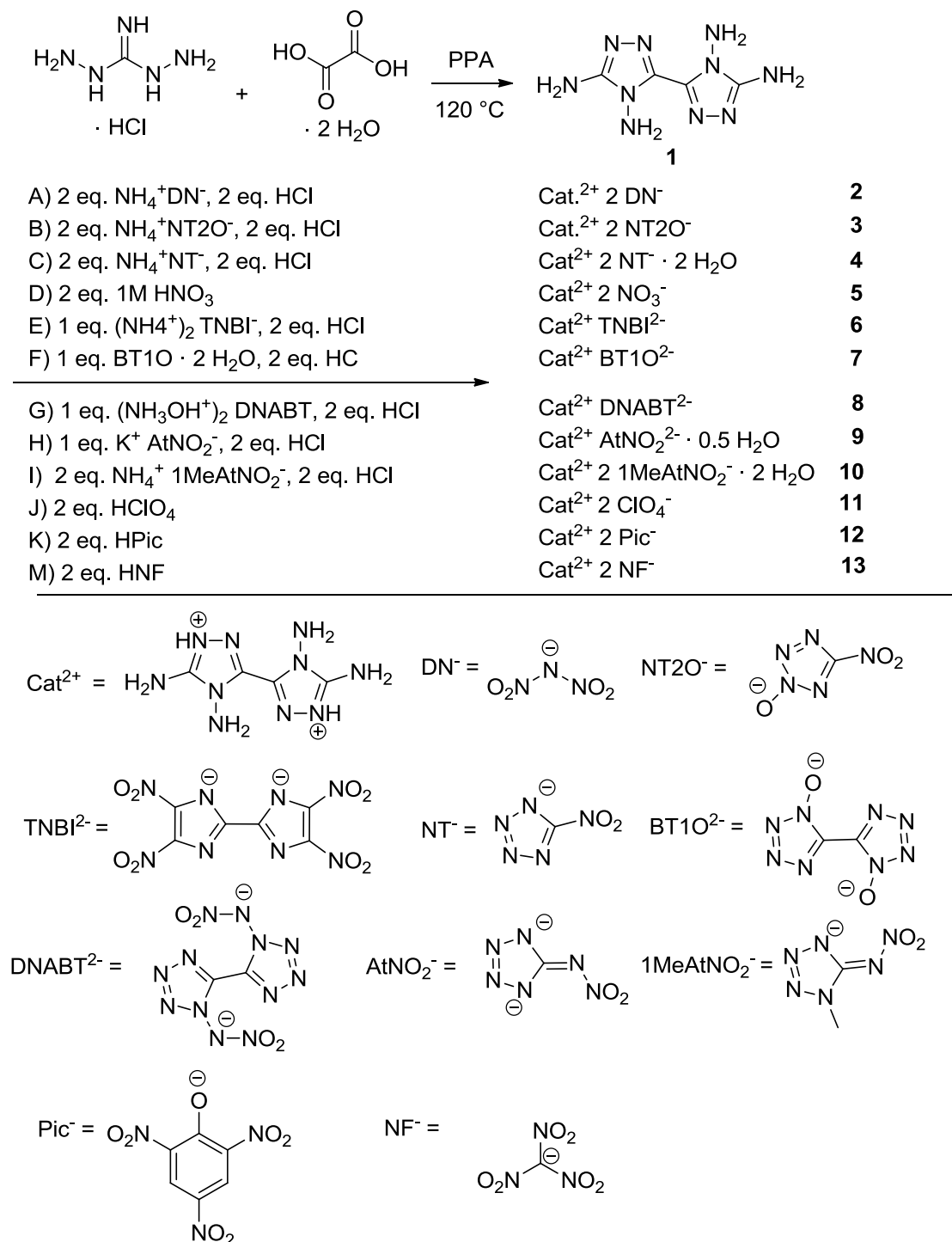
R. Centore *et al.*^[9] reported the facile synthesis of 4,4',5,5'-tetraamino-3,3'-bi-1,2,4-triazole (**1**). This compound has not yet been used as building block in the development of new energetic materials, although it has been characterized by its decomposition point, elemental analysis and mass spectroscopy. Detailed characterization using X-ray diffraction, elemental analysis and ^{13}C NMR spectrometry, as well as the investigation of the energetic properties of compound **1**, have not yet been reported. We report the synthesis of the temperature-stable nitrogen-rich salts of 4,4',5,5'-tetraamino-3,3'-bi-1,2,4-triazole and a detailed investigation of the properties of the resulting energetic materials.

8.2 Results and Discussion

8.2.1 Synthesis

4,4',5,5'-Tetraamino-3,3'-bi-1,2,4-triazole (**1**) was synthesized according to an improved version of a previously published procedure.^[9] By using phosphoric acid (100%) and phosphorus pentoxide, polyphosphoric acid is formed and can be used as a solvent. Diaminoguanidine monohydrochloride and oxalic acid were finely ground in a mortar and then added to the polyphosphoric acid. The temperature was kept at 120 °C overnight to

form **1**. The energetic salts were formed by simple metathesis reactions using compound **1** and different energetic anions, as illustrated in Scheme 1.



Scheme 1. Synthesis of compound **1** and its salts **2–13** via metathesis reactions

4,4',5,5'-Tetraamino-3,3'-bi-1,2,4-triazolium dinitramide **2**, 4,4',5,5'-tetraamino-3,3'-bi-1,2,4-triazolium dinitrotetrazolate-2*N*-oxide **3**, 4,4',5,5'-tetraamino-3,3'-bi-1,2,4-triazolium dinitrotetrazolate **4** and 4,4',5,5'-tetraamino-3,3'-bi-1,2,4-triazolium di-1-methylnitriminotetrazolate dihydrate **10** were formed by a 2:1 stoichiometric reaction of the

respective anions, compound **1** and two equivalents of hydrochloric acid in water. The protonation of compound **1** leads to a better solubility in water. 4,4',5,5'-Tetraamino-3,3'-bi-1,2,4-triazolium dinitrate **5**, 4,4',5,5'-tetraamino-3,3'-bi-1,2,4-triazolium diperchlorate **11**, 4,4',5,5'-tetraamino-3,3'-bi-1,2,4-triazolium dipicrate **12** and 4,4',5,5'-tetraamino-3,3'-bi-1,2,4-triazolium dinitroformate **13** were formed by adding two equivalents of the anion to one equivalent of compound **1** under aqueous conditions. The nitrogen-rich compounds 4,4',5,5'-tetraamino-3,3'-bi-1,2,4-triazolium tetranitrobis-imidazolate **6**, 4,4',5,5'-tetraamino-3,3'-bi-1,2,4-triazolium 5,5'-bitetrazole-1,1'-dioxide **7**, 4,4',5,5'-tetraamino-3,3'-bi-1,2,4-triazolium 1,1'-dinitramino-5,5'-bitetrazolate **8** and 4,4',5,5'-tetraamino-3,3'-bi-1,2,4-triazolium 5-nitrimino-1*H*-tetrazolate hemihydrate **9** were formed by a 1:1 stoichiometric reaction of the respective anions with compound **1** and two equivalents of hydrochloric acid in water.

8.2.2 Crystal Structures

The crystal structures of compounds **2–10** and **13** were determined by low-temperature X-ray diffraction. Selected parameters of the X-ray determinations are given in Tables S1–S4 in the (ESI). The cif files were deposited^[10] with CCDC nos 1029064 (**2**), 1029053 (**3**), 1029066 (**4**), 1029061 (**5**), 1029060 (**6**), 1029062 (**7**), 1029053 (**7·2H₂O**), 1029058 (**8**), 1029056 (**9**), 1029055 (**9a**), 1029057 (**9b**), 1029054 (**10**) and 1029059 (**13**).

4,4',5,5'-Tetraamino-3,3'-bi-1,2,4-triazolium dinitramide (**2**) crystallizes from water in the triclinic space group *P*–1 with a density of 1.860 g cm^{–3} at 173 K and one molecule per unit cell. The density of compound **2** is in the same range as previously reported dinitramides. For example, ammonium dinitramide with a density of 1.856 g cm^{–3} at 173 K^[11] or hydrazinium dinitramide (1.83 g cm^{–3}, 298K)^[12] show similar densities to the newly reported compound **2**. The torsion angle of N3–C2–C2ⁱ–N1ⁱ is 0.5(2)°, showing that a nearly planar ring system is formed by the two triazoles. Through the aromaticity of the ring system, the triazoles form almost regular pentagons with angles near to 108° and with almost equal bond lengths between the ring atoms of 1.3–1.4 Å. The connecting C–C bond of the triazole rings with a length of 1.445(3) Å is significantly shorter than a C–C single bond (1.54 Å). Similar C–C bond lengths can be observed in salts **3–10** and **13**. Compared with the linking C–C bonds in other 1,2,4-triazoles – for example, 3,3'-dinitro-1,1'-dihydroxy-5,5'-bi-1,2,4-triazole and its derivatives with C–C bond lengths between 1.463(2) and 1.438(6) Å – the bond lengths in compound **2–10** and **13** are very similar.^[8a, 13] The distance C1–N5 is 1.317(2) Å and is thus remarkably shorter than the distance of the carbon to the nitrogen of the nitro group in 3,3'-dinitro-1,1'-dihydroxy-5,5'-bi-1,2,4-triazole and its derivatives, which have bond lengths

between 1.454(5) and 1.427(5) Å.^[8a] Moreover, the C1–N5 bond length is shorter than other C_(triazole)–N_(amino) distances (1.351(3) Å) of comparable compounds reported previously.^[14] Compounds **3–10** and **13** also show bond lengths around 1.31 Å for the equivalent C–N distance. Fig. 2 shows the molecular unit of compound **2** with selected bond lengths and selected bond angles in the caption.

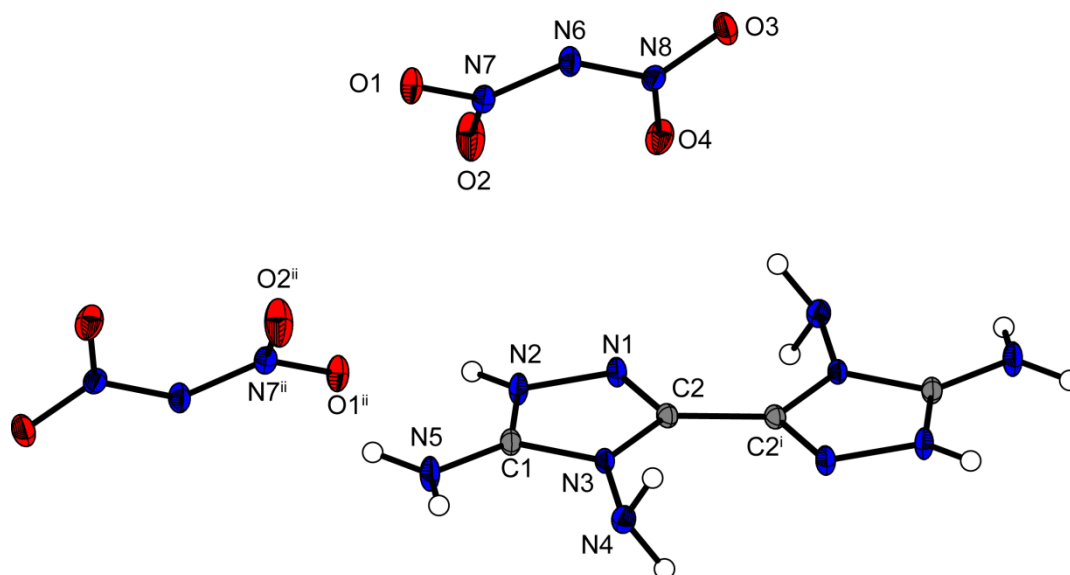


Figure 2. Molecular unit of **2**. Ellipsoids are drawn at the 50% probability level. Selected bond lengths [Å]: N1–N2 1.379(3), N2–C1 1.327(3), C1–N3 1.348(0), N3–C2 1.382(7), C2–N1 1.297(2), C2–C2ⁱ 1.445(3), N3–N4 1.400(2), C1–N5 1.317(2); selected bond angles [°]: N1–N2–C1 111.92(13), N2–C1–N3 106.07(13), C1–N3–C2 106.55(14), N3–C2–N1 111.45(12), C2–N1–N2 104.00(13).

The anhydrous crystal structure of 4,4',5,5'-tetraamino-3,3'-bi-1,2,4-triazolium dinitrotetrazolate-2*N*-oxide (**3**) is described by the triclinic space group *P*–1 with a density of 1.833 g cm^{–3} at 173 K and one molecule per unit cell. Compound **3** almost reaches the density of the highly energetic hydroxylammonium nitrotetrazolate-2*N*-oxide with a density of 1.850(2) g cm^{–3}.^[8c] In relation to the nitrogen-rich guanidinium, aminoguanidinium or diaminoguanidinium nitrotetrazolate-2*N*-oxides with densities of 1.6978(4), 1.697(2) and 1.6867(3) g cm^{–3}, respectively, which are more stable than the hydroxylammonium salt, the density of **3** is significantly higher.^[8c] The torsion angle of N9–C3–C3ⁱ–N6ⁱ is 0°, making the bicyclic ring system completely planar, similar to that of the cation in compound **2**. The angles of the ring system and the bond lengths behave in the same way as described for compound **2**. Likewise, the bond lengths and bond angles of the anion correspond to previously reported data.^[5] The molecular unit is shown in Fig. 3, with selected bond lengths and bond angles in the caption.

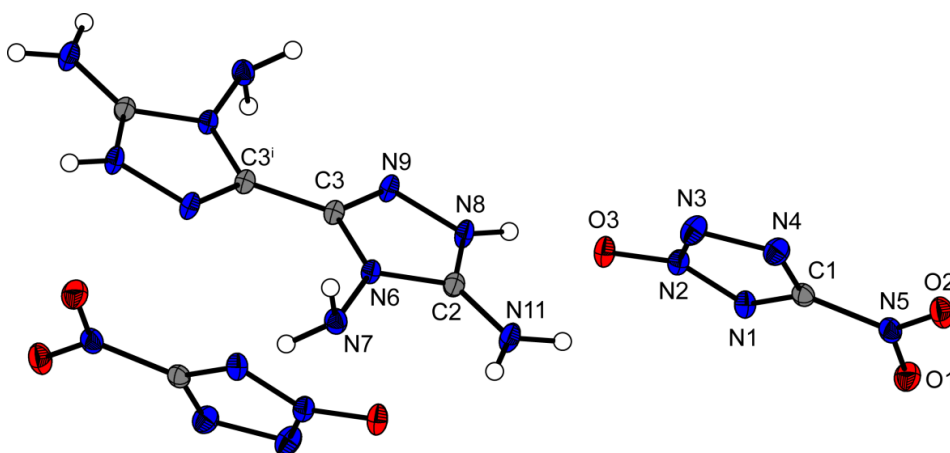


Figure 3. Molecular unit of **3**. Ellipsoids are drawn at the 50% probability level. Selected bond lengths [Å]: C1–N1 1.330(2), N1–N2 1.324(0), N2–N3 1.338(4), N3–N4 1.336(6), N4–C1 1.317(2), N5–C1 1.441(2), C3–N6 1.380(2), N6–C2 1.358(2), C2–N8 1.330(3), N8–N9 1.380(1), N9–C3 1.302(3), N6–N7 1.400(2), C3–C3ⁱ 1.447(2) C2–N11 1.313(2); selected bond angles [°]: N9–C3–N6 111.47(13), C3–N6–C2 106.46(15), N6–C2–N8 106.09(14), C2–N8–N9 111.74(14), N8–N9–C3 104.24(14), N1–C1–N4 116.17(14), C1–N4–N3 104.48(13), N4–N3–N2 105.46(12), N3–N2–N1 114.54(12), N2–N1–C1 99.34(13).

The energetic compound 4,4',5,5'-tetraamino-3,3'-bi-1,2,4-triazolium dinitrate (**5**) crystallizes anhydrously from water in the triclinic space group *P*–1 with one molecule per unit cell and a density of 1.779 g cm^{–3} at 173 K. The density of compound **5** is lower than those of compound **2** and **3**. Compared with hydroxylammonium nitrate with a density of 1.841 g cm^{–3},^[15] compound **5** has a lower density, whereas compound **5** has a higher density than guanidinium nitrate (1.410 g cm^{–3}).^[16] With a torsion angle of 1.4(2)° of the plane N1–C1–C1ⁱ–N3ⁱ, the two triazoles are tilted only slightly more towards each other than in the compounds **2**–**4**. The bond angles and bond lengths of the bicyclic ring system match the reported data. Fig. 4 shows the molecular unit of compound **5**.

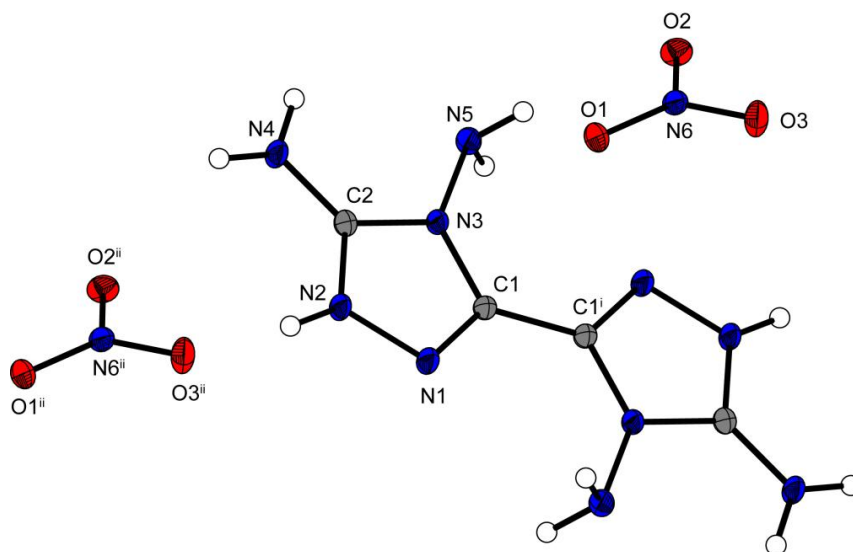


Figure 4. Molecular unit of **5**. Ellipsoids are drawn at the 50% probability level. Selected bond length [Å]: C1–C1ⁱ 1.454(6), C2–N4 1.318(8).

The anhydrous salt 4,4',5,5'-tetraamino-3,3'-bi-1,2,4-triazolium tetranitro-bisimidazolate (**6**) crystallizes in the monoclinic space group $P2_1/c$ with two molecules per unit cell. Compound **6** has a high density of 1.879 g cm^{-3} at 173 K. The high density may be rationalized as being a result of the strong intra- and intermolecular interactions that arise through the hydrogen-bond network formed by the combination of the four amino groups of the cation and the four nitro-groups of the anion, resulting in very long hydrogen bridges. Only the hydrazinium salt of tetranitrobisimidazolate, with a density of 1.826 g cm^{-3} (298K)^[17] showed a density in the range of compound **6**; the other nitrogen-rich salts, such as the guanidinium ($\rho = 1.701 \text{ g cm}^{-3}$ at 298K) or aminoguanidinium salt ($\rho = 1.698 \text{ g cm}^{-3}$ at 298K) clearly have lower densities.^[17] The torsion angles of the two bicyclic ring systems show that two nearly planar moieties are formed. The C–C bond of the anion linking the two rings is in the same dimension as the bond of the cation and is comparable with the bond lengths of other tetranitrobisimidazoles.^[18] Fig. 5 shows the molecular unit of compound **6** with selected torsion angles and hydrogen bond lengths in its caption.

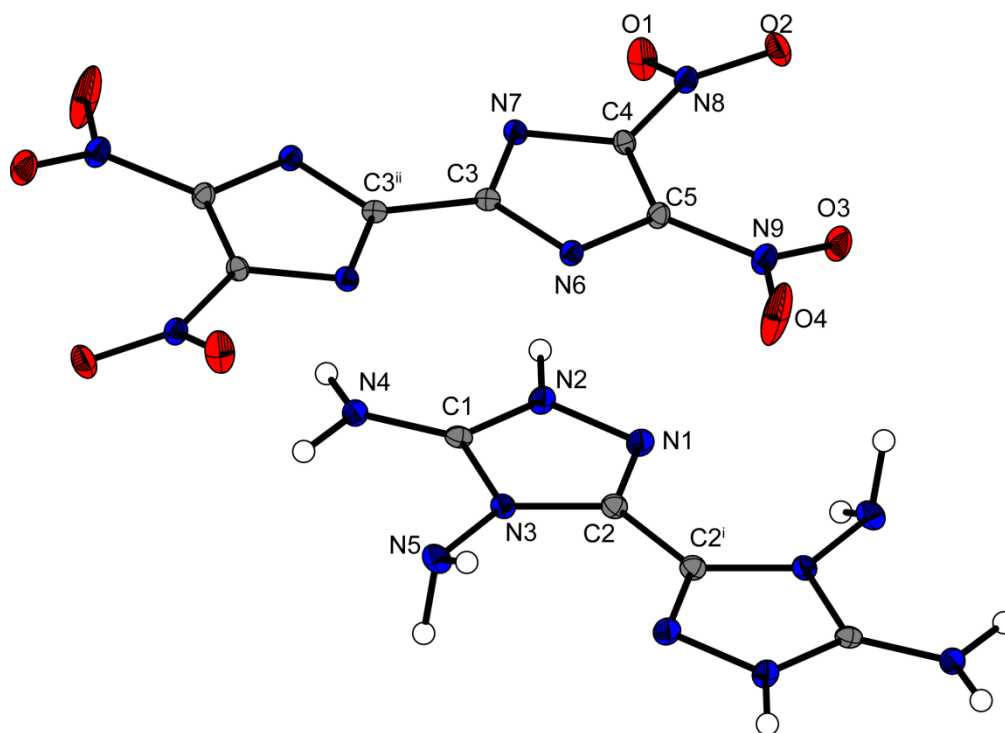


Figure 5. Molecular unit of **6**. Ellipsoids are drawn at the 50% probability level. Selected bond lengths [Å]: C2–C2ⁱ 1.452(3), C3–C3ⁱ 1.460(3), C1–N4 1.307(3); Selected torsion angles [°]: N1–C2–C2ⁱ–N3ⁱ 1.7(3), N7–C3–C3ⁱ–N6ⁱ 0.9(3); selected hydrogen bond lengths (H···A) [Å]: N2–H2–O4 2.15(3), N4–H4^(a)–O2 2.56(3), N4–H4^(a)–O3 2.17(4), N4–H4^(a)–O1 2.51(3), N5–H5^(a)–O1 2.48(3), N5–H5^(a)–O2 2.43(3), N5–H5^(a)–O3 2.49(3); symmetry codes (i) 1–x, 1–y, –z (ii) 1–x, 1–y, 1–z.

4,4',5,5'-Tetraamino-3,3'-bi-1,2,4-triazolium 5,5'-bitetrazole-1,1'-dioxide (**7**) forms anhydrous crystals as well as crystals containing two water moieties when crystallized from water

(7·2 H₂O). The water-free compound **7** crystallizes in the triclinic space group *P*–1 with a density of 1.686 g cm^{–3} at 173 K and one molecule per unit cell. The structure of the di-anion has been discussed previously.^[19,20] Compared with other energetic salts of 5,5'-bitetrazole-1,1'-dioxide, *e.g.* the hydroxylammonium salt TKX-50 ($\rho_{173\text{ K}} = 1.915\text{ g cm}^{-3}$), the density of compound **7** is fairly low.^[19] However, compared with the thermally stable diguanidinium salt 5,5'-bitetrazole-1,1'-dioxide with a density of 1.639 g cm^{–3},^[20] compound **7** shows a slightly higher density. Fig. 6 shows the molecular unit of **7**, with selected bond lengths and torsion angles in the caption. The molecular unit of **7**·2H₂O is illustrated in Fig. S2 in the ESI.

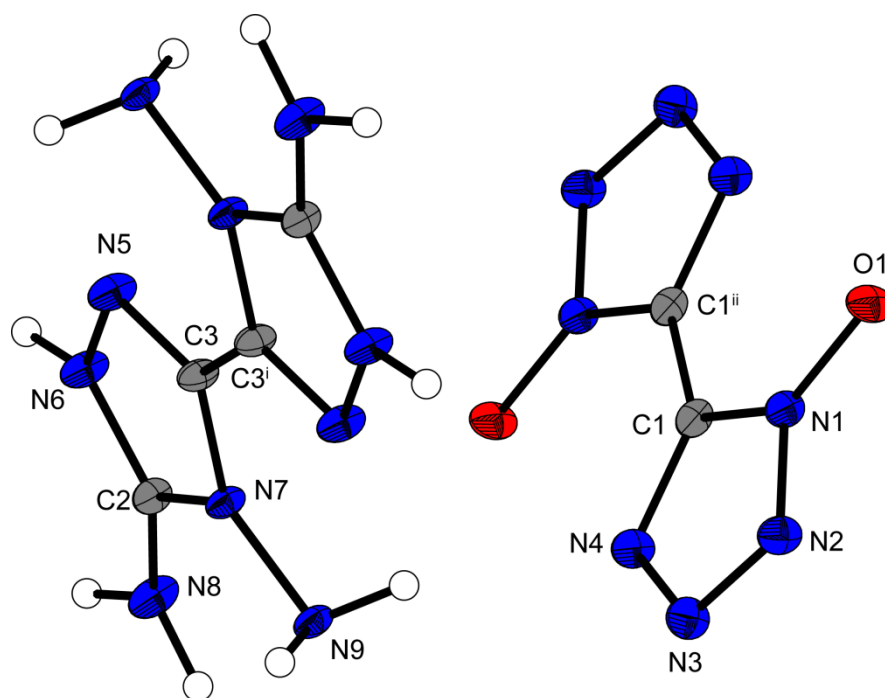


Figure 6. Molecular unit of **7**. Ellipsoids are drawn at the 50% probability level. Selected bond lengths [Å]: C3–C3ⁱ 1.45.1(2), C2–N8 1.312(3), O1–N1 1.318(2), C1–C1ⁱⁱ 1.446(3), N1–C1 1.347(2), N1–N2 1.345(2), N2–N3 1.314(2), N3–N4 1.342(2), N4–C1 1.333(2); selected torsion angles [°]: N7–C3–C3ⁱ–C5ⁱ 1.3(3), N1–C1–C1ⁱ–N1ⁱ 0.5(3); symmetry codes: (i) –x, 1–y, 1–z; (ii) 1–x, 1–y, z.

The anhydrous energetic compound 4,4',5,5'-tetraamino-3,3'-bi-1,2,4-triazolium 1,1'-dinitramino-5,5'-bitetrazolate (**8**) crystallizes from water in the triclinic space group *P*–1 with a density of 1.778 g cm^{–3} and one formula unit per unit cell. Dipotassium 1,1'-dinitramino-5,5'-bitetrazolate with a density of 2.172 g cm^{–3} is the only previously reported compound containing this anion.^[4a] The anion of **8** has a larger torsion angle than the corresponding cation, forming a planar cation and a slightly tilted anion. The molecular unit of compound **8** is shown in Fig. 7.

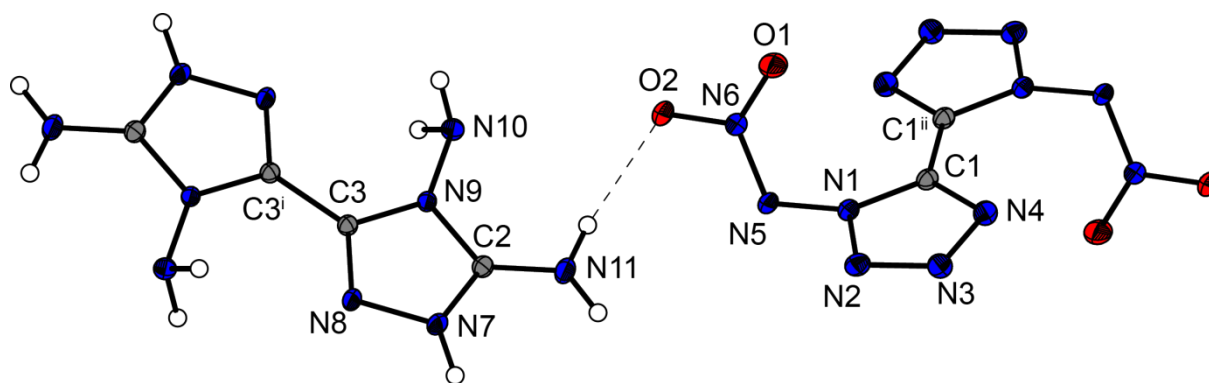


Figure 7. Molecular unit of **8**. Ellipsoids are drawn at the 50% probability level. Selected bond lengths [Å]: C1–C1ⁱ 1.443(3), C3–C3ⁱ 1.448(2) C2–N11 1.317(2); selected torsion angles [°]: N4–C1–C1ⁱ–N1ⁱ 1.7(3), N8–C3–C3ⁱ–N9ⁱ 0.2(2); symmetry code: (i) 2–x, 1–y, –z (ii) –x, –y, 2–z.

The crystal structures of compounds **4**, **7·2H₂O**, **9–10** and **13** were determined and are presented in the ESI.

8.2.3 Thermal Analysis and Compatibilities

To identify the decomposition temperatures of compound **1–13**, differential thermal analysis (DTA) with a heating rate of 5 °C min^{–1} was used. The results are shown in Fig. 8 and 10.

The decomposition temperature of the neutral compound **1** is very high (342 °C) and thus exceeds the decomposition temperature of the explosives **RDX** ($T_{\text{dec.}} = 204$ °C)^[21] and hexanitrostilbene ($T_{\text{dec.}} = 316$ °C).^[22] The dinitramide **2** decomposes at 200 °C. Dinitramide-based ionic energetic materials oftentimes lack thermal stability. One exception is **FOX-12**. Its decomposition temperature of 215 °C has been reported at a heating rate of 10 °C min^{–1}.^[23] For better comparison of **2** with **FOX-12**, ammonium dinitramide (**ADN**) and guanidinium dinitramide (**GDN**), these compounds were re-measured on our instrument at a heating rate of 5 °C min^{–1} (Fig. 8). **FOX-12** showed an onset decomposition temperature of 201 °C, which is virtually the same temperature as compound **2**. **GDN** and **ADN** had lower decomposition temperatures of 149 and 147 °C. Table 1 compares the thermal stability (although being a 1:2 dinitramide salt) with other nitrogen-rich dinitramides.

Compounds **4**, **9** and **10** containing two water moieties each, dehydrate at 89, 93 and 104 °C, respectively. The highest decomposition temperature of the energetic salts of compound **1** was measured for compound **6** ($T_{\text{dec.}} = 290$ °C). After compound **6**, compounds **5**, **7**, **11** and **12** also showed very high thermal stabilities, with onset decomposition temperatures of 275, 279, 286 and 284 °C, respectively. In comparison to the 1-methylnitriminotetrazolate **10**, which shows a fairly low onset of decomposition at 209 °C, nitriminotetrazolate **9** has a higher onset

of decomposition at 232 °C. This agrees with the decomposition temperatures of reported nitrogen-rich 1-methylnitrimino-tetrazolates with onset temperatures of around 210 °C.^[24]

Table 1. Decomposition temperatures of various nitrogen-rich dinitramides ^[27] in comparison to compound **2**^a

Dinitramide	$T_{\text{dec. (onset) [°C]}}$
2	200
FOX-12	201 (215 at 10 °C min ⁻¹) (ref. 23)
A DN	147
G DN	149
TAG DN	180 (ref. 27a)
1,5-DAT DN	135 (ref. 27b)
1-Me-AT DN	145 (ref. 27b)
2-Me-AT DN	148 (ref. 27c)
5-AT DN	117 (ref. 27c)
Tz DN	110 (ref. 27c)
3,5-DATr DN	164 (ref. 27d)
3,6-DHyTT DN	152 (ref. 27e)

^a DN = dinitramide, A = ammonium, G = guanidinium, TAG = triaminoguanidinium, 1,5-DAT = 1,5-diaminotetrazolium, 1-Me-AT = 1-methyl-5-aminotetrazolium, 2-Me-AT = 2-methyl-5-aminotetrazolium, 5-AT = 5-aminotetrazolium, Tz = tetrazolium, 3,5-DATr = 3,5-diaminotriazolium, 3,6-DHyTT = 3,6-dihydrazino-tetrazinium

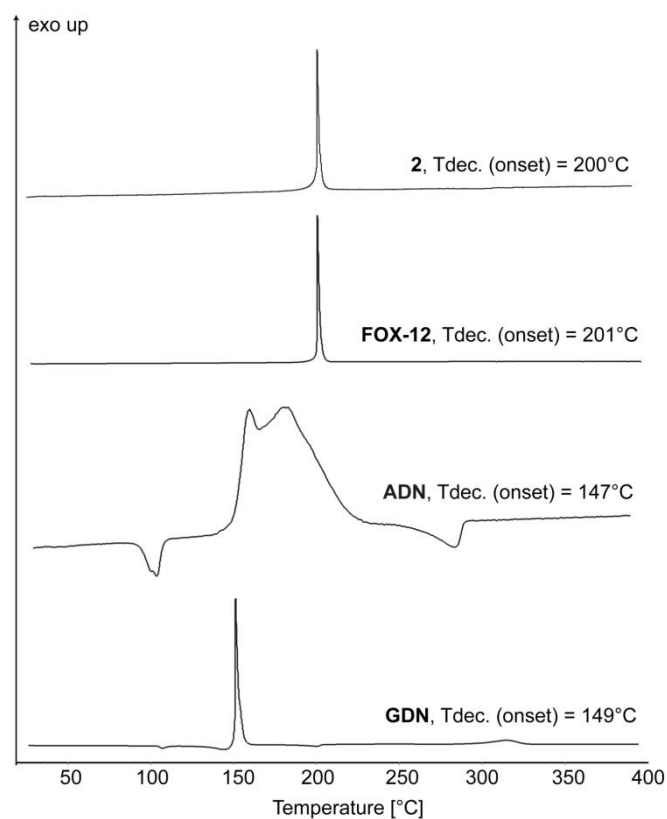


Figure 8. DTA plots of compound **2** compared with other nitrogen-rich dinitramide salts, such as *N*-guanylurea-dinitramide (**FOX-12**), ammonium dinitramide (**ADN**) and guanidinium dinitramide (**GDN**) measured with a heating rate of 5 °C min⁻¹.

The nitrotetrazolate **4** decomposes at a temperature of 225 °C and thus shows a higher thermal stability than all other reported non-metal nitrotetrazolate salts, with guanidinium nitrotetrazolate being the most temperature stable ($T_{\text{dec.}} = 212$ °C).^[5] Thermal stabilization of the anion in compound **8** could be achieved through cation metathesis. Although the potassium salt K_2DNABT decomposes at 200 °C,^[4a] the new energetic compound **8** is thermally stable up to a temperature of 223 °C. Compared with the nitrogen-rich salts, only the ammonium salt $(\text{NH}_4)_2\text{DNABT}$ lies in the range of the thermal stability of compound **8**, whereas the hydroxylammonium salt $(\text{NH}_3\text{OH})_2\text{DNABT}$ reveals a much lower decomposition temperature of 170 °C.^[25] The onset decomposition temperature of the nitrotetrazolate-2*N*-oxide **3** is 220 °C, showing a much higher thermal stability than other comparable nitrotetrazolate-2*N*-oxides, such as the guanidinium salt ($T_{\text{dec.}} = 211$ °C), the aminoguanidinium salt ($T_{\text{dec.}} = 185$ °C), the diaminoguanidinium salt ($T_{\text{dec.}} = 174$ °C), the triaminoguanidinium salt ($T_{\text{dec.}} = 153$ °C) or the ammonium salt ($T_{\text{dec.}} = 173$ °C).^[8c] Compared with **RDX**, with a decomposition temperature of 204 °C,^[21] salts **2–12** have at least an equivalent thermal stability. Only the nitroformate **13** decomposes at 94 °C, which is slightly lower than the ammonium (116 °C), guanidinium (113 °C) and triaminoguanidinium (105 °C) salt, but higher than the corresponding aminoguanidinium (71 °C) and diaminoguanidinium (82 °C) salt.^[26]

All explosives have to be coated for practical applications. A prominent mixture of **RDX** and **TNT** (ca. 60:40) is called Composition B. A compatibility test of compound **2** with **TNT** revealed that the decomposition temperature of the **2**/**TNT** mixture is virtually the same as for pure compound **2** with respect to both the onset and top of the peak. It can be concluded that dinitramide **2** is compatible with **TNT** (Fig. 9.)

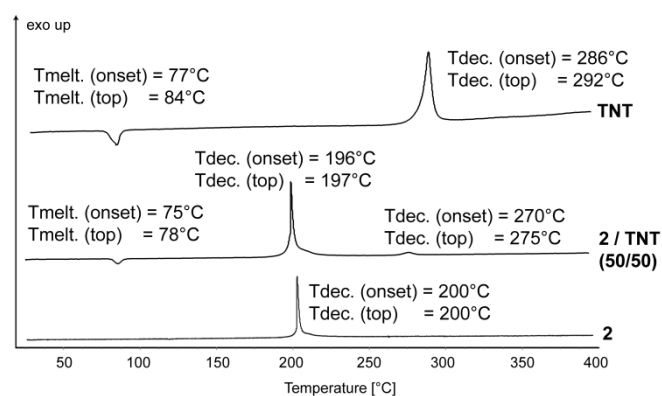


Figure 9. Compatibility measurements of dinitramide **2** with **TNT**

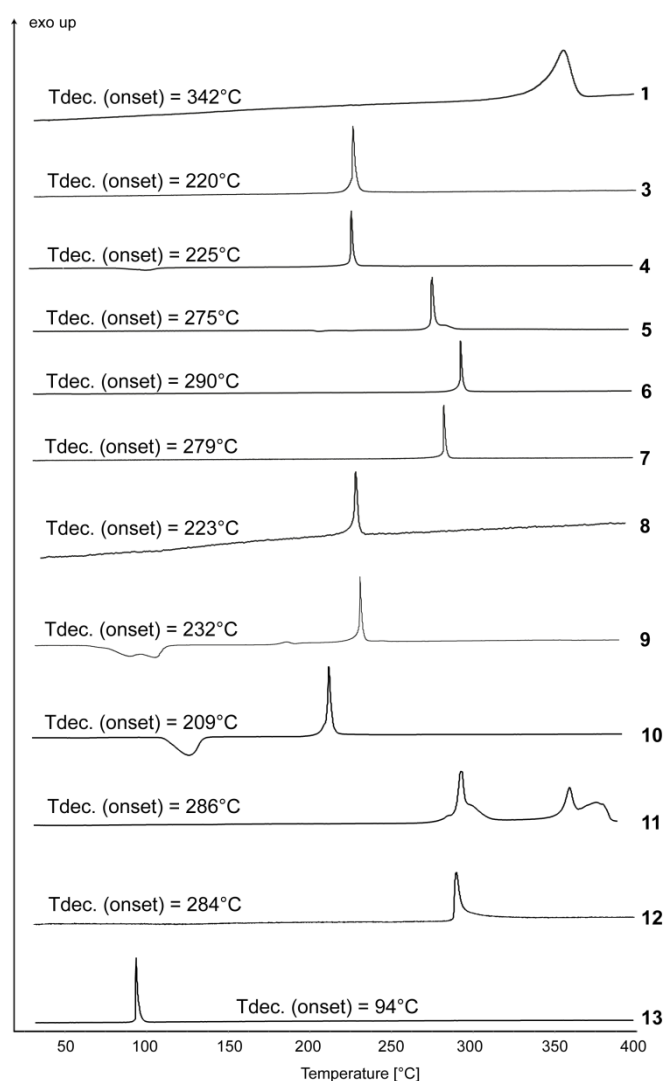


Figure 10. DTA plots of compounds **1** and **3–13** measured with a heating rate of $5\text{ }^{\circ}\text{C min}^{-1}$.

8.2.4 Sensitivities

Compounds **1–13** were tested for their sensitivity towards friction and impact using the BAM methods as described in the ESI. Compounds **1–13** showed a wide range of sensitivities towards impact. Although the neutral compound **1** and compounds **6**, **7** and **9** can be classified as insensitive towards impact ($<40\text{ J}$), compounds **2**, **3**, **8** and **11** show very high sensitivities from 6 J (**3**) to up to 3 J (**8**). The dinitramide **2**, with an impact sensitivity of 5 J , is in the range of sensitivities towards impact observed for other nitrogen-rich dinitramides (**ADN**, 5 J ;^[28] **TAG DN**, 2 J).^[27a] The impact sensitivity of compound **3** (6 J) is comparable with the impact sensitivities of the corresponding hydroxylammonium or ammonium salts with impact sensitivities of 4 and 7 J , respectively, but does not reach the stability of the diaminoguanidinium nitrotetrazolate-2*N*-oxide (20 J) or the guanidinium salt, which is

insensitive.^[8c] Compound **8** shows the highest sensitivity towards impact stimuli with 3 J, which is a result of the highly sensitive anion. The corresponding hydroxylammonium and ammonium salts have an impact sensitivity of 2 J and thus lie in the same range as compound **8**.^[25]

Compound **13** shows a sensitivity of 4 J. Compounds **4**, **10** and **12** are fairly insensitive, with sensitivities >30 J. Compared with previously reported nitrogen-rich salts of 1-methyl-5-nitrimino-tetrazole, an impact sensitivity of up to 35 J is very high, especially as the aminoguanidinium or triaminoguanidinium salts have values of about 10 J.^[24] The nitrate salt **5** (15 J) has a moderate sensitivity towards friction. The compounds **2**, **3**, **8**, **11** and **13** thus at least lie in the range of **RDX** (7.5 J)^[29] or have higher stabilities towards impact.

Except for compounds **8** and **11**, the energetic salts and the neutral compound **1** are insensitive towards friction (360 N). The friction insensitivity of the dinitramide compound **2** is notable, as previously reported nitrogen-rich salts, such as triaminoguanidinium dinitramide (24 N)^[27a] or ammonium dinitramide (72 N),^[28] have high sensitivities towards friction. In addition, the friction insensitivity of the nitrotetrazolate-2*N*-oxide **3** far exceeds the values reported for other nitrogen-rich nitrotetrazolate-2*N*-oxides, which range from guanidinium nitrotetrazolate-2*N*-oxide (252 N) to the hydroxylammonium salt with a friction sensitivity of 60 N.^[8c] The perchlorate (**11**) and nitroformate (**13**) salts have a slightly higher sensitivity towards friction stimuli (240 and 160 N). Compounds **1–7** and **9–12** have a much lower sensitivity towards friction than **RDX** ($FS_{RDX} = 120$ N).^[29] The ESD measurements show that compounds **1–7** and **9–13** are less sensitive towards electrostatic discharge (**1**, **5**, **7** and **9** = 1.5 J; **2**, **3** and **13** = 0.8 J; **12** = 0.75 J; **11** = 0.6 J; **10** = 0.5 J; **6** = 0.4 J; **4** = 0.3 J) than the sensitive compound **8** (0.05 J) or **RDX** (0.2 J).

8.2.5 Energetic performance

The values for the enthalpies of formation were calculated using the atomization method with electronic energies (CBS-4M method) at room temperature (see ESI). The heats and energies of formation for compounds **1–3**, **5–8**, **11** and **13** are given in Table 2.

The detonation parameters of compounds **1–3**, **5–8**, **11** and **13** were calculated using the program package EXPLO5 (version 6.02).^[30] The program is based on the chemical equilibrium steady-state model of detonation. It uses the Becker–Kistiakowsky–Wilson equation of state for gaseous detonation products and Cowan–Fickett's equation of state for solid carbon. For these calculations, the low-temperature X-ray densities were converted to

room temperature values with the equation $\rho_{298\text{K}} = \rho_{\text{T}}/(1 + \alpha_{\text{V}}(298 - T_0))$; $\alpha_{\text{V}} = 1.5 \times 10^{-4} \text{ K}^{-1}$.^[31] To verify this approximation, crystals of compound **2** were measured at 100, 173 and 298 K (see ESI). The measured X-ray density of 1.819 g cm^{-3} (298 K) is almost the same as the recalculated density of 1.826 g cm^{-3} (298 K). The marginal influence on the calculated detonation performances is shown in Table 2.

The calculated detonation parameters are summarized in Table 2 and compared with the values calculated for **FOX-12** and **RDX**. The energetic performances of compounds **6–8**, **11** and **13** are discussed in detail in the ESI.

Compared with the energetic salts, compound **1** has a fairly high heat of formation of 472 kJ mol^{-1} . The dinitramide **2** has a heat of formation of 302 kJ mol^{-1} . Compared with **ADN** (heat of formation -150 kJ mol^{-1}), or hydroxylammonium dinitramide (heat of formation -34 kJ mol^{-1}), the calculated heat of formation of compound **2** is significantly higher.^[12] A higher value is also obtained compared with **RDX** and **FOX-12**, which have heats of formation of 70 and -355 kJ mol^{-1} , respectively. Compound **3** has a highly positive heat of formation of 761 kJ mol^{-1} .

For neutral compound **1**, a fairly high detonation velocity of 8944 m s^{-1} and a detonation pressure of 285 kbar were calculated. The highest detonation velocity of 9053 m s^{-1} in this work was calculated for dinitramide **2**. This was also higher than that of **RDX** (8861 m s^{-1}) and **FOX-12** (8323 m s^{-1}). When comparing the detonation pressures, compound **2** showed a value in the range of **RDX** (345 kbar) and a much higher value than **FOX-12** (265 kbar). Compared with **RDX**, compound **3** had a very similar detonation velocity of 8857 m s^{-1} and a slightly lower detonation pressure of 306 kbar. The corresponding hydroxylammonium salt had a higher detonation velocity (9499 m s^{-1}) and detonation pressure (410 kbar).^[8c] The other reported nitrotetrazolate-2N-oxides had detonation parameters in the range of compound **3** ($\text{NH}_4\text{NT}_2\text{O}$ $p_{\text{CJ}} = 322 \text{ kbar}$, $D = 8885 \text{ m s}^{-1}$) or had lower values (the G^+ , AG^+ , DAG^+ , TAG^+ salts).^[8c] The nitrate **5** had a detonation velocity of 8334 m s^{-1} and a detonation pressure of 260 kbar. The lowest detonation pressure (221 kbar) and velocity (8081 m s^{-1}) of the compounds were for compound **7**.

A small-scale reactivity test (SSRT; see ESI for detailed setup) was conducted to assess the explosive performance of **2** compared with **RDX** and **FOX-12**. From measuring the volumes of the dents (Table 3), it can be concluded that the small-scale explosive performance of **2** is slightly lower than that of commonly used **RDX**, but far exceeds that of **FOX-12**.

Table 2. Energetic Properties and detonation parameters of compounds **1–3, 5–8, 11** and **13** compared to RDX and FOX-12.

	1	2	3	5	6	7	8	11	13	RDX	FOX-12
Formula	C ₄ H ₈ N ₁₀	C ₄ H ₁₀ N ₁₆ O ₈	C ₆ H ₁₀ N ₂₀ O ₆	C ₄ H ₁₀ N ₁₂ O ₆	C ₁₀ H ₁₀ N ₁₈ O ₈	C ₆ H ₁₀ N ₁₈ O ₂	C ₆ H ₁₀ N ₂₂ O ₄	C ₄ H ₁₀ N ₁₀ O ₈ Cl ₂	C ₆ H ₁₀ N ₁₆ O ₁₂	C ₃ H ₆ N ₆ O ₆	C ₂ H ₇ N ₇ O ₅
FW [g mol ⁻¹]	196.17	410.22	458.11	322.20	510.30	366.26	454.29	397.09	498.24	222.12	209.12
IS [J] ^a	40	5	6	15	40	40	3	5	4	7.5	30
FS [N] ^b	360	360	360	360	360	360	10	240	160	120	350
ESD [J] ^c	1.5	0.8	0.8	1.5	0.4	1.5	0.05	0.9	0.8	0.20	1.5
N [%] ^d	71.40	54.63	61.13	52.17	49.41	68.84	67.83	35.27	44.98	37.84	46.89
Q [%] ^e	-97.87	-19.50	-38.40	-34.76	-53.30	-65.52	-45.79	-16.11	-16.06	-21.61	-19.13
T _{dec.} [°C] ^f	342	200	220	275	290	279	223	286	94	204	201
ρ [g cm ⁻³] (298K) ^g	1.68 (pyc.)	1.826 (1.819) ^h	1.799	1.746	1.844	1.655	1.745	1.870	1.837	1.806	1.754
Δ _f H° [kJ mol ⁻¹] ⁱ	472.0	301.5 (302.8) ^h	761.2	-153.2	20.9	597.4	1107.7	-23.1	173.4	70.3	-355.0
Δ _f U° [kJ kg ⁻¹] ^j	2520.3	837.7 (840.9) ^h	1758.3	-367.7	258.6	1733.7	2536.6	35.4	442.5	417.0	-1585.0
EXPLO V6.02 values:											
-Δ _E U° [kJ kg ⁻¹] ^k	3101	4955 (4956) ^h	4696	3871	3533	3262	4672	4589	5226	5845	3694
T _E [K] ^l	2088	3407 (3422) ^h	3293	2790	2668	2446	3266	3492	3642	3810	2703
p _{CJ} [kbar] ^m	258	338 (338) ^h	306	260	260	221	288	299	343	345	265
D [m s ⁻¹] ⁿ	8944	9053 (9022) ^h	8857	8334	8237	8081	8804	8290	8879	8861	8323
V ₀ [L kg ⁻¹] ^o	812	843 (843) ^h	822	867	736	819	833	792	780	785	893

a impact sensitivity (BAM drophammer, 1 of 6); b friction sensitivity (BAM friction tester, 1 of 6); c electrostatic discharge device (OZM); d nitrogen content; e oxygen balance; f decomposition temperature from DTA (β = 5°C); g recalculated from low temperature X-ray densities (ρ_{298K} = ρ_T / (1 + α_V(298-T₀); α_V = 1.5 · 10⁻⁴ K⁻¹); h in parenthesis values for the density obtained from the X-ray measurement at 298K; i calculated (CBS-4M) heat of formation; j calculated energy of formation; k energy of explosion; l explosion temperature; m detonation pressure; n detonation velocity; o assuming only gaseous products.

Table 3. Values for the SSRT and toxicity test of compound **2** compared to **FOX-12** and **RDX**

SSRT		
Compound	Weight [mg]	Dent [mg SiO ₂]
2	524	772
FOX-12	503	579
RDX	504	858
Toxicity assessment:		
Compound	EC ₅₀ (15 min)	EC ₅₀ (30 min)
2	-	3.78
FOX-12	2.15	3.58
RDX	0.237	0.239

The toxicity to aquatic life was investigated using the luminescent marine bacterium *Vibrio fischeri* (see ESI).^[32] For the dinitramide **2** and **FOX-12** we observed EC₅₀ values of 3.78 and 3.58 g L⁻¹ after an incubation time of 30 min. A compound can be considered as non-toxic if EC₅₀ is >1.00 g L⁻¹. The toxicity test shows the low toxicity of **2** and **FOX-12** compared with **RDX** (Table 3).

8.2.6 Spectroscopy

Compounds **1–13** were characterized by ¹H NMR and ¹³C NMR spectroscopy. Compound **1** shows two broad signals at 5.91 and 5.81 ppm representing two –NH₂ groups each. These values match the chemical shifts reported previously (5.90 and 5.80 ppm).^[9] Carbon resonances of the poorly soluble compound **1** could only be observed in a ¹³C NMR long-time measurement (pulse delay >2 s, >8000 scans). The resulting spectrum shows two sharp peaks at 155.4 (C–NH₂) and 139.4 ppm (C–C).

The ¹H-NMR spectra of compounds **2–5**, **8** and **11–13**, which all contain only N-connected protons, each reveals two similar broad signals with chemical shifts of 8.64–8.56 and 6.16–6.08 ppm. With two broad signals at 8.10 and 6.17 ppm, the energetic salt **6** shows chemical shifts that are slightly shifted up-field compared with the signals of most of the compounds. The proton signals of compounds **7** and **9** are slightly shifted up-field to 7.65 and 6.00 ppm and 7.82 and 6.05 ppm, respectively. In comparison, compound **10**, which is the 1-methyl derivative of compound **9**, shows an even greater chemical shift up-field to 6.89 and 4.64 ppm.

The chemical shifts of the carbon atoms of the cations in compounds **2–13** are slightly shifted up-field compared with the neutral compound **1**. The chemical shifts of all carbons in the cations of compounds **2–13** show very sharp signals in a similar range. The carbon of the C–NH₂ group shows a chemical shift between 153.6 and 151.9 ppm, whereas the chemical shift of the C–C carbon lies between 138.5 and 137.7 ppm.

IR and Raman spectra for compounds **1–13** were measured and the frequencies were assigned according to commonly observed values.^[5,33]

In the IR spectrum of compound **1**, the stretching vibration of the N–H bond is observed between 3500 and 3300 cm⁻¹, whereas the deformation vibration shows a strong band at 1537 cm⁻¹ in the IR spectrum and a very weak band at 1551 cm⁻¹ in the Raman spectrum. The strongest band observed in the IR spectrum is the C=N stretch at 1626 cm⁻¹. Another characteristic band of the triazole ring is observed at 1317 cm⁻¹, representing the C–N stretch.

These values are very similar to those reported for substituted 1,2,4-triazoles.^[34] The vibration of the carbon–amine bond appears at 1085 cm⁻¹ and the C–C vibration of the carbons linking the two rings together occurs at 1022 cm⁻¹. These bands can all be observed at very similar values for the cations of compounds **2–13**.

The ¹³C NMR peaks and the IR and Raman bands of the anions all match the previously published values and are discussed in detail in the ESI.

8.3 Experimental Part

The general methods and procedures as well as the synthesis of compounds **3–13** are described in the ESI.

4,4',5,5'-Tetraamino-3,3'-bi-1,2,4-triazole (**1**)

4,4',5,5'-Tetraamino-3,3'-bi-1,2,4-triazole (**1**) was synthesized by a slightly modified version of a previously published procedure.^[9] Phosphorus pentoxide (10 g, 70.4 mmol) was slowly dissolved in phosphoric acid (30 g, 306 mmol) preheated to 50 °C. A finely ground mixture of oxalic acid dihydrate (3.15 g, 25.0 mmol, 1.0 equiv.) and diaminoguanidine monohydrochloride (8.29 g, 66 mmol, 2.6 equiv.) was slowly added to the preheated solution. After complete addition, the viscous mixture was slowly heated to 120 °C and the evolution of gaseous HCl was observed. The mixture was kept at 120 °C for 4 h and was then cooled to room temperature with stirring. Ice water (150 mL) was poured into the mixture and a white precipitate was formed. About 75 mL of 10 M NaOH was used to neutralize the reaction mixture, changing the color of the suspension from white to brown. The precipitate was filtered, washed repeatedly with water and air-dried to obtain the crude compound **1** as a brownish solid. Yield: 1.39 g, 7.09 mmol, 28%. To purify, the crude product was recrystallized with hydrochloric acid or glacial acetic acid. Compound **1** (1000 mg, 5.10 mmol, 1.00 equiv.) was added slowly to glacial acid. The mixture was heated until compound **1** completely dissolved. The mixture was removed from the heating bath and was left to cool to room temperature. After filtration and repeated washing with water, the residue was dried in a nitrogen flow before drying overnight in an oven at 100 °C. The solid was then suspended in 50 mL of water and made alkaline with about 1 mL of 10 M NaOH. The suspension was filtered and the residue was air-dried to produce pure compound **1** as a white solid. Yield: 696 mg, 3.55 mmol, 70%.

DTA (5 °C min⁻¹) onset: 342 °C (dec.); **IR** (ATR, cm⁻¹): $\tilde{\nu}$ = 3782 (vw), 3400 (m), 3341 (m), 3278 (m), 3142 (w), 2348 (vw), 1626 (vs.), 1537 (s), 1478 (m), 1421 (w), 1317 (w), 1252

(vw), 1232 (vw), 1085 (m), 1022 (m), 987 (vs.), 935 (m), 799 (vw), 778 (vw), 723 (m), 678 (vw), 664 (vw); **Raman** (1064 nm, 300 mW, 25 °C, cm⁻¹): $\tilde{\nu}$ = 3258 (4), 3171 (3), 1592 (100), 1551 (11), 1510 (4), 1393 (4), 1289 (7), 1087 (10), 1034 (6), 811 (16), 712 (6), 621 (3), 374 (3), 330 (4), 268 (4), 110 (12), 93 (7); **¹H NMR** ([D₆]DMSO): δ = 5.91 (br s, 4H), 5.81 ppm (br s, 4H); **¹³C NMR** ([D₆]DMSO): δ = 155.4 (s, C–NH₂), 139.4 ppm (s, C–C); **MS** *m/z* (DEI⁺): 196.2 (C₄H₈N₁₀); **EA** (C₄H₈N₁₀, 196.17) calcd.: C 24.49, H 4.11, N 71.40%; found: C 25.04, H 4.04, N 69.93%; **Sensitivities**: IS: 40 J, FS: 360 N, ESD: 1.5 J (at grain sizes <100 μm).

4,4',5,5'-Tetraamino-3,3'-bi-1,2,4-triazolium dinitramide (2)

To a suspension of 4,4',5,5'-tetraamino-3,3'-bi-1,2,4-triazole (**1**) (392 mg, 2.00 mmol, 1.00 equiv.) and ammonium dinitramide (496 mg, 4.00 mmol, 2.00 equiv.) in water was added 1 mL of 1 M hydrochloric acid. The mixture was heated until all components were dissolved and the mixture was left to crystallize overnight. The product was formed as slightly brownish crystals. Yield: 416 mg, 1.01 mmol, 51%.

DTA (5 °C min⁻¹) onset: 200 °C (dec.); **IR** (ATR, cm⁻¹): $\tilde{\nu}$ = 3278 (m), 3142 (m), 3088 (m), 2854 (m), 1695 (vs.), 1602 (m), 1596 (m), 1554 (m), 1516 (s), 1470 (m), 1417 (m), 1352 (m), 1339 (m), 1306 (m), 1258 (m), 1172 (s), 1082 (w), 992 (vs.), 954 (m), 790 (m), 778 (m), 706 (w), 672 (w), 672 (w); **Raman** (1064 nm, 300 mW, 25 °C, cm⁻¹): $\tilde{\nu}$ = 3176 (1), 1695 (2), 1642 (100), 1560 (2), 1532 (1), 1436 (6), 1377 (1), 1339 (2), 1288 (14), 1124 (2), 1079 (7), 1022 (2), 805 (20), 713 (7), 602 (6), 492 (1), 415 (1), 387 (2), 328 (3), 286 (2), 264 (2), 175 (3), 150 (7), 150 (7), 121 (12), 90 (11); **¹H NMR** ([D₆]DMSO): δ = 8.56 (br s, 4H), 6.08 ppm (br s, 6H); **¹³C NMR** ([D₆]DMSO): δ = 152.0 (s, C–NH₂), 137.8 ppm (s, C–C); **MS** *m/z* (FAB⁻): 106.0 (N₃O₄⁻), *m/z* (FAB⁺): 197.0 (C₄H₉N₁₀⁺); **EA** (C₄H₁₀N₁₆O₈, 410.22) calcd.: C 11.71, H 2.46, N 54.63%, found: C 12.04, H 2.55, N 53.96%; **Sensitivities**: IS: 5 J. FS: 360 N. ESD: 0.8 J (at grain sizes <100 μm).

8.4 Conclusions

The aromatic, nitrogen-rich 4,4',5,5'-tetraamino-3,3'-bi-1,2,4-triazole (**1**) was synthesized from commercially available diaminoguanidine hydrochloride and oxalic acid in polyphosphoric acid. Compound **1** shows an excellent thermal stability in both its neutral (342 °C) and protonated forms. Through simple anion metathesis several new energetic salts (**2–13**) were obtained and characterized in detail. These energetic ionic derivatives were extensively characterized for their physico-chemical properties (stability, sensitivity, compatibility) and detonation parameters based on their enthalpies of formation calculated

using the EXPLO5 computer code. The dinitramide salt **2** has a heat of formation of 301.5 kJ mol⁻¹, a detonation pressure of 338 kbar and a detonation velocity of 9053 m s⁻¹, which are remarkably high compared with other nitrogen-rich dinitramide salts, such as **FOX-12**. Moreover, dinitramide **2** was measured to be less toxic than **RDX** in aqueous media. Fundamental compatibility tests demonstrate the compatibility of **2** with **TNT**.

The high decomposition temperature (200 °C, determined by DTA at a heating rate of 5 °C min⁻¹) of dinitramide **2** is better than nearly all the dinitramides reported previously. The high thermal stability of these energetic salts shows the great value of compound **1** over other nitrogen-rich cations, such as guanidine, aminoguanidine or triaminoguanidine, in the synthesis of new ionic energetic materials.

8.5 Notes and References

- [1] a) W. E. Bachmann and J. C. Sheehan, *J. Am. Chem. Soc.*, 1949, **71**, 1842–1845; b) E. P. Burrows and E. E. Brueggemann, *J. of Chromatogr.*, 1985, **329**, 285–289; c) A. T. Nielsen, A. P. Chafin, S. L. Christian, D. W. Moore, M. P. Nadler, R. A. Nissan, D. J. Vanderah, R. D. Gilardi, C. F. George and J. L. Flippen-Anderson, *Tetrahedron*, 1998, **54**, 11793–11812.
- [2] T. Fendt, N. Fischer, T. M. Klapötke and J. Stierstorfer, *Inorg. Chem.*, 2011, **50**, 1447–1458.
- [3] a) H. Gao and J. M. Shreeve, *Chem. Rev.*, 2011, **111**, 7377–7436; b) R. Haiges, S. Schneider, T. Schroer and K. O. Christe, *Angew. Chem.*, 2004, **116**, 5027–5032; *Angew. Chem. Int. Ed.*, 2004, **43**, 4919–4924; c) D. E. Chavez, M. A. Hiskey, D. L. Naud and D. Parrish, *Angew. Chem.*, 2008, **120**, 8431–8433; *Angew. Chem. Int. Ed.*, 2008, **47**, 8307–8309; d) M. B. Talawar, R. Sivabalan, T. Mukundan, H. Muthurajan, A. K. Sikder, B. R. Gandhe and A. Subhananda Rao, *J. Hazard. Mater.*, 2009, **161**, 589–607; e) O. S. Bushuyev, P. Brown, A. Maiti, R. H. Gee, G. R. Peterson, B. L. Weeks and L. J. Hope-Weeks, *J. Am. Chem. Soc.*, 2012, **134**, 1422–1425; f) C. Li, L. Liang, K. Wang, C. Bian and J. Zhang, *J. Mat. Chem. A*, 2014, **2**, 18097–18105.
- [4] a) D. Fischer, T. Klapötke and J. Stierstorfer, *Angew. Chem.*, 2014, **126**, 8311–8314; *Angew. Chem. Int. Ed.*, 2014, **53**, 8172–8175. b) M. Göbel and T. M. Klapötke, *Z. Anorg. Allg. Chem.*, 2007, **633**, 1006–1017; c) M. Härtel, T. M. Klapötke, D. Piercey and J. Stierstorfer, *Z. Anorg. Allg. Chem.*, 2012, **638**, 2008–2014.

- [5] T. M. Klapötke, P. Mayer, C. M. Sabaté, J. M. Welch and N. Wiegand, *Inorg. Chem.*, 2008, **47**, 6014–6027.
- [6] D. E. Chavez, M. A. Hiskey, and R. D. Gilardi, *Angew. Chem.*, 2000, **112**, 1861–1863; *Angew. Chem. Int. Ed.*, 2000, **39**, 1791–1793.
- [7] a) A. Hammerl, M. A. Hiskey, G. Holl, T. M. Klapötke, K. Polborn, J. Stierstorfer and J. J. Weigand, *Chem. Mater.* 2005, **17**, 3784–3793; b) L. Liang, K. Wang, C. Bian, L. Ling and Z. Zhou, *Chem. Eur. J.* 2013, **19**, 14902–14910; c) L. Liang, H. Huang, K. Wang, C. Bian, J. Song, L. Ling, F- Zhao and Z. Zhou, *J. Mater. Chem.* 2012, **22**, 21954–21964.
- [8] a) A. A. Dippold and T. M. Klapötke, *J. Am. Chem. Soc.*, 2013, **135**, 9931–9938; b) J. Zhang and J. M. Shreeve *J. Am. Chem. Soc.*, 2014, **136**, 4437–4445; c) M. Göbel, K. Karaghiosoff, T. M. Klapötke, D. G. Piercey and J. Stierstorfer, *J. Am. Chem. Soc.*, 2010, **132**, 17216–17226; d) J. Song, Z. Zhou, X. Dong, H. Huang, D. Cao, L. Liang, K. Wang, J. Zhang, F. Chen and Y. Wu, *J. Mater. Chem.* 2012, **22**, 3201–3209.
- [9] R. Centore, A. Carella and S. Fusco, *Struct. Chem.*, 2011, **22**, 1095–1103.
- [10] The cif files can be obtained free of charge from the Cambridge Crystallographic Data Centre via www.ccdc.cam.ac.uk/data_request/cif.
- [11] H. Östmark, U. Bemm, A. Lenglet, R. Sandén and N. Wingborg, *J. Energ. Mater.*, 2000, **18**, 123–138.
- [12] R. J. Schmidt, J. C. Battaro, P. E. Penwell, The Development of New Protecting/Leaving Groups and Application to the Synthesis of Cage Nitramines, SRI International Project 6654, ADA261496, 1993.
- [13] A. Dippold and T. M. Klapötke, *Chem. Eur. J.*, 2012, **18**, 16742–16753.
- [14] A. A. Dippold, T. M. Klapötke, *Chem. Asian. J.*, 2013, **8**, 1463–1471.
- [15] A. Rheingold, J. Cronin and T. Brill, *Acta Cryst.*, 1987, **C43**, 402–404.
- [16] A. Katrusiak, *Acta Cryst.*, 1994, **C50**, 1161–1163.
- [17] S. H. Kim and J. S. Kim, *Bull. Korean Chem. Soc.*, 2013, **34**, 2503–2506.
- [18] T. M. Klapötke, A. Preimesser and J. Stierstorfer, *Z. Anorg. Allg. Chem.*, 2012, **638**, 1278–1286.

- [19] N. Fischer, D. Fischer, T.M. Klapötke, D. G. Piercey and J. Stierstorfer, *J. Mater. Chem.*, 2012, **22**, 20418–20422.
- [20] N. Fischer, T. Klapötke, M. Reymann and J. Stierstorfer, *Eur. J. Inorg. Chem.*, 2013, 2167–2180.
- [21] J. P. Agrawal, *High Energy Materials*, Wiley-VCH, Weinheim, 1st edn, 2010, 189.
- [22] K. Shipp, *J. Org. Chem.*, 1964, **29**, 2620–2623.
- [23] H. Östmark, A. Helte, T. Carlsson, R. Adolfsson, L. Bodin, C. Eldstätter, H. Edvinsson, J. Lundgreen and H. Örnhed, *FOI Technical Report*, N-guanyllurea dinitramide (FOX-12): properties 2007, FOI-R--2312—SE, Project No. E20503.
- [24] T. M. Klapötke, J. Stierstorfer and A. U. Wallek, *Chem. Mater.*, 2008, **20**, 4519–4530.
- [25] Dennis Fischer, private communication.
- [26] M. Göbel and T. M. Klapötke, *Z. Anorg. Allg. Chem.*, 2007, **633**, 1006–1017.
- [27] (a) T. M. Klapötke and J. Stierstorfer, *Chem. Phys.*, 2008, **10**, 4340–4346; (b) T. M. Klapötke and J. Stierstorfer, *Eur. J. Inorg. Chem.*, 2008, 26, 4055–4062. (c) T. M. Klapötke and J. Stierstorfer, *Dalton Trans.*, 2009, **4**, 643–653. (d) T. M. Klapötke, F. A. Martin, N. T. Mayr and J. Stierstorfer, *Z. Anorg. Allg. Chem.*, 2010, **636**, 2555–2564. (e) J. C. Oxley, J. L. Smith and H. Chen, *Thermochimica Acta*, 2002, **384**, 91–99.
- [28] U. Teipel, T. Heintz and H. H. Krause, *Propellants Explos. Pyrotech.*, 2000, **25**, 81–85.
- [29] J. Köhler and R. Meyer, *Explosivstoffe*, Wiley-VCH, Weinheim, 9th edn, 1998, 166–168.
- [30] M. Sućeska, EXPLO5.06 program, Zagreb, Croatia, 2013.
- [31] C. Xue, J. Sun, B. Kang, Y. Liu, X. Liu, G. Song and Q. Xue, *Propellants Explos. Pyrotech.*, 2010, **35**, 333–338.
- [32] G. I. Sunahara, S. Dodard, M. Sarrazin, L. Paquet, G. Ampleman, S. Thiboutot, J. Hawari and A. Y. Renoux, *Ecotoxicol. Environ. Saf.* 1998, **39**, 185–194.
- [33] a) M. Hesse, H. Meier and B. Zeeh, *Spektroskopische Methoden in der Organischen Chemie*, Thieme, Stuttgart, New York, 7th edn, 2005; b) G. Socrates, *Infrared and Raman Characteristic Group Frequencies: Tables and Charts*, John Wiley & Sons, Chichester, 3rd edn, 2004.
- [34] Y. Murthi, R. Agnihotri, D. Pathak, *American Journal of Chemistry* 2011, **1**, 42–46.

8.6 Supplementary information

The analytical methods and general procedures are described in the appendix of this thesis.

8.6.1 Experimental work

4,4',5,5'-Tetraamino-3,3'-bi-1,2,4-triazole (**1**)

4,4',5,5'-Tetraamino-3,3'-bi-1,2,4-triazole (**1**) was synthesized according to the literature:^[1]

Phosphorus pentoxide (10 g, 70.4 mmol) was slowly dissolved in phosphoric acid (30 g, 306 mmol), which was preheated to 50 °C. A finely ground mixture of oxalic acid dihydrate (3.15 g, 25.0 mmol, 1.0 eq) and diaminoguanidine monohydrochloride (8.29 g, 66 mmol, 2.6 eq.) was slowly added to the preheated solution. After complete addition, the viscous mixture was slowly heated to 120 °C and gas evolution of HCl was observed. The mixture was kept at 120 °C for 4 h and was then cooled to room temperature under stirring. 150 mL ice water was poured into the mixture and a white precipitate was formed. About 75 mL of 10 M NaOH was used to neutralize the reaction mixture, changing the color of the suspension from white to brown. The precipitate was filtered, washed repeatedly with water and air dried to obtain crude compound **1** as a brownish solid. Yield: 1.39 g, 7.09 mmol, 28%.

For purification the crude product was recrystallized with hydrochloric acid or glacial acetic acid. Compound **1** (1000 mg, 5.10 mmol, 1.00 eq.) was added slowly to glacial acid. The mixture was heated until compound **1** completely dissolved. The mixture was removed from the heating bath and was left to cool to room temperature. After filtration and repeated washing with water the residue was dried in a nitrogen flow before drying the substance in oven at 100 °C over night. Then the solid was suspended in 50 mL water and basified with about 1 mL of 10 M NaOH. The suspension was filtered and the residue was air dried to obtain pure compound **1** as a white solid. Yield: 696 mg, 3.55 mmol, 70%.

DTA (5 °C min⁻¹) onset: 342 °C (dec.); **IR** (ATR, cm⁻¹): $\tilde{\nu}$ = 3782(vw), 3400(m), 3341(m), 3278(m), 3142(w), 2348(vw), 1626(vs), 1537(s), 1478(m), 1421(w), 1317(w), 1252(vw), 1232(vw), 1085(m), 1022(m), 987(vs), 935(m), 799(vw), 778(vw), 723(m), 678(vw), 664(vw); **Raman** (1064 nm, 300 mW, 25 °C, cm⁻¹): $\tilde{\nu}$ = 3258(4), 3171(3), 1592(100), 1551(11), 1510(4), 1393(4), 1289(7), 1087(10), 1034(6), 811(16), 712(6), 621(3), 374(3), 330(4), 268(4), 110(12), 93(7); **¹H NMR** ([D₆]DMSO): δ = 5.91 (br s, 4H), 5.81 ppm (br s, 4H); **¹³C NMR** ([D₆]DMSO): δ = 155.4 (s, C–NH₂), 139.4 ppm (s, C–C); **MS** *m/z* (DEI⁺): 196.2 (C₄H₈N₁₀); **EA** (C₄H₈N₁₀, 196.17) calcd.: C 24.49, H 4.11, N 71.40%; found: C 25.04, H 4.04, N 69.93%; **Sensitivities**: IS: 40 J, FS: 360 N, ESD: 1.5 J (at grain sizes: <100 μ m).

4,4',5,5'-Tetraamino-3,3'-bi-1,2,4-triazolium dinitramide (2)

To a suspension of 4,4',5,5'-tetraamino-3,3'-bi-1,2,4-triazole (**1**) (392 mg, 2.00 mmol, 1.00 eq.) and ammonium dinitramide (496 mg, 4.00 mmol, 2.00 eq.) in water was added 1 mL 1 M hydrochloric acid. The mixture was heated until all components were dissolved and the mixture was left to crystallize over night. The product was obtained in form of slightly brownish crystals. Yield: 416 mg, 1.01 mmol, 51%.

DTA (5 °C min⁻¹) onset: 200 °C (dec.); **IR** (ATR, cm⁻¹): $\tilde{\nu}$ = 3278(m), 3142(m), 3088(m), 2854(m), 1695(vs), 1602(m), 1596(m), 1554(m), 1516(s), 1470(m), 1417(m), 1352(m), 1339(m), 1306(m), 1258(m), 1172(s), 1082(w), 992(vs), 954(m), 790(m), 778(m), 706(w), 672(w), 672(w); **Raman** (1064 nm, 300 mW, 25 °C, cm⁻¹): $\tilde{\nu}$ = 3176(1), 1695(2), 1642(100), 1560(2), 1532(1), 1436(6), 1377(1), 1339(2), 1288(14), 1124(2), 1079(7), 1022(2), 805(20), 713(7), 602(6), 492(1), 415(1), 387(2), 328(3), 286(2), 264(2), 175(3), 150(7), 150(7), 121(12), 90(11); **¹H NMR** ([D₆]DMSO): δ = 8.56 (br s, 4 H), 6.08 ppm (br s, 6 H); **¹³C NMR** ([D₆]DMSO): δ = 152.0 (s, C–NH₂), 137.8 ppm (s, C–C); **MS** m/z (FAB⁻): 106.0 (N₃O₄⁻), m/z (FAB⁺): 197.0 (C₄H₉N₁₀⁺); **EA** (C₄H₁₀N₁₆O₈, 410.22) calcd.: C 11.71, H 2.46, N 54.63%; found: C 12.04, H 2.55, N 53.96%; **Sensitivities**: IS: 5 J, FS: 360 N, ESD: 0.8 J (at grain sizes <100 μ m).

4,4',5,5'-Tetraamino-3,3'-bi-1,2,4-triazolium nitrotetrazolate-2-oxide (3)

To 4,4',5,5'-tetraamino-3,3'-bi-1,2,4-triazole (**1**) (392 mg, 2.00 mmol, 1.00 eq.) and ammonium nitrotetrazolate-2-oxide (592 mg, 4.00 mmol, 2.00 eq.) in water 1 mL 2 M hydrochloric acid was added and the suspension was heated until all components dissolved. The reaction mixture was cooled to room temperature and was then left to crystallize over night, yielding yellow crystals. Yield: 631 mg, 1.38 mmol, 69%.

DTA (5 °C min⁻¹) onset: 220 °C (dec.); **IR** (ATR, cm⁻¹): $\tilde{\nu}$ = 3432(m), 3379(s), 3294(m), 3106(s), 2673(m), 1757(w), 1704(s), 1613(s), 1540(vs), 1532(vs), 1467(m), 1456(m), 1426(s), 1403(vs), 1381(s), 1305(vs), 1257(s), 1232(vs), 1091(m), 1075(s), 1049(s), 975(s), 904(s), 904(s), 822(m), 761(m), 707(m), 701(s), 664(s); **Raman** (1064 nm, 300 mW, 25 °C, cm⁻¹): $\tilde{\nu}$ = 3299(2), 1715(2), 1637(42), 1592(3), 1535(5), 1460(6), 1424(29), 1401(63), 1385(20), 1308(14), 1292(10), 1234(7), 1122(4), 1091(9), 1073(49), 1052(28), 982(100), 843(3), 804(20), 761(4), 720(4), 705(4), 610(4), 610(4), 604(5), 489(3), 338(5), 275(3), 240(5), 206(7), 179(4), 144(11), 125(24), 104(21), 72(17); **¹H NMR** ([D₆]DMSO): δ = 8.64 (br s, 4 H), 6.14 ppm (br s, 6 H); **¹³C NMR** ([D₆]DMSO): δ = 157.4 (s, C–NO₂), 152.0 (s, C–NH₂), 137.9 ppm (s, C–C); **MS** m/z (FAB⁻): 130.0 (CN₅O₃⁻), m/z (FAB⁺): 197.0 (C₄H₉N₁₀⁺);

EA ($\text{C}_6\text{H}_{10}\text{N}_{20}\text{O}_6$, 458.28) calcd.: C 15.73, H 2.20, N 61.13%; found: C 16.05, H 2.24, N 60.57%; **Sensitivities**: IS: 6 J, FS: 360 N, ESD: 0.8 J (at grain sizes 100 – 500 μm).

4,4',5,5'-Tetraamino-3,3'-bi-1,2,4-triazolium nitrotetrazolate dihydrate (4)

To a suspension of 4,4',5,5'-tetraamino-3,3'-bi-1,2,4-triazole (**1**) (196 mg, 1.00 mmol, 1.00 eq.) and ammonium nitrotetrazolate (264 mg, 2.00 mmol, 2.00 eq.) in water 1 mL 2 M hydrochloric acid was added and the reaction mixture was heated until all solid materials were dissolved. After crystallization over night compound **4** was obtained in form of brownish crystals. Yield: 312 mg, 0.67 mmol, 67%.

DTA (5 $^{\circ}\text{C min}^{-1}$) onset: 89 $^{\circ}\text{C}$ ($-\text{H}_2\text{O}$), 225 $^{\circ}\text{C}$ (dec.); **IR** (ATR, cm^{-1}): $\tilde{\nu}$ = 3568(m), 3338(m), 3250(m), 3143(m), 2946(w), 2850(w), 2755(m), 1697(vs), 1611(m), 1584(w), 1538(vs), 1511(w), 1494(w), 1436(m), 1417(s), 1316(s), 1264(w), 1179(w), 1167(w), 1098(w), 1049(w), 1028(w), 984(s), 984(s), 937(m), 838(s), 785(w), 736(vw), 712(w), 671(w); **Raman** (1064 nm, 300 mW, 25 $^{\circ}\text{C}$, cm^{-1}): $\tilde{\nu}$ = 3264(2), 1709(4), 1648(100), 1605(5), 1540(8), 1484(4), 1414(94), 1335(2), 1314(6), 1298(12), 1178(3), 1168(6), 1134(6), 1089(6), 1077(4), 1067(3), 1063(3), 1049(85), 1043(38), 1031(7), 944(2), 837(10), 802(22), 802(22), 774(5), 716(10), 692(4), 614(3), 538(5), 451(5), 422(3), 380(5), 330(10), 280(7), 260(10), 175(11), 123(30), 86(76), 64(22); **$^1\text{H NMR}$** ($[\text{D}_6]\text{DMSO}$): δ = 8.64 (br s, 4 H), 6.16 ppm (br s, 6 H); **$^{13}\text{C NMR}$** ($[\text{D}_6]\text{DMSO}$): δ = 168.8 (s, C- NO_2), 152.0 (s, C- NH_2), 137.8 ppm (s, C-C); **MS** m/z (FAB^-): 114.0 (CN_5O_2^-), m/z (FAB^+): 197.0 ($\text{C}_4\text{H}_9\text{N}_{10}^+$); **EA** ($\text{C}_6\text{H}_{14}\text{N}_{20}\text{O}_6$, 462.31) calcd.: C 15.59, H 3.05, N 60.59%; found: C 15.84, H 3.06, N 59.48%; **Sensitivities**: IS: 35 J, FS: 360 N, ESD: 0.30 J (at grain sizes <100 μm).

4,4',5,5'-Tetraamino-3,3'-bi-1,2,4-triazolium dinitrate (5)

4,4',5,5'-Tetraamino-3,3'-bi-1,2,4-triazole (**1**) (140 mg, 0.71 mmol 1.00 eq.) was added to 0.75 mL of a 2 M HNO_3 in 5 mL water. The suspension was heated to reflux and left standing overnight to yield colorless crystals. Yield: 0.20 g, 0.62 mmol, 87%.

DTA (5 $^{\circ}\text{C min}^{-1}$) onset: 275 $^{\circ}\text{C}$ (dec.); **IR** (ATR, cm^{-1}): $\tilde{\nu}$ = 3329(s), 3253(m), 3201(m), 3115(m), 2913(m), 2620(m), 1756(vw), 1685(s), 1611(m), 1575(m), 1523(w), 1406(m), 1313(vs), 1294(s), 1249(s), 1148(m), 1095(w), 1047(m), 981(m), 942(m), 849(m), 820(m), 778(m), 778(m), 736(vw), 723(w), 685(m), 666(m); **Raman** (1064 nm, 300 mW, 25 $^{\circ}\text{C}$, cm^{-1}): $\tilde{\nu}$ = 3235(3), 1703(5), 1656(6), 1639(100), 1588(7), 1539(3), 1461(6), 1384(3), 1289(13), 1128(6), 1085(9), 1067(4), 1051(39), 1034(3), 952(3), 800(21), 728(5), 712(10), 614(5), 576(3), 415(4), 383(4), 340(5), 340(5), 266(5), 172(14), 142(22), 128(24), 111(22),

69(6); **¹H NMR** ([D₆]DMSO): δ = 8.57 (br s, 4 H), 6.14 ppm (br s, 6 H); **¹³C NMR** ([D₆]DMSO): δ = 152.0 (s, C–NH₂), 137.8 ppm (s, C–C); **MS** m/z (FAB[–]): 62.0 (NO₃[–]), m/z (FAB⁺): 197.0 (C₄H₉N₁₀⁺); **EA** (C₄H₁₀N₁₂O₆, 322.20) calcd.: C 14.91, H 3.13, N 52.17%; found: C 15.17, H 3.08, N 51.56%; **Sensitivities**: IS: 15 J, FS: 360 N, ESD: 1.5 J (at grain sizes 100 – 500 μ m).

4,4',5,5'-Tetraamino-3,3'-bi-1,2,4-triazolium tetranitrobisimidazolate (6)

4,4',5,5'-Tetraamino-3,3'-bi-1,2,4-triazole (**1**) (196 mg, 1.00 mmol, 1.00 eq.), ammonium tetranitro-bisimidazolate (348 mg, 1 mmol, 1.00 eq.) and 2 mL 1 M hydrochloric acid were added to 1.5 L of water. The formed suspension was refluxed for 5 min and a yellowish solution was formed. The solution was left to cool to room temperature and cooled to 5 °C overnight. Filtration of the solution yielded yellow crystals of compound **6**. Yield: 290.0 mg, 0.57 mmol, 57 %.

DTA (5 °C min^{–1}) onset: 290 °C (dec.); **IR** (ATR, cm^{–1}): $\tilde{\nu}$ = 3379(w), 2919(w), 1699(s), 1528(m), 1497(m), 1487(s), 1386(s), 1366(vs), 1300(s), 1237(s), 1215(s), 1114(m), 1062(m), 973(m), 899(m), 853(m), 809(vs), 751(m), 695(m), 675(w); **Raman** (1064 nm, 300 mW, 25 °C, cm^{–1}): $\tilde{\nu}$ = 1808(2), 1641(31), 1620(12), 1550(100), 1539(50), 1507(8), 1489(34), 1387(15), 1351(19), 1297(63), 1269(30), 1236(61), 1112(3), 1069(4), 1035(6), 1024(14), 874(19), 810(4), 803(4), 770(4), 760(5), 755(5), 704(3), 704(3), 617(2), 524(3), 394(5), 342(3), 263(5), 199(8), 118(12), 101(16); **¹H NMR** ([D₆]DMSO): δ = 8.10 (br s, 4 H), 6.17 ppm (br s, 4 H); **¹³C NMR** ([D₆]DMSO): δ = 152.8 (s, C–NH₂ Cation), 141.7 (s, C–C_{Anion}), 139.4 (s, C=C_{Anion}), 138.1 ppm (s, C–C_{Cation}); **MS** m/z (ESI[–]): 313.0 (C₆HO₈N₈[–]), m/z (ESI⁺): 197.1 (C₄H₉N₁₀⁺); **EA** (C₁₀H₁₀N₁₈O₈, 510.31) calcd.: C 23.54, H 1.98, N 49.41%; found: C 23.76, H 2.18, N 48.53%; **Sensitivities**: IS: 40 J, FS: 360 N, ESD 0.4 J (at grain sizes 100 – 500 μ m).

4,4',5,5'-Tetraamino-3,3'-bi-1,2,4-triazolium 5,5'-bitetrazole-1,1'-dioxide (7)

A clear solution of 5,5'-di-1,1'-hydroxytetrazole dihydrate (206 mg, 1.00 mmol, 1.0 eq.) and 4,4',5,5'-tetraamino-3,3'-bi-1,2,4-triazole (**1**) (196 mg, 1.00 mmol, 1.00 eq.) was prepared by dissolving the components in water (150 mL) while heating. The reaction mixture was refluxed for 10 min. and was then left to crystallize over night, yielding compound **7** as colorless crystals. Yield: 340 mg, 0.92 mmol, 92%.

DTA (5 °C min^{–1}) onset: 279 °C (dec.); **IR** (ATR, cm^{–1}): $\tilde{\nu}$ = 3360(w), 2964(m), 2671(w), 1694(vs), 1596(w), 1529(w), 1468(w), 1400(m), 1348(m), 1302(w), 1282(w), 1263(vw),

1236(s), 1225(m), 1171(m), 1065(vw), 1041(w), 1001(m), 970(s), 924(m), 787(w), 773(w), 732(m), 732(m), 714(w), 669(w); **Raman** (1064 nm, 300 mW, 25 °C, cm⁻¹): $\tilde{\nu}$ = 3214(3), 1709(4), 1633(100), 1603(73), 1598(72), 1575(5), 1558(4), 1537(3), 1457(6), 1437(6), 1297(13), 1281(7), 1247(10), 1234(17), 1142(17), 1110(11), 1089(10), 1005(6), 808(25), 770(6), 740(2), 714(5), 607(5), 607(5), 418(5), 404(5), 384(4), 342(6), 290(5), 275(7), 264(4), 198(4), 134(30), 121(33), 102(12), 94(11), 67(12); **¹H NMR** ([D₆]DMSO): δ = 7.65 (br s, 6 H), 6.00 ppm (br s, 4 H); **¹³C NMR** ([D₆]DMSO): δ = 153.6 (s, C–NH₂ Cation), 138.5 (C–C_{Cation}), 135.2 (s, C–C_{Anion}); **MS** m/z (FAB⁻): 169.0 (C₂HN₈O₂⁻), m/z (FAB⁺): 197.0 (C₄H₉N₁₀⁺); **EA** (C₆H₁₀N₁₈O₂, 366.26): C 19.68, H 2.75%, N 68.84; found: C 20.12, H 2.76, N 68.41%; **Sensitivities**: IS: 40 J, FS: 360 N, ESD: 1.5 J (at grain sizes <100 μm).

4,4',5,5'-Tetraamino-3,3'-bi-1,2,4-triazolium 1,1'-dinitramino-5,5'-bitetrazolate (8)

4,4',5,5'-Tetraamino-3,3'-bi-1,2,4-triazole (**1**) (196 mg, 1.00 mmol, 1.00 eq.) and dihydroxylammonium 1,1'-dinitramino-5,5'-bitetrazolate (324 mg, 1.00 mmol, 1.00 eq.) were dissolved in water under heating and the solution was left to stand overnight yielding colorless crystals of compound **8**. Yield: 276 mg, 0.61 mmol, 61%.

DTA (5 °C min⁻¹) onset: 223 °C (dec.); **IR** (ATR, cm⁻¹): $\tilde{\nu}$ = 3417(m), 3331(s), 3215(s), 3137(m), 2932(m), 2733(m), 2350(w), 2290(m), 1698(vs), 1616(s), 1530(m), 1485(w), 1416(s), 1361(s), 1285(vs), 1254(vs), 1162(m), 1119(m), 1035(w), 993(s), 962(m), 874(m), 770(s), 770(s), 710(s), 666(w); **Raman** (1064 nm, 300 mW, 25 °C, cm⁻¹): $\tilde{\nu}$ = 3237(1), 1705(3), 1648(100), 1611(66), 1585(6), 1540(3), 1448(9), 1433(4), 1295(13), 1264(18), 1254(15), 1141(7), 1082(15), 1023(24), 989(4), 894(3), 805(11), 722(5), 711(5), 608(4), 520(7), 456(3), 411(3), 411(3), 375(3), 321(8), 304(7), 279(5), 263(5), 175(4), 154(11), 134(29), 114(47), 94(35), 65(7); **¹H NMR** ([D₆]DMSO): δ = 8.60 (br s, 4 H), 6.13 ppm (br s, 4 H); **¹³C NMR** ([D₆]DMSO): δ = 151.9 (s, C–NH₂ Cation), 140.5 (s, C–C_{Anion}), 137.7 ppm (s, C–C_{Cation}); **MS** m/z (FAB⁻): 255.0 (C₂HN₁₂O₄⁻), m/z (FAB⁺): 197.0 (C₄H₉N₁₀⁺); **EA** (C₆H₁₀N₂₂O₄, 454.30) calcd.: C 15.86, H 2.22, N 67.83%; found: C 16.06, H 2.24, N 67.83%; **Sensitivities**: IS: 3 J, FS: 10 N, ESD: 50 mJ (at grain sizes 100 – 500 μm).

4,4',5,5'-Tetraamino-3,3'-bi-1,2,4-triazolium nitriminotetrazolate hemihydrate (9)

To a suspension of 4,4',5,5'-tetraamino-3,3'-bi-1,2,4-triazole (**1**) (392 mg, 2.00 mmol, 1.00 eq.) and potassium nitriminotetrazolate (672 mg, 4.00 mmol, 2.00 eq.) in water 1 mL 2 M hydrochloric acid was added. The suspension was heated until all solid materials were dissolved, before the mixture was left to crystallize over night and compound **9** was obtained as brownish crystals. Yield: 243 mg, 0.71 mmol, 71%.

DTA (5 °C min⁻¹) onset: 232 °C; **IR** (ATR, cm⁻¹): $\tilde{\nu}$ = 3491(m), 3447(s), 3356(s), 3320(s), 2926(m), 1703(s), 1644(s), 1607(s), 1552(m), 1520(m), 1486(m), 1445(s), 1391(w), 1321(vs), 1298(s), 1241(s), 1142(m), 1095(m), 1055(m), 1043(m), 1026(s), 975(m), 964(m), 964(m), 930(s), 873(m), 781(w), 772(w), 745(w), 721(w), 709(m), 698(w), 674(w), 656(vw); **Raman** (1064 nm, 300 mW, 25 °C, cm⁻¹): $\tilde{\nu}$ = 3359(2), 1709(2), 1642(24), 1615(30), 1600(100), 1576(8), 1559(15), 1543(8), 1523(17), 1481(4), 1446(3), 1410(6), 1399(8), 1392(8), 1351(8), 1289(10), 1245(3), 1124(6), 1103(5), 1087(9), 1061(10), 1030(6), 1002(6), 1002(6), 886(4), 800(26), 755(4), 719(5), 617(4), 476(4), 426(4), 376(3), 325(3), 262(5), 246(5), 168(8), 119(20), 85(12), 73(21); **¹H NMR** ([D₆]DMSO): δ = 7.82 (br s, 4 H), 6.05 ppm (br s, 6 H); **¹³C NMR** ([D₆]DMSO): δ = 157.7 (s, C=N–NO₂), 153.3 (s, C–NH₂), 138.4 ppm (s, C–C); **MS** m/z (FAB⁻): 129.0 (CHN₆O⁻), m/z (FAB⁺): 197.0 (C₄H₉N₁₀⁺); **EA** (C₁₀H₂₂N₃₂O₅, 670.51) calcd.: C 17.91, H 3.31, N 66.85%; found: C 17.34, H 3.81, N 62.00%; **Sensitivities**: IS: 40 J, FS: 360 N, ESD: 1.5 J (at grain sizes 500 – 1000 μ m).

4,4',5,5'-Tetraamino-3,3'-bi-1,2,4-triazolium 1-methyl-5-nitriminotetrazolate dihydrate (10)

4,4',5,5'-Tetraamino-3,3'-bi-1,2,4-triazole (**1**) (392 mg, 2.00 mmol, 1.00 eq.), ammonium 1-methylnitriminotetrazolate (644 mg, 4.00 mmol, 2.00 eq.) and 1 mL 2 M hydrochloric acid were dissolved in water under heating and the solution was left to crystallize over night to give compound **10** as colorless needles. Yield: 804 mg, 1.66 mmol, 83%.

DTA (5 °C min⁻¹) onset: 104 °C (–H₂O), 209 °C (dec.); **IR** (ATR, cm⁻¹): $\tilde{\nu}$ = 3331(m), 1695(s), 1600(m), 1505(m), 1459(m), 1351(s), 1332(vs), 1296(s), 1241(m), 1110(m), 1049(w), 1028(m), 986(s), 959(m), 911(m), 877(m), 775(m), 750(w), 735(w), 691(m), 671(m); **Raman** (1064 nm, 300 mW, 25 °C, cm⁻¹): $\tilde{\nu}$ = 2965(3), 1695(3), 1649(100), 1496(34), 1457(16), 1408(4), 1342(7), 1303(15), 1142(6), 1109(8), 1050(5), 1030(41), 987(4), 879(5), 802(18), 751(4), 745(3), 714(8), 701(7), 491(7), 452(3), 368(4), 331(9), 331(9), 296(12), 262(5), 242(4), 204(7), 178(9), 113(27), 87(25), 70(14), 63(8); **¹H NMR** ([D₆]DMSO): δ = 6.89 (br s, 4 H), 5.99 (br s, 6 H), 1.30 ppm (s, 3H, –CH₃); **¹³C NMR** ([D₆]DMSO): δ = 155.4 (s, C=N–NO₂), 152.9 (s, C–NH₂), 138.2 ppm (s, C–C), 32.9 ppm (s, –CH₃); **MS** m/z (FAB⁻): 143.0 (C₂H₃N₆O₂⁻), m/z (FAB⁺): 197.0 (C₄H₉N₁₀⁺); **EA** (C₈H₂₀N₂₂O₆, 520.40) calcd.: C 18.46, H 3.87, N 59.22%; found: C 18.72, H 3.81, N 58.82%; **Sensitivities**: IS: 35 J, FS: 360 N, ESD: 0.5 J (at grain sizes 500 – 1000 μ m).

4,4',5,5'-Tetraamino-3,3'-bi-1,2,4-triazolium diperchlorate (11)

To 4,4',5,5'-tetraamino-3,3'-bi-1,2,4-triazole (**1**) (196 mg, 1.00 mmol, 1.00 eq.) in 50 mL water 4 mL 1 M perchloric acid was added and the solution was heated until all solid components were dissolved. The solution was left to crystallize over night to yield compound **11** as colorless needles. Yield: 317 mg, 0.80 mmol, 40%.

DTA (5 °C min⁻¹) onset: 286 °C (dec.); **IR** (ATR, cm⁻¹): $\tilde{\nu}$ = 3625(vw), 3557(vw), 3417(m), 3349(m), 3307(m), 3213(m), 1703(s), 1615(m), 1564(w), 1528(w), 1486(vw), 1375(vw), 1313(w), 1257(vw), 1099(vs), 1045(vs), 986(s), 956(m), 928(m), 782(w), 693(w), 673(w); **Raman** (1064 nm, 300 mW, 25 °C, cm⁻¹): $\tilde{\nu}$ = 3314(3), 1716(3), 1652(100), 1569(4), 1544(2), 1450(10), 1296(17), 1138(5), 1075(6), 929(37), 806(26), 719(11), 630(8), 604(4), 467(9), 459(8), 381(4), 334(4), 285(2), 260(2), 87(31); **¹H NMR** ([D₆]DMSO): δ = 8.61 (br s, 4 H), 6.08 ppm (br s, 6 H); **¹³C NMR** ([D₆]DMSO): δ = 152.0 (s, C–NH₂), 137.9 ppm (s, C–C); **MS** *m/z* (FAB⁻): 99.1 (ClO₄⁻), *m/z* (FAB⁺): 197.0 (C₄H₉N₁₀⁺); **EA** (C₄H₁₀Cl₂N₁₀O₈, 397.09) calcd.: C 12.10, H 2.54, N 35.27, Cl 17.86%; found: C 12.32, H 2.55, N 35.24 C 18.22%; **Sensitivities**: IS: 5 J, FS: 240 N, ESD: 0.6 J (at grain sizes 100 – 500 μm).

4,4',5,5'-Tetraamino-3,3'-bi-1,2,4-triazolium dipicrate (12)

4,4',5,5'-Tetraamino-3,3'-bi-1,2,4-triazole (**1**) (196.2 mg, 1.00 mmol, 1.00 eq.) and picric acid (448.2 mg, 2.00 mmol, 2.00 eq.) were dissolved in water under heating so that a clear solution was observed. The solution was cooled down to room temperature and left standing over night to yield compound **12** in form of a yellowish solid. Yield: 484 mg, 0.74 mmol, 74%.

DTA (5 °C min⁻¹) onset: 284 °C (dec.); **IR** (ATR, cm⁻¹): $\tilde{\nu}$ = 3329(m), 3194(m), 3076(m), 1695(s), 1630(s), 1616(s), 1565(s), 1520(s), 1474(s), 1422(s), 1363(s), 1326(vs), 1265(vs), 1160(s), 1086(s), 1060(m), 978(m), 928(m), 916(s), 837(m), 790(s), 776(m), 744(m), 744(m), 714(s), 681(m); **Raman** (1064 nm, 300 mW, 25 °C, cm⁻¹): $\tilde{\nu}$ = 3074(2), 1640(32), 1545(28), 1497(12), 1435(5), 1368(33), 1340(48), 1315(100), 1273(30), 1165(17), 1118(5), 1089(10), 1064(7), 945(14), 929(14), 827(31), 800(8), 766(3), 748(3), 720(9), 605(6), 548(3), 363(7), 363(7), 339(11), 273(3), 205(7), 156(14), 101(20); **¹H NMR** ([D₆]DMSO): δ = 8.59 (s, 6 H), 6.13 ppm (br s, 4 H); **¹³C NMR** ([D₆]DMSO): δ = 160.8 (s, C₁–O), 152.0 (s, C–NH₂), 141.8 (s, C₄–NO₂), 137.8 (s, C–C), 125.2 (s, C_{2,6}–NO₂), 124.3 ppm (s, C_{3,5}–H); **MS** *m/z* (FAB⁻): 228.0 (C₆H₂N₃O₇⁻), *m/z* (FAB⁺): 197.0 (C₄H₉N₁₀⁺); **EA** (C₁₆H₁₄N₁₆O₁₄, 654.38) calcd.: C 29.37, H 2.16, N 34.25%; found: C 29.36, H 2.24, N 34.03%; **Sensitivities**: IS: 30 J, FS: 360 N, ESD: 0.75 J (at grain sizes <100 μm).

4,4',5,5'-Tetraamino-3,3'-bi-1,2,4-triazolium dinitroformate (13)

4,4',5,5'-Tetraamino-3,3'-bi-1,2,4-triazole (**1**) (196.2 mg, 1.00 mmol, 1.00 eq.) and trinitromethane (302 mg, 2.00 mmol, 2.00 eq.) were dissolved in 50 mL of water under heating until a clear solution was observed. The solution was stirred for further 30 min and then left for crystallization to give yellow crystals. Yield: 350 mg, 0.70 mmol, 70%.

DTA (5 °C min⁻¹) onset: 94 °C (dec.); **IR** (ATR, cm⁻¹): $\tilde{\nu}$ = 3435(m), 3315(s), 3249(s), 1690(vs), 1606(m), 1517(s), 1481(s), 1402(s), 1384(m), 1317(m), 1231(vs), 1152(s), 1132(vs), 1078(s), 976(s), 864(s), 780(s), 729(s), 689 (m); **Raman** (1064 nm, 300 mW, 25 °C, cm⁻¹): $\tilde{\nu}$ = 3328(2), 3277(3), 1650(100), 1608(8), 1559(5), 1517(4), 1467(8), 1449(7), 1386(22), 1353(12), 1294(33), 1277(32), 1255(32), 1163(14), 1146(15), 1059(4), 868(60), 804(17), 785(14), 721(7), 604(4), 472(11), 426(9), 426(9), 381(7), 325(11), 272(10), 172(16), 146(24), 109(33), 81(46); **¹H NMR** ([D₆]DMSO): δ = 8.61 (s, 6 H), 6.13 ppm (br s, 4 H); **¹³C NMR** ([D₆]DMSO): δ = 152.0 (s, C–NH₂), 150.3 (s, C(NO₂)₃), 137.8 ppm(s, C–C); **MS** m/z (FAB⁻): 150.0 (CN₃O₆⁻), m/z (FAB⁺): 197.0 (C₄H₉N₁₀⁺); **EA** (C₆H₁₀N₁₀O₁₂, 498.24) calcd.: C 14.46, H 2.02, N 44.98%; found: C 14.54, H 2.03, N 44.95%; **Sensitivities**: IS: 4 J, FS: 160 N, ESD: 0.8 J (at grain sizes <100 μm).

8.6.2 X-ray Diffraction

8.6.2.1 Crystallographic data and refinement parameters

Table S1. Crystallographic data and refinement parameters of compound **2** at different temperatures.

	2 (173K_1)	2 (173K_2)	2 (100K)	2 (298K)
Formula	C ₄ H ₁₀ N ₁₆ O ₈	C ₄ H ₁₀ N ₁₆ O ₈	C ₄ H ₁₀ N ₁₆ O ₈	C ₄ H ₁₀ N ₁₆ O ₈
FW [g mol ⁻¹]	410.28	410.28	410.28	410.28
Crystal system	triclinic	triclinic	triclinic	triclinic
Space Group	<i>P</i> −1	<i>P</i> −1	<i>P</i> −1	<i>P</i> −1
Color / Habit	colorless, plate	colorless, plate	colorless, plate	colorless, plate
Size [mm]	0.03 × 0.10 × 0.20	0.10 x 0.10 x 0.10	0.10 x 0.10 x 0.10	0.10 x 0.10 x 0.10
<i>a</i> [Å]	6.5168(5)	6.5155(8)	6.5046(9)	6.5597(12)
<i>b</i> [Å]	7.7826(5)	7.7748(11)	7.7010(13)	7.984(2)
<i>c</i> [Å]	8.5072(6)	8.5036(11)	8.4831(13)	8.5813(19)
α [°]	97.717(6)	97.677(11)	97.897(13)	97.31(2)
β [°]	107.340(6)	107.306(11)	107.262(13)	107.895(19)
γ [°]	112.140(7)	112.194(12)	111.478(14)	113.84(2)
<i>V</i> [Å ³]	366.35(6)	365.76(10)	362.85(12)	374.52(18)
<i>Z</i>	1	1	1	1
$\rho_{\text{calc.}}$ [g cm ⁻³]	1.860	1.863	1.878	1.819
μ [mm ⁻¹]	0.171	0.171	0.171	0.171
<i>F</i> (000)	210	210	210	210
$\lambda_{\text{MoK}\alpha}$ [Å]	0.71073	0.71073	0.71073	0.71073
<i>T</i> [K]	173	173	100	298
ϑ min-max [°]	4.4, 26.5	4.4, 26.5	4.5, 26.5	4.4, 26.5
Dataset <i>h</i> ; <i>k</i> ; <i>l</i>	−8:8; −9:9; −10:10	−4:8; −9:9; −10:9	−4:8; −9:9; −10:9	−4:8; −9:9; −10:9
Reflect. coll.	5373	1997	1969	2030
Independ. refl.	1510	1498	1482	1537
<i>R</i> _{int}	0.026	0.016	0.017	0.017
Reflection obs.	1320	1183	1225	1046
No. parameters	147	147	147	147
<i>R</i> ₁ (obs)	0.0336	0.0402	0.0384	0.0630
<i>wR</i> ₂ (all data)	0.0855	0.1012	0.1013	0.1720
<i>S</i>	1.06	1.06	1.06	1.02
Resd. Dens.[e Å ⁻³]	−0.34, 0.38	−0.25, 0.29	−0.27, 0.26	−0.42, 0.50
Device type	Oxford XCalibur3 CCD	Oxford XCalibur3 CCD	Oxford XCalibur3 CCD	Oxford XCalibur3 CCD
Solution	SIR-2004	SIR-2004	SIR-2004	SIR-2004
Refinement	SHELXL-97	SHELXL-97	SHELXL-97	SHELXL-97
Absorpt. corr.	multi-scan	multi-scan	multi-scan	multi-scan
CCDC	1029064	1035376	1035375	1035377

Table S2. Crystallographic data and refinement parameters of compounds **3–6**.

	3	4	5	6
Formula	C ₆ H ₁₀ N ₂₀ O ₆	C ₆ H ₁₄ N ₂₀ O ₆	C ₄ H ₁₀ N ₁₂ O ₆	C ₁₀ H ₁₀ N ₁₈ O ₈
FW [g mol ⁻¹]	458.34	462.37	322.24	510.36
Crystal system	triclinic	monoclinic	triclinic	monoclinic
Space Group	<i>P</i> –1	<i>P</i> 2 ₁ / <i>c</i>	<i>P</i> –1	<i>P</i> 2 ₁ / <i>c</i>
Color / Habit	colorless, plate	colorless, block	colorless, plate	yellow, plate
Size [mm]	0.05 × 0.14 × 0.28	0.19 × 0.29 × 0.32	0.04 × 0.20 × 0.30	0.02 × 0.06 × 0.10
<i>a</i> [Å]	6.6569(6)	6.2655(3)	6.6825(4)	5.2141(4)
<i>b</i> [Å]	8.3735(8)	8.2526(4)	6.9310(4)	9.8545(6)
<i>c</i> [Å]	8.5943(8)	17.2616(8)	7.0089(5)	17.7329(11)
α [°]	88.177(8)	90	73.212(6)	90
β [°]	68.659(9)	92.655(5)	89.114(6)	98.076(2)
γ [°]	69.429(8)	90	75.819(5)	90
<i>V</i> [Å ³]	415.22(8)	891.58(7)	300.79(4)	902.12(10)
<i>Z</i>	1	2	1	2
ρ_{calc} [g cm ⁻³]	1.833	1.722	1.779	1.879
μ [mm ⁻¹]	0.159	0.149	0.160	0.163
<i>F</i> (000)	234	476	166	520
$\lambda_{\text{MoK}\alpha}$ [Å]	0.71073	0.71073	0.71073	0.71073
<i>T</i> [K]	173	173	173	173
ϑ min-max [°]	4.9, 26.5	4.1, 26.5	4.3, 26.5	2.3, 26.4
Dataset <i>h</i> ; <i>k</i> ; <i>l</i>	–8:8; –10:9; –10:10	–7:7; –10:7; –21:21	–8:8; –8:8; –8:8	–6:6; –12:12; –22:22
Reflect. coll.	3195	6534	4404	23035
Independ. refl.	1718	1834	1242	1845
<i>R</i> _{int}	0.024	0.026	0.024	0.079
Reflection obs.	1381	1594	1086	1391
No. parameters	165	173	120	183
<i>R</i> ₁ (obs)	0.0359	0.0346	0.0313	0.0370
<i>wR</i> ₂ (all data)	0.0913	0.0915	0.0898	0.1108
<i>S</i>	1.07	1.10	1.09	1.11
Resd. Dens.[e Å ⁻³]	–0.23, 0.19	–0.37, 0.29	–0.22, 0.26	–0.28, 0.28
Device type	Oxford XCalibur3 CCD	Oxford XCalibur3 CCD	Oxford XCalibur3 CCD	Oxford XCalibur3 CCD
Solution	SIR-2004	SIR-2004	SIR-2004	SIR-2004
Refinement	SHELXL-97	SHELXL-97	SHELXL-97	SHELXL-97
Absorpt. corr.	multi-scan	multi-scan	multi-scan	multi-scan
CCDC	1029053	1029066	1029061	1029060

Table S3. Crystallographic data and refinement parameters of compounds **7–9**.

	7	7 · 2 H₂O	8	9
Formula	C ₆ H ₁₀ N ₁₈ O ₂	C ₆ H ₁₄ N ₁₈ O ₄	C ₆ H ₁₀ N ₂₂ O ₄	C ₁₀ H ₂₂ N ₃₂ O ₅
FW [g mol ⁻¹]	366.32	402.35	454.36	679.60
Crystal system	triclinic	monoclinic	triclinic	monoclinic
Space Group	<i>P</i> –1	<i>P</i> 2 ₁ / <i>c</i>	<i>P</i> –1	<i>C</i> 2/ <i>c</i>
Color / Habit	colorless, block	colorless, needle	colorless, plate	colorless, plate
Size [mm]	0.03 × 0.10 × 0.10	0.03 × 0.03 × 0.13	0.02 × 0.16 × 0.40	0.05 × 0.20 × 0.35
<i>a</i> [Å]	6.3741(7)	8.9220(7)	6.3892(6)	28.2349(8)
<i>b</i> [Å]	7.8143(8)	14.3723(8)	8.2420(7)	12.8429(3)
<i>c</i> [Å]	8.4826(8)	6.7226(6)	8.4392(7)	7.2379(3)
α [°]	66.716(9)	90	81.266(7)	90
β [°]	69.319(9)	110.555(10)	75.251(7)	94.715(3)
γ [°]	76.365(9)	90	85.638(7)	90
<i>V</i> [Å ³]	360.81(7)	806.99(11)	424.46(7)	2615.71(15)
<i>Z</i>	1	2	1	4
$\rho_{\text{calc.}}$ [g cm ⁻³]	1.686	1.656	1.778	1.703
μ [mm ⁻¹]	0.137	0.139	0.150	0.140
<i>F</i> (000)	188	416	232	1384
$\lambda_{\text{MoK}\alpha}$ [Å]	0.71073	0.71073	0.71073	0.71073
<i>T</i> [K]	173	173	173	173
ϑ min-max [°]	4.2, 26.5	4.3, 26.5	4.1, 26.5	4.3, 26.5
Dataset <i>h</i> ; <i>k</i> ; <i>l</i>	–7:7; –9:9; –10:10	–11:11; –16:18; –4:8	–8:8; –10:10; –10:10	–35:35; –16:16; –9:9
Reflect. coll.	2719	3575	6245	19744
Independ. refl.	1478	1671	1750	2706
<i>R</i> _{int}	0.030	0.023	0.036	0.032
Reflection obs.	1099	1372	1390	2355
No. parameters	138	155	165	257
<i>R</i> ₁ (obs)	0.0403	0.0356	0.0356	0.0318
<i>wR</i> ₂ (all data)	0.095	0.0801	0.0862	0.0874
<i>S</i>	1.02	1.04	1.02	1.03
Resd. Dens.[e Å ⁻³]	–0.20, 0.23	–0.21, 0.22	–0.27, 0.18	–0.19, 0.24
Device type	Oxford XCalibur3	Oxford XCalibur3	Oxford XCalibur3	Oxford XCalibur3
	CCD	CCD	CCD	CCD
Solution	SIR-2004	SIR-2004	SIR-2004	SIR-2004
Refinement	SHELXL-97	SHELXL-97	SHELXL-97	SHELXL-97
Absorpt. corr.	multi-scan	multi-scan	multi-scan	multi-scan
CCDC	1029062	1029063	1029058	1029056

Table S4. Crystallographic data and refinement parameters of compounds **9a–10** and **13**.

	9a	9b	10	13
Formula	C ₁₆ H ₃₆ N ₅₄ O ₁₀	C ₁₀ H ₂₈ N ₃₂ O ₈	C ₈ H ₂₀ N ₂₂ O ₆	C ₆ H ₁₀ N ₁₆ O ₁₂
FW [g mol ⁻¹]	1144.99	724.64	520.46	498.24
Crystal system	monoclinic	triclinic	triclinic	monoclinic
Space Group	<i>P</i> 2 ₁ / <i>c</i>	<i>P</i> -1	<i>P</i> -1	<i>P</i> 2 ₁ / <i>c</i>
Color / Habit	colorless, stab	colorless block	colorless, block	colorless, plate
Size [mm]	0.11 × 0.12 × 0.31	0.38 × 0.40 × 0.40	0.35 × 0.21 × 0.14	0.32 × 0.27 × 0.03
<i>a</i> [Å]	10.9541(3)	9.2750(7)	6.4916(3)	16.8271(4)
<i>b</i> [Å]	19.7090(4)	9.5238(8)	7.9296(4)	12.0361(3)
<i>c</i> [Å]	20.4037(7)	9.8392(8)	10.1535(5)	8.7485(3)
α [°]	90	109.650(7)	87.069(4)	90
β [°]	104.295(3)	96.080(6)	77.437(4)	93.252(2)
γ [°]	90	116.486(8)	84.279(4)	90
<i>V</i> [Å ³]	4268.7(2)	698.14(13)	507.37(4)	1769.00(9)
<i>Z</i>	4	1	1	4
ρ _{calc.} [g cm ⁻³]	1.782	1.724	1.703	1.871
μ [mm ⁻¹]	0.149	0.146	0.144	0.176
<i>F</i> (000)	2360	376	270	1016
λ _{MoKα} [Å]	0.71073	0.71073	0.71073	0.71073
<i>T</i> [K]	173	173	173	173
θ min-max [°]	4.1, 26.5	4.2, 26.5	4.1, 26.5	4.2, 26.5
Dataset <i>h</i> ; <i>k</i> ; <i>l</i>	-13:13; -22:24; -25:22	-11:11; -11:11; -11:12	-8:8; -9:9; -12:12	-21:21; -15:15; -10:10
Reflect. coll.	22613	5502	7429	26371
Independ. refl.	8801	2872	2089	3649
<i>R</i> _{int}	0.025	0.019	0.019	0.030
Reflection obs.	6673	2371	1909	3154
No. parameters	865	282	203	347
<i>R</i> ₁ (obs)	0.0376	0.0328	0.0302	0.0299
w <i>R</i> ₂ (all data)	0.0990	0.0874	0.0764	0.0778
<i>S</i>	1.03	1.02	1.08	1.05
Resd. Dens. [e Å ⁻³]	-0.26, 0.33	-0.24, 0.30	-0.26, 0.26	-0.26, 0.21
Device type	Oxford XCalibur3	Oxford XCalibur3	Oxford XCalibur3	Oxford XCalibur3
	CCD	CCD	CCD	CCD
Solution	SIR-2004	SIR-2004	SIR-2004	SIR-2004
Refinement	SHELXL-97	SHELXL-97	SHELXL-97	SHELXL-97
Absorpt. corr.	multi-scan	multi-scan	multi-scan	multi-scan
CCDC	1029055	1029057	1029054	1029059

8.6.2.3 Crystal structures of compounds **4**, **7** · 2 H₂O, **9–10** and **13**

4,4',5,5'-Tetraamino-3,3'-bi-1,2,4-triazolium nitrotetrazolate dihydrate (**4**)

The energetic salt 4,4',5,5'-tetraamino-3,3'-bi-1,2,4-triazolium nitro-tetrazolate crystallizes from water in the monoclinic space group $P2_1/c$ with two water moieties and two molecules per unit cell. The torsion angle of N1–C1–C1ⁱ–N3ⁱ is equal to 0.6(2)° yielding a planar structure. The molecular unit of compound **4** is illustrated in Figure S1.

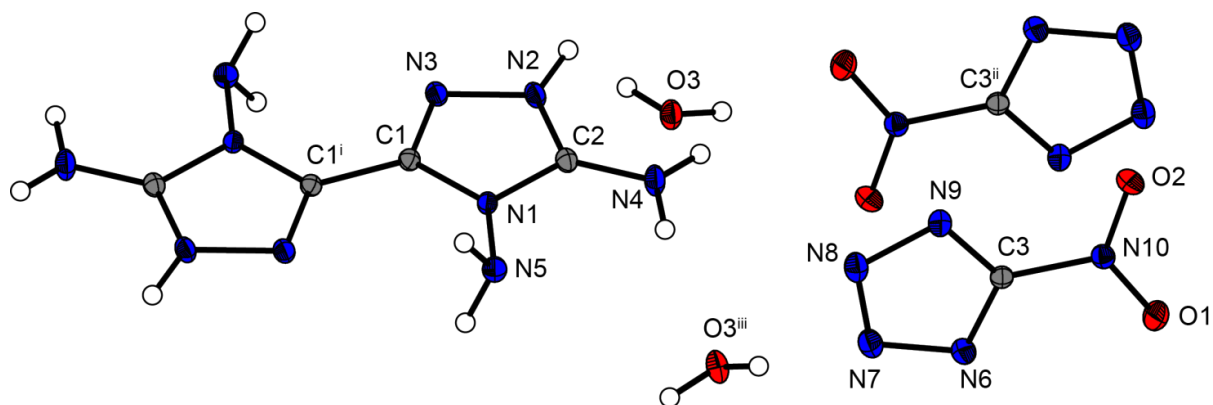


Figure S1. Molecular unit of **4**. Ellipsoids are drawn at the 50% probability level. Selected bond lengths [Å]: C1–C1ⁱ 1.446(9), C2–N4 1.315(8), C3–N10 1.444(9).

4,4',5,5'-Tetraamino-3,3'-bi-1,2,4-triazolium bistetrazolate-1-oxide dihydrate (**7** · 2 H₂O)

The energetic salt **7** crystallizes from water as water free structure and as a dihydrate (**7** · 2 H₂O) in the monoclinic space group $P2_1/c$ with two water moieties and two molecules per unit cell. The molecular unit of compound **7** · 2 H₂O is illustrated in Figure S2.

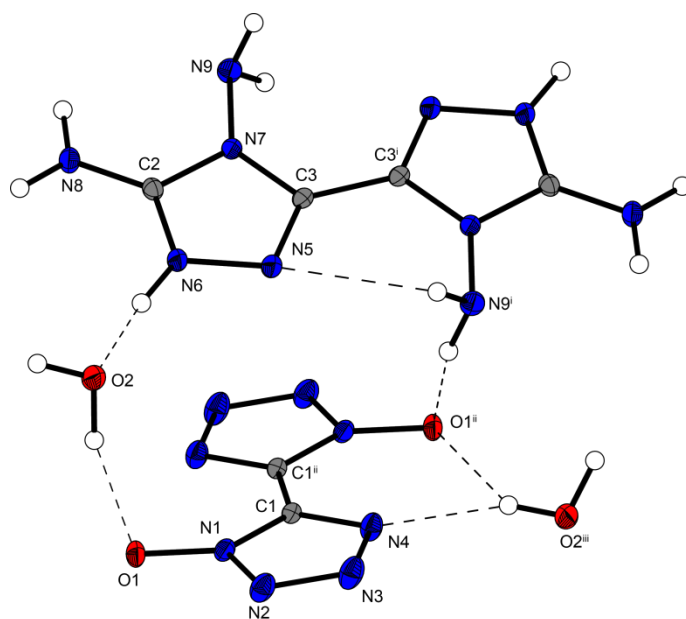


Figure S2. Molecular unit of **7** · 2 H₂O. Ellipsoids are drawn at the 50% probability level.

4,4',5,5'-Tetraamino-3,3'-bi-1,2,4-triazolium 5-nitrimino-1*H*-tetrazolate hemihydrate (**9**)

4,4',5,5'-Tetraamino-3,3'-bi-1,2,4-triazolium 5-nitrimino-1*H*-tetrazolate hemihydrate (**9**) crystallizes in a stoichiometric composition of 1:1 in the monoclinic space group *C2/c* with 0.5 moieties of water per unit cell. The density of compound **9** at 173 K amounts to 1.703 g cm⁻³ and thus exhibits the exact same density as the 1-methyl derivative **10**. Energetic nitriminotetrazolates, as the hydroxylammonium salt with a density 1.785 g cm⁻³ or the hydrazinium salt with a lower density of 1.635 g cm⁻³,^[2] show very different densities. Since compound **9** crystallizes with crystal water, the comparison of the densities is just a rough point of reference. The cation forms a planar system with a torsion angle of N9–C2–C4–N12 equal to 0.5(2)°. The bond length of C1 to the N5 of the nitrimino-group is similar to the lengths of similar salts reported in literature.^[2] The molecular unit of compound **9** is illustrated in Figure S3.

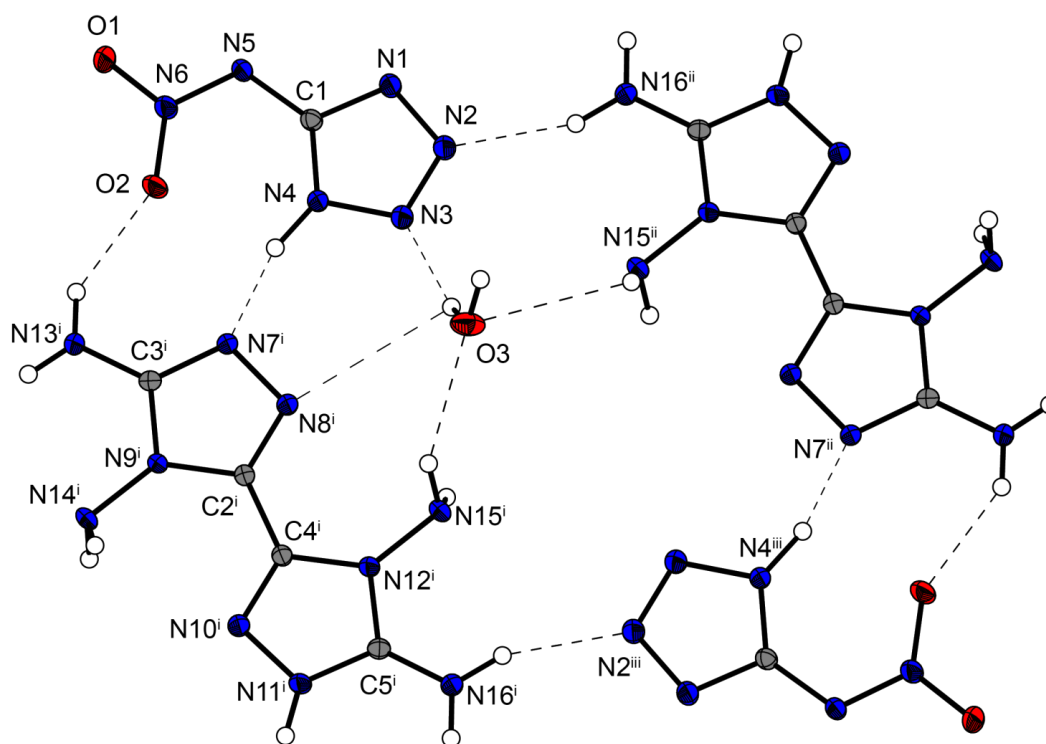


Figure S3. Molecular structure of **9**. Ellipsoids are drawn at the 50% probability level. Selected bond lengths [Å]: C2–C4ⁱ 1.445(8), C5ⁱ–N16ⁱ 1.313(6) C1–N5 1.370(1); selected torsion angle [°]: N9–C2–C4–N12 0.5(2).

Further crystal structures of the 5-nitriminotetrazolate salt were obtained (**9a** and **9b**) and are displayed in Figures S4 and S5

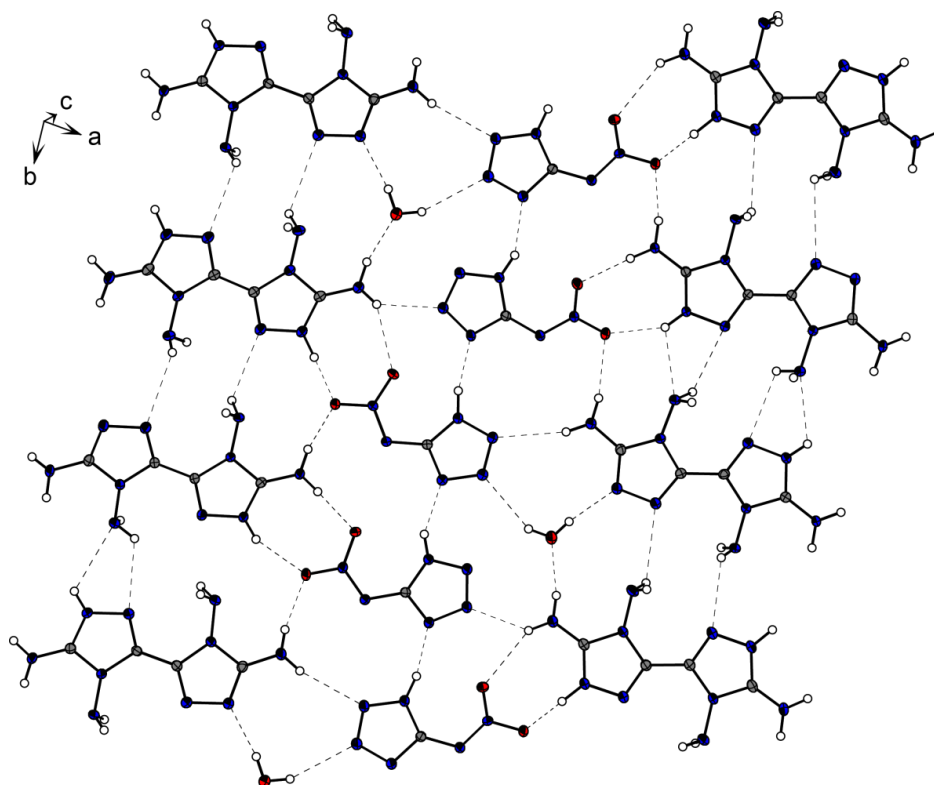


Figure S4. Structure of **9a**. Ellipsoids are drawn at the 50% probability level.

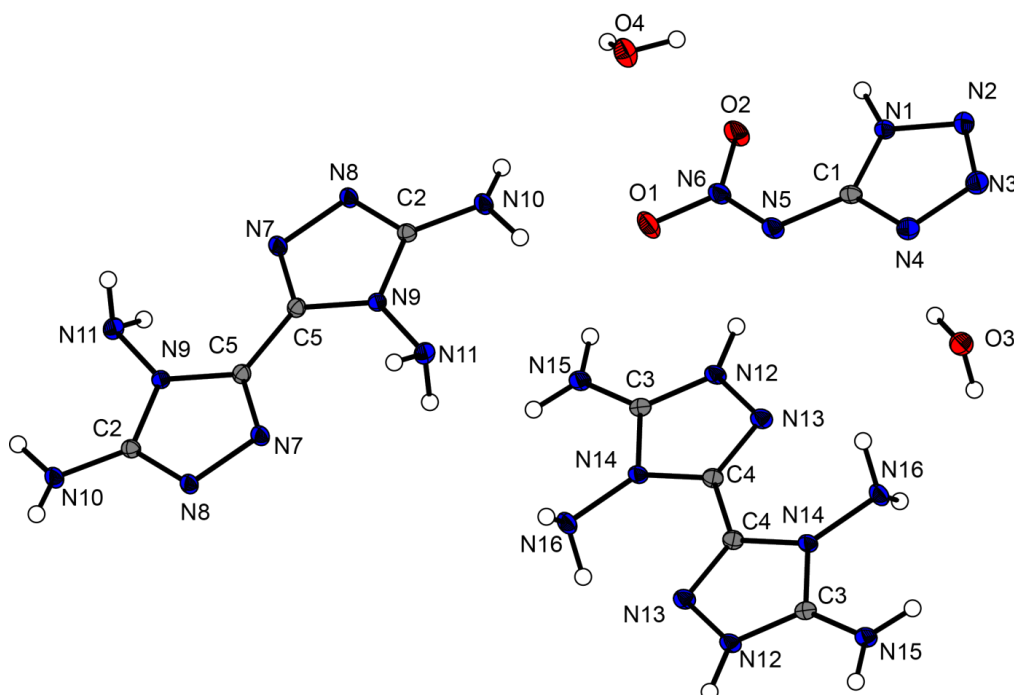


Figure S5. Structure of **9b**. Ellipsoids are drawn at the 50% probability level.

4,4',5,5'-Tetraamino-3,3'-bi-1,2,4-triazolium 1-methyl-5-nitriminotetrazolate dihydrate (10)

The energetic compound 4,4',5,5'-tetraamino-3,3'-bi-1,2,4-triazolium 1-methylnitriminotetrazolate crystallizes from water in the triclinic space group $P\bar{1}$ with two water moieties and a density of 1.703 g cm^{-3} at 173 K. The bond length C3–N10 corresponds more to the length of a C=N double bond and is similar to the length of reported 1-methylnitriminotetrazoles.^[3] The molecular unit of compound **10** is illustrated in Figure S6.

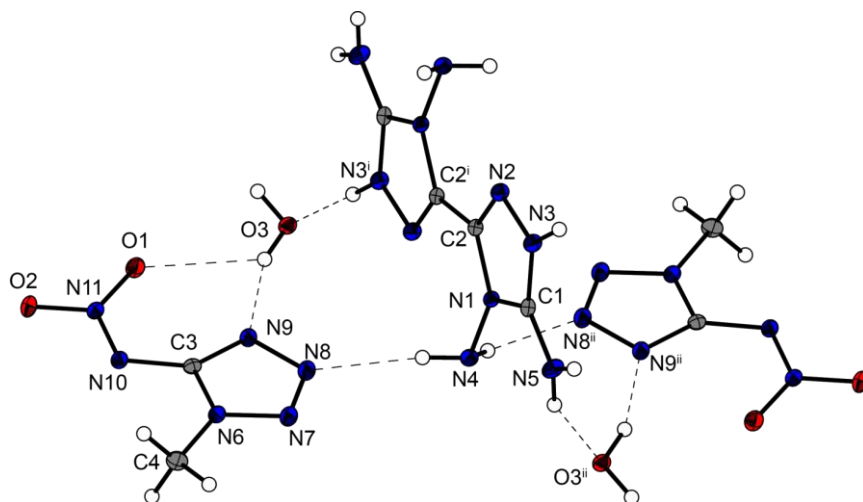


Figure S6. Molecular unit of **10**. Ellipsoids are drawn at the 50% probability level. Selected bond lengths [Å]: C2–C2ⁱ 1.451(2), C1–N5 1.321(1), C3–N10 1.376(0); selected hydrogen-bridge-bond-lengths [Å]: O3–H3B–O1 1.97, O3–H3B–O2 2.63(2), O3–H3A–O1 2.45(2).

4,4',5,5'-Tetraamino-3,3'-bi-1,2,4-triazolium dinitroformate (13)

4,4',5,5'-Tetraamino-3,3'-bi-1,2,4-triazolium dinitroformate (**13**) crystallizes in the monoclinic space group $P2_1/c$ with a density of 1.871 g cm^{-3} at 173 K. The molecular unit of compound **13** is illustrated in Figure S7.

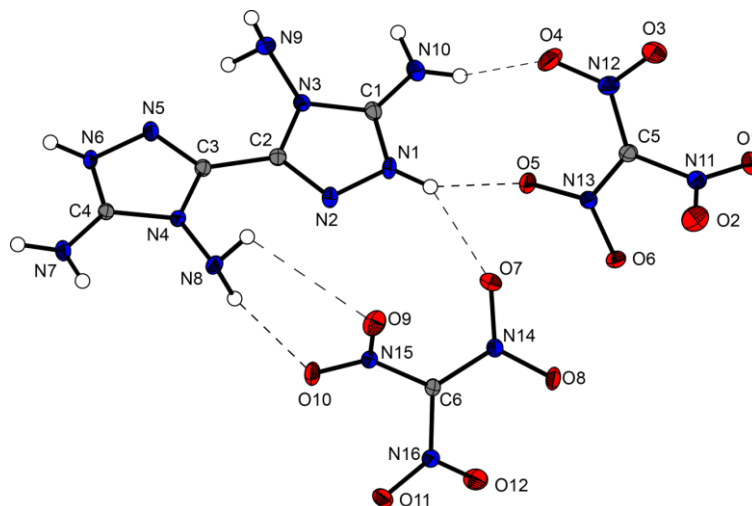


Figure S7. Molecular structure of **13**. Ellipsoids are drawn at the 50% probability level.

8.6.3 Electron Microscopy

First morphological investigations of compound **2** were carried out on a JSM-6500F scanning electron microscope (SEM) (JEOL Ltd., Tokyo, Japan) with a field emission source operated at 4.0 to 12.0 kV. All images shown are secondary electron images in the Figures S8a–S8d. The average chemical composition was studied with an energy-dispersive X-ray spectrometry (EDS) detector model 7418 (Oxford instruments, Oxfordshire, UK). Powders were placed on a brass sample carrier fixed with self-adhesive carbon plates (Plano, Wetzlar, Germany). The samples were sputtered with carbon (sputter device: BAL-TEC MED 020, BAL-TEC AG, Balzers, Netherlands) before loading them into the SEM chamber, since the reaction products were not electrically conducting.

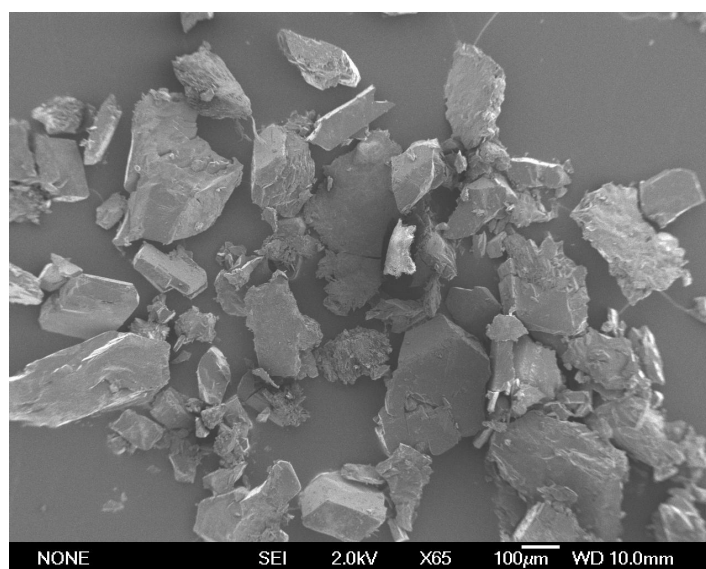


Figure S8a. Morphology of compound **2**.

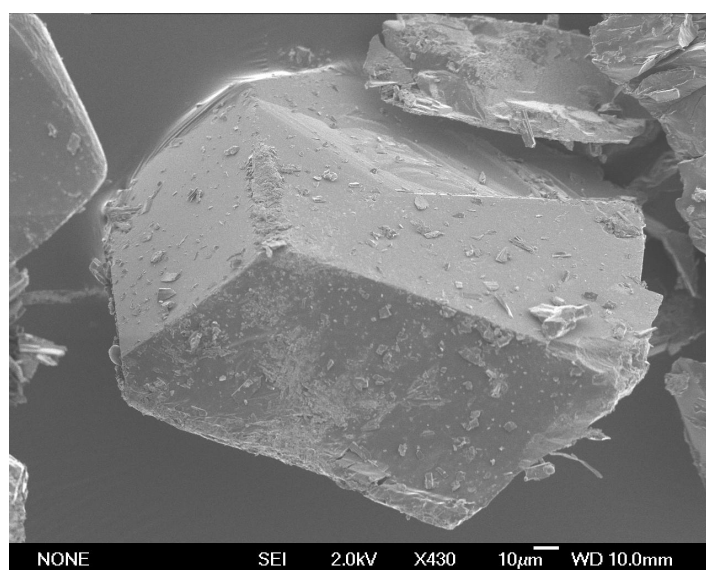


Figure S8b. Morphology of compound **2**.

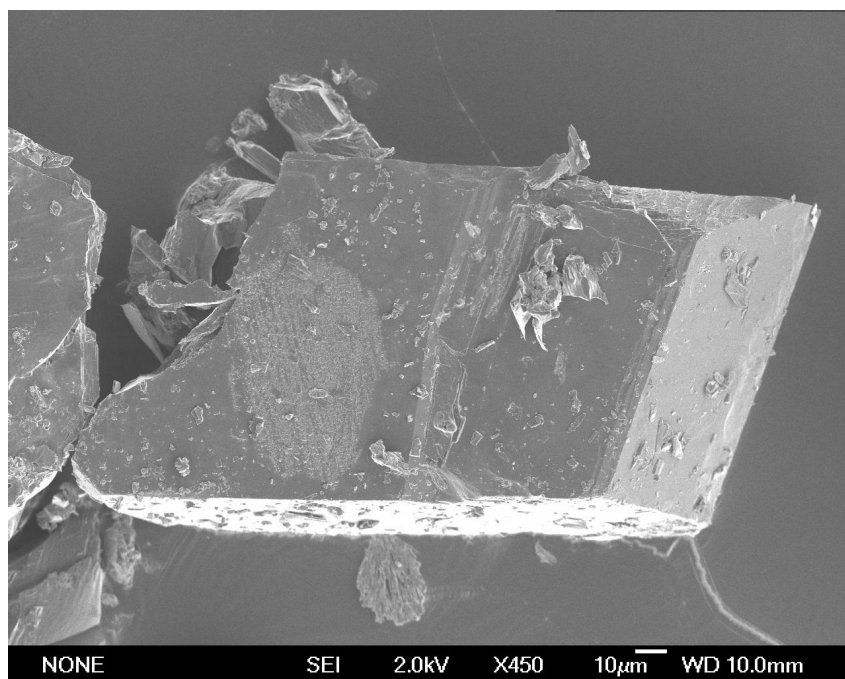


Figure S8c. Morphology of compound 2.

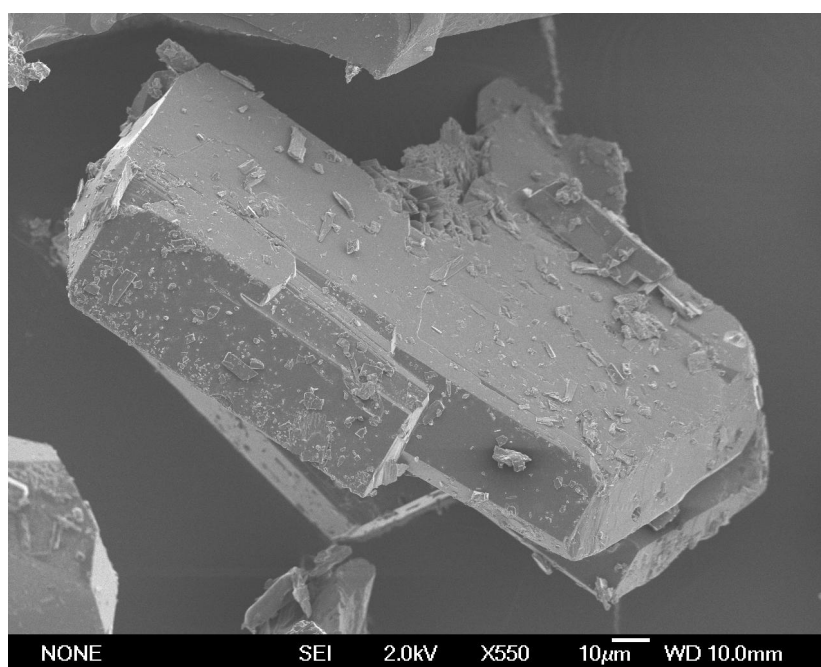


Figure S8d. Morphology of compound 2.

8.6.4 Explosive performance

8.6.4.1 Heat of formation calculations

General information about the heat of formation calculations can be found in the appendix of this thesis. The calculation results are summarized in Table S5.

Table S5. Calculation results

M	$-H^{298}$ ^[a] / a.u.	$\Delta_f H^\circ(\text{g}, \text{M})$ / kJ mol^{-1} ^[b]	V_M / nm^3 ^[c]	$\Delta U_L, \Delta H_L$ (4); ^[d] ΔH_{sub} ^[e] (3) / kJ mol^{-1}	$\Delta_f H^\circ(\text{s})$ ^[f] / kJ mol^{-1}	Δn ^[g]	$\Delta_f U(\text{s})$ ^[f] / kJ kg^{-1}
BDAT	703.707615	587.6		115.6	472.0	9.0	2520.3
BDAT ²⁺	704.327388	2032.9					
DN [−]	464.499549	−124.0					
BDAT ²⁺ DN [−]		1787.5	0.373	1478.5, 1485.9	301.5	17	837.7
NT2O [−]	536.798772	83.0					
BDAT NT2O		2201.6	0.423	1433.0, 1440.4	761.2	18	1758.3
NO₃ [−]	280.080446	−313.6					
BDAT ²⁺ (NO₃ [−]) ₂		1408.3	0.306	1554.0, 1561.5	−153.2	14	−367.7
TNBI ^{2−}	1266.677508	−33.9					
BDAT ²⁺ TNBI ^{2−}		1760.0	0.460	1658.7, 1672.6	87.3	18	258.6
BT1O ^{2−}	663.703743	587.7					
BDAT ²⁺ BT1O ^{2−}		2381.6	0.368	1769.8, 1783.7	597.9	15	1733.7
DNABT ^{2−}	1032.612357						
BDAT		2768.8	0.432	1656.2, 1661.1	1107.7	18.0	2536.6
DNABT ^{2−}							
ClO₄ [−]	760.171182	−278.2					
BDAT ²⁺ (ClO₄ [−]) ₂		1476.5	0.359	1492.2, 1499.6	−23.1	15.0	35.4
C(NO₂)₃ [−]	652.767406	−220.9					
BDAT C(NO₂)₃ [−]		1591.1	0.451	141.2, 1417.7	173.4	19.0	442.7

^[a] CBS-4M electronic enthalpy; ^[b] gas phase enthalpy of formation; ^[c] molecular volumes taken from X-ray structures and corrected to room temperature; ^[d] lattice energy and enthalpy (calculated using Jenkins and Glasser equations); ^[e] enthalpy of sublimation (calculated by Trouton rule); ^[f] standard solid state enthalpy of formation; ^[g] solid state energy of formation.

8.6.4.2 Energetic Performance

In comparison to other reported nitrotetrazolate-2*N*-oxides, the heat of formation of salt **3** (761 kJ mol^{-1}) is exceptionally high, since the highest heat of formation is exhibited by the triaminoguanidinium nitrotetrazolate-2*N*-oxide (471.5 kJ mol^{-1}), the ammonium salt reaches as low as 152.0 kJ mol^{-1} .^[4] The value for the high energetic hydroxylammonium salt lies between these two heats of formation ($\Delta_f H_m^\circ = 218.7 \text{ kJ mol}^{-1}$). The nitrate **5** shows a negative heat of formation of $-153.2 \text{ kJ mol}^{-1}$. The nitrogen-rich ammonium and hydroxylammonium nitrates show smaller values with $-365.5 \text{ kJ mol}^{-1}$ ^[5] and $-364.3 \text{ kJ mol}^{-1}$ ^[6] in comparison to compound **5**. Compound **6** reveals a heat of formation of 20.9 kJ mol^{-1} . In comparison to the values reported for the aminoguanidinium (171.1 kJ mol^{-1}), diaminoguanidinium (399.3 kJ mol^{-1}) and triaminoguanidinium salts (638.7 kJ mol^{-1}) this value is surprisingly small.^[7] The 5,5'-bitetrazole-1,1'-dioxide **7** shows a

much higher heat of formation of $597.4 \text{ kJ mol}^{-1}$ lying slightly under the heats of formation of the corresponding hydrazinium and aminoguanidinium salts with of $677.7 \text{ kJ mol}^{-1}$ and $668.6 \text{ kJ mol}^{-1}$.^[8] Other reported salts, like the ammonium or the guanidinium salts, as well as RDX show much smaller heats of formation.^[8] The highest heat of formation in this report is exhibited by compound **8** with $1107.7 \text{ kJ mol}^{-1}$. This value not only exceeds the value of K_2DNABT ($326.4 \text{ kJ mol}^{-1}$) but also the heat of formation of RDX by far.^[9] The perchlorate **11** reveals a slightly negative heat of formation of $-23.1 \text{ kJ mol}^{-1}$, whereas the hydroxyammonium perchlorate has a much higher negative heat of formation of $-277.0 \text{ kJ mol}^{-1}$.^[10]

Compound **6** exhibits a detonation velocity of 8237 m s^{-1} and a detonation pressure of 260 kbar thus located within the range of previously reported TNBI salts.^[7] The hydroxylammonium ($p_{\text{CJ}} = 311 \text{ kbar}$, $D = 8362 \text{ m s}^{-1}$), the diaminoguanidinium ($p_{\text{CJ}} = 286 \text{ kbar}$, $D = 8377 \text{ m s}^{-1}$) and the triaminoguanidinium salts ($p_{\text{CJ}} = 281 \text{ kbar}$, $D = 8388 \text{ m s}^{-1}$) show slightly higher detonation parameters, whereas the guanidinium ($p_{\text{CJ}} = 266 \text{ kbar}$, $D = 8070 \text{ m s}^{-1}$) and the aminoguanidinium salts ($p_{\text{CJ}} = 268 \text{ kbar}$, $D = 8138 \text{ m s}^{-1}$) show lower detonation velocities and detonation pressures in the same range as compound **6**.^[7] Compared to compound **7**, other 5,5'-bitetrazole-1,1'-dioxide all show equal if not much larger detonation pressures and velocities than compound **7**.^[7] Only the corresponding guanidinium, aminoguanidinium and triaminoguanidinium salts with detonation pressures of 233 kbar, 243 kbar and 246 kbar as well as with detonation velocities of 7917 m s^{-1} , 8111 m s^{-1} and 8028 m s^{-1} respectively are in the range of the parameters of compound **7**.^[8] In comparison the high performance hydroxylammonium salt has a significantly higher detonation pressure of 331 kbar and a fairly higher detonation velocity of 8764 m s^{-1} .^[8] The detonation pressure of salt **8** (288 kbar) is lower compared to RDX and with 8804 m s^{-1} the detonation velocity is in the range of RDX. Compared to the potassium salt K_2DNABT , the velocity is much higher (8330 m s^{-1}), whereas the detonation pressure of the potassium salt is a little higher (317 kbar).^[9] The perchlorate **11** with a detonation velocity of 8290 m s^{-1} and a detonation pressure of 299 kbar.

8.6.4.3 Small scale shock reactivity test

The Small-Scale Shock Reactivity Test (SSRT)^[11,12] was introduced by researchers at IHDIV, DSWC (Indian Head Division, Naval Surface Warfare Center). The SSRT measures the shock reactivity (explosiveness) of energetic materials, often well-below critical diameter, without requiring a transition to detonation. The test setup combines the benefits from a lead block

test^[13] and a gap test.^[14] In comparison to gap tests, the advantage is the use of a much smaller sample size of the tested explosive (ca. 500 mg). The sample volume V_s is recommended to be 0.284 mL (284 mm³). For our test setup no possible attenuator (between detonator and sample) and air gap (between sample and aluminum block) was used. The used sample weight m_s was calculated using the formula $V_s \times \rho_{\text{Xray}} \times 0.95$. The dent sizes (see Figure S9) were measured by filling them with powdered SiO₂ and measuring the resulting weight.



Figure S9. Aluminum block of the SSRT before (left) and after (right) detonation of dinitramide 2.

8.6.5 Toxicity assessment

The *Luminescent Bacteria Inhibition Test* offers a possibility to determine the environmental acceptability of new energetic materials to aquatic organisms whereat a marine bacteria is used as a representative for marine organisms. In this test the decrease of the luminescence of the liquid-dried bacteria is determined after 15 min and 30 min at different concentrations of the test compounds and is compared to a control measurement of a 2% NaCl stock solution.

The sample dilution sequence corresponds to DIN 38412 L34, which ranges from 1:2 to 1:32 dilution of the compound in the test system. For a better reproducibility, all dilution steps were made in duplicate. The change of intensity of bacterial luminescence in the absence (controls) and in the presence (samples) of the tested substances after different incubation times (15 min, 30 min) were recorded. The controls (2% NaCl only) were measured for calculating the correction factor, which is necessary to consider the normal decrease of luminescence without any toxic effect per time.

The EC₅₀ value gives the concentration of each compound where the bacterial luminescence is inhibited by 50% and is calculated by plotting I against the concentration of the test

substance in a diagram with a logarithmic scale, where Γ = inhibition (in %) / 100 – inhibition (in %) and c = concentration of the test sample. The EC_{50} value is identical with the intersection of the resulting graph with the X-axis ($\Gamma = 0$).

For better comparison of the resulting toxicities, we also determined the toxic effect of RDX and FOX-12 to the bacterial strain under the same conditions applied for the toxicity assessment of nitramide **2**. To imitate the natural environment of the employed marine bacterium as good as possible, the samples need to be diluted with a 2% (w/v) sodium chloride solution. Since RDX is barely soluble in water, a stock solution in acetone was prepared, which was further diluted with the sodium chloride solution to a mixture containing 200 ppm RDX in water/acetone 99/1 (v/v).

8.6.6 Spectroscopy

NMR Spectroscopy

The peak observed in the ^{13}C NMR spectrum of compound **3** at 157.4 ppm belongs to the nitrotetrazolate-2*N*-oxide anion. This chemical shift is very similar to the ones observed in the guanidinium salt (157.6 ppm) or the triaminoguanidinium salt (157.1 ppm) for the carbon of the nitrotetrazolate-2*N*-oxide.^[4] The carbon-peak of the nitrotetrazolate anion in compound **4** appears at 168.8 ppm and is only slightly downshifted in comparison to chemical shifts in other nitrogen-rich nitrotetrazolates with chemical shifts between 169.5 and 169.0 ppm.^[15] The tetranitrobisimidazolate anion in compound **6** exhibits two peaks representing six carbon-atoms in the ^{13}C NMR spectrum at 141.7 (C–C) and 139.4 (C=C) due to the high symmetry of the anion. Depending on the cation, the comparable nitrogenous salts show a very different peak distribution making a comparison between the energetic compounds difficult.^[16] The peak of the carbons of the 5,5'-bitetrazole-1,1'-dioxide anion of compound **7** appear at 135.2 ppm in the ^{13}C NMR spectrum, thus lying in the range of other reported nitrogen-cations, like the bis(guanidinium) salt (134.6 ppm) or the dihydrazinium salt with a chemical shift of 134.9 ppm.^[8] The free acid 1*H*,1*H*-5,5-bitetrazole-1,1-diol dihydrate also shows a very similar chemical shift of 135.8 ppm.^[8] The peaks of the carbons of the anion in compound **8** appear at 140.5 ppm. In comparison to the 5-nitrimino-1*H*-tetrazolate of compound **9** with a chemical shift of the carbon of 157.7 ppm, the 1-methyl derivative **10** shows a chemical shift of the carbon, which amounts to 155.4 ppm. This downshift probably arises through the inductive effect of the methyl-group, pushing electron density into the ring. The carbon-signal of the methyl-group is observed at 32.9 ppm, so that the chemical shift of both peaks lies in the range of the chemical shifts of the 1-methylnitriminotetrazolate-carbons in other nitrogenous

compounds, which equal to 157.7 and 33.1 ppm.^[7] The picric acid anion in compound **12** leads to four additional peaks in the ¹³C NMR spectrum, which show similar chemical shifts compared to the shifts of picric acid.^[17]

IR and Raman Spectroscopy

For the dinitramide anion in compound **2** $\nu(\text{NO}_2)$ is observed at 1532 and 1339 cm^{-1} in the Raman spectrum as well as at similar values in the IR spectrum according to the values reported in literature.^[18] In the IR and Raman spectra of compounds **3** and **4** a number of bands occur in the range of 1540–700 cm^{-1} , which show the characteristic pattern of $\nu(\text{NN})$, $\nu(\text{NCN})$, $\gamma(\text{CN})$ and δ aromatic ring vibrations of the tetrazole and the tetrazole–2*N*–oxide rings.³⁵ Additionally the O–H band of the crystal water in compound **4** can be observed at 3106 cm^{-1} . The nitrate anion in compound **5** can be easily identified through a distinct band at 1406 cm^{-1} in the IR spectrum, showing the valence vibration. The C–NO₂ stretch of the anion of compound **6** can be observed with a very strong band at 1550 cm^{-1} and medium band at 1351 cm^{-1} in the Raman spectrum. These bands can also be observed with reversed intensities in the IR spectrum. The usually strongest aromatic C=C stretch band can be observed in the IR spectrum at 1497 cm^{-1} . The characteristic C–C stretch probably overlaps with the C–C stretch of the cation and thus only a single band is observed for the two vibrations at 1024 cm^{-1} . The tetrazole derivatives in compounds **7**, **8**, **9** and **10** show similar absorption patterns in the range of 1540 to 700 cm^{-1} compared to the ones observed for compound **3** and **4** for the tetrazole–rings. The C–C absorption of compound **7** and **8** occurs at 1001 and 993 cm^{-1} , thus in the range of the C–C band of the cation, so that the two bands probably overlap. Compounds **7**, **8** and **9** all exhibit a weak band at around 1530 cm^{-1} in both IR and Raman spectra representing the NO₂ stretch of the nitrimino–group. In compound **10** this absorption seems to be shifted to around 1500 cm^{-1} in the vibrational spectra. Characteristic for the anion in compound **10** are the bands of the –CH₃ group at around 2900 cm^{-1} (broad band), 1468 cm^{-1} (δ C–H), 1400 cm^{-1} (symmetric deformation vibration of CH₃). The absorption at 3360 cm^{-1} indicates the presence of crystal water in compound **10**. The presence of the perchlorate anion in compound **11** is indicated by the bands at 929, 1075 and 1138 cm^{-1} in the Raman spectrum. These bands correlate in reasonable agreement with the bands reported for inorganic perchlorate compounds.^[18] In the vibrational spectra of compound **12** the characteristic vibrations of the C=C stretch vibrations of the aromatic ring can be observed at 1616, 1565 and 1520 cm^{-1} and thus stand in good agreement to the values reported in literature.^[19] The C–NO₂ stretch can be observed in the Raman spectra at 1545 and 1368 cm^{-1} .

Lastly the characteristic C–O stretch vibration occurs in both IR and Raman spectra between 1150 and 1040 cm⁻¹.

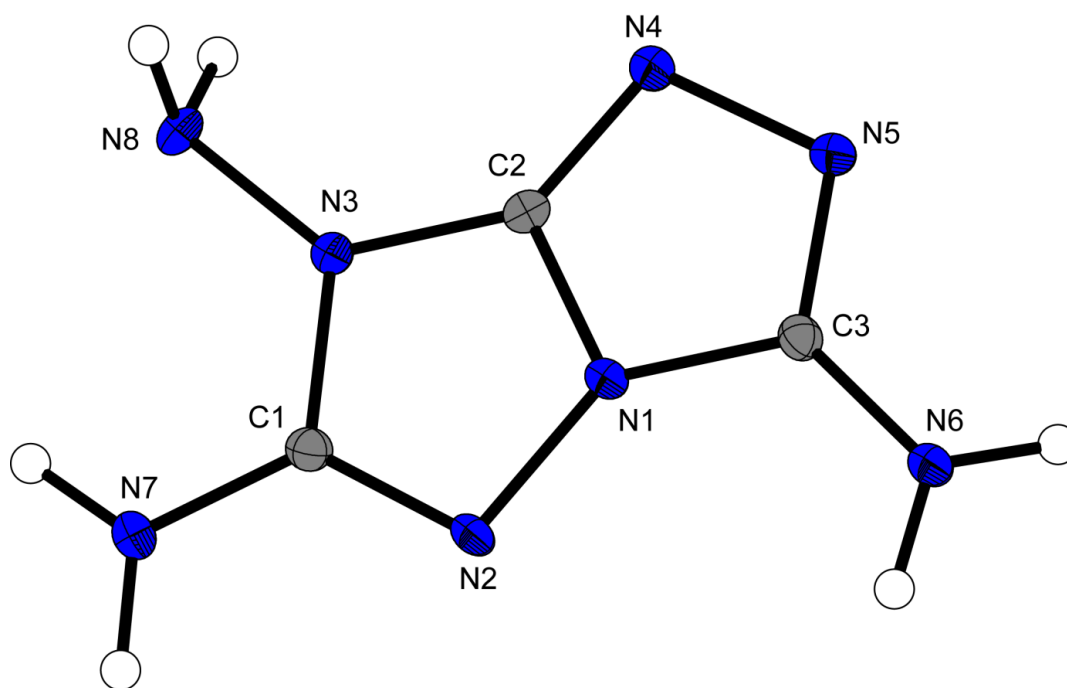
8.6.7 References

- [1] R. Centore, A. Carella, S. Fusco, *Struct. Chem.* **2011**, 22, 1095–1103.
- [2] (a) N. Fischer, T. M. Klapötke, D. G. Piercey, J. Stierstorfer, *Z. Anorg. Allg. Chem.* **2012**, 638, 302–310; (b) N. Fischer, T. M. Klapötke, J. Stierstorfer, *Z. Anorg. Allg. Chem.* **2011**, 637, 1273–1276.
- [3] T. M. Klapötke, J. Stierstorfer, A. Wallek, *Chem. Mater.* **2008**, 20, 4519–4530.
- [4] M. Göbel, K. Karaghiosoff, T. M. Klapötke, D. G. Piercey, Nitrotetrazolate, *J. Am. Chem. Soc.* **2010**, 132, 17216–17226.
- [5] D. E. Wilcox, L. A. Bromley, *J. Chem. Eng.* **1963**, 55, 32–39.
- [6] V. Rafeev, Y. Rubtsov, *Russ. Chem. Bull.* **1993**, 42, 1811–1815.
- [7] T. M. Klapötke, A. Preimesser, J. Stierstorfer, *Z. Anorg. Allg. Chem.* **2012**, 638, 1278–1286.
- [8] N. Fischer, T. Klapötke, M. Reymann, J. Stierstorfer, *Eur. J. Inorg. Chem.* **2013**, 2013, 2167–2180.
- [9] D. Fischer, T. Klapötke, J. Stierstorfer, *Angew. Chem.* **2014**, 126, 8311–8314.
- [10] M. Zimmer, E. Baroody, G. Carpentier, R. Robb, *J. Chem. Eng. Data* **1968**, 13, 212–214.
- [11] J. E. Felts, H. W. Sandusky, R. H. Granholm, *AIP Conf. Proc.* **2009**, 1195, 233.
- [12] H. W. Sandusky, R. H. Granholm, D. G. Bohl, IHTR 2701, Naval Surface Warfare Center, Indian Head, MD, 12 Aug 2005.
- [13] R. Mayer, J. Köhler, A. Homburg, *Explosives*, 5th ed., Wiley VCH, Weinheim, **2002**, 197–200.
- [14] R. Mayer, J. Köhler, A. Homburg, *Explosives*, 5th ed., Wiley VCH, Weinheim, **2002**, 148.
- [15] T. M. Klapötke, P. Mayer, C. M. Sabaté, J. M. Welch, N. Wiegand, *Inorg. Chem.* **2008**, 47, 6014–6027.
- [16] S. Kim, J. Kim, *Bull. Korean Chem. Soc.* **2013**, 34, 2503–2506.

- [17] M. I. Saleh, E. Kusrini, R. Adnan, B. Saad, B. M. Yamin, H. K. Fun, , *J. Mol. Struct.* **2007**, 837, 169–178.
- [18] F. A. Miller, C. H. Wilkins, *Anal. Chem.* **1952**, 42, 1253–1294.
- [19] M. Hesse, H. Meier and B. Zeeh, *Spektroskopische Methoden in der Organischen Chemie*, Thieme, Stuttgart, New York, 7th edn, 2005.

3,6,7-Triamino-[1,2,4]triazolo[4,3-b][1,2,4]triazolium - a non-toxic, high performance energetic building block with excellent stabilities

published in *Chem. Eur. J.* **2015**, *21*, 9219–9228. (DOI: 10.1002/chem.201500982)



Abstract: A novel strategy for the design of energetic materials that uses fused amino-substituted triazoles as energetic building blocks is presented. The 3,6,7-triamino-7*H*-[1,2,4]triazolo[4,3-*b*][1,2,4]triazolium (TATOT) motif can be incorporated into many ionic, nitrogen-rich materials to form salts with advantages such as remarkably high stability towards physical or mechanical stimuli, excellent calculated detonation velocity, and toxicity low enough to qualify them as “green explosives”. Neutral TATOT can be synthesized in a convenient and inexpensive two-step protocol in high yield. To demonstrate the superior properties of TATOT, 13 ionic derivatives were synthesized and their chemical- and physicochemical properties (e.g., sensitivities towards impact, friction and electrostatic discharge) were investigated extensively. Low toxicity was demonstrated for neutral TATOT and its nitrate salt. Both are insensitive towards impact and friction and the nitrate salt combines outstanding thermal stability (decomposition temperature = 280 °C) with promising calculated energetic values.

Keywords: Energetic materials · Triazoles · Amino · Crystal Structure · Cations

9.1 Introduction

Since the discovery of trinitrotoluene (TNT, Figure 1), the development of explosives and other new energetic materials has been a continuously growing research topic in the large field of materials science.^[1] A new secondary explosive should possess a high heat of formation and density, which results in a high detonation pressure and detonation velocity. Furthermore, it must be less sensitive towards impact and friction than **RDX** (Figure 1) and its thermal stability should surpass the 200 °C benchmark. Recently, environmental concerns have become increasingly important, which means that new explosive materials should only release environmentally benign decomposition products on detonation.^[2]

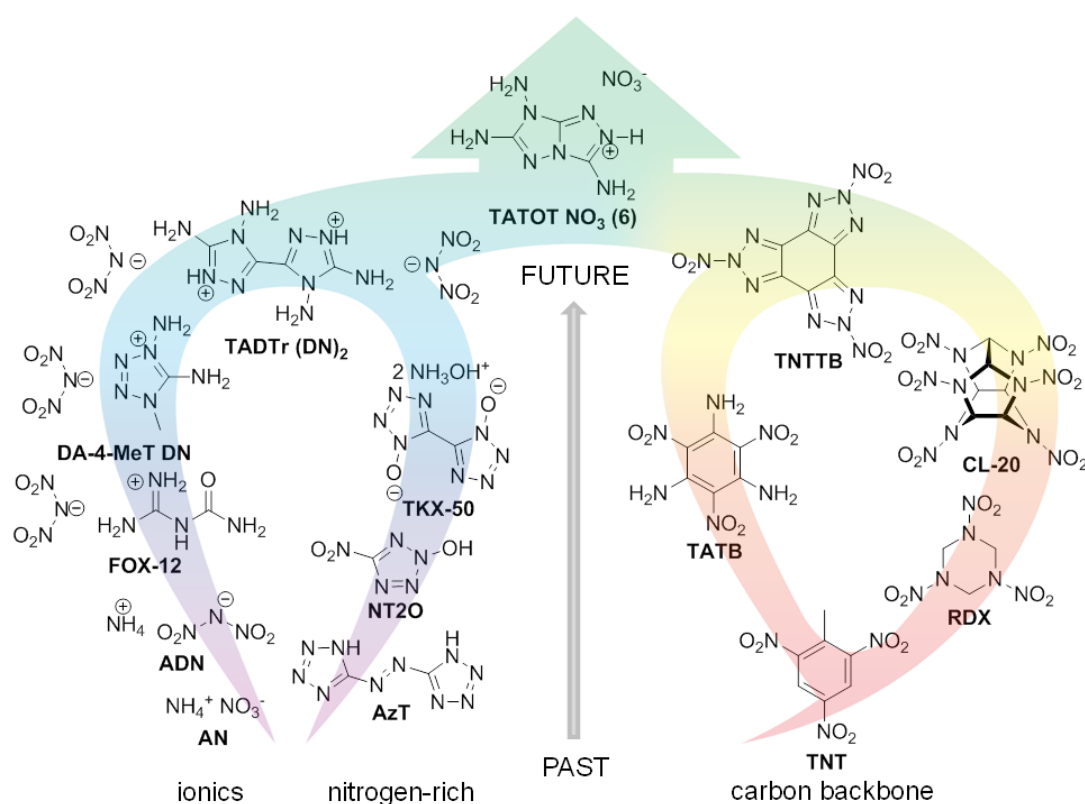


Figure 1. Selected chemical structures of secondary explosives, which give an overview of different concepts and research strategies used during the development of new secondary explosives. A combination of strategies, i) ionic compounds (**AN**, **ADN**, **FOX-12**, **DA-4-MeTDN**), ii) nitrogen-rich heterocycles (**AzT**) with *N*-oxides (**NT20**, **TKX-50**), iii) introduction of amino- (**TADTr (DN)₂**, **TATB**), nitro- (**TNT**, **TATB**), and nitramino functional groups (**RDX**, **CL-20**, **TNTTB**), iv) hydrogen-bonding network (**FOX-12**, **TATB**), v) caged (**CL-20**) and fused (**TNTTB**) molecules, results in the ionic, aromatic, nitrogen-rich, energetic, environmentally friendly, fused heterocyclic compound **TATOT NO₃**.

Several concepts have been used in the past two decades to improve the properties of secondary explosives^[3] (Figure 1): i) ionic compounds with nitrogen-rich cations, such as ammonium, hydrazinium, and hydroxylammonium, can lead to higher densities and stabilities due to their high lattice energy (e.g., **AN**, **ADN**,^[3a,b] **FOX-12**,^[3c] **DA-4-MeTDN**),^[3d]

ii) nitrogen-rich heterocycles (**AzT**)^[3e] with an *N*-oxide functionality (**NT2O**,^[3f,g] **TKX-50**),^[3h] iii) large hydrogen-bonding networks in the solid state (e.g., **TATB**,^[3i] **FOX-12**), and iv) use of aromaticity to further increase the stability of energetic compounds (e.g., **TKX-50**, **TNT**, **TATB**, **TNTTB**,^[3j] **TADTr (DN)₂**).^[3k]

However, the most recent studies focus on new energetic anions that are often functionalized with nitro- (e.g., **NT2O**) or nitramino (e.g., **TNTTB**) moieties combined with known, non-aromatic, nitrogen-rich cations, such as ammonium, hydroxylammonium (e.g., **TKX-50**), or hydrazinium.^[1a,b,3f,h,4] New ionic explosives that comprise nitro- and nitramino moieties coupled with hydrazinium or hydroxylammonium cations might not meet the criteria for “green explosives”.

Examples of aromatic nitrogen-rich cations in energetic compounds are di- or triaminotriazolium ions, as well as amino- or diaminotetrazolium ions.^[5] Recently, Shreeve et al. reported energetic materials based on tris(triazolo)benzene^[3j] and 3,6-dinitropyrazolo[4,3-*c*]pyrazole,^[3l] which showed good thermal stabilities. Recently, we reported TADTr, which is exceptionally thermally stable, up to 342 °C in its neutral form.^[3k]

In our continuing effort to synthesize energetic materials with high thermal stability and good energetic performance, we decided to investigate 3,6,7-triamino-7*H*-[1,2,4]triazolo-[4,3-*b*][1,2,4]triazole (TATOT), a system consisting of two fused triazole rings and three amino moieties. Potts and Hirsch first reported the synthesis of TATOT in the 1960s;^[6] recent investigations focused on TATOT and similar compounds have been conducted by Centore et al.^[7] Herein, we report a detailed investigation of the triaminotriazolotriazole system that utilizes TATOT as an energetic building block. Scheme 1 shows the synthesis and characterization of numerous ionic derivatives, which all meet the required criteria for mechanical (impact sensitivity (*IS*) ≥ 7.5 J, friction sensitivity (*FS*) ≥ 120 N) or thermal (decomposition temperature (*T*_{dec.}) ≥ 200 °C) stimuli, and most show excellent explosive properties.

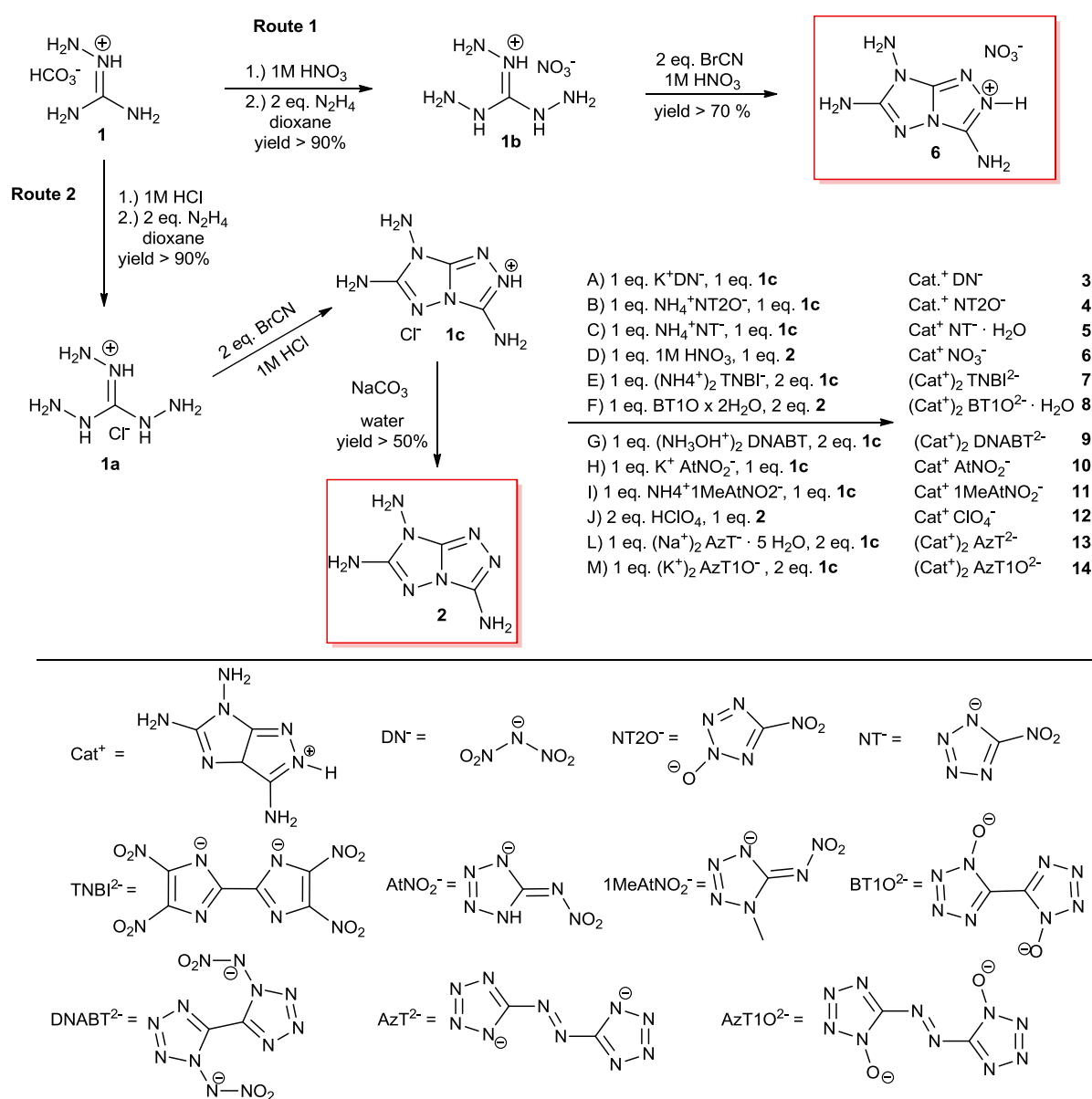
9.2 Results and Discussion

9.2.1 Synthesis

TATOT (**2**) is synthesized by a quick and convenient reaction using water as the solvent.^[6] Triaminoguanidine hydrochloride (**1 a**) is dissolved in 1 M hydrochloric acid, then cyanogen bromide is added. The reaction mixture is first heated to 60 °C, then heated at reflux for 1 h. The mixture is allowed to cool to ambient temperature and, after alkaline workup with sodium

carbonate, neutral **2** is obtained in good yield (Scheme 1, route 2). Nitrate **6** can be synthesized by a less-expensive, more-feasible, and even-more-efficient route from triaminoguanidine nitrate (**1b**) solvated in 1 M nitric acid (Scheme 1, route 1). All the products can be used as obtained and do not require further purification (e.g., column chromatography). Compound **2** and its salts show low water solubility, which facilitates isolation and purification.

The energetic salts **3–5**, **7**, **9–11**, and **13–14** were obtained by simple anion metathesis of **1c** with different energetic anions, whereas compounds **6**, **8**, and **12** were obtained by addition of the appropriate acid to the free base **2** (Scheme 1).



Scheme 1. Synthesis of nitrate **6** (route 1; total yield > 60 %) and compounds **2–14** (route 2).

TATOT dinitramide (**3**) is obtained by a 1:1 stoichiometric reaction with the monohydrochloride salt **1 c** in ethanol. TATOT 5-nitrotetrazole-2-oxide (**4**), TATOT 5-nitrotetrazolate monohydrate (**5**), TATOT 5-nitriminotetrazolate (**10**), and TATOT 1-methyl-5-nitriminotetrazolate (**11**) are obtained by a 1:1 stoichiometric reaction of **1 c** with the required anion in water. TATOT nitrate (**6**) and TATOT perchlorate (**12**) salts are formed by addition of nitric acid (1 equiv) or perchloric acid (1 equiv), respectively, to **2**, whereas di-TATOT bitetrazole-1-oxide (**8**) is obtained by a 2:1 stoichiometric reaction of the free base **2** with 1,1'-dihydroxy-5,5'-bitetrazole. Di-TATOT tetranitro-biimidazolate (**7**), di-TATOT 1,1'-dinitramino-5,5'-bitetrazolate (**9**), di-TATOT 5,5'-azotetrazolate (**13**), and di-TATOT 5,5'-azotetrazole-1,1'-dioxide (**14**) are formed by dissolving **1** (2 equiv) and the appropriate anion (1 equiv) in water.

9.2.2 Crystal Structures

During this work the crystal structures of compounds **2**, **4–6**, **8**, **9**, **11–13** were obtained. Selected data and parameters from the low temperature X-ray data collection and refinement are given in Tables S1–S3 (Supporting Information).^[8]

Compound **2** crystallizes from water in the triclinic space group *P*–1 with a density of 1.757 g cm^{–3} at 173 K and two molecules per unit cell. The molecular unit of **2** with selected bond lengths and angles is shown in Figure 2. With bond lengths of 1.306(2) to 1.434(9) Å, the distances between the ring atoms of the 1,2,4-triazoles lie between the length of formal C–N and N–N single and double bonds (C–N: 1.47 Å, C=N: 1.22 Å; N–N: 1.48 Å, N=N: 1.20 Å), which indicates the aromaticity of the ring system.^[9] The bond angles in the two rings all lie near 108°; the N1–N2–C1 angle shows the greatest deviation (100.97(13)°). A planar ring system is formed with an N5–N4–C2–N3 torsion angle of 180.00(19)°. Thus, like bitriazoles,^[9] fused triazoles form planar ring systems. The torsion angle of the amino groups is slightly larger than 0° (1–5°), thus the amino groups are slightly tilted out of the plane of the ring system. All the amino groups participate in hydrogen bonds, whereas in the ring system only N2, N4, and N5 act as hydrogen-bond acceptors. The lengths of the hydrogen bonds are in the range of the sum of the van der Waals radii ($r_w(\text{N})+r_w(\text{N})=3.20$ Å), thus a strong hydrogen-bond network is formed.^[9]

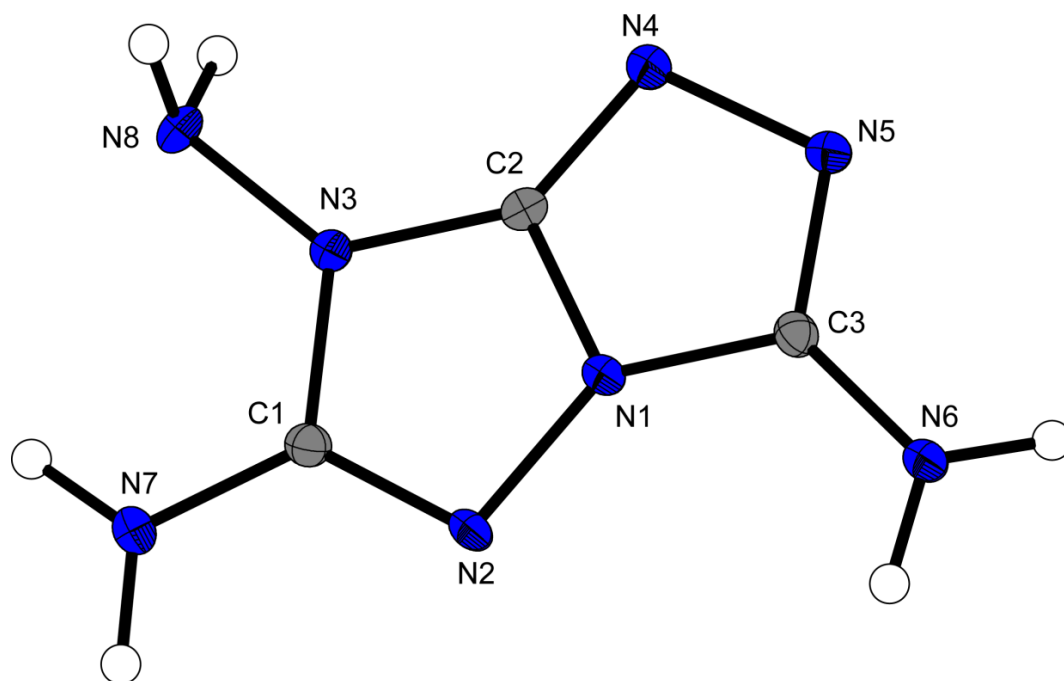


Figure 2. Molecular unit of **2**. Ellipsoids are drawn at the 50% probability level. Selected bond lengths of **2** [Å]: N1–C2 1.343(2), N1–N2 1.408(5), N2–C1 1.327(2), C1–N3 1.383(2), N3–C2 1.370(2), C2–N4 1.306(2), N4–N5 1.434(9), N5–C3 1.318(2), C3–N1 1.366(1); selected torsion angle of **2** [°]: N5–N4–C2–N3 180.

Compound **4** crystallizes from water in the orthorhombic space group $P2_12_12_1$ with a density of 1.765 g cm^{-3} at 173 K and four molecules per unit cell. The molecular unit of **4** with and selected hydrogen bond lengths, is illustrated in Figure 3. Compared to the high-energy hydroxylammonium salt ($\rho = 1.850 \text{ g cm}^{-3}$), this density is fairly low. On the other hand, ammonium nitrotetrazole-2*N*-oxide shows a lower density ($\rho = 1.730 \text{ g cm}^{-3}$), similar to the more-stable nitrogen-rich guanidinium- ($\rho = 1.698 \text{ g cm}^{-3}$), aminoguanidinium- ($\rho = 1.697 \text{ g cm}^{-3}$), diaminoguanidinium- ($\rho = 1.687 \text{ g cm}^{-3}$), and triaminoguanidinium salts ($\rho = 1.6391 \text{ g cm}^{-3}$).^[3f] The hydrogen-bond network in **4** is built up a little differently due to the new donor introduced into the ring-system through protonation. Only N10 of the cation acts as a hydrogen-bond acceptor, whereas the other hydrogen bonds are all intermolecular bonds to the nitrotetrazolate-2-oxide anion. Additionally, the geometry of the cation is slightly different than in the free base **2**. The protonated triazole component is slightly distorted relative to neutral **2**. The bond length N8–C4 (1.347(3) Å) is slightly shorter, whereas the C4–N9 bond (1.344(3) Å) is significantly longer than the corresponding lengths in **2** (C3–N1: 1.366(1) Å, N5–C3: 1.318(2) Å). Also, the N9–N10 bond length in **4** (1.412(2) Å) shows a deviation from that in neutral **2** (1.434(9) Å). Similarly, the bond angles around the protonated nitrogen atom show small deviations of around 4° relative to in the free base **2**. The

nitrotetrazolate-2*N*-oxide anion shows the same bond lengths and bond angles as reported in literature.^[3f]

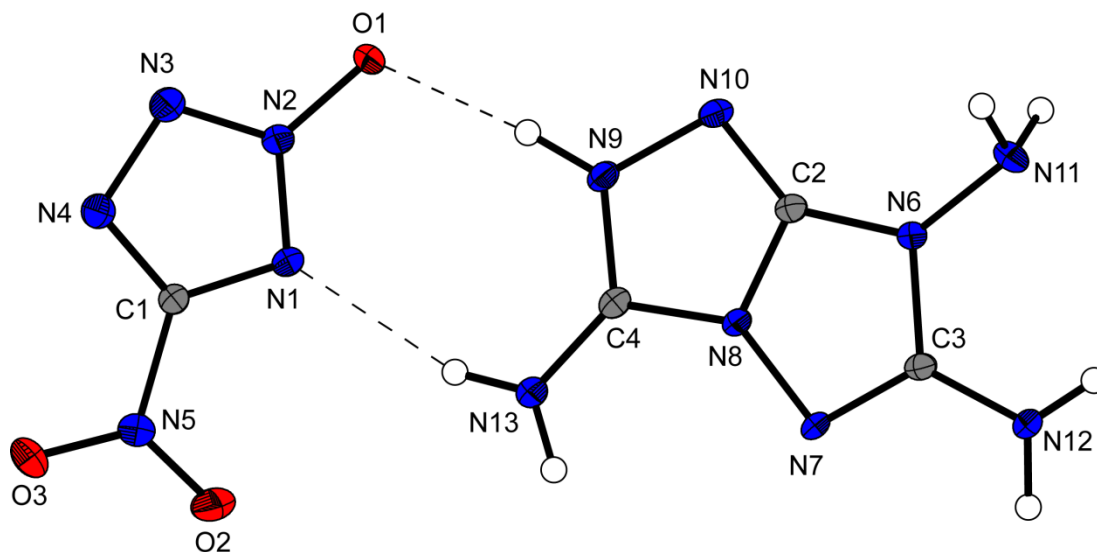


Figure 3. Molecular unit of **4**. Ellipsoids are drawn at the 50% probability level. Selected bond lengths [Å]: C2–N8 1.350(3); selected hydrogen bond lengths (D–H···A) [Å]: N12–N12A···N10 2.989(3), N13–N13A···N1 2.941(2), N9–N9A···O1 2.808(2); selected bond angles [°]: N8–C4–N9 104.14(16), C4–N9–N10 112.82(17).

Compound **5** crystallizes as monohydrate from water in the monoclinic space group *C2/c* and eight molecular units per unit cell. The molecular unit of **5** with selected bond lengths and angles is illustrated in Figure 4. The density at 173 K is 1.742 g cm^{−3}, which is much higher than the density of the corresponding triaminoguanidinium monohydrate ($\rho = 1.599 \text{ g cm}^{-3}$).^[10] The bond lengths and angles of the counterion correspond to the data reported in literature.^[10] Likewise, the geometry of the cation lies in the range of the data reported for compound **4**, showing small deviations from the free base **2** near the protonated nitrogen atom N8. Additionally, the length of the C2–N9 bond, at which the two triazoles are fused together is slightly longer than in the free base **2** or in **4**. The C3–N8–N7 bond angle (113.69(13)°) is even larger than the corresponding angle in **4**, whereas the angle N9–C3–N8 shows a similar value to that in **4**.

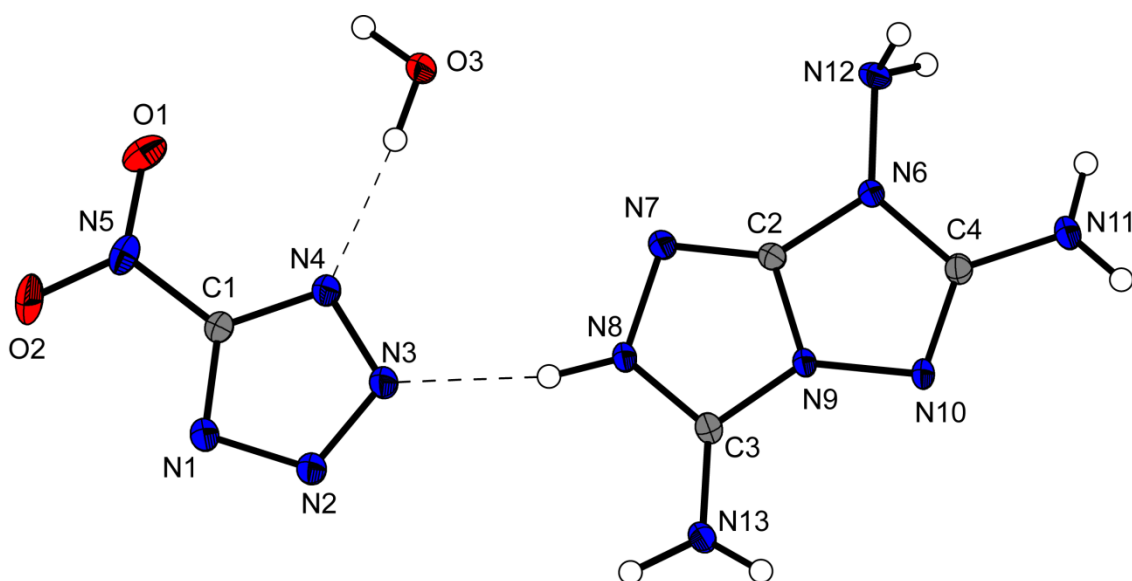


Figure 4. Molecular unit of **5**. Ellipsoids are drawn at the 50% probability level. Selected bond lengths [Å]: C2–N9 1.353(1), N9–C3 1.349(2), C3–N8 1.336(2), N8–N7 1.415(5); selected bond angles (°): N9–C3–N8 104.26(12), N8–N7–C2 99.87(12)

Anhydrous compound **6** crystallizes from water in the orthorhombic space group *Pnma* with four formula units per unit cell. The molecular unit of **6** with selected bond lengths and angles is illustrated in Figure 5. The density of **6** ($\rho = 1.812 \text{ g cm}^{-3}$ at 173 K) is higher than the density of guanidinium nitrate ($\rho = 1.410 \text{ g cm}^{-3}$),^[11] and is similar to that of the highly energetic compound hydroxylammonium nitrate ($\rho = 1.841 \text{ g cm}^{-3}$).^[12] Strikingly the torsion angles of this molecule reveal a perfectly planar molecule, with every torsion angle of the cation equal to 0.00°. The geometry of the cation is comparable to the geometry of the cation in compound **4**, and has similar bond angles and lengths.

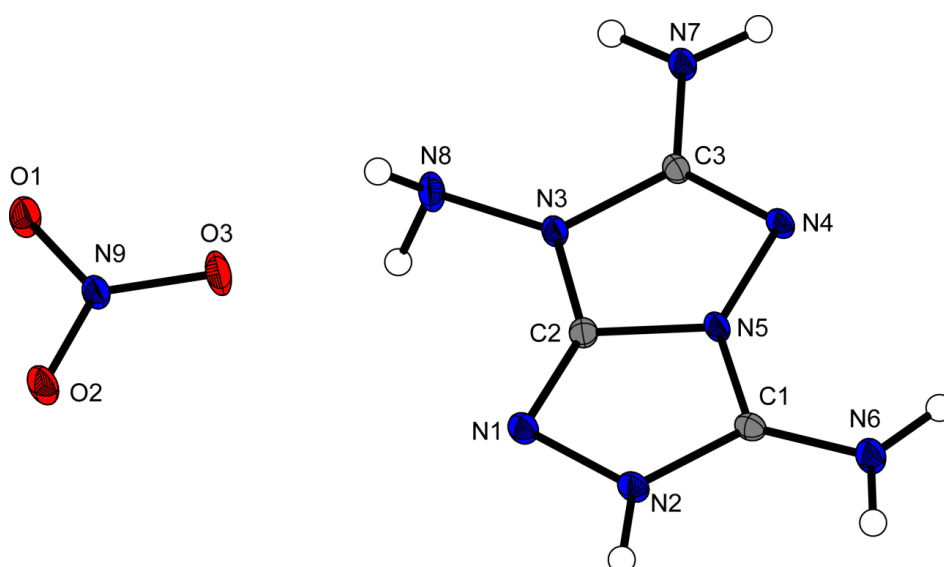


Figure 5. Molecular unit of **6**. Ellipsoids are drawn at the 50% probability level. Selected bond lengths [Å]: C2–N5 1.350(2), C1–N2 1.341(8), N2–N1 1.413(4); selected bond angles [°] C1–N2–N1 113.47(12), N5–C1–N2 104.13(13).

The energetic salt **8** crystallizes from water in the triclinic space group $P\bar{1}$ with two water moieties and one molecule per unit cell. The molecular unit and selected bond lengths and angles is illustrated in Figure 6. The density of the crystal is 1.692 g cm^{-3} at 173 K. As reported for the cations above, the protonated ring is slightly distorted relative to the free base **2**. The length of the C–C bond connecting the two tetrazole moieties in the anion is between a formal C–C single bond and a C=C double bond ($\text{C1}^{\text{ii}}\text{--}\text{C1}^{\text{iii}} = 1.439(0)\text{ \AA}$), which lies in the range of bond lengths reported for neutral 1,1'-dihydroxy-5,5'-bitetrazole ($\text{C--C} = 1.454(2)\text{ \AA}$).^[13] The cation ring system and the anion form two nearly planar structures with N6--N5--C3--N8 and $\text{N1}^{\text{ii}}\text{--}\text{C1}^{\text{ii}}\text{--}\text{C1}^{\text{iii}}\text{--}\text{N4}^{\text{iii}}$ torsion angles of $179.11(10)^\circ$ and $1.3(2)^\circ$, respectively.

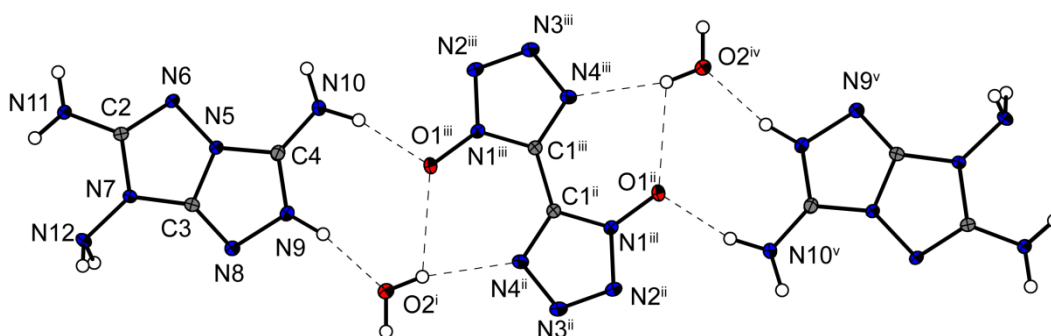


Figure 6. Molecular unit of **8**. Ellipsoids are drawn at the 50% probability level. Selected bond lengths [\AA]: C3--N5 $1.352(3)$, N5--C4 $1.349(9)$, C4--N9 $1.343(2)$, N9--N8 $1.410(7)$; selected bond angles [$^\circ$]: N5--C4--N9 $104.24(10)$, C4--N9--N8 $113.15(10)$, N9--N8--C3 $100.67(10)$.

Compound **9** crystallizes from water in the monoclinic space group $P2_1/n$ with two formula units per unit cell. The molecular unit of **9** with selected bond lengths and angles is shown in Figure 7. The density at 173 K is 1.792 g cm^{-3} , which is lower than that of the potassium salt K_2DNABT ($\rho = 2.172\text{ g cm}^{-3}$ at 100 K).^[14] The hydroxylammonium salt $(\text{NH}_3\text{OH})_2\text{ DNABT}$ and the ammonium salt $(\text{NH}_4)_2\text{ DNABT}$ also show higher densities ($\rho = 1.877$ and 1.814 g cm^{-3} , respectively).^[15] The tetrazole units of the anion form a completely planar structure with an $\text{N11--C4--C4}^{\text{ii}}\text{--}\text{N14}^{\text{ii}}$ torsion angle of $0.0(2)^\circ$. The nitro groups are twisted out of this plane by $78.66(15)^\circ$, as reported in the literature.^[14] The triazole rings of the cation are slightly tilted towards each other with a torsion angle of $177.94(11)^\circ$. The $\text{N4}^{\text{i}}\text{--}\text{N5}^{\text{i}}$ bond length of $1.405(8)\text{ \AA}$ is slightly smaller than in compounds **2–8**. The $\text{C4--C4}^{\text{ii}}$ bond length is equal to that in K_2DNABT ($1.451(5)\text{ \AA}$).^[14]

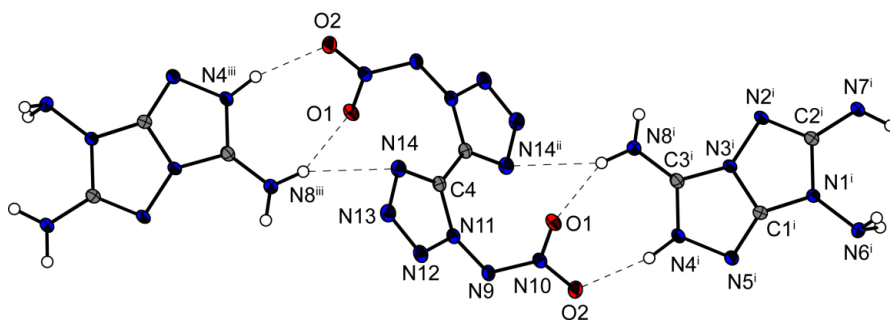


Figure 7. Molecular unit of **9**. Ellipsoids are drawn at the 50% probability level. Selected bond lengths [Å]: N3ⁱ–C1ⁱ 1.349(7), N3ⁱ–C3ⁱ 1.345(3), C3ⁱ–N4ⁱ 1.336(7), N4ⁱ–N5ⁱ 1.405(8), C4–C4^a 1.451(5); selected bond angles [°]: N3ⁱ–C3ⁱ–N4ⁱ 104.28(10), C3ⁱ–N4ⁱ–N5ⁱ 113.63(10).

Anhydrous compound **11** crystallizes from water in the monoclinic space group $P2_1/c$ with four molecules per unit cell. The molecular unit of **11** with selected bond lengths, bond angles, and torsion angles is illustrated in Figure 8. This compound displays the lowest density of the compounds in this report ($\rho = 1.685 \text{ g cm}^{-3}$ at 173 K). However, the other nitrogen-rich guanidinium, diaminoguanidinium, and triaminoguanidinium 1-methylnitriminotetrazolate salts exhibit significantly lower densities ($\rho = 1.550$, 1.605, and 1.569 g cm^{-3} , respectively).^[16] The C3–N9–C4–N7 torsion angle of the cation ($177.88(10)^\circ$) reveals an almost-planar ring system. The tetrazole ring of the anion also forms a planar moiety, whereas the nitramine unit is twisted out of the plane by $10.9(2)^\circ$. In contrast, the amine units of the cation lie in the same plane as the ring system. The bond lengths in the tetrazolate ring system are between 1.29 and 1.37 Å and match the data reported in literature.^[16] The bond lengths and angles between the ring atoms in the cation have similar values to those of compound **9**.

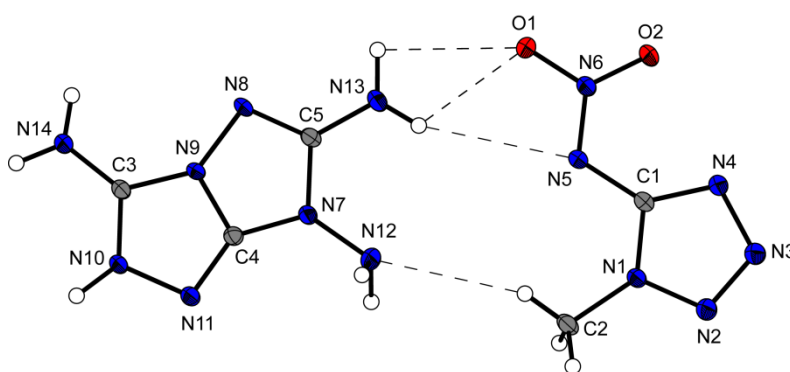


Figure 8. Molecular unit of **11**. Ellipsoids are drawn at the 50% probability level. Selected bond lengths [Å]: C4–N9 1.353(9), N9–C3 1.353(9), C3–N10 1.340(2), N10–N11 1.404(7); selected bond angles [°]: N10–N11–C4 100.41(10), N11–N10–C3 113.53(10), N10–C3–N9 104.39(11) selected torsion angles [°]: N12–N7–C4–N11 0.6(3), N12–N7–C5–N13 3.1(2), N8–N9–C3–N14 1.6(3), N6–N5–C1–N4 10.9(2), N2–N1–C1–N4 0.72(14).

Perchlorate salt **12** crystallizes from water in the triclinic space group $P\bar{1}$ with two formula units per unit cell. The molecular unit of **12** with selected bond lengths, bond angles, and

torsion angles is illustrated in Figure 9. The density at 173 K ($\rho = 1.808 \text{ g cm}^{-3}$) is relatively small compared with the density reported for the commonly used salt ammonium perchlorate ($\rho = 1.951 \text{ g cm}^{-3}$),^[17] whereas the calculated density of hydroxylammonium perchlorate ($\rho = 2.13 \text{ g cm}^{-3}$)^[18] is significantly higher. However, compound **12** has a similar density as hydrazinium perchlorate ($\rho = 1.84 \text{ g cm}^{-3}$) and a much higher density than triaminoguanidinium perchlorate ($\rho = 1.67 \text{ g cm}^{-3}$).^[19] The two triazoles are tilted slightly towards each other with an N2-N3-C1-N4 torsion angle of $176.96(18)^\circ$. The amino groups are significantly twisted out of the plane up to 10.3° . The bond angles and lengths of the cation are similar to the values reported for **9**. The perchlorate anion has a slightly distorted tetrahedral geometry with O-Cl-O bond angles between 111.99° and 107.56° and Cl-O bond lengths between 1.406 and 1.459 Å.

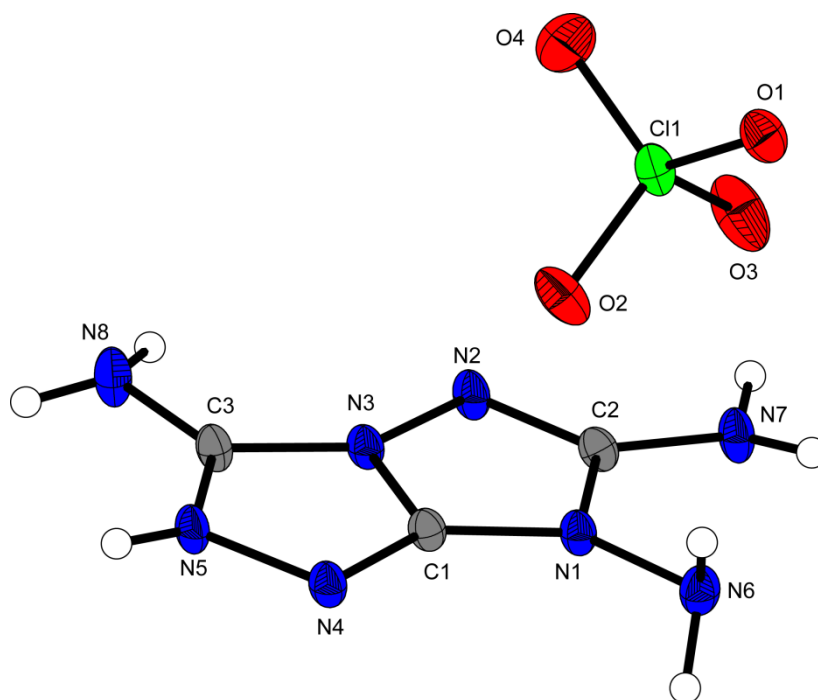


Figure 9. Molecular unit of **12**. Ellipsoids are drawn at the 50% probability level. Selected bond lengths [Å]: C1–N3 1.355(3), N3–C3 1.341(3), C3–N5 1.337(3), N5–N4 1.409(2), C11–O1 1.438(3), C11–O2 1.435(2), C11–O3 1.459(3), C11–O4 1.406(3); selected bond angles [$^\circ$]: N3–C3–N5 104.20(18), N4–N5–C3 113.58(18), N5–N4–C1 100.38(16), O1–C11–O4 111.99(16), O2–C11–O4 111.17, O3–C11–O4 107.89(17); selected torsion angles [$^\circ$]: N6–N1–C1–N4 10.3(5), N3–N2–C2–N7 178.4(2), N2–N3–C3–N8 7.6(4).

Salt **13** crystallizes from water in the monoclinic space group $P2_1/c$ with two molecular moieties per unit cell. The molecular unit of **13** with selected bond lengths, angles, torsion angles, and hydrogen-bond lengths is illustrated in Figure 10. The density of **13** ($\rho = 1.756 \text{ g cm}^{-3}$) is significantly higher than the density of the corresponding ammonium, guanidinium, or triaminoguanidinium salts ($\rho = 1.562$, 1.569 , and 1.634 g cm^{-3} , respectively).^[20] A direct comparison with the hydroxylammonium salt was not possible

because the hydroxylammonium salt cocrystallizes with two water moieties.^[21] The two rings of the cation are tilted slightly towards each other with a torsion angle of 176.67(17)°, whereas the anion displays a completely planar system. The amino groups of the cation are slightly less twisted outward than in **12**. The geometry of the cation is very similar to those of the other cations in this report. The bond length of the diazene bond (N5=N5ⁱ: 1.255(2) Å) lies in the range found for the corresponding diguanidinium and di(triaminoguanidinium) salts.^[20] The crystal structure analysis also revealed numerous N–H···N hydrogen bonds. Several hydrogen bonds are formed in the crystal structure, including one intramolecular bond, a cation–cation bond, and various anion–cation bonds.

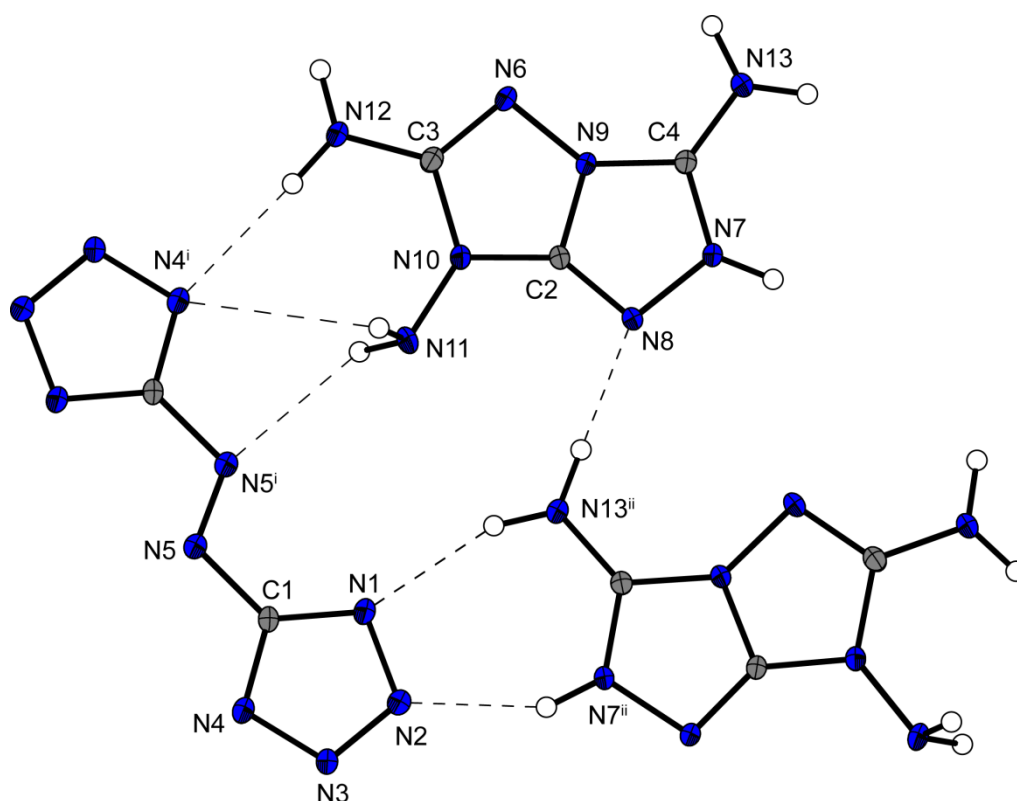


Figure 10. Molecular unit of **13**. Ellipsoids are drawn at the 50% probability level. Selected bond lengths [Å]: C2–N9 1.345(2), N9–C4 1.357(2), C4–N7 1.335 (2), N8–N7 1.406(2); selected bond angles [°]: N9–C4–N7 104.65(15), C4–N7–N8 113.02(15), N7–N8–C2 100.74(15); selected torsion angles [°]: N11–N10–C2–N8 5.4(4), N6–N9–C4–N13 7.4(4), C2–N10–C3–N12 175.19(16), C1–N5–N5ⁱ–C1ⁱ 0.00(86); selected hydrogen bonds d(D–H···A) [Å]: N7–H7···N2 2.824(2), N11–N11A···N12 3.211(3), N11–N11A···N5 3.026(2), N11–N11B···N1 3.179(2), N12–N12A···N4 3.163(2), N12–N12B···N3 2.967(2), N13–N13A···N8 2.883(2), N13–N13B···N1 2.989(2).

Compound **14** crystallizes from water in the monoclinic space group *C2/c* with four cation/anion pairs per unit cell. The molecular unit of **14** with selected bond lengths, bond angles, torsion angles, and hydrogen bond lengths is represented in Figure 11. The density of **14** ($\rho = 1.763 \text{ g cm}^{-3}$) is slightly higher than the density of azotetrazolate **13**, which reveals that introduction of a 1,1'-dioxide functionality slightly improves the density. A slightly lower

density is observed compared with the corresponding hydroxylammonium ($\rho = 1.778 \text{ g cm}^{-3}$) or ammonium salts ($\rho = 1.800 \text{ g cm}^{-3}$).^[22] The torsion angle of the cation reveals an almost-planar ring system with the amino groups slightly twisted out of the plane. The anion reveals a planar system in which the oxygen atoms are slightly twisted outwards at an angle of 1.6° . The bond lengths and angles of the cation are consistent with the data reported for the energetic salts. The only exception is that the C1–N4 bond is slightly longer than the reported distances for the corresponding bond lengths in the other cations studied. The N13ⁱ–N13ⁱⁱ diazene bond length (1.269(2) Å) is even longer than the diazene bond length in **13**. The hydrogen-bond network formed in **14** is different to that found for **13** due to the presence of the oxygen atoms. In addition to hydrogen bonds to oxygen, two very strong intermolecular hydrogen bonds between the triazoles of the two cations are formed (N5ⁱⁱ–H5ⁱⁱ...N2: 2.890(2) Å and N6–H6...N4ⁱⁱⁱ: 2.867(2) Å).

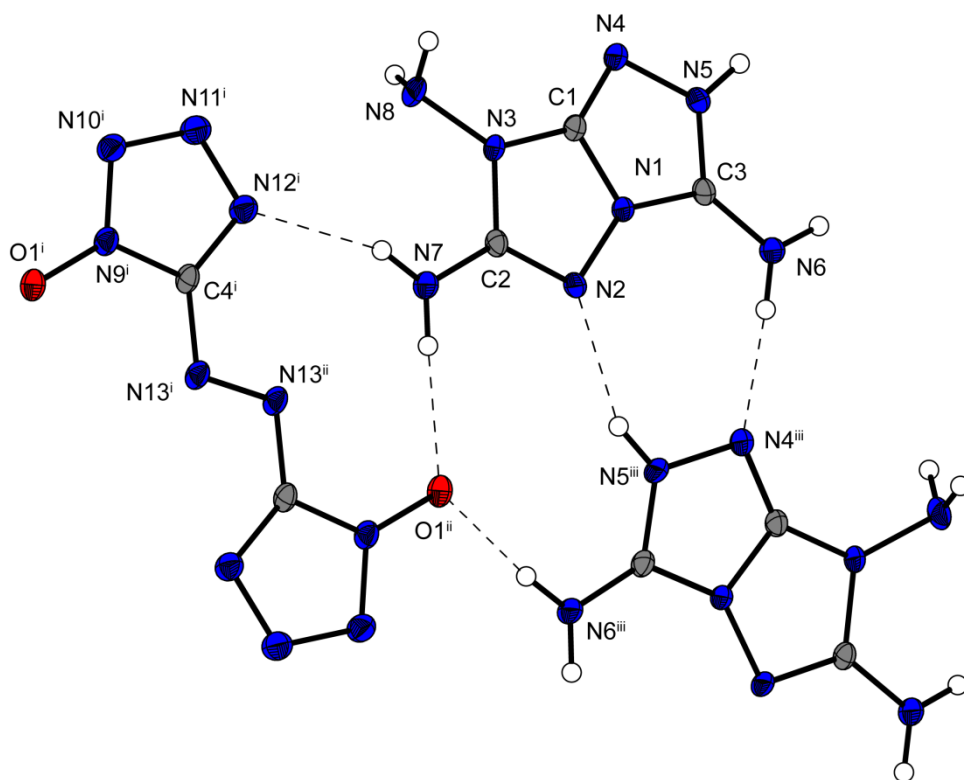


Figure 11. Molecular unit of **14**. Ellipsoids are drawn at the 50% probability level. Selected bond lengths [Å]: C1–N1 1.348(2), N1–C3 1.363(2), C3–N5 1.338(3), N5–N4 1.413(2), N9ⁱ–O1ⁱ 1.306(2), N13–N13ⁱⁱ 1.269(2); selected bond angles [°]: N1–C3–N5 104.04(16), C3–N5–N4 113.27(16), N5–N4–C1 100.75(15); selected torsion angles [°]: N2–N1–C3–N6 4.2(4), N1–N2–C2–N7 179.2(2), N8–N3–C1–N4 10.1(4); selected hydrogen bonds [Å]: N5–H5...N2 2.890(2), N6–H6...N4 2.867(2), N7–H7...N8 2.853(3).

9.2.3 Spectroscopy

NMR spectroscopy

All NMR spectra were recorded in solution in $[D_6]DMSO$. In addition to 1H and ^{13}C NMR spectroscopy, HMBC experiments were carried out to ensure the correct assignment of all the protons and carbon atoms. For example (Figure 12), the 1H NMR spectrum of **6** reveals four signals at $\delta = 13.31$ (H_A), 8.19 (H_B), 7.23 (H_C), and 5.78 ppm (H_D). In the ^{13}C NMR spectrum nitrate **6** shows resonances at $\delta = 160.3$ (C_1), 147.6 (C_2), and 141.3 ppm (C_3). The assignments were confirmed by gauge independent atomic orbital (GIAO) quantum chemical calculations. The chemical shifts of **3–5** and **7–14** all lie in the same range and are discussed in the Supporting Information

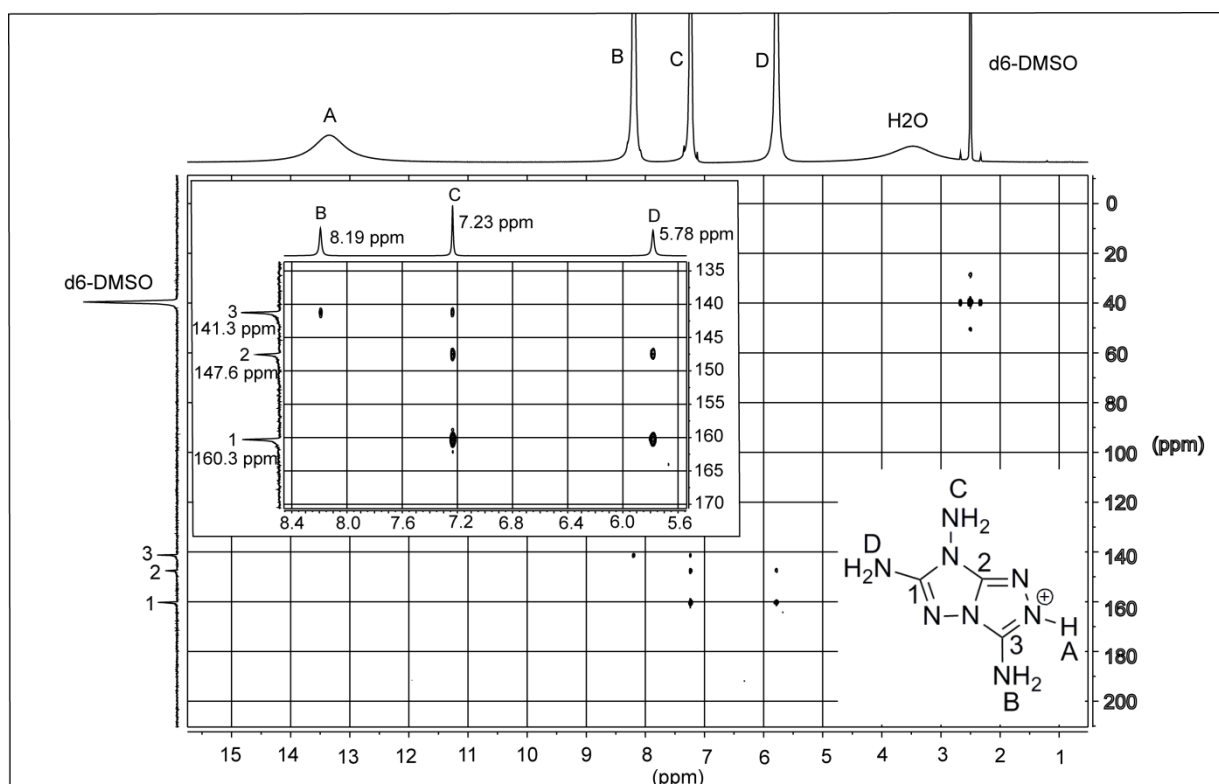


Figure 12. Assignment of the peaks in the HMBC spectrum of **6**

IR and Raman spectroscopy

IR and Raman spectra for compounds **2–14** were measured and the frequencies were assigned according to commonly observed values reported in the literature.^[23] Compound **2** shows the N–H bond stretching vibration between $\nu = 3500$ and 3100 cm^{-1} in the IR spectrum, whereas the deformation vibration of the N–H bond is found as the strongest band at $\nu = 1569\text{ cm}^{-1}$ in the IR spectrum. In the Raman spectrum, this deformation vibration appears as a weak band at $\nu = 1584\text{ cm}^{-1}$. The C–N stretching vibration of the triazole ring is visible as a very strong

band at $\nu = 1616 \text{ cm}^{-1}$ in the IR spectrum, whereas the same vibration is present as a weak band at $\nu = 1611 \text{ cm}^{-1}$ in the Raman spectrum. The second important vibration of the ring system is the C–N stretch, which appears at $\nu = 1293 \text{ cm}^{-1}$ in both vibrational spectra. Similar values for the vibrational data have been found for previously reported substituted 1,2,4-triazoles.^[24] The band at $\nu = 1502 \text{ cm}^{-1}$ arises from the N–NH₂ stretch in the IR spectrum, whereas the characteristic C–NH₂ vibration is found at $\nu = 1078 \text{ cm}^{-1}$ in both vibrational spectra. In compounds **3–14**, similar values to those described for compound **2** were observed for the cations and are discussed in the Supporting Information.

9.2.4 Physiochemical and energetic properties

All the materials investigated are highly energetic compounds, therefore their energetic behaviors were investigated.

Thermal behavior and sensitivities

The thermal behavior and sensitivities of all the compounds studied were investigated and reported. A detailed description of the setup is presented in the Supporting Information. It can be seen from Table 1 that all the compounds have a decomposition temperature ($T_{\text{dec.}}$) $\geq 200 \text{ }^{\circ}\text{C}$ and, therefore, meet the required criteria for replacing **RDX**. Nitrate salt **6** shows an exceptionally high thermal stability ($T_{\text{dec.}} = 280 \text{ }^{\circ}\text{C}$). The long-term stability of **6** was determined ($75 \text{ }^{\circ}\text{C}$ for 48 h), according to interim hazard classification (IHC). No mass loss was observed and no significant change in the elemental composition was observed before or after the measurement.

In terms of the sensitivities, all the compounds, except **9**, meet the required criteria towards mechanical stimuli ($IS \geq 7.5 \text{ J}$ and $FS \geq 120 \text{ N}$). Notably, neutral compound **2**, as well as the energetic salts **4–8**, **10**, **11**, **13**, and **14**, are insensitive to friction ($FS \geq 360 \text{ N}$).

Heats of formation and detonation parameters

The heats of formation were calculated theoretically by using the atomization equation [Eq. (1)] and CBS-4M electronic enthalpies.

$$\Delta_f H^\circ_{(\text{g}, \text{M}, 298)} = H_{(\text{M}, 298)} - \sum H^\circ_{(\text{atoms}, 298)} + \sum \Delta_f H^\circ_{(\text{atoms}, 298)} \quad (1)$$

Calculation of the detonation parameters was performed with the EXPLO5 (version 6.02) program package.^[25] The parameters of the Becker–Kistiakowsky–Wilson equation of state (BKW EOS) in EXPLO5 V6.02 are calibrated particularly for the formation of nitrogen, which is the main product from compounds with a high nitrogen content.^[26] The EXPLO5

detonation parameters of compounds **2**, **4**, **6**, **9**, and **11–14** were calculated by using the room-temperature density values obtained from the X-ray structures as described in Table 1 and in reference [27] and are summarized in Table 1, alongside a comparison with the values calculated for **RDX**. For a complete discussion on the methods used see the Supporting Information.

With regards to the calculated detonation velocities (D), surprisingly, the free base **2** exhibits the highest value ($D = 9385 \text{ m s}^{-1}$). The detonation pressure (p_{CJ}) of 297 kbar lies in the range of the detonation pressures of the energetic salts, which have values between 269 and 315 kbar. The neutral compound **2** possess a lower detonation pressure than **RDX** ($p_{CJ\text{RDX}} = 345 \text{ kbar}$) but a significantly higher detonation velocity ($D_{\text{RDX}} = 8861 \text{ m s}^{-1}$). The detonation velocity of **4** ($D = 8814 \text{ m s}^{-1}$) is similar to that of **RDX**, whereas the detonation pressure ($p_{CJ} = 290 \text{ kbar}$) is slightly lower. The corresponding stable, nitrogen-rich guanidinium (G^+), aminoguanidinium, diaminoguanidinium, and triaminoguanidinium (TAG^+) salts all show lower detonation velocities ($D = 8201 [G^+\text{NT2O}]$ to $8768 \text{ m s}^{-1} [TAG^+\text{NT2O}]$) and detonation pressures ($p_{CJ} = 266 [G^+\text{NT2O}]$ to $294 \text{ kbar} [TAG^+\text{NT2O}]$) than **4**.^[3f] However, **4** has poorer energetic properties than highly energetic hydroxylammonium nitrotetrazolate-2*N*-oxide salt ($D = 9499 \text{ m s}^{-1}$; $p_{CJ} = 390 \text{ kbar}$).^[3f] The nitrate salt **6** exhibits a very high detonation velocity ($D = 9005 \text{ m s}^{-1}$), which is significantly higher than the detonation velocity of the highly energetic hydrazinium hydrate salt ($D = 8690 \text{ m s}^{-1}$) or the commonly used salt ammonium nitrate ($D = 5270 \text{ m s}^{-1}$).^[28] Unfortunately, the detonation pressure of **6** ($p_{CJ} = 302 \text{ kbar}$) is somewhat lower than that of **RDX** ($p_{CJ} = 345 \text{ kbar}$). The highly energetic compound **9** reveals promising energetic properties with a detonation velocity of 9242 m s^{-1} and the highest detonation pressure of the compounds studied ($p_{CJ} = 320 \text{ kbar}$). The detonation velocity is significantly higher than the detonation velocity of the dipotassium salt ($D = 8330 \text{ m s}^{-1}$) or **RDX** ($D = 8861 \text{ m s}^{-1}$), whereas the detonation pressure is in the same range as the detonation pressure of $K_2\text{DNABT}$ ($p_{CJ} = 317 \text{ kbar}$) and only slightly lower than the detonation pressure of **RDX**. Compound **11** reveals a relatively low detonation velocity ($D = 8760 \text{ m s}^{-1}$) and the lowest detonation pressure ($p_{CJ} = 269 \text{ kbar}$). These values are similar to the detonation pressure ($p_{CJ} = 273 \text{ kbar}$) and the detonation velocity ($D = 8770 \text{ m s}^{-1}$) of the corresponding triaminoguanidinium salt.^[16] The more-stable guanidinium, aminoguanidinium, and diaminoguanidinium salts all reveal lower values for the detonation velocity and detonation pressure.^[16]

Table 1. Energetic Properties and detonation parameters of compounds **2**, **4**, **5**, **6**, **9** and **11-14** compared to **RDX**.

	2	4	6	9	11	12	13	14	RDX
Formula	C ₃ H ₆ N ₈	C ₄ H ₇ N ₁₃ O ₃	C ₃ H ₇ N ₉ O ₃	C ₈ H ₁₄ N ₂₈ O ₄	C ₅ H ₁₀ N ₁₄ O ₂	C ₃ H ₇ N ₈ O ₄ Cl	C ₈ H ₁₄ N ₂₆	C ₈ H ₁₄ N ₂₆ O ₂	C ₃ H ₆ N ₆ O ₆
FW [g mol ⁻¹]	154.13	285.18	217.15	566.38	298.23	254.59	474.37	506.37	222.12
IS [J] ^a	40	25	40	7.5	8	9	20	30	7.5
FS [N] ^b	360	360	360	108	360	216	360	360	120
ESD [J] ^c	1.5	1.0	0.75	0.08	1.0	0.6	1.25	1.5	0.20
N [%] ^d	72.70	63.85	58.05	69.24	65.75	44.01	76.77	71.92	37.84
Ω [%] ^e	-93.43	-47.69	-47.89	-53.67	-69.75	-34.57	-77.58	-66.35	-21.61
T _{dec.} [°C] ^f	245	222	280	224	237	264	200	210	210
ρ [g cm ⁻³] (298K) ^g	1.725	1.732	1.779	1.759	1.654	1.775	1.724	1.731	1.806
Δ _f H° [kJ mol ⁻¹] ^h	446.7	691.7	261.5	1845.5	783.9	314.6	1811.8	1834.1	70.3
Δ _f U° [kJ kg ⁻¹] ⁱ	2872.0	2525.3	1312.7	3359.1	2736.7	1331.1	3924.0	3724.9	417.0
EXPLO5 V6.02 values:									
-Δ _E U° [kJ kg ⁻¹] ^j	3559	5040	4663	5170	4602	5072	4327	4926	5845
T _E [K] ^k	2284	3412	3062	3388	2970	3654	2776	3154	3810
p _{C-J} [kbar] ^l	297	290	302	320	269	281	307	315	345
D [m s ⁻¹] ^m	9385	8814	9005	9242	8760	8312	9360	9289	8861
V _o [L kg ⁻¹] ⁿ	813	835	870	834	845	817	811	824	785

a impact sensitivity (BAM drophammer, 1 of 6); b friction sensitivity (BAM friction tester, 1 of 6); c electrostatic discharge device (OZM); d nitrogen content; e oxygen balance; f decomposition temperature from DTA (β = 5°C); g recalculated from low temperature X-ray densities ($\rho_{298K} = \rho T / (1 + \alpha V(298 - T_0))$; $\alpha_V = 1.5 \cdot 10^{-4} \text{ K}^{-1}$); h in parenthesis values for the density obtained from the X-ray measurement at 298K; i calculated (CBS-4M) heat of formation; j calculated energy of formation; k energy of explosion; l explosion temperature; m detonation pressure; n detonation velocity; o assuming only gaseous products.

Perchlorate salt **12** had the lowest detonation velocity ($D = 8312 \text{ m s}^{-1}$) and a fairly low detonation pressure ($p_{CJ} = 281 \text{ kbar}$), therefore does not fulfill the requirements to replace **RDX**. In contrast, azotetrazolate **13** possesses the highest detonation velocity ($D = 9360 \text{ m s}^{-1}$), which greatly exceeds the detonation velocity of **RDX** and even of the highly energetic dihydrazinium salt ($D = 6330 \text{ m s}^{-1}$).^[29] Compound **14** exhibits a slightly lower detonation velocity ($D = 9289 \text{ m s}^{-1}$) than compound **13**, whereas the detonation pressure of **14** ($p_{CJ} = 315 \text{ kbar}$) is slightly higher than the detonation pressure of **13**. Compound **14** possesses a competitive detonation pressure compared to the corresponding highly energetic ammonium, hydroxylammonium, and hydrazinium salts,^[22] which exhibit high detonation pressures of 338, 375, and 329 kbar, respectively. The detonation velocities of the ammonium and hydrazinium salts ($D = 9032$ and 9066 m s^{-1} , respectively) are slightly lower, whereas the dihydroxylammonium salt exhibits the highest value ($D = 9348 \text{ m s}^{-1}$).^[22] **RDX** cannot compete with the detonation velocity of **14**, but has a slightly higher detonation pressure.

9.2.5 Toxicity Assessment

Neutral **2** and nitrate salt **6** exhibit high thermal stability, insensitivity towards impact and friction, as well as good energetic performances. The toxicity of **2** and **6** was determined by using the known method with *Vibrio fischeri* NRRL-B-11177.^[9] The half-maximal effective concentration (EC_{50}) of both compounds after 30 min of incubation time (**2**: 4.83 g L^{-1} ; **6**: 3.36 g L^{-1}) is much higher than toxic **RDX** (0.22 g L^{-1}) and also above the benchmark of 1.0 g L^{-1} at which a compound is considered non-toxic.

9.3 Conclusions

Crucially, a higher detonation velocity was calculated for **2**, **6**, **9**, **13**, and **14** than for **RDX**. It can be concluded from the results shown in Table 1 that all the compounds studied, except **9**, meet the required criteria for mechanical ($IS \geq 7.5 \text{ J}$, $FS \geq 120 \text{ N}$) or thermal ($T_{\text{dec.}} \geq 200 \text{ }^{\circ}\text{C}$) stimuli, which demonstrates the great advantage of this aromatic system that forms many hydrogen bonds. The most promising compounds for potential applications are **6** and the azotetrazolates **13** and **14**. Salts **6**, **13**, and **14** combine good stability with high calculated detonation velocities ($D \geq 9000 \text{ m s}^{-1}$) and detonation pressures ($p_{CJ} \approx 300 \text{ kbar}$).

It has been demonstrated that TATOT cation can be used as an inexpensive alternative to commonly used nitrogen-rich cations, such as guanidines and amines, due to several key features: stability towards high temperatures and mechanical stimuli, low (or no) toxicity, and

high energetic performance. These advantages make TATOT a next-generation energetic building block.

9.4 Experimental Section

Complete experimental section can be found in the Supporting Information.

Caution! All the compounds investigated are potentially explosive energetic materials, although no hazards were observed during the preparation and handling of these compounds. Nevertheless, this necessitates additional meticulous safety precautions (earthed equipment, Kevlar gloves, Kevlar sleeves, face shield, leather coat, and ear plugs).

3,6,7-Triamino-7H-[1,2,4]triazolo[4,3-*b*][1,2,4]triazole hydrochloride (**1c**)^[6]

Compound **1a** (70 g, 0.5 mol, 1.00 equiv) was dissolved in 2 M hydrochloric acid (750 mL). Cyanogen bromide (105.9 g, 1.0 mol, 2.00 equiv) was added and the solution was heated to 60 °C with stirring, then kept at 60 °C for 2 h. After heating the reaction mixture at reflux for 1 h the solution was cooled to 0 °C in an ice bath. At 0 °C, **1c** (50.3 g, 0.26 mol, 53%) was deposited as white plates.

¹H NMR ([D₆]DMSO): δ = 13.41 (br s, 1H, H-2), 8.22 (s, 2 H, H-9), 7.30 (s, 2 H, H-11), 5.84 ppm (s, 2 H, H-10); ¹³C NMR ([D₆]DMSO): δ = 160.2 (s, C-6), 147.4 (s, C-8), 141.1 ppm (s, C-3); MS *m/z* (FAB⁻): 35.0 (Cl⁻), *m/z* (FAB⁺): 155.2 (C₃H₆N₈⁺).

3,6,7-Triamino-7H-[1,2,4]triazolo[4,3-*b*][1,2,4]triazole (**2**)^[6]

Neutral compound **2** was obtained by neutralizing a solution of **1c** (50.3 g, 0.264 mol, 2.00 equiv) in water (500 mL) with sodium carbonate (14.0 g, 0.132 mol, 1.00 equiv). The solution was heated at reflux, then left to crystallize to give compound **2** (32.3 g, 0.210 mol, 80%).

DTA (5 °C min⁻¹) onset: 245 °C (dec.); **IR** (ATR, cm⁻¹): $\tilde{\nu}$ = 3411(w), 3298(m), 3181(m), 3141(m), 2735(w), 2361(w), 2339(w), 1616(vs), 1569(vs), 1502(s), 1403(m), 1346(m), 1293(m), 1241(w), 1158(w), 1106(m), 1078(w), 968(m), 946(m), 847(w), 729(w), 704(m), 667(w), 667(w), 659(w); **Raman** (1064 nm, 300 mW, 25 °C, cm⁻¹): $\tilde{\nu}$ = 3300(7), 3191(14), 3148(6), 1660(11), 1646(14), 1611(27), 1584(21), 1498(5), 1413(10), 1402(14), 1296(18), 1247(12), 1121(12), 1081(4), 984(7), 949(7), 852(44), 711(5), 677(21), 624(22), 604(26), 401(19), 306(22), 306(22), 177(10), 109(100); ¹H NMR ([D₆]DMSO): δ = 6.38 (s, 2 H, H-11), 5.59 (s, 2 H, H-10), 5.46 ppm (s, 2H, H-9); ¹³C NMR ([D₆]DMSO): δ = 158.5 (s, C-6), 149.1 (s, C-8), 143.5 ppm (s, C-3); MS *m/z* (DEI⁺): 154.1 (C₃H₆N₈); **EA** (C₃H₆N₈, 154.13)

calcd.: C 23.38, H 3.92, N 72.20%; found: C 23.67, H 3.85, N 72.20%; **Sensitivites**: IS: 40 J, FS: 360 N, ESD: 1.5 J (at grain sizes < 100 μm).

3,6,7-Triamino-7H-[1,2,4]triazolo[4,3-*b*][1,2,4]triazolium nitrotetrazole-2-oxide (4)

Ammonium nitrotetrazolate-2-oxide (296 mg, 2.00 mmol, 1.00 equiv)^[9] and **1 c** (381 mg, 2.00 mmol, 1.00 equiv) were dissolved in water and heated to 90 °C. The resulting clear solution was left to crystallize overnight to yield **4** (404 mg, 1.42 mmol, 71%) as yellow needles.

DTA (5 °C min⁻¹) onset: 222 °C (dec.); **IR** (ATR, cm⁻¹): $\tilde{\nu}$ = 3430(m), 3362(m), 3295(m), 3244(m), 3161(m), 3066(m), 2968(m), 2734(m), 2363(w), 2342(w), 1702(s), 1693(s), 1664(s), 1643(vs), 1604(m), 1552(s), 1529(s), 1471(s), 1457(m), 1422(vs), 1395(m), 1368(m), 1319(s), 1319(s), 1232(s), 1148(m), 1080(m), 1048(m), 1025(m), 1008(m), 976(m), 845(s), 799(w), 773(s), 723(m), 697(s), 658(w); **Raman** (1064 nm, 300 mW, 25 °C, cm⁻¹): $\tilde{\nu}$ = 3246(2), 1706(4), 1668(3), 1645(4), 1561(4), 1534(4), 1482(5), 1475(5), 1459(5), 1423(100), 1403(21), 1386(5), 1321(10), 1264(9), 1151(2), 1101(41), 1052(12), 1009(68), 978(3), 849(14), 764(4), 726(1), 682(2), 682(2), 624(10), 604(7), 492(5), 431(2), 396(7), 350(1), 309(5), 261(4), 242(5), 200(6), 171(14), 96(34), 74(14), 65(12); **¹H NMR** ([D₆]DMSO): δ = 13.37 (br s, 1 H, H-2), 8.21 (s, 2 H, H-9), 7.24 (s, 2H, H-11), 5.77 ppm (s, 2 H, H-10); **¹³C NMR** ([D₆]DMSO): δ = 160.2 (s, C-6), 157.2 (s, C_{Anion}), 147.4 (s, C-8), 141.1 ppm (s, C-3); **MS** m/z (FAB⁻): 130.0 (CN₅O₃⁻), m/z (FAB⁺): 155.2 (C₃H₇N₈⁺); **EA** (C₄H₇N₁₃O₃, 285.19) calcd.: C 16.85, H 2.47, N 63.85%; found: C 17.29, H 2.50, N 63.76%; **Sensitivites**: IS: 25 J, FS: 360 N, ESD: 1.0 J (at grain sizes 100–500 μm).

3,6,7-Triamino-7H-[1,2,4]triazolo[4,3-*b*][1,2,4]triazolium nitrate (6)

HNO₃ (2 M, 1 mL) was added to a suspension of **2** (2.0 mmol, 308 mg) in water (20 mL). The mixture was heated at reflux and the solution was left to stand. Compound **6** (400 mg, 1.84 mmol, 92%) crystallized as colorless plates.

DTA (5 °C min⁻¹) onset: 280 °C (dec.); **IR** (ATR, cm⁻¹): $\tilde{\nu}$ = 3348(m), 3290(m), 3223(m), 3166(m), 3134(m), 3053(m), 2998(m), 2873(m), 2745(m), 2362(m), 2342(m), 1773(vw), 1767(vw), 1698(m), 1670(s), 1634(vs), 1583(m), 1552(m), 1512(m), 1427(w), 1398(s), 1344(vs), 1300(s), 1300(s), 1163(m), 1073(m), 1050(m), 978(m), 912(s), 843(m), 819(m), 767(m), 724(w), 715(m), 700(m), 676(w), 668(w); **Raman** (1064 nm, 300 mW, 25 °C, cm⁻¹): $\tilde{\nu}$ = 3352(3), 3294(3), 3246(4), 3233(5), 3205(3), 1707(6), 1671(13), 1639(10), 1586(7), 1559(9), 1513(3), 1458(8), 1427(5), 1396(4), 1383(5), 1377(5), 1305(9), 1255(25), 1166(4),

1082(7), 1072(8), 1055(68), 914(3), 846(44), 718(11), 700(3), 680(9), 616(40), 603(19), 395(14), 336(5), 309(16), 255(9), 200(15), 164(47), 98(100); **¹H NMR** ([D₆]DMSO): δ = 13.31 (br s, 1 H, H-2), 8.20 (s, 2 H, H-9), 7.24 (s, 2 H, H-11), 5.78 ppm (s, 2 H, H-10); **¹³C NMR** ([D₆]DMSO): δ = 160.2 (s, C-6), 147.5 (s, C-8), 141.2 ppm (s, C-3); **MS** m/z (FAB⁻): 62.0 (NO₃⁻), m/z (FAB⁺): 155.0 (C₃H₇N₈⁺); **EA** (C₃H₇N₉O₃, 217.15) calcd.: C 16.59, H 3.25, N 58.05%; found: C 16.87, H 3.22, N 57.81%; **Sensitivities**: IS: 40 J, FS: 360 N, ESD: 0.75 J (at grain sizes 100–500 μ m).

9.5 References

- [1] a) J. P. Agrawal, *High Energy Materials: Propellants, Explosives and Pyrotechnics*, Wiley-VCH, 1st ed., Weinheim, **2010**; b) C. B. Jones, R. Haiges, T. Schroer, K. O. Christe, *Angew. Chem. Int. Ed.* **2006**, *45*, 4981–4984; *Angew. Chem.* **1999**, *111*, 2112–2118; c) R. P. Singh, R. D. Verma, D. T. Meshri, J. M. Shreeve, *Angew. Chem. Int. Ed.* **2006**, *45*, 3584–3601; *Angew. Chem.* **2006**, *118*, 3664–3682; d) J. Zhang, J. M. Shreeve, *J. Am. Chem. Soc.* **2014**, *136*, 4437–4445; e) Y. Li, C. Qi, S. Li, H. Zhang, C. Sun, Y. Yu, S. Pang, *J. Am. Chem. Soc.* **2010**, *132*, 12172–12173.
- [2] a) J. Giles, *Nature* **2004**, *427*, 580–581; b) M. B. Talawar, R. Sivabalan, T. Mukundan, H. Muthurajan, A. K. Sikder, B. R. Gandhe, A. Subhananda Rao, *J. Hazard. Mat.* **2008**, *161*, 589–607.
- [3] a) S. Venkatachalam, G. Santhosh, K. N. Ninan, *Propellants Explos. Pyrotech.* **2004**, *29*, 178–187; b) Karl. O. Christe, W. W. Wilson, M. A. Petrie, H. H. Michels, J. C. Bottaro, R. Gilardi, *Inorg. Chem.* **1996**, *35*, 5068–5071; c) H. Östmark, A. Helte, T. Carlsson, R. Adolfsson, L. Bodin, C. Eldstätter, H. Edvinsson, J. Lundgreen, H. Örnhed, FOI Technical Report, N-guanylurea dinitramide (FOX-12): properties **2007**, FOI-R–2312—SE; d) T. M. Klapötke, P. Mayer, A. Schulz, J. J. Weigand, *J. Am. Chem. Soc.* **2005**, *127*, 2032–2033; e) A. Hammerl, M. A. Hiskey, G. Holl, T. M. Klapötke, K. Polborn, J. Stierstorfer, J. J. Weigand, *Chem. Mater.* **2005**, *17*, 3787–3793; f) M. Göbel, K. Karaghiosoff, T. M. Klapötke, D. G. Piercey, J. Stierstorfer, *J. Am. Chem. Soc.* **2010**, *132*, 17216–17226; g) J. C. Bottaro, M. Petrie, P. E. Penwell, A. L. Dodge, R. Malhotra, NANA/HEDM Technology: Late Stage Exploratory Effort, Report No. A466714; SRI International: Menlo Park, CA, **2003**; h) N. Fischer, D. Fischer, T. M. Klapötke, D. G. Piercey, J. Stierstorfer, *J. Mater. Chem.* **2012**, *22*, 20418–20422; i) P. F. Pagoria, G. S. Lee, A. R. Mitchell, R. D. Schmidt, *Thermochimica Acta* **2002**, *384*, 187–204; j) V. Thottempudi, F. Forohor, D. A. Parrish, J. M. Shreeve, *Angew. Chem. Int. Ed.* **2012**, *51*,

- 9881–9885; *Angew. Chem.* **2012**, 124, 10019–10023; k) T. M. Klapötke, P. C. Schmid, S. Schnell, J. Stierstorfer, *J. Mater. Chem. A* **2015**, 3, 2658–2668; l) J. Zhang, D. A. Parrish, J. M. Shreeve, *Chem. Asian J.* **2014**, 9, 2953–2960.
- [4] a) R. Wang, H. Xu, Y. Guo, R. Sa, J. M. Shreeve, *J. Am. Chem. Soc.* **2010**, 132, 11904–11905; b) V. Thottempudi, J. M. Shreeve, *J. Am. Chem. Soc.* **2011**, 133, 19982–19992; c) Y. Guo, G. H. Tao, Z. Zeng, H. Gao, J. M. Shreeve, *Chem. Eur. J.* **2010**, 16, 3753–3762.
- [5] a) L. Liang, K. Wang, C. Bian, L. Ling, Z. Zhou, *Chem. Eur. J.* **2013**, 19, 14902–14910; b) C. Bian, M. Zhang, C. Li, Z. Zhou, *J. Mat. Chem* **2014**, 3, 163–169; c) Y.-H. Joo, B. Twamley, S. Garg, J. M. Shreeve, *Angew. Chem. Int. Ed.* **2008**, 47, 6236–6239; *Angew. Chem.* **2008**, 120, 6332–6335.
- [6] K. T. Potts, C. Hirsch, *J. Org. Chem.* **1968**, 33, 143–150.
- [7] R. C. Centore, S. Fusco, A. Capobianco, V. Piccialli, S. Zaccaria, A. Peluso, *Eur. J. Org. Chem.* **2013**, 3721–3728.
- [8] CCDC-1045074 (**2**), 1045070 (**4**), 1045069 (**5**), 1045073 (**6**), 1045071 (**8**), 1045067 (**9**), 1045072 (**11**), 1045068 (**12**), 1045066 (**13**), and 1045065 (**14**) contain the supplementary crystallographic data for this paper. These data can be obtained free of charge from The Cambridge Crystallographic Data Centre via www.ccdc.cam.ac.uk/data_request/cif.
- [9] A. Dippold, T. M. Klapötke, *Chem Eur. J.* **2012**, 18, 16742–16753.
- [10] T. M. Klapötke, P. Mayer, C. M. Sabaté, J. M. Welch, N. Wiegand, *Inorg. Chem.* **2008**, 47, 6014–6027.
- [11] A. Katrusiak, *Acta Crystallogr. Sect. C* **1994**, C50, 1161–1163.
- [12] A. Rheingold, J. Cronin, T. Brill, *Acta Crystallogr. Sect. C* **1987**, C43, 402–404.
- [13] N. Fischer, T. M. Klapötke, M. Reymann, J. Stierstorfer, *Eur. J. Inorg. Chem.* **2013**, 2167–2180.
- [14] D. Fischer, T. M. Klapötke, J. Stierstorfer, *Angew. Chem. Int. Ed.* **2014**, 53, 8172–8175; *Angew. Chem.* **2014**, 126, 8311–8314.
- [15] D. Fischer, private communication.
- [16] T. M. Klapötke, J. Stierstorfer, A. Wallek, *Chem. Mater.* **2008**, 20, 4519–4530.

- [17] J. Lundgren, R. Liminga, *Acta Crystallogr. Sect. B* **1979**, B35, 1023–1027.
- [18] B. Dickens, *Acta Crystallogr. Sect. B* **1969**, B25, 1875–1882.
- [19] H. Gao, C. Ye, C. Piekarski, C. M. Piekarski, J. M. Shreeve, *J. Phys. Chem. C* **2007**, 111, 10718–10731.
- [20] A. Hammerl, G. Holl, M. Kaiser T. M. Klapötke, P. Mayer, H. Nöth, H. Piotrowski, M. Sluter, *Z. Naturforsch. Sect. B* **2001**, 56B, 857–870.
- [21] N. Fischer, K. Hüll, T. M. Klapötke, J. Stierstorfer, G. Laus, M. Hummel, *Dalton Trans.* **2012**, 41, 11201–11211.
- [22] D. Fischer, T. M. Klapötke, D. G. Piercey, J. Stierstorfer, *Chem. Eur. J.* **2013**, 19, 4602–4613.
- [23] (a) J. W. Ochterski, G. A. Petersson, and J. A. Montgomery Jr., *J. Chem. Phys.* **1996**, 104, 2598; (b) J. A. Montgomery Jr., M. J. Frisch, J. W. Ochterski G. A. Petersson, *J. Chem. Phys.* **2000**, 112, 6532; c) M. Hesse, H. Meier, B. Zeeh, *Spektroskopische Methoden in der Organischen Chemie*, 7th ed., Thieme, Stuttgart, New York, **2005**. d) G. Socrates, *Infrared and Raman Characteristic Group Frequencies: Tables and Charts*, 3rd ed., John Wiley & Sons, Chichester, **2004**.
- [24] Y. Murtim, R. Agnihotri, D. Pathak, *Am. J. of Chem.* **2011**, 1, 42–46.
- [25] M. Sućeska, EXPLO5 V6.02 program, Zagreb, Croatia, **2014**.
- [26] Muhamed Sućeska, private communication.
- [27] C. Xue, J. Sun, B. Kang, Y. Liu, X. Liu, G. Song, Q. Xue, *Propellants Explos. Pyrotech.* **2010**, 35, 333–338.
- [28] J. Köhler, *Explosivstoffe*, 9th ed., Wiley-VCH, New York, **1998**, 166.
- [29] A. Hammerl, T. M. Klapötke, H. Nöth, M. Warchhold, *Inorg. Chem.* **2001**, 40, 3570–3575.

9.6 Supplementary information

The analytical methods and general procedures are described in the appendix of this thesis.

9.6.1 Experimental work

Figure S1 shows the atom labeling for the NMR resonance assignments of compound **2**^[1] and the cation of **3–14**. Figure S2 is displayed to give a quick overview over compounds **1–14**

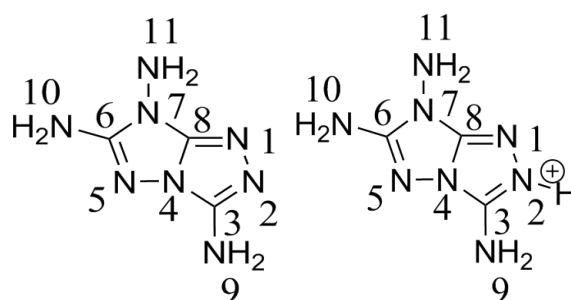


Figure S1. Chemical structures of 3,6,7-triamino-7H-[1,2,4]triazolo[4,3-b][1,2,4]triazole and 3,6,7-triamino-7H-[1,2,4]triazolo[4,3-b][1,2,4]triazolium.

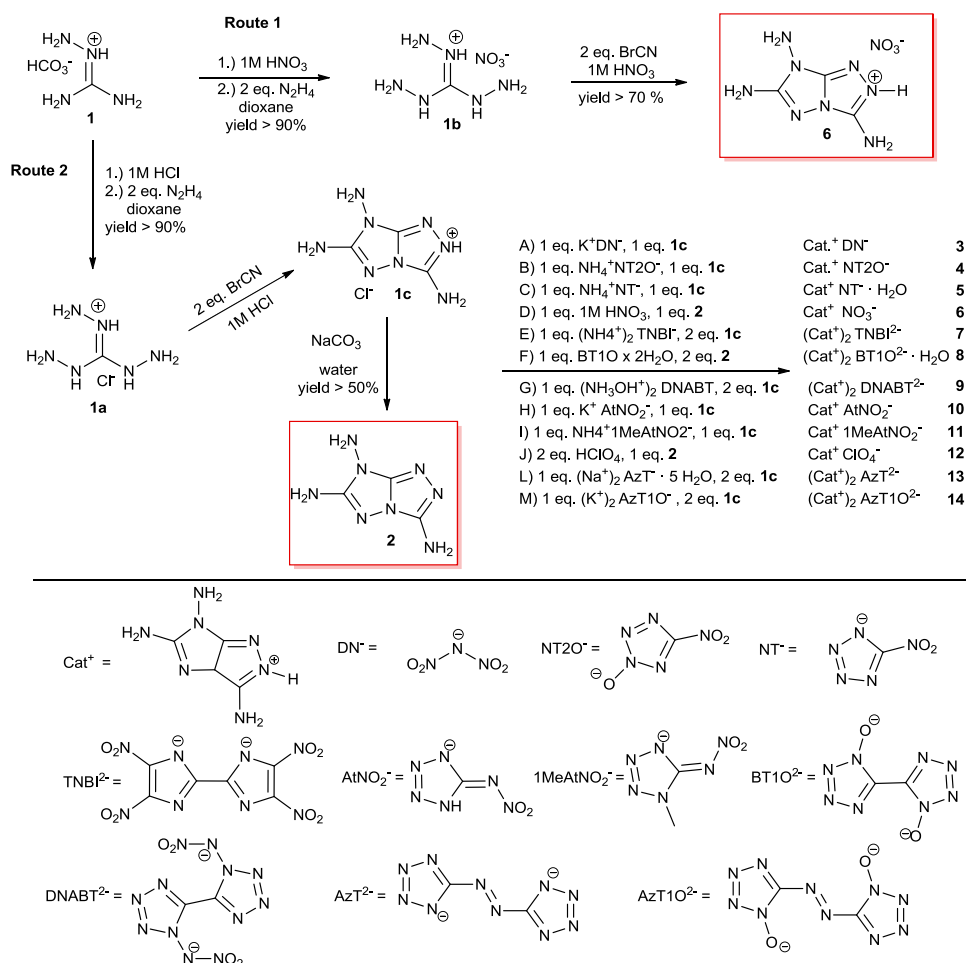


Figure S2. Synthetic pathway towards nitrate **6** (route 1, total yield > 60%) and compounds **2–14** (route 2).

The synthesis of compounds **1c**, **2**, **4** and **6** is described in Chapter 9.4.

3,6,7-Triamino-7*H*-[1,2,4]triazolo[4,3-*b*][1,2,4]triazolium dinitramide (**3**)

3,6,7-Triamino-7*H*-[1,2,4]triazolo[4,3-*b*][1,2,4]triazole monohydrochloride (**1c**) (190 mg, 1.00 mmol, 1.00 eq.) and potassium dinitramide (145 mg, 1.00 mmol, 1.00 eq.) were dissolved in boiling ethanol forming a white precipitate of potassium chloride. The boiling suspension was filtered to remove the potassium chloride from the reaction mixture. The resulting clear solution was left to crystallize yielding compound **3** as a slightly brownish powder. Yield: 136 mg, 0.52 mmol, 52%. Recrystallization in solvents such as water, ethanol, methanol and DMF did not yield single crystals suitable for X-Ray diffraction.

DTA (5 °C min⁻¹) onset: 197 °C; **IR** (ATR, cm⁻¹): $\tilde{\nu}$ = 3371(m), 3343(m), 3282(m), 3237(m), 3116(m), 2953(m), 2749(w), 1995(w), 1694(s), 1659(s), 1638(vs), 1579(m), 1551(m), 1515(vs), 1504(vs), 1437(m), 1419(s), 1301(w), 1258(w), 1202(s), 1173(vs), 1058(w), 1031(s), 1031(s), 1011(s), 978(s), 965(s), 939(m), 862(m), 840(m), 816(m), 762(m), 749(m), 720(m), 700(m); **Raman** (1064 nm, 300 mW, 25 °C, cm⁻¹): $\tilde{\nu}$ = 3252(5), 1708(7), 1667(7), 1640(10), 1559(8), 1511(7), 1486(3), 1440(12), 1382(6), 1318(61), 1256(37), 1171(5), 1150(5), 1090(4), 1060(6), 1035(6), 1015(6), 990(5), 969(16), 915(2), 901(2), 842(25), 819(18), 819(18), 759(2), 720(3), 678(7), 610(25), 558(2), 495(15), 471(2), 450(4), 392(10), 319(12), 307(12), 252(12), 194(11), 159(51), 92(100); **¹H NMR** ([D₆]DMSO): δ = 13.32 (br s, 1 H, H-2), 8.19 (s, 2 H, H-9), 7.23 (s, 2 H, H-11), 5.76 ppm (s, 2 H, H-10); **¹³C NMR** ([D₆]DMSO): δ = 160.2 (s, C-6), 147.4 (s, C-8), 141.1 ppm (s, C-3); **MS** m/z (FAB⁻): 106.1 (N₃O₄⁻), m/z (FAB⁺): 155.3 (C₃H₇N₈⁺); **EA** (C₃H₇N₁₁O₄, 261.16) calcd.: C 13.80, H 2.70, N 59.00%; found: C 14.16, H 2.78, N 57.34%; **Sensitivities**: IS: 4 J, FS: 288 N, ESD: 0.8 J (at grain sizes < 100 μ m).

3,6,7-Triamino-7*H*-[1,2,4]triazolo[4,3-*b*][1,2,4]triazolium nitrotetrazolate monohydrate (**5**)

3,6,7-Triamino-7*H*-[1,2,4]triazolo[4,3-*b*][1,2,4]triazole monohydrochloride (**1c**) (381 mg, 2.00 mmol, 1.00 eq.) and ammonium nitrotetrazolate (264 mg, 2.00 mmol, 1.00 eq.) were dissolved in water under heating. The solution was left to crystallize yielding the energetic compound **5** in form of yellow crystals. Yield: 447 mg, 1.66 mmol, 83%.

DTA (5 °C min⁻¹) onset: 154 °C (-H₂O), 232 °C (dec.); **IR** (ATR, cm⁻¹): $\tilde{\nu}$ = 3440(m), 3347(m), 3274(m), 3250(m), 3157(m), 3103(s), 3004(m), 2913(m), 2759(m), 2363(w), 2243(w), 2106(w), 1685(s), 1644(vs), 1608(m), 1580(s), 1524(s), 1507(s), 1444(s), 1424(s), 1382(m), 1319(s), 1194(m), 1194(m), 1174(m), 1127(w), 1057(m), 1037(m), 1017(m),

922(s), 834(s), 786(m), 731(w), 720(vw), 681(m); **Raman** (1064 nm, 300 mW, 25 °C, cm⁻¹): $\tilde{\nu}$ = 3179(2), 1698(5), 1663(7), 1610(3), 1536(6), 1510(3), 1448(10), 1425(100), 1403(5), 1385(5), 1321(7), 1305(6), 1279(3), 1263(11), 1196(3), 1176(4), 1108(4), 1071(35), 1058(24), 1041(10), 927(2), 841(16), 773(3), 773(3), 721(2), 662(4), 628(8), 601(13), 540(3), 456(3), 415(8), 385(1), 327(5), 248(4), 210(4), 172(7), 129(55), 113(51), 73(8); **¹H NMR** ([D₆]DMSO): δ = 13.32 (br s, 1 H, H-2), 8.21 (s, 2 H, H-9), 7.24 (s, 2H, H-11), 5.77 ppm (s, 2 H, H-10); **¹³C NMR** ([D₆]DMSO): δ = 168.7 (s, C_{Anion}), 160.1 (s, C-6), 147.4 (s, C-8), 141.0 ppm (s, C-3); **MS** m/z (FAB⁻): 114.1 (CN₅O₂⁻), m/z (FAB⁺): 155.0 (C₃H₇N₈⁺); **EA** (C₄H₉N₁₃O₃, 287.20) calcd.: C 16.73, H 3.16, N 63.40%; found: C 17.20, H 3.07, N 63.32%; **Sensitivities**: IS: 20 J, FS: 360 N, ESD: 1 J (at grain sizes 100–500 μm).

3,6,7-Triamino-7H-[1,2,4]triazolo[4,3-*b*][1,2,4]triazolium tetranitrobiimidazolate (7)

3,6,7-Triamino-7H-[1,2,4]triazolo[4,3-*b*][1,2,4]triazole monohydrochloride (**1c**) (762 mg, 4.00 mmol, 2.00 eq.) and diammonium tetranitrobiimidazolate (696 mg, 2.00 mmol, 1.00 eq.).^[2] The suspension was refluxed, giving a clear yellowish solution. The solution was left to crystallize over night. The energetic compound **7** was received as a yellow solid. Yield: 484 mg, 0.78 mmol, 39%.

DTA (5 °C min⁻¹) onset: 275 °C (dec.); **IR** (ATR, cm⁻¹): $\tilde{\nu}$ = 3433(w), 3395(w), 3371(w), 3331(m), 3276(m), 3248(m), 3221(m), 3175(m), 3095(m), 2670(w), 2361(w), 2341(w), 1687(m), 1657(s), 1649(s), 1634(vs), 1583(m), 1552(w), 1529(m), 1518(m), 1492(s), 1470(s), 1377(vs), 1377(vs), 1346(m), 1324(m), 1302(s), 1264(m), 1206(vs), 1167(m), 1110(m), 1031(m), 1016(m), 978(w), 943(m), 893(w), 855(m), 840(w), 809(s), 753(w), 726(m), 704(s), 684(m); **Raman** (1064 nm, 300 mW, 25 °C, cm⁻¹): $\tilde{\nu}$ = 1699(1), 1668(2), 1559(100), 1541(17), 1530(8), 1491(6), 1475(23), 1395(10), 1378(6), 1346(13), 1299(45), 1266(11), 1224(42), 1213(58), 1108(5), 1068(3), 1017(13), 942(2), 867(15), 842(3), 814(1), 771(3), 757(5), 757(5), 692(3), 620(4), 524(2), 451(2), 404(5), 394(5), 323(2), 313(2), 261(2), 250(2), 206(4), 199(5), 174(4), 91(13), 73(12); **¹H NMR** ([D₆]DMSO): δ = 8.29 (s, 2 H, H-9), 7.23 (s, 2H, H-11), 5.79 ppm (s, 2 H, H-10); **¹³C NMR** ([D₆]DMSO): δ = 160.1 (s, C-6), 147.4 (s, C-8), 144.2 (s, C-NO₂ Anion), 141.2 (s, C-3), 140.4 ppm (s, C-C_{Anion}); **MS** m/z (FAB⁻): 313.0 (C₆HN₈O₈⁻), m/z (FAB⁺): 155.0 (C₃H₇N₈⁺); **EA** (C₁₂H₁₄N₂₄O₈, 622.40) calcd.: C 23.16, H 2.27, N 54.01%; found: C 23.44, H 2.37, N 53.96%; **Sensitivities**: IS: 25 J, FS: 360 N, ESD: 0.6 J (at grain sizes < 100 μm).

Di-3,6,7-triamino-7H-[1,2,4]triazolo[4,3-*b*][1,2,4]triazolium bitetrazole-1,1'-dioxide dihydrate (8)

A suspension of 3,6,7-triamino-7*H*-[1,2,4]triazolo[4,3-*b*][1,2,4]triazole (**2**) (616 mg, 4.00 mmol, 2.00 eq.) and 1*H*,1*H'*-[5,5'-bi-1,1'-hydroxytetrazole] (340 mg, 2.00 mmol, 1.00 eq.)^[3] in water was heated until all starting material was dissolved. The resulting clear solution was left to crystallize over night, yielding compound **8** as colorless crystals. Yield: 551 mg, 1.15 mmol, 58%.

DTA (5 °C min⁻¹) onset: 169 °C (–H₂O), 255 °C (dec.); **IR** (ATR, cm⁻¹): $\tilde{\nu}$ = 3492(m), 3406(m), 3319(s), 3111(m), 2853(m), 2725(m), 2361(m), 2341(m), 1692(s), 1677(s), 1657(vs), 1632(s), 1613(vs), 1574(s), 1514(m), 1469(w), 1422(s), 1343(s), 1272(w), 1227(s), 1168(m), 1107(w), 1070(m), 1070(m), 1049(m), 1000(m), 974(m), 844(m), 803(m), 726(s), 706(s), 675(w); **Raman** (1064 nm, 300 mW, 25 °C, cm⁻¹): $\tilde{\nu}$ = 3325(2), 3119(2), 1686(7), 1663(9), 1611(100), 1587(5), 1577(3), 1509(2), 1462(5), 1426(2), 1384(5), 1355(2), 1302(5), 1270(9), 1232(40), 1150(27), 1130(11), 1118(6), 1009(10), 980(2), 851(21), 782(11), 739(3), 739(3), 687(5), 635(17), 620(5), 602(9), 422(7), 412(10), 334(6), 286(6), 258(4), 197(5), 173(8), 128(32), 117(37), 96(42), 89(37), 79(36); **¹H NMR** ([D₆]DMSO): δ = 7.59 (br s, 2 H, H–9), 7.01 (s, 4 H, H–11), 5.73 ppm (br s, 2 H, H–10); **¹³C NMR** ([D₆]DMSO): δ = 159.8 (s, C–6), 147.9 (s, C–8), 142.1 (s, C–3), 135.0 ppm (s, C–C_{Anion}); **MS** *m/z* (FAB[–]): 169.0 (C₂HN₈O₂[–]), *m/z* (FAB⁺): 155.3 (C₃H₇N₈⁺); **EA** (C₈H₁₆N₂₄O₃, 496.38): C 19.36, H 3.25, N 67.72%; found: C 19.11, H 3.45, N 65.16%; **Sensitivities**: IS: 35 J, FS: 360 N, ESD: 1.5 J (at grain sizes 100–500 μm).

Di-3,6,7-triamino-7*H*-[1,2,4]triazolo[4,3-*b*][1,2,4]triazolium 1,1'-dinitramino-5,5'-bitetrazolate (9**)**

3,6,7-Triamino-7*H*-[1,2,4]triazolo[4,3-*b*][1,2,4]triazole monohydrochloride (**1c**) (381 mg, 1.00 mmol, 1.00 eq.) and dihydroxylammonium 1,1'-dinitramino-5,5'-bitetrazolate (324 mg, 1.00 mmol, 1.00 eq.)^[4] were suspended and heated until a clear solution was formed. The solution was left to crystallize yielding compound **9** as colorless crystals. Yield: 346 mg, 0.61 mmol, 61%.

DTA (5 °C min⁻¹) onset: 224 °C (dec.); **IR** (ATR, cm⁻¹): $\tilde{\nu}$ = 3398(m), 3328(m), 3244(m), 3217(m), 3152(m), 2361(m), 2340(m), 1682(s), 1658(vs), 1651(vs), 1596(m), 1555(w), 1536(w), 1449(w), 1380(s), 1358(s), 1294(vs), 1264(s), 1165(w), 1131(m), 1038(w), 1013(m), 914(m), 914(m), 873(m), 838(m), 773(w), 709(m), 696(m), 670(w); **Raman** (1064 nm, 300 mW, 25 °C, cm⁻¹): $\tilde{\nu}$ = 3331(5), 3246(9), 1696(9), 1656(11), 1625(9), 1610(77), 1597(8), 1584(7), 1546(3), 1514(3), 1447(16), 1429(5), 1305(7), 1295(5), 1279(33), 1255(32), 1150(7), 1090(17), 1049(4), 1037(4), 1024(41), 1008(3), 991(7), 991(7),

916(2), 891(4), 841(20), 748(4), 725(5), 699(3), 665(10), 631(5), 618(21), 599(18), 514(13), 456(4), 402(11), 380(5), 317(12), 302(10), 262(9), 244(4), 140(50), 126(49), 111(38), 95(100), 83(75); **¹H NMR** ([D₆]DMSO): δ = 13.29 (br s, 2H, H-2), 8.20 (s, 4H, H-9), 7.23 (s, 4 H, H-11), 5.77 ppm (s, 4 H, H-10); **¹³C NMR** ([D₆]DMSO): δ = 160.2 (s, C-6), 147.4 (s, C-8), 141.1 (s, C-3), 140.4 ppm (s, C-C_{Anion}); **MS** m/z (FAB⁻): 257.3 (C₂HN₂₂O₄⁻), m/z (FAB⁺): 155.0 (C₃H₇N₈⁺); **EA** (C₈H₁₄N₂₈O₄, 566.39) calcd.: C 16.96, H 2.49, N 69.24%; found: C 17.04, H 2.51, N 69.10%; **Sensitivities**: IS: 7.5 J, FS: 108 N, ESD: 80 mJ (at grain sizes < 100 μ m).

3,6,7-Triamino-7H-[1,2,4]triazolo[4,3-*b*][1,2,4]triazolium nitriminotetrazolate (10)

A clear solution of potassium 5-nitriminotetrazolate (336 mg, 2.00 mmol, 1.00 eq.)^[5] and 3,6,7-triamino-7H-[1,2,4]triazolo[4,3-*b*][1,2,4]triazole monohydrochloride (**1c**) (381 mg, 2.00 mmol, 1.00 eq.) in hot water was prepared. The solution was left to crystallize overnight yielding colorless crystals of compound **10**. Yield: 476 mg, 1.67 mmol, 83%.

DTA (5 °C min⁻¹) onset: 235 °C (dec.); **IR** (ATR, cm⁻¹): $\tilde{\nu}$ = 3362(m), 3168(m), 2361(m), 2338(m), 1694(s), 1652(vs), 1516(s), 1451(w), 1416(s), 1338(s), 1316(vs), 1232(s), 1146(w), 1097(w), 1055(s), 1023(m), 998(m), 978(m), 867(m), 847(m), 771(w), 747(w), 720(w), 720(w), 701(m), 668(w); **Raman** (1064 nm, 300 mW, 25 °C, cm⁻¹): $\tilde{\nu}$ = 3288(3), 3199(3), 1700(4), 1667(4), 1651(5), 1592(5), 1531(100), 1452(6), 1424(6), 1404(5), 1376(12), 1352(11), 1344(11), 1325(21), 1293(3), 1254(14), 1151(5), 1101(4), 1079(4), 1061(6), 1035(27), 1006(23), 872(4), 872(4), 849(17), 738(5), 701(2), 683(3), 616(9), 603(8), 495(2), 426(10), 395(7), 382(5), 341(3), 335(4), 319(7), 243(8), 102(65), 90(75); **¹H NMR** ([D₆]DMSO): δ = 8.20 (s, 2H, H-9), 7.24 (s, 2H, H-11), 5.78 ppm (s, 2H, H-10); **¹³C NMR** ([D₆]DMSO): δ = 160.2 (s, C-6), 157.9 (s, C_{Anion}), 147.4 (s, C-8), 141.1 ppm (s, C-3); **MS** m/z (FAB⁻): 129.2 (CHN₆O₂⁻), m/z (FAB⁺): 155.0 (C₃H₇N₈⁺); **EA** (C₄H₈N₁₄O₂, 284.20) calcd.: C 16.90, H 2.84, N 69.00%; found: C 16.83, H 3.10, N 66.67%; **Sensitivities**: IS: 15 J, FS: 360 N, ESD: 0.7 J (at grain sizes 100–500 μ m).

3,6,7-Triamino-7H-[1,2,4]triazolo[4,3-*b*][1,2,4]triazolium 1-methyl-5-nitriminotetrazolate (11)

3,6,7-Triamino-7H-[1,2,4]triazolo[4,3-*b*][1,2,4]triazole monohydrochloride (**1c**) (381 mg, 2.00 mmol, 1.00 eq.) and ammonium 1-methyl-5-nitriminotetrazolate (322 mg, 2.00 mmol, 1.00 eq.)^[6] were dissolved in hot water and left to crystallize over night yielding compound **11** as colorless crystals. Yield: 252 mg 0.84 mmol, 42%.

DTA (5 °C min⁻¹) onset: 235 °C (dec.); **IR** (ATR, cm⁻¹): $\tilde{\nu}$ = 3425(m), 3389(m), 3337(m), 3257(m), 3096(m), 2694(m), 2361(m), 2340(m), 1688(s), 1672(s), 1651(vs), 1631(s), 1557(m), 1512(s), 1464(s), 1454(m), 1418(m), 1408(m), 1388(s), 1359(s), 1344(s), 1315(vs), 1295(vs), 1295(vs), 1257(s), 1232(m), 1169(m), 1109(m), 1093(m), 1060(m), 1037(m), 988(m), 935(s), 880(m), 842(s), 773(w), 751(vw), 738(w), 724(m), 708(m), 691(m), 668(w); **Raman** (1064 nm, 300 mW, 25 °C, cm⁻¹): $\tilde{\nu}$ = 3271(2), 3224(4), 3107(4), 3097(3), 3086(3), 3042(4), 2960(9), 1698(12), 1674(4), 1646(12), 1630(8), 1568(6), 1547(7), 1518(89), 1466(23), 1420(10), 1409(10), 1402(7), 1388(10), 1378(9), 1326(13), 1300(39), 1261(30), 1261(30), 1242(10), 1172(2), 1113(22), 1101(15), 1071(7), 1063(8), 1038(74), 990(5), 976(5), 939(3), 882(15), 845(32), 754(16), 740(4), 724(4), 694(25), 669(7), 621(34), 601(16), 499(14), 459(7), 402(19), 370(9), 351(4), 309(17), 291(24), 268(8), 239(19), 204(6), 172(10), 125(62), 102(82), 87(90), 73(100); **¹H NMR** ([D₆]DMSO): δ = 8.19 (s, 2 H, H-9), 7.24 (s, 2H, H-11), 5.79 (s, 2H, H-10), 3.67 ppm (s, 3 H, -CH₃); **¹³C NMR** ([D₆]DMSO): δ = 160.2 (s, C-6), 157.2 (s, C_{Anion}), 147.5 (s, C-8), 141.2 (s, C-3), 32.7 ppm (s, -CH₃); **MS** m/z (FAB⁻): 143.0 (C₂H₃N₆O₂⁻), m/z (FAB⁺): 155.2 (C₃H₇N₈⁺); **EA** (C₅H₁₀N₁₄O₂, 298.23) calcd.: C 20.14, H 3.38, N 65.75%; found: C 20.42, H 3.35, N 65.76%; **Sensitivities**: IS: 8 J, FS: 360 N, ESD: 1 J (at grain sizes < 100 μ m).

3,6,7-Triamino-7H-[1,2,4]triazolo[4,3-*b*][1,2,4]triazolium perchlorate (**12**)

3,6,7-Triamino-7H-[1,2,4]triazolo[4,3-*b*][1,2,4]triazole (**2**) (308 mg, 2.00 mmol, 1 eq.) was dissolved in water. 2 mL 1 M perchloric acid was added and the solution was left to crystallize over night yielding compound **12** in form of colorless crystals. Yield: 423 mg, 1.66 mmol, 83%.

DTA (5 °C min⁻¹) onset: 264 °C (dec.); **IR** (ATR, cm⁻¹): $\tilde{\nu}$ = 3380(m), 3310(m), 3263(m), 3185(m), 2361(w), 2341(w), 1687(m), 1654(s), 1567(m), 1511(w), 1446(w), 1402(w), 1325(w), 1264(w), 1162(vw), 1074(vs), 1028(s), 878(m), 844(m), 726(m), 713(m), 685(m), 669(w), 669(w); **Raman** (1064 nm, 300 mW, 25 °C, cm⁻¹): $\tilde{\nu}$ = 3408(3), 3382(3), 3311(10), 3264(8), 3201(6), 1697(10), 1650(31), 1603(5), 1574(16), 1515(5), 1446(8), 1413(12), 1401(12), 1366(3), 1305(18), 1265(79), 1161(4), 1101(9), 1065(10), 1008(4), 981(7), 936(73), 874(2), 874(2), 848(37), 805(2), 787(2), 727(5), 703(5), 680(12), 607(39), 534(3), 468(19), 426(4), 400(22), 321(20), 261(5), 219(4), 178(9), 107(100); **¹H NMR** ([D₆]DMSO): δ = 13.29 (br s, 1 H, H-2), 8.20 (s, 2 H, H-9), 7.22 (s, 2 H, H-11), 5.75 ppm (s, 2 H, H-10); **¹³C NMR** ([D₆]DMSO): δ = 160.2 (s, C-6), 147.5 (s, C-8), 141.2 ppm (s, C-3); **MS** m/z (FAB⁻): 99.0 (ClO₄⁻), m/z (FAB⁺): 155.2 (C₃H₇N₈⁺); **EA** (C₃H₇ClN₈O₄, 254.59) calcd.: C

14.15, H 2.77, N 44.01%; found: C 14.45, H 2.75, N 43.91%; **Sensitivities**: IS: 9 J, FS: 216 N, ESD: 0.6 J (at grain sizes 500–1000 μm).

3,6,7-Triamino-7*H*-[1,2,4]triazolo[4,3-*b*][1,2,4]triazolium 5,5'-azotetrazolate (13)

3,6,7-Triamino-7*H*-[1,2,4]triazolo[4,3-*b*][1,2,4]triazole monohydrochloride (**1c**) (381 mg, 2.00 mmol, 1.00 eq.) and sodium 5,5'-azotetrazolate pentahydrate (300 mg, 1.00 mmol, 1 eq.) were suspended in water. The suspension was heated until all solid materials were dissolved and a clear solution was formed. The solution was left to crystallize, yielding energetic salt **13** in form of yellow crystals. Yield: 285 mg, 0.60 mmol, 60%.

DTA (5 $^{\circ}\text{C min}^{-1}$) onset: 200 $^{\circ}\text{C}$ (dec.); **IR** (ATR, cm^{-1}): $\tilde{\nu}$ = 3360(m), 3275(m), 3198(m), 3087(s), 2761(m), 2247(m), 2131(m), 2106(m), 1713(s), 1676(vs), 1651(vs), 1592(s), 1507(s), 1445(s), 1423(m), 1381(s), 1307(m), 1198(m), 1160(m), 1124(m), 1093(m), 1080(w), 1048(m), 1048(m), 1032(m), 1001(m), 869(m), 850(m), 838(m), 782(w), 770(m), 732(w), 721(m), 710(m), 668(w); **Raman** (1064 nm, 300 mW, 25 $^{\circ}\text{C}$, cm^{-1}): $\tilde{\nu}$ = 1717(2), 1673(1), 1607(1), 1499(4), 1486(59), 1472(3), 1445(5), 1403(25), 1364(100), 1339(4), 1305(2), 1247(3), 1200(2), 1162(2), 1090(39), 1075(3), 1060(24), 913(13), 886(4), 853(3), 682(2), 626(5), 597(3), 597(3), 421(2), 383(1), 327(4), 263(2), 234(1), 203(2), 165(5), 124(23), 103(11), 88(5), 76(5); **$^1\text{H NMR}$** ($[\text{D}_6]\text{DMSO}$): δ = 7.75 (s, 4H, H-9), 7.10 (s, 4H, H-11), 5.75 ppm (s, 4 H, H-10); **$^{13}\text{C NMR}$** ($[\text{D}_6]\text{DMSO}$): δ = 172.2 (s, C-N_{Anion}), 159.9 (s, C-6), 147.7 (s, C-8), 141.6 ppm (s, C-3); **MS** m/z (FAB⁻): 165.0 ($\text{C}_2\text{HN}_{10}^-$), m/z (FAB⁺): 155.3 ($\text{C}_3\text{H}_7\text{N}_8^+$); **EA** ($\text{C}_8\text{H}_{14}\text{N}_{26}$, 474.38): C 20.26, H 2.97, N 76.77%; found: C 20.30, H 3.00, N 76.68%; **Sensitivities**: IS: 20 J, FS: 360 N, ESD: 1.25 J (at grain sizes 100–500 μm).

3,6,7-Triamino-7*H*-[1,2,4]triazolo[4,3-*b*][1,2,4]triazolium 5,5'-azotetrazole-1,1'-dioxide (14)

3,6,7-Triamino-7*H*-[1,2,4]triazolo[4,3-*b*][1,2,4]triazole monohydrochloride (**1c**) (381 mg, 2.00 mmol, 1.00 eq.) and potassium 5,5'-azotetrazole-1,1'-dioxide (274 mg, 1.00 mmol, 1 eq.) were added to water and the suspension was heated until a clear solution occurred. The solution was left to crystallize, yielding compound **14** as red crystals. Yield: 329 mg, 0.65 mmol, 65%.

DTA (5 $^{\circ}\text{C min}^{-1}$) onset: 210 $^{\circ}\text{C}$ (dec.); **IR** (ATR, cm^{-1}): $\tilde{\nu}$ = 3354(m), 3161(m), 3100(s), 2862(s), 2705(m), 2117(w), 1705(s), 1670(s), 1650(vs), 1626(s), 1576(s), 1512(m), 1469(s), 1454(m), 1425(s), 1403(s), 1360(s), 1260(s), 1209(s), 1178(m), 1137(s), 1078(m), 1058(s), 1058(s), 1003(m), 977(m), 908(w), 858(s), 776(s), 728(s), 718(s), 677(m); **Raman** (1064 nm,

300 mW, 25 °C, cm^{-1}): $\tilde{\nu}$ = 1659(1), 1468(6), 1389(100), 1256(1), 1197(14), 1164(2), 1144(8), 1073(6), 1017(3), 981(1), 961(1), 917(14), 861(1), 768(0), 726(1), 687(1), 624(2), 599(1), 577(1), 431(1), 365(1), 325(1), 271(1), 271(1), 232(1), 188(1), 136(3), 86(9); **^1H NMR** ($[\text{D}_6]$ DMSO): δ = 8.11 (s, 4H, H-9), 7.22 (s, 4H, H-11), 5.76 ppm (s, 4H, H-10); **^{13}C NMR** ($[\text{D}_6]$ DMSO): δ = 160.1 (s, C-6), 154.1 (s, C_{Anion}), 147.5 (s, C-8), 141.3 ppm (s, C-3); **MS** m/z (FAB^-): 197.0 ($\text{C}_2\text{HN}_{10}\text{O}_2^-$), m/z (FAB^+): 155.0 ($\text{C}_3\text{H}_7\text{N}_8^+$); **EA** ($\text{C}_8\text{H}_{14}\text{N}_{26}\text{O}_2$, 506.38): C 18.98, H 2.79, N 71.92%; found: C 19.11, H 2.90, N 71.84%; **Sensitivities**: IS: 30 J, FS: 360 N, ESD: 1.5 J (at grain sizes 100–500 μm).

9.6.2 X-ray Diffraction

Crystallographic data and refinement parameters

Table S1. Crystallographic data and refinement parameters of compound **2** and **4–6**.

	2	4	5	6
Formula	C ₃ H ₆ N ₈	C ₄ H ₇ N ₁₃ O ₃	C ₄ H ₉ N ₁₃ O ₃	C ₃ H ₇ N ₉ O ₃
FW [g mol ^{−1}]	154.16	285.23	287.24	217.18
Crystal system	triclinic	orthorhombic	monoclinic	orthorhombic
Space Group	<i>P</i> −1	<i>P</i> 2 ₁ 2 ₁ 2 ₁	<i>C</i> 2/ <i>c</i>	<i>Pnma</i>
Color / Habit	colorless, plate	colorless, plate	colorless, block	colorless, plate
Size [mm]	0.04 × 0.15 × 0.40	0.03 × 0.15 × 0.40	0.11 × 0.22 × 0.31	0.04 × 0.28 × 0.40
<i>a</i> [Å]	6.2227(9)	6.4957(3)	14.0322(6)	18.7962(13)
<i>b</i> [Å]	7.0199(10)	6.7948(3)	6.8633(4)	6.1218(7)
<i>c</i> [Å]	7.9513(8)	24.3270(14)	22.8093(9)	6.9176(5)
α [°]	75.676(10)	90.0	90.0	90.0
β [°]	69.579(12)	90.0	94.113(4)	90.0
γ [°]	64.263(15)	90.0	90.0	90.0
<i>V</i> [Å ³]	291.32(8)	1073.72(9)	2191.04(18)	795.99(12)
<i>Z</i>	2	4	8	4
ρ_{calc} [g cm ^{−3}]	1.757	1.765	1.742	1.812
μ [mm ^{−1}]	0.134	0.150	0.147	0.157
<i>F</i> (000)	160	584	1184	448
$\lambda_{\text{MoK}\alpha}$ [Å]	0.71073	0.71073	0.71073	0.71073
<i>T</i> [K]	173	173	173	173
ϑ min-max [°]	4.5, 27.0	4.3, 26.5	4.2, 26.5	4.3, 29.0
Dataset <i>h</i> ; <i>k</i> ; <i>l</i>	−7:7; −8:8; −10:9	−8:8; −8:8; −20:30	−17:17; −3:8; −28:27	−25:25; −8:3; −8:9
Reflect. coll.	2286	8354	4302	3411
Independ. refl.	1252	1319	2265	1149
<i>R</i> _{int}	0.025	0.035	0.023	0.025
Reflection obs.	976	1203	1817	958
No. parameters	124	209	217	110
<i>R</i> ₁ (obs)	0.0403	0.0279	0.0400	0.0345
<i>wR</i> ₂ (all data)	0.1060	0.0642	0.0995	0.0919
<i>S</i>	1.01	1.05	1.03	1.03
Resd. Dens.[e Å ^{−3}]	−0.24, 0.18	−0.15, 0.16	−0.20, 0.23	−0.23, 0.36
Device type	Oxford XCalibur3	Oxford XCalibur3	Oxford XCalibur3	Oxford XCalibur3
	CCD	CCD	CCD	CCD
Solution	SIR-92	SIR-92	SIR-92	SIR-92
Refinement	SHELXL-97	SHELXL-97	SHELXL-97	SHELXL-97
Absorpt. corr.	multi-scan	multi-scan	multi-scan	multi-scan
CCDC	1045074	1045070	1045069	1045073

Table S2. Crystallographic data and refinement parameters of compounds **8**, **9**, **11** and **12**.

	8	9	11	12
Formula	C ₈ H ₁₈ N ₂₄ O ₄	C ₈ H ₁₄ N ₂₈ O ₄	C ₅ H ₁₀ N ₁₄ O ₂	C ₃ H ₇ ClN ₈ O ₄
FW [g mol ⁻¹]	514.46	566.47	298.27	254.62
Crystal system	triclinic	monoclinic	monoclinic	triclinic
Space Group	<i>P</i> -1	<i>P</i> 2 ₁ / <i>n</i>	<i>P</i> 2 ₁ / <i>c</i>	<i>P</i> -1
Color / Habit	colorless, block	colorless, block	colorless, block	colorless, block
Size [mm]	0.10 × 0.25 × 0.25	0.15 × 0.20 × 0.35	0.15 × 0.15 × 0.20	0.04 × 0.15 × 0.25
<i>a</i> [Å]	6.0528(3)	11.4127(3)	5.7700(1)	5.8695(4)
<i>b</i> [Å]	7.3217(4)	8.2095(2)	27.1687(6)	8.0942(6)
<i>c</i> [Å]	12.2072(6)	12.0033(4)	7.5970(2)	10.8828(7)
α [°]	103.679(5)	90.0	90.0	101.625(6)
β [°]	104.207(4)	110.998(3)	99.165(3)	103.341(6)
γ [°]	94.027(5)	90.0	90.0	104.721(6)
<i>V</i> [Å ³]	504.82(5)	1049.94(6)	1175.73(5)	467.60(6)
<i>Z</i>	1	2	4	2
ρ_{calc} [g cm ⁻³]	1.692	1.792	1.685	1.808
μ [mm ⁻¹]	0.139	0.148	0.137	0.429
<i>F</i> (000)	266	580	616	260
$\lambda_{\text{MoK}\alpha}$ [Å]	0.71073	0.71073	0.71073	0.71073
<i>T</i> [K]	173	173	173	173
ϑ min-max [°]	4.2, 26.5	4.2, 26.5	4.2, 26.5	4.2, 27.5
Dataset <i>h</i> ; <i>k</i> ; <i>l</i>	-7:7; -9:9; -15:15	-14:14; -10:10; -15:15	-7:7; -34:34; -9:9	-7:7; -10:10; -14:13
Reflect. coll.	7340	14701	16770	3644
Independ. refl.	2094	2173	2427	2141
<i>R</i> _{int}	0.021	0.025	0.034	0.025
Reflection obs.	1874	1931	2111	1768
No. parameters	200	209	230	210
<i>R</i> ₁ (obs)	0.0311	0.0287	0.0327	0.0428
<i>wR</i> ₂ (all data)	0.0858	0.0735	0.0865	0.1115
<i>S</i>	1.04	1.03	1.05	1.05
Resd. Dens.[e Å ⁻³]	-0.19, 0.25	-0.21, 0.20	-0.21, 0.20	-0.31, 0.45
Device type	Oxford XCalibur3	Oxford Calibur3	Oxford XCalibur3	Oxford Calibur3
	CCD	CCD	CCD	CCD
Solution	SIR-92	SIR-92	SIR-92	SIR-92
Refinement	SHELXL-97	SHELXL-97	SHELXL-97	SHELXL-97
Absorpt. corr.	multi-scan	multi-scan	multi-scan	multi-scan
CCDC	1045071	1045067	1045072	1045068

Table S3. Crystallographic data and refinement parameters of compounds **13** and **14**.

	13	14
Formula	C ₈ H ₁₄ N ₂₆	C ₈ H ₁₄ N ₂₆ O ₂
FW [g mol ⁻¹]	474.45	506.45
Crystal system	monoclinic	monoclinic
Space Group	<i>P</i> 2 ₁ / <i>c</i>	<i>C</i> 2/ <i>c</i>
Color / Habit	yellow, plate	orange, needle
Size [mm]	0.04 × 0.18 × 0.23	0.04 × 0.08 × 0.40
<i>a</i> [Å]	4.6597(3)	19.9367(18)
<i>b</i> [Å]	24.5519(13)	10.8102(11)
<i>c</i> [Å]	7.8831(5)	9.5549(8)
α [°]	90.0	90.0
β [°]	95.706(6)	112.096(9)
γ [°]	90.0	90.0
<i>V</i> [Å ³]	897.39(9)	1908.0(3)
<i>Z</i>	2	4
$\rho_{\text{calc.}}$ [g cm ⁻³]	1.756	1.763
μ [mm ⁻¹]	0.136	0.142
<i>F</i> (000)	488	1040
$\lambda_{\text{MoK}\alpha}$ [Å]	0.71073	0.71073
<i>T</i> [K]	173	173
ϑ min-max [°]	4.2, 26.5	4.3, 26.5
Dataset <i>h</i> ; <i>k</i> ; <i>l</i>	−5:5; −16:30; −9:8	−24:14; −13:9; −11:11
Reflect. coll.	3314	3671
Independ. refl.	1842	1966
<i>R</i> _{int}	0.027	0.026
Reflection obs.	1429	1517
No. parameters	182	191
<i>R</i> ₁ (obs)	0.0445	0.0436
<i>wR</i> ₂ (all data)	0.1090	0.1153
<i>S</i>	1.09	1.03
Resd. Dens.[e Å ⁻³]	−0.27, 0.24	−0.28, 0.24
Device type	Oxford XCalibur3	Oxford XCalibur3
	CCD	CCD
Solution	SIR-92	SIR-92
Refinement	SHELXL-97	SHELXL-97
Absorpt. corr.	multi-scan	multi-scan
CCDC	1045066	1045065

9.6.3 Electron Microscopy

First morphological investigations of compound **6** were carried out on a JSM-6500F scanning electron microscope (SEM) (JEOL Ltd., Tokyo, Japan) with a field emission source operated at 4.0 to 12.0 kV. All images shown are secondary electron images in the Figures S3a–S3d. The average chemical composition was studied with an energy-dispersive X-ray spectrometry (EDS) detector model 7418 (Oxford instruments, Oxfordshire, UK). Powders were placed on a brass sample carrier fixed with self-adhesive carbon plates (Plano, Wetzlar, Germany). The samples were sputtered with carbon (sputter device: BAL-TEC MED 020, BAL-TEC AG, Balzers, Netherlands) before loading them into the SEM chamber, since the reaction products were not electrically conducting.

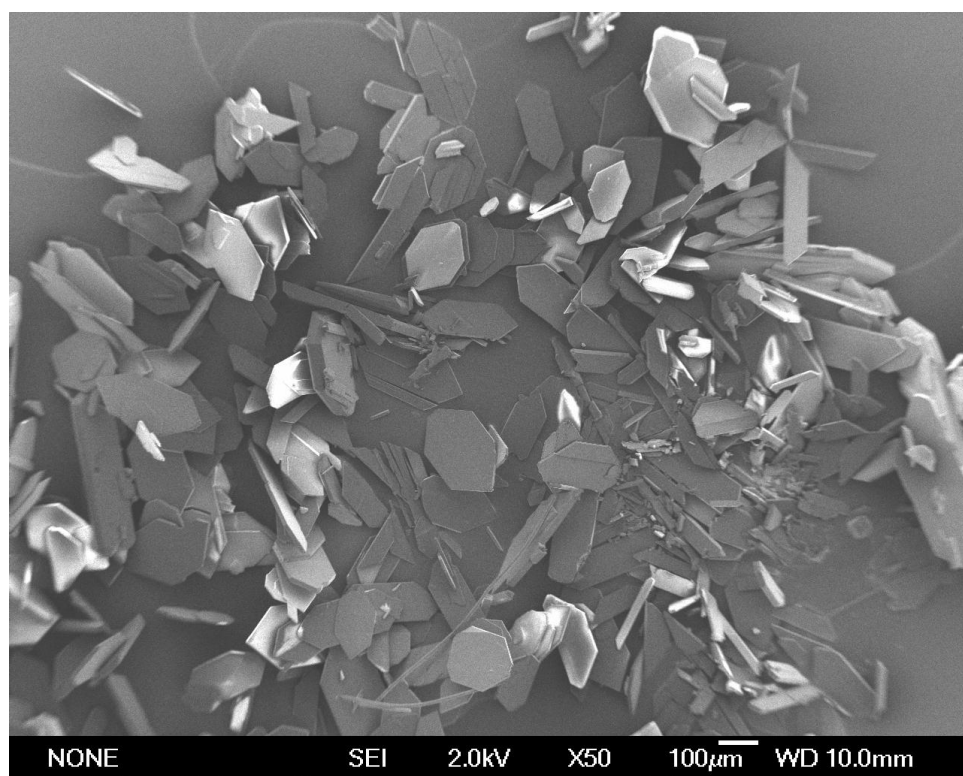


Figure S3a. Morphology of compound 6.

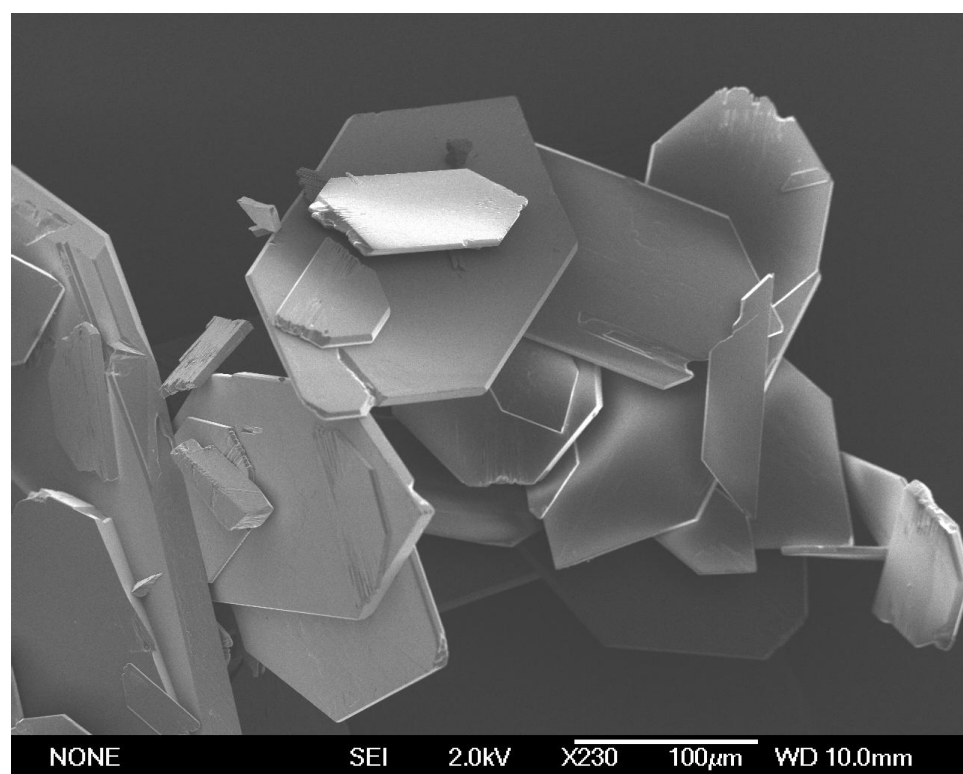


Figure S3b. Morphology of compound 6.

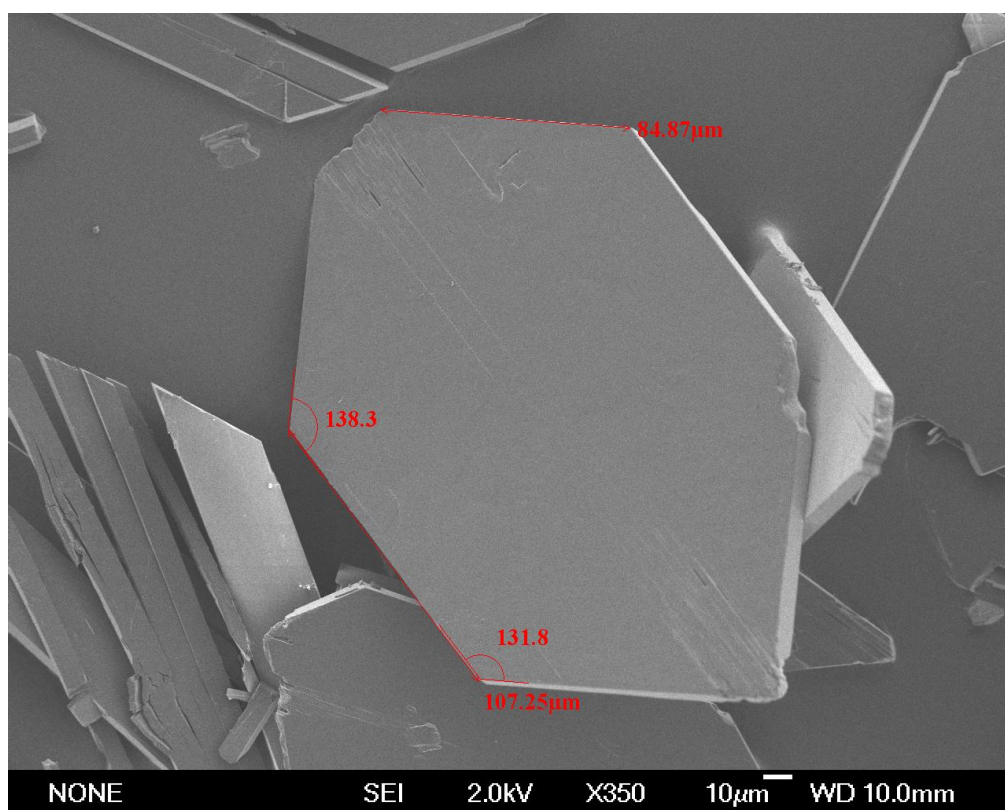


Figure S3c. Morphology of compound **6**.

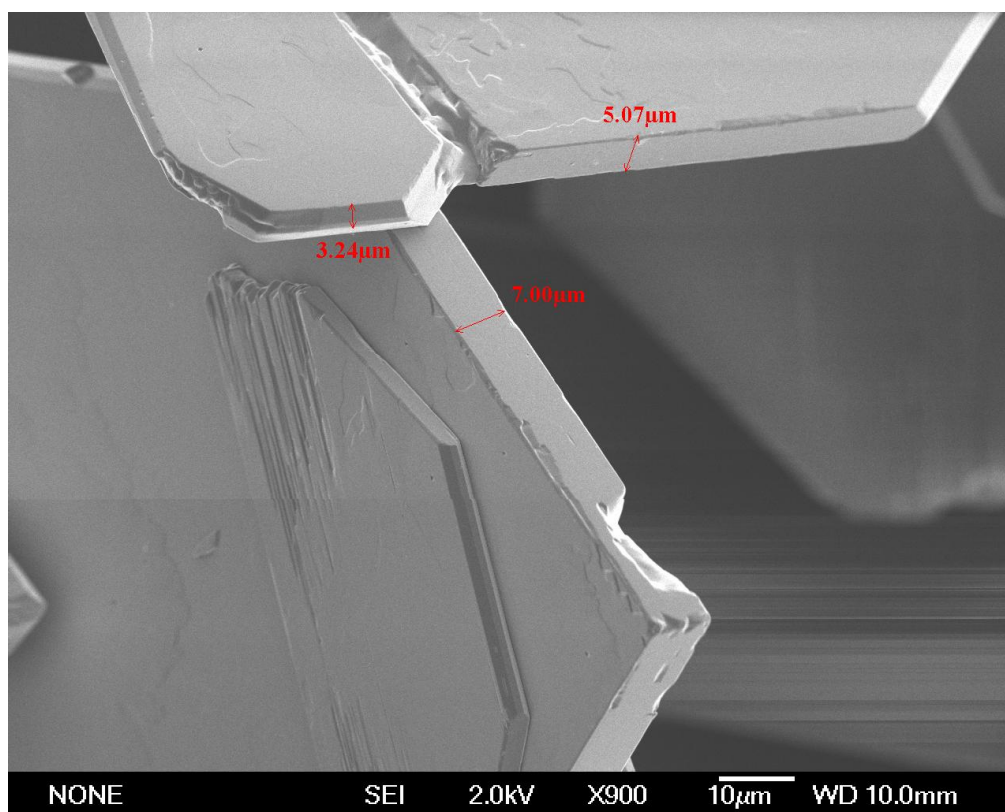


Figure S3d. Morphology of compound **6**.

9.6.4 Explosive performance

9.6.4.1 Heat of formation calculations

General information about the heat of formation calculations can be found in the introduction of this thesis. The calculation results are summarized in Table S4.

Table S4. Calculation results

M	$-H^{298}$ ^[a] / a.u.	$\Delta_f H^\circ(\text{g}, \text{M})$ / kJ mol ⁻¹ ^[b]	V_M / nm ³ ^[c]	$\Delta U_L, \Delta H_L$ (4); ^[d] ΔH_{sub} ^[e] (3) / kJ mol ⁻¹	$\Delta_f H^\circ(\text{s})$ ^[f] / kJ mol ⁻¹	Δn ^[g]	$\Delta_f U(\text{s})$ ^[f] / kJ kg ⁻¹
TATOT	555.095762	540.1		97.4	442.7	7.0	2984.8
TATOT ⁺	555.474133	1080.0					
ClO₄⁻	760.171182	-278.2					
TATOT ClO₄⁻		801.8	0.238	482.3, 487.2	314.6	10.0	1331.1
NT2O⁻	536.798772	81.8C					
TATOT NT2O⁻		1161.9	0.273	465.2, 470.2	691.7	11.5	2525.3
NO₃⁻	280.080446						
1-MeAtNO₂⁻	556.194636	165.1					
TATOT 1-MeAtNO₂⁻		1245.1	0.295	456.2, 461.2	783.9	13.0	2736.7
DNABT²⁻	1032.612357						
(TATOT)₂ DNABT		2896.0	0.535	1043.1, 1050.5	1845.5	23.0	3359.1
AzBT²⁻	622.850742	767.9					
(TATOT)₂ AzT		2928.0	0.457	1108.7, 1116.6	1811.8	20.0	3924.0
AzBT1O²⁻	773.024382	764.2					
(TATOT)₂ AzT1O		2924.3	0.486	1082.7, 1090.2	1834.1	21.0	3724.9

^[a] CBS-4M electronic enthalpy; ^[b] gas phase enthalpy of formation; ^[c] molecular volumes taken from X-ray structures and corrected to room temperature; ^[d] lattice energy and enthalpy (calculated using Jenkins and Glasser equations); ^[e] enthalpy of sublimation (calculated by Trouton rule); ^[f] standard solid state enthalpy of formation; ^[g] solid state energy of formation.

9.6.4.2 Thermal analysis and sensitivities

To identify the decomposition temperatures of compound **2–14** differential thermal analysis (DTA) with a heating rate of 5 °C min⁻¹ was employed. The neutral compound revealed a decomposition onset temperature of 245 °C and thus confirmed the value of 250 °C (dec.) reported in literature.^[1] Compared to commonly used RDX with a decomposition temperature of 210 °C, this value is fairly high.^[7]

The energetic salts **3–14** show a wide range of decomposition temperatures. Before decomposing, compounds **5** and **8** dehydrate at temperatures of 154 °C and 169 °C. Since no crystal structure could be obtained for compound **10** it can only be assumed, that the endotherm peak at 173 °C marks the point of dehydration. The highest decomposition temperature of the energetic salts of **2** is found for the nitrate **6** with 280 °C. Compound **6** exhibits a high thermal stability compared to ammonium nitrate with a decomposition temperature of 210 °C and even lies in the range of the decomposition temperature of the very stable guanidinium nitrate ($T_{\text{dec.}} = 305$ °C).^[8] Compound **7** also lies in the range of the nitrate

6 with an onset decomposition temperature of 275 °C. Except for the corresponding guanidinium salt ($T_{\text{dec.}} = 328$ °C) other reported nitrogen-rich salts of tetranitrobiimidazole show significantly smaller decomposition temperatures reaching as low as 152 °C for the triaminoguanidinium salt.^[2] Compound **12** decomposes at 264 °C, compared to the commonly used ammonium salt, which decomposes at 150 °C, the temperature found for the perchlorate **12** is much higher.^[9] Compounds **8**, **10** and **11** decompose in the range of the neutral compound **2** with onset decomposition temperatures of 255, 235 and 237 °C respectively. Compared to the neutral compound 5-nitriminotetrazole ($T_{\text{dec.}} = 122$ °C) a significant stabilization is reached in the energetic salt **10**.^[10] The 1-methyl derivative of **10**, compound **11**, shows a very similar onset temperature of 235 °C. This is in accordance to other salts reported in the literature, for instance the temperature difference observed in the hydroxylammonium salts of 5-nitriminotetrazolate ($T_{\text{dec.}} = 172$ °C) and 1-methylnitriminotetrazolate ($T_{\text{dec.}} = 185$ °C) are very close as well. Overall the compounds **10** and **11** show significantly higher decomposition temperatures than corresponding nitrogen-rich salts.^[11,12] With an onset decomposition temperature of 255 °C, compound **8** reveals a smaller thermal stability than the corresponding temperature stable ammonium and guanidinium salts which decompose at 290 and 274 °C respectively.^[3] On the other hand the diaminoguanidinium ($T_{\text{dec.}} = 204$ °C) and triaminoguanidinium salts ($T_{\text{dec.}} = 210$ °C) reveal smaller decomposition temperatures than compound **8**.^[3] The nitrotetrazolate **5** exhibits a decomposition temperature of 232 °C, which compared to other reported nitrogen-rich salts of 5-nitrotetrazolate, is fairly high. The guanidinium salt, with the highest value, reveals a decomposition temperature of 212 °C, whereas the values for the other salts reach as low as 96 °C (TAG-salt).^[13] In comparison the nitrotetrazolate-2-oxide reveals a smaller decomposition onset of 222 °C. Compared to the hydroxylammonium or ammonium salts, which decompose at 173 and 157 °C, compound **4** has a high thermal stability.^[14] Also the more temperature stable guanidinium or aminoguanidinium salts ($T_{\text{dec.}} = 211$ and 185 °C respectively) do not reach the decomposition temperature of nitrotetrazolate-2-oxide **4**.^[14] Compound **9** reveals a decomposition temperature of 224 °C and thus has a slightly higher thermal stability than the ammonium salt ($T_{\text{dec.}} = 220$ °C), whereas the high energetic hydroxylammonium salt decomposes at 170 °C and thus exhibits a significantly lower thermal stability.^[15] When comparing the azotetrazolate **13** ($T_{\text{dec.}} = 200$ °C) and the azotetrazolate-1,1'-dioxide **14** ($T_{\text{dec.}} = 210$ °C), a slightly higher thermal stability of compound **14** is noticed. Except for the diguanidinium 5,5'-azotetrazolate with a higher decomposition temperature of 242 °C, the temperature-stable energetic salts (aminoguanidinium, diaminoguanidinium and

triaminoguanidinium) decompose in the range of the decomposition temperature of **13**, with $T_{\text{dec.}} = 218, 196$ and $203\text{ }^{\circ}\text{C}$ respectively.^[16] The diammonium 5,5'-azotetrazolate-1,1'-dioxide exhibits a much higher decomposition of $250\text{ }^{\circ}\text{C}$, whereas the hydroxylammonium and hydrazinium salts reveal lower thermal stabilities than **14**, with $T_{\text{dec.}} = 190$ and $187\text{ }^{\circ}\text{C}$ respectively.^[17] The dinitramide **3** is the only compound reported with a decomposition temperature beneath $200\text{ }^{\circ}\text{C}$ ($T_{\text{dec.}} = 197\text{ }^{\circ}\text{C}$). However compared to other nitrogen-rich dinitramides, for example ADN, GDN and *N*-guanylurea-dinitramide (FOX-12) with decomposition temperatures of $147, 149$ and $201\text{ }^{\circ}\text{C}$, the value obtained for compound **3** is fairly high. Overall, all energetic compounds at least lie in the range (compounds **3, 9, 13** and **14**) of the decomposition temperature of RDX ($T_{\text{dec.}} = 210\text{ }^{\circ}\text{C}$),^[7] if not even significantly higher thermal stabilities are reached (compounds **2, 4, 5, 6, 7, 8, 10, 11** and **12**).

Compounds **1–14** were tested for their sensitivity towards friction and impact by employment of BAM methods. The neutral compound **2** is classified as completely insensitive towards impact (40 J). Next to the free base **2**, compound **6** reveals insensitivity towards impact. With an impact sensitivity of 35 J compound **8** is also not very sensitive towards friction. The corresponding ammonium, guanidinium and aminoguanidinium, like compound **8**, are not very sensitive towards impact, with impact sensitivities of 35 J , $> 40\text{ J}$ and 40 J respectively.^[3] On the other hand compared to the high energetic hydrazinium salt (9 J) or the diaminoguanidinium salt (12 J) compound **8** is much more stable.^[3] Compound **14** reveals a stability towards impact up to 30 J , and thus is much more stable towards impact than the nitrogen-rich hydroxylammonium, ammonium or hydrazinium salts, which exhibit impact sensitivities of 15 J , 3 J and 3 J respectively.^[16] In comparison to the reported 5,5'-azotetrazolate **13** with an impact sensitivity of 20 J , the 5,5'-azotetrazole-1,1'-dioxide derivative is also more stable. Compounds **4, 7** ($IS = 25\text{ J}$) and **5** ($IS = 20\text{ J}$) reveal similar sensitivities towards impact. The impact sensitivity of **4** thus lies in the range of the corresponding aminoguanidinium and diaminoguanidinium salts ($IS = 20\text{ J}, 25\text{ J}$), but does not reach the stability of the guanidinium or diaminoguanidinium salt which are both completely insensitive.^[14] The tetranitrobiimidazolate **7** is a little more stable than the aminoguanidinium or diaminoguanidinium salts, which exhibit impact sensitivities of 20 J and 17 J respectively whereas **7** is much more stable than the ammonium ($IS = 9\text{ J}$) or triaminoguanidinium salts ($IS = 6\text{ J}$).¹⁰ The nitrotetrazolate **5** is less stable than the corresponding 2*N*-oxide **4**. Compound **10** also reveals a decent stability towards impact of up to 15 J and thus is much more insensitive than the corresponding hydroxylammonium ($IS = 2\text{ J}$) and hydrazinium salt ($IS = 3\text{ J}$).^[18,19] Compound **9, 11** and the perchlorate **12** exhibit

similar impact sensitivities with 7.5 J, 8 J and 9 J. Compared to the impact sensitivity the ammonium ($IS = 2$ J) and hydroxylammonium salt ($IS = 2$ J), compound **9** exhibits a fairly higher stability towards impact.^[15] The impact sensitivity of **11** lies in the range of the corresponding diaminoguanidinium and triaminoguanidinium salt with impact sensitivities of 7.5 J and 6 J.^[11] The highest sensitivity towards impact is displayed by the dinitramide **3** with 4 J and thus lies in the range of other nitrogen-rich dinitramides (ADN: 5 J,^[20] TAG DN: 2 J).^[21] Compound **3** is the only compound with a higher impact sensitivity than RDX ($IS = 7.5$ J).^[22] The other compounds reveal higher stability towards impact up to complete insensitive energetic compounds (**6** and **8**).

The neutral compound **2** as well as all energetic salts except compounds **3**, **9** and **12** are insensitive to friction (insensitive up to 360 N). For compounds **5**, **7**, **8** and **11** this result corresponds with values of a number of other nitrogen-rich salts, which are reported in literature.^[2,3,11] In contrast to compound **14** the hydroxylammonium and hydrazinium 5,5'-azotetrazolate-1,1'-dioxide salts reveal high sensitivities towards friction of 54 and 20 N respectively.^[16] Compound **4** reveals a surprisingly high stability, which is unexpected because other nitrogen-rich salts of nitrotetrazolate-2*N*-oxide exhibit friction sensitivities between 252 N (guanidinium salt) and 60 N (hydroxylammonium salt).^[14] The insensitivity of compound **10** towards friction is rather surprising, since the reported compounds to some extent show very high sensitivities towards friction (hydrazinium salt FS : 56 N, hydroxylammonium salt FS : 40 N).^[10,12] Striking is the friction insensitivity of the dinitramide compound **3** ($FS = 288$ N) compared to previously reported nitrogen-rich salts, exemplarily the triaminoguanidinium dinitramide (24 N)^[21] or ammonium dinitramide (72 N)^[20] being sensitive to friction. The perchlorate with a stability towards friction of 216 N is also fairly stable towards friction. Compound **9** ($FS = 108$ N) exhibits a remarkably high stability towards friction compared to the corresponding hydroxylammonium and ammonium salts which show extremely high sensitivities ($FS = 5$ N).^[15] Only compound **9** exhibits a marginally higher sensitivity towards friction than RDX ($FS = 120$ N),^[22] whereas the other reported energetic compounds are either completely insensitive towards friction or just show a slight sensitivity (compounds **3** and **12**).

The ESD measurements show that compounds **2–8** and **10–12** are less sensitive towards electrostatic discharge (**2**, **8**, **14**: 1.5 J, **13**: 1.25 J, **4**, **5**, **11**: 1 J, **6**: 0.75 J, **10**: 0.7 J, **7**, **12**: 0.6 J) than the high energetic compound **9** (0.08 J) or RDX (0.2 J).

9.6.5 Toxicity assessment

The *Luminescent Bacteria Inhibition Test* offers a possibility to determine the environmental acceptability of new energetic materials to aquatic organisms whereat a marine bacteria is used as a representative for marine organisms. In this test the decrease of the luminescence of the liquid-dried bacteria is determined after 15 min and 30 min at different concentrations of the test compounds and is compared to a control measurement of a 2% NaCl stock solution.

The sample dilution sequence corresponds to DIN 38412 L34, which ranges from 1:2 to 1:32 dilution of the compound in the test system. For a better reproducibility, all dilution steps were made in duplicate. The change of intensity of bacterial luminescence in the absence (controls) and in the presence (samples) of the tested substances after different incubation times (15 min, 30 min) were recorded. The controls (2% NaCl only) were measured for calculating the correction factor, which is necessary to consider the normal decrease of luminescence without any toxic effect per time.

The EC_{50} value gives the concentration of each compound where the bacterial luminescence is inhibited by 50% and is calculated by plotting Γ against the concentration of the test substance in a diagram with a logarithmic scale, where $\Gamma = \text{inhibition (in \%)} / 100 - \text{inhibition (in \%)}$ and $c = \text{concentration of the test sample}$. The EC_{50} value is identical with the intersection of the resulting graph with the X-axis ($\Gamma = 0$).

For better comparison of the resulting toxicities, we also determined the toxic effect of RDX to the bacterial strain under the same conditions applied for the toxicity assessment of neutral **2** and nitrate **6** as displayed in Table S5. To imitate the natural environment of the employed marine bacterium as good as possible, the samples need to be diluted with a 2% (w/v) sodium chloride solution. Since RDX is barely soluble in water, a stock solution in acetone was prepared, which was further diluted with the sodium chloride solution to a mixture containing 200 ppm RDX in water/acetone 99/1 (v/v).

Table S5. Toxicity values of compounds **2** and **6** compared to **RDX**

	EC_{50} (15 min)	EC_{50} (30 min)
2	5.015	4.837
6	3.564	3.363
RDX	0.237	0.239

9.6.6 Spectroscopy

NMR Spectroscopy

Compounds **1–14** were characterized by ^1H NMR and ^{13}C NMR spectroscopy. The protons and carbons are assigned corresponding to the numeration illustrated in Figure S1. Three signals can be found for compound **2** in the ^1H NMR spectrum at 6.38 (H–11), 5.59 (H–10) and 5.46 ppm (H–9), representing the protons of the amino-groups. In comparison to the neutral compound, the protons H–9 in the energetic salts are strongly upshifted. Additionally the proton signals of H–11 and H–10 are also found at slightly upshifted values. Compounds **1, 3–6, 9** and **12** all reveal four proton signals with similar chemical shifts in each compound of 13.41–13.29 ppm (H–2), 8.22–8.19 ppm (H–9), 7.30–7.22 ppm (H–11) and 5.84–5.75 ppm (H–10). Compounds **7** and **10** show three signals in the ^1H NMR spectrum at very similar chemical shifts in each compound of 8.20–8.19 ppm (H–9), 7.24–7.23 ppm (H–11), 5.79–5.78 ppm (H–10). The energetic salt **11** reveals three chemical shifts in the same range in the ^1H NMR spectrum (8.19, 7.24 and 5.79 ppm) as in compounds **7, 8** and **10**, however, a fourth signal is found, which represents the methyl-group of the anion at 3.67 ppm. The same chemical shift is found in the corresponding, nitrogen-rich diaminoguanidinium and triaminoguanidinium salts with a chemical shift of 3.67 ppm representing the methyl-group.^[11] The chemical shift of the signal of the protons H–9 in compound **14** is slightly downshifted compared to the other energetic salts to a value of 8.11 ppm. The protons H–11 and H–10 are found at similar chemical shifts as in the other energetic salts with values of 7.22 and 5.76 ppm respectively. The chemical shifts of the protons H–9 and H–11 in the energetic compound **13** are downshifted to 7.75 and 7.10 ppm, whereas the protons H–10 are found at a similar chemical shift as in the other energetic salts reported with a value of 7.75 ppm. The same observation can be made for compound **8**, in which the protons H–9 and H–11 are downshifted even further to 7.59 and 7.01 ppm, whereas the protons H–10 are found at similar values as in the reported compounds ($\delta = 5.73$ ppm).

In the ^{13}C NMR spectrum of the free base **2**, three signals are found at 158.5 (C–6), 149.1 (C–8) and 143.5 (C–3) respectively. In all energetic salts, the signal for C–6 is slightly upshifted, whereas the signals for C–8 and C–3 are slightly downshifted. The chemical shifts of all carbons in the cations of compounds **1** and **3–12** exhibit very sharp signals in a similar range. The carbon C–6 shows a chemical shift between 160.2 and 159.8 ppm, whereas the carbon C–8 can be found at chemical shifts between 147.4 and 147.9 ppm and C–3 exhibits chemical shifts of 142.1 to 141.0 ppm. The carbon peaks of the anions all match the values of the literature. For instance, the peak observed in the ^{13}C NMR spectrum of compound **4** at 157.2 ppm belongs to the carbon of the anion and reveals a similar chemical shift as found for carbon of the nitrotetrazolate-2*N*-oxide in the guanidinium salt (157.6 ppm) or the

triaminoguanidinium salt (157.1 ppm).^[14] The peak at 168.7 ppm in the ^{13}C NMR spectrum of energetic salt **5** can be assigned to the nitrotetrazolate anion, which also exhibits similar chemical shifts for the corresponding triaminoguanidinium salt (169.1 ppm) or the hydrazinium salt (169.0 ppm).^[23] The signals at 144.3 and 140.4 ppm in ^{13}C NMR spectrum of compound **7** can be assigned to the carbons of the anions. The signal at 144.3 ppm is formed by the C–NO₂ carbon, whereas the peak at 140.4 ppm belongs to the C–C carbon.^[2] Similar values are found in reported nitrogen-rich salts, for example in the guanidinium (144.1 [C–NO₂] and 140.8 ppm [C–C]) or aminoguanidinium salts (144.5 [C–NO₂] and 140.6 ppm [C–C]).^[2] In the ^{13}C NMR spectrum of compound **8**, the peak at 150.0 ppm can be assigned to the anion, for which similar chemical shifts are found in various nitrogen-rich salts, for example the biammonium salt (134.8 ppm) or the bihydrazinium salt (134.9 ppm) just to point out two of them.^[3] For the carbon of the anion in compound **9** a chemical shift of 140.4 ppm is found. This value is within the same range as for 3,4-diamino-5-(3,4-diamino-1,2,4-triazol-5-yl)-1,2,4-triazolium 1,1'-dinitramino-5,5'-bitetrazolate (140.5 ppm) described in section one of this report. The anion of compound **10** reveals a chemical shift of 157.9 ppm and thus exhibits a value similar to the hydroxylammonium and hydrazinium salt with a chemical shift of the carbon of 158.3 and 158.4 ppm respectively.^[10,12] In comparison, the chemical shift of the corresponding carbon in the 1-methyl derivative of **10**, is slightly downshifted to a value of 157.2 ppm. The peak at 32.7 ppm arises through the –CH₃ group. Similar values are exhibited by various nitrogen-rich compounds of 1-methylnitriminotetrazolate, for example the guanidinium salt with peaks at 157.6 ppm (CN₄) and 33.1 ppm (–CH₃) or the aminoguanidinium salt with peaks at 157.7 ppm (CN₄) and 33.1 ppm (–CH₃) just to name two examples.^[11] With 172.2 ppm the peak of the anion of compound **13** is strongly upshifted compared to all reported energetic salts, except for compound **5**. The carbons of the anion in the corresponding guanidinium and triaminoguanidinium salts reveal peaks, even further upshifted, than the anion-peak of **13** with signals at 172.9 and 173.3 ppm respectively.^[24] In comparison to compound **13**, the chemical shift of the carbon of the 1-oxide derivative is downshifted by about 18 ppm to 154.1 ppm. This value is according to the chemical shift of the corresponding carbon in the ammonium, hydroxylammonium and hydrazinium salt with chemical shifts of 153.8, 153.6 and 153.9 ppm respectively.^[16]

IR and Raman Spectroscopy of compounds 3–14

In compounds **3–14**, similar values as described for compound **2** can be observed for the cations. The dinitramide anion can be identified by vibrational spectrometry through the

bands at 1559 and 1318 cm^{-1} in the Raman spectrum and through similar values in the IR-spectrum (1515 and 1301 cm^{-1}). These values correspond to the values reported in literature for the dinitramide anion.^[25] Compounds **4** and **5** reveal a number of bands between 1540–700 cm^{-1} , which show the characteristic pattern of $\nu(\text{NN})$, $\nu(\text{NCN})$, $\gamma(\text{CN})$ and δ aromatic ring vibrations of the tetrazole and the tetrazole-2-oxide rings in both vibrational spectra.^[23] The weak band of the OH-vibration of the crystal water in compound **5** can be found at 3103 cm^{-1} in the IR-spectrum. According to literature, the nitrate anion **6** can be identified through a strong broad absorption in the IR-spectrum with a maximum at 1344 cm^{-1} , and through a sharp, strong absorption at 1055 cm^{-1} in the Raman spectrum.^[26] Compound **7** exhibits the C–C stretch at 1031 cm^{-1} , whereas the aromatic C=C stretch is found at 1492 cm^{-1} . In the Raman spectrum the characteristic C–NO₂ vibration is found with a very strong band at 1559 cm^{-1} and a medium band at 1346 cm^{-1} , whereas the corresponding bands in the IR-spectrum show reversed intensities. Similar absorption patterns as observed for energetic salts **4** and **5** can be found in the tetrazole derivative anions of compounds **8–11** and **13–14** in the range of 1540 to 700 cm^{-1} for the tetrazole rings. The band at 1000 cm^{-1} in the IR-spectrum of **8** and at 1013 cm^{-1} in the IR-spectrum of energetic compound **9** can be assigned to the C–C bond in the respective molecule. With bands at 1009 cm^{-1} respectively 1024 cm^{-1} in the Raman spectrum of **8** and **9**, the vibration of the C–C bond is found in a similar range. At 1168 cm^{-1} the valence vibration of the C–O bond of **8** can be observed in the IR-spectrum. The band of the crystal water of compound **8** is found in the range of 3100 cm^{-1} . Compounds **9** and **10** exhibit a weak band at around 1530 cm^{-1} in both IR and Raman spectra representing the NO₂ stretch of the nitrimino-group. In compound **11** this absorption seems to be shifted to around 1515 cm^{-1} in both vibrational spectra. The anion of compound **11** reveals the characteristic bands of the –CH₃ group at around 2900 cm^{-1} (broad band), 1468 cm^{-1} (δ C–H), 1400 cm^{-1} (symmetric deformation vibration of CH₃). In compound **14**, the azo-bond is found at 1576 cm^{-1} , as described in literature.^[27] In compound **13** this band cannot be observed, which according to literature is often the case.^[27] The C–O valence vibration of compound **14** occurs at 1137 cm^{-1} . The bands at 936, 1065 and 1101 cm^{-1} found in the Raman spectrum of **12** indicate the presence of perchlorate and agree with reasonable deviation with the reported values.^[25]

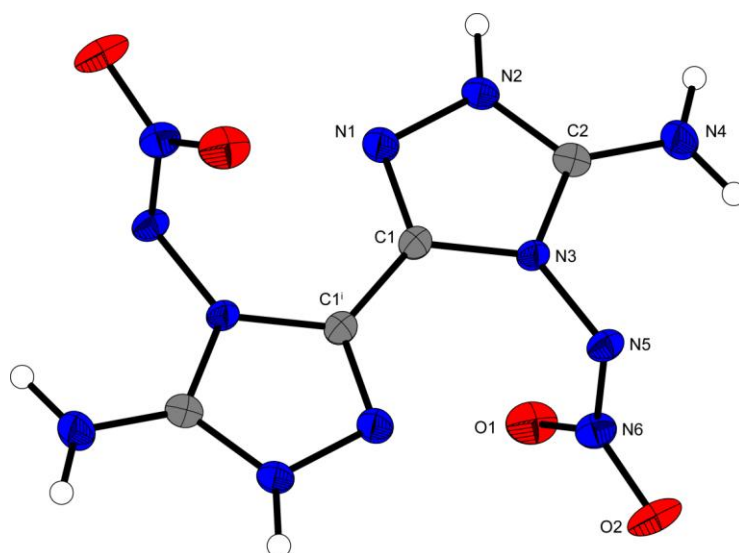
9.6.7. References

- [1] K. Potts, C. Hirsch, *J. Org. Chem.* **1968**, 33, 143–150
- [2] T. M. Klapötke, A. Preimesser, J. Stierstorfer, *Z. Anorg. Allg. Chem.* **2012**, 638, 1278–1286.
- [3] N. Fischer, T. M. Klapötke, M. Reymann, J. Stierstorfer, *Eur. J. Inorg. Chem.* **2013**, 2167–2180.
- [4] D. Fischer, T. M. Klapötke, J. Stierstorfer, *Angew. Chem. Int. Ed.* **2014**, 53, 8172–8175; *Angew. Chem.* **2014**, 126, 8311–8314.
- [5] T. M. Klapötke, Insensitive high-performance replacements for RDX in explosive and propellant formulations, Interim Technical Report, United States Army, **2007**.
- [6] A. Dippold, T. M. Klapötke, *Chem Eur. J.* **2012**, 18, 16742–16753.
- [7] R. Reed, *J. Org. Chem.* **1958**, 23, 775–777.
- [8] M. Udupa, *Thermochim. Acta.* **1982**, 53, 383–385.
- [9] P. Jacobs, H. Whitehead, *Chem. Rev.* **1969**, 69, 551–590.
- [10] N. Fischer, T. M. Klapötke, J. Stierstorfer, *Z. Anorg. Allg. Chem.* **2011**, 637, 1273–1276.
- [11] T. M. Klapötke, J. Stierstorfer, A. Wallek, *Chem. Mater.* **2008**, 20, 4519–4530.
- [12] N. Fischer, T. M. Klapötke, D. G. Piercey, J. Stierstorfer, *Z. Anorg. Allg. Chem.* **2012**, 638, 302–310.
- [13] A. Dippold, T. M. Klapötke, *Chem Eur. J.* **2012**, 18, 16742–16753.
- [14] M. Göbel, K. Karaghiosoff, T. M. Klapötke, D. G. Piercey, J. Stierstorfer, *J. Am. Chem. Soc.* **2010**, 132, 17216–17226.
- [15] D. Fischer, private communication.
- [16] D. Fischer, T. M. Klapötke, D. G. Piercey, J. Stierstorfer, *Chem. Eur. J.* **2013**, 19, 4602–4613
- [17] V. Rafeev, Y. Rubtsov, *Russ. Chem. Bull.* **1993**, 42, 1811–1815.
- [18] N. Fischer, T. M. Klapötke, J. Stierstorfer, *Z. Anorg. Allg. Chem.* **2011**, 637, 1273–1276.

- [19] N. Fischer, T. M. Klapötke, D. G. Piercey, J. Stierstorfer, *Z. Anorg. Allg. Chem.* **2012**, 638, 302–310.
- [20] U. Teipel, T. Heintz, H. Krause, *Propellants Explos. Pyrotech.* **2000**, 25, 81–85.
- [21] T. M. Klapötke, J. Stierstorfer, *Phys. Chem. Chem. Phys.* **2008**, 10, 4340–4346.
- [22] J. Köhler, *Explosivstoffe*, 9. Ed., Wiley-VCH, New York, **1998**, 166.
- [23] T. M. Klapötke, P. Mayer, C. M. Sabaté, J. M. Welch, N. Wiegand, *Inorg. Chem.* **2008**, 47, 6014–6027.
- [24] A. Hammerl, G. Holl, M. Kaiser T. M. Klapötke, P. Mayer, H. Nöth, H. Piotrowski, M. Sluter, *Z. Naturforsch.* **2001**, 56B, 857–870.
- [25] F. Miller, C. Wilkins, *Anal. Chem.* **1952**, 24, 1253–1294.
- [26] K. Karaghiosoff, T. M. Klapötke, P. Mayer, C. M. Sabaté, A. Penger, J. M. Welch, *Inorg. Chem.* **2008**, 47, 1007–1019.
- [27] a) M. Hesse, H. Meier, B. Zeeh, *Spektroskopische Methoden in der Organischen Chemie*, 7th edn., Thieme, Stuttgart, New York, **2005**. b) G. Socrates, *Infrared and Raman Characteristic Group Frequencies: Tables and Charts*, 3rd edn., John Wiley & Sons, Chichester, **2004**.

Energetic Materials Based on 5,5'-Diamino-4,4'-nitramino-3,3'-bi-1,2,4-triazole

published in *Chem. Asian J.* **2016**, *11*, 844–851. (DOI: 10.1002/asia.201500701)



Abstract: A simple and straightforward synthesis of 5,5'-diamino-4,4'-dinitramino-3,3'-bi-1,2,4-triazole by the selective nitration of 4,4',5,5'-tetraamino-3,3'-bi-1,2,4-triazole is presented. The interaction of the amino and nitramino groups improves the energetic properties of this functionalized bitriazole. For a deeper investigation of these properties, various nitrogen-rich derivatives were synthesized. The new compounds were investigated and characterized by spectroscopy (¹H and ¹³C NMR, IR, Raman), elemental analysis, mass spectrometry, differential thermal analysis (DTA), X-ray analysis, and impact and friction sensitivities (IS, FS). X-ray analyses were performed and deliver insight into structural characteristics with which the stability of the compounds can be explained. The standard enthalpies of formation were calculated for all compounds at the CBS-4M level of theory, revealing highly positive heats of formation. The energetic performance of the new molecules was predicted with the EXPLO5 V6.02 computer. A small-scale shock reactivity test (SSRT) and a toxicity test gave a first impression of the performance and toxicity of selected compounds.

Keywords: Energetic materials · Triazoles · Structure elucidation · N-Heterocycles · Sensitivities

10.1 Introduction

When developing new energetic materials, three major principles should be taken into account: i) sufficient oxygen for the oxidation of the carbon backbone as in RDX^[1] or PETN^[2] (Figure 1), ii) build up strained ring or cage systems to maximize the density as well the energy output as used in CL-20^[3] (Figure 1), and iii) formation of nitrogen-rich compounds, as TKX-50^[4] (Figure 1). Contrary to conventional materials such as the carcinogenic and toxic RDX, nitrogen-rich compounds release mostly environmentally benign dinitrogen after decomposition.^[5] Other than the energetic performance and environmental concerns, the safe handling is another key aspect for the development of new energetic materials. Modern energetic materials should have decomposition temperatures over 200 °C, as well as low sensitivities to mechanical stimuli as impact (>7.5 J) or friction (>120 N).

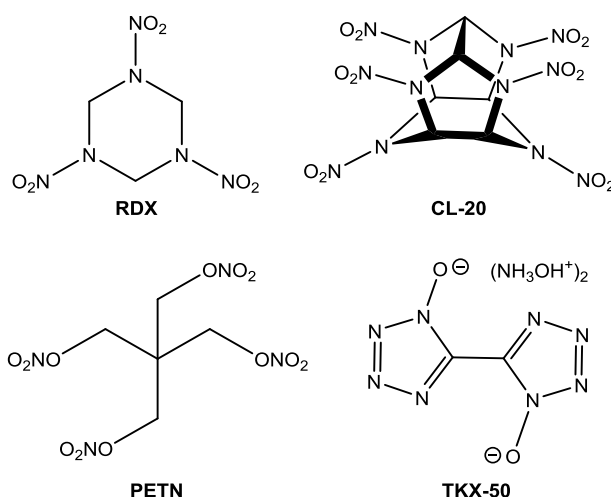


Figure 1. High energy density materials 1,3,5-trinitro-1,3,5-triazinane (RDX), pentaerythritol tetranitrate (PETN), hexanitrohexaazaisowurtzitane (CL-20) and dihydroxylammonium 5,5'-bistetrazole-1,1'-diolate (TKX-50).

Beside the nitrogen-rich tetrazole, triazoles have been used successfully as energetic building blocks in the past.^[6] By implementing nitro^[7] (Figure 2 A), nitramino^[8] or *N*-oxides^[9] (Figure 2 B) moieties, the energetic performance and the oxygen balance of the target molecule can be optimized.

With a system that comprises both nitro and amino groups, a good thermal stability can be achieved through the formation of a strong hydrogen-bonding network as observed in TATB^[10] (Figure 2 C). Recently, aminated derivatives of 5,5'-dinitro-bi-1,2,3-triazoles as the 2,2'-diamino-5,5'-dinitro-bi-1,2,3-triazole (Figure 2 D) have been reported as materials that may be potential replacements for RDX.^[11] We recently reported on the 4,4',5,5'-tetraamino-3,3'-bi-1,2,4-triazole^[12] (Figure 2 E) that shows excellent thermal stabilities ($T_{\text{dec}} > 340$ °C).

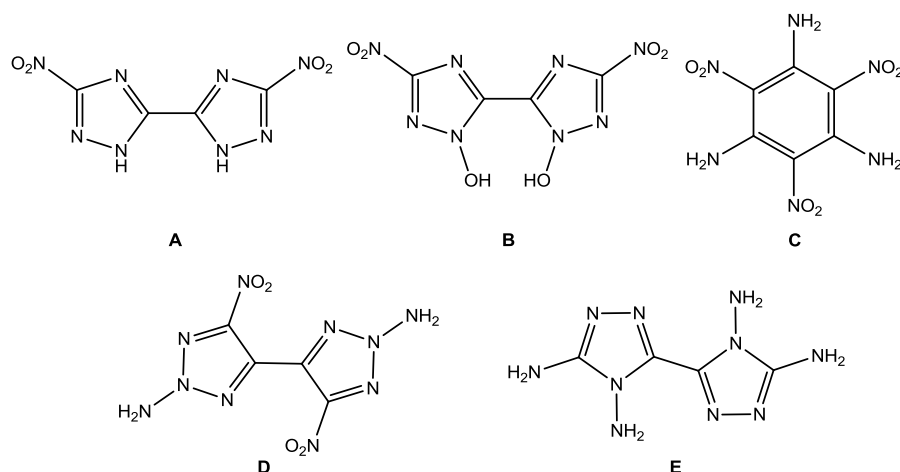


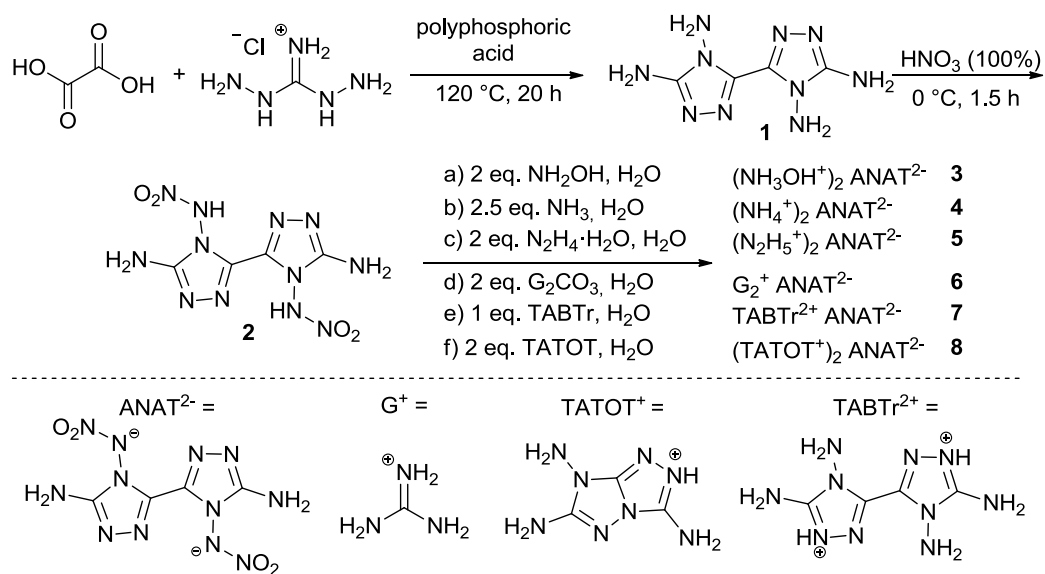
Figure 2. Energetic derivatives 3,3'-dinitro-5,5'-bi-1,2,4-triazole (A), 3,3'-dinitro-5,5'-bi-1,2,4-triazole-1,1'-diol (MAD-X, B), 1,3,5-triamino-2,4,6-trinitrobenzene (TATB, C), 4,4'-bi-(2-amino-5-nitro-1,2,3-2*H*-triazole) (D), 4,4',5,5'-tetraamino-3,3'-bi-1,2,4-triazole (E).

This work focuses on novel 5,5'-diamino-4,4'-dinitramino-3,3'-bi-1,2,4-triazole and energetic salts thereof. We report on the simple and straightforward method of the selective *N*-amino nitration of 4,4',5,5'-tetraamino-3,3'-bi-1,2,4-triazole to increase the energetic performance, while preserving the thermal stability of this system.

10.2 Results and Discussion

10.2.1 Synthesis

The preparation of 5,5'-diamino-4,4'-dinitramino-3,3'-bi-1,2,4-triazole **2** and its energetic salts **3–8** is displayed in Scheme 1. 1,3-Diaminoguanidine hydrochloride and oxalic acid were dissolved in polyphosphoric acid and heated to give 4,4',5,5'-tetraamino-3,3'-bi-1,2,4-triazole **1**.^[12] Compound **1** was slowly added to ice-cooled 100 % HNO₃ and stirred at 0 °C for 1.5 h. Afterwards the solution was quenched with ice-water and the formed precipitate was filtered off yielding pure 5,5'-diamino-4,4'-dinitramino-3,3'-bi-(1,2,4-triazole) **2**. Compound **2** can be used as obtained and does not require further purification such as chromatography, or recrystallization.



Scheme 1. Synthesis route towards compound **1–8**.

The energetic salts **3–8** were prepared by simple salt-metathesis of the neutral compound **2** and selected energetic cations. Therefore **2** was suspended in water and the corresponding base was added (Scheme 1, reactions a–f). The suspension was heated until a clear solution appeared and then left for crystallization to obtain dihydroxylammonium 5,5'-diamino-4,4'-dinitramino-3,3'-bi-1,2,4-triazolate (**3**), diammonium 5,5'-diamino-4,4'-dinitramino-3,3'-bi-1,2,4-triazolate (**4**), dihydrazinium 5,5'-diamino-4,4'-dinitramino-3,3'-bi-1,2,4-triazolate (**5**), diguanidinium 5,5'-diamino-4,4'-dinitramino-3,3'-bi-1,2,4-triazolate (**6**), 4,4',5,5'-tetraamino-3,3'-bi-1,2,4-triazolium 5,5'-diamino-4,4'-dinitramino-3,3'-bi-1,2,4-triazolate (**7**) and di-(3,6,7-triamino-[1,2,4]triazolo[4,3-b][1,2,4]triazolium) 5,5'-diamino-4,4'-dinitramino-3,3'-bi-1,2,4-triazolate dihydrate (**8·2 H₂O**).

10.2.2 Crystal Structures

The crystal structures of compounds **2**, **3**, **6**, **7** and **8·2 H₂O** were determined. Tables S1-S2 in the Supporting Information gather selected data and parameters of the X-ray measurements.

5,5'-Diamino-4,4'-dinitramino-3,3'-bi-1,2,4-triazole (**2**) crystallizes from water in the orthorhombic space group *Pbca* with four molecules per unit cell and a density of 1.789 g cm⁻³ at 173 K. The molecular unit of **2** is illustrated in Figure 3. **2** has a zwitterionic structure with a formal negative charge at the nitrogen atom N5 atom and a protonated nitrogen atom N2. The C1–C1ⁱ and the C2–N4 bonds are shorter than common C–C/C–N single bonds but in the same range as the recently reported bond length of **1**.^[12] The observed bond lengths of N3–N5 (1.398(2) Å) and N5–N6 (1.348(2) Å) are between the values for a N–N single bond (1.47 Å) and a N=N double bond (1.25 Å) due to electron delocalization in

the triazole ring. The N3–C1–C1ⁱ–N3ⁱ and N1–N2–C2–N4 torsion angles are nearly 180°, which means both ring systems and the amino groups are located in plane. The two nitramino groups are tilted out of the plane by 78°. Moreover, intramolecular hydrogen bonds are built up from the amino group to the nitramino moiety as well as the N2 atom.

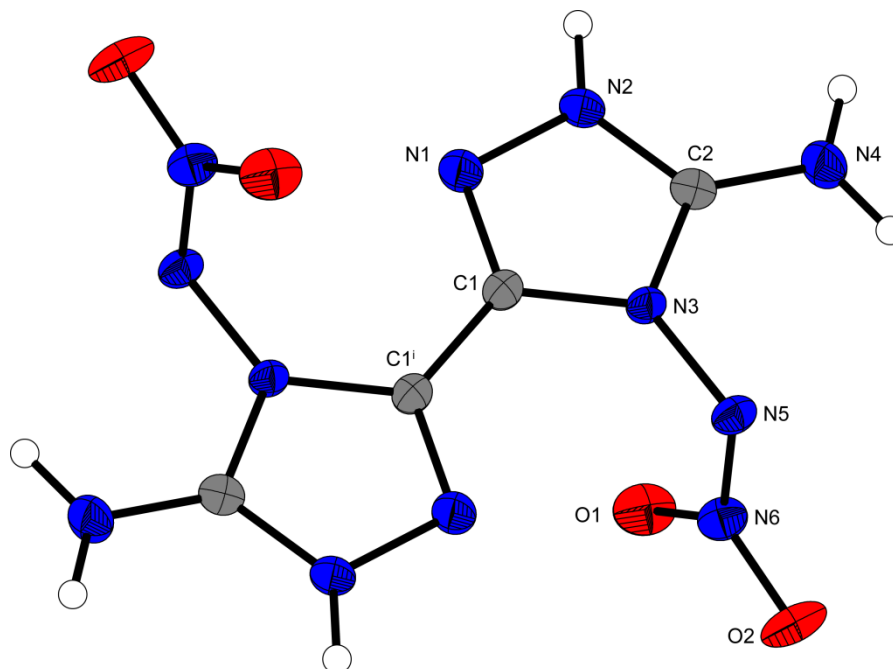


Figure 3. Molecular unit of **2**. Ellipsoids are drawn at the 50 % probability level. Selected bond lengths (Å): C1–C1ⁱ 1.449(2), N4–C2 1.313(2), N3–N5 1.398(2), N5–N6 1.348(2); selected bond angles (°): N3–C1–C1ⁱ 124.06(14), N5–N3–C1 130.38(13), O1–N6–N5 122.42(14), N3–N5–N6 108.59(12), N3–C2–N4 125.40(15); selected hydrogen bond lengths [Å] and angles [°] (D–H⋯A, *d*(D–H), *d*(H⋯A), *d*(D⋯A), (D–H⋯A)): N4–H4B⋯N2: 0.86(2), 2.67(2), 3.75(2), 148(2); N4–H4A⋯O1 0.91(2), 2.02(2), 2.887(2), 158(2); selected torsion angles (°): C1–N3–N5–N6 78.2(2), N3–C1–C1ⁱ–N3ⁱ 180.00(14), N1–N2–C2–N4 178.38(16).

Recrystallization from water yielded single crystals of dihydroxylammonium 5,5'-diamino-4,4'-dinitramino-3,3'-bi-1,2,4-triazolate (**3**), as illustrated in Figure 4. **3** crystallizes in the orthorhombic space group *Pbca* with four molecules per unit cell and has a density of 1.796 g cm^{−3} at 173 K. The bond lengths of the anion are in same the range as those of zwitterionic **2**. Similar to **2** the anion is in plane except for the nitramino groups, which are twisted out of the plane by approximately 73°. In contrast to **2** the N5 atom is tilted out of the plane by the torsion angle N5–N3–C1–N2=12°. An intensive hydrogen bond network is formed between the hydroxylammonium cations, the amino- and nitramino moieties.

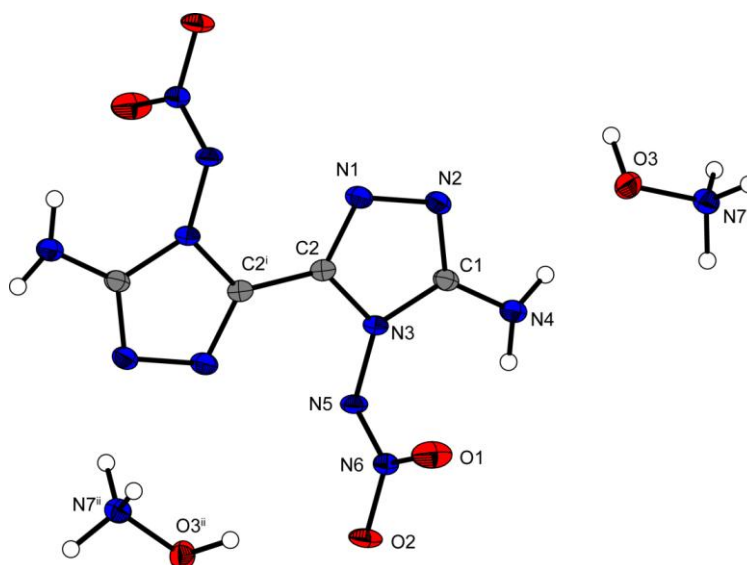


Figure 4. Molecular unit of **3**. Ellipsoids are drawn at the 50 % probability level. Selected bond lengths (Å): C2–C2ⁱ 1.446(2), N3–N5 1.409(2), N5–N6 1.314(2), N4–C1 1.341(2); selected bond angles (°): N3–C2–C2ⁱ 124.66(12), N5–N3–C2 126.69(12), N3–N5–N6 109.86(11), O1–N6–N5 126.65(12), N3–C1–N4 124.23(13), selected hydrogen bond lengths [Å] and angles [°] (D–H \cdots A, *d*(D–H), *d*(H \cdots A), *d*(D \cdots A), (D–H \cdots A)): O3ⁱⁱ–H3ⁱⁱ \cdots O2 0.91(2), 1.74(2), 2.634(2), 165(2); N4–H4 A \cdots O1 0.86(2), 2.03(2), 2.884(2), 171(2); N4–H4B \cdots O3 0.85(2), 2.34(2), 3.152(2), 161(2); selected torsion angles (°): N3–C2–C2ⁱ–N3ⁱ 179.98(15), C2–N3–N5–N6 –107.93(15), N1–N2–C1–N4 –179.14(13), N5–N3–C1–N2 167.52(12).

Diguanidinium 5,5'-diamino-4,4'-dinitramino-3,3'-bi-1,2,4-triazolate (**6**) crystallizes from water in the triclinic space group *P*–1 with a density of 1.687 g cm^{–3} at 173 K and one molecule per unit cell. The crystal structure is shown in Figure 5. All bond lengths and angles are similar to the neutral compound **2**. Also, the anion of **6** is in plane except for the two nitramino groups.

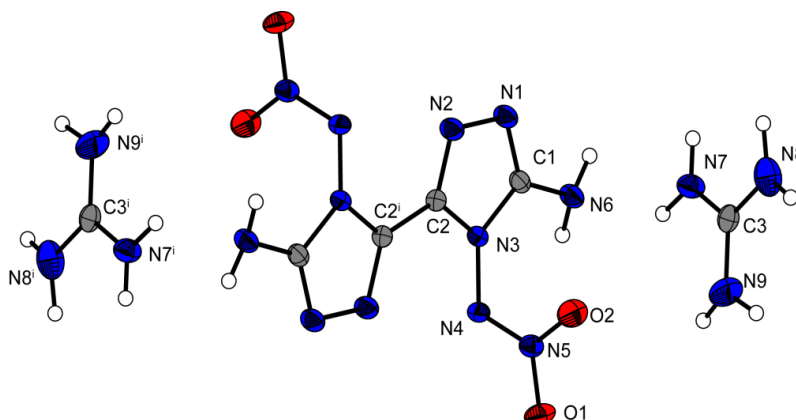


Figure 5. Molecular unit of **6**. Ellipsoids are drawn at the 50 % probability level. Selected bond lengths (Å): C2–C2ⁱ 1.449(2), N3–N4 1.405(2), N4–N5 1.321(2), N6–C1 1.356(2); selected bond angles (°): N3–C2–C2ⁱ 124.59(12), N4–N3–C2 129.81(11), O1–N5–N4 116.09(11), N3–N4–N5 108.65(10), N3–C1–N6 122.88(12); selected hydrogen bond lengths [Å] and angles [°] (D–H \cdots A, *d*(D–H), *d*(H \cdots A), *d*(D \cdots A), (D–H \cdots A)): N6–H6 A \cdots O2 0.90(2), 2.21(2), 3.069(2), 160(2); N6–H6B \cdots N1 0.86(2), 2.18(2), 3.019(2), 165(2); N9–H9A \cdots O2 0.88(2), 2.48(2), 3.031(2), 121(2); N9–H9B \cdots O1 0.90(3), 2.16(3), 3.028(2), 162(3); N9–H9B \cdots O2 0.90(3), 2.32(3), 3.044(2), 138(3); selected torsion angles (°): N3–C2–C2ⁱ–N3ⁱ 179.98(14), C2–N3–N4–N5 –99.16(15), N2–N1–C1–N6 –175.74(13).

4,4',5,5'-Tetraamino-3,3'-bi-1,2,4-triazolium 5,5'-diamino-4,4'-dinitramino-3,3'-bi-1,2,4-triazolate (**7**) crystallizes in the triclinic space group $P\bar{1}$ with one molecule per unit cell and a density of 1.850 g cm^{-3} at 173 K. The molecular unit is displayed in Figure 6. The cation molecule is completely planar and the bond lengths and angles are similar to other recently reported derivatives.^[12] All bond lengths and angles of the anion match with the values of **2**. The anion is in plane except for the nitramino group. The N10 atom is tilted by 11° out of the triazole plane, indicated by the torsion angle N7-C4-N8-N10. In this molecule the nitramino groups are more bent (torsion angle C4-N8-N10-N11= 74°) relative to the triazole plane than in the compounds **3–6**. Hydrogen bonds are formed from the N4 amino group and to the N10 atom and the nitramino group. Further hydrogen bonds are made up from the N9 amino group to the N10 and N5 atom. As a consequence, the nitramino group is stabilized through three different hydrogen bonds, which could explain the high thermal stability.

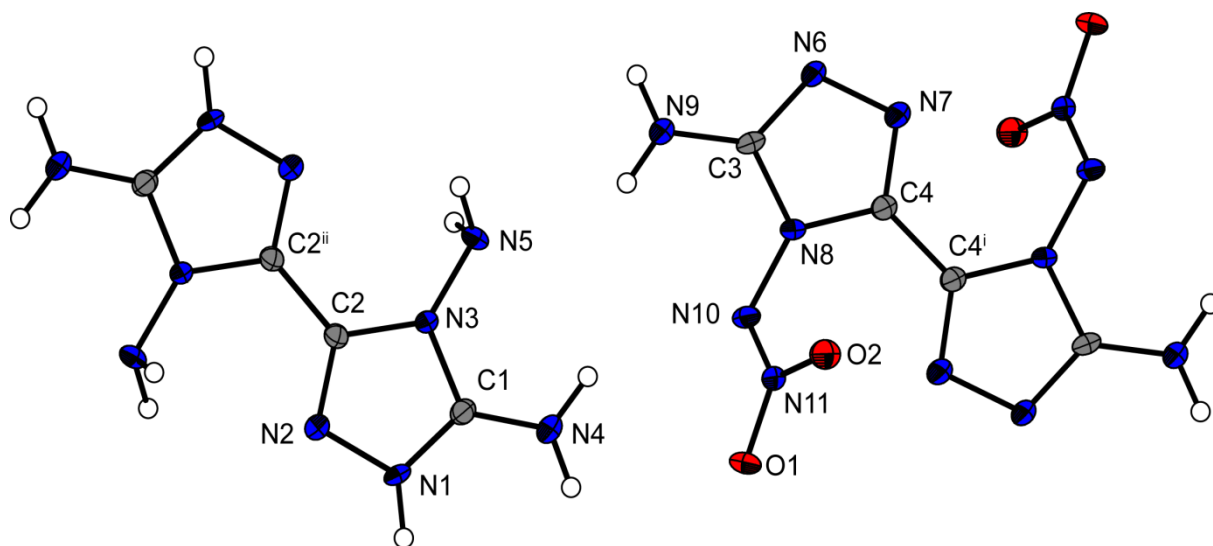


Figure 6. Molecular unit of **7**. Ellipsoids are drawn at the 50 % probability level. Selected bond lengths (Å): C4–C4ⁱ 1.448(3), N8–N10 1.401(2), N10–N11 1.338(2), N9–C3 1.337(3), C2–C2ⁱⁱ 1.444(3), N3–N5 1.406(2), N4–C1 1.330(3); selected bond angles (°): N8–C4–C4ⁱ 123.8(2), N10–N8–C4 128.99(16), N8–N10–N11 109.49(14), O1–N11–N10 114.61(15), N8–C3–N9 124.8(2), N3–C2–C2ⁱⁱ 123.95(17), N5–N3–C2 131.44(17), N3–C1–N4 123.9(2); selected hydrogen bond lengths [Å] and angles [°] (D–H⋯A, $d(\text{D–H})$, $d(\text{H}⋯\text{A})$, $d(\text{D}⋯\text{A})$, $(\text{D–H}⋯\text{A})$): N4–H4B⋯O1 0.87(3), 2.44(3), 3.203(3), 147(2); N4–H4A⋯N10 0.92(3), 2.46(3), 3.271(2), 147(2); N9–H9A⋯N10 0.88(3), 2.60(3), 2.919(3), 102(2); N9–H9A⋯N5 0.88(3), 2.35(3), 3.114(3), 145(3); selected torsion angles (°): N8–C4–C4ⁱ–N8ⁱ $-180.00(18)$, C4–N8–N10–N11 $74.0(2)$, N7–N6–C3–N9 $179.4(2)$, N3–C2–C2ⁱⁱ–N3ⁱⁱ $-180.00(19)$, N2–N1–C1–N4 $179.4(2)$, N5–N3–C1–N1 $172.84(18)$, N7–C4–N8–N10 $168.87(17)$.

Di(3,6,7-triamino-[1,2,4]triazolo[4,3-b][1,2,4]triazolium) 5,5'-diamino-4,4'-dinitramino-3,3'-bi-1,2,4-triazolate dihydrate (**8·2 H₂O**) crystallizes from water in the monoclinic space group $C2/c$ with a density of 1.737 g cm^{-3} at 173 K and four molecules per unit cell. The crystal structure is displayed in Figure 7. The bond lengths and angles of the cation correspond to the values given in the literature.^[13] The bond lengths of the anion are very similar to compound

2. However, both triazole rings in the anion of compound **8** are tilted against each other by 27° (N3-C1-C1ⁱ-N3ⁱ). Additionally the N4 atom of the nitramino group is bent by 12° (N1-C2-N3-N4) out of the triazole plane. As in the other compounds the nitramino groups are twisted out of the plane by nearly 85° (C1-N3-N4-N5).

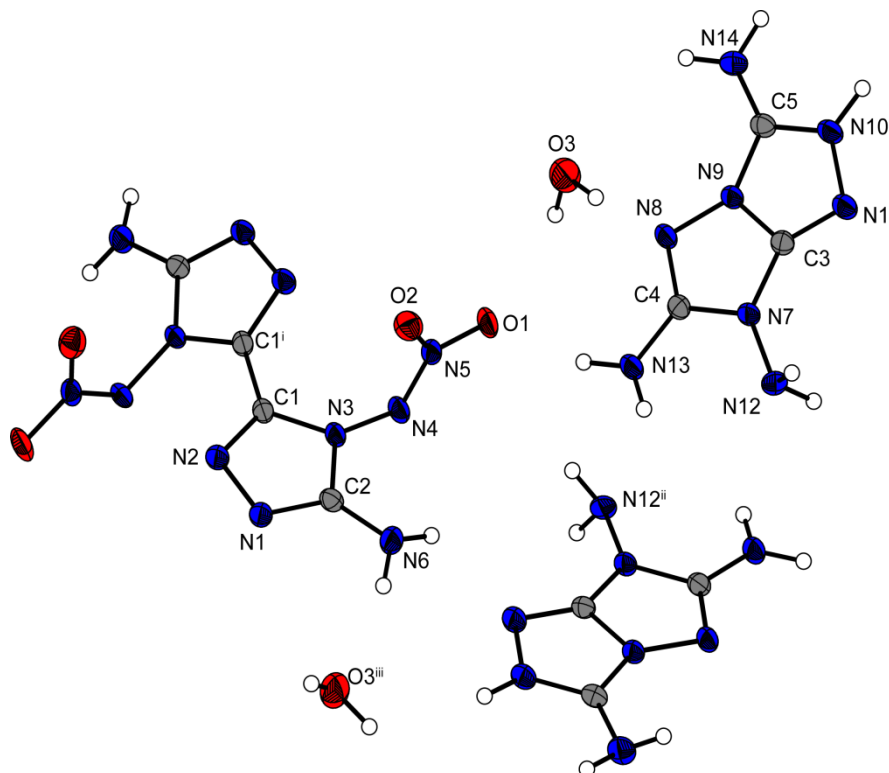


Figure 7. Molecular unit of **8·2 H₂O**. Ellipsoids are drawn at the 50 % probability level. Selected bond lengths (Å): C1–C1ⁱ 1.449(2), N3–N4 1.403(2), N4–N5 1.326(2), N6–C2 1.342(2), N13–C4 1.327(2), N14–C5 1.346(2), N7–N12 1.397(2); selected bond angles (°): N3–C1–C1ⁱ 123.44(13), N4–N3–C2 125.05(12), N3–N4–N5 109.59(12), O1–N5–N4 114.99(13), N3–C2–N6 123.58(14), N8–C4–N13 125.39(14), N12–N7–C3 129.74(12), N10–C5–N14 128.06(14); selected hydrogen bond lengths [Å] and angles [°] (D–H···A, *d*(D–H), *d*(H···A), *d*(D···A), (D–H···A)): O3–H3B···N8 0.91(3), 2.02(3), 2.926(2), 175(2); N6–H6A···O2 0.86(2), 2.27(2), 3.132(2), 177(2); N6–H6B···O3 0.89(3), 2.26(3), 3.125(2), 166(2); N13–H13B···O1 0.93(2), 1.95(2), 2.858(2), 165(2); N14–H14 A···O3 0.88(3), 2.15(3), 2.980(2), 158(2); selected torsion angles (°): N3–C1–C1ⁱ–N3ⁱ 152.29(14), C1–N3–N4–N5 94.45(17), N2–N1–C2–N6 178.81(14), N11–N10–C5–N14 –176.83(14), N9–N8–C4–N13 178.50(14), N12–N7–C4–N8 179.98(13), N1–C2–N3–N4 –167.82(13).

10.2.3 Thermal Analysis and Sensitivities

Due to safety issues, new explosives should be as heat resistant as possible. To identify the decomposition temperatures of compounds **2–8**, differential thermal analysis (DTA) with a heating rate of 5 °C min^{–1} was used. The results are shown in Figure 8. The decomposition temperatures are given as absolute onset temperatures.

Compound **8·2 H₂O** dehydrates at 163 °C, has a melting point at 185 °C and decomposes at a temperature of 200 °C. Beside **8**, all compounds have a higher decomposition temperature

than RDX ($T_{\text{dec}} = 205\text{ }^{\circ}\text{C}$).^[14] The neutral compound **2** shows an excellent thermal stability ($T_{\text{dec}} = 259\text{ }^{\circ}\text{C}$) compared to other nitro substituted triazoles such as the previously reported bis(3-nitroamino-1,2,4-triazole)methane^[15] ($T_{\text{dec}} = 198\text{ }^{\circ}\text{C}$) or 3,3'-dinitro-5,5'-bi-1,2,4-triazole-1,1'-diol^[9] ($T_{\text{dec}} = 191\text{ }^{\circ}\text{C}$). The measured decomposition temperatures of the dihydroxylammonium salt **3** ($T_{\text{dec}} = 210\text{ }^{\circ}\text{C}$) and the dihydrazinium salt **5** ($T_{\text{dec}} = 220\text{ }^{\circ}\text{C}$) are similar to that of RDX. Higher thermal stabilities were determined for the diammonium salt **4** ($T_{\text{dec}} = 278\text{ }^{\circ}\text{C}$) and the diguanidinium salt **6** ($T_{\text{dec}} = 266\text{ }^{\circ}\text{C}$), which is common for these cations.^[16] Compound **7** shows the best thermal stability of the present set of compounds with a decomposition temperature of $296\text{ }^{\circ}\text{C}$ which is in the range of the commonly used high temperature explosive hexanitrostilbene ($T_{\text{dec}} = 316\text{ }^{\circ}\text{C}$).^[17]

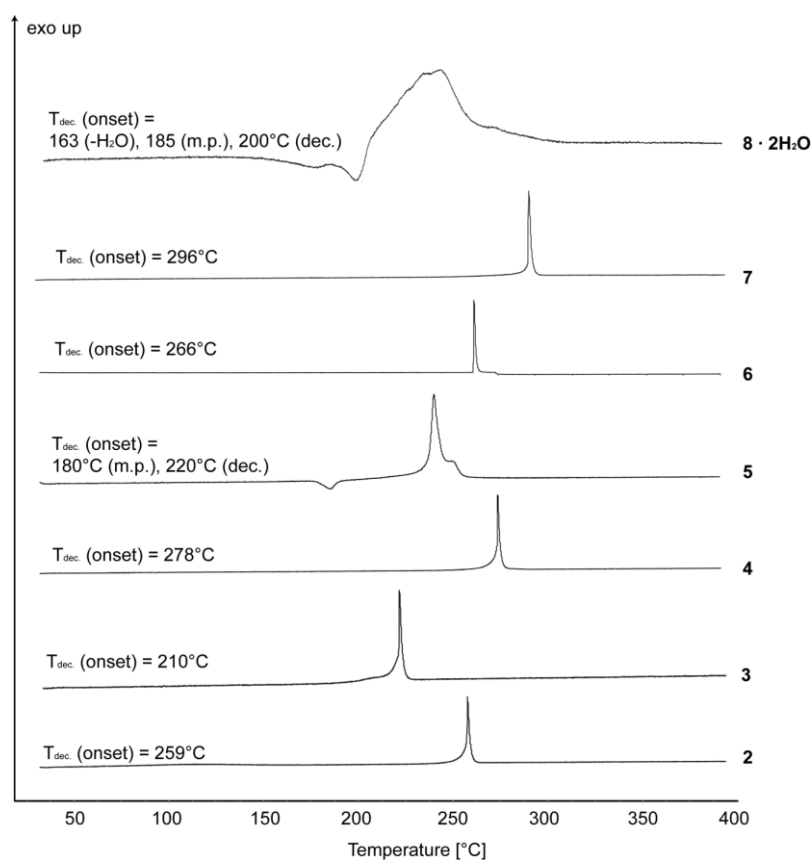


Figure 8. DTA plots of compounds **2–8** measured with a heating rate of $5^{\circ}\text{C min}^{-1}$.

Due to safety issues, new explosives should be less sensitive than contemporary explosives. The neutral compound **2** ($IS = 9\text{ J}$) as well as the salts **3** ($IS = 8\text{ J}$) and **5** ($IS = 9\text{ J}$) are less or equally sensitive toward impact as RDX ($IS = 7.5\text{ J}$). The ammonium salt **4** ($IS = 4\text{ J}$) is the only compound exhibiting a higher impact sensitivity than RDX. Compounds **2** ($FS = 120\text{ N}$), **3** ($FS = 288\text{ N}$), **4** ($FS = 324\text{ N}$) and **5** ($FS = 240\text{ N}$) are less sensitive towards friction than commonly used RDX ($FS = 120\text{ N}$). For compounds **6** ($IS = 40\text{ J}$, $FS = 360\text{ N}$), **7** ($IS = 35\text{ J}$, $FS = 360\text{ N}$) and **8** ($IS = 30\text{ J}$, $FS = 360\text{ N}$) a low friction and impact sensitivity was observed.

Except for zwitterionic **2** ($ESD = 0.15$ J), all compounds show lower sensitivity against electrical discharge than RDX ($ESD = 0.20$ J).

10.2.4 Physiochemical and energetic properties

The heats and energies of formation are given in Table 1. The values were calculated by the atomization method using electronic energies (CBS-4M method). Calculation of the detonation parameters was performed with the program package EXPLO5 (version 6.02).^[18] The parameters of the Becker-Kistiakowsky-Wilson equation of state in EXPLO5 V6.02 are calibrated particularly for the formation of nitrogen, which is the main product from compounds with a high nitrogen content.^[19] The EXPLO5 detonation parameters of compounds **2–8** were calculated by using pycnometrical measured densities of the water free compounds or the room-temperature density values obtained from the X-ray structures as described in Table 1 and in reference [20]. The detonation parameters are summarized in Table 1, alongside a comparison with the values calculated for RDX. For a complete discussion on the methods used see the Supporting Information.

All discussed compounds have a highly positive heat of formation $\Delta_f H^\circ$ in the range from 516.8 kJ mol⁻¹ (**6**) to 1674.0 kJ mol⁻¹ (**8**). The hydroxylammonium salt (**3**), the ammonium salt (**4**) and the guanidinium salt (**6**) have lower heat of formations compared to the neutral **2** ($\Delta_f H^\circ = 691.9$ kJ mol⁻¹). Remarkable high heats of formation were calculated for compound **7** ($\Delta_f H^\circ = 922.9$ kJ mol⁻¹) and compound **8** ($\Delta_f H^\circ = 1674.0$ kJ mol⁻¹).

The calculated detonation pressure p_{CJ} for compounds **2–8** are ranging from 259 kbar (**6**) to 340 kbar (**3**). The highest detonation pressures were achieved for the hydroxylammonium salt (**3**) (340 kbar) and the hydrazinium salt (**5**) (330 kbar). Both values are similar to the detonation pressure of RDX (345 kbar). The calculated p_{CJ} values of the thermally most stable compound **7** (310 kbar) and the neutral compound **2** (312 kbar) are somewhat lower than the detonation pressure of RDX.

Compounds **2–8** reveal satisfying calculated values for the detonation velocity D in the range from 8846 m s⁻¹ (**2**) to 9497 m s⁻¹ (**5**). All compounds show a detonation velocity similar to or higher than that of RDX ($D = 8861$ m s⁻¹). The most promising results were calculated for the hydroxylammonium salt (**3**) with $D = 9313$ m s⁻¹ and the hydrazinium salt (**5**) with $D = 9497$ m s⁻¹. Moreover, the high temperature stable salt **7** has a detonation velocity of $D = 9191$ m s⁻¹.

Table 1. Energetic properties of compounds **2–8** compared with those of **RDX**.

	2	3	4	5	6	7	8	RDX
Formula	C ₄ H ₆ N ₁₂ O ₄	C ₄ H ₁₂ N ₁₄ O ₆	C ₄ H ₁₂ N ₁₄ O ₄	C ₄ H ₁₄ N ₁₆ O ₄	C ₆ H ₁₆ N ₁₈ O ₄	C ₈ H ₁₄ N ₂₂ O ₄	C ₁₀ H ₁₈ N ₂₈ O ₄	C ₃ H ₆ N ₆ O ₆
FW [g mol ⁻¹]	286.17	352.23	320.23	350.26	404.31	482.34	594.44	222.12
<i>IS</i> [J] ^a	9	8	4	9	40	35	30	7.5
<i>FS</i> [N] ^b	120	288	324	240	360	360	360	120
<i>ESD</i> [J] ^c	0.15	1.5	1.0	0.85	1.5	0.75	1.0	0.20
<i>N</i> [%] ^d	58.73	55.67	61.24	63.98	62.36	63.89	65.98	37.84
<i>Q</i> [%] ^e	-39.14	-36.34	-49.96	-50.25	-63.32	-63.03	-67.29	-21.61
<i>T</i> _{dec.} [°C] ^f	259	210	278	180 (m.p.) 220 (dec.)	266	296	185 (m.p.) 200 (dec.)	210
ρ [g cm ⁻³] (298K) ^g	1.756	1.763	1.67 (pyc.)	1.71 (pyc.)	1.656	1.816	1.71 (pyc.)	1.806
$\Delta_f H^\circ$ [kJ mol ⁻¹] ^h	691.9	654.5	524.5	821.5	516.8	922.9	1674.0	70.3
$\Delta_f U^\circ$ [kJ kg ⁻¹] ⁱ	2513.1	1970.7	1752.9	2465.8	1394.7	2016.1	2920.3	417.0
EXPLO5 V6.02 values:								
$-\Delta_f U^\circ$ [kJ kg ⁻¹] ^j	5520	5936.2	4889	5413	4030	4169	4746	5845
<i>T</i> _E [K] ^k	3771	3679	3123	3250	2657	2774	3065	3810
<i>p</i> _{C-J} [kbar] ^l	312	340	284	330	259	310	290	345
<i>D</i> [m s ⁻¹] ^m	8846	9313	8883	9497	8662	9191	8977	8861
<i>V</i> ₀ [L kg ⁻¹] ⁿ	808	897	909	928	889	822	828	785
SSRT:								
Weight [mg]	504	506	-	-	-	512	-	504
Dent [mg SiO ₂]	633	664	-	-	-	475	-	858
Toxicity:								
EC ₅₀ (15 min) [g L ⁻¹]	0.129	0.751	-	-	-	- ^o	-	0.327
EC ₅₀ (15 min) [g L ⁻¹]	0.065	0.346	-	-	-	- ^o	-	0.239

a impact sensitivity (BAM drophammer, 1 of 6); *b* friction sensitivity (BAM friction tester, 1 of 6); *c* electrostatic discharge device (OZM); *d* nitrogen content; *e* oxygen balance; *f* decomposition temperature from DTA ($\beta = 5^\circ\text{C}$); *g* recalculated from low temperature X-ray densities ($\rho_{298\text{K}} = \rho_T / (1 + \alpha_V(298 - T_0))$; $\alpha_V = 1.5 \cdot 10^{-4} \text{ K}^{-1}$); *h* in parenthesis values for the density obtained from the X-ray measurement at 298K; *i* calculated (CBS-4M) heat of formation; *j* calculated energy of formation; *k* energy of explosion; *l* explosion temperature; *m* detonation pressure; *n* detonation velocity; *o* assuming only gaseous products.

A small-scale shock reactivity test (SSRT; see supporting information for detailed setup) was conducted to assess the explosive performance of **2**, **3** and **6** compared with RDX. From measuring the volumes of the dents (Table 1), it can be concluded that the small-scale explosive performances of **2** and **3** are slightly lower than that of commonly used RDX. Moreover the small-scale explosion of **2**, **3** and RDX show more potential as salt **7**.

10.2.5 Toxicity assessment

The toxicity to aquatic life of **2** and **3** was investigated using the luminescent marine bacterium *Vibrio fischeri* (see supporting information).^[21] The half-maximal effective concentration (*EC50*) of neutral **2** is lower than that of RDX (see Table 1), which means **2** is more toxic than RDX. Thus the hydroxylammonium salt **3** has a higher *EC50* value after an incubation time of 15 min and 30 min, which implies that compound **3** is considered less toxic than RDX.

10.2.6 NMR spectroscopy

All compounds described were characterized by using multinuclear NMR spectroscopy. Chemical shifts are given with respect to TMS (¹H, ¹³C) in [D₆]DMSO as the solvent. The ¹H NMR spectrum of the zwitterionic **2** shows a broad signal at 14.30 ppm for the two protonated triazole carbon atoms. Further there is a sharp signal at 8.43 ppm, which indicates the two amino groups. In the ¹³C NMR spectrum two resonances were observed at 152.8 ppm (C–NH₂) and at 137.6 ppm (C–C). Both ¹³C shifts are in the same dimension as reported for the precursor **1**.^[12] Additionally a sharp signal in the ¹⁴N NMR was detected at $\delta = -4.7$ ppm, which can be related to the nitro groups. For the energetic salts **3–8** similar values can be observed: the ¹H chemical shifts of the amino groups of the anion in compounds **3–8** are between 6.56 ppm and 5.50 ppm. The characteristic ¹³C signals of the anions in **3–8** range from 153.9–150.6 ppm (C–NH₂) and 138.3–137.2 ppm (C–C).

10.2.7 Vibrational Spectroscopy

IR and Raman spectra for compounds **2–8** were measured and the frequencies were assigned according to commonly observed values reported in the literature.^[22] In the IR spectrum of compound **2** the asymmetric and the symmetric stretching vibrations of the primary amine were found at 3434 and 3214 cm⁻¹. Similar bands can be found for salts **3–8**: 3436 and 3326 cm⁻¹ (**3**), 3565 and 3133 cm⁻¹ (**4**), 3291 and 3045 cm⁻¹ (**5**), 3457 and 3263 cm⁻¹ (**6**), 3439 and 3143 cm⁻¹ (**7**) and 3398 and 3243 cm⁻¹ (**8**). The nitro group was verified by the very strong N–O stretching vibration at 1273 cm⁻¹ for compound **2** and in the region from 1278–

1293 cm^{-1} for salts **3–8**. Typical triazole ring vibrations occur in the regions between 1575–1400 cm^{-1} for neutral **2** and in similar region for salts **3–8**.

The strongest signal in the Raman spectrum indicates a C=N stretch vibration at around 1630 cm^{-1} for **2–8**. Moreover the amine deformation vibration was found at 1617 cm^{-1} . The absorption at 1284–1250 cm^{-1} could be attributed to the N–O vibration.

10.3 Conclusions

In conclusion, we reported on the feasible and straightforward synthesis of 5,5'-diamino-4,4'-dinitramino-3,3'-bi-(1,2,4-triazole) (**2**) and nitrogen-rich salts thereof. It is possible to selectively nitrate the *N*-amino groups of 4,4',5,5'-tetraamino-3,3'-bi-1,2,4-triazole in high purity and good yields. A full structural and spectroscopic characterization of the target molecule **2** and its derivatives deliver insight into structural characteristics and strong intermolecular interactions. The introduction of the N–NO₂ group next to the C–NH₂ group was found to be an effective method to improve the density while retaining the thermal stability of this molecule through a strong hydrogen-bonding network. Using calculated heats of formation and experimentally obtained crystal densities, the detonation parameters (heat of explosion, explosion temperature, detonation pressure, and velocity) were calculated for compounds **2–8**. The detonation pressure $p_{\text{CJ}} = 259$ (**8**) – 340 kbar (**2**) and detonation velocity $D = 8883$ (**3**) – 9497 m s^{-1} (**4**) are superior over the unnitrated 4,4',5,5'-tetraamino-3,3'-bi-1,2,4-triazole and comparable to the values of RDX ($p_{\text{CJ}} = 345$ kbar, $D = 8861$ m s^{-1}). Decomposition temperatures range from 200 °C (**8**) – 297 °C (**7**). The most promising derivative for potential RDX replacement is the hydroxyl-ammonium salt **3** that has stabilities and energetic properties comparable to RDX yet a lower toxicity than RDX. Also notable is the high thermal stability of energetic salt **7** ($T_{\text{dec.}} = 297$ °C) which is not expected for a triazole with an N–N bonded NO₂ group.

10.4 Experimental Section

General information is provided in the Supporting Information. 4,4',5,5'-Tetraamino-3,3'-bi-1,2,4-triazole (**1**) was synthesized according to the literature.^[12]

10.4.1 5,5'-Diamino-4,4'-dinitramino-3,3'-bi-(1,2,4-triazole) (**2**)

HNO₃ (100%, 80 mL) was placed in a 500 mL three-neck round-bottom flask and cooled to –10 °C. Next, **1** (10.0 g, 50.98 mmol) was slowly added with the temperature not rising above 0 °C. After complete addition, the orange solution was stirred for 90 min at –5 °C. Afterwards the solution was poured onto 300 g of ice and stirred for about 10–15 min. In the solution of

ice water and HNO₃ **2** precipitated as a colorless solid. The precipitate was filtered off, and washed with ice-cooled water, ethanol and ether (3×30 mL respectively) to give a slightly yellowish powder of pure **2**. Yield: 10.1 g (35.29 mmol, 69%). Recrystallization in boiling water yielded colorless crystals suitable for X-Ray diffraction.

DTA (5 °C min⁻¹) onset: 259 °C (dec.); **IR** (ATR, cm⁻¹): $\tilde{\nu}$ = 3434(w), 3214(w), 2715(w), 1688(s), 1515(w), 1440(m), 1273(vs), 1237(m), 1093(w), 1047(w), 997(s), 886(m), 782(m), 705(m); **Raman** (1064 nm, 300 mW, 25 °C, cm⁻¹): $\tilde{\nu}$ = 1695(4), 1645(8), 1630(100), 1617(11), 1582(6), 1466(7), 1284(13), 1127(6), 988(11), 530(9), 269(8), 188(8), 146(15), 125(24), 112(22), 94(41), 73(26); **¹H NMR** ([D₆]DMSO): δ = 14.43 (br s, 2H, N–H), 8.43 ppm (s, 4 H, –NH₂); **¹³C NMR** ([D₆]DMSO): δ = 149.1 (s, C–NH₂), 136.5 ppm (s, C–C); **¹⁴N NMR** ([D₆]DMSO): δ = –4.7 ppm (s, –NO₂); **MS** *m/z* (ESI[–]): 285.1 (C₄H₅N₁₂O₄[–]); *m/z* (ESI⁺): 287.1 (C₄H₇N₁₂O₄⁺); **EA** (C₄H₆N₁₂O₄, 286.17) calcd.: C 16.79, H 2.11, N 58.74%, found: C 16.72, H 2.38, N 57.03%; **Sensitivities**: IS: 9 J, FS: 120 N, ESD: 0.15 J.

Dihydroxylammonium 5,5'-diamino-4,4'-dinitramino-3,3'-bi(1,2,4-triazolate) (3)

2 (1.14 g, 4.00 mmol) was suspended in 40 mL of water. Hydroxylamine (528 mg of a 50% w/v solution in H₂O, 8.00 mmol) was added. The solvent was left for crystallization and **3** precipitated as colorless crystals. Yield: 1.06 g, 3.01 mmol, 75%.

DTA (5 °C min⁻¹) onset: 205 °C (dec.); **IR** (ATR, cm⁻¹): $\tilde{\nu}$ = 3436(w), 3326(m), 3116(m), 2688(m), 1603(s), 1551(m), 1532(m), 1468(m), 1354(s), 1293(vs), 1227(m), 1159(s), 1126(m), 1057(m), 1003(s), 979(m), 877(m), 775(m), 715(w); **Raman** (1064 nm, 400 mW, 25 °C, cm⁻¹): $\tilde{\nu}$ = 1649(8), 1597(100), 1571(20), 1506(5), 1403(3), 1252(10), 1115(8), 1067(9), 1014(8), 1000(24), 801(6), 628(2), 541(5), 268(6), 190(6), 163(10), 139(10), 139(10), 122(21), 104(29), 73(7); **¹H NMR** ([D₆]DMSO): δ = 8.91 (br s, 8H, NH₃OH⁺), 6.20 ppm (s, 4 H, –NH₂); **¹³C NMR** ([D₆]DMSO): δ = 152.8 (C–NH₂), 137.6 ppm (C–C); **MS** *m/z* (FAB[–]): 285.0 (C₄H₅N₁₂O₄[–]); *m/z* (FAB⁺): 34.0 (NH₄O⁺); **EA** (C₄H₁₂N₁₄O₆, 252.11) calcd.: C 13.64, H 3.43, N 55.67%; found: C 13.93, H 3.39, N 55.60%; **Sensitivities**: IS: 8 J; FS: 288 N; ESD: 1.5 J.

Diammonium 5,5'-diamino-4,4'-dinitramino-3,3'-bi(1,2,4-triazolate) (4)

2 (1.14g, 4.00 mmol) was suspended in 50 mL of water. 5 mL of a 2 M NH₃ solution (10 mmol, 2.5 equiv.) were added and the suspension was stirred at ambient temperature until a clear solution appeared. The solution was left for crystallization for four days and **4** precipitated as small colorless crystals. Yield: 0.87 g, 2.72 mmol, 68%.

DTA (5 °C min⁻¹) onset: 278 °C (dec.); **IR** (ATR, cm⁻¹): $\tilde{\nu}$ = 3565(vw), 3133(m), 1638(m), 1570(w), 1480(w), 1415(m), 1366(s), 1281(vs), 1226(s), 1100(m), 1029(m), 996(w), 966(w), 878(m), 778(m), 717(w), 662(w); **Raman** (1064 nm, 400 mW, 25 °C, cm⁻¹): $\tilde{\nu}$ = 1612(80), 1591(100), 1575(14), 1256(14), 1103(8), 1041(10), 1002(31), 793(7), 539(7), 276(7), 108(32), 90(33), 76(29). **¹H NMR** ([D₆]DMSO): δ = 7.15 (br s, 8H, NH₄⁺), 6.52 ppm (s, 4 H, -NH₂); **¹³C NMR** ([D₆]DMSO): δ = 151.9 (C-NH₂), 137.4 ppm (C-C); **¹⁴N NMR** ([D₆]DMSO): δ = -358 ppm (NH₄⁺); *m/z* (FAB⁻): 285.0 (C₄H₅N₁₂O₄⁻), *m/z* (FAB⁺): 18.0 (NH₄⁺); **EA** (C₄H₁₂N₁₄O₄, 320.23) calcd.: C 15.00, H 3.78, N 61.24%, found: C 15.25, H 3.81, N 58.99%; **Sensitivities**: IS: 4 J; FS: 324 N; ESD: 1.0 J.

Dihydrazinium 5,5'-diamino-4,4'-dinitramino-3,3'-bi(1,2,4-triazolate) (5)

2 (1.14 g, 4.00 mmol) was suspended in 40 mL of water and a hydrazinium hydroxide solution (0.40 g, 8 mmol, 2.0 equiv.) was added. The solution was left for crystallization and **5** precipitated as a colorless needles, too small for X-Ray diffraction. Yield: 0.80 g, 2.28 mmol, 57%.

DTA (5 °C min⁻¹) onset: 180 °C (m.), 220 °C (dec.); **IR** (ATR, cm⁻¹): $\tilde{\nu}$ = 3291(m), 3045(m), 1659(m), 1562(m), 1459(w), 1416(w), 1361(s), 1314(s), 1286(vs), 1226(m), 1149(w), 1096(s), 1057(s), 1013(m), 962(s), 873(m), 810(m), 761(m), 747(m), 706(s), 655(vw); **Raman** (1064 nm, 300 mW, 25 °C, cm⁻¹): $\tilde{\nu}$ = 1581(100), 1564(51), 1501(6), 1400(4), 1324(4), 1257(16), 1173(8), 1091(7), 1071(13), 1010(28), 966(4), 886(3), 809(7), 719(4), 622(5), 536(7), 372(8), 263(5), 180(7), 149(23), 120(13), 120(13), 103(16), 88(13), 75(8); **¹H NMR** ([D₆]DMSO): δ = 7.17 (br s, 10H, N₂H₅⁺), 5.50 ppm (s, 4H, -NH₂); **¹³C NMR** ([D₆]DMSO): δ = 153.9 (C-NH₂), 138.3 ppm (C-C); **MS** *m/z* (FAB⁻): 285.0 (C₄H₁₃N₁₆O₄⁻), *m/z* (FAB⁺): 33.0 (N₂H₅⁺); **EA** (C₄H₁₄N₁₆O₄, 350.26) calcd.: C 13.72, H 4.03, N 63.98%; found: C 14.05, H 3.95, N 63.06%; **Sensitivities**: IS: 9 J; FS: 240 N; ESD: 0.85 J.

Diguanidinium 5,5'-diamino-4,4'-dinitramino-3,3'-bi(1,2,4-triazolate) (6)

2 (1.14 g, 4.00 mmol) was suspended in 50 mL of water. Guanidinium carbonate (721 mg, 8.00 mmol) was added and the suspension was heated until a clear solution appeared and no more CO₂ development was observed. Slight impurities were filtered off and the solution was left for crystallization. **6** precipitated as large colorless needles. Yield: 1.29 g, 3.19 mmol, 80%.

DTA (5 °C min⁻¹) onset: 266 °C (dec.); **IR** (ATR, cm⁻¹): $\tilde{\nu}$ = 3457(w), 3404(w), 3341(m), 3263(m), 3128(m), 1655(s), 1618(s), 1556(s), 1457(m), 1364(s), 1285(vs), 1212(m), 1128(m),

1049(m), 997(m), 965(m), 874(m), 703(m); **Raman** (1064 nm, 400 mW, 25°C, cm⁻¹): $\tilde{\nu}$ = 1625(5), 1612(10), 1598(100), 1582(9), 1572(5), 1549(16), 1500(2), 1251(6), 1149(4), 1085(4), 1060(8), 1012(15), 998(14), 795(4), 208(3), 145(19), 100(16); **¹H NMR** ([D₆]DMSO): δ = 7.17 (s, 12H, -NH₂), 5.64 ppm (s, 4 H, -NH₂); **¹³C NMR** ([D₆]DMSO): δ = 158.0 (C-NH₂), 153.5 (CH₆N₃⁺) 137.6 ppm (C-C); **MS** *m/z* (FAB⁻): 285.1 (C₄H₅N₁₂O₄⁻), *m/z* (FAB⁺): 60.1 (CH₆N₃⁺); **EA** (C₆H₁₆N₁₈O₄, 404.32) calcd.: C 17.82, H 3.99, N 62.36%, found: C 18.10, H 3.97, N 62.08%; **Sensitivities**: IS: 40 J; FS: 360 N; ESD: 1.5 J.

4,4',5,5'-Tetraamino- 3,3'-bi(1,2,4-triazolium 5,5'-diamino-4,4'-dinitramino-3,3'-bi(1,2,4-triazolate) (7)

1 (0.78 g, 4.00 mmol, 2.0 equiv.) was suspended in 4.50 L of hot water. **2** (1.14 g, 4.00 mmol) was added and the suspension was heated until a clear solution was formed. The solution was filtered and the solvent was left for crystallization. **6** precipitated as colorless needles. Yield: 1.61 g, 3.33 mmol, 83%.

DTA (5 °C min⁻¹) onset: 296 °C (dec.); **IR** (ATR, cm⁻¹): $\tilde{\nu}$ = 3439(w), 3338(m), 3291(m), 3143(m), 1619(m), 1552(w), 1497(w), 1474(m), 1403(s), 1278(vs), 1218(s), 1081(s), 1020(vs), 997(s), 801(m), 773(m), 730(w), 704(m); **Raman** (1064 nm, 400 mW, 25°C, cm⁻¹): $\tilde{\nu}$ = 1641(96), 1614(100), 1499(3), 1425(3), 1290(8), 1245(9), 1132(19), 1097(10), 1008(21), 884(3), 801(13), 736(6), 696(5), 632(4), 315(6), 279(10), 202(11), 163(22), 140(43), 106(24), 89(21), 89(21), 74(19); **¹H NMR** ([D₆]DMSO): δ = 7.65 (s, 4H, -NH₂, cat.⁺), 6.56 (s, 4H, -NH₂, anion), 5.89 (s, 4H, -NH₂, Cat.⁺); **¹³C NMR** ([D₆]DMSO): δ = 155.1 (s, C-NH₂, cat.⁺), 150.6 (s, C-NH₂, anion), 139.4 (s, C-C, cat.⁺), 137.2 (s, C-C, anion); **MS** *m/z* (ESI⁻): 285.1 (C₄H₅N₁₂O₄⁻); *m/z* (ESI⁺): 197.1 (C₄H₉N₁₀⁺); **EA** (C₈H₁₄N₂₂O₄, 482.16) calcd.: C 19.92, H 2.93, N 63.89%; found: C 20.14, H 2.96, N 63.89%; **Sensitivities**: IS: 35 J; FS: 360 N; ESD: 0.75 J.

Di-(3,6,7-triamino-[1,2,4]triazolo[4,3-*b*][1,2,4]triazolium) 5,5'-diamino-4,4'-dinitramino-3,3'-bi(1,2,4-triazolate) dihydrate (8·2 H₂O)

2 (1.14 g, 4.00 mmol) and **TATOT**^[13] (1.23 g, 8.00 mmol, 2.0 equiv.) were dissolved in 200 mL of water. The solution was left for crystallization and **8·2 H₂O** precipitated as orange-brown crystals. Yield: 2.15 g, 3.41 mmol, 85%.

DTA (5 °C min⁻¹) onset: 180 °C (m), 220 °C (dec.); **IR** (ATR, cm⁻¹): $\tilde{\nu}$ = 3560(w), 3398(m), 3296(m), 3243(m), 3133(m), 1629(vs), 1563(m), 1515(w), 1471(m), 1437(w), 1383(s), 1340(m), 1278(vs), 1251(s), 1231(m), 1157(w), 935(m), 881(m), 842(w), 704(m), 666(w);

Raman (1064 nm, 400 mW, 25°C, cm⁻¹): $\tilde{\nu}$ = 3182(3), 3140(3), 1651(8), 1613(8), 1597(100), 1579(18), 1387(5), 1280(11), 1252(11), 1130(5), 1063(12), 1010(27), 847(7), 796(6), 624(8), 536(4), 418(6), 367(5), 321(9), 245(9), 153(42), 136(32), 136(32), 89(23), 69(13); **¹H NMR** ([D₆]DMSO): δ = 7.01 (s, 4H, N-NH₂, cat.⁺), 6.85 (s, 4H, C-NH₂, cat.⁺), 6.68 (s, 4H, -NH₂, anion), 5.69 ppm (s, 4H, C-NH₂, cat.⁺); **¹³C NMR** ([D₆]DMSO): δ = 159.9 (C-NH₂, cat.⁺), 152.2 (C_q, anion), 148.6 (C-NH₂, cat.⁺), 142.6 (C-NH₂, cat.⁺), 137.8 ppm (C-C, anion); **MS** m/z (FAB⁻): 285.0 (C₄H₁₃N₁₆O₄⁻); m/z (FAB⁺): 155.1 (C₃H₉N₈⁺); **EA** (C₁₀H₂₂N₂₈O₆, 630.48): C 19.05, H 3.52, N 62.21%; found: C 19.35, H 3.52, N 61.66%; **Sensitivities**: IS: 30 J; FS: 360 N; ESD: 1.0 J.

10.5 References

- [1] W. E. Bachmann, J. C. Sheehan, *J. Am. Chem. Soc.* **1949**, 71, 1842–1845.
- [2] B. Tollens, P. Wigand, *Liebigs Ann. Chem.* **1891**, 265, 316–340.
- [3] A. T. Nielsen, R. A. Nissan, D. J. Vanderah, C. L. Coon, R. D. Gilardi, C. F. George, J. Flippen-Anderson, *J. Org. Chem.* **1990**, 55, 1459–1466.
- [4] N. Fischer, D. Fischer, T. M. Klapötke, D. G. Piercey, J. Stierstorfer, *J. Mater. Chem.* **2012**, 22, 20418–20422.
- [5] a) J. Giles, *Nature* **2004**, 427, 580–581; b) M. B. Talawar, R. Sivabalan, T. Mukundan, H. Muthurajan, A. K. Sikder, B. R. Gandhe, A. Subhananda Rao, *J. Hazard. Mater.* **2009**, 161, 589–607.
- [6] H. Xue, B. Twamley, J. M. Shreeve, *Inorg. Chem.* **2005**, 44, 7009–7013; b) N. Sasidharan, B. Hariharanath, A. G. Rajendran, *Thermochim. Acta* **2011**, 520, 139–144; c) H. Xue, H. Gao, B. Twamley, J. M. Shreeve, *Chem. Mater.* **2007**, 19, 1731–1739; d) Y. Tang, J. M. Shreeve, *Chem. Eur. J.* **2015**, 21, 7285–7291; e) A. A. Dippold, D. Izsák, T. M. Klapötke, *Chem. Eur. J.* **2013**, 19, 12042–12051.
- [7] A. A. Dippold, T. M. Klapötke, N. Winter, *Eur. J. Inorg. Chem.* **2012**, 2012, 3474–3484.
- [8] A. A. Dippold, T. M. Klapötke, *Chem. Eur. J.* **2012**, 18, 16742–16753.
- [9] A. A. Dippold, T. M. Klapötke, *J. Am. Chem. Soc.* **2013**, 135, 9931–9938.
- [10] A.R. Mitchell, P.F. Pagoria, R.D. Schmidt, U.S. Patent No. 5,569,783 (29 October 1996).

- [11] C. He, J. M. Shreeve, *Angew. Chem. Int. Ed.* **2015**, 54, 6260–6264; *Angew. Chem.* **2015**, 127, 6358–6362.
- [12] T. M. Klapötke, P. C. Schmid, S. Schnell, J. Stierstorfer, *J. Mater. Chem. A* **2015**, 3, 2658–2668.
- [13] T. M. Klapötke, P. C. Schmid, S. Schnell, J. Stierstorfer, *Chem Eur. J.* **2015**, *in press*, DOI:10.1002/chem.201500982.
- [14] H. Maruizumi, D. Fukuma, K. Shirota, N. Kubota, *Propellants, Explos., Pyrotech.* **1982**, 7, 40–45.
- [15] E. L. Metelkina, T. A. Novikova, S. N. Berdonosova, D. Y. Berdonosov, V. S. Grineva, *Russ. J. Org. Chem.* **2004**, 40, 1412–1414.
- [16] K. Hafner, T. M. Klapötke, P. C. Schmid, J. Stierstorfer, *Eur. J. Inorg. Chem.* **2015**, *in press*, DOI:10.1002/ejic.201500338.
- [17] K. G. Shipp, *J. Org. Chem.* **1964**, 29, 2620–2623.
- [18] M. Suceska, EXPLO5V6.02 program, Brodarski Institute, Zagreb, Croatia, **2014**.
- [19] Muhamed Suceska, private communication.
- [20] C. Xue, J. Sun, B. Kang, Y. Liu, X. Liu, G. Song, Q. Xue, *Propellants, Explos., Pyrotech.* **2010**, 35, 333–338.
- [21] G. I. Sunahara, S. Dodard, M. Sarrazin, L. Paquet, G. Ampleman, S. Thiboutot, J. Hawari and A. Y. Renoux, *Ecotoxicol. Environ. Saf.* **1998**, 39, 185–194.
- [22] a) S. Bienz, L. Bigler, T. Fox in *Spektroskopische Methoden in der organischen Chemie*, 8th ed., Georg Thieme Verlag, Stuttgart, New York, **2012**; b) G. Socrates in *Infrared and Raman Characteristic Group Frequencies: Tables and Charts*, 3rd ed., John Wiley & Sons, Chichester, **2004**; c) M. Hesse, H. Meier, B. Zeeh, in *Spektroskopische Methoden in der Organischen Chemie*, 7th ed., Thieme, Stuttgart, New York, **2005**.

10.6 Supplementary information

The analytical methods and general procedures are described in the appendix of this thesis.

10.6.1 Crystallographic data and refinement parameters

Table S1. Crystallographic data and refinement parameters of compound **2**, **3** and **4b**.

	2	3	4b
Formula	C ₄ H ₆ N ₁₂ O ₄	C ₄ H ₁₂ N ₁₄ O ₆	C ₄ H ₉ N ₁₃ O ₆
FW [g mol ⁻¹]	286.21	252.11	339.27
Crystal system	orthorhombic	orthorhombic	monoclinic
Space Group	<i>Pbca</i>	<i>Pbca</i>	<i>C2/c</i>
Color / Habit	colorless, block	colorless, block	colorless, block
Size [mm]	0.05×0.10×0.20	0.15×0.25×0.30	0.15 × 0.19 × 0.29
<i>a</i> [Å]	9.0563(5)	11.2979(9)	16.3573(10)
<i>b</i> [Å]	10.2770(7)	6.8967(7)	9.2230(5)
<i>c</i> [Å]	11.4144(8)	16.7190(13)	9.8708(6)
α [°]	90.0	90.0	90.0
β [°]	90.0	90.0	116.962(5)
γ [°]	90.0	90.0	90.0
<i>V</i> [Å ³]	1062.36(12)	1302.7(2)	1327.28(14)
<i>Z</i>	4	4	4
$\rho_{\text{calc.}}$ [g cm ⁻³]	1.789	1.796	1.698
μ [mm ⁻¹]	0.156	0.161	0.156
<i>F</i> (000)	584	728	704
$\lambda_{\text{MoK}\alpha}$ [Å]	0.71073	0.71073	0.71073
<i>T</i> [K]	173	173	173
ϑ min-max [°]	4.2, 26.5	4.2, 26.5	4.2, 26.2
Dataset <i>h</i> ; <i>k</i> ; <i>l</i>	−11:7; −12:12; −14:14	−14:11; −6:8; −20:19	−20:15; −11:11; −12:12
Reflect. coll.	7912	5264	4913
Independ. refl.	1099	1353	1335
<i>R</i> _{int}	0.052	0.033	0.030
Reflection obs.	894	1122	1126
No. parameters	103	133	135
<i>R</i> ₁ (obs)	0.0352	0.0329	0.0354
<i>wR</i> ₂ (all data)	0.0843	0.0869	0.0873
<i>S</i>	1.06	1.07	1.06
Resd. Dens.[e Å ⁻³]	−0.24, 0.24	−0.21, 0.31	−0.25, 0.15
Device type	Oxford XCalibur3 CCD	Oxford XCalibur3 CCD	Oxford XCalibur3 CCD
Solution	SIR-92	SIR-92	SIR-92
Refinement	SHELXL-97	SHELXL-97	SHELXL-97
Absorpt. corr.	multi-scan	multi-scan	multi-scan

Table S2. Crystallographic data and refinement parameters of compound **6–8**.

	6	7	8
Formula	C ₆ H ₁₆ N ₁₈ O ₄	C ₈ H ₁₄ N ₂₂ O ₄	C ₁₀ H ₂₂ N ₂₈ O ₆
FW [g mol ⁻¹]	404.32	482.16	630.48
Crystal system	triclinic	triclinic	monoclinic
Space Group	<i>P</i> -1	<i>P</i> -1	<i>C</i> 2/ <i>c</i>
Color / Habit	colorless, block	colorless, plate	yellow, plate
Size [mm]	0.40×0.40×0.45	0.05×0.12×0.40	0.04×0.33×0.40
<i>a</i> [Å]	4.7356(3)	7.0525(7)	16.6037(9)
<i>b</i> [Å]	7.8357(5)	7.4726(11)	6.7266(5)
<i>c</i> [Å]	11.3245(7)	9.2053(10)	21.7277(11)
α [°]	106.827(6)	75.464(11)	90.00
β [°]	97.813(5)	67.744(10)	96.391(5)
γ [°]	90.181(5)	89.029(10)	90.00
<i>V</i> [Å ³]	398.09(5)	432.96(10)	2411.6(3)
<i>Z</i>	1	1	4
$\rho_{\text{calc.}}$ [g cm ⁻³]	1.687	1.850	1.737
μ [mm ⁻¹]	0.141	0.153	0.145
<i>F</i> (000)	210	248	1304
$\lambda_{\text{MoK}\alpha}$ [Å]	0.71073	0.71073	0.71073
<i>T</i> [K]	173	173	173
ϑ min-max [°]	4.3, 26.5	4.2, 26.8	4.2, 26.5
Dataset <i>h</i> ; <i>k</i> ; <i>l</i>	−5:5; −9:9; −14:14	−6:8; −9:9; −14:14	−16:20; −7:8; −27:17
Reflect. coll.	5882	2402	4993
Independ. refl.	1641	1816	2500
<i>R</i> _{int}	0.033	0.013	0.037
Reflection obs.	1410	1470	2112
No. parameters	159	178	243
<i>R</i> ₁ (obs)	0.0334	0.0440	0.0372
<i>wR</i> ₂ (all data)	0.0863	0.1173	0.1030
<i>S</i>	1.09	1.08	1.06
Resd. Dens.[e Å ⁻³]	−0.33, 0.20	−0.50, 0.41	−0.27, 0.28
Device type	Oxford XCalibur3 CCD	Oxford XCalibur3 CCD	Oxford XCalibur3 CCD
Solution	SIR-92	SIR-92	SIR-92
Refinement	SHELXL-97	SHELXL-97	SHELXL-97
Absorpt. corr.	multi-scan	multi-scan	multi-scan

10.6.2 Crystal Structure of compound 4b

A crystal structure of ammonium salt **4** was obtained from water, with only one ammonium cation and two water moieties. The structure of **4b** is illustrated in Figure S1

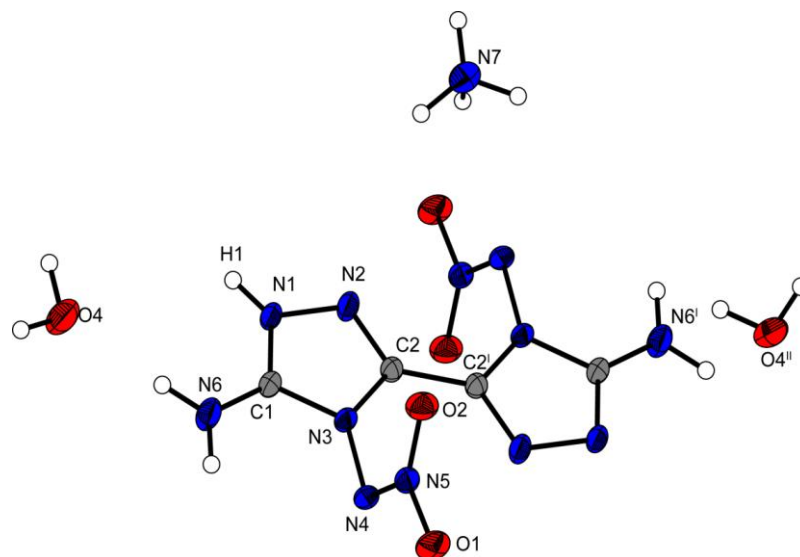


Figure S1. Molecular unit of **4b**. Ellipsoids are drawn at the 50% probability level.

10.6.2 Heat of formation calculations

General information about the heat of formation calculations can be found in the appendix of this thesis. The calculation results are summarized in Table S2.

Table S3. Calculation results

M	$-H^{298}$ ^[a] / a.u.	$\Delta_f H^\circ(\text{g}, \text{M})$ / kJ mol^{-1} ^[b]	V_M / nm^3 ^[c]	$\Delta U_L, \Delta H_L$ (4); ΔH_{sub} ^[e] (3) / kJ mol^{-1} ^[d]	$\Delta_f H^\circ(\text{s})$ ^[f] / kJ mol^{-1}	Δn ^[g]	$\Delta_f U(\text{s})$ ^[f] / kJ kg^{-1}
2	1112.213392	791.9		100.0	691.9	11.0	2513.1
Hx ⁺	131.863249	686.4					
A ²⁻	1111.140196	542.9					
3		1915.8	0.332	1253.9, 1261.3	654.5	16.0	1970.7
NH ₄ ⁺	56.796608	635.3					
4		1813.5	0.313	1282.0, 1289.4	524.2	15.0	1752.9
N ₂ H ₅ ⁺	112.030523	773.4					
5		2089.8	0.327	1260.8, 1268.2	821.5	17.0	2465.8
G ⁺	205.453192	571.2					
6		1685.3	0.406	1161.1, 1168.5	516.8	19.0	1394.8
TABTr ²⁺	704.327388	2032.9					
7		2575.8	0.441	1648.0, 1652.9	922.9	20.0	2016.2
TATOT ⁺	555.474133	1080.0					
8		2703.0	0.564	1021.6, 1029.1	1674.0	25.0	2920.3

^[a] CBS-4M electronic enthalpy; ^[b] gas phase enthalpy of formation; ^[c] molecular volumes taken from X-ray structures and corrected to room temperature; ^[d] lattice energy and enthalpy (calculated using Jenkins and Glasser equations); ^[e] enthalpy of sublimation (calculated by Trouton rule); ^[f] standard solid state enthalpy of formation; ^[g] solid state energy of formation.

10.6.3 Toxicity assessment

The *Luminescent Bacteria Inhibition Test* offers a possibility to determine the environmental acceptability of new energetic materials to aquatic organisms whereat a marine bacteria is used as a representative for marine organisms. In this test the decrease of the luminescence of the liquid-dried bacteria is determined after 15 min and 30 min at different concentrations of the test compounds and is compared to a control measurement of a 2% NaCl stock solution.

The sample dilution sequence corresponds to DIN 38412 L34, which ranges from 1:2 to 1:32 dilution of the compound in the test system. For a better reproducibility, all dilution steps were made in duplicate. The change of intensity of bacterial luminescence in the absence (controls) and in the presence (samples) of the tested substances after different incubation times (15 min, 30 min) were recorded. The controls (2% NaCl only) were measured for calculating the correction factor, which is necessary to consider the normal decrease of luminescence without any toxic effect per time.

The EC_{50} value gives the concentration of each compound where the bacterial luminescence is inhibited by 50% and is calculated by plotting Γ against the concentration of the test substance in a diagram with a logarithmic scale, where $\Gamma = \text{inhibition (in \%)} / 100 - \text{inhibition (in \%)}$ and $c = \text{concentration of the test sample}$. The EC_{50} value is identical with the intersection of the resulting graph with the X-axis ($\Gamma = 0$).

For better comparison of the resulting toxicities, we also determined the toxic effect of RDX to the bacterial strain under the same conditions applied for the toxicity assessment of neutral **2** and salt **3**. To imitate the natural environment of the employed marine bacterium as good as possible, the samples need to be diluted with a 2% (w/v) sodium chloride solution. Since RDX is barely soluble in water, a stock solution in acetone was prepared, which was further diluted with the sodium chloride solution to a mixture containing 200 ppm RDX in water/acetone 99/1 (v/v).

10.6.4 Small scale shock reactivity test

The Small-Scale Shock Reactivity Test (SSRT)^[1,2] was introduced by researchers at IHDIV,DSWC (Indian Head Division, Naval Surface Warfare Center). The SSRT measures the shock reactivity (explosiveness) of energetic materials, often well-below critical diameter, without requiring a transition to detonation. The test setup combines the benefits from a lead block test and a gap test. In comparison to gap tests, the advantage is the use of a much smaller sample size of the tested explosive (ca. 500 mg). The sample volume V_s is

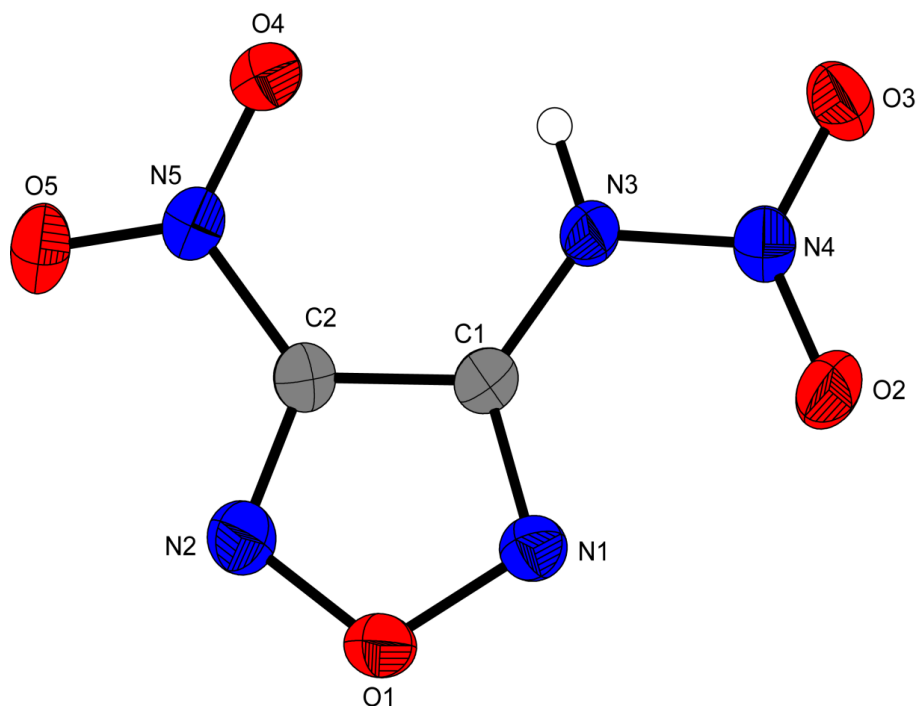
recommended to be 0.284 mL (284 mm³). For our test setup no possible attenuator (between detonator and sample) and air gap (between sample and aluminum block) was used. The used sample weight m_s was calculated using the formula $V_s \times \rho_{\text{Xray}} \times 0.95$. The dent sizes were measured by filling them with powdered SiO₂ and measuring the resulting weight.

10.6.5 References

- [1] J. E Felts, H. W. Sandusky, R. H. Granholm, *AIP Conf. Proc.* **2009**, 1195, 233.
- [2] H. W. Sandusky, R. H. Granholm, D. G. Bohl, IHTR 2701, Naval Surface Warfare Center, Indian Head, MD, 12 Aug **2005**.

Crystal Structures of Furazanes

published in *Crystals* **2015**, *5*, 518–432. (DOI: 10.3390/cryst5040418)



Abstract: Several nitrogen-rich salts of 3-nitramino-4-nitrofurazane and dinitraminoazoxyfurazane were synthesized and characterized by various spectroscopic methods. The crystal structures were determined by low temperature single crystal X-ray diffraction. Moreover the sensitivities toward thermal and mechanical stimuli were determined by differential thermal analysis (DTA) and BAM (Bundesanstalt für Materialforschung und -prüfung) methods. The standard enthalpies of formation were calculated for all compounds at the CBS-4M level of theory, and the energetic performance was predicted with the EXPLO5 V6.02 computer code.

Keywords: X-ray · energetic · furazane · nitrogen-rich salts · nitramino

11.1 Introduction

Modern energetic materials need to fulfill several criteria to become potential replacements for commonly used Research Department explosive (RDX). In addition to having excellent detonation velocities and pressures, new secondary explosives must comply with certain safety criteria, such as a decomposition temperature over 200 °C and low sensitivity to mechanical stimuli as impact (> 7.5 J) or friction (> 120 N). In recent years, the growth in environmental concern has resulted in the desire for energetic materials that release environmentally benign dinitrogen after decomposition^[1]. Forming the energetic salt of a neutral compound can improve the performance of explosives without compromising their safety^[2]. We recently reported on the two nitrogen-rich cations 4,4',5,5'-tetraamino-3,3'-bi-triazolium^[3] and 3,6,7-triamino[1,2,4]triazolo[4,3-b][1,2,4]triazolium^[4], which can form thermally stable energetic salts. With these two nitrogen-rich cations in hand, we have now synthesized several new ionic furazanes to increase the decomposition temperatures of previously known 3-nitramino-4-nitrofurazan **4**^[5] and dinitraminoazoxyfurazan **10**^[6]. Moreover, we report on the crystal structures of the 3-nitramino-4-nitrofurazan **4** as well as its hydroxylammonium **5** and ammonium **6** salt. Although compounds **4–6** have been previously described in the literature^[5,7], X-ray analyses deliver insight into structural characteristics that could explain the high density of this interesting class of energetic molecules.

11.2 Results and Discussion

11.2.1 Synthesis

The preparations of the energetic derivatives of 3-nitramino-4-nitrofurazan **4** and dinitraminoazoxyfurazan **10** are displayed in Figure 1.

Glyoxal was stirred with 4.3 equivalents of hydroxylammonium chloride under basic conditions to give diaminoglyoxime **1**^[8]. Compound **1** was heated in an autoclave to build the furazan ring eliminating one molecule of water to give diaminofurazan **2**^[8]. To obtain compound **3**, compound **2** was oxidized with persulfuric acid and Na₂WO₄^[9]. Compound **3** can be easily nitrated under relatively “mild” conditions with N₂O₅ to give 3-nitramino-4-nitrofurazan **4**^[5]. The energetic salts hydroxylammonium 3-nitramino-4-nitrofurazan **5**, ammonium 3-nitramino-4-nitrofurazan (**6**), 4,4',5,5'-tetraamino-3,3'-bi-triazolium di-3-nitramino-4-nitrofurazan **7** and 3,6,7-triamino-[1,2,4]triazolo[4,3-b][1,2,4]triazolium 3-nitramino-4-nitrofurazan **8** can be synthesized by treating compound **4** with the respective base.

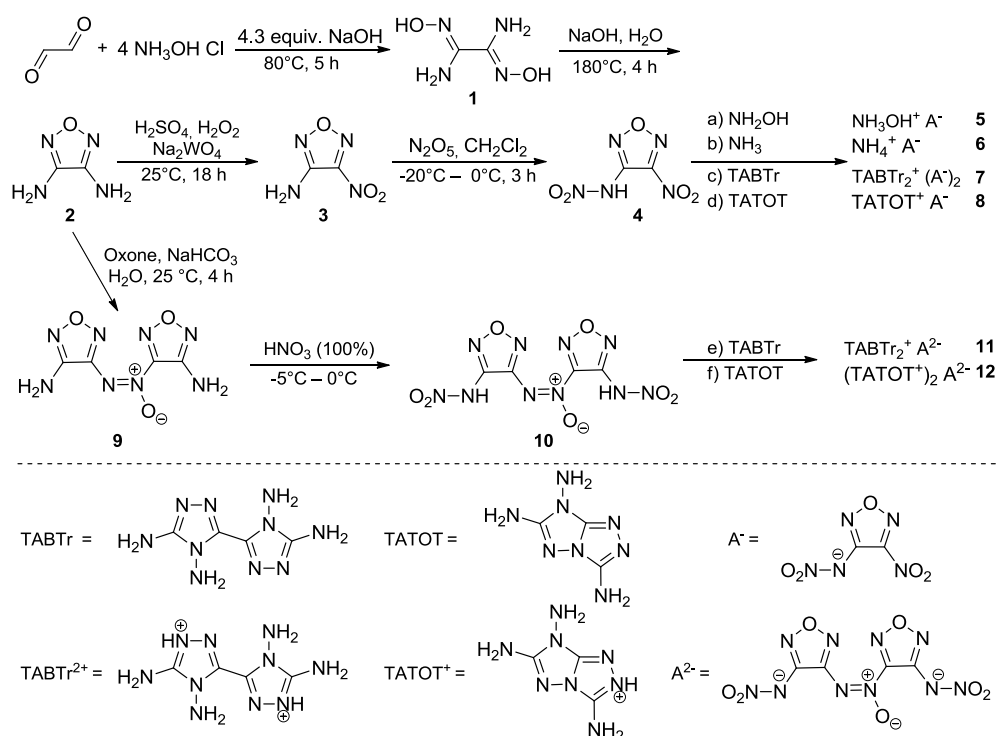


Figure 1. Synthesis of 3-nitramino-4-nitrofurazan **4** and dinitraminoazoxyfurazan **10** as well as their energetic salts.

Diaminofurazane **2** was treated with Oxone® and sodium bicarbonate as described by Chavez et. al. to give diaminazoxyfurazan **9**^[10]. Compound **9** was then stirred in nitric acid (100%) to nitrate the two amino groups to obtain dinitraminoazoxyfurazan **10**^[6]. Two thermally stable derivatives 4,4',5,5'-tetraamino-3,3'-bi-triazolium dinitraminoazoxyfurazan **11** and di-3,6,7-triamino-[1,2,4]triazolo[4,3-b][1,2,4]triazolium dinitraminoazoxy-furazan **12** were obtained by treating the acid **10** with the corresponding bases.

11.2.2 Crystal Structure

The crystal structures of compounds **3–6**, **8** and **12** were determined. Tables S1–S2 in the Supporting Information gather selected data and parameters of the X-ray measurements. Once crystals were obtained for each compound, we did not attempt to search for additional polymorphs of each.

The compound 3-amino-4-nitraminofurazan **3** crystallizes in the orthorhombic space group $\text{Pna}2_1$ with a cell volume of 938.26 \AA^3 and eight molecular units per unit cell (Figure 2). The calculated density at 173 K is $1.842 \text{ g}\cdot\text{cm}^{-3}$, which is similar to the previously reported density of $1.84 \text{ g}\cdot\text{cm}^{-3}$ (X-ray analysis at 153 K)^[11]. Compound **3** is planar, only the nitro moiety is slightly tilted against the furazan plane by a torsion angle of $\text{O2-N3-C1-C2} = 4.4^\circ$.

Short hydrogen bonding can be observed between the amino and nitro groups, similar bond distances have been reported for other furazanes in the literature^[6]. A more detailed description of the structure can be found in the literature^[11].

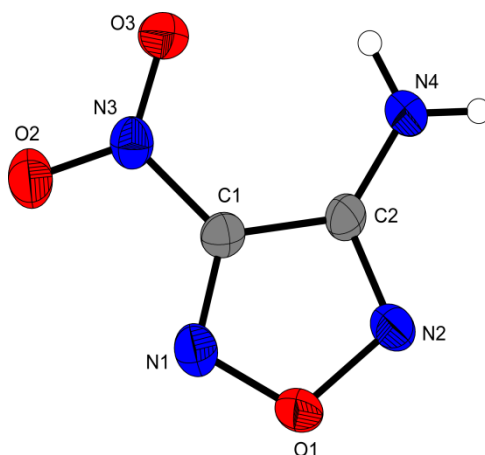


Figure 2. Molecular unit of **3**. Ellipsoids are drawn at the 50% probability level. Selected bond distances (Å): O1–N1 1.352(4), O1–N2 1.409(5), C1–C2 1.428(6), N4–N2 1.331(7), N3–C1 1.450(5), O2–N3 1.226(5); selected bond angles (°): N1–O1–N2 111.1(3), N1–C1–C2 111.8(3), N3–C1–C2 128.1(4), N4–C2–C1 129.5(4); selected hydrogen bond distances [Å] and angles [°] (D–H...A, d(D–H), d(H...A), d(D...A), (D–H...A)): N4–H4A...O3: 0.87(5), 2.38(5), 2.919(5), 120(4); N4–H4A...N1 0.87(5), 2.29(2), 3.084(6), 152(5); selected torsion angles (°): N2–O1–N1–C1 0.6(4), O2–N3–C1–C2 4.4(5), O1–N2–C2–N4 179.2(4).

The compound 3-nitramino-4-nitrofurazan **4** crystallizes in the orthorhombic space group *Pbca* with a cell volume of 1177.45 Å³ and eight molecular units per unit cell. The calculated density at 173 K is 1.975 g·cm^{−3}, which is comparable to the density reported in the literature: 1.93 g·cm^{−3} (gas pycnometer)^[5] and 1.95 g·cm^{−3}^[7]. The small discrepancies are likely due to the different temperatures at which the densities were measured. The molecular unit of **4** is displayed in Figure 3.

The nitro- and nitramino groups in compound **4** are only slightly tilted against the furazan ring as shown by the torsion angles O4–B5–C2–C1 = 4.2°, C1–N3–N4–O2 = 179.4° and C1–N3–N4–O2 = 3.9°. Together with the planar furazan ring (N2–O1–N1–C1 = 0.5°) the complete compound forms an almost planar unit, which might be one of the reasons that can explain the high density of this compound. Another reason might be the hydrogen-bonds of N3–H3...O4 and N3–H3...O3. The bond distances of the furazan ring (C1–C2 = 1.420 Å) and the nitro group (N5–C2 1.444 Å, O5–N5 = 1.215 Å) are similar to those in other nitrofurazanes as compound **3**. The bond distances of the nitramino moiety (O2–N4 = 1.210 Å, N3–N4 = 1.370 Å) are also in the same range compared to other nitramino moieties in heterocyclic ring systems^[6,12].

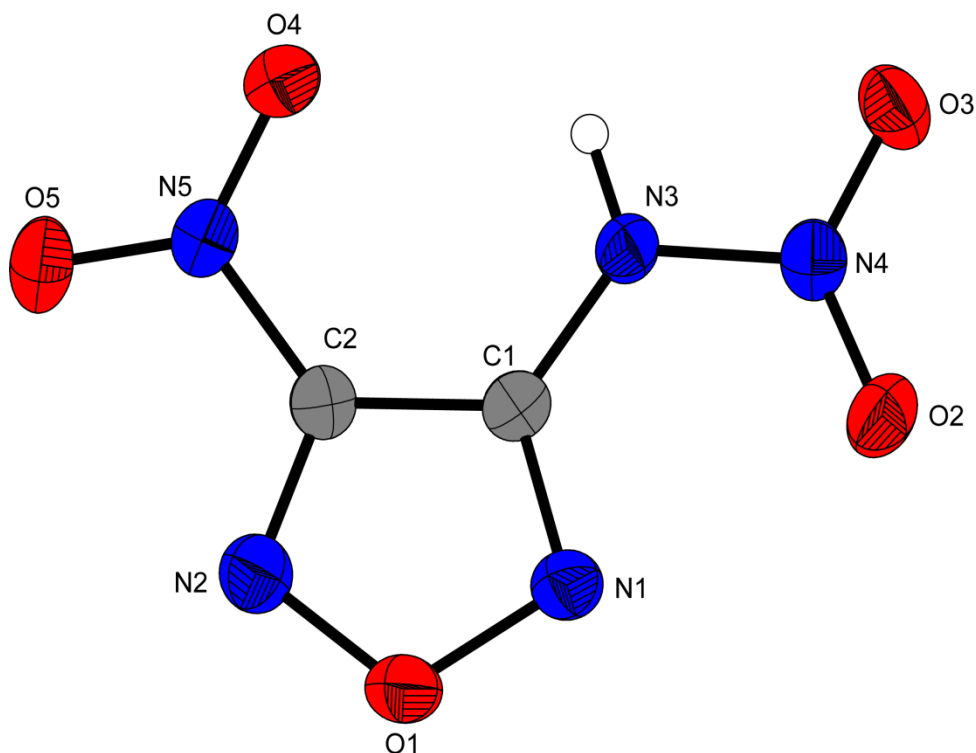


Figure 3. Molecular unit of **4**. Ellipsoids are drawn at the 50% probability level. Selected bond distances (Å): O2–N4 1.210(2), N3–N4 1.370(2), N3–C1 1.365(2), N5–C2 1.444(2), O5–N5 1.215(2), C1–C2 1.420(3); selected bond angles (°): N2–C2–N5 111.23 (17), N3–C1–C2 107.69(16), N1–O1–N2 112.26(14); selected hydrogen bond distances [Å] and angles [°] (D–H...A, d(D–H), d(H...A), d(D...A), (D–H...A)): N3–H3...O4: 0.85(3), 2.29(2), 2.787(2), 111.8(2); N3–H3...O3 0.85(3), 2.21(3), 3.016(2), 159(2); selected torsion angles (°): N2–O1–N1–C1 0.5(2), O4–N5–C2–C1 4.2(3), C1–N3–N4–O2 179.4(2), C1–N3–N4–O3 3.9 (3).

Hydroxylammonium 3-nitramino-4-nitrofurazan **5** crystallizes in the monoclinic space group *Pc* with a cell volume of 361.86 Å³ and two molecular units per unit cell. The calculated density at 173 K is 1.910 g·cm^{−3}, which is comparable to the reported values in the literature: 1.875 g·cm^{−3} (X-ray analysis)^[5] and 1.89 g·cm^{−3}^[7]. The slightly higher density values of **5** might be because of the different temperatures at which the densities were measured. The molecular unit of **5** is displayed in Figure 4.

Similar to neutral compound **4**, the furazan unit in **5** is planar (N2–O2–N1–C1 = 1.1°), whereas the nitro- and nitramino groups are slightly tilted against the furazan ring as indicated by the torsion angles of O5–N5–C2–N2 = 5.1° and N4–N3–C1–C2 = 171.7°, C1–N3–N4–O3 = 2.5°. Hydrogen-bonding can for example be observed between the hydrogen atoms of the hydroxylammonium cation and the O4 of the nitramino moiety. The bond distances of the furazan ring (C1–C2 = 1.432 Å), the nitro group (N5–C2 = 1.451 Å, O6–N5 = 1.243 Å) and the nitramino moiety (N3–N4 = 1.307 Å, O4–N4 = 1.280 Å) are in accordance with parent compound **4**.

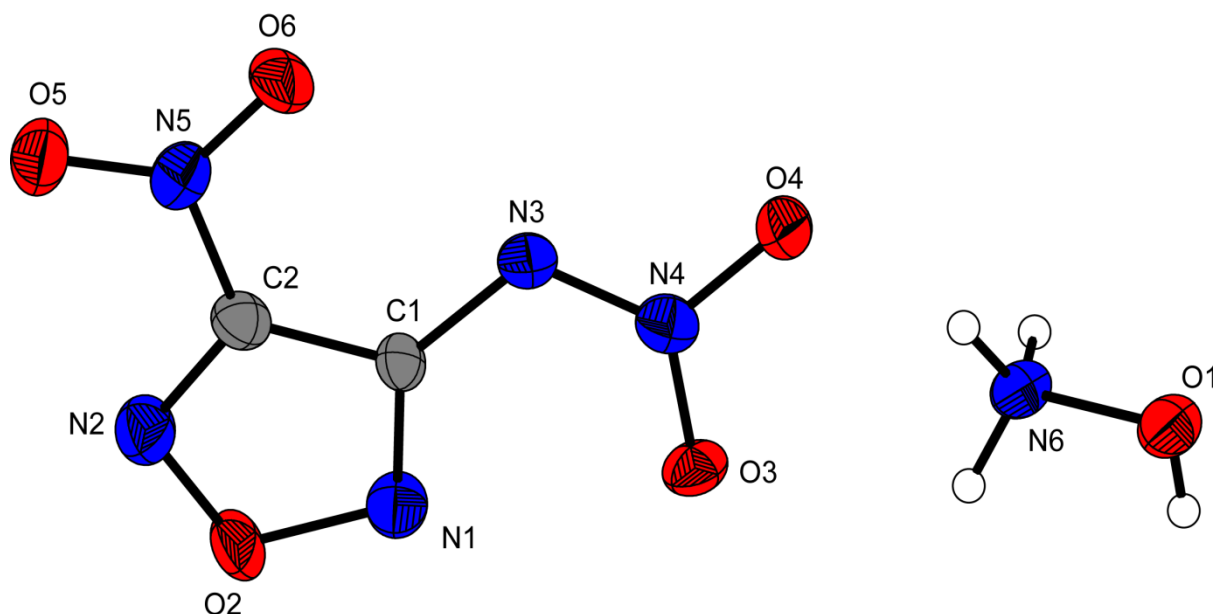


Figure 4. Molecular unit of **5**. Ellipsoids are drawn at the 50% probability level. Selected bond distances (Å): N5–C2 1.451(8), O6–N5 1.243(6), N3–C1 1.385(7), N3–N4 1.307(2), O4–N4 1.280(6), C1–C2 1.432(8); selected bond angles (°): N1–O2–N2 111.8(4), N2–C2–N5 119.7(5), N1–C1–N3 129.7(5), O3–N4–N3 125.5(5); selected hydrogen bond distances [Å] and angles [°] (D–H...A, d(D–H), d(H...A), d(D...A), (D–H...A)): N6–H6B...O4: 0.910, 2.440, 2.892(6), 111.00; O1–H4A...O4 0.73(6), 1.94(6), 2.653(6), 169(6); selected torsion angles (°): N2–O2–N1–C1 1.1(6), O5–N5–C2–N2 5.1(8), N4–N3–C1–C2 171.7(5), C1–N3–N4–O3 2.5(8).

Ammonium 3-nitramino-4-nitrofurazan **6** crystallizes in the monoclinic space group $P2_1/n$ with a cell volume of 704.59 Å³ and four molecular units per unit cell. The calculated density at 173 K is 1.811 g·cm^{−3}, which is virtually the same as the reported density in the literature: 1.82 g·cm^{−3}^[7], but significantly lower than of hydroxylammonium salt **5**. The molecular unit of compound **6** is illustrated in Figure 5.

As in salt **5** and neutral compound **4**, the furazan ring in **6** has a planar structure (N2–O1–N1–C1 = 0.27°). While the nitramino group is only slightly tilted against the furazan plane (N5–N4–C1–N1 = 5.5°, C1–N4–N5–O5 = 2.9°), the nitro group is tilted strongly against the plane by a torsion angle of O2–N3–C2–N2 = 29.5°. A reason for this might be the strong hydrogen bonds between the hydroxylammonium cation and the oxygen atoms O3 and O4 of the nitro group. More hydrogen bonds can be observed between the cation and the nitramino moiety. Even though the nitro group is strongly tilted against the plane, the bond distances of the furazan ring (C1–C2 = 1.4293 Å), the nitro group (N3–C2 = 1.451 Å, O3–N3 = 1.217 Å) and nitramino moiety (N4–N5 = 1.3179 Å, O4–N4 = 1.257 Å) are comparable to parent compound **4** and salt **5**.

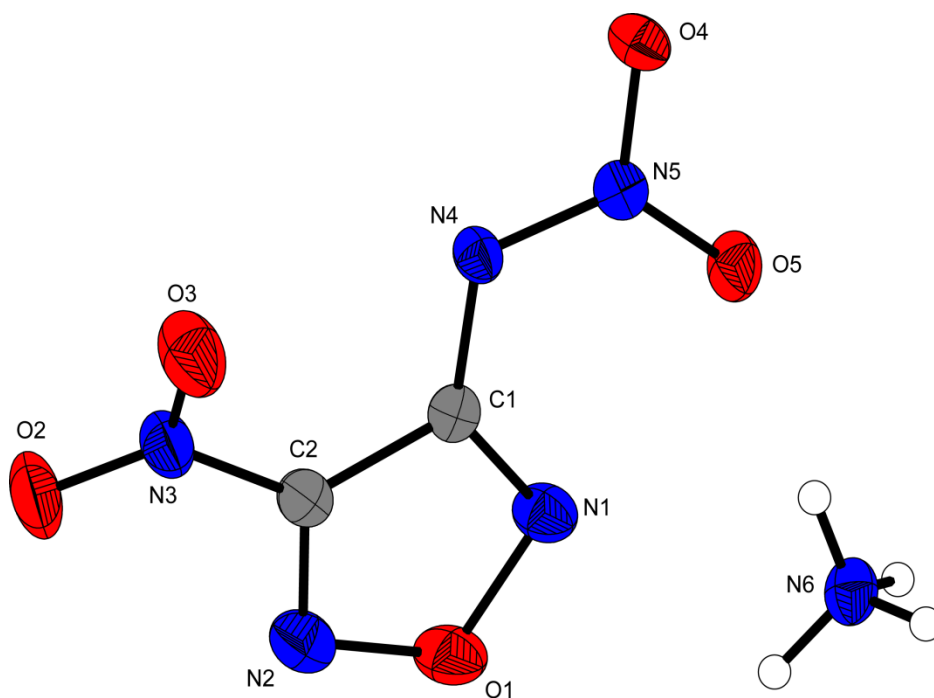


Figure 5. Molecular unit of **6**. Ellipsoids are drawn at the 50% probability level. Selected bond distances (Å): C1–C2 1.4293(17), N3–C2 1.451(2), O3–N3 1.217(2), N4–C1 1.3684(15), N4–N5 1.3179(15), O4–N4 1.2570(14); selected bond angles (°): N1–O1–N2 111.72(10), N2–C2–N3 119.64(11), N1–C1–N4 132.09(11), O5–N5–N4 124.25(11); selected hydrogen bond distances [Å] and angles [°] (D–H...A, d(D–H), d(H...A), d(D...A), (D–H...A)): N6–H4A...O3: 0.87(2), 2.51(3), 3.249 (2), 143(2); N6–H4A...O2: 0.87(2), 2.38(3), 3.043 (2), 133.6(18); N4–H4B...O5 0.91(2), 2.09(2), 2.993(2), 176(2); selected torsion angles (°): N2–O1–N1–C1 0.27(14), N5–N4–C1–N1 5.5(2), O2–N3–C2–N2 29.5(2), C1–N4–N5–O5 2.9(2).

3,6,7-Triamino-[1,2,4]triazolo[4,3-b][1,2,4]triazolium 3-nitramino-4-nitrofuran **8** crystallizes in the monoclinic space group $P2_1$ with a cell volume of 619.21 Å³ and two molecular units per unit cell. The calculated density at 173 K is 1.766 g·cm^{−3}, which is lower than the density of salts **5** and **6**. The molecular unit of compound **8** is shown in Figure 6.

In compound **8**, the furazan ring is also planar (N2–O1–N1–C1 = 0.27°), whereas the nitro (O5–N3–C2–C1 = 157.9°) and nitramino (N5–N4–C1–C2 = 50.6°, O2–N5–N4–C1 = 7.4°) moieties are strongly tilted out of the furazan plane. The cation has a planar structure except for the two protons located at N13 as reported previously in the literature^[4]. All the three amino groups in the cation form hydrogen bonds to the nitro and nitramino groups of the anion, resulting in a strong hydrogen-bonding network. This effect was expected because it was already observed for other energetic salts of the 3,6,7-triamino-[1,2,4]triazolo[4,3-b][1,2,4]triazolium cation^[4] and can explain the higher thermal stability of compound **8** compared to that of salts **5** and **6**. The bond distances of the furazan ring (C1–C2 = 1.422 Å), the nitro group (C2–N3 = 1.441 Å, O4–N3 = 1.211 Å) and the nitramino group (O3–N5 = 1.227 Å, N4–N5 = 1.300 Å) are virtually the same as in parent compound **4** or salts **5** and **6**. The bond distances of the cation fit the values of the literature^[4].

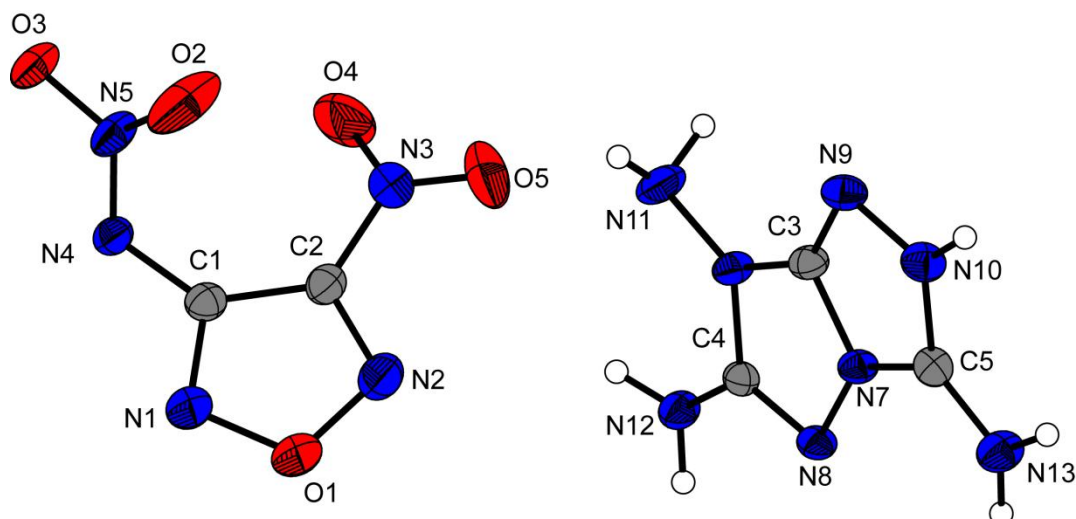


Figure 6. Molecular unit of **8**. Ellipsoids are drawn at the 50% probability level. Selected bond distances (Å): C1–C2 1.422(3), N4–C1 1.381(3), N4–N5 1.300(3), O3–N5 1.277(3), C2–N3 1.441(3), O4–N3 1.211(3); selected bond angles (°): N1–O1–N2 111.64(19), N2–C2–N3 138.4(2), O2–N5–N4 123.3(2), N4–C1–C2 134.1(2); selected hydrogen bond distances [Å] and angles [°] (D–H⋯A, d(D–H), d(H⋯A), d(D⋯A), (D–H⋯A)): N10–H10⋯O3: 0.79(3), 2.08(3), 2.869(2), 175(3); N11–H11A⋯N2 0.87(4), 2.42(4), 3.190(3), 148(3); N12–H12A⋯O5 0.88(3), 2.58(3), 3.345(3), 147(3); selected torsion angles (°): N2–O1–N1–C1 1.2(3), O2–N5–N4–C1 7.4(4), N5–N4–C1–C2 50.6(4), O5–N3–C2–C1 157.9(2).

Di-3,6,7-triamino-[1,2,4]triazolo[4,3-b][1,2,4]triazolium dinitraminoazoxyfuran **12** crystallizes in the triclinic space group P-1 with a cell volume of 561.13 Å³ and one molecular units per unit cell. The calculated density at 173 K is 1.807 g·cm⁻³, which is somewhat lower than the density of the corresponding hydroxylammonium salt: 1.883 g·cm⁻³ (X-ray analysis at 173 K).^[6] The molecular unit of compound **12** is displayed in Figure 7.

In compound **12**, the N=N connected furazan rings are tilted against each other by a torsion angle of 38.2° (N3i–N3–NC2–C1). O4 is in the same plane as the furazan ring which is located further away (O4–N3–C3i–C2i = 1.0°) and twisted against the furazan ring which is closer to O4 (O4–N3–C2–C1 = 37.0°). The two nitramino moieties are also tilted out of the furazan plane by 44.0° (N6–N5–C1–C2). The two cations have a planar structure except for the two protons located at N13 as reported previously in the literature^[4]. As in salt **8**, an intensive hydrogen bond network is formed between the three amino groups of the cation and the nitro and nitramino groups of the anion, which makes the salt **12** stable up to 266 °C. The bond distances of the anion (C1–C2 = 1.432 Å, N5–C1 = 1.380 Å, N5–N6 = 1.306 Å, O2–N6 = 1.244 Å, C2–N3 = 1.416 Å, N3–O4 = 1.199 Å), are in accordance with other dinitraminoazoxyfurazanes^[6]. The bond distances of the cation are in good agreement with literature values.^[4]

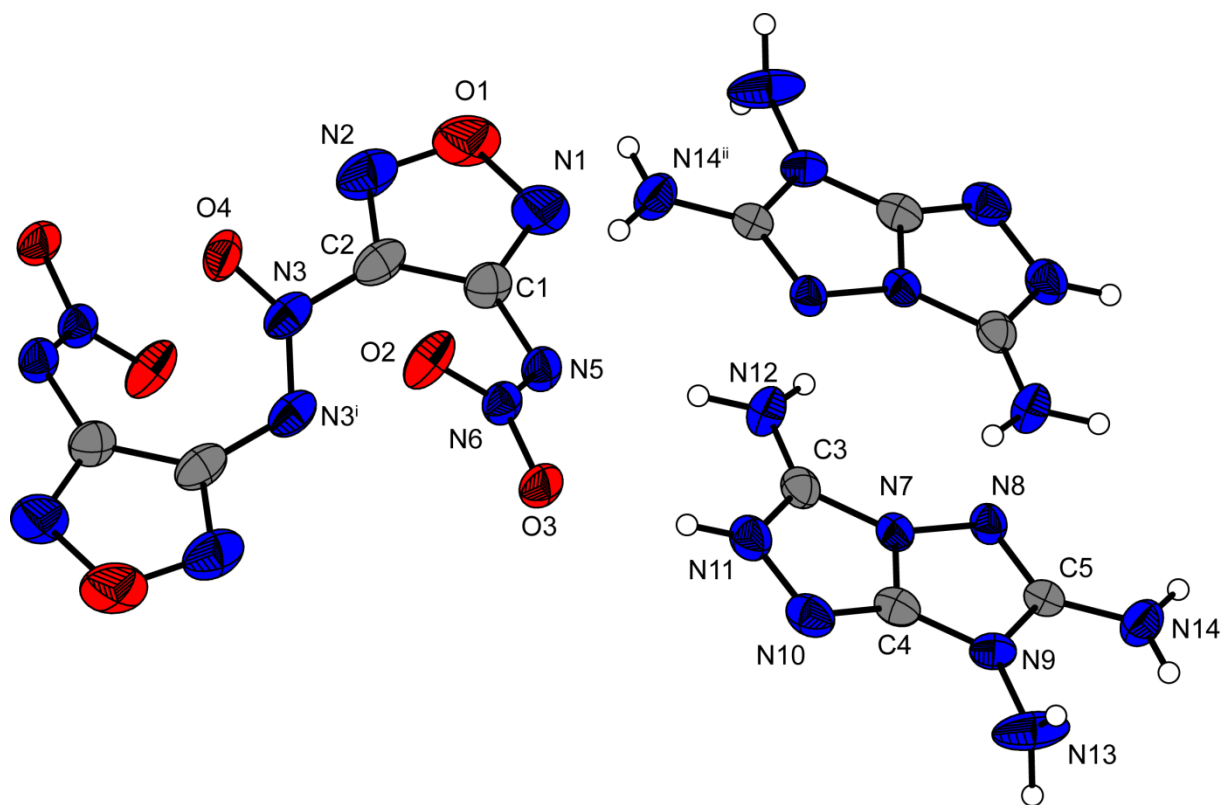


Figure 7. Molecular unit of **12**. Ellipsoids are drawn at the 50% probability level. Selected bond distances (Å): C1–C2 1.432(4), N5–C1 1.380(3), N5–N6 1.306(3), O2–N6 1.244(3), C2–N3 1.416(4), N3–O4 1.199(4), N3–N3i 1.268(3); selected bond angles (°): N3i–N3–C2 115.2(2), N4–N3–C2 111.9(3), N6–N5–C1 113.2(2); selected hydrogen bond distances [Å] and angles [°] (D–H \cdots A, d(D–H), d(H \cdots A), d(D \cdots A), (D–H \cdots A)): N11–H11 \cdots O3: 0.89(2), 1.95(3), 2.814(3), 164(3); N12–H12A \cdots N5 0.90(4), 2.11(2), 3.001(3), 171(3); N12–H12B \cdots O2 0.86(4), 2.48(3), 3.163(3), 137(3); selected torsion angles (°): N3i–N3–C2–C1 38.2(4), O4–N3–C3i–C2i 1.0(4), O4–N3–C2–C1 37.0(4), N6–N5–C1–C2 44.0(4), C1–N5–N6–O2 5.7(3).

11.2.3 Thermal Analysis and Sensitivities

Considering safety issues explosives should be heat resistant. To identify the decomposition temperatures of compounds **3–12**, differential thermal analysis (DTA) with a heating rate of 5 °C·min^{−1} was used. The results are shown in Figure 8. The decomposition temperatures are given as absolute onset temperatures.

Compound **3** decomposes at 143 °C, whereas 3-nitramino-4-nitrofurazan **4** as well as its hydroxylammonium **5** and hydrazinium salt **6** decompose between 65 °C and 140 °C. The thermal stability of 3-nitramino-4-nitrofurazan could be enhanced by introducing thermally stable cations as demonstrated by compounds **7** and **8** with a decomposition onset at 176 °C and 193 °C. Moreover compounds **11** and **12** surpass a decomposition temperature of 200 °C, which can be considered as benchmark for new potential secondary explosives.

Sensitivities of compounds **3–12** were determined and are displayed in Table 1. The impact sensitivities for the derivatives of 3-nitramino-4-nitrofurazan **4** range from 3 J (**7**) to 10 J (**5**).

The two energetic salts of dinitraminoazoxyfuran **10** show similar and slightly lower impact sensitivities with 15 J (**11**) and 10 J (**12**). The friction sensitivities lie between 120 N (**4**) and 360 N (**12**), except for the hydroxylammonium **5** and ammonium **6** salt, both of which comprise a friction sensitivity of 72 N.

Although all structures are dominated by a large variety of hydrogen bonds and other electrostatic interactions all investigated compounds were found to be sensitive toward various outer stimuli. Except for energetic polymorphs in our opinion it is still very challenging to correlate sensitivities and structural motives. For neutral compounds some strategies have been described e.g. by Politzer *et al.* They correlated impact sensitivity *versus* electrostatic surface potentials or molecular volumes^[13]. However, these methods have not successfully been applied for energetic salts, which deviate significantly from standard energetic motifs, such as those found in traditional explosives, such as TNT and RDX.

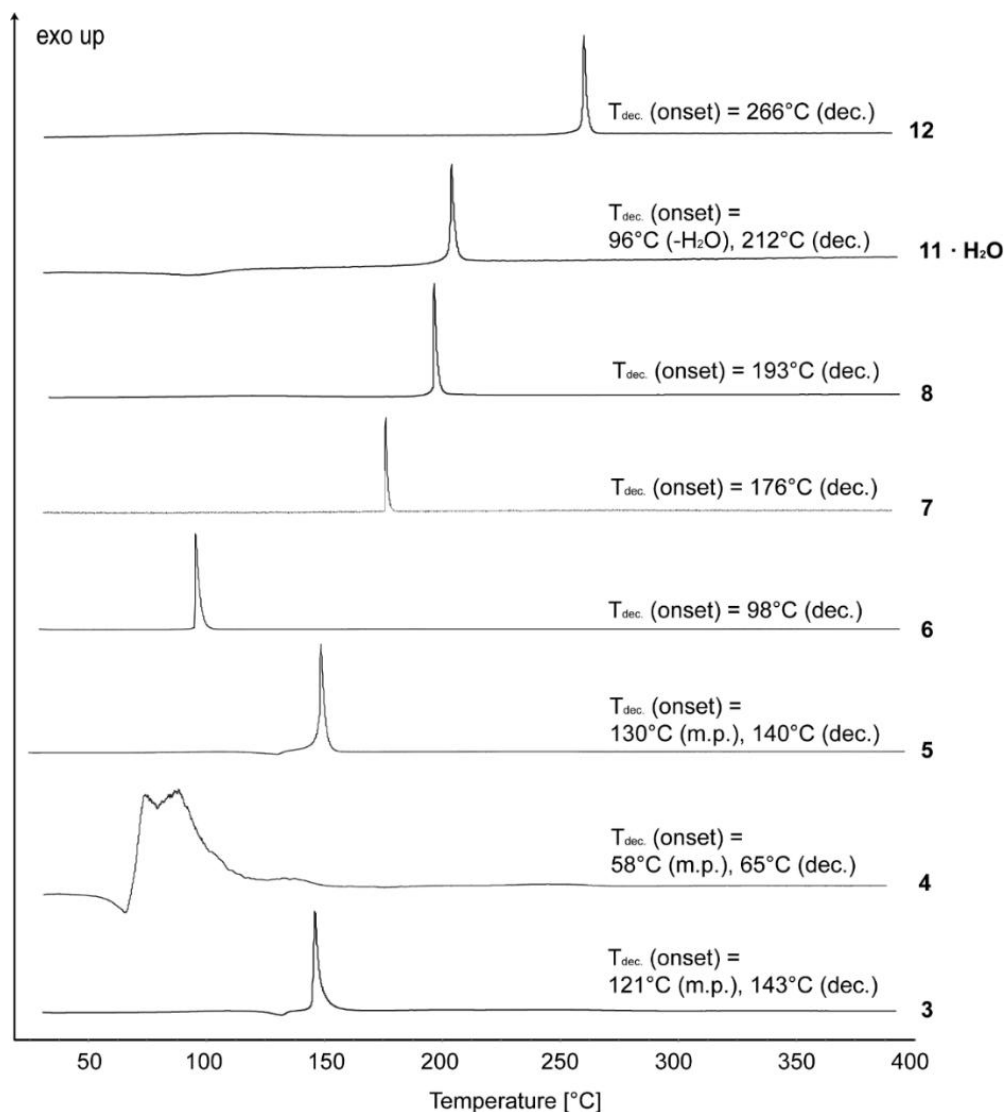


Figure 8. Differential thermal analysis (DTA) plots of compounds **3–12** measured with a heating rate of 5 °C·min⁻¹.

11.2.4 Physiochemical and energetic properties

The heats and energies of formation are given in Table 1. Calculation of the detonation parameters as detonation velocity D and detonation pressure p_{CJ} was performed with the program package EXPLO5 (version 6.02).^[14] The EXPLO5 detonation parameters of compounds **2–12** were calculated by using pycnometrical measured densities of the water free compounds or the room-temperature density values obtained from the X-ray structures as described in Table 1 and in reference [15]. For a complete discussion on the methods used see the Supporting Information.

The densities range from $1.69 \text{ g}\cdot\text{cm}^{-3}$ (**7**) to $1.939 \text{ g}\cdot\text{cm}^{-3}$ (**4**) and are summarized in Table 1 with the calculated explosion parameters for **3–8** and **11–12**, alongside a comparison with the values calculated for RDX. The recalculated low temperature X-ray densities of compounds **4–6** have only small deviation compared to the values reported in the literature: $1.939 \text{ g}\cdot\text{cm}^{-3}$ (**4**) *versus* $1.93 \text{ g}\cdot\text{cm}^{-3}$ (gas pycnometer)^[5] and $1.95 \text{ g}\cdot\text{cm}^{-3}$ ^[7]; $1.875 \text{ g}\cdot\text{cm}^{-3}$ (**5**) *versus* $1.875 \text{ g}\cdot\text{cm}^{-3}$ (X-ray analysis)^[5] and $1.89 \text{ g}\cdot\text{cm}^{-3}$ ^[7]; $1.778 \text{ g}\cdot\text{cm}^{-3}$ (**6**) *versus* $1.82 \text{ g}\cdot\text{cm}^{-3}$ ^[7].

All compounds reported in Table 1 show a highly positive heat of formation from $156.7 \text{ kJ}\cdot\text{mol}^{-1}$ (**3**) to $1706.7 \text{ kJ}\cdot\text{mol}^{-1}$ (**12**), which are all higher than the heat of formation of RDX ($70.3 \text{ kJ}\cdot\text{mol}^{-1}$). The high heat of formation of salt **12** can be explained by the large number of N–N bonds.

The detonation velocities and pressures range from $D = 8330 \text{ m}\cdot\text{s}^{-1}$ (**7**)– $9589 \text{ m}\cdot\text{s}^{-1}$ (**5**) and $p_{\text{CJ}} = 277 \text{ kbar}$ (**7**)– 407 kbar (**5**). Notably is the discrepancy between the calculated detonation velocities and pressures compared to the previously reported values in the literature:^[7] $D = 9438 \text{ m}\cdot\text{s}^{-1}$ (**4**) *versus* $D = 9860 \text{ m}\cdot\text{s}^{-1}$ (lit.), $D = 9589 \text{ m}\cdot\text{s}^{-1}$ (**5**) *vs.* $D = 10010 \text{ m}\cdot\text{s}^{-1}$ (lit.), $D = 9011 \text{ m}\cdot\text{s}^{-1}$ (**6**) *versus* $D = 9880 \text{ m}\cdot\text{s}^{-1}$ (lit.), $p_{\text{CJ}} = 398 \text{ kbar}$ (**4**) *versus* $p_{\text{CJ}} = 464 \text{ kbar}$ (lit.), $p_{\text{CJ}} = 407 \text{ kbar}$ (**5**) *versus* $p_{\text{CJ}} = 478 \text{ kbar}$ (lit.), $p_{\text{CJ}} = 349 \text{ kbar}$ (**6**) *versus* $p_{\text{CJ}} = 465 \text{ kbar}$ (lit.). A potential reason for these discrepancies are the different computer codes used for the calculation of the detonation parameters^[17]. The thermally stable salt **12** shows a detonation velocity comparable to that of RDX.

Table 1. Physico-chemical properties of compounds **3–8** and **11–12** compared with those of Research Department explosive (RDX).

	3	4	5	6	7	8	11	12	RDX
Formula	C ₂ H ₂ N ₄ O ₃	C ₂ HN ₅ O ₅	C ₂ H ₄ N ₆ O ₆	C ₂ H ₄ N ₆ O ₅	C ₈ H ₁₀ N ₂₀ O ₁₀	C ₅ H ₇ N ₁₃ O ₅	C ₈ H ₁₀ N ₂₀ O ₇	C ₁₀ H ₁₄ N ₂₆ O ₇	C ₃ H ₆ N ₆ O ₆
FW [g mol ⁻¹]	130.06	175.06	208.09	192.09	546.29	329.19	498.29	610.39	222.12
IS [J] ^a	10	4	10	7	3	6	15	10	7.5
FS [N] ^b	360	120	72	72	252	324	240	360	120
ESD [J] ^c	0.3	0.3	0.5	0.8	0.75	1.2	0.25	0.5	0.20
N [%] ^d	43.08	40.01	40.39	43.75	51.28	55.31	56.22	59.66	37.84
Ω [%] ^e	-24.60	-4.57	0.00	-8.33	-32.22	-41.31	-44.95	-52.43	-21.61
T _{dec.} [°C] ^f	121(m.p.) 143(dec.)	58(m.p.) 65(dec.)	140	98	176	193	212	266	210
ρ [g cm ⁻³] (298K) ^g	1.808	1.939	1.875	1.778	1.69 (pyc.)	1.733	1.79 (pyc.)	1.774	1.806
Δ _f H° [kJ mol ⁻¹] ⁱ	156.7	263.6	254.7	199.9	834.1	715.9	715.4	1706.7	70.3
Δ _f U° [kJ kg ⁻¹] ^j	1290.7	1583.7	1319.3	1137.4	1617.6	2268.9	1527.8	2891.6	417.0
EXPLO V6.02 values:									
-Δ _E U° [kJ kg ⁻¹] ^k	5712	6555	7018	6348	5262	5484	4578	5538.7	5845
T _E [K] ^l	4015	4768	4627	4292	3790	3760	3253	3658.5	3810
p _{C-J} [kbar] ^m	333	398	407	349	277	297	286	311	345
D [m s ⁻¹] ⁿ	8769	9438	9589	9011	8330	8649	8580	8965	8861
V ₀ [L kg ⁻¹] ^o	743	733	815	810	788	796	780	800	785

a impact sensitivity (BAM drophammer, 1 of 6); b friction sensitivity (BAM friction tester, 1 of 6); c electrostatic discharge device (OZM); d nitrogen content; e oxygen balance; f decomposition temperature from DTA ($\beta = 5^\circ\text{C}$); g recalculated from low temperature X-ray densities ($\rho_{298\text{K}} = \rho T / (1 + \alpha V(298 - T_0))$; $\alpha_V = 1.5 \cdot 10^{-4} \text{ K}^{-1}$); h in parenthesis values for the density obtained from the X-ray measurement at 298K; i calculated (CBS-4M) heat of formation; j calculated energy of formation; k energy of explosion; l explosion temperature; m detonation pressure; n detonation velocity; o assuming only gaseous products.

11.3 Experimental Section

Compound **9** and **10** were prepared as described in the literature^[6,10].

3-Amino-4-Nitrofurazan (**3**)

Compound **3** was synthesized according to the literature^[9].

DTA (5 °C min⁻¹) onset: 121 °C (m.), 143 °C (dec.), literature: 120 °C (m.), 170 °C (dec.)^[9]; **IR** (ATR, cm⁻¹): $\tilde{\nu}$ = 3471 (m), 3447 (m), 3337 (m), 2957 (w), 2923 (w), 2854 (w), 1717 (w), 1634 (s), 1521 (s), 1499(s), 1464 (m), 1436 (m), 1369 (vs), 1348 (s), 1230 (w), 1210 (s), 1097 (m), 1039 (s), 870 (w), 832 (vs), 764 (m), 728 (w), 680 (w), 662 (w); **¹H NMR** ([D₆]DMSO): δ = 6.98 ppm (s, 2H, -NH₂); **¹³C NMR** ([D₆]DMSO): δ = 153.3 (C-NO₂), 151.5 ppm (C-NH₂); **¹⁴N NMR** ([D₆]DMSO): δ = -28.8 ppm (C-NO₂); **MS** *m/z* (DEI⁺): 130.1 (C₂H₂N₄O₃); **EA** (C₂H₂N₄O₃, 130.06) calcd.: C 18.47, H 1.55, N 43.08%, found: C 18.64, H 1.69, N 43.05%; **Sensitivities**: IS: 10 J; FS: 360 N; ESD: 0.3 J.

3-Nitramino-4-nitrofurazan (**4**)

Compound **4** was synthesized via a revised literature procedure^[5].

A dry 100ml three-neck flask was equipped with a stirrer, thermometer and two stoppers. 60–70 mL of methylene chloride was added and cooled to -20 °C. To the cooled methylene chloride was added N₂O₅ (2.3 g, 21.3 mmol, 1.2 equiv.). When the N₂O₅ was fully dissolved, **3** (2.3 g, 17.7 mmol, 1.0 equiv.) was added slowly over a period of 2–5 minutes, while the temperature was kept at -20 °C. The yellowish solution was put in ice bath and warmed slowly to 0–5 °C, then it was stirred for 3 h at 0–5 °C. The solvents were removed under a constant nitrogen flow to yield 2.04 g (11.65 mmol, 66%) of **4**.

DTA (5 °C min⁻¹) onset: 65 °C (dec.), literature: 60 °C (m.), 101.5 °C (dec.)^[5]; **IR** (ATR, cm⁻¹): $\tilde{\nu}$ = 3617 (vw), 3271 (m), 2930 (w), 2714 (w), 1625 (s), 1604 (s), 1545 (m), 1496 (vs), 1378 (m), 1329 (vs), 1302 (vs), 1201 (m); 1177 (s), 1168 (m), 1053 (m), 997 (m), 942 (s), 888 (w), 836 (s), 802 (s), 748 (s); **Raman** (1064 nm, 400 mW, 25 °C, cm⁻¹): $\tilde{\nu}$ = 1606 (13), 1588 (5), 1552 (11), 1500 (38), 1458 (5), 1441 (60), 1425 (7), 1386 (45), 1302 (13), 1057 (8), 1008 (9), 839 (25), 823 (3), 803 (5), 761 (5), 476 (7), 413 (10), 351 (5), 327 (7), 227 (8), 90 (100); **¹H NMR** ([D₆]DMSO): δ = 10.36 ppm (s, 1H, -NH); **¹³C NMR** ([D₆]DMSO): δ = 157.3 (C-NO₂), 153.1 ppm (C-NH-NO₂); **¹⁴N NMR** ([D₆]DMSO): δ = -14.6 (N-NO₂), -28.9 ppm (C-NO₂); **MS** *m/z* (FAB⁻): 174.0 (C₂N₅O₅⁻), *m/z* (DEI⁺): 175.0 (C₂HN₅O₅); **EA** (C₂HN₅O₅, 175.06) calcd.: C 13.72, H 0.58, N 40.01%, found: C 14.05, H 1.26, N 38.90%; **Sensitivities**: IS: 4 J; FS: 120 N; ESD: 0.3 J.

Hydroxylammonium 3-nitramino-4-nitrofurazan (5)

Compound **5** was synthesized as described in the literature^[5].

DTA (5 °C min⁻¹) onset: 149 °C (dec.), literature: 132 °C (m.), 162.9 °C (dec.)^[5]; **IR** (ATR, cm⁻¹): $\tilde{\nu}$ = 3070 (m), 2866 (m), 2719 (m), 2400 (w), 1623 (w), 1577 (s), 1506 (s), 1451 (m), 1410 (m), 1380 (s), 1285 (vs), 1203 (vs), 1175 (s), 1047 (m), 1023 (s), 1007 (s), 943 (m), 848 (m), 808 (s), 771 (s), 748 (m), 704 (m); **Raman** (1064 nm, 400 mW, 25 °C, cm⁻¹): $\tilde{\nu}$ = 3071 (4), 2989 (4), 1625 (4), 1583 (10), 1535 (19), 1468 (10), 1453 (100), 1440 (24), 1427 (8), 1413 (20), 1385 (12), 1358 (20), 1339 (24), 1206 (10), 1181 (6), 1051 (14), 1026 (56), 1010 (15), 892 (6), 851 (20), 815 (6), 770 (7), 496 (11), 417 (10), 391 (8), 335 (16), 253 (10), 225 (11), 166 (29), 136 (21), 92 (64), 77 (36), 65 (37). **¹H NMR** ([D₆]DMSO): δ = 10.06 (s, 3H, NH₃-OH⁺), 9.87 ppm (s, 1H, NH₃-OH⁺); **¹³C NMR** ([D₆]DMSO): δ = 157.0 (C-NO₂), 153.5 ppm (C-N-NO₂); **MS** *m/z* (FAB⁻): 174.1 (C₂N₅O₅⁻), *m/z* (FAB⁺): 34.0 (NH₄O⁺); **EA** (C₂H₆N₆O₄, 178.11) calcd.: C 11.54, H 1.94, N 40.39%, found: C 12.00, H 1.98, N 40.04%; **Sensitivities**: IS: 10 J; FS: 72 N; ESD: 0.5 J.

Ammonium 3-nitramino-4-nitrofurazan (6)

Compound **6** was synthesized with a similar method as described in the literature^[5].

DTA (5 °C min⁻¹) onset: 97 °C (dec.), literature: 121 °C (dec.)^[5]; **IR** (ATR, cm⁻¹): $\tilde{\nu}$ = 3324 (w), 3062 (w), 1579 (m), 1544 (w), 1464 (m), 1412 (s), 1370 (m), 1341 (s), 1278 (vs), 1205 (m), 1043 (m), 933 (m), 830 (m), 799 (s), 778 (m), 768 (m); **Raman** (1064 nm, 400 mW, 25 °C, cm⁻¹): $\tilde{\nu}$ = 3139 (2), 1572 (12), 1531 (16), 1465 (100), 1413 (22), 1366 (20), 1347 (26), 1296(7), 1206(7), 1045(19), 1010 (51), 934 (4), 830 (19), 802 (7), 741 (4), 496 (8), 422 (7), 386 (5), 334 (14), 249 (10), 218 (14), 162 (24), 128 (38), 105 (80), 84 (69); **¹H NMR** ([D₆]DMSO): δ = 7.08 ppm (s, NH₄⁺); **¹³C NMR** ([D₆]DMSO): δ = 157.3 (C-NO₂), 153.6 ppm (C-N-NO₂); **MS** *m/z* (FAB⁻): 174.0 (C₂N₅O₅⁻), *m/z* (FAB⁺): 18.1 (NH₄⁺); **EA** (C₂H₆N₆O₃, 162.11) calcd.: C 12.51, H 2.10, N 43.75%, found: C 12.91, H 2.14, N 43.48%; **Sensitivities**: IS: 7 J; FS: 72 N; ESD: 0.8 J.

4,4',5,5'-Tetraamino-3,3'-bi-triazolium di-3-nitramino-4-nitrofurazan (7)

Freshly prepared **4** (350 mg, 2.0 mmol) and 4,4',5,5'-tetraamino-3,3'-bi-triazole^[3] (196 mg, 1.0 mmol) were dissolved in approximately 400 mL of water, while the water was not warmed above 30 °C. The solution was left in an open beaker to slowly evaporate the water to yield 470 mg (0.86 mmol, 86%) of **7**.

DTA (5 °C min⁻¹) onset: 176 °C (dec.); **IR** (ATR, cm⁻¹): $\tilde{\nu}$ = 3460 (w), 3347 (w), 3245 (m), 3187 (m), 1703 (s), 1623 (w), 1572 (s), 1525 (m), 1451 (m), 1419 (s), 1389 (m), 1358 (m), 1335 (m), 1280 (vs), 1199 (m), 1093 (w), 1045 (w), 999 (s), 972 (m), 940 (m), 828 (m), 800 (m), 776 (m); **Raman** (1064 nm, 300 mW, 25 °C, cm⁻¹): $\tilde{\nu}$ = 3268 (2), 1665 (6), 1650 (100), 1634 (12), 1616 (16), 1584 (8), 1527 (12), 1452 (72), 1419 (10), 1392 (11), 1361 (16), 1335 (58), 1303 (14), 1047 (10), 1017 (36), 831 (13), 803 (21), 721 (7), 721 (7), 415 (7), 379 (4), 337 (15), 247 (4), 217 (5), 111 (50). **¹H NMR** ([D₆]DMSO): δ = 8.55 (s, 4H, -NH₂), 5.50 ppm (s, 4H, -NH₂); **¹³C NMR** ([D₆]DMSO): δ = 157.2 (C-NO₂), 153.5 (C-N-NO₂), 152.0 (C-NH₂), 137.7 ppm (C-C); **¹⁴N NMR** ([D₆]DMSO): δ = -12.1 (N-NO₂), -27.4 ppm (C-NO₂); **MS** *m/z* (ESI⁻): 174.0 (C₂N₅O₅⁻), *m/z* (ESI⁺): 197.1 (C₄H₉N₁₀⁺); **EA** (C₈H₁₀N₂₀O₁₀, 546.09) calcd.: C 17.59, H 1.85, N 51.28%; found: C 17.87, H 1.87, N 51.11%; **Sensitivities**: IS: 3 J; FS: 252 N; ESD: 0.75 J.

3,6,7-Triamino-[1,2,4]triazolo[4,3-b][1,2,4]triazolium 3-nitramino-4-nitrofurazan (8)

Freshly prepared **4** (280 mg, 1.6 mmol) and 3,6,7-triamino-[1,2,4]triazolo[4,3-b][1,2,4]triazole^[4] (246 mg, 1.6 mmol) were dissolved in 100 mL of water, while the water was not warmed above 30 °C. The solution was left for crystallization to yield 350 mg (1.06 mmol, 66%) of **8** as colorless crystals.

DTA (5 °C min⁻¹) onset: 193 °C (dec.); **IR** (ATR, cm⁻¹): $\tilde{\nu}$ = 3422 (m), 3364 (w), 3293 (m), 3239 (m), 3175 (m), 3134 (m), 1706 (s), 1674 (s), 1648 (s), 1579 (s), 1540 (m), 1458 (m), 1414 (m), 1368 (vs), 1298 (vs), 1207 (m), 1049 (m), 1035 (m), 1016 (m), 976 (w), 845 (m), 822 (s), 776 (m), 740 (m), 722 (m), 704 (m), 695 (m), 666 (w); **Raman** (1064 nm, 300 mW, 25 °C, cm⁻¹): $\tilde{\nu}$ = 3244 (7), 1699 (8), 1673 (7), 1575 (10), 1543 (16), 1462 (73), 1427 (12), 1373 (15), 1306 (15), 1263 (23), 1209 (15), 1053 (32), 1019 (10), 849 (31), 825 (17), 765 (7), 681 (7), 619 (22), 602 (18), 502 (22), 390 (21), 303 (18), 244 (8), 244 (8), 217 (12), 137 (100), 99 (54), 85 (43); **¹H NMR** ([D₆]DMSO): δ = 13.14 (br, s, 1H, N-H), 8.16 (s, 2H, -NH₂), 7.21 (s, 2H, -NH₂), 5.76 ppm (s, 2H, -NH₂); **¹³C NMR** ([D₆]DMSO): δ = 160.2 (C-NH₂), 157.2 (C-N-NO₂), 153.5 (C-NO₂), 147.5 (C_q), 141.2 ppm (C-NH₂); **¹⁴N NMR** ([D₆]DMSO): δ = -12.1 (N-NO₂), -27.5 ppm (C-NO₂); **MS** *m/z* (FAB⁻): 174.1 (C₂N₅O₅⁻), *m/z* (FAB⁺): 155.2 (C₃H₇N₈⁺); **EA** (C₅H₇N₁₃O₅, 329.07): C 18.24, H 2.14, N 55.31%; found: C 18.42, H 2.21, N 55.32%; **Sensitivities**: IS: 6 J; FS: 324 N; ESD: 1.2 J.

4,4',5,5'-Tetraamino-3,3'-bi-triazolium dinitraminoazoxyfurazan (11)

4,4',5,5'-Tetraamino-3,3'-bi-triazole^[3] (0.78 g, 4.00 mmol, 2.0 equiv.) was suspended in 4.0 L of hot water. Compound **10** (0.64 g, 2.00 mmol) was added and the suspension was heated

until a clear solution was formed. The solution was filtered and the solvent was evaporated in air. **11** precipitated as an orange powder. Yield: 1.17 g, 1.7 mmol, 85%.

DTA (5 °C min⁻¹) onset: 212 °C (dec.); **IR** (ATR, cm⁻¹): $\tilde{\nu}$ = 3604 (w), 3528 (w), 3357 (w), 3202 (w), 3052 (w), 1698 (s), 1610 (m), 1555 (m), 1524 (m), 1445 (m), 1426 (s), 1389 (s), 1262 (br, vs), 1172 (m), 1123 (w), 1017 (m), 985 (s), 936 (s), 817 (m), 784 (m), 753 (m), 707 (m); **Raman** (1064 nm, 300 mW, 25 °C, cm⁻¹): $\tilde{\nu}$ = 1655 (81), 1632 (13), 1556 (8), 1526 (19), 1475 (97), 1459 (31), 1436 (97), 1390 (32), 1335 (41), 1315 (100), 1296 (18), 1271 (12), 1083 (6), 1042 (10), 1020 (28), 1006 (16), 956 (7), 862 (13), 820 (9), 803 (24), 754 (5), 712 (7), 497 (9), 478 (8), 399 (6), 263 (6), 231 (10), 129 (23); **¹H NMR** ([D₆]DMSO): δ = 8.53 (s, 4H, -NH₂), 6.12 ppm (s, 4H, -NH₂); **¹³C NMR** ([D₆]DMSO): δ = 155.1 (C-N(O)-N), 153.9 (C-N-N(O)), 152.0 (C-NH_{2 cat.}), 151.2 (C-N-NO₂), 137.8 (C-C_{cat.}); **¹⁴N NMR** ([D₆]DMSO): δ = -13.4 (N-NO₂), -66.8 ppm (N-N(O)); **MS** *m/z* (FAB⁻): 285.0 (C₄H₁₃N₁₆O₄⁻); **EA** (C₈H₁₀N₂₀O₇·H₂O, 516.31) calcd.: C 18.61, H 2.34, N 54.26%; found: C 18.82, H 2.85, N 53.64%; **Sensitivities**: IS: 20 J; FS: 240 N; ESD: 0.25 J.

Di-3,6,7-triamino-[1,2,4]triazolo[4,3-b][1,2,4]triazolium dinitraminoazoxyfurazan (**12**)

3,6,7-Triamino-[1,2,4]triazolo[4,3-b][1,2,4]triazole^[4] (0.61 g, 4.0 mmol) was suspended in 300 mL of hot water. Compound **10** (0.64 g, 2.00 mmol) was added and the suspension was heated until a clear solution was formed. The solution was filtered and the solvent was evaporated in air. **12** precipitated as colorless crystals (1.03 g, 3.3 mmol, 82%).

DTA (5 °C min⁻¹) onset: 266 °C (dec.); **IR** (ATR, cm⁻¹): $\tilde{\nu}$ = 3436 (w), 3384 (m), 3226 (m), 3116 (m), 2757 (w), 1690 (vs), 1652 (vs), 1566 (m), 1496 (s), 1477 (m), 1400 (s), 1365 (s), 1319 (s), 1286 (vs), 1188 (m), 1138 (m), 1060 (m), 1038 (m), 1012 (m), 981 (m), 931 (m), 879 (w), 846 (m), 810 (m), 770 (m), 733 (w), 707 (m); **Raman** (1064 nm, 300 mW, 25 °C, cm⁻¹): $\tilde{\nu}$ = 1649 (11), 1568 (11), 1539 (19), 1497 (25), 1480 (39), 1445 (77), 1420 (18), 1348 (12), 1326 (13), 1257 (19), 1193 (18), 1049 (40), 879 (9), 851 (23), 757 (14), 620 (21), 598 (15), 491 (18), 413 (8), 394 (10), 328 (13), 309 (17), 228 (12), 187 (23), 129 (77), 101 (100), 76 (33); **¹H NMR** ([D₆]DMSO): δ = 13.29 (s, 2H, N-H), 8.19 (s, 4H, -NH₂), 7.22 (s, 4H, -NH₂), 5.77 ppm (s, 4H, -NH₂); **¹³C NMR** ([D₆]DMSO): δ = 160.1 (C-NH₂), 155.0 (C-N(O)-N), 153.9 (C-N-N(O)), 151.2 (C-N-NO₂), 147.4 (C_q), 141.1 ppm (C-NH₂); **¹⁴N NMR** ([D₆]DMSO): δ = -12.7 (N-NO₂), -66.1 ppm (N-N(O)); **MS** *m/z* (FAB⁻): 285.0 (C₄H₁₃N₁₆O₄⁻); **EA** (C₁₀H₁₄N₂₆O₇, 610.40) calcd.: C 19.68, H 2.31, N 59.66%; found: C 19.74, H 2.45, N 59.66%; **Sensitivities**: IS: 10 J; FS: 360 N; ESD: 0.5 J.

11.4 Conclusions

Energetic derivatives of 3-nitramino-4-nitrofurazan and dinitraminoazoxyfurazan were investigated in the search for more thermally stable materials. The crystal structures were determined by low temperature single crystal X-ray diffraction and show the stabilizing effect of a strong hydrogen-bonding network formed by the 3,6,7-triamino-[1,2,4]triazolo[4,3-b][1,2,4]triazolium cation. Moreover, the X-ray structures of highly dense hydroxylammonium and ammonium 3-nitramino-4-nitrofurazan were reported. Even though neutral **4** and salt **5** have excellent detonation parameters (D 9500 m·s⁻¹, p_{CJ} 400 kbar), their application is unlikely because of their low thermal stability. To our dismay, thermally more stable salts **7** and **8** fell short of a decomposition temperature of 200 °C. However the dinitraminoazoxyfurazan **12** shows a high thermal stability due to an extensive hydrogen bonding network, with sufficient stability against impact and friction, and yet a detonation velocity $D = 9000$ m·s⁻¹, which is similar to RDX.

11.5 References

- [1] Giles, J. Green explosives: Collateral damage. *Nature* **2004**, 427, 580–581.
- [2] Gao, H.; Shreeve, J.M. Azole based energetic salts. *Chem. Rev.* **2011**, 11, 7377–7436.
- [3] Klapötke, T.M.; Schmid, P.C.; Schnell, S.; Stierstorfer, J. Thermal stabilization of energetic materials by the aromatic nitrogen-rich 4,4',5,5'-tetraamino-3,3'-bi-1,2,4-triazolium cation. *J. Mat Chem. A* **2015**, 3, 2658–2668.
- [4] Klapötke, T.M.; Schmid, P.C.; Schnell, S.; Stierstorfer, J. 3,6,7-Triamino-[1,2,4]triazolo[4,3-b][1,2,4]triazole: A non-toxic, high-performance energetic building block with excellent stability. *Chem Eur. J.* **2015**, 21, 9219–9228
- [5] Willer, R.L.; Day, R.S.; Park, D.J. Liquid gun propellants. *U.S. Patent* 5,460,669, 24 October 1995.
- [6] Fischer, D.; Klapötke, T.M.; Reymann, M.; Stierstorfer, J. Dense energetic nitraminofurazanes. *Chem. Eur. J.* **2014**, 20, 6401–6411.
- [7] Willer, R. Calculation of the density and detonation properties of C, H, N, O and F compounds: Use in the design and synthesis of new energetic materials. *J. Mex. Chem. Soc.* **2009**, 53, 108–119.

- [8] Glyoxime, Diaminofurazan and some Energetic Derivatives, by AXT. Available online: http://www.sciencemadness.org/member_publications/energetic_glyoxime_and_diaminofurazan_derivatives.pdf (accessed on 31 July 2015).
- [9] Novikova, T.S.; Mel'nikova, T.M.; Kharitonova, O.V.; Kulagina, V.O.; Aleksandrova, N.S.; Sheremetev, A.B.; Pivina, T.S.; Khmel'nitskii, L.I.; Novikov, S.S. An effective method for the oxidation of aminofurazans to nitrofurazans. *Mendeleev Commun.* **1994**, *4*, 138–140.
- [10] Beal, R.W. Structures and chemistry of amino and nitro furazanes. Master's Thesis, University of Delaware, Newark, DE, USA, 2000.
- [11] Francois, E.G.; Chavez, D.E.; Sandstrom, M.M. The development of a new synthesis process for 3,3'-Diamino-4,4'-azoxyfurazan (DAAF). *Propellants Explos. Pyrotech.* **2010**, *35*, 529–534.
- [12] Batsanov, A.S.; Struchkov, Y.T. Crystal structure of 3,4-diaminofurazan and 3-aminon-4-nitrofurazan. *J. Struct. Chem.* **1985**, *26*, 52–56.
- [13] Klapötke, T.M.; Leroux, M.; Schmid, P.C.; Schnell, S.; Stierstorfer, J. Energetic materials based on 5,5'-diamino-4,4'-dinitramino-3,3'-bi(1,2,4-triazole). *Chem. Asian J.* **2015**, doi: 10.1002/asia.201500701.
- [14] Murray, S.; Politzer, P. *Chemistry and Physics of Energetic Materials*; Bulusu, S.N., Ed.; Kluwer: Dordrecht, The Netherlands, 1990; pp. 157–173.
- [15] Murray, J.S.; Politzer, P. Impact sensitivity and crystal lattice compressibility/free space. *J. Mol. Model* **2014**, *20*, 2223–2227.
- [16] Xue, C.; Sun, J.; Kang, B.; Liu, Y.; Liu, X.; Song, G.; Xue, Q. The β - δ -phase transition and thermal expansion of octahydro-1,3,5,7-tetranitro-1,3,5,7-tetrazocine. *Propellants Explos. Pyrotech.* **2010**, *35*, 333–338.
- [17] *EXPLO5V6.02 program*; Brodarski Institute: Zagreb, Croatia, 2014.

11.6 Supplementary information

The analytical methods and general procedures are described in the appendix of this thesis.

11.6.1 Crystallographic data and refinement parameters

Table S1. Crystallographic data and refinement parameters of compound **3–5**.

	3	4	5
Formula	C ₂ H ₂ N ₄ O ₃	C ₄ H ₁₂ N ₁₄ O ₆	C ₂ H ₄ N ₆ O ₆
FW [g mol ⁻¹]	130.08	175.08	208.11
Crystal system	orthorhombic	orthorhombic	monoclinic
Space Group	<i>Pna</i> 2 ₁	<i>Pbca</i>	<i>Pc</i>
Color / Habit	yellow, platelet	colorless, block	colorless, plate
Size [mm]	0.04×0.08×0.22	0.05×0.18×0.39	0.04 × 0.24 × 0.33
<i>a</i> [Å]	14.9183(9)	5.0351(3)	5.6470(9)
<i>b</i> [Å]	5.3962(3)	8.9523(4)	10.8713(15)
<i>c</i> [Å]	11.6551(8)	26.1215(11)	6.0744(8)
α [°]	90.0	90.0	90.0
β [°]	90.0	90.0	103.985(15)
γ [°]	90.0	90.0	90.0
<i>V</i> [Å ³]	938.26(10)	1177.45(10)	361.86(9)
<i>Z</i>	8	8	2
$\rho_{\text{calc.}}$ [g cm ⁻³]	1.789	1.975	1.910
μ [mm ⁻¹]	0.171	0.193	0.187
<i>F</i> (000)	528	704	212
$\lambda_{\text{MoK}\alpha}$ [Å]	0.71073	0.71073	0.71073
<i>T</i> [K]	173	173	173
θ min-max [°]	4.2, 26.5	4.3, 26.5	4.2, 27.0
Dataset <i>h</i> ; <i>k</i> ; <i>l</i>	−18:18; −6:6; −14:14	−6:6; −10:11; −32:32	−4:7; −13:9 ; −7:7
Reflect. coll.	6140	7539	1401
Independ. refl.	1019	1216	779
<i>R</i> _{int}	0.059	0.039	0.038
Reflection obs.	822	1002	592
No. parameters	179	113	132
<i>R</i> ₁ (obs)	0.0398	0.0400	0.0502
<i>wR</i> ₂ (all data)	0.1020	0.0975	0.0996
<i>S</i>	1.08	1.12	1.05
Resd. Dens.[e Å ⁻³]	−0.22, 0.22	−0.20, 0.26	−0.26, 0.26
Device type	Oxford XCalibur3 CCD	Oxford XCalibur3 CCD	Oxford XCalibur3 CCD
Solution	SIR-92	SIR-92	SIR-92
Refinement	SHELXL-97	SHELXL-97	SHELXL-97
Absorpt. corr.	multi-scan	multi-scan	multi-scan
CCDC	1415341	1415340	1415342

Table S2. Crystallographic data and refinement parameters of compound **6**, **8** and **12**.

	6	8	12
Formula	C ₂ H ₄ N ₆ O ₅	C ₅ H ₇ N ₁₃ O ₅	C ₁₀ H ₁₄ N ₂₆ O ₇
FW [g mol ⁻¹]	192.11	329.24	610.47
Crystal system	monoclinic	monoclinic	triclinic
Space Group	<i>P</i> 2 ₁ / <i>n</i>	<i>P</i> 2 ₁	<i>P</i> -1
Color / Habit	colorless, block	yellow, platelet	yellow, block
Size [mm]	0.10×0.14×0.35	0.02×0.30×0.35	0.08×0.19×0.38
<i>a</i> [Å]	10.3798(4)	7.4532(4)	6.6964(8)
<i>b</i> [Å]	5.1636(2)	6.8696(3)	7.4364(8)
<i>c</i> [Å]	13.8832(6)	12.3413(5)	12.9964(12)
α [°]	90	90	77.394(9)
β [°]	108.754(4)	101.495(5)	77.827(9)
γ [°]	90	90	63.649(11)
<i>V</i> [Å ³]	704.59(5)	619.21(5)	561.13(12)
<i>Z</i>	4	2	1
ρ_{calc} [g cm ⁻³]	1.811	1.766	1.807
μ [mm ⁻¹]	0.173	0.155	0.153
<i>F</i> (000)	392	336	312
$\lambda_{\text{MoK}\alpha}$ [Å]	0.71073	0.71073	0.71073
<i>T</i> [K]	173	173	173
ϑ min-max [°]	4.2, 26.0	4.2, 26.5	4.2, 26.4
Dataset <i>h</i> ; <i>k</i> ; <i>l</i>	−12:11; −6:6; −10:17	−9:7; −8:7; −15:15	−8:8; −9:8 ; −16:16
Reflect. coll.	3423	5017	4006
Independ. refl.	1377	1395	2291
<i>R</i> _{int}	0.020	0.027	0.020
Reflection obs.	1194	1280	1803
No. parameters	134	236	227
<i>R</i> ₁ (obs)	0.0296	0.0274	0.0518
<i>wR</i> ₂ (all data)	0.0740	0.0692	0.1197
<i>S</i>	1.09	1.03	1.10
Resd. Dens.[e Å ⁻³]	−0.18, 0.22	−0.16, 0.18	−0.24, 0.32
Device type	Oxford XCalibur3 CCD	Oxford XCalibur3 CCD	Oxford XCalibur3 CCD
Solution	SIR-92	SIR-92	SIR-92
Refinement	SHELXL-97	SHELXL-97	SHELXL-97
Absorpt. corr.	multi-scan	multi-scan	multi-scan
CCDC	1415343	1057626	1057627

11.6.2 Heat of formation calculations

General information about the heat of formation calculations can be found in the appendix of this thesis. The calculation results are summarized in Table S3.

Table S3. Calculation results

M	$-H^{298}$ ^[a] / a.u.	$\Delta_f H^\circ(\text{g}, \text{M})$ / kJ mol ⁻¹ ^[b]	V_M / nm ³ ^[c]	$\Delta U_{L_s} \Delta H_L$ (4); ^[d] ΔH_{sub} ^[e] (3) / kJ mol ⁻¹	$\Delta_f H^\circ(\text{s})$ ^[f] / kJ mol ⁻¹	Δn ^[g]	$\Delta_f U(\text{s})$ ^[f] / kJ kg ⁻¹
ANF (3)	521.26512	235.0		78.2	156.7	4.5	1290.7
NNF(4)	725.520689	327.2		63.6	263.6	5.5	1583.7
NNF ⁻	725.027281	89.3					
Hx ⁺	131.863249	686.4					
5		775.7	0.184	516.0, 521.0	254.7	8.0	1319.3
NH ₄ ⁺	56.796608	635.3					
6		724.6	0.179	519.7, 524.7	199.9	7.5	1137.4
TABTr ²⁺	704.327388	2032.9					
7		2211.5	0.507	1369.9, 1377.4	834.1	20.0	1617.6
TATOT ⁺	555.474133	1080.0					
8		1169.3	0.315	448.4, 453.4	715.9	12.5	2268.9
DNAAF ²⁻	1224.647003	570.3					
11		2603.2	0.448	1882.9, 1887.8	715.4	18.5	1527.8
12		2730.4	0.572	1016.3	1023.7	23.5	2891.6

^[a] CBS-4M electronic enthalpy; ^[b] gas phase enthalpy of formation; ^[c] molecular volumes taken from X-ray structures and corrected to room temperature; ^[d] lattice energy and enthalpy (calculated using Jenkins and Glasser equations); ^[e] enthalpy of sublimation (calculated by Trouton rule); ^[f] standard solid state enthalpy of formation; ^[g] solid state energy of formation.

Appendix: General Information

12.1 Materials and Methods

Caution! The compounds discussed in this thesis may be energetic materials with sensitivities toward shock and friction. Therefore, proper safety precautions (face shield, earthened equipment and shoes, Kevlar gloves and ear plugs) have to be applied while synthesizing and handling the described compounds. Specifically, compounds described having the azido group are extremely sensitive and have to be handled very carefully.

All chemicals and solvents were employed as received (Sigma-Aldrich, Fluka, Acros) without further purification unless otherwise stated.

12.2 NMR spectroscopy

^1H and ^{13}C NMR spectra were recorded using a JEOL Eclipse 270, JEOL EX 400 or a JEOL Eclipse 400 instrument. The chemical shifts quoted in ppm in the text refer to tetramethylsilane (^1H , ^{13}C).

12.3 Vibrational spectroscopy

Infrared spectra were measured using a Perkin Elmer Spectrum One FT-IR spectrometer as KBr pellets. Raman spectra were recorded on a Bruker MultiRAM Raman Sample Compartment D418 equipped with a Nd-YAG-Laser (1064 nm) and a LN-Ge diode as detector.

12.5 Mass spectrometry and elemental analysis

Mass spectra of the described compounds were measured at a JEOL MStation JMS 700 using either DEI or FAB technique. To measure elemental analyses a Netsch STA 429 simultaneous thermal analyzer was employed.

12.6 Differential thermal analysis

Differential thermal analysis (DTA) measurements to determine the decomposition temperatures of the materials were performed at a heating rate of 5°C min^{-1} with an OZM Research DTA 552-Ex instrument.

12.7 Differential scanning calorimetry

Differential scanning calorimetry (DSC) measurements to determine the decomposition temperatures of the compounds (about 1.5 mg of each energetic material) were performed in covered Al-containers containing a hole (0.1 mm) in the lid for gas release and a nitrogen

flow of 20 mL per minute on a Linseis PT 10 DSC calibrated with standard pure indium and zinc at a heating rate of 5°C min⁻¹.

12.8 Sensitivity testing

The impact sensitivity tests were carried out according to STANAG 4489^[1] modified instruction^[2] using a BAM (Bundesanstalt für Materialforschung) drophammer.^[3] The friction sensitivity tests were carried out according to STANAG 4487^[4] modified instruction^[5] using the BAM friction tester. The classification of the tested compounds results from the “UN Recommendations on the Transport of Dangerous Goods”.^[6] Additionally all compounds were tested upon the sensitivity towards electrical discharge using the Electric Spark Tester ESD 2010 EN.^[7]

12.9 X-Ray diffraction: instrument and refinement software

Suitable single crystal of synthesized compounds were picked from the crystallization mixtures and mounted in Kel-F oil, transferred to the N₂ stream of an Oxford Xcalibur3 diffractometer with a Spellman generator (voltage 50 kV, current 40 mA) and a KappaCCD detector. The data collection was performed using the CRYSLIS CCD software^[8], the data reduction using the CRYSLIS RED software^[9]. The structure was solved with SIR-92^[10], refined with SHELXL-97^[11] and finally checked using the PLATON software^[12] integrated in the WINGX software suite.^[13] The non-hydrogen atoms were refined anisotropically and the hydrogen atoms were mostly located and freely refined. The absorptions were corrected using a SCALE3 ABSPACK multi-scan method.^[14]

12.10 Heat of formation calculations

Heats of formation of ionic compounds were calculated using the atomization method (equation S1) using room temperature CBS-4M enthalpies summarized in Table S2.^[15,16]

$$\Delta_f H^\circ_{(g, M, 298)} = H_{(Molecule, 298)} - \sum H^\circ_{(Atoms, 298)} + \sum \Delta_f H^\circ_{(Atoms, 298)} \quad (S1)$$

Table S2. CBS-4M electronic enthalpies for atoms C, H, N and O and their literature values for atomic $\Delta H^\circ_f{}^{298} / \text{kJ mol}^{-1}$

	$-H^{298} / \text{a.u.}$	NIST ^[17]
H	0.500991	218.2
C	37.786156	717.2
N	54.522462	473.1
O	74.991202	249.5

Quantum chemical calculations were carried out using the Gaussian G09 program package.^[18] The enthalpies (H) and free energies (G) were calculated using the complete basis set (CBS)

method of Petersson and coworkers in order to obtain very accurate energies. The CBS models use the known asymptotic convergence of pair natural orbital expressions to extrapolate from calculations using a finite basis set to the estimated CBS limit. CBS-4 begins with an HF/3-21G(d) geometry optimization; the zero point energy is computed at the same level. It then uses a large basis set SCF calculation as a base energy, and an MP2/6-31+G calculation with a CBS extrapolation to correct the energy through second order. An MP4(SDQ)/6-31+ (d,p) calculation is used to approximate higher order contributions. In this study, we applied the modified CBS.

For neutral compounds the sublimation enthalpy, which is needed to convert the gas phase enthalpy of formation to the solid state one, was calculated by the *Trouton* rule.^[19] In the case of the ionic compounds, the lattice energy (U_L) and lattice enthalpy (ΔH_L) were calculated from the corresponding X-ray molecular volumes according to the equations provided by *Jenkins* and *Glasser*.^[20] With the calculated lattice enthalpy the gas-phase enthalpy of formation was converted into the solid state (standard conditions) enthalpy of formation. These molar standard enthalpies of formation (ΔH_m) were used to calculate the molar solid state energies of formation (ΔU_m) according to equation S2.

$$\Delta U_m = \Delta H_m - \Delta n RT \quad (\text{S2})$$

(Δn being the change of moles of gaseous components)

12.11 References

- [1] NATO standardization agreement (STANAG) on explosives. *Impact sensitivity tests*. No. 4489, 1st ed., Sept. 17, 1999.
- [2] WIWEB-Standardarbeitsanweisung 4-5.1.02, Ermittlung der Explosionsgefährlichkeit, hier der Schlagempfindlichkeit mit dem Fallhammer, Nov. 8, 2002.
- [3] <http://www.bam.de>
- [4] NATO standardization agreement (STANAG) on explosive. *Friction sensitivity tests*. No. 4487, 1st ed., Aug. 22, 2002.
- [5] WIWEB-Standardarbeitsanweisung 4-5.1.03, Ermittlung der Explosionsgefährlichkeit oder der Reibeempfindlichkeit mit dem Reibeapparat, Nov. 8, 2002.
- [6] Impact: Insensitive > 40 J, less sensitive ≥ 35 J, sensitive ≥ 4 J, very sensitive ≤ 3 J; friction: Insensitive > 360 N, less sensitive = 360 N, sensitive < 360 N a. > 80 N, very

sensitive ≤ 80 N, extreme sensitive ≤ 10 N; according to the UN recommendations on the transport of dangerous goods. (+) Indicates: not safe for transport.

- [7] <http://www.ozm.cz>
- [8] CrysAlis CCD, Oxford Diffraction Ltd., Version 1.171.27p5 beta (release 01-04-2005 CrysAlis171.NET) (compiled Apr 1 2005,17:53:34).
- [9] CrysAlis RED, Oxford Diffraction Ltd., Version 1.171.27p5 beta (release 01-04-2005 CrysAlis171.NET) (compiled Apr 1 2005,17:53:34).
- [10] A. Altomare, G. Cascarano, C. Giacovazzo, A. Guagliardi, *J. Appl. Cryst.* **1993**, 26, 343–350.
- [11] Sheldrick, G. M. SHELXL-97. Program for the refinement of crystal structures. University of Göttingen, Germany, 1997.
- [12] Spek, A. L. PLATON, A multipurpose crystallographic tool, Utrecht University, Utrecht, The Netherlands, **1999**.
- [13] Farrugia, L. J. WinGX suite for small molecule single-crystal crystallography. *J. Appl. Cryst.* **1999**, 32, 837.
- [14] SCALE3 ABSPACK - An Oxford Diffraction program (1.0.4,gui:1.0.3) (C), Oxford Diffraction Ltd., **2005**.
- [15] (a) J. W. Ochterski, G. A. Petersson, and J. A. Montgomery Jr., *J. Chem. Phys.* **1996**, 104, 2598–2619; (b) J. A. Montgomery Jr., M. J. Frisch, J. W. Ochterski G. A. Petersson, *J. Chem. Phys.* **2000**, 112, 6532–6542.
- [16] (a) L. A. Curtiss, K. Raghavachari, P. C. Redfern, J. A. Pople, *J. Chem. Phys.* **1997**, 106, 1063–1079; (b) E. F. C. Byrd, B. M. Rice, *J. Phys. Chem. A* **2006**, 110, 1005–1013; (c) B. M. Rice, S. V. Pai, J. Hare, *Comb. Flame* **1999**, 118, 445–458.
- [17] P. J. Lindstrom, W. G. Mallard (Editors), NIST Standard Reference Database Number 69, <http://webbook.nist.gov/chemistry/> (accessed June **2011**).
- [18] M. J. Frisch, G. W. Trucks, H. B. Schlegel, G. E. Scuseria, M. A. Robb, J. R. Cheeseman, G. Scalmani, V. Barone, B. Mennucci, G. A. Petersson, H. Nakatsuji, M. Caricato, X. Li, H.P. Hratchian, A. F. Izmaylov, J. Bloino, G. Zheng, J. L. Sonnenberg, M. Hada, M. Ehara, K. Toyota, R. Fukuda, J. Hasegawa, M. Ishida, T. Nakajima, Y. Honda, O. Kitao, H. Nakai, T. Vreven, J. A. Montgomery, Jr., J. E. Peralta, F. Ogliaro, M. Bearpark, J. J. Heyd, E. Brothers, K. N. Kudin, V. N. Staroverov, R. Kobayashi, J.

- Normand, K. Raghavachari, A. Rendell, J. C. Burant, S. S. Iyengar, J. Tomasi, M. Cossi, N. Rega, J. M. Millam, M. Klene, J. E. Knox, J. B. Cross, V. Bakken, C. Adamo, J. Jaramillo, R. Gomperts, R. E. Stratmann, O. Yazyev, A. J. Austin, R. Cammi, C. Pomelli, J. W. Ochterski, R. L. Martin, K. Morokuma, V. G. Zakrzewski, G. A. Voth, P. Salvador, J. J. Dannenberg, S. Dapprich, A. D. Daniels, O. Farkas, J.B. Foresman, J. V. Ortiz, J. Cioslowski, D. J. Fox, Gaussian 09 A.02, Gaussian, Inc., Wallingford, CT, USA, **2009**.
- [19] M. S. Westwell, M. S. Searle, D. J. Wales, D. H. Williams, *J. Am. Chem. Soc.* **1995**, *117*, 5013–5015; (b) F. Trouton, *Philos. Mag.* **1884**, *18*, 54–57.
- [20] (a) H. D. B. Jenkins, H. K. Roobottom, J. Passmore, L. Glasser, *Inorg. Chem.* **1999**, *38*, 3609–3620. (b) H. D. B. Jenkins, D. Tudela, L. Glasser, *Inorg. Chem.* **2002**, *41*, 2364–2367.

List of publications

Publications

- [1] G. K. S. Prakash,* L. Gurung, P. C. Schmid, F. Wang, T. E. Thomas, C. Panja, T. Mathew, G. A. Olah, *ipso*-Nitrosation of Arylboronic Acids with Chlorotrimethylsilane and Sodium Nitrite, *Tetrahedron Lett.* **2014**, 55, 1975–1978. (DOI: 10.1016/j.tetlet.2014.01.138)
- [2] D. Fischer, T. M. Klapötke,* M. Reymann, P. C. Schmid, J. Stierstorfer, M. Sućeska, Synthesis of 5-(1*H*-Tetrazolyl)-1-hydroxy-tetrazole and Energetically Relevant Nitrogen-Rich Ionic Derivatives, *Propellants Explos. Pyrotech.* **2014**, 39, 550–557. (DOI: 10.1002/prop.201300152)
- [3] M. Joas, S. Kießling, T. M. Klapötke,* P. C. Schmid, J. Stierstorfer, Energetic Complexes of 5-(4-Amino-1,2,4-triazol-3-on-5-yl)tetrazole and Ionic Derivatives of its 2*N*-Oxide, *Z. Anorg. Allg. Chem.* **2014**, 640, 2759–2765. (DOI: 10.1002/zaac.201400417)
- [4] T. M. Klapötke,* M. Q. Kurz, R. Scharf, P. C. Schmid, J. Stierstorfer, M. Sućeska, 5-(1*H*-Tetrazolyl)-2-Hydroxy-Tetrazole: A Selective 2*N*-Monoxidation of Bis(1*H*-Tetrazole), *ChemPlusChem* **2015**, 80, 97–106. (DOI: 10.1002/cplu.201402124)
- [5] T. M. Klapötke,* M. Q. Kurz, P. C. Schmid, J. Stierstorfer, Energetic Improvements by *N*-Oxidation: Insensitive Amino-Hydroximoyl-Tetrazole-2*N*-Oxides, *J. Energ. Mat.* **2015**, 33, 191–201. (DOI: 10.1080/07370652.2014.963743)
- [6] T. M. Klapötke,* P. C. Schmid, S. Schnell, J. Stierstorfer, Thermal stabilization of energetic materials by the aromatic nitrogen-rich 4,4',5,5'-tetraamino-3,3'-bi-1,2,4-triazolium cation, *J. Mater. Chem. A* **2015**, 3, 2658–2668. (DOI: 10.1039/C4TA05964F)
- [7] T. M. Klapötke,* P. C. Schmid, S. Schnell, J. Stierstorfer, 3,6,7-Triamino-[1,2,4]triazolo[4,3-*b*][1,2,4]triazole: A Non-toxic, High-Performance Energetic Building Block with Excellent Stability, *Chem. Eur. J.* **2015**, 21, 9219–9228. (DOI: 10.1002/chem.201500982)
- [8] K. Hafner, T. M. Klapötke,* P. C. Schmid, J. Stierstorfer, Synthesis and Characterization of Asymmetric 1,2-Dihydroxy-5,5'-bitetrazole and Selected Nitrogen-Rich Derivatives, *Eur. J. Inorg. Chem.* **2015**, 17, 2794–2803. (DOI: 10.1002/ejic.201500338)
- [9] T. M. Klapötke,* P. C. Schmid, J. Stierstorfer, Crystal Structures of Highly Energetic Furazanes, *Crystals* **2015**, 5, 518–432. (DOI: 10.3390/cryst5040418)
- [10] T. M. Klapötke,* M. Leroux, P. C. Schmid, J. Stierstorfer, Energetic Materials Based on 5,5'-Diamino-4,4'-dinitramino-3,3'-bi-1,2,4-triazole, *Chem. Asian J.* **2016**, 11, 844–851. (DOI: 10.1002/asia.201500701)
- [11] T. M. Klapötke,* P. C. Schmid, J. Stierstorfer, N. Szimhardt, Synthesis and Characterization of Tetrahedral Zn(II) Complexes with 3,6,7-Triamino-7*H*-[1,2,4]triazolo[4,3-*b*][1,2,4]triazole as Nitrogen-rich Ligand, *Z. Anorg. Allg. Chem.* **2016**, 642, 383–389. (DOI: 10.1002/zaac.201600006)

The authors of [2] – [11] are listed in alphabetical order. P. C. Schmid is the first author of [2] – [10].

Oral presentations

- [1] T. M. Klapötke, P. C. Schmid, J. Stierstorfer, M. Sućeska, Novel energetic bistetrazole-*N*-oxides - synthesis and characterization, *New Trends in Research of Energetic Materials*, 17th Seminar, Pardubice, Czech Republic, **2014**.
- [2] T. M. Klapötke, P. C. Schmid, J. Stierstorfer, New energetic aminotriazoles, *New Trends in Research of Energetic Materials*, 18th Seminar, Pardubice, Czech Republic, **2015**.

Poster presentations

- [1] T. M. Klapötke, P. C. Schmid, J. Stierstorfer, Investigations on the effect of 2*N*-oxides in aminohydroximoly-tetrazoles, *New Trends in Research of Energetic Materials*, 18th Seminar, Pardubice, Czech Republic, **2015**.
- [2] S. Kießling, T. M. Klapötke, P. C. Schmid, J. Stierstorfer, Enhancing the Energetic Properties of 5-(4-amino-1,2,4-triazol-3-on-5-yl)tetrazole by *N*-oxidation, *New Trends in Research of Energetic Materials*, 18th Seminar, Pardubice, Czech Republic, **2015**.
- [3] T. M. Klapötke, P. C. Schmid, J. Stierstorfer, Investigations on the Energetic Performance and Thermal Stability of *N*-bonded Nitramines, *New Trends in Research of Energetic Materials*, 19th Seminar, Pardubice, Czech Republic, **2016**.